Synthèse et caractérisation de glycopolymères à base d'oligoalginates en milieu aqueux

Ali Ghadban

UNIVERSITÉ DE GRENOBLE

THÈSE

Pour obtenir le grade de

DOCTEUR DE L'UNIVERSITÉ DE GRENOBLE

Spécialité : **Science des polymères**

Arrêté ministériel : 7 août 2006

Présentée par

« Ali GHADBAN»

Thèse dirigée par **« Alain HEYRAUD»** et
codirigée par **«Luca ALBERTIN»**

préparée au sein du **Centre de Recherches sur les Macromolécules Végétales (CERMAV), CNRS**
dans **l'École Doctorale de Chimie et Sciences du Vivant**

Synthèse et caractérisation de glycopolymères à base d'oligoalginates en milieu aqueux

Thèse soutenue publiquement le **« 20 janvier 2012 »**,
devant le jury composé de:

Monsieur Serge PEREZ
Directeur de Recherche, European Synchrotron Radiation Facility,
(Examinateur)
Monsieur Laurent FONTAINE
Professeur, Université du Maine,
(Examinateur)
Monsieur Alain DURAND
Professeur, Ecole Nationale Supérieure des Industries Chimiques,
(Rapporteur)
Monsieur Sébastien VIDAL
Chargé de Recherche, Université Claude Bernard Lyon 1,
(Rapporteur)

to my family for their unlimited support

and

to the Sultan of the last and the final age

Table of contents

Abstract

The synthesis of oligoalginate derived glycomonomers (AlgiMERs) and their conventional and Reversible Addition Fragmentation chain Transfer (RAFT) polymerizations in aqueous solution were investigated. Firstly, the starting oligoalginates were transformed either into the corresponding glycosylamines or into amino-alditols (via reductive amination). At this stage, optimized amination protocols were identified by carrying out a systematic study on a simpler uronic acid (D-glucuronic acid). Secondly, the obtained amino sugars were reacted with an electrophile bearing a polymerizable vinyl group to yield AlgiMERs.

The resulting glycomonomers did not homopolymerize even in high ionic strength and for long reaction times, but their conventional radical copolymerization with *N*-(2-hydroxyethyl methacrylamide) HEMAm led to high molecular weight glycopolymers ($M_w \approx 1.5 \times 10^6$ Da) containing up to 50 % by mass of oligoalginate. A kinetic study confirmed that the consumption of both monomers followed a first order kinetic and that oligoalginate-derived monomers were incorporated early on in the polymerization process. Based on these results, the investigation was extended to the reversible-deactivation radical copolymerization in aqueous solution and well defined gradient glycopolymers were obtained (M_n = 12 000 Da – 90 000 Da; PDI ≤ 1.20).

Finally, I could prove that a synthetic polymer carrying oligo(1→4)-α-L-guluronan residues gels in the presence of Ca^{2+} ions and affords a transparent and stable hydrogel.

Acknowledgement

Many thanks to the French minister of education for the three years scholarship and to the “Réseau de Recherche Chimie pour le développement durable” that backed up us during my first year of my thesis as well.

My sincere appreciation goes to Alain Heyraud and Luca Albertin who supervised me as it should be and gave me the chance to jump into the world of polymers. Both Alain’s old hands on alginates and his fruitful suggestions guided me several times. Being together in the same boat, *i.e.* thirst for science, Luca was not only a supervisor of mine but also was an honest friend. His constructive comments together with his subtle ideas pushed me further to work harder and to be as good as he wanted me to be. He always tried to keep me away from his problems even in his worst times. All my acquired *organization skills* during my stay in CEMRAV are due to him, *grazie* Luca. I am equally thankful to Pr. M. Rinaudo whose endless donation to science will never stop. She was always there to answer any question and I owe the little I know in rheology to her. Furthermore, I would like to thank Isabelle Jeacomine for her assistance in nuclear magnetic resonance acquisitions together with Dr. Bernard Brasme and Stephanie Boullanger for the mass spectroscopy analyses. I would like to express my gratitude to Phillipe Colin-Morel and Lauren Buon who analyzed my size exclusion chromatography samples and to Luca who familiarized me with the instrument. Last but not least, I would like to thank Eric Bayma for the thermo-gravimetric analyses.

Not to forget as well all my colleagues in CERMAV who stayed beside me since the first day of my Ph.D. where we spent memorable times together. Thank you all.

Keys to symbols and constants

[A]	concentration of species A
$[A]_0$	initial concentration of species A
$[P\text{-}X]_0$	initial initiator/control agent concentration
A_δ^i	area of a methine signal of compound *i* having a chemical shift δ
A	virial coefficient or area
C	chain transfer constant
c	concentration
c^0	initial concentration
C^*	critical concentration
D_c	proportion of dead chains
d*n*/d*c*	differential refractive index increment
E	Young's modulus
F	force
f	initiator efficiency or mole fraction of monomer in the feed mixture
F	mole fraction of monomer in polymer
F_m	weight fraction of monomer in polymer
G'	storage modulus
G''	loss modulus
H	optical constant
I_2	initiator
$I^{\cdot}$	primary radical
J	coupling constant
k	rate constant
M	monomer molecule
M_n	number average molecular weight
M_w	weight average molecular weight
m	mass
N_A	avogadro's number

n	refractive index
P_i	dead i-mer macromolecule
P	degree of polymerization, purity, or scattering function
p	pressure
R_p	rate of polymerization
R_t	rate of termination
R_{tr}	rate of chain transfer
$R_i^{\cdot}$	growing i-mer macroradical
R	rayleigh's ratio or universal constant
R_g	radius of gyration
r	reactivity ratio
S	chain transfer agent or normalizing constant
S	surface area
t	time
T	temperature
ν	kinetic chain length or Poisson's ratio
ν	initiator's degree of functionality
V	elution volume
δ	contribution of disproportionation to the overall termination process
$[\eta]$	intrinsic viscosity
η_{sp}	specific viscosity
σ	swelling ratio
x	conversion or mole fraction
λ	wavelength
π	osmotic pressure

Keys to abbreviations and acronyms

ATRP	atom transfer radical polymerization
AIBN	2,2'-azobis-isobutyronitrile
ACPA	4,4'-azobis-cyanopentanoic acid
Ai	initiator used in ATRP holding the number i
BSA	bovine serum albumin
BA	butyl acrylate
BS-DBN	2-(Benzoyloxy)-1-(phenylethyl)-di- tert-butyl nitroxide
COSY	correlated spectroscopy
CPADB	4-cyano-4-[(phenylcarbonothioyl)sulfanyl] pentanoic acid
CPATTC	4-cyano-4-{[(ethylsulfanyl)carbonothioyl]sulfanyl} pentanoic acid
CMC	critical micelle concentration
CSA	camphorsulfonic acid
ConA	concanavalin A
CD14	cluster of differentiation 14
DNA	deoxyribonucleic acid
DCP	dicumyl peroxide
DODA	*N*,*N*-di(octadecyl)amine
DP	degree of polymerization
DLS	dynamic light scattering
DMAc	dimethyl acetamide
DMF	dimethyl formamide
Da	Dalton
DRI	differential refractive index
DVB	divinylbenzene
DMSO	dimethyl sulfoxide
dHbipy	4,4'-Di-*n*-heptyl-2,2'-bipyridine
dDbipy:	4,4'-Bis(1-decyl)-2,2'-bipyridine
ESI	electrospray ionization

fimH	fimbrial lectin
Glc	D-glucose
GlcA	D-glucuronic acid
$GulA_x$	oligoguluronan block with DP_n = x
Ii	initiator holding number i
ISTD	internal standard
IV	intrinsic viscosity
$ManA_x$	oligomannuronan block with DP_n = x
FTIR	fourier transform infrared
HEMA	*N*-(2-hydroxyethyl)methacrylate
HEMAm	*N*-(2-hydroxyethyl)methacrylamide
HMBC	heteronuclear multiple bond correlation
HMQC	heteronuclear multiple quantum correlation
KPS	potassium persulfate
Li	ligand holding number i
LCST	lower critical solution temperature
RDRP	reversible-deactivation radical polymerization
LS	light scattering
MALDI-ToF	matrix-assisted laser desorbtion ionisation - time of flight
MW	molecular distribution
MWD	molecular weight distribution
MWCO	molecular weight cut off
Mi	monomer holding number i
MWNT	multiwalled carbon nanotube
MMA	methyl methacrylate
MA	methacrylate
$M_{n,th}$	theoretical number average molecular weight
MALLS	multi angle laser light scattering
NIPAAm	*N*-isopropylacrylamide
NMP	nitroxide mediated polymerization or *N*-methyl-2-pyrrolidone
NMR	nuclear magnetic resonance
Ni	initiator used in NMP holding the number i

NOESY	nuclear overhauser effect spectroscopy
NIPAAm	*N*-isopropylacrylamide
OligoG	oligoguluronan
OligoM	oligomannuronan
PDI	polydispersity index
PFS	pentafluorostyrene
PPO	poly propylene oxide
PMDETA	N,N,N',N",N"-pentamethyldiethylenetriamine
PEG	polyethylene glycol
PE	petroleum ether
PMi	polyMi
ppm	part per million
PSF	polysulfone
QD	quantum dot
ROP	ring opening polymerization
ROMP	ring opening metathesis polymerization
RAFT	reversible addition fragmentation chain transfer
RCA_{120}	*Ricinus communis* agglutinin
Ri	RAFT agent holding number i
RI	refractive index
RT	room temperature
St	styrene
SEC	size exclusion chromatography
SG1	*N*-tert-butyl-*N*-(1-diethylphosphono-2,2-dimethylpropyl)
SEM	scanning electron microscopy
SFM	scanning force microscopy
SDS	sodium dodecyl sulfate
SV	specific viscosity
SCVCP	self condensing vinyl copolymerization
SPR	plasmon resonance measurements
TEA	triethyl amine
TEMPO	2,2,6,6-Tetramethylpiperidine-1-oxyl

TFA	tri-fluoroacetic acid
THF	tetrahydrofuran
TEM	transmission electron microscopy
TBAF	tetra-*n*-butylammonium fluoride
TGA	thermal gravimetric analysis
TEMPO	2,2,6,6-tetramethylpiperidine-1-oxyl
TLR2	toll-like receptor 2
TLR4	toll-like receptor 4
TNF	tumor necrosis factor
VLA	*N*-(p-vinylbenzyl)-[O-β-D-galactopyranosyl-(1→4)]-D-gluconamide
VA-080	2,2'-Azobis{2-methyl-N-[1,1-bis(hydroxymethyl)-2-hydroxyethl]propionamide}
WGA	wheat germ agglutinin

Chapter 1: Introduction to the thesis

1.1 The rationale

One drawback to the use of natural polysaccharides is the intrinsic variability of their physicochemical properties. Factors such as the source species, the conditions of growth, the period of harvest and the extraction process all result in a different structure and composition of the polymer. An original approach to the use of biopolymers as a primary source of functional materials would be to depolymerize a natural polysaccharide into well-defined oligomers, separate them on the basis of their size and chemical nature, functionalize them with a suitable functional group at the chain-end, and re-polymerize them (in a reversible-deactivation fashion) as to obtain neo-polysaccharides with well-defined macromolecular architecture and composition. In this context, control of the macromolecular architecture will be essential to bestow the resulting glycopolymer with suitable physico-chemical properties.

Through careful molecular and process design, the resulting biohybrid materials could combine the best of synthetic polymers (e.g. flexible design, precise architecture, pre-determined composition and functionality, reproducible properties) and of polysaccharides (e.g. renewable sourcing, biodegradability, biological recognition, high persistence length, and complexation of metal ions).

1.2 The doctoral project

Within the working hypothesis exposed above, alginate is a perfectly appropriate object of research since it combines very interesting properties (e.g. complexation of divalent cations), with great structural and compositional variability, and the possibility to be depolymerized into chemically homogeneous oligomers of different nature and size. In fact, the latter can be obtained on a multi-gram scale by simple acid hydrolysis and selective precipitation.

Hence, well-defined oligoglycuronans were obtained from the depolymerization of alginate, [1] separated on the basis of their size and chemical nature, [2] functionalized at the chain-end with a group suitable for radical polymerization and re-polymerized in a reversible-deactivation fashion as to obtain hybrid polymers with well-defined and original

macromolecular architecture and composition. ***A fundamental aspect of this work is that virtually all syntheses*** [3] ***and all polymerizations were realized in water (or water/organic mixtures) without resorting to protective group chemistry.*** This choice was motivated by the challenge of developing environmentally friendly synthetic strategies and to make the know-how developed in this thesis readily accessible to the widest possible public, including scientists with no specific expertise in carbohydrate chemistry and industrial companies.

Thus, oligoglycuronans were transformed into the corresponding glycosylamines (**Chapter 5**) and 1-amino-1-deoxy alditols directly in aqueous solution (**Chapter 6**) and the latter were converted to oligoalginate-derived monomers (AlgiMERs; **Chapter 7**) without the need for protective group chemistry. Both in Chapter 5 and in Chapter 6 an optimization study is described which was aimed at minimizing the amount of reagents used and (or) at maximizing the yield of amine. The conventional radical (co)polymerization of some AlgiMERs was then examined and high molar mass graft copolymers were obtained that contained up to 50% by mass of oligosaccharide residues (**Chapter 8**). The study was then extended to the RAFT copolymerization of N-(2-hydroxyethyl)methacrylamide with methacrylamide-type AlgiMERs and well-defined glycopolymers with a predetermined molar mass were obtained (**Chapter 9**). Finally, the rheological properties of the polymers obtained in Chapters 8 and 9 were briefly investigated both in solution and in the gel state. **Chapter 10** contains all conclusions that were drawn from the study.

This thesis merges fields of research (*i.e.* polysaccharides, carbohydrate chemistry and radical polymerization) that normally interest different audiences. As a complement to the presentation of experimental results, the interested reader will find an introduction to alginates in **Chapter 2** and to conventional radical and RAFT polymerization in **Chapter 3**. Also, a short review of the synthesis of well-defined glycopolymers by reversible-deactivation radical polymerization techniques can be found in **Chapter 4**.

1.3 Publications from this thesis

(1) Ghadban, A.; Albertin, L.; Moussavou Mounguengui, R. W.; Peruchon, A.; Heyraud, A., Synthesis of β-D-glucopyranuronosylamine in aqueous solution: Kinetic study and synthetic potential. *Carbohydr. Res.* **2011,** *346* (15), 2384–2393.

(2) Ghadban, A.; Albertin, L.; Condamine, E.; Moussavou Mounguengui, R. W.; Heyraud, A., NMR and MS study of the formation of β-D-glucopyranuronosylamine in aqueous solution. *Can. J. Chem.* **2011,** *89* (8), 987-1000.

1.4 References

(1) Haug, A.; Larsen, B.; Smidsroed, O. *Acta Chem. Scand.* **1966**, *20*, 183.

(2) The first two parts the project were contracted-out to a company, since they are based on well-established scientific knowledge and practice.

(3) The sole exception was the synthesis of RAFT agents.

Chapter 2: Alginates

Table of contents

The interested reader can also refer to the comprehensive reviews on alginate written by Draget et al., [1] Rehm [2] and Rinaudo. [3]

2.1 Chemical structure and depolymerization

Also known as *alginic acid* or *algin*, alginate is an unbranched heteropolysaccharide present in the cell wall of brown algae (e.g. *laminaria hyperborea*, *Ascophyllum nodosum*) and produced (in a partially acetylated form) by some soil bacteria (e.g. *Pseudomonas* and *Azotobacter vinelandii*). Alginate is a polyelectrolyte composed of two repeating units (Figure 2.1): β-D-mannuronic acid (M unit) and its epimer at C5, α-L-guluronic acid (G unit). Both units are present as hexopyranose ring but while mannuronic acid mostly adopts a $^4C_1$ ring conformation, guluronic acid mostly adopts a $^1C_4$ one. Within the polymer chain, these two units are linked in position (1→4) and give rise to homopolymeric blocks (MM and GG) and to mixed (mostly alternating) MG blocks. [4]

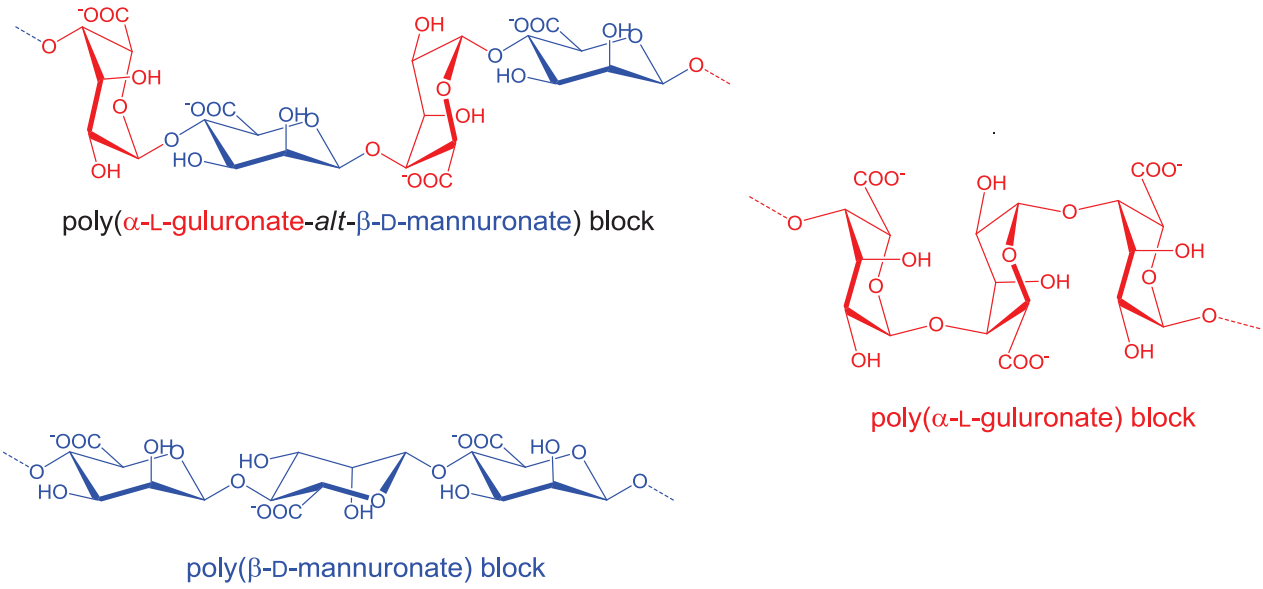

Figure 2.1 *Different arrangements of repeating units within the alginate chain.* [4]

Fisher and Dorfel [5] first determined the composition of alginate samples by total acid hydrolysis [6] followed by separation of the constituting monosaccharides by paper chromatography and their colorimetric quantification with tetrazolium chloride. The separation and quantification methods proved impractical though, and Huag et al. [7] successfully replaced them with anion exchange chromatography and the orcinol colorimetric

method. Later, the same group investigated the partial hydrolysis of alginate [8] and identified the conditions leading to the isolation of fairly pure (1→4)-β-D-mannuronan and (1→4)-α-L-guluronan oligosaccharides. In particular, upon hydrolysis for 2 h at 100°C in HCl 0.3 N they obtained:

- A soluble fraction which was later identified as consisting of mixed MG blocks. [4b]
- An insoluble fraction which proved more resistant toward acid hydrolysis. The latter was re-solubilized by the addition of alkali and fractionated by adjusting the pH at 2.85. At this pH, GG blocks precipitate while MM blocks stay in solution. In this way, fairly pure (1→4)-α-L-guluronan and (1→4)-β-D-mannuronan oligosaccharides with $DP_n \cong 20$ could be obtained (purity ~90%). [8b]

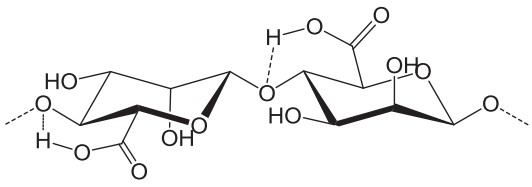

Figure 2.2 *Model suggested by Smidsrod et al. [4a] showing the intramolecular catalyzed acid hydrolysis of alginates.*

In the same study it was noticed that the hydrolysis of alginates at pH > 2 is faster than that of neutral polysaccharides under the same conditions. It was thus suggested the reaction was catalyzed by the undissociated carboxyl groups via intramolecular hydrogen bonding (Figure 2.2). [4a] Obviously, this hypothesis necessitates the presence of a carboxyl group in the vicinity of the glycosidic bond and the effect strictly depends on the conformation of monosaccharide units and the configuration of C5. Indeed, it was found that rate of hydrolysis follows the order: [4b,9]

$$MM > GM > MG > GG$$

In more recent work Chhatbar et al. [10] examined the partial acid hydrolysis of alginates in oxalic acid (0.15 mol L^{-1}) or sulfuric acid (0.25 mol L^{-1}) assisted by microwave irradiation. They obtained results comparable with those from previous literature but in much shorter times (4 minutes).

Enzymatic hydrolysis can be used as an alternative or as a complement to acid hydrolysis for compositional studies of alginates and the preparation of oligoglycuronans.

Alginate lyases catalyze a β-elimination reaction that splits the 1→4 glycosidic linkage and leaves a double bond at the non-reducing end of the molecule (Scheme 2.1). [1] Enzymes which depolymerize alginates could be obtained from various bacteria, brown algae and from marine mollusks. [11] Generally talking, enzymes from bacterial origins have preference for cleaving the α-L-guluronic acid linkage, whereas those purified from algae and mollusks have greater affinity to β-D-mannuronic acid linkage. The glycal unit obtained from enzymatic degradation is identical for both M and G blocks. [1]

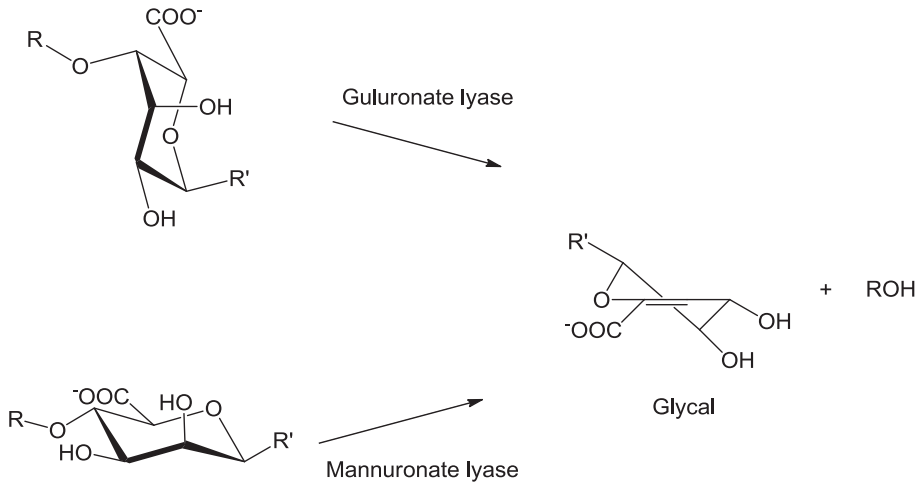

Scheme 2.1 *Glycal formation after the enzymatic degradation of alginates.*

For illustration, Boyd et al. [11] described the specificity of an extracellular lyase towards poly α-L-guluronates. The lyase in question, after random degradation led to the formation of unsaturated di and tri-saccharide with small amounts of tetra-saccahrides after its action upon poly-G blocks. On the other hand, the lyase did not show any action on the mannuronate blocks and had an extensive action on MG blocks. Another example on the preparation of either mannuronate blocks (poly-M blocks) with DP ≈ 30, or strictly alternating sequences of mannuronic and guluronic acid (poly-MG blocks) with DP > 20 by the action of a polymannuronate lyase on two *Pseudomonas aeruginosa* alginates was reported by Heyraud et al. [12]

The two methods described above are the most familiar and known methods to obtain oligoalginates from alginates, yet there are other methods to obtain these oligomers as well:

Degradation of sodium alginates by γ-irradiation [13] and by oxidative-reductive methods [13, 14] have been also investigated. The variation of viscosity has been monitored

throughout the degradation processes, where a decrease in viscosity with time was observed. Howells et al. [13] showed that the prepared oligomers prepared by either method have gross chemical and biological properties similar to those obtained by hydrolytic methods. Smidsrods et al. [14] showed after testing various reducing agents that ascorbic acid was very effective in degrading alginates, where a decrease of viscosity from 20 dl g^{-1} to 2.5 dl g^{-1} was observed in 3 hours.

Smidsrod et al. [15] also described the degradation of alginates in the solid state. They observed that thermal depolymerization of alginate in the solid state was found to be catalyzed simultaneously by protons and hydroxide ions and independently from the oxygen content in the reaction medium; suggesting that acid hydrolysis and β-elimination were the primary mechanisms involved in the depolymerization reaction.

Matsushima et al. [16] reported the partial depolymerization of alginates in *subcritical water* (25 MPa at 250 °C for 88 ms) where under such conditions M-G and G-M linkages were selectively cleaved. As a result, they obtained almost homopolymers of guluronic acid (98%) after selective preparation at pH 2.95 together with water soluble mannuronic acid rich heteropolymers purified by dialysis. According to the authors, by varying the reaction conditions the M/G ratio could be controlled. Recently, oligomers rich in M, G and MG blocks were obtained in 90% yields using a photochemical reaction (UV/TiO_2 at pH7 for 3 hours). [17] The authors monitored the change in molecular weights of the degraded alginate samples by polyacrylamide gel electrophoresis. Recently, the decomposition of alginates under hydrothermal conditions (180-240 °C) was examined. [18] They observed that at lower temperatures (180 °C), monosaccharides as mannuronic and guluronic acid formed with a preferential formation for mannuronic acid. Furthermore, SEC, HPLC and MS analyses showed evidence for smaller molecules as glycolic, lactic acids that formed during the course of the reaction.

2.2 Solution properties of alginates

Alginates isolated from different sources differ in their molar mass and in the length and distribution of the different blocks. For instance, the composition (M / G ratio) and the sequence distribution of the units vary between different algae, between different tissues of the same algae and according to seasonal and growth conditions. The extraction process plays

a role as well, and some degradation is unavoidable. This structural variability is reflected in the variation of the physico-chemical properties of alginates and considerably hinders the production of alginate with standardized properties on a large scale.

2.2.1 Solubility in aqueous solution

The solubility of alginates depends on two things: the pH, due to the presence of the carboxyl functionality in the polymer, and the ionic strength of the solution. Potentiometric titrations revealed that the dissociation constants, pK_a, for mannuornic and guluronic acid monomers were 3.38 and 3.65 respectively in 0.1 M NaCl [1] which are consistent with those for alginates. It is worth noting that the pK_a can slightly differ depending on the concentration of the alginate and the ionic strength of the solution. Thus pH values below the pK_a values cause precipitation of the polymer, whereas controlled addition of protons in the medium can trigger the formation of acid gels. [19] Moreover, alginates with alternating sequences precipitate at low pH values, for *e.g.* alginates from *A. nodosum* are soluble at pH as low as 1.4. This is due to the difficulties in the formation of the crystalline regions in the alternating sequence, contrary to the homopolymeric blocks where the formed crystalline regions are stabilized by H-bonding which causes precipitation. Thus the solubility of alginates is dependent on the MG block whose presence assures the solubility at low pH. Furthermore, the ionic strength of the solution plays an important role in the solubility of alginates. For instance, alginates rich in mannuronic acid could be precipitated and fractionated out in high ionic strength medium due to the salting out effect. [20] Thus the hardness of water also affects the solubility of alginates due to its rich contents in mono and divalent cations. However, alginates could be solubilized at $[Ca^{2+}]$ above 3mM in the presence of a complexing agent as citrate. [1]

2.2.2 Selectivity to ions

One of the interesting properties of alginates is its capability to form gels in the presence of certain multivalent counterions as Ca, Sr, Ba, while Mg ions does not form gels. Most monovalent counterions (except Ag^+) form soluble alginates while divalent ions form gels or precipitates. [3] The affinity of alginates to counterions was found as follows: [21, 22]

$$Pb > Cu > Cd > Ba > Sr > Ca > Ni, Co, Zn > Mn$$

Furthermore, it has been shown that the gelling effect is related to the abundance of the G residues in the chain, in other words the selectivity of alginates increased markedly with increasing content of G residues in the chain. In addition, the selectivity coefficients of Ca to K ions, k_K^{Ca}, for polymannuronate and polyguluronate were different with $k_K^{Ca} = 4.2$ and $k_K^{Ca} =$ 71 respectively. [22] Moreover, the selectivity coefficients of divalent ions were also established for the polyguluronate blocks ($k_{Mg}^{Sr} = 150$, $k_{Mg}^{Ca} = 40$, $k_{Ca}^{Sr} = 7$) and those for polymannuronate blocks showed values close to unity. [23] Interestingly, experiments to study the binding affinity of Ca^{2+} to D-mannuronic acid and L-guluronic acid did not show any Ca-binding affinities which emphasize the fact that the selectivity of binding ions is dependent on the polymeric nature. [22] For that, Grant et el. [24] tried to explain this phenomenon and attributed that to the so-called "egg-box" model, based upon the conformation of the guluronate residues in space (Figure 2.3).

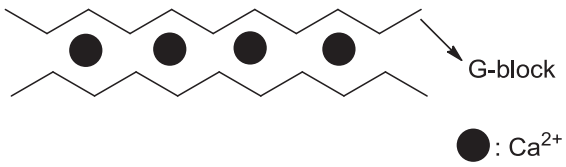

Figure 2.3 *Egg box model reported by Grant et al. [24] showing the calcium interaction with the α-L-guluronic-box block.*

In conclusion, L-guluronic acid is basically responsible for the formation of the gels in the chains.

2.2.3 Solution properties

Alginate salts resulting from monovalent counter ions as Na and K are soluble in water and result in viscous solutions depending on the size of the polymer, its concentration and the ionic strength of solution. Thus its intrinsic viscosity together with its molecular weight could be calculated according to Mark Houwnik relation:

$$[\eta] = KM^a \tag{1.1}$$

where $[\eta]$ is the intrinsic viscosity, M is the molecular weight, and K and a are constants depending on the nature of the polymer, solvent and temperature. The constant a from Eq. 1.1 lies between 0.5 for a polymer dissolved in a theta solvent to about 0.8 in very good solvent. [25] Furthermore, this constant also gives information about the rigidity of the chain. For most

flexible polymers, $0.5 \leq a \leq 0.8$ and for semi flexible polymers $a > 0.8$ reaching a limit value of 1.8 for rigid rod like polymers. For instance, Smidsrod et al. [26] gave, after light scattering experiments on an alginate sample containing 38 % G units, the following parameters: a = 0.98 and $K = 2.44 \times 10^{-3}$. Mackie et al. [27] showed that K and a parameters depend on the M/G ratio, where a increasing and K decreasing with G content increase. [3] Finally, Smidsrod et al. [28] gave information about the relative extension of alginate blocks in solution after light scattering and viscosity measurements where the extension of alginate blocks at a given ionic strength is:

$$GG > MM > MG$$

This sequence was theoretically demonstrated by the authors by the rotation hindrance around the glycosidic bond when the L-guluronic acid residues adopt the $^1C_4$ conformation. This explains the high stiffness (rigidity) of the G block adopting a diaxial conformation. It is worth noting that the expansion of an alginate, even in excess salt, is larger than that of a neutral polysaccharide, where it has been found by Smidsrod et al. [28] that at very high ionic strengths, a = 0.84 which corresponds to a neutral alginate molecule, yet it stays very extended.

2.3 Ionic gel formation

In general a gel is defined as a 3D network of macromolecules swollen by a solvent. Two cross-linking methods exist:

a) chemically via covalent bond formation
b) or physically by crosslinking between chains. The formation of physical gels is sometimes reversible, contrary to chemical gels.

Due to its ability to complex divalent cations, alginates rich in G residues are able to form gels. R. Kohn [29] showed, after monitoring the variation of the activity coefficient of Ca^{2+} (γCa^{2+}) with *DP* for β-D-mannuronic and α-L-guluronic acid blocks, that a specific interaction of Ca ions with G blocks is observed at *DP* values above 20. Subsequently, this cross-linking induces an increase in viscosity and a decrease in the volume occupied by the gel. The mechanism for Ca^{2+} complexation is still a debate and mostly involves the interaction of a calcium ion with different oxygen atoms of two adjacent guluronic acid units in both

chains entering in the inter-chain binding to Ca^{2+} as adopted by the egg-box model (Figure 2.4). [3]

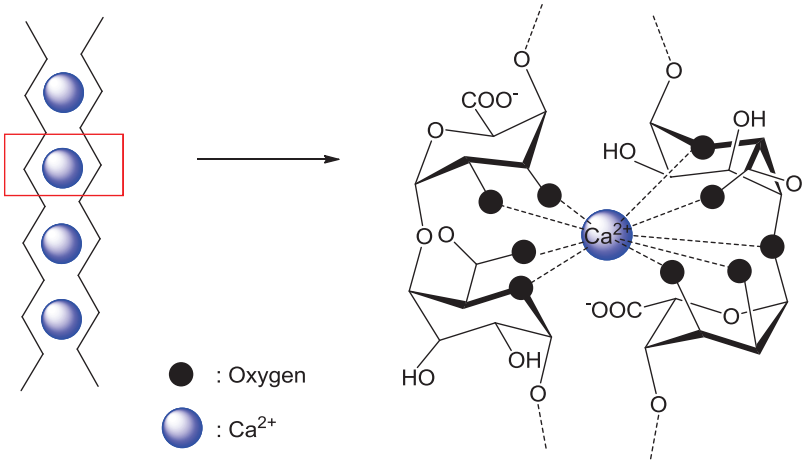

Figure 2.4 *Interaction of Ca ions with the oxygen atoms of two G blocks adopting the egg-box model as reported by Braccini et al. [30] in their paper.*

Gels are generally formed by two methods: the diffusion and the internal setting methods. In the former method, the cross-linking cation is left to diffuse from an outer reservoir to an alginate solution as with dialysis or by a drop wise addition of an alginate solution over a $CaCl_2$ solution. On the other hand, in an internal setting method the release of the cross-linking cation (Ca^{2+}) in an alginate solution is triggered and controlled by a change in pH or in the presence of a chelating agent. [31] The main difference between the two methods is the gelling kinetics which is very rapid in the case of diffusion setting and this result in an inhomogeneous distribution of alginate within the gel with the highest concentration being at the surface and gradually decreases towards the center. Nonetheless, this is useful for immobilization purposes. [32]

The quality of the obtained gel depends on the nature of the alginate. In other words the stability of gels and their physical properties depend on the content of G residues in the chain and the length of the G block and that will be reflected on the stiffness of the obtained gel. [33] Interestingly, the polyelectrolyte nature of alginates can influence the electrostatic interaction, under favorable conditions, with other charged molecules (e.g. proteins). These types of interactions can stabilize more the mixture and increase the strength of the corresponding gels resulting in a phase transition and thus altering the rheological behavior. [1] For instance, in their studies involving gelling of bovine serum (BSA) and alginate in both the sodium and calcium forms, Neiser et al. [34] referred the increase in the Young's modulus at

known pH and ionic strength to electrostatic interaction between the alginate and the protein. It is worth noting that BSA/Ca-alginate gels were stronger than BSA/Na-alginate gels at all conditions, and stronger than pure BSA gels up to higher pH values.

2.4 Stability of alginates

As mentioned before, one of the methods to degrade alginates is achieved by varying the pH of the solution. At around neutral pH alginate solutions are stable, and their stability is affected by the change in pH. For instance, Smidsrod et al. [35] showed that degradation of alginates was maximum at pH values below 5 and above 10 after subjecting an alginate sample isolated from *laminaria digitata* at 68 °C to different pH. The drop in viscosity was a clear evidence for the degradation process. In acidic conditions, alginates degrade by the cleavage of the glycosidic bond whereas in basic conditions degradation is assured by β-elimination resulting in the formation of a glycal (Scheme 2.1). Further studies established by the Trondheim group focused on the degradation under basic conditions. [36] In their study they noticed that the degradation was dependent on two major requirements: the counter-ion (Na, Ca, Mg) present and the nature of solution (ionic strength, concentration, species). First, they have noticed that above pH 11 the rate of degradation was proportional to the concentration of hydroxyl ions present. The presence of carbonate and phosphate ions showed a catalytic effect and an increase in the rate of degradation was observed, whereas amine sources as methyl and triethyl amines had marginal effects on the degradation. On the other hand, increasing the ionic strength of solution increased the rate of degradation and that was referred to the increased withdrawing character of the carboxyl group once screened and that was supported by the idea that alginate methyl esters degrade at a faster rate than alginates (10^4-10^5 faster). Moreover, by exhanging the Mg counter ion of an alginate with Na a drop in the rate of degradation was observed. It is worth noting that at pH 10 there was no influence for degradation by β-elimination where the authors referred any degradation below that pH to an oxidative-reductive degradation. [37] Since degradation reactions are temperature sensitive, autoclaving is generally not recommended for alginates where sterile filters are used in sterilizing alginates in solutions. [1] As claimed by McCleary et al. [38] that the elimination reaction is not stereospecific, since the glycosyloxy group is a poor leaving group and the

ionization of H-5 is probably easy. That is why a mechanism approximating to E1cB (Elimination Unimolecular conjugate Base) type is to be expected as shown in Scheme 2.2.

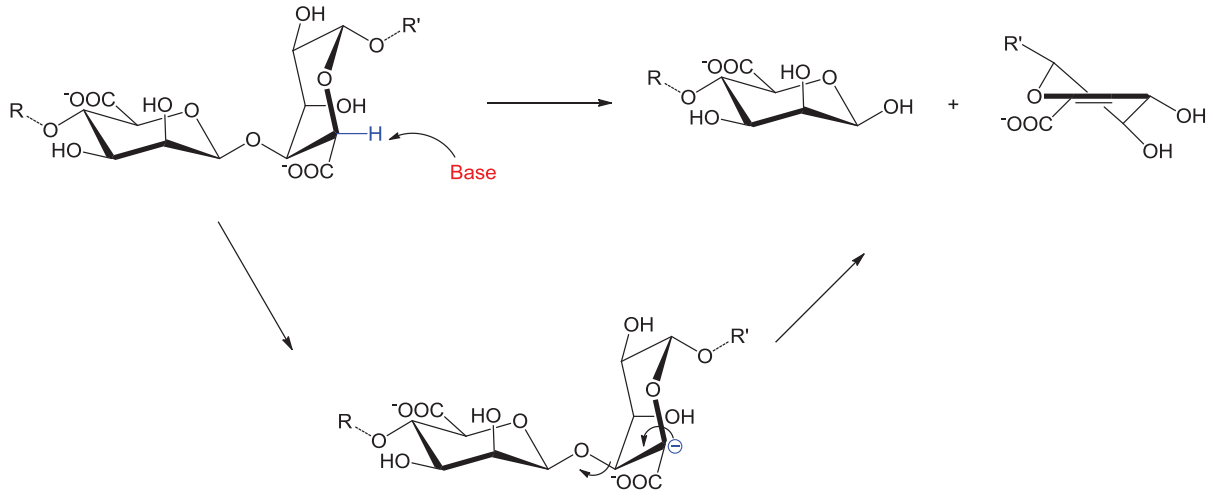

Scheme 2.2 *Mechanism for the degradation of alginates suggested by McCleary et al.* [38]

2.5 Biological activity

Concerning the biological activity of oligo- and poly(uronic acids), it is demonstrated that alginate and alginate-derived oligosaccharides are potent immune-stimulating agents and elicit cytokine production by monocytes. [39] In particular, (1→4)-β-D-mannuronan stimulates monocytes to produce tumor necrosis factor alpha (TNF-α), interleukin-1 (IL-1), and IL-6, and its potency increases with molecular size. By contrast, (1→4)-α-L-guluronan displays no such activity but acts as antagonists to mannuronan. It is now understood that both saccharides bind to the surface receptor CD14, [40] toll-like receptor 2 (TLR2) and TLR4 [41] and that optimal immunostimulating activity is determined both by the molecular size and by the conformation of the carbohydrate. Hence, attaching oligo(1→4)-β-D-mannuronan of low activity to particles enhances their TNF inducing potency by 2–4 log units. [42] Interestingly, both oligo(1→4)-β-D-mannuronan and oligo(1→4)-α-L-guluronan having an unsaturated unit at their non-reducing end induce cytokine secretion from mouse macrophage cells (cell line RAW264.7) in a size-dependent manner, whereas the corresponding saturated oligosaccharides display fairly low activity. Based on these studies, Jiang et al. have recently synthesized two oligo(1→4)-β-D-mannuronan derived neoglycolipids as potential TLR ligands. [43] Alginate oligomers have also been reported to act as elicitors of plant [44] and

Bifidobacteria [45] growth, and two patents [46] claim that oligo(1→4)-α-L-guluronan is effective in treating mucus hyper-viscosity in the respiratory tract, and in enhancing cervical mucus penetrability by spermatozoa. Finally, the biological activity of sulphated oligo(uronic acid)s have also been investigated: They appear to induce an indirect antitumor response by modulating the host-mediated immune defenses, [47] they exhibit a significant anticoagulant activity in vitro, as well as an anti-inflammatory activity in cotton pellet-induced granuloma in rats. [48]

2.6 Application

Given the large number of applications in food, pharmaceuticals, cosmetics and other industrial domains, [3] alginates should be considered as one of the most versatile polysaccharides.

Due to its gel-forming ability, viscosifying properties and stabilization of aqueous mixtures, dispersions and emulsions [1] alginates are used as food additives (E 400 - E 404) to improve, modify and stabilize the texture of foods. [49] The only alginate derivative used in food is propylene glycol alginate (PGA) which is obtained from the partial esterification of the carboxyl groups by propylene oxide. [50]

Alginates have been exploited as films or fibers in wound dressings for halting blood flow. [51] Interestingly, these fibers/films are able to absorb up to 20 times their weight and are resistant to oil penetration due to the hydrophilic character granted by the hydroxyl and carboxyl groups. Besides, calcium alginate revealed usefulness in making models of teeth in dental practice, limbs and other body parts in prosthetics. [3,1] Furthermore, alginates are used as immobilizing matrices in various biotechnological processes. For instance, mixing a cell suspension with a sodium alginate solution followed by dripping the resulting mixture in a solution rich in divalent cations (Ca^{2+}) entrap the cells in a three dimensional network. [32] Like that the gel acts as a barrier between the cells and the immune system of the host. Different cells have been suggested for gel immobilization including parathyroid cells for treatment of hypocalcemia (low serum calcium levels in the blood) and dopamine-producing adrenal chromaffin cells for treatment of Parkinson's disease. [1] Moreover, major interest in trapping insulin producing cells has been investigated for the treatment of Type I diabetes. [52]

Not to forget the use of alginates as a viscosifyer in textile printing, in paper coating for surface regularity, in welding as a binding agent and finally its ammonium form is used in can sealing because of its low ash content. [1]

2.7 Conclusion

From a chemical point of view, alginates look very simple as it contains only two sugar residues, β-D-mannuronic acid and α-L-guluronic acid linked in a 1-4 linkage but they possess various properties depending on the abundance of each block, the M/G ratio and their sequence. In this chapter an overview on alginate is reported. The first part of this chapter discussed the methods described in literature for de-polymerizing alginates into oligoalginates. Some of these methods comprise: acid, enzymatic, γ irradiation, and hydrothermal techniques. Based on literature, alginates possess interesting properties in solution and their solubility was found to be dependent on the pH and the ionic strength. For instance, an alginate solution whose pH is below the pK_a (3.38-3.65) tends to precipitate. Furthermore, alginates with monovalent counter ions, except for Ag^+, tend to form soluble viscous solutions depending on the size of the polymer, its concentration and the ionic strength. Moreover, the selectivity of alginates to counter ions was shown to be higher with divalent cations as Cu, Sr and Ca. This selectivity results in the formation of ionic gels whose formation is dependent on the abundance of G blocks. It was also shown the best pH range that assures the stability of alginates in solution is 5.5-9, where at low pH alginates degrade by acid hydrolysis and under basic conditions pH > 10 they undergo degradation by β-elimination. Finally, some applications and biological interests of alginates were reported.

2.8 References

(1) Draget, I. K.; Smidsroed, O.; Skjak-Braek, G. In *Biopolymers: Polysaccharides II*; Vandamme, E. J., De Baets, S., Steinbuchel, A., Eds.; Wiley-VCH, 2002, pp 215-244; Vol. 6.

(2) Rehm, B. H. A. In *Polysaccharides II: Polysaccharides from Eurokaryotes*; Vandamme, E. J., De Baets, S., Steinbuchel, A., Eds.; Eds. Wiley-VCH: Weinheim, 2002; Vol. 6.

(3) Rinaudo, M. In *Comprehensive Glycoscience: From Chemistry to System Biology*; Boons, G. J., Lee, Y. C., Suzuki, A., Taniguchi, N., Voragen, A. G. J., Eds.; Elsevier Ltd, 2007, pp 691-735; Vol. 2.

(4) (a) Smidsroed, O.; Haug, A.; Larsen, B. *Acta Chemica Scandinavica (1947-1973)* **1966**, *20*, 1026(b) Larsen, B.; Smidsroed, O.; Haug, A.; Painter, T. J. *Acta Chem. Scand.* **1969**, *23*, 2375.

(5) Fischer, F. G.; Dorfel, H. *Hoppe-Seyler's Zeitschrift fuer Physiologische Chemie* **1955**, *302*, 186.

(6) H_2SO_4 80% for 18 h at room temperature, then H_2SO_4 2 mol L^{-1} for 5 h at 100 °C.

(7) Haug, A.; Larsen, B. *Acta Chem. Scand.* **1962**, *16*, 1908.

(8) (a) Haug, A.; Larsen, B.; Smidsroed, O. *Acta Chem. Scand.* **1966**, *20*, 183(b) Haug, A.; Larsen, B.; Smidsroed, O. *Acta Chem. Scand.* **1967**, *21*, 691.

(9) Smidsroed, O.; Larsen, B.; Painter, T. J.; Haug, A. *Acta Chem. Scand.* **1969**, *23*, 1573.

(10) Chhatbar, M.; Meena, R.; Prasad, K.; Siddhanta, A. K. *Carbohydr. Polym.* **2009**, *76*, 650.

(11) (a) Boyd, J.; Turvey, J. R. *Carbohydr. Res.* **1977**, *57*, 163(b) Boyd, J.; Turvey, J. R. *Carbohydr. Res.* **1978**, *66*, 187.

(12) Heyraud, A.; Colin-Morel, P.; Gey, C.; Chavagnat, F.; Guinand, M.; Wallach, J. *Carbohydrate Research* **1998**, *308*, 417.

(13) Humphreys, E. R.; Howells, G. R. *Carbohyd. Res.* **1971**, *16*, 65.

(14) Smidsroed, O.; Haug, A.; Larsen, B. *Acta Chemica Scandinavica* **1963**, *17*, 2628.

(15) Holme, H. K.; Lindmo, K.; Kristiansen, A.; Smidsrod, O. *Carbohydrate Polymers* **2003**, *54*, 431.

(16) Matsushima, K.; Minoshima, H.; Kawanami, H.; Ikushima, Y.; Nishizawa, M.; Kawamukai, A.; Hara, K. *Industrial & Engineering Chemistry Research* **2005**, *44*, 9626.

(17) Burana-osot, J.; Hosoyama, S.; Nagamoto, Y.; Suzuki, S.; Linhardt, R. J.; Toida, T. *Carbohydr Res* **2009**, *344*, 2023.

(18) Aida, T. M.; Yamagata, T.; Watanabe, M.; Smith, R. L., Jr. *Carbohydr. Polym.* **2010**, *80*, 296.

(19) Draget, K. I.; Skjåk Bræk, G.; Smidsrød, O. *Carbohydrate Polymers* **1994**, *25*, 31.

(20) Haug, A. *Acta Chemica Scandinavica* **1959**, *13*, 601.

(21) Smidsroed, O.; Haug, A. *Acta Chem. Scand.* **1968**, *22*, 1989.

(22) Kohn, R.; Furda, I.; Haug, A.; Smidsroed, O. *Acta Chem. Scand.* **1968**, *22*, 3098.

(23) Haug, A.; Smidsroed, O. *Acta Chem. Scand.* **1970**, *24*, 843.

(24) Grant, G. T.; Morris, E. R.; Rees, D. A.; Smith, P. J. C.; Thom, D. *FEBS Letters* **1973**, *32*, 195.

(25) Cowie, J. M. G. *Polymers: Chemistry and physics of modern materials*; 2nd ed.; Blackie Academic and professional: London, UK, 1991.

(26) Smidsroed, O.; Haug, A. *Acta Chem. Scand.* **1968**, *22*, 797.

(27) Mackie, W.; Noy, R.; Sellen, D. B. *Biopolymers* **1980**, *19*, 1839.

(28) Smidsroed, O.; Glover, R. M.; Whittington, S. G. *Carbohyd. Res.* **1973**, *27*, 107.

(29) Kohn, R. *Pure and Applied Chemistry* **1975**, *42*, 371.

(30) Braccini, I.; Perez, S. *Biomacromolecules* **2001**, *2*, 1089.

(31) Ingar Draget, K.; Østgaard, K.; Smidsrød, O. *Carbohydrate Polymers* **1990**, *14*, 159.

(32) Smidsrød, O.; Skja˚k-Br˙k, G. *Trends in Biotechnology* **1990**, *8*, 71.

(33) Martinsen, A.; Skjaak-Braek, G.; Smidsroed, O. *Biotechnol. Bioeng.* **1989**, *33*, 79.

(34) (a) Neiser, S.; Draget, K. I.; Smidsrød, O. *Food Hydrocolloids* **1999**, *13*, 445(b) Neiser, S.; Draget, K. I.; Smidsrød, O. *Food Hydrocolloids* **1998**, *12*, 127.

(35) Haug, A.; Larsen, B.; Smidsroed, O. *Acta Chemica Scandinavica* **1963**, *17*, 1466.

(36) Haug, A.; Larsen, B.; Smidsroed, O. *Acta Chemica Scandinavica* **1967**, *21*, 2859.

(37) Smidsroed, O.; Haug, A.; Larsen, B. *Acta Chemica Scandinavica* **1963**, *17*, 1473.

(38) McCleary, C. W.; Rees, D. A.; Samuel, J. W. B.; Steele, I. W. *Carbohydr. Res.* **1967**, *5*, 492.

(39) (a) Otterlei, M.; Sundan, A.; Skjaak-Braek, G.; Ryan, L.; Smidsroed, O.; Espevik, T. *Infection and Immunity* **1993**, *61*, 1917(b) Otterlei, M.; Oestgaard, K.; Skjaak-Braek, G.; Smidsroed, O.; Soon-Shiong, P.; Espevik, T. *Journal of Immunotherapy (1991-1992)* **1991**, *10*, 286.

(40) Espevik, T.; Otterlei, M.; Skjaak-Braek, G.; Ryan, L.; Wright, S. D.; Sundan, A. *European Journal of Immunology* **1993**, *23*, 255.

(41) (a) Iwamoto, M.; Kurachi, M.; Nakashima, T.; Kim, D.; Yamaguchi, K.; Oda, T.; Iwamoto, Y.; Muramatsu, T. *FEBS Lett.* **2005**, *579*, 4423(b) Flo, T. H.; Ryan, L.; Latz, E.; Takeuchi, O.; Monks, B. G.; Lien, E.; Halaas, O.; Akira, S.; Skjak-Brak, G.; Golenbock, D. T.; Espevik, T. *Journal of Biological Chemistry* **2002**, *277*, 35489.

(42) (a) Flo, T. H.; Ryan, L.; Kilaas, L.; Skjak-Braek, G.; Ingalls, R. R.; Sundan, A.; Golenbock, D. T.; Espevik, T. *Infection and Immunity* **2000**, *68*, 6770(b) Berntzen, G.; Flo, T. H.; Medvedev, A.; Kilaas, L.; Skjak-Break, G.; Sundan, A.; Espevik, T. *Clinical and Diagnostic Laboratory Immunology* **1998**, *5*, 355.

(43) (a) Xu, R.; Jiang, Z.-H. *Carbohydr. Res.* **2008**, *343*, 7(b) Jiang, Z.-H.; Xu, R.; Wilson, C.; Brenk, A. *Tetrahedron Letters* **2007**, *48*, 2915.

(44) (a) Natsume, M.; Kamo, Y.; Hirayama, M.; Adachi, T. *Carbohydr. Res.* **1994**, *258*, 187(b) Yonemoto, Y.; Tanaka, H.; Yamashita, T.; Kitabatake, N.; Ishida, Y.; Kimura, A.; Murata, K. *Journal of Fermentation and Bioengineering* **1993**, *75*, 68.

(45) Akiyama, H.; Endo, T.; Nakakita, R.; Murata, K.; Yonemoto, Y.; Okayama, K. *Biosci., Biotechnol., Biochem.* **1992**, *56*, 355.

(46) (a) Taylor, C.; Draget, K. I.; Smidsrød, O. In *PCT*; NTNU Technology Transfer AS, Norway: WO, 2007, p.22(b) Taylor, C.; Draget, K. I.; Smidsrød, O. In *PCT*; NTNU Technology Transfer AS, Norway: WO, 2007, p. 25.

(47) Hu, X.; Jiang, X.; Hwang, H.; Liu, S.; Guan, H. *European Journal of Phycology* **2004**, *39*, 67.

(48) Zhao, X.; Yu, G.; Guan, H.; Yue, N.; Zhang, Z.; Li, H. *Carbohydrate Polymers* **2007**, *69*, 272.

(49) E is the code for food additives in the EU regulation.

(50) Steiner, A. B.; US Patent 2, 215, Ed., 1947.

(51) Thomas, S. J. *Journal of wound care* **1992**, *1*, 29.

(52) (a) Soon-Shiong, P.; Heintz, R. E.; Merideth, N.; Yao, Q. X.; Yao, Z.; Zheng, T.; Murphy, M.; Moloney, M. K.; Schmehl, M.; Harris, M.; Mendez, R.; Sandford, P. A. *The Lancet* **1994**, *343*, 950(b) Soon-Shiong, P.; Feldman, E.; Nelson, R.; Heintz, R.; Yao, Q.; Yao, Z.; Zheng, T.; Merideth, N.; Skjak-Braek, G.; Espevik, T. *Proceedings of the National Academy of Sciences* **1993**, *90*, 5843.

Chapter 3: Reversible-deactivation radical polymerization

Table of contents

3.1 Conventional radical polymerization

Conventional radical polymerization is described as the addition of primary radical to an olefinic monomer to generate a chain carrier which can propagate further under certain conditions to form a mcromolecular chain. It is composed of three major steps: initiation, propagation and termination.

3.1.1 Initiation

In the initiation step primary radicals are generated either by a hemolytic cleavage of relatively weak bonds under thermal or photochemical conditions, or by a redox process. The formed primary radicals can propagate to form the polymer chains (Scheme 3.1).

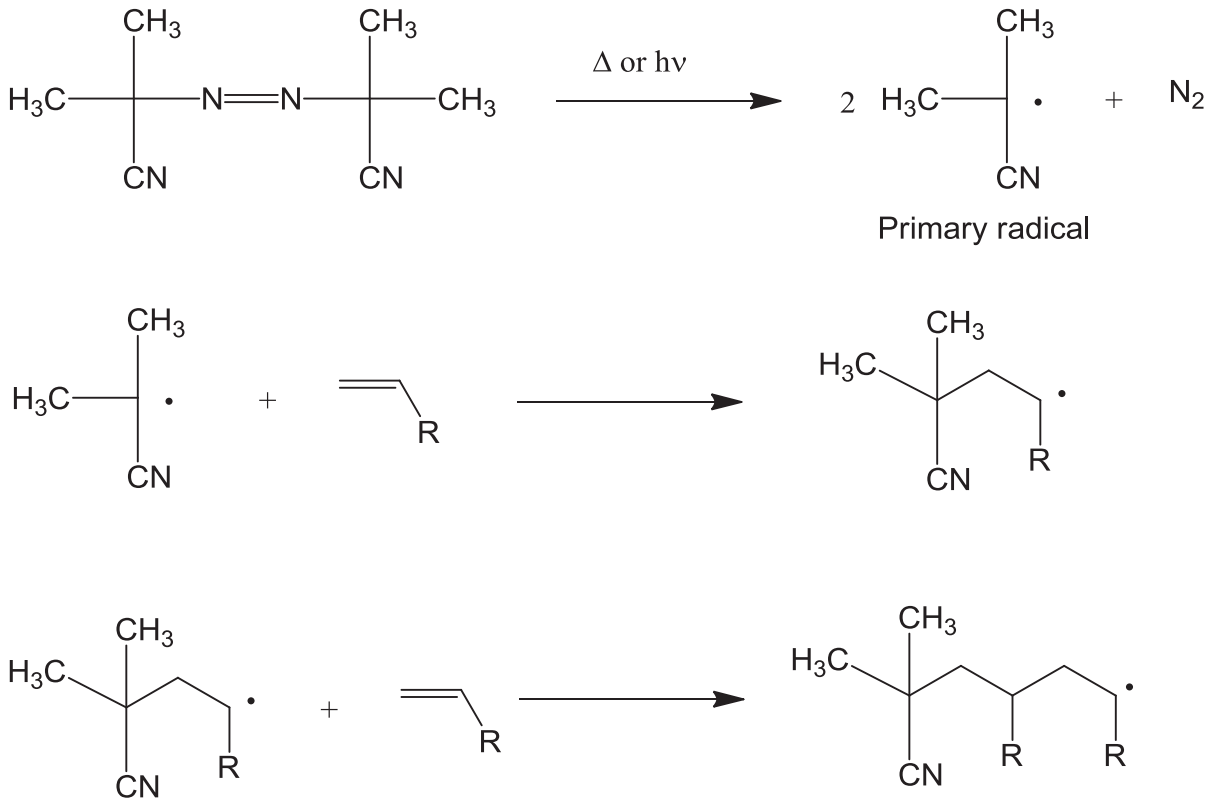

Scheme 3.1 *Decomposition of an azo-initiator (2,2'-azobis(2-isobutyronitrile)) to generate primary radicals that induce polymerization.*

3.1.2 Propagation

Once the primary radical adds to the first monomer, the newly formed chain carrier starts to propagate by adding furthers monomer units ending in a long polymer chain in short

period (chains over than 1000 units can be produced in 0.01s). [1] This step is referred to as propagation.

3.1.3 Termination

Since the life time of propagating radicals is short, they are deactivated by either bimolecular combination or via an abstraction of a proton at an α position from the radical center via disproportionation to give two dead chains (Scheme 3.2). It is noteworthy to mention the possibility of termination by chain transfer of the active chains to other molecules (solvent, initiator, monomer, etc) or by reaction with impurities as inhibitors. [1]

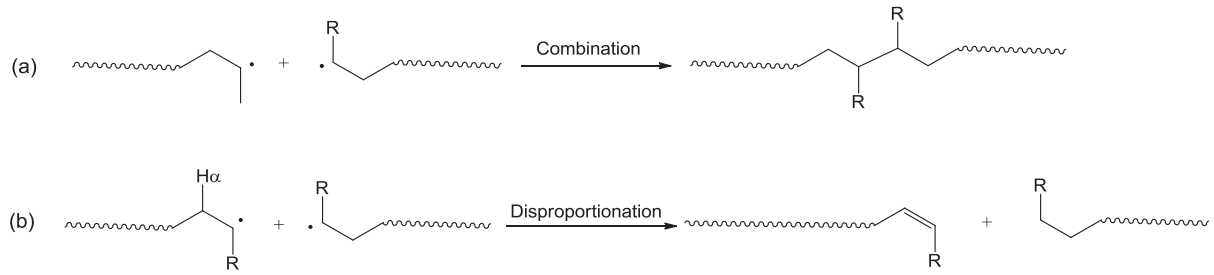

Scheme 3.2 *Termination of two growing radicals by (a) combination and (b) disproportionation.*

3.1.4 Chain transfer

Chain transfer reactions lead to dead chains on one hand, accompanied with a generation of another radical on the other hand. This is to say, that the free radical is not destroyed and is merely transferred, and if the newly formed radical center is active enough it can grow up new chains. This happens when the propagating radical abstracts a weakly bonded atom from another molecule, so called transfer agent, in order to form a more stable covalent bond. The transfer agent can be monomer, solvent, impurities, polymer chain or on purpose added chain transfer agent as in the case of reversible-deactivation radical polymerizations (Scheme 3.3).

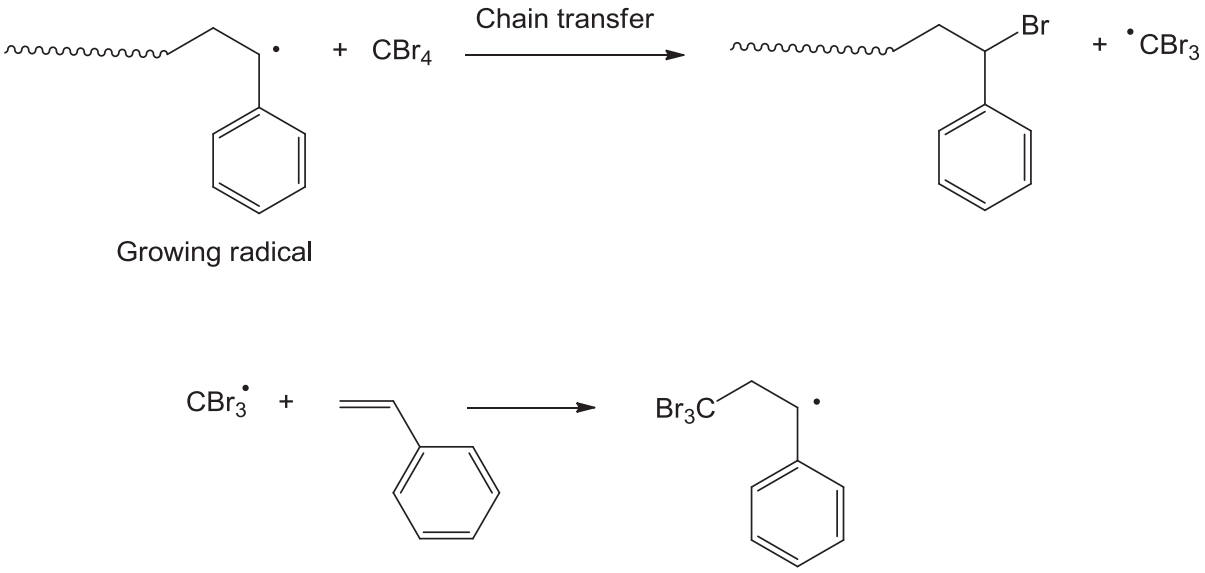

Scheme 3.3 *Chain transfer reaction of a growing polystyrene radical to the solvent (CBr_4).*

3.1.5 Kinetics of free radical polymerization

The following section on the kinetics is based on the thesis of Luca Albertin whose data were extracted from two book sections. [2]

3.1.5.1 Rate of polymerization

The three basic steps in the polymerization process (initiation, propagation and termination) can be expressed in general terms as shown from Scheme 3.4. The scheme can generally be applied to *homogenous polymerizations* in the limit of *low conversion* and is based on a number of simplifying assumptions:

1. The polymerization is made-up of a single step, irreversible reactions.
2. Radical reactivity (and the related kinetic constants) is chain-length and conversion independent.
3. A steady-state free-radicals concentration is rapidly established in the early stage of the process.
4. Monomer consumption is only due to the propagation process.
5. The concentration of primary radicals is constant throughout the polymerization.
6. Primary radicals are only involved in the initiation process, which is must faster than the initiator decomposition ($k_i \gg k_d$).

7. Intramolecular chain transfer and de-polymerization reactions are negligible.

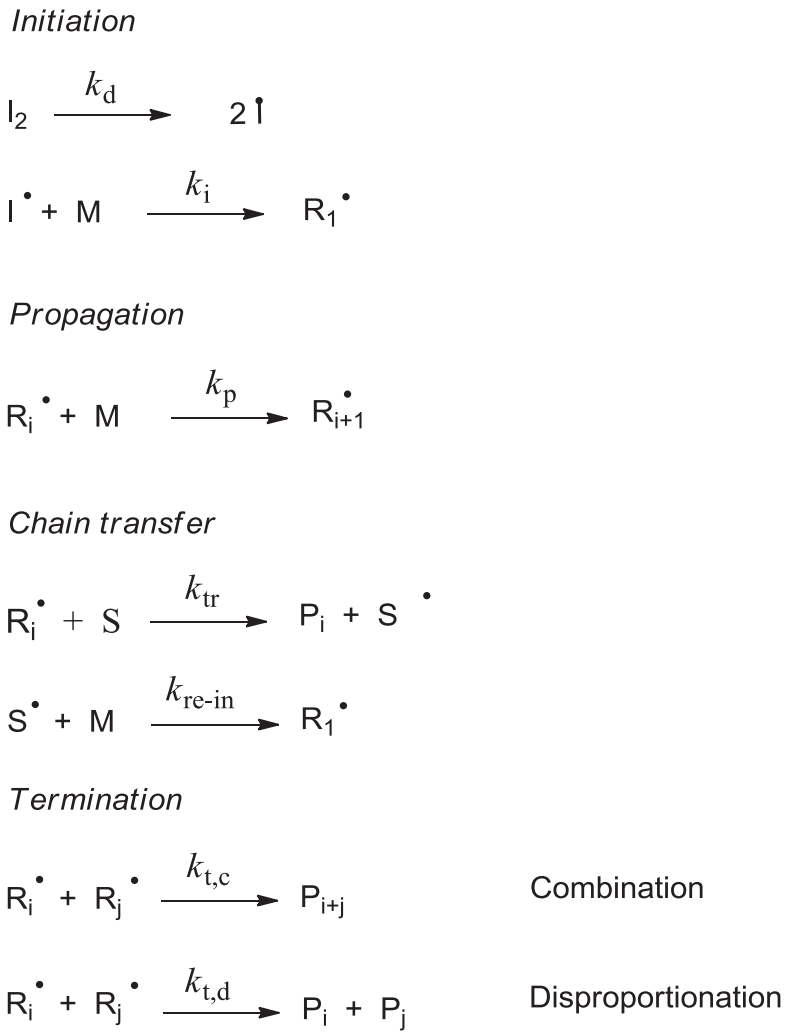

Scheme 3.4 *Elementary reactions that take place during a radical polymerization reaction. The symbols' meaning can be found in the Key to Symbols and Constants.*

Thus we can say that the *rate of polymerization*, R_p, can be expressed as follows:

$$R_p = -\frac{d[M]}{dt} = k_p[R^{\bullet}][M] \tag{3.1}$$

where $[R^{\bullet}]$ represents the total concentration of growing macroradicals, irrespective of their chain length. In a steady state, the rate of radical formation (R_i) is exactly counterbalanced by the rate of destruction (R_t), i.e. $R_i=R_t$. Thus for a thermal reaction:

$$2k_t[R^{\bullet}]^2 = 2k_d f[I_2] \tag{3.2}$$

From equation 3.2 we can express $[R^{\bullet}]$ as:

$$[R^{\bullet}] = \left(f \frac{k_d}{k_t} \right)^{1/2} [I_2]^{1/2} \tag{3.3}$$

By substituting for [R•] in equation 3.1 we get:

$$R_p = -\frac{d[M]}{dt} = k_p \left(f \frac{k_d}{k_t} \right)^{1/2} [I_2]^{1/2} [M] \tag{3.4}$$

From equation 3.4, the rate of polymerization is proportional to the monomer concentration and the square root of the initiator concentration. Finally, from equation 3.4 we can express the variation of monomer's concentration with time as follows:

$$\ln\left(\frac{[M]_0}{[M]} \right) = k_p \left(f \frac{k_d}{k_t} \right)^{1/2} [I_2]^{1/2} t \tag{3.5}$$

3.1.5.2 Degree of polymerization

In order to calculate the *number average degree of polymerization*, $\overline{P}_n$, in a steady state polymerization, it is worth knowing the number of propagation steps that occur before termination. For that the *kinetic chain length*, ν, in the absence of transfer reactions is defined as:

$$\nu = \frac{\text{number of polymerized monomer units}}{\text{number of initiating steps}} \tag{3.6}$$

In general ν will vary with time, but at any moment it will be equal to the ratio between the initiation and the propagation rate:

$$\nu = \frac{R_p}{R_i} = \frac{k_p[R^{\bullet}][M]}{2 f k_d [I_2]} \tag{3.7}$$

Elimination of [R•] by means of Eq. 3.3 leads to the expression:

$$\nu = \frac{k_p}{\sqrt{2 f k_d k_t}} \frac{[M]}{\sqrt{[I_2]}} \tag{3.8}$$

The average value $\bar{\nu}$ observed after a reaction time t will be equal to the integral of ν between 0 and t, but in the limit of low conversion the monomer and initiator concentration can be considered to be constant and:

$$\bar{\nu} = \frac{k_p}{\sqrt{2fk_d k_t}} \int_0^t \frac{[M]}{\sqrt{[I_2]}}\, dt \cong \frac{k_p}{\sqrt{2fk_d k_t}} \frac{[M]}{\sqrt{[I_2]}} \tag{3.9}$$

We deduce from Eq. 3.9 that the chain length of a macromolecule is directly proportional to the monomer concentration and inversely proportional to the square root of the initiator. Thus, disregarding any transfer reactions we can say that:

1- If termination occurs by disproportionation, one polymer molecule is produced per every chain initiated, then:

$$\bar{P}_n = \bar{\nu} \tag{3.10}$$

2- If termination occurs via combination then one polymer chain is produced per two chains initiated, then:

$$\bar{P}_n = 2\bar{\nu} \tag{3.11}$$

3- Any mixture of these both mechanisms can be described by using the value δ:

$$\bar{P}_n = \frac{2}{1+\delta}\bar{\nu} \tag{3.12}$$

Where δ represents the contribution of disproportionation to the overall termination process:

$$\delta = \frac{k_{t,d}}{k_{t,d} + k_{t,c}} \tag{3.13}$$

Taking chain transfer into account, the *number average degree of polymerization*, $\bar{P}_n$, can be described as:

$$\bar{P}_n = \frac{\text{total number of polymerized monomer units}}{\text{half the number of formed end groups}} \tag{3.14}$$

The various reactions within the polymerization process generate different amounts of end groups per initiation step:

a) Initiation: 1 end group.

b) Propagation: 0 end groups.
c) Transfer: 2 end groups.
d) Termination by disproportionation: 1 end group.
e) Termination by combination: 0 end groups.

What is more important in a chain transfer phenomenon is a decrease in the chain length. If k_{tr} is much larger than k_p then a very small polymer is formed. Besides, the chain re-initiation process could be slower which results in a slower R_p. However, the influence on P_n is the most dramatic and it can be estimated by considering all the transfer processes (to solvent, monomer, chain transfer agent, etc) in the Mayo equation as follows:

$$\frac{1}{P_n} = \frac{1}{P_n^0} + Cs\frac{[S]}{[M]} \tag{3.15}$$

Where P_n^0 represents the *number average degree of polymerization* in the absence of chain transfer agents (CTA), C_S is the chain transfer constant to CTA and S is the CTA. The above equation is a simplified form, where the main assumption is that transfer to chain transfer agent predominates and all other terms enter in $1/P_n^0$.

3.1.6 Polydispersity index (PDI)

The polydispersity index is a measure of the breadth of a chain length distribution and of a polymer's molecular heterogeneity. It is defined as the ratio between weight and number average degrees of polymerization. It can be expressed as:

$$\sigma_n^2 = \overline{P}_w \overline{P}_n - \overline{P}_n{}^2 \tag{3.16}$$

$$PDI = \frac{\overline{P}_w}{\overline{P}_n} = 1 + \frac{\sigma_n{}^2}{\overline{P}_n{}^2} \tag{3.17}$$

where σ_n^2 is the variance of the *number distribution function*. That is to say that the PDI is equal to one plus the coefficient of variation of the *number distribution function*. $\overline{P}_w$ is always greater than (or equal to) $\overline{P}_n$ since the variance is always positive (Eq. 3.16) and that suggests that the PDI is always greater than (equal to) unity. The same analysis can be carried out for the *weight distribution function* that results in:

$$\overline{P}_n \leq \overline{P}_w \leq \overline{P}_z \tag{3.18}$$

Equality of the three chain length distributions is only met when all chains are of the same length. In this case, the polymer is said to be "monodisperse", and since $\sigma_n^2 = 0$, its polydispersity index will have the minimum value of 1. The reverse reasoning is not necessarily true though, and an experimental value close to 1 for PDI does not necessarily indicate a nearly monodisperse polymer. In fact, this will only be the case if the polymer has a unimodal distribution function, while it will be meaningless in the presence of a multimodal distribution. Finally, it is worth noting that while many biological macromolecules like proteins and nucleic acids are rigorously monodisperse, today's synthetic polymers can only approach monodispersity.

3.2 Conventional radical copolymerization

This ideas of this section has been adopted from a book chapter by Cowie et al. [1] So far, the emphasis has been on homopolymers. An alternative approach is to synthesize polymers bearing more than one monomer thus resulting in products which exhibit properties of both homopolymers. This is known as *copolymerization*.

3.2.1 Composition and general characteristics

Even in the simplest case where a copolymer bearing two types of monomers, variety of structures could be attained:

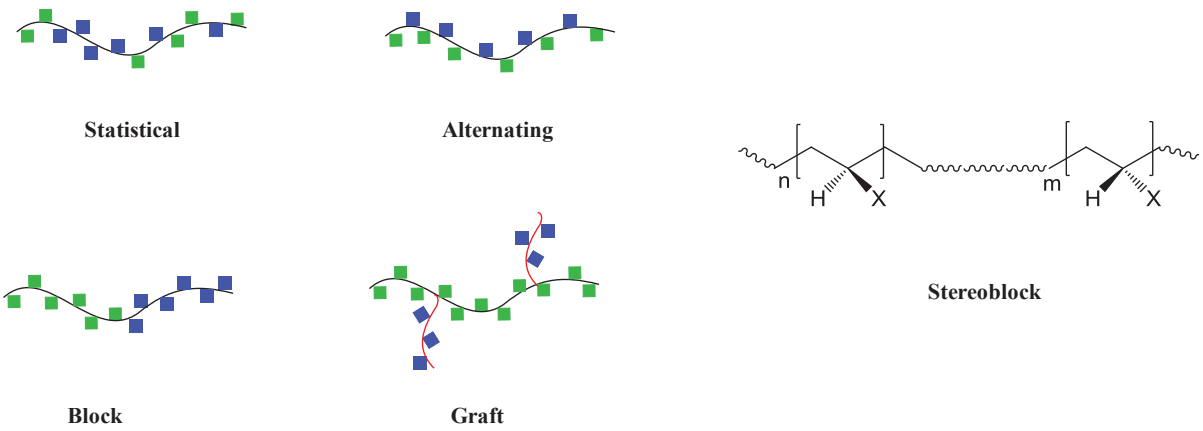

Figure 3.1 *Types of copolymers obtained from conventional radical polymerization.*

i) *Statistical copolymers*: are formed when random propagation occurs thus making the monomers enter statistically in the polymer.

ii) *Alternating copolymers*: are obtained when the two monomer units are alternately distributed in the polymers.

iii) *Block copolymers*: where a block of one monomer is joined to another block of the other monomer.

iv) *Graft copolymers*: are non linear or branched block copolymers that are obtained by attaching chains of one monomer to the chains of another homopolymer.

v) *Stereoblock copolymers*: A very special structure can be obtained from one monomer where now the distinguishing feature of each block is its tacticity.

In general block and graft copolymers exhibit properties of both homopolymers, whereas the random and alternating polymers have characteristics which are more of a compromise between the extremes. Besides, the factors affecting copolymerization are more complex than those affecting homopolymerization. For instance, styrene can inhibit the polymerization of vinyl acetate in a copolymerization solution of both monomers. On the other hand, some bulky monomers that do not tend to homopolymerize can copolymerize, as maleic anhydride and stilbene. [1,3]

3.2.2 The copolymer equation

Sticking to the terminal model where it is assumed that the terminal unit of a propagating polymer radical is the only factor influencing its reactivity (radical reactivity is independent of the chain length), and that side reactions are not significant, four types of propagation reactions in the free-radical copolymerization of any two given monomers (**M_1** and **M_2**) exist:

$$R\mathrm{M}_i^{\bullet} + \mathrm{M}_j \xrightarrow{K_{i,j}} R\mathrm{M}_i\mathrm{M}_j^{\bullet} \qquad (i, j = 1 \text{ or } 2) \tag{3.19}$$

where k_{11} and k_{22} are the rate constants for the *self-propagating* reactions and, k_{12} and k_{21} are the rate constants of the corresponding *cross-propagating* reactions. Under steady state conditions, we can estimate the rate of consumption of **M_1** from the initial reaction mixture by:

$$-\frac{d[\mathrm{M}_1]}{dt} = k_{11}[\mathrm{M}_1][\mathrm{M}_1^{\bullet}] - k_{21}[\mathrm{M}_1][\mathrm{M}_2^{\bullet}] \tag{3.20}$$

and for **M₂** by:

$$-\frac{d[\mathrm{M}_2]}{dt} = k_{22}[\mathrm{M}_2][\mathrm{M}_2^{\bullet}] - k_{12}[\mathrm{M}_2][\mathrm{M}_1^{\bullet}] \tag{3.21}$$

Assuming that in steady-state conditions:

$$k_{21}[\mathrm{M}_1][\mathrm{M}_2^{\bullet}] = k_{12}[\mathrm{M}_2][\mathrm{M}_1^{\bullet}] \tag{3.22}$$

Thus by dividing equation (3.20) by (3.21) we obtain the *copolymer equation*:

$$\frac{d[\mathrm{M}_1]}{d[\mathrm{M}_2]} = \left(\frac{[\mathrm{M}_1]}{[\mathrm{M}_2]}\right)\{(r_1[\mathrm{M}_1] + [\mathrm{M}_2])/([\mathrm{M}_1] + r_2[\mathrm{M}_2])\} \tag{3.23}$$

where $r_1 = k_{11}/k_{12}$ and $r_2 = k_{22}/k_{21}$. The quantities r_1 and r_2 are the relative reactivity ratios *i.e.* the reactivity of the propagating species with its own monomer to the reactivity of the propagating species with other monomer.

The *copolymer equation* provides a means of calculating the amount of each monomer in the copolymer by knowing the reactivity ratios of both monomers. Thus, by saying that **M₁** is more reactive than **M₂**, then **M₁** will be more rapidly incorporated in the copolymer and its amount in the feed will be less thus creating a drift in composition. Hence, the copolymer equation could be written based on the composition of monomers in the feed and in the copolymer as follows:

$$F_1 = \left(r_1 f_1^2 + f_1 f_2\right)/\left(r_1 f_1^2 + 2 f_1 f_2 + r_2 f_2^2\right) \tag{3.24}$$

where F_1 is defined as the mole fraction of **M₁** added to the copolymer at a given time, and f_1 and f_2 are the mole fractions of **M₁** and **M₂** in the feed mixture, respectively.

3.2.3 Reactivity ratios and copolymer structure

For unknown reactivity ratios of two given monomers one can calculate for them by analyzing the composition of the copolymer formed by running a series of copolymerizations that are stopped at low conversion with a known [**M₁**] / [**M₂**] ratio. Wide ranging values for the reactivity ratios could be obtained which have influence on the structure of the formed copolymer:

In the case where $r_1 \approx r_2 \approx 1$ the growing radical has no preference of adding one monomer on the other, in other words: $k_{11} \approx k_{12}$ and $k_{22} \approx k_{21}$. Under such conditions $F_1 = f_1$

and the copolymerization proceeds in a random way. In this case, the plot of F_1 versus f_1 is linear passing through origin and that is the behavior of an ideal copolymer (when $r_1r_2 = 1$). On the other hand, a drift in composition is observed in cases where $r_1 > 1$ and $r_2 < 1$ but $r_1r_2 = 1$ and as the difference in reactivity ratios between both monomers becomes larger, random copolymers become increasingly difficult to prepare.

In the case where both reactivity ratios are less than unity (r_1 and $r_2 < 1$), here copolymerization is favored. Furthermore, in the extreme case where $r_1 = r_2 = 0$, alternating copolymers are formed. For systems lying in the range $0 < r_1r_2 < 1$ a special case is observed. Hence, the closer the product of the reactivity ratios to zero is the more the monomer alternates in the chain and the copolymer composition plots (F_1 vs. f_1) for these types of systems are sigmoidal where they intersect with the linear plot of an ideal case (F_1 vs. f_1 is linear) at a point "P" indicating the *azeotropic copolymer composition*. At this point the composition of the copolymer is constant throughout the whole reaction and is independent from the feed where no drift in composition is observed, contrary to other cases.

Finally, in the case where r_1 and r_2 are greater than unity ($r_1r_2 >> 1$) homo-segments or blocks of each monomer form up the copolymer and in extreme cases homopolymerization may predominate.

3.2.4 Structural effects on the reactivity ratios

The relative reactivity of a monomer can be correlated by *resonance stability*, the *polarity* of the double bond and *steric* effects.

3.2.4.1 Resonance effect

The stability of a radical can be affected by the groups in the vicinity of the radical. The more the delocalization of the radical by resonance, the more it becomes stable, thus the lower its reactivity. In other words, highly conjugated monomers (as styrene and butadiene) are very reactive monomers but will form stable and so relatively un-reactive radicals. The stability of the radicals is shown in Figure 3.2.

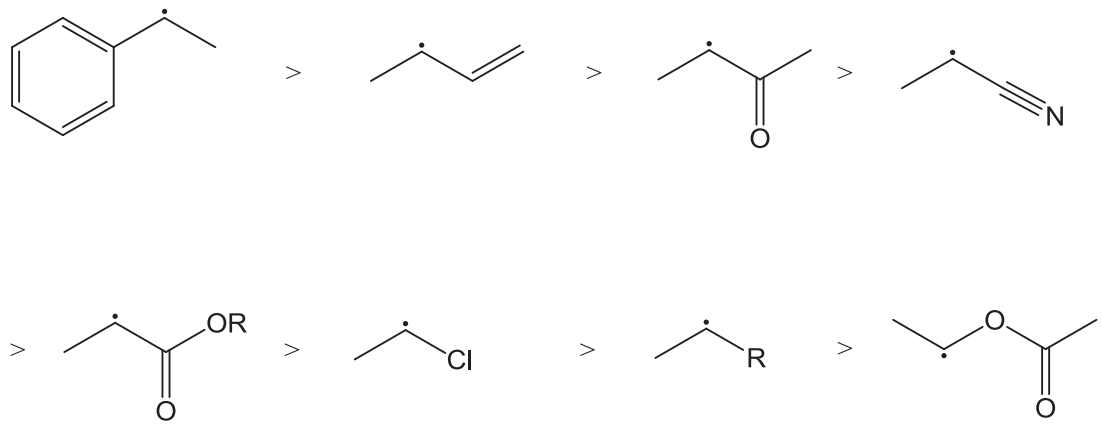

Figure 3.2 *Decreasing stability of radicals.*

3.2.4.2 Polarity effect

In this case as well, the polarity of the double bond is determined by the side groups. Thus, electron withdrawing side groups (-COOR, -CN, -$COCH_3$) decrease the electron density of the double bond contrary to electron donating groups (-CH_3, -OR, -$OCOCH_3$). Hence, two monomers with widely differing polarities tend to alternate strongly, *i.e.* one monomer bearing an electron donating group and the other bearing an electron withdrawing group.

3.2.4.3 Steric hindrance

Substituents on the double bond strongly retard the addition on the substituted carbon. However, the polarity of the double bond helps to overcome the *steric* hindrance. For example, bulky monomers as maleic anhydride and stiblene cannot homopolymerize, but due to the strong polar interaction they tend to copolymerize.

3.3 Reversible-deactivation radical polymerization

The first demonstration of reversible-deactivation polymerization could be traced to Szwarc in 1956 that described the polymerization of styrene in THF using a naphthyl initiator. [4] Reversible-deactivation polymerization provides polymers with controlled composition, architecture and molecular weight distribution, contrary to conventional radical polymerization. Ideally, the mechanism of a reversible-deactivation polymerization lacks chain breaking reactions (no irreversible chain transfer and termination) where all chains are initiated at the beginning of polymerization and propagate at similar rates until the

consumption of all monomer. [5] This polymerization is associated with an increase of molecular weight (MW) with conversion where narrow molecular weight distributions (MWD) could be obtained (Poisson like distribution). In this case, $\overline{P}_n$ is a simple function of the monomer consumed and of the initial amount of initiator: [6]

$$\overline{P}_n = \frac{1}{\nu}\frac{[M]_0 - [M]}{[I]_0} = \frac{1}{\nu}\frac{[M]_0}{[I]_0}c \qquad (3.25)$$

where ν is the initiator functionality.

3.3.1 General features of reversible-deactivation radical polymerization

A series of criteria to distinguish reversible-deactivation radical polymerization were set by Quirk and Lee [7] (as summarized by Moad and Solomon [8] in their book), although there is no single criterion which is satisfactory to tell whether a given polymerization is living or not as judged by the authors: [7]

(a) Reversible-deactivation radical polymerization (RDRP) can proceed until all monomer is consumed and can be continued if further monomer is added.
(b) In RDRP molecular weight increases linearly with conversion, an aspect not seen in conventional radical polymerization where the longest chains are formed at the early stages of polymerization, and thus the molecular weight decreases with time.
(c) The concentration of active species is constant with time, *i.e.* the kinetics follows a pseudo first order plots (same observed in free radical polymerization).
(d) RDRP provides narrow MWD with time.
(e) End group functionalities are retained in RDRP, thus helping in calculating the number of living chains.

RDRP processes are distinguished from conventional free radical polymerization (RP) by involving some form of *reversible activation (or deactivation) reaction*. [9] As shown in Scheme 3.5, the end-capped "dormant" chain P-X is in equilibrium with the free polymer radical $P^{\bullet}$, which undergoes propagation (in the presence of monomer) until it is deactivated back to its dormant form. The rate constants of activation (k_{act}) and deactivation (k_{deact}) are both defined as pseudo-first order constants, having the unit s^{-1}. In this scheme, every dormant chain is activated every k_{act}^{-1} second (typically 10-10^3) and deactivated back to the dormant

state after a "transient" lifetime (τ) of k_{deact}^{-1} second (typically 0.1-10 ms). For the quasi-equilibrium

$$k_{act}\,[\text{P-X}] = k_{deact}\,[\text{P}^{\bullet}]\,[\text{X}^{\bullet}] \tag{3.26}$$

to hold, the concentration of free macro-radicals must be around 10^{-5} that of the dormant chains. As a result, most potentially active chains (*i.e.* living chains) will be in the dormant state, and the number of active and temporarily deactivated *chain carriers* (dormant chains) will be practically identical. In general, after each activation-deactivation cycle the chain length of P-X will have increased, and if the frequency of these cycles is large enough over the polymerization time, every chain will nearly have equal chance to grow, resulting in a linear increase of MW with conversion. Moreover, if all chains are initiated at low monomer conversion and only a small amount of chain-terminating reactions take place, narrow polydispersity polymer will be obtained and its PDI will decrease with conversion. [10]

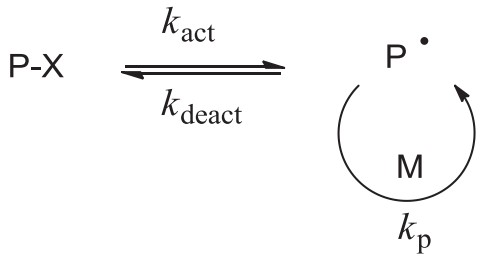

Scheme 3.5 *Activation and de-activation step that occurs in a reversible-deactivation radical process.*

The following section describes one reversible-deactivation radical polymerization technique with a reversible chain transfer step *i.e.* RAFT polymerization, with a comparison between the three most versatile reversible-deactivation radical polymerization techniques shown in Table 3.1. [10]

Table 3.1 *A general comparison between the three most known reversible-deactivation radical polymerization techniques.* [10]

Technique	Monomers	Conditions	Initiators / control agents	Additives
RAFT	Nearly all	Elevated *T* for less reactive monomers (≥60 °C); waterborne systems; sensitive to oxygen	Dithioesters: thermally and photo unstable, relatively expensive, coloured polymers, odour release	Conventional radical initiator
ATRP	No monomers producing non-stabilised radicals (e.g. vinyl acetate)	Large *T* range (-30 to 150 °C); waterborne systems; some tolerance to oxygen and inhibitor with Mt^0	Alkyl (pseudo)halides: thermally and photostable, inexpensive, halogen exchange may enhance cross-propagation	Transition metal catalyst: should be removed at the end of the polymerization.
NMP	Styrene, acrylates and acrylamides	Elevated *T* (≥90 °C); waterborne systems; sensitive to oxygen	Alkoxyamines: thermally unstable, expensive	None; may be accelerated with acyl compounds or radical initiators

3.3.2 Reversible Addition Fragmentation chain Transfer (RAFT) polymerization

Reversible-deactivation radical polymerization using thiocarbonylthio RAFT agents (Figure 3.3) was first described in 1998, where a normal RP was shown to bear an activation deactivation behavior in the presence of the suitable RAFT agent. [11]

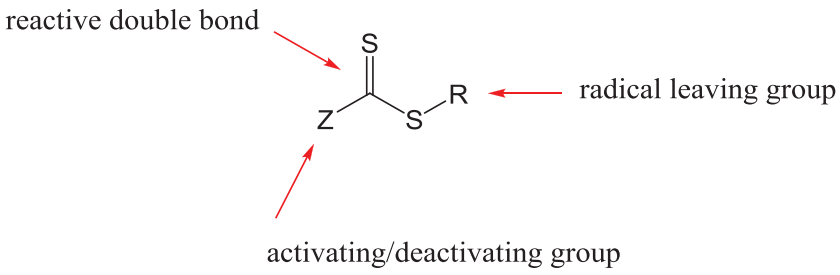

Figure 3.3 *General structure of a RAFT agent.*

The RAFT process offers the same versatility and convenience as conventional free-radical polymerization being applicable to the same range of monomers (e.g., (meth)acrylates, styrenes, acrylamides, vinyls), solvents, functional groups (e.g., OH, CO_2H, NR_2, NCO) and reaction conditions (e.g., bulk, solution, suspension and emulsion). The RAFT process yields thiocarbonylthio-terminated polymers that can be chain extended to yield a variety of copolymers (e.g., AB, ABA blocks, gradient). [12]

3.3.2.1 Mechanism of RAFT process

A main feature of the mechanism of RAFT polymerization is the sequence of reversible equilibria shown in Scheme 3.6. Similarly to conventional radical polymerization, RAFT polymerization has the same elementary steps (initiation, propagation and termination). In the early stages of polymerization, addition of the growing radical $P_n^{\bullet}$ to the RAFT agent **1** takes place leading to the formation of the intermediate **2** whose stability is affected by the Z group of the RAFT agent. What follows is a fragmentation at the β position from the radical to give the adduct **3** with another radical $R^{\bullet}$ that is supposed to reinitiate polymerization. The newly released radical into solution ($R^{\bullet}$) grows a polymer chain as well, and can in its turn add to the newly formed RAFT agent **3**; where after a number of addition-fragmentation steps a fast equilibrium takes place between the growing chains ($P_n^{\bullet}$ and $P_m^{\bullet}$) and the dormant adduct **3** that provides equal probability for all chains to grow and allows the formation of narrow dispersity polymers. It is noteworthy to state that radicals are neither formed nor destroyed in the chain equilibrium step. [8] By choosing the right experimental conditions, most of the chains should retain their thiocarbonylthio group.

Initiation

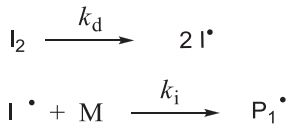

Propagation

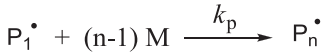

Reversible chain transfer (pre-equilibrium)

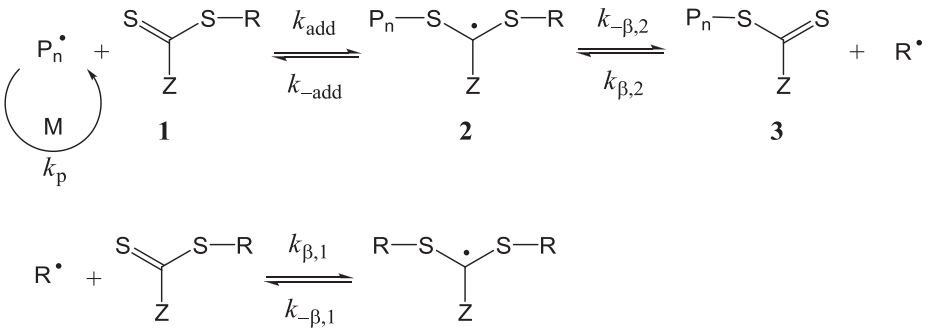

Reinitiation

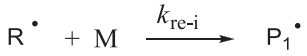

Chain equilibrium

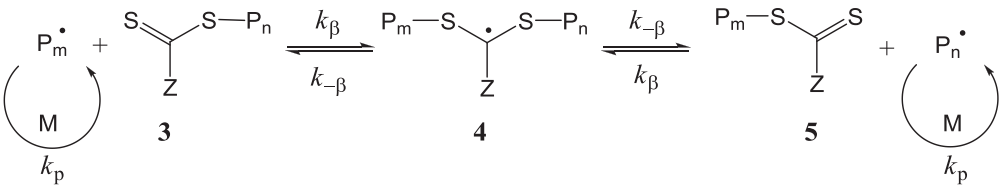

Termination

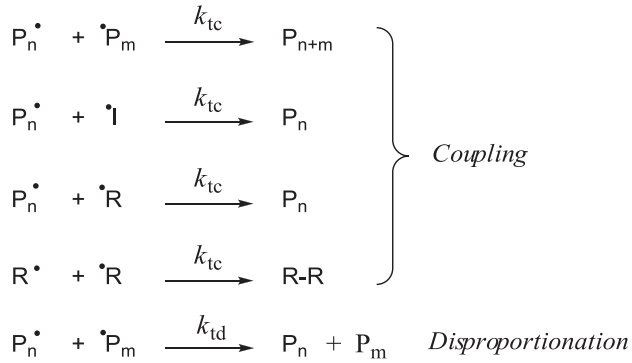

Scheme 3.6 *Mechanism of RAFT polymerization.*

For very active RAFT agents, the R$^{\bullet}$ that is supposed to reinitiate polymerization can also add to the RAFT agents (**1** or **3**), thus direct application of the Mayo method will underestimate the transfer coefficient and a different approach is required, where the transfer constant will be dependent on the concentration of transfer agent and the monomer conversion. [13] The chain transfer constant to the RAFT agent (C_{tr}) is given by the ratio of the rate constant for chain transfer (k_{tr}) to that for propagation (k_p):

$$C_{tr} = \frac{k_{tr}}{k_p} \tag{3.27}$$

and in chain transfer by addition-fragmentation (Scheme 3.6), the rate constant for chain transfer (k_{tr}) is given by the following expression: [14]

$$k_{tr} = k_{add} \frac{k_{\beta,2}}{k_{-add} + k_{\beta,2}} \tag{3.28}$$

3.3.2.2 Degree of livingness

In order to attain polymer chains with thiocarbonylthio end groups one should avoid formation of dead chains. For this aim, besides choosing the right RAFT agent, the polymerization should be conducted at low radical flux [12,15] and the ratio of the RAFT agent to that of the initiator is supposed to be high enough to avoid termination reactions (dead chain formation) since dead chains, when formed, are normally derived from initiator initiated chains not from R$^{\bullet}$ initiated chains. Analysis of the RAFT mechanism (Scheme 3.6) reveals that the total number of polymer chains produced will be equal to the number initiated by initiator derived radicals plus the number initiated by the RAFT agent derived radicals (R$^{\bullet}$). Hence, the proportion of dead chains (D_c) will be given by the ratio of the number of initiator derived radicals $2f([I]_0 - [I]_t)$ to the number of RAFT agent molecules ([RAFT]) plus the initiator derived radicals (Eq. 3.30), where: [12]

$$[I]_t = [I]_0 e^{-k_d t} \tag{3.29}$$

$$D_c = \frac{2f([I]_0 - [I]_t)}{[RAFT] + 2f([I]_0 - [I]_t)} \tag{3.30}$$

The number of dead chains is reduced to one half this value (i.e. D_c) when termination is by combination.

3.3.2.3 Types of RAFT agents

Depending on the Z group of the RAFT agent (Figure 3.3), different types are obtained:

a) dithioesters (Z = aryl, alkyl)

b) trithiocarbonates (Z = SR)

c) dithiocarbonates / xanthates (Z = OR)

d) dithiocarbamates ($Z = NR_2$)

All RAFT agents described above are highly dependent on the Z and R groups, and thus for and efficient RAFT polymerization the following should be considered: [8]

1- Both the initial RAFT agent (**1**) and the polymeric RAFT agent (**3**) should have a reactive C=S double bond (*i.e.* high k_{add}).
2- Fragmentation of the intermediate radicals (**2** and **4**) should be rapid (i.e. high k_β and a weak S-R bond).
3- The adduct **2** should favor the formation of the product (*i.e.* $k_\beta \geq k_{add}$).
4- The formed $R^\bullet$ should be able to reinitiate the polymerization.

For instance, dithioester RAFT agents (Z = Ar) results in retardation when high concentration of RAFT agent is used. However, using a trithiocarbonate RAFT agent results in less retardation under similar conditions. [14a] Also, dithioacetate and RAFT agents with Z = alkyl or aralkyl also give less retardation but have lower transfer constants that can lead to polydisperse polymers. For extra information on RAFT agents and the types of monomers that can be used with, see the reviews by Moad et al. [16]

3.3.3 Macromolecular design by RAFT polymerization

The synthetic versatility of RAFT will be discussed on the basis of two features of the obtained materials: composition (*i.e.* the relative amount and distribution of the monomers making up the macromolecule) and topology (*i.e.* the way in which constituent parts of the macromolecule are interrelated and arranged). Far from being exhaustive, the following section rather aims to review general strategies used in macromolecular design via RAFT.

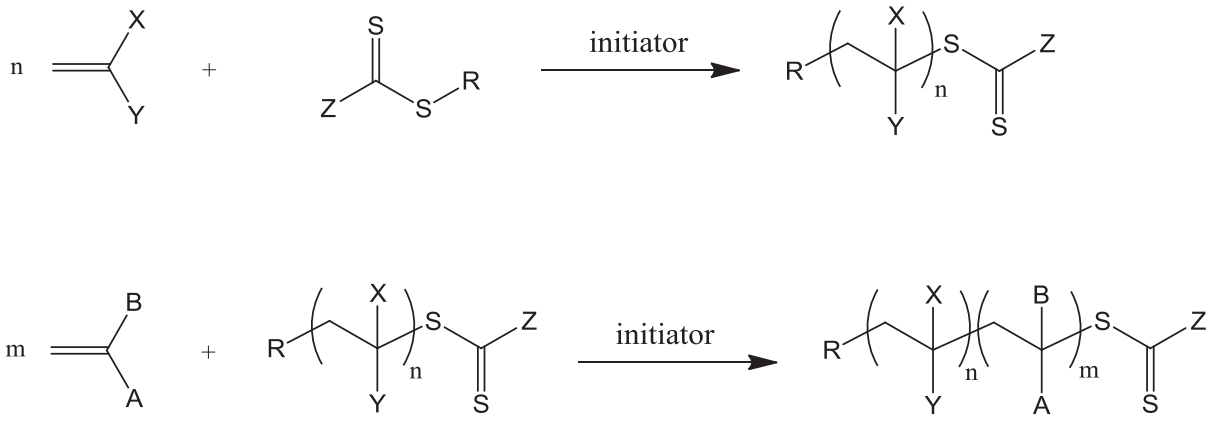

Scheme 3.7 *Example on the synthesis of (up) homopolymer and (down) an AB block copolymer via RAFT.*

3.3.3.1 Homopolymers

By choosing the right RAFT agent with the right monomer, narrow polydispersity polymers could be obtained with a control over molecular weight. [14a] Moreover, besides its versatility to wide window of monomers, RAFT polymerization of monomers generating non stable radicals as vinyl acetates and esters have been also polymerized. [17] Also, as a consequence of the RAFT mechanism the prepared polymers will be α,ω-functionalized, with the dithiocarbonyl-fragment and the R group of the RAFT agent will be on the α and ω positions respectively, where a desired functionality can be introduced. [18]

3.3.3.2 Block copolymers

Polymers bearing the end functionality group (obtained by RAFT polymerization) can be chain extended in the presence of the same monomer or a different one. In the latter case, the result is a diblock copolymer of the form poly(A-*b*-B). [19] In analogy, triblock copolymers could be obtained by extending the poly(A-*b*-B) using a third monomer resulting in a triblock copolymer of the form ABC or ABA. [20] In an easier route to get triblock copolymers is to use a symmetric trithiocarbonate RAFT agent, [21] where in two steps one can obtain the triblock copolymer rather than obtaining it via three steps. Three RAFT agent designs are amenable for this strategy as shown from Scheme 3.8. In one of them a central R-group is sided by two dithioester subsistents and polymer chains grow directly from it. [20a] In another one, a central Z-group is sided by two dithiocarbonyl subsistents and polymer chains grow away from it. [22] In the last one, symmetrically substituted trithiocarbonates promote polymer growth away from the RAFT agent's core. [20b] In RAFT polymerization, the order of constructing the blocks

of a block copolymer is very important, [13] where the propagating radical of the first block should have a better hemolytic cleavage with respect to the second block. It is worth noting that besides, problem of macroRAFT agents with low transfer constants is mitigated by using a starved feed polymerization protocol in order to maximize the concentration of [macro-RAFT]:[monomer]; thus it is important to use a RAFT agent with minimal retardation. [8,14a]

Central R-group

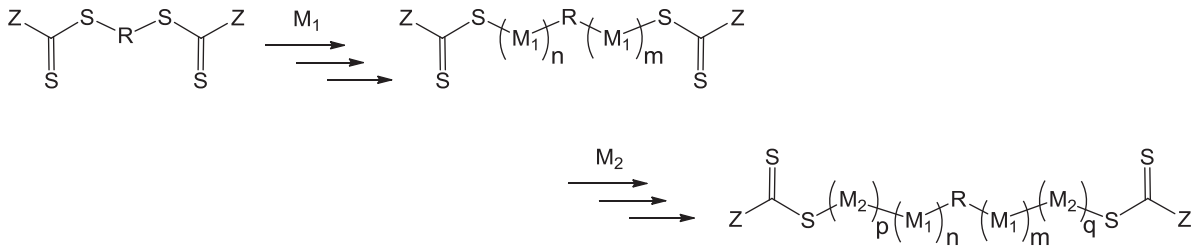

Peripheral R-group

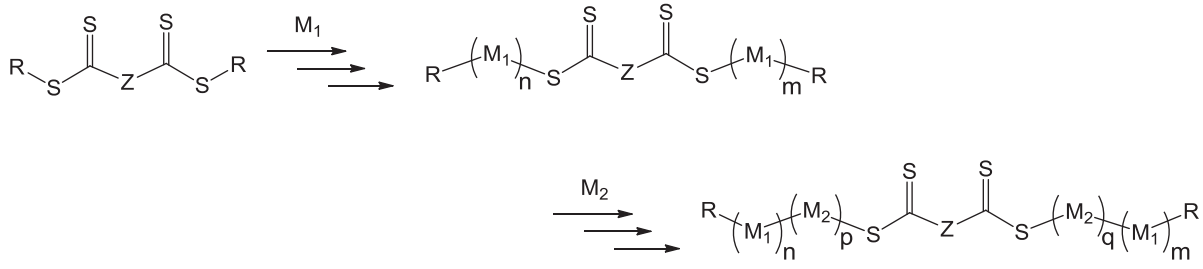

Symmetric trithiocarbonates

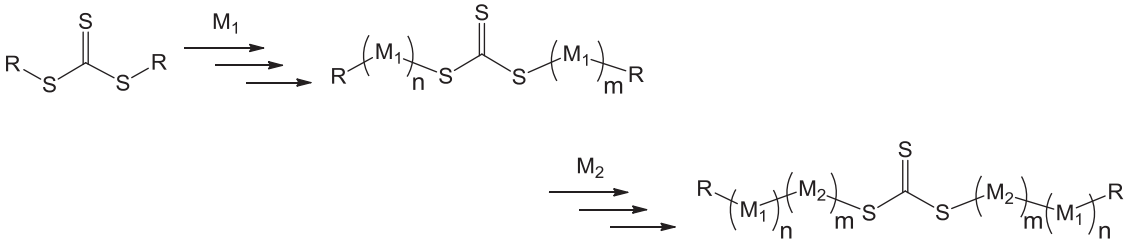

Scheme 3.8 *Design of three RAFT agents for the two step synthesis of ABA triblock copolymers via RAFT.* [20,22]

3.3.3.3 Random and Gradient copolymers

It has been shown from ^{1}H-NMR analysis [23] that the RAFT process does not alter the composition of copolymers in random copolymerizations when compared to copolymerizations without the RAFT agent. [12]

3.3.3.4 Star polymers

Star copolymers with various architectures could be obtained by different approaches as the following (Scheme 3.9): [8]

a) The *core first* approach requires a core containing the right functionality where the number of arms is indicated by the number of functionalities of the core. [24] Since the propagating radicals are attached to the core though, an unavoidable consequence with this method is that coupling termination reactions lead to star-star coupled products.
b) The *arm first* approach where a self assembly of the grown arms takes place to form the core. [25] A distinctive advantage of this strategy is the avoidance of any star-star coupling reaction.
c) Self condensing vinyl polymerization where hyperbranched polymers are obtained. [8,26]
d) The synthesis of dendritic polymers by an iterative approach. [8]

Core first

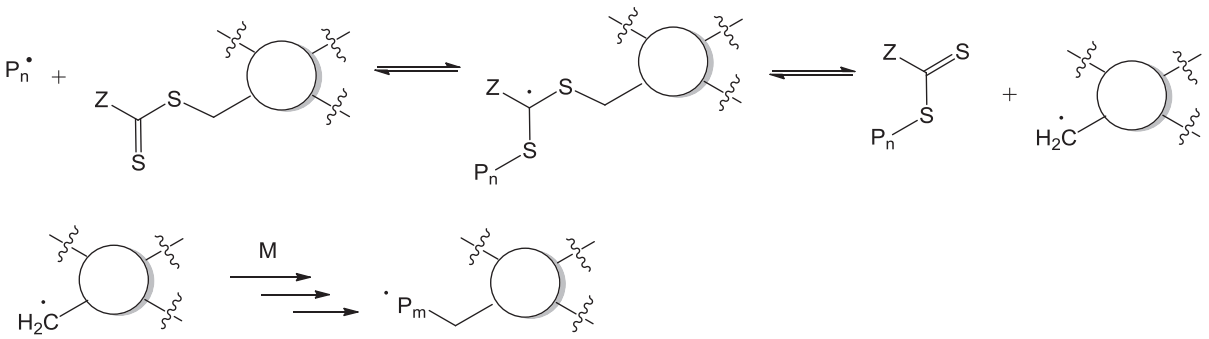

Arm first

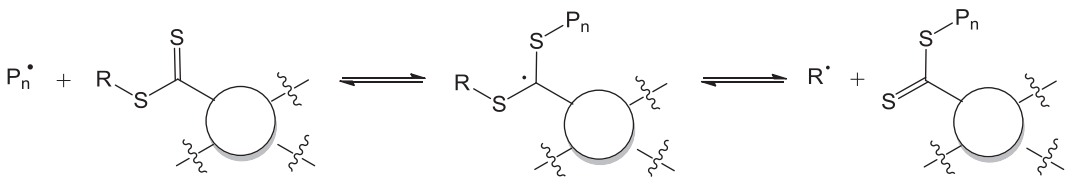

Scheme 3.9 *The core and the arm first approaches used in the synthesis of star polymers.* [24a,25b]

3.3.3.5 Graft copolymers / Polymer brushes

Graft polymerization involving reversible-deactivation radical processes use the same basic approaches of conventional radical polymerization and it is divided into three main parts: [8]

a) *Grafting through* approach where a propagating species reacts with a pendant instauration on another polymer chain, for example the copolymerization of two macromonomers. The resulting polymers in most cases are said to form polymer brushes. [27]

b) *Grafting from* approach where active sites are created on the polymer chain from which new polymerization is initiated. The advantages of growing polymers directly on the surfaces result in well defined grafts, in reversible-deactivation polymerization, and stability due to the covalent linkage of the polymer chain to the surface. The grafting could be obtained either from polymer surface, [28] or from an inorganic surface as silica particles (Scheme 3.10) where bimolecular termination is a problem. [29]

c) *Grafting to* approach involves the attachment of an end functionalized polymer with reactive surface groups on the substrate. For instance, taking the advantage of the thiol functionality of a macroRAFT agent to adhere it to a gold nanoparticle. [30]

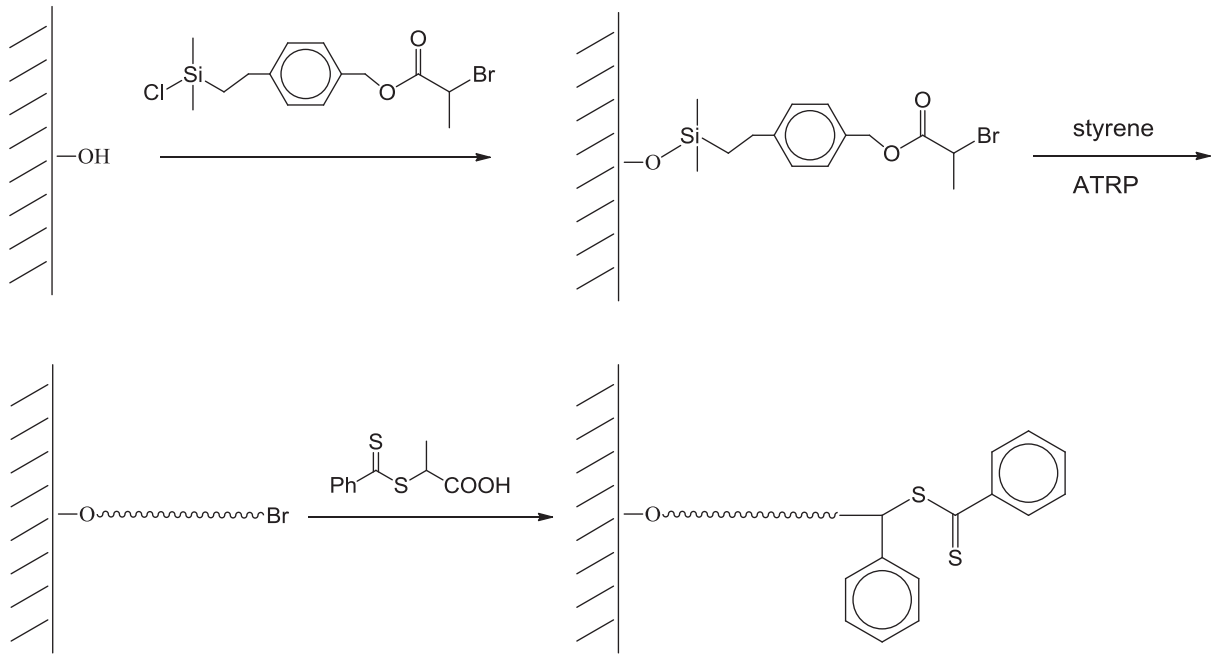

Scheme 3.10 *Original strategy used by T. Fukuda and co-workers for attaching a RAFT agent onto a silica substrate.* [29]

3.3.3.6 Post-polymerization modification

Taking advantage of either the chemical functionality of the RAFT agent or that of the polymerized monomer different bio-conjugates could be obtained: [31]

The first approach deals with the hydrolysis of the thiocarbonylthio group of the RAFT agent (after polymerization) in the presence of a nucleophile (amine) or a reducing agent ($NaBH_4$) to release a thiol moiety that can be exploited in nucleophilic or radical reactions (thio-ene, thiol-yne, and disulfide bond formation). [32]

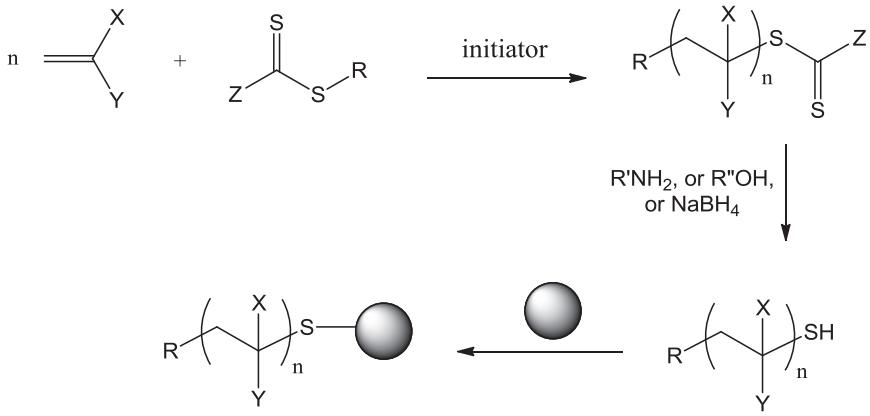

Scheme 3.11 *Modification of the thiocarbonylthio group after polymerization.*

The second approach takes advantage of the use of a functionalized RAFT agent for the polymerization. Reactive Z or/and R groups of the (macro)RAFT agent could react with another molecule carrying a suitable functional group. [33]

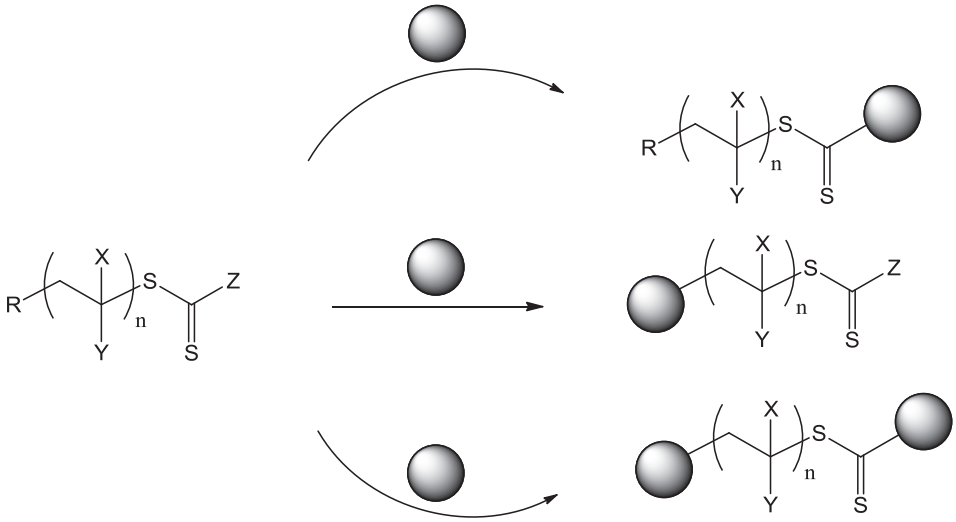

Scheme 3.12 *Schematic representation for the reaction of a macroRAFT agent with a suitable functionality with another molecule.*

The final approach describes the use of functionalized monomers after polymerization in the synthesis of novel conjugates. [34]

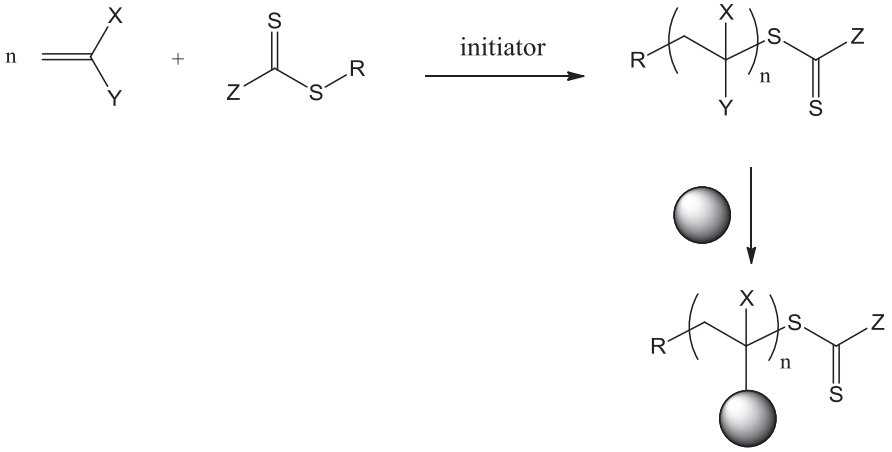

Scheme 3.13 *Schematic representation for the direct synthesis of bio-conjugates using functionalized monomers.*

3.4 Conclusion

Reversible-deactivation radical polymerization techniques, NMP, ATRP and RAFT, have shown a great importance in the field of radical polymerization where control over molecular weight and design are nowadays crucial for a wide number of applications. This chapter had described the mechanism and the kinetics of conventional radical polymerization together with the mechanism of RAFT polymerization. Besides, the ability to control

architecture using this polymerization technique (from homopolymers to block copolymers to star polymers, etc) has been also summarized up.

3.5 References

(1) Cowie, J. M. G. *Polymers: Chemistry and physics of modern materials*; 2nd ed.; Blackie Academic and professional: London, UK, 1991.

(2) (a) Guita, M.; Ciardelli, F.; Mantia, F. L.; Pedemonte, E. *Fondamenti di Scienza dei polimeri*; AIM: Pisa, Italy, 1998(b) Barner-Kowollik, C.; Vana, P.; Davis, T. P. *Handbook of radical polymerization*; Eds John Wiley and Sons, Inc.: Hoboken, USA, 2002; pp 187-262.

(3) Rzayev, Z. M.; Zeinalov, I. P.; Medyakova, L. V.; Babayev, A. I.; Agayev, M. M. *Polymer Science U.S.S.R.* **1981**, *23*, 689.

(4) Szwarc, M. *Nature (London, United Kingdom)* **1956**, *178*, 1168.

(5) Moad, G.; Rizzardo, E.; Thang, S. H. *Accounts of Chemical Research* **2008**, *41*, 1133.

(6) Szwarc, M. *J. Polym. Sci., Part A Polym. Chem.* **1998**, *36*, ix.

(7) Quirk, R. P.; Lee, B. *Polym. Int.* **1992**, *27*, 359.

(8) Moad, G.; Solomon, D. H. *The chemistry of radical polymerization: Second fully revised edition*; 2nd ed.; Elsevier Ltd., 2006.

(9) Fukuda, T.; Goto, A.; Tsujii, Y. *Handbook of radical polymerization*; Eds John Wiley and Sons, Inc.: Hoboken, USA, 2002; pp 407-462.

(10) Matyaszewski, K. *Handbook of radical polymerization*; Eds John Wiley and Sons, Inc.: Hoboken, USA, 2002; pp 361-406.

(11) (a) Le, T. P.; Moad, G.; Rizzardo, E.; Thang, S. H.; (E. I. Du Pont de Nemours & Co., USA; Le, Tam Phuong; Moad, Graeme; Rizzardo, Ezio; Thang, San Hoa). Application: WO, 1998(b) Chiefari, J.; Chong, Y. K.; Ercole, F.; Krstina, J.; Jeffery, J.; Le, T. P. T.; Mayadunne, R. T. A.; Meijs, G. F.; Moad, C. L.; Moad, G.; Rizzardo, E.; Thang, S. H. *Macromolecules* **1998**, *31*, 5559.

(12) Chiefari, J.; Rizzardo, E. *Handbook of radical polymerization*; Eds John Wiley and Sons, Inc.: Hoboken, USA, 2002; pp 629-690.

(13) Chong, Y. K.; Krstina, J.; Le, T. P. T.; Moad, G.; Postma, A.; Rizzardo, E.; Thang, S. H. *Macromolecules* **2003**, *36*, 2256.

(14) (a) Moad, G.; Chiefari, J.; Chong, Y. K.; Krstina, J.; Mayadunne, R. T. A.; Postma, A.; Rizzardo, E.; Thang, S. H. *Polymer International* **2000**, *49*, 993(b) Moad, C. L.; Moad, G.; Rizzardo, E.; Thang, S. H. *Macromolecules* **1996**, *29*, 7717.

(15) Vana, P.; Davis, T. P.; Barner-Kowollik, C. *Macromol. Theory Simul.* **2002**, *11*, 823.

(16) (a) Moad, G.; Rizzardo, E.; Thang, S. H. *Australian Journal of Chemistry* **2005**, *58*, 379(b) Moad, G.; Rizzardo, E.; Thang, S. H. *Aust. J. Chem.* **2009**, *62*, 1402(c) Moad, G.; Rizzardo, E.; Thang, S. H. *Aust. J. Chem.* **2006**, *59*, 669.

(17) (a) Albertin, L.; Kohlert, C.; Stenzel, M.; Foster, L. J. R.; Davis, T. P. *Biomacromolecules* **2004**, *5*, 255(b) Destarac, M.; Charmot, D.; Franck, X.; Zard, S. Z. *Macromolecular Rapid Communications* **2000**, *21*, 1035.

(18) Stenzel, M. H.; Davis, T. P.; Fane, A. G. *Journal of Materials Chemistry* **2003**, *13*, 2090.

(19) (a) Prazeres, T. J. V.; Beija, M.; Charreyre, M.-T.; Farinha, J. P. S.; Martinho, J. M. G. *Polymer* **2010**, *51*, 355(b) Sun, X.-L.; He, W.-D.; Pan, T.-T.; Ding, Z.-L.; Zhang, Y.-J. *Polymer* **2010**, *51*, 110.

(20) (a) Chong, B. Y. K.; Le, T. P. T.; Moad, G.; Rizzardo, E.; Thang, S. H. *Macromolecules* **1999**, *32*, 2071(b) Mayadunne, R. T. A.; Rizzardo, E.; Chiefari, J.; Krstina, J.; Moad, G.; Postma, A.; Thang, S. H. *Macromolecules* **2000**, *33*, 243.

(21) Zheng, L.; Chai, Y.; Liu, Y.; Zhang, P. *e-Polymers* **2011**, No pp given.

(22) Fleet, R.; McLeary, J. B.; Grumel, V.; Weber, W. G.; Matahwa, H.; Sanderson, R. D. *Macromolecular Symposia* **2007**, *255*, 8.

(23) (a) Vosloo, J. J.; Tonge, M. P.; Fellows, C. M.; D'Agosto, F.; Sanderson, R. D.; Gilbert, R. G. *Macromolecules* **2004**, *37*, 2371(b) Rizzardo, E.; Chiefari, J.; Chong, B. Y. K.; Ercole, F.; Krstina, J.; Jeffery, J.; Le, T. P. T.; Mayadunne, R. T. A.; Meijs, G. F.; Moad, C. L.; Moad, G.; Thang, S. H. *Macromol. Symp.* **1999**, *143*, 291.

(24) (a) Kuriyama, A.; Otsu, T. *Polym. J. (Tokyo)* **1984**, *16*, 511(b) Chen, M.; Ghiggino, K. P.; Launikonis, A.; Mau, A. W. H.; Rizzardo, E.; Sasse, W. H. F.; Thang, S. H.; Wilson, G. J. *J. Mater. Chem.* **2003**, *13*, 2696(c) Liu, J.; Tao, L.; Xu, J.; Jia, Z.; Boyer, C.; Davis, T. P. *Polymer* **2009**, *50*, 4455.

(25) (a) Wu, Z.-M.; Liang, H.; Lu, J.; Deng, W.-L. *J. Polym. Sci., Part A Polym. Chem.* **2010**, *48*, 3323(b) Moad, G.; Mayadunne, R. T. A.; Rizzardo, E.; Skidmore, M.; Thang, S. H. *Macromolecular Symposia* **2003**, *192*, 1(c) Zheng, G.; Pan, C. *Polymer* **2005**, *46*, 2802.

(26) Semsarilar, M.; Ladmiral, V.; Perrier, S. *Macromolecules (Washington, DC, United States)* **2010**, *43*, 1438.

(27) (a) Shinoda, H.; Matyjaszewski, K.; Okrasa, L.; Mierzwa, M.; Pakula, T. *Macromolecules* **2003**, *36*, 4772(b) Khousakoun, E.; Gohy, J.-F.; Jerome, R. *Polymer* **2004**, *45*, 8303.

(28) (a) Takolpuckdee, P.; Westwood, J.; Lewis, D. M.; Perrier, S. *Macromol. Symp.* **2004**, *216*, 23(b) Perrier, S.; Takolpuckdee, P.; Westwood, J.; Lewis, D. M. *Macromolecules* **2004**, *37*, 2709.

(29) Tsujii, Y.; Ejaz, M.; Sato, K.; Goto, A.; Fukuda, T. *Macromolecules* **2001**, *34*, 8872.

(30) (a) Sumerlin, B. S.; Lowe, A. B.; Stroud, P. A.; Zhang, P.; Urban, M. W.; McCormick, C. L. *Langmuir* **2003**, *19*, 5559(b) Lowe, A. B.; Sumerlin, B. S.; Donovan, M. S.; McCormick, C. L. *Journal of the American Chemical Society* **2002**, *124*, 11562.

(31) Bulmus, V. *Polymer Chemistry* **2011**, *2*, 1463.

(32) (a) Hoyle, C. E.; Bowman, C. N. *Angewandte Chemie International Edition* **2010**, *49*, 1540(b) Spain, S. G.; Albertin, L.; Cameron, N. R. *Chemical Communications* **2006**,

4198(c) Boyer, C.; Davis, T. P. *Chemical Communications (Cambridge, United Kingdom)* **2009**, 6029.

(33) (a) Golden, A. L.; Battrell, C. F.; Pennell, S.; Hoffman, A. S.; J. Lai, J.; Stayton, P. S. *Bioconjugate Chemistry* **2010**, *21*, 1820(b) Aqil, A.; Qiu, H.; Greisch, J.-F.; Jerome, R.; De Pauw, E.; Jerome, C. *Polymer* **2008**, *49*, 1145(c) Xu, J.; Boyer, C.; Bulmus, V.; Davis, T. P. *J. Polym. Sci., Part A Polym. Chem.* **2009**, *47*, 4302.

(34) (a) Alidedeoglu, A. H.; York, A. W.; Rosado, D. A.; McCormick, C. L.; Morgan, S. E. *J. Polym. Sci., Part A Polym. Chem.* **2010**, *48*, 3052(b) Abdelkader, O.; Moebs-Sanchez, S.; Queneau, Y.; Bernard, J.; Fleury, E. *J. Polym. Sci., Part A Polym. Chem.* **2011**, *49*, 1309.

Chapter 4: Well defined glycopolymers from reversible-deactivation radical polymerization of vinyl glycomonomers

Table of contents

4.1 Introduction

Synthetic polymers containing carbohydrates as pendant or terminal groups are referred to as glycopolymers (Figure 4.1). [1]

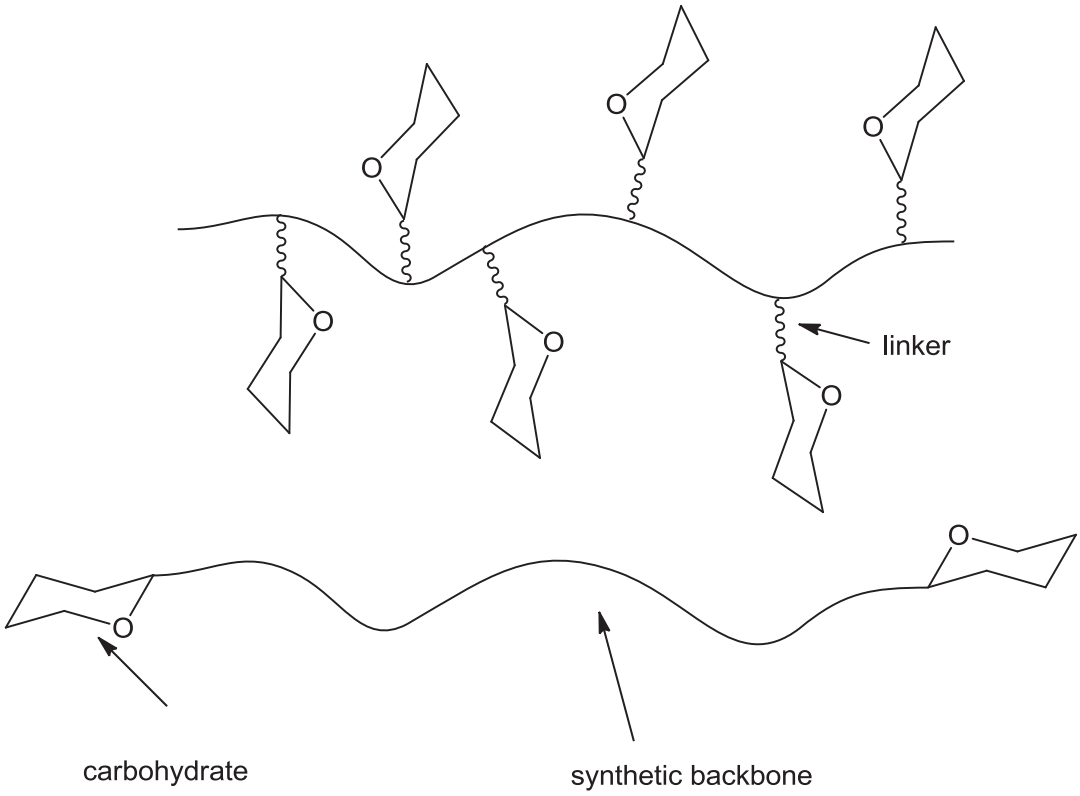

Figure 4.1 *General structure of a glycopolymer.*

Glycopolymers are of great interest in biological, biochemical and biomedical uses and that is due to the so-called "biomimetic approach" that gave these glycopolymers applications including matrices for encapsulation, stabilization and active ingredients release, [2] macromolecular drugs [3] and drug delivery systems, [4] biosensitive [5] and biocatalytic hydrogels, [6] and surface modifiers. [7]

Although essential, the presence of appropriate functional group in a glycopolymer is usually insufficient to bestow it with the biological and physiochemical properties required by a given application. As a matter of fact, control of macromolecular architecture has proven essential to enable sophisticated functions and to allow a precise correlation between those functions and the polymer structure. [8] For this reason, over the past 13 years the scope of glycopolymers synthesis and application was greatly expanded by the advent of reversible-deactivation polymerization techniques that are tolerant to impurities and/or functional

groups. These glycopolymers have been obtained from different reversible-deactivation polymerization techniques as: Living cationic, [9] Living anionic, [10] Ring-Opening Metathesis (ROMP), [8a,11] Ring-Opening, (ROP), [12] and Reversible-deactivation Radical Polymerization (RDRP). [13] However, living cationic and anionic polymerization techniques are relatively laborious, expensive and not suited to industrial scale-up. For instance, anionic polymerization generally requires aprotic solvents and all reactants must be of the highest purity. Monomers must not contain acidic protons or strongly electrophilic functionalities and reactions are very sensitive to oxygen and usually require sub-ambient temperatures. Likewise, cationic polymerization has the same problems with the addition that the propagating species are inherently unstable and prone to side reactions. [14] On the other hand, some of the inherent limitations in ionic polymerization could be avoided by resorting to ROMP which is tolerant to a variety of functional groups. [11c] However, this method is limited to strained monomers such as norbornene and cyclobutene, and imposes a significant cost on their preparation. Ring-opening polymerization (ROP) takes a part as well in the synthesis of well-defined glycopolymers where heterocyclic compounds with the appropriate ring-strain, bond type and reactivity may undergo cationic or anionic ring-opening polymerization depending on their nature. [14] For instance, Okada and co-workers reported the synthesis of well-defined glycopepetides via ROP. [12b,15] Unique to this method is the possibility to synthesize monodisperse, stereo-regular glycopeptides using primary amines as initiators. Although this technique was adopted for the synthesis of glycopolymers with a biodegradable backbone, yet it requires long polymerization times and the use of protected monomers. Finally, reversible-deactivation radical polymerization techniques are more tolerant to a wide range of protected or unprotected monomers (as methacrylamides, acrylamides, methacrylates, acrylates, styrenes, and vinyl esters) and functionalities, and can be performed in almost any solvent (water, organic) over a wide temperature range depending on the method of choice. Herein, the synthesis of glycopolymers from three reversible-deactivation radical polymerization techniques; Nitroxide Mediated Polymerization (NMP), Atom Transfer Radical Polymerization (ATRP), and Reversible Addition Fragmentation chain Transfer (RAFT) is described. It is worth noting that the latest update of this chapter dates to June 2011.

To facilitate the consultation of this chapter, a scheme with the structure of the compounds cited and a table summarizing polymerization experiments are placed in each section. The following abbreviations were used:

1- **M1** stands for monomer 1 and P**M1** stands for poly(monomer 1).
2- **Ni** stands for: initiator/control agents used in NMP.
3- **Ai** stands for: initiator/control agents used in ATRP.
4- **Ri** stands for: Chain transfer agents used in RAFT polymerization.

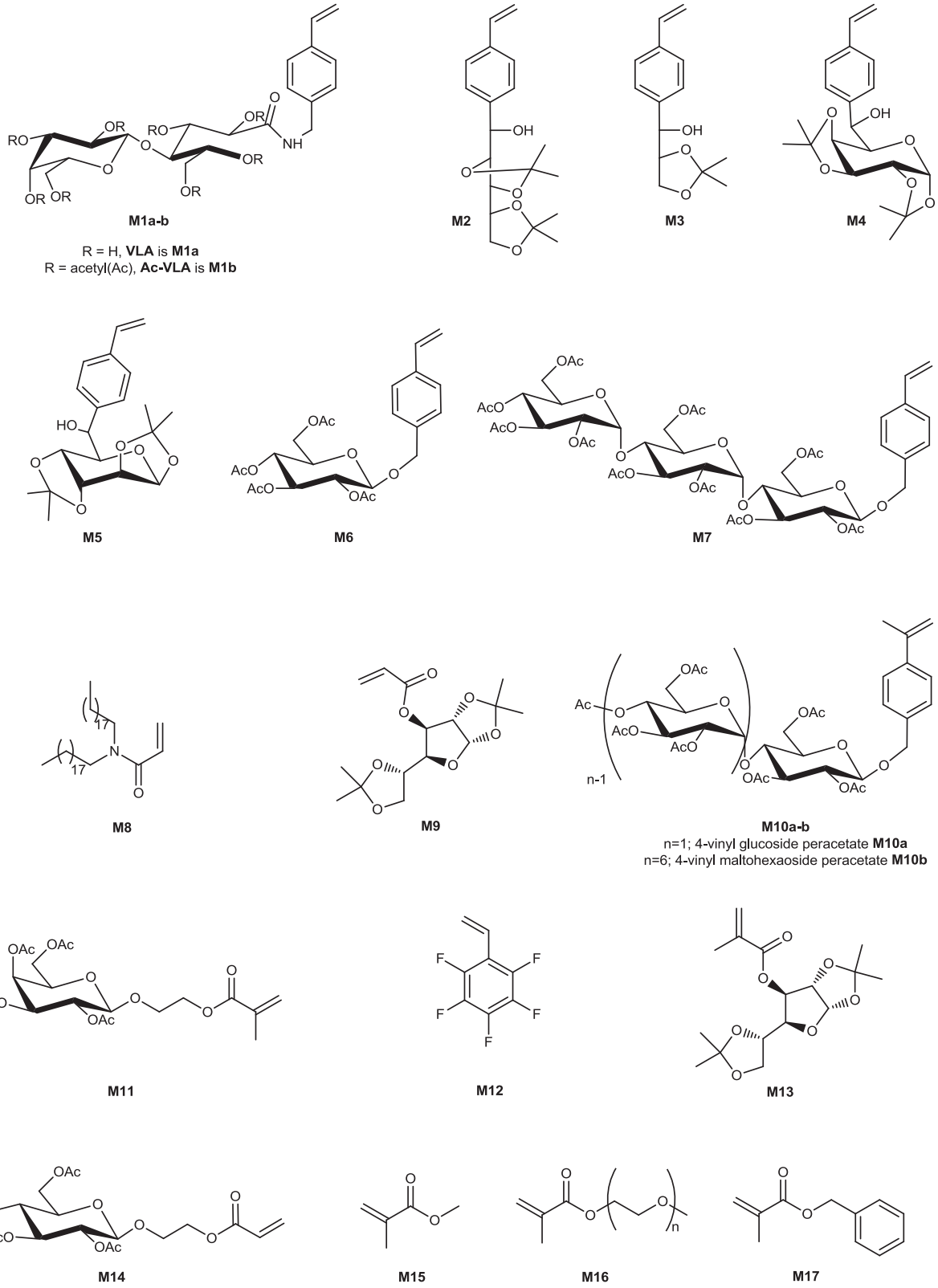

Figure 4.2 *Structural formulas of glycomonomers and related co-monomers polymerized by reversible-deactivation radical polymerization techniques.*

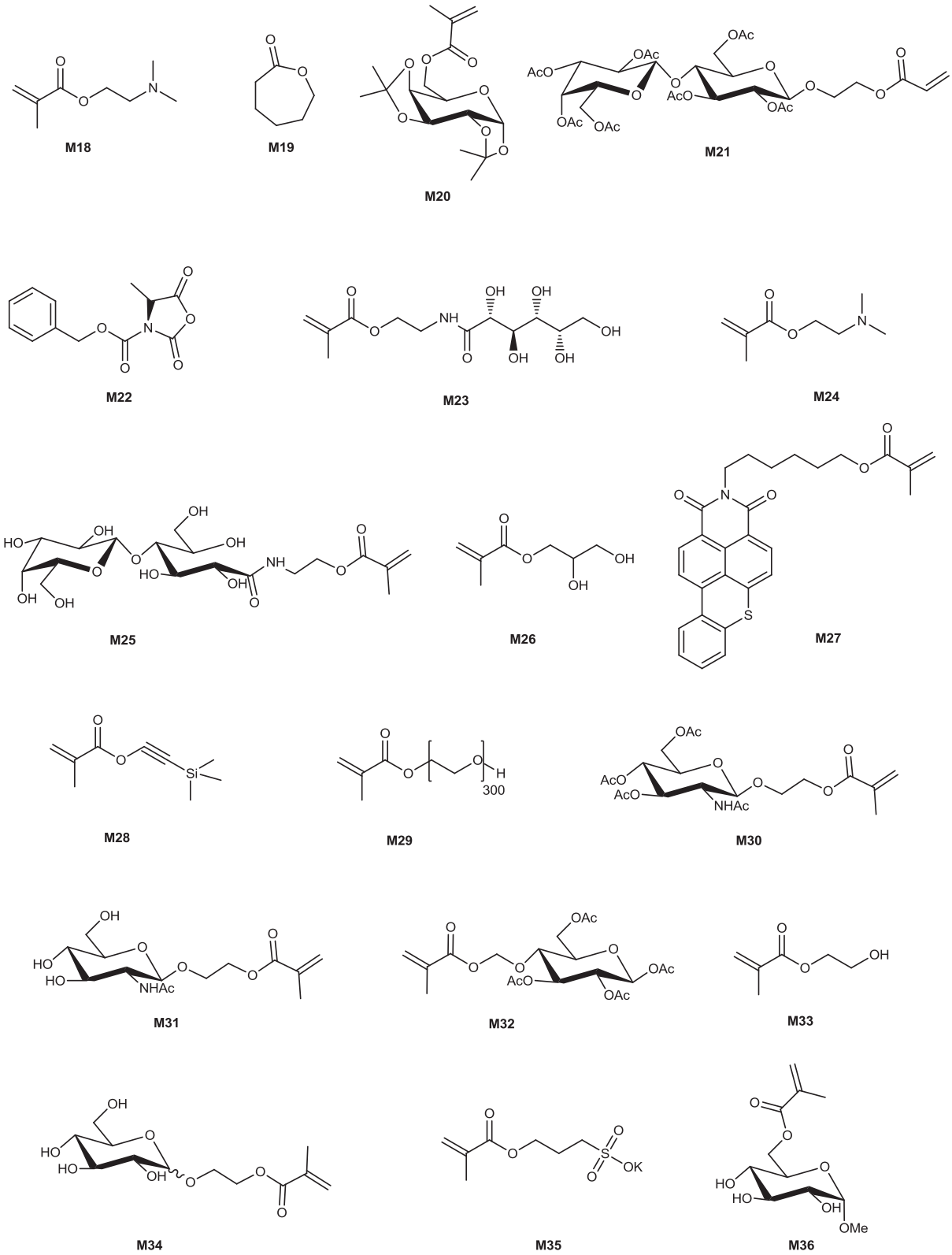

Figure 4.2 *Continued.*

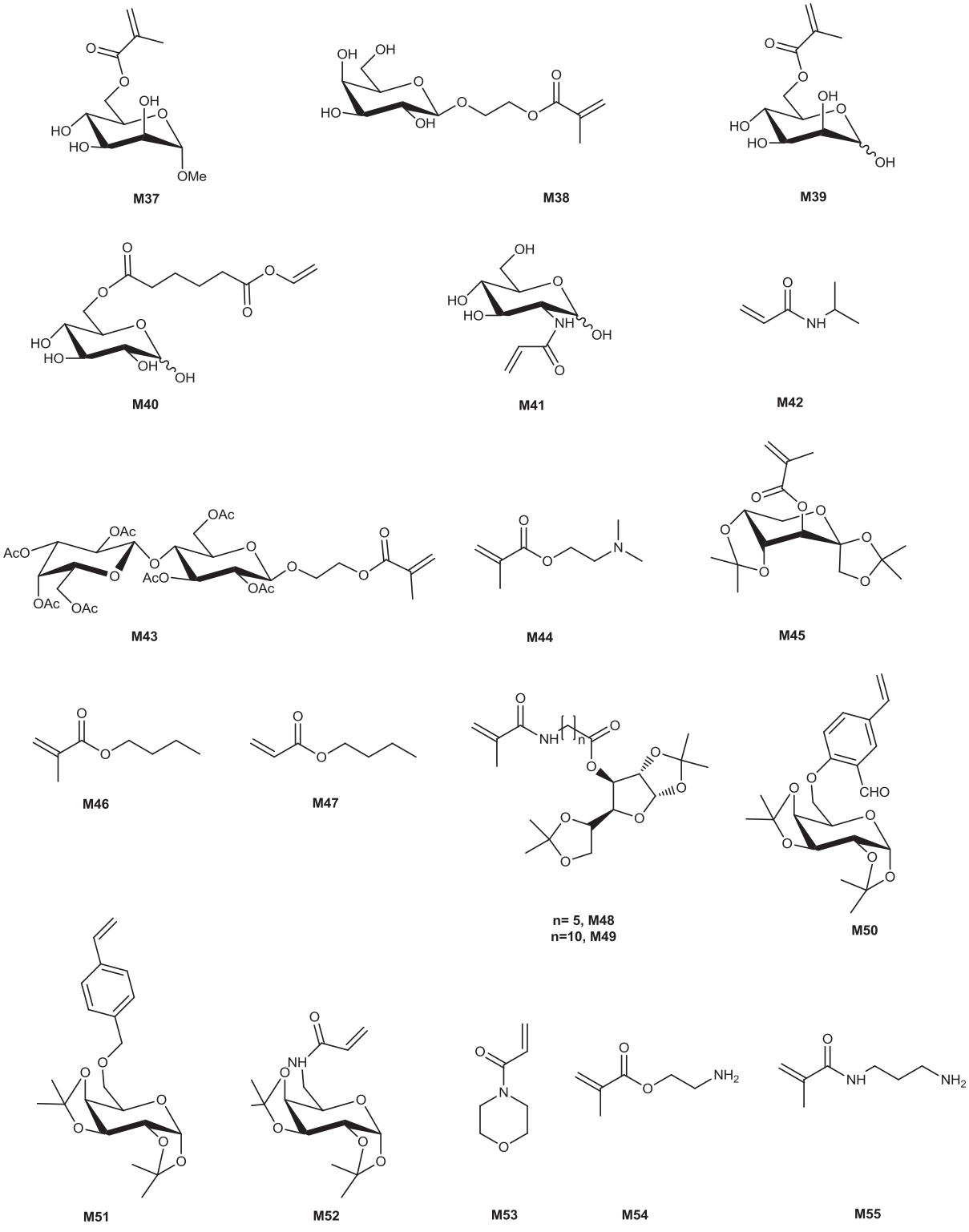

Figure 4.2 *Continued.*

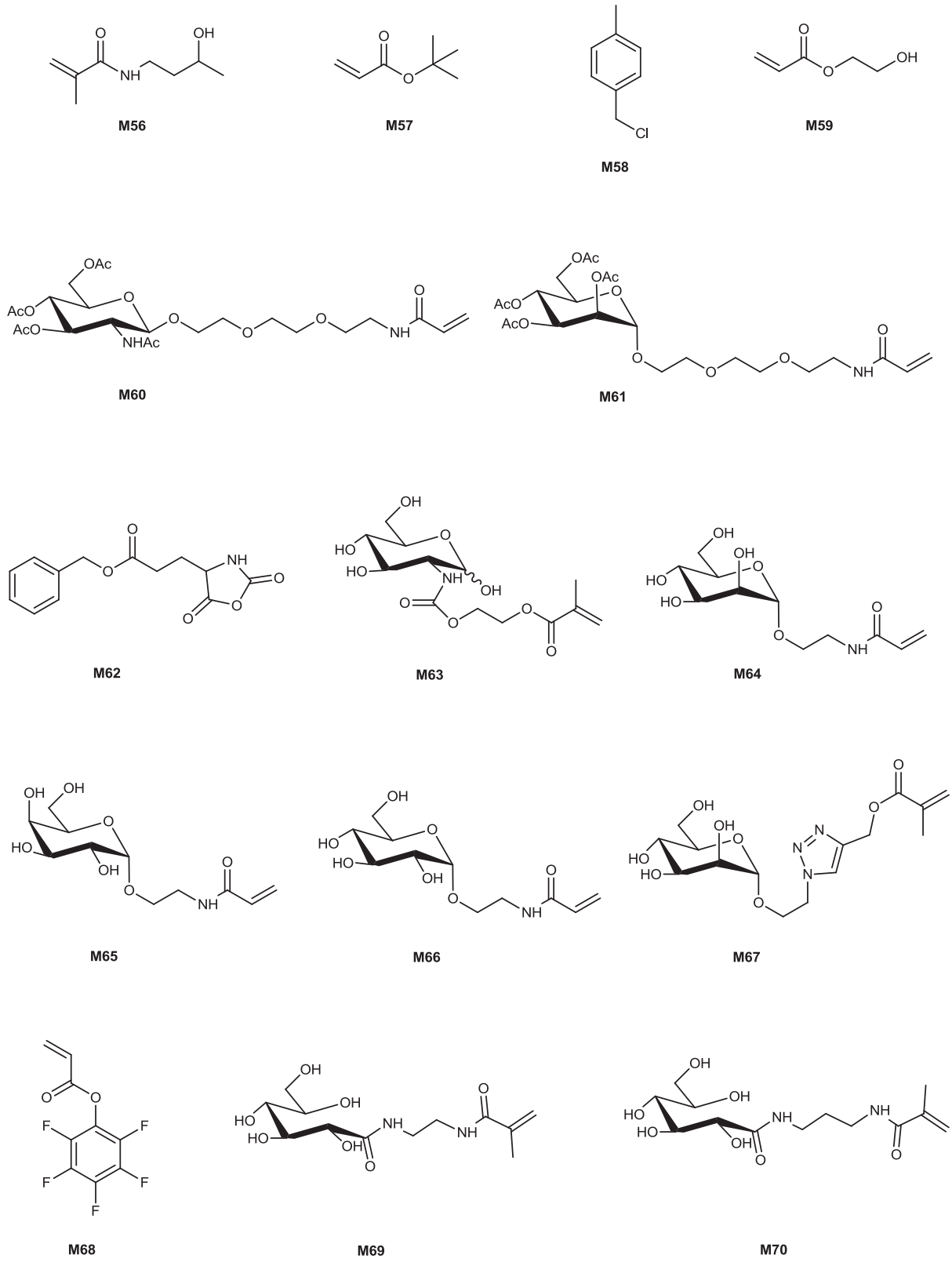

Figure 4.2 *Continued.*

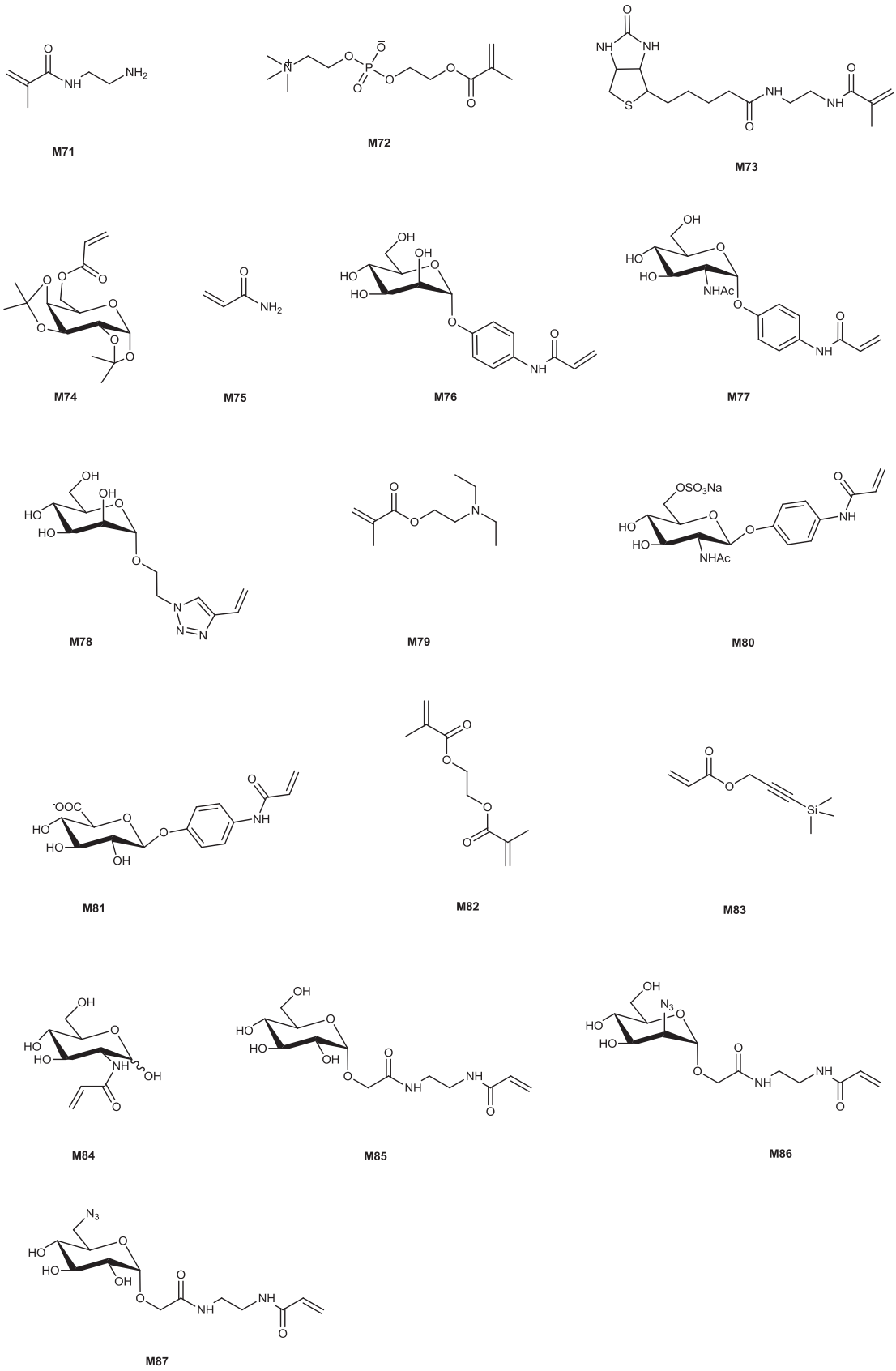

Figure 4.2 *Continued.*

4.2 Well defined glycopolymers from NMP

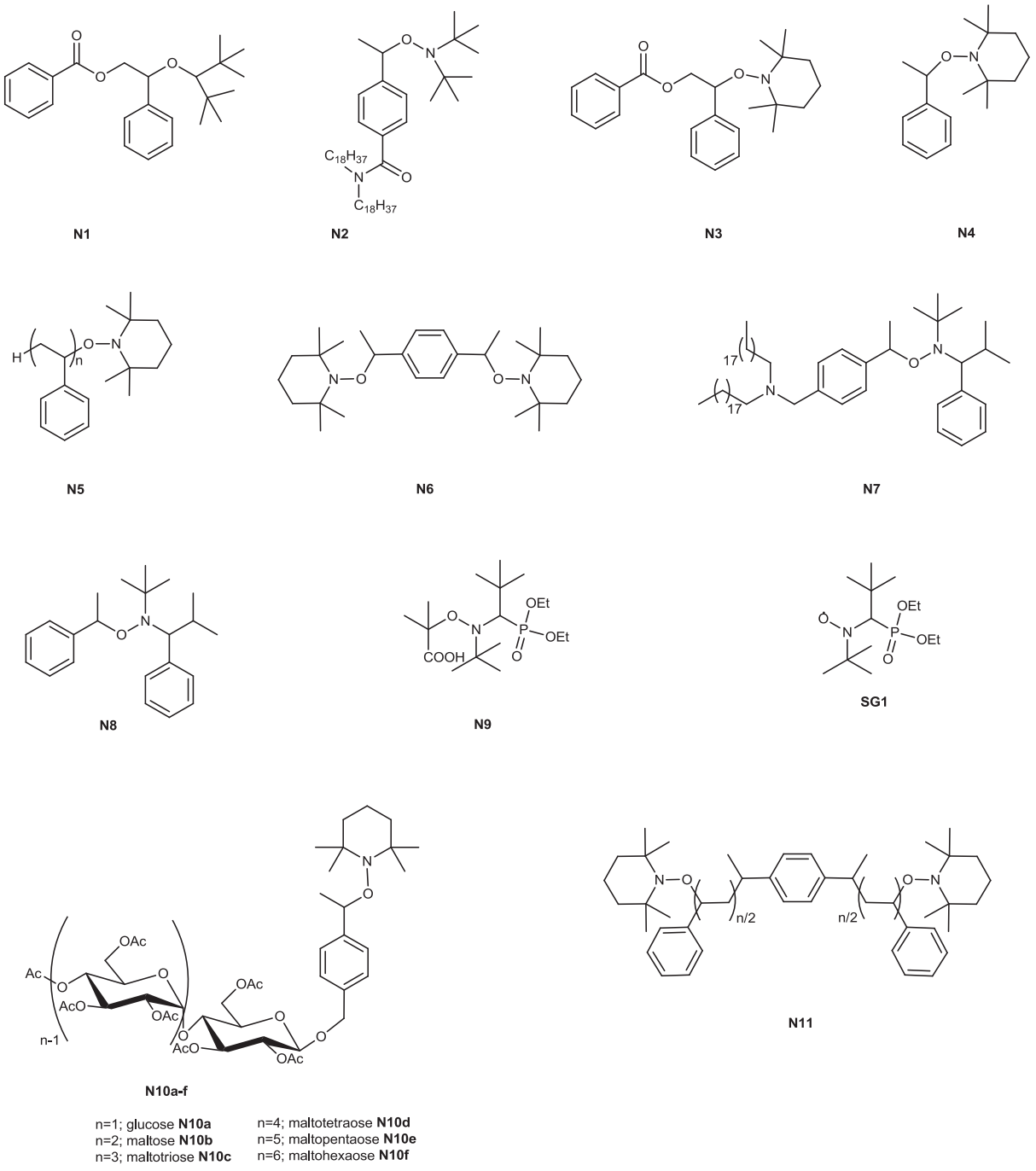

Figure 4.3 *Initiators involved in the synthesis of well defined glycopolymers by NMP.*

Table 4.1 *Summary of Nitroxide Mediated Polymerization (NMP) experiments described in literature.*

Entry	Monomer(s)	Control agent	Additive	M_n ($\times 10^{-3}$)	M_n / $M_{n,th}$ [a]	Conv. %	PDI	Structure[b]	Ref.
1	**M1a**	N1	DCP	7.5	-	35	1.3	homop.	13e
2	**M1b**	N1	DCP	12.5	-	90	1.1	homop.	13e
3	**M1b**	N2	DCP	12	-	90	≤ 1.2	homop.	16
4	**M1b**	N3	-	40	-	50	≤ 1.3	homop.	17
5	**M2**	N4	-	7	-	74	1.2	homop.	18
6	**M5**	N4	-	34	-	90	2	homop.	19
7	**M6**	N5	CSA	12.7	-	-	1.1	Block AB	20
8	**M7**	N5	CSA	16.2	-	-	1.2	Block AB	20
9	**M6/St**	N6	CSA	34.3	-	17	1.17	Block ABA	21
10	**M6/St**	N6	CSA	20	-	18	1.12	Block ABA	21
11	**M6/St**	N6	CSA	14.2	-	10	1.1	Block ABA	21
12	**St**	N10a-f	-	5-25	-	≅ 40	1.1	homop.	22
13	**M10**	N11	DCP	21	-	73	1.16	Block ABA	23
14	**M10**	N11	DCP	31.8	-	84	1.11	Block ABA	23
15	**M9**	N7	-	9	-	60	1.2	homop.	24
16	**M9/M8**	N8	-	13.8	-	55	1.2	A-*co*-B	24
17	**M11/10% St**	N9	-	40.6	-	45	1.26	A-*co*-B	25
18	**St**	P(**M11**$_{0.9}$-co-S$_{0.1}$)[c]	-	85.3	-	51	1.44	(A-*co*-B)-*b*-C	25
19	**M12**	N9	-	35	0.44	78	1.03	homop.	26
20	**St**	P**M12**$_{16}$[c]	-	17.8	1.02	66	1.21	Block AB	26
21	**M12**	P**St**$_{46}$[c]	-	7.1	0.56	76	1.16	Block AB	26

a: degree of control where $M_{n,th}$ is the theoretical targeted molar mass, b: homop. stands for homopolymer, c: macroinitiator.

4.2.1 Protected glycomonomers

4.2.1.1 Styrenic monomers

In 1997 Fukuda's group at Kyoto University (Japan) first described the NMP of a styrene derivative carrying a (1→4)-β-D-galactoside moiety **M1a** in DMF at 90 °C using N1 as a mediator and DCP (dicumyl peroxide) as an accelerator. [13e] However, the monomer conversion was low and only polymers with low molecular weights were obtained. By contrast, the polymerization of the protected monomer **M1b** under the same conditions proceeded after reversible-deactivation cycles to high conversion, giving higher molecular weights between 2000 and 40000 Da, and narrower polydispersities (Entries 1-2, Table 4.1). The same polymerization was repeated in 1,2-dichloroethane using an alkoxyamine initiator with a dioctadecyl group **N2** (Entry 3, Table 4.1). [16] The resulting polymer **DODA-**P**M1b** had a low polydispersity (1.1 ≤ PDI ≤ 1.2), with M_n between 3000 and 12000 Da. After deprotecting the polymer, liposomes were obtained showing specific recognition by *Ricinus communis*, a β-D-galactose binding lectin.

Encouraged by the potential of the glycocluster effect between lectins and P**M1a** studies on the same monomer were extended in DMF using **N3** as a unimodal initiator (130 °C, 24 hours, no accelerator). [17] While the conventional free radical polymerization provided glycopolymers with large polydispersities, NMP of **M1b** yielded polymers with fairly low polydispersities (PDI < 1.3). From Table 4.1 (Entry 4), we notice that the highest conversion was 50 % after 24 hours and M_n did not exceed 40000 Da. This was attributed, as judged by the authors, to the steric hindrance of the lactose unit. As expected, P**M1a** showed a strong and specific glycocluster effect to RCA_{120} (*β*-galactose specific lectin).

After Hirao et al. [10b] demonstrated the anionic "living" polymerization of styrene derivatives containing acetal protected monosaccharide residues (acetal-protected glucofuranose, galactopyranose, fructopyranose, and sorbofuranose) and after knowing their benefit application in biomedicine and biomaterials, Y.M. Chen and G. Wulff published two articles [18-19] in which four isopropylidene protected styrene derivatives with a monosaccharide moiety (**M2-M5**) were polymerized in bulk for 24 hours at 130 °C with **N4** as an initiator. From the kinetic studies, these polymerizations possessed the characteristics of reversible-deactivation radical polymerizations. From Table 4.1 (Entries 5-6) we can see that the prepared polymers had relatively low polydispersities as compared to classical free radical

polymerizations while that of monomer **M5** was an exception. The corresponding protected polymers showed a thermal stability up to 150 °C and their corresponding deprotected forms were obtained by the treatment with TFA/H_2O (9:1, v/v) solution. Block copolymers with styrene were also prepared and following deprotection of the sugar block, amphiphilic block copolymers were obtained whose surface properties were investigated. [19]

The synthesis of amphiphilic block glycopolymers was also the subject of a published article by T. Kakuchi et al. [20] The article described the polymerization of 4-vinylbenzyl glucoside **M6** and 4-vinylbenzyl maltohexaoside peracetate **M7** in xylene at 120 °C with a TEMPO terminated polystyrene oligomer **N5** (M_n = 8100 Da, PDI = 1.17) as a macromolecular initiator. The resulting P**St**-*b*-P**M6** and P**St**-*b*-P**M7** had a M_n of 12700 Da and 16200 Da respectively, and the polydispersity indices remained quite low (Entries 7-8, Table 4.1). De-acetylation with sodium methoxide in dry THF, provided amphiphilic blocks copolymers containing glucose and maltohexaose as hydrophilic segments that formed reversed micelle-like aggregate in toluene and micelle-like aggregates in water. In an extension to this work, the same group used the bi-functional initiator **N6** to prepare TEMPO-terminated P**M6** (M_n = 8500 Da, PDI = 1.09) that was subsequently chain extended with styrene to afford P**St**-*b*-P**M6**-*b*-P**St** tri-block copolymers of various chain lengths (M_n = 12500, 17900 and 29400 Da; PDI_s = 1.14-1.17). [21] The yields for both polymerization steps were quite low in spite of using camphorsulfonic acid as an accelerator (Entry 9-11, Table 4.1).

A series of glycoconjugated TEMPO adducts, **N10a-f**, was synthesized and used as the initiators for the polymerization of styrene for 6 hours at 120 °C to afford end-functionalized P**St**'s with the acetyl saccharides (Entry 12, Table 4.1). [22] The resulting acelyated polymers were obtained with controlled molecular weights, which fairly agreed with the predicted values, ranging from 4,800 to 25,000 Da, with narrow polydispersities and quantitative end functionality. The end-functionalized P**St**'s with saccharides, which were obtained by selective deprotection by sodium methoxide in THF, formed polymeric reverse micelles consisting of a saccharide-core and P**St**-shell in chloroform and toluene. It was demonstrated that the aggregation property, such as the average molar mass obtained by laser light scattering and aggregation number values was strongly related to the degree of polymerization *DP* and the number of the glucose residues.

The same group in the same year came out with a novel type of glycoconjugated macromolecular architecture, an amphiphilic ABA triblock copolymer containing pendant glucose and maltohexaose units by a two step TEMPO mediated polymerization (Entries 13-14, Table 4.1). [23] First styrene was polymerized with **N6** as an initiator at 120 °C for 5 hours to obtain a polystyrene macro-initiator **N11**. In the presence of the latter initiator **N11** and DCP as an accelerator, 4-vinyl (glucoside or maltohexaoside) peracetate **M10a-b** was polymerized in dichlorobenzene at 120 °C for 5 hours to yield their corresponding ABA triblock copolymer with pendant acetyl saccharide units on both sides of the chain end. The corresponding polymers were modified by deacetylation into amphiphilic ABA triblock glycopolymers.

4.2.1.2 (Meth)acrylate monomers

Hawker and co-workers [24] examined the NMP of 1,2,5,6-di (isopropylidene)-D-glucose-2-propenoate **M9** in DMF at 105 °C due to the use of an α-hydrido alkoxyamine initiator **N7** functionalized with a lipophilic DODA group. The kinetics of the polymerization was investigated allowing after hydrolysis, controlled molecular weight, low-polydispersity lipo-glycopolymers to be prepared. The overall polymerization rate was quite slow with 60 % conversion after 50 hours of reaction. Amphiphilic statistical copolymer of **M9** with N, N'-di(octadecyl)acrylamide **M8** was also prepared. The resulting co-polymer was obtained with M_n of about 13800 Da with 55 % yield and with a polydispersity of 1.2 (Entries 15-16, Table 4.1). Well-defined lipo-glycopolymers were obtained after the removal of the alkoxy amine end chain with tributylin hydride (Bu_3SnH) and deprotecting the glucose unit by TFA. Finally the surface and membrane-forming properties characterized for the application of these new lipo-glycopolymers in biosensors.

Ting et al. [25] reported the synthesis of a novel galactose based amphiphilic glycopolymer. A methacryloyl galactose monomer **M11** was first copolymerized with styrene in the presence of **N9** as an initiator in dioxane at 85 °C to afford copolymers P(**M11**$_{0.9}$-*co*-**St**$_{0.1}$) with fairly low polydispersities (Entries 17-18, Table 4.1). The latter prepared macroinitiator was chain extended with styrene in the same solvent at 115 °C for 3.8 hours to get after 51 % monomer conversion diblock copolymers P(**M11**$_{0.9}$-*co*-**St**$_{0.1}$)-*b*-P**St** whose polydispersities were relatively high. Deprotection of the latter diblock copolymer using sodium methoxide in MeOH/DCM mixture yielded amphiphilic glycopolymers that auto-

assembled into micelles. The biofunctionality of β-galactose moieties on micelles were screened using peanut agglutinin, a lectin specific for conjugating β-galactose.

4.2.2 Glycopolymers from the post-polymerization approach

Becer et al. described the synthesis of glycopolymers bearing thio-glucoside units using a convergent method. [26] First, the glycopolymers were obtained by the polymerization of the **St** and **M12** (pentaflurorostyrene) into their corresponding polymers or copolymers in the presence of a bloc builder **N9** as an initiator in THF at 110 °C for a period of 5 hours. What followed was a nucleophilic attack of a thiol-glycoside (2,3,4,6-tetra-*O*-acetyl-1-thio-*β*-D-glucopyranose), at the *para* position of the pentafluorostyrene ring to obtain the title glycopolymers. The obtained glycopolymers were deprotected by sodium methoxide in DMF and purified by precipitation in cold EtOH. According to SEC results, all synthesized polymers exhibited narrow molar mass distributions with polydispersity indices ranging from 1.03 to 1.2 with a fairly accordance between the theoretical molar mass and the experimental one (Entries 19-21, Table 4.1). Some copolymers showed self-assembly behavior into regular nanospheres with diameters ranging from 70 to 720 nm by applying a nanoprecipitation technique. Recently, the same group [27] also managed to incorporate a thio-galactoside to homo and block copolymers of styrene and **M12** using the same method. The water-insoluble P**St** block copolymers were drop-casted to form stable films. The coated substrates were used to study the attachment of 3T3 fibroblasts and MC3T3-E1 preosteoblasts (strain of tissue cultures).

4.3 Well defined glycopolymers from ATRP

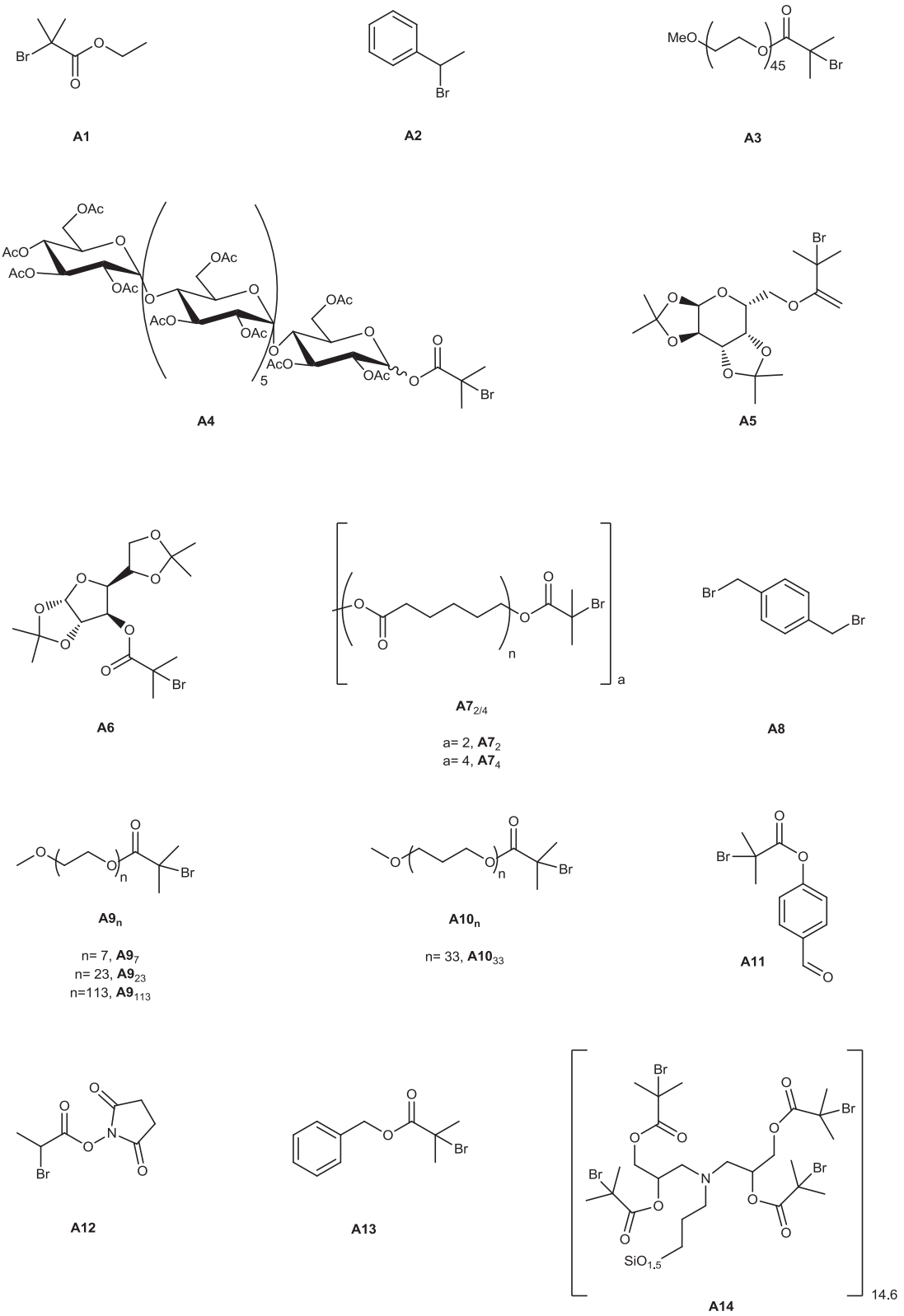

Figure 4.4 *Initiators involved in the synthesis of well defined glycopolymers by ATRP.*

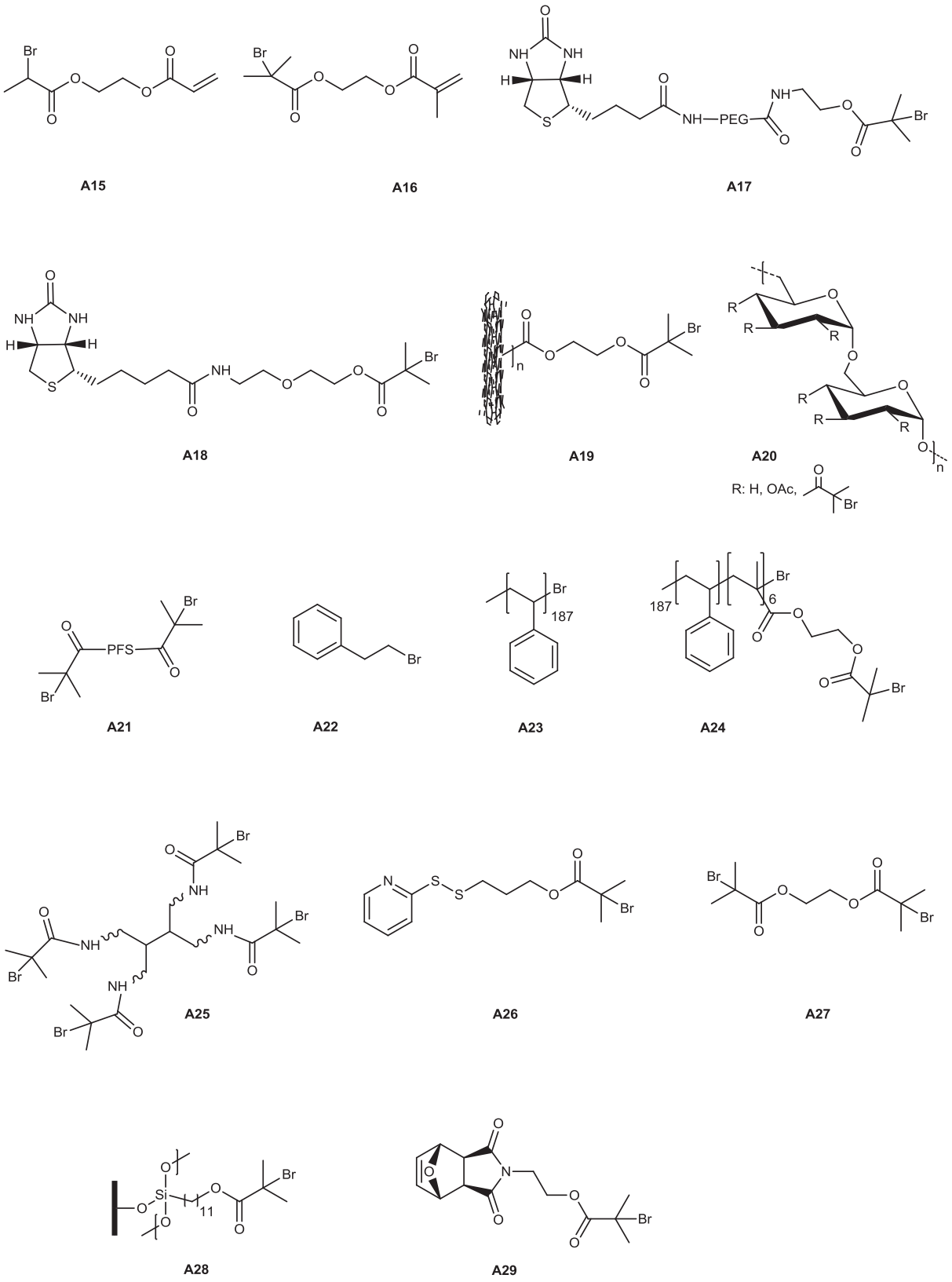

Figure 4.4 *Continued.*

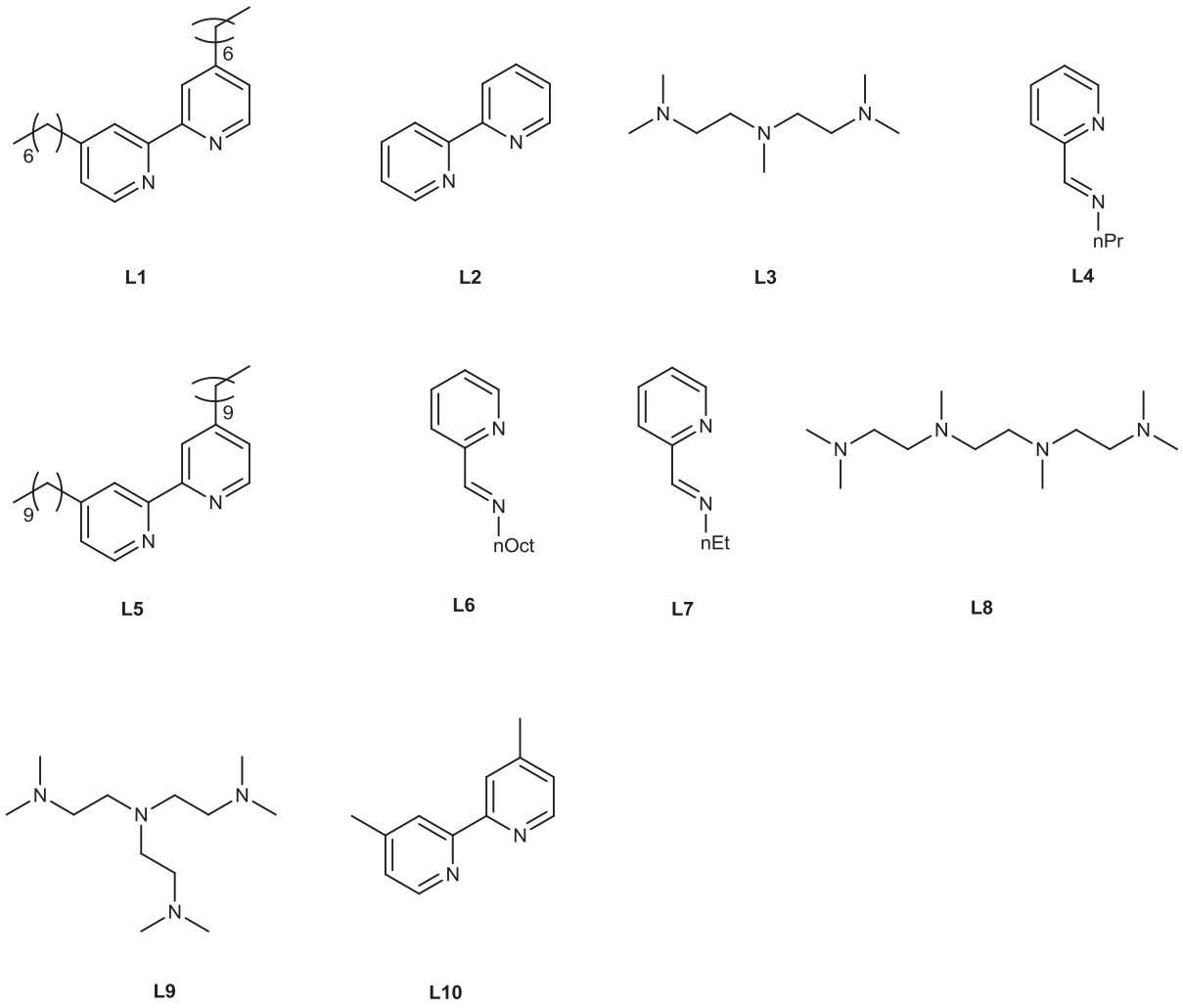

Figure 4.5 *Commercial ligands involved in the synthesis of well defined glycopolymers by ATRP.*

Table 4.2 *Summary of Atom Transfer Radical Polymerization (ATRP) experiments described in literature.*

Entry	Monomer(s)	Control agent	Additive	M_n ($\times 10^{-3}$)	M_n / $M_{n,th}$ [a]	Conv. %	PDI	Structure[b]	Ref.
1	**M13**	A1	$CuBr(L1)_2$	75	0.45	83	1.82	homop.	13f
2	**M14**	A2	$CuBr(L2)_2$	5.2	1.06	55	1.26	homop.	28
3	**M14**	A2	$CuBr(L2)_2$	11.8	1.01	52	1.27	homop.	28
4	**M14**	A2	$CuBr(L2)_2$	24.8	1.00	55	1.34	homop.	28
5	**M15**	A4	$CuBr(L4)_2$	10.1	0.92	87	1.09	Block AB	29
6	**M16**	A4	$CuBr(L4)_2$	11.5	0.84	80	1.15	Block AB	29
7	**M13**	A4	$CuBr(L4)_2$	16.5	0.65	88	1.21	Block AB	29
8	**M18**	A4	$CuBr(L4)_2$	-	-	82	-	Block AB	29
9	**St**	A4	$CuBr(L4)_2$	10.7	1.20	91	1.48	Block AB	29
10	**M19**	I1	$Sn(Oct)_2$	6.6	1.12	-	1.14	homop.	30
11	**M19**	I2	$Sn(Oct)_2$	13.7	1.15	-	1.12	homop.	30
12	**M20**	$A7_2$	$CuBr(L5)_2$	20.1	-	65	1.19	Block ABA	30
13	**M20**	$A7_4$	$CuBr(L5)_2$	35.0	-	51	1.17	4 arm star	30
14	**M21**	A8	$CuBr(L2)_2$	20.6	1.22	58	1.29	homop.	31
15	**M21**	A8	$CuBr(L2)_2$	9.31	1.26	96	1.24	homop.	31
16	**M22**	$PM21_{10}$	-	14.26	1.14	73	1.38	Block ABA	31
17	**M13**	A12	$CuBr(L6)_2$	7.1[c]	-	90	1.14	homop.	32
18	**M13**	A12	$CuBr(L6)_2$	14.7	-	90	1.31	homop.	32
19	**M20**	A12	$CuBr(L6)_2$	7.5	-	95	1.08	homop.	32
20	**M20**	A12	$CuBr(L6)_2$	13.4	-	99	1.10	homop.	32
21	**M13/M28**	A12	$CuBr(L6)_2$	6.1	-	90	1.25	A-*co*-B	32
22	**M20/M27**	A12	$CuBr(L6)_2$	6.1	-	90	1.15	A-*co*-B	32
23	**M13**	A14	$CuBr(L8)_2$	416	-	8	1.17	Star	33
24	**M13**	A14	$CuBr(L8)_2$	601	-	6	1.26	Star	33
25	**M9**	A1	$CuBr(L3)_2$	6.6	1.2	88	1.13	homop.	34
26	**M9**	A1	$CuBr(L3)_2$	18.5	1.3	93	1.25	homop.	34

27	**M9**	A1	$CuBr(L3)_2$	31		84	1.37	homop.	34
28[c]	**M9**	A15	$CuBr(L3)_2$	6.6	-	98	1.92	Hyper branched	34
29[d]	**M9**	A15	$CuBr(L3)_2$	13	-	96	1.95	Hyper branched	34
30[c]	**M13**	A16	$(PPh_3)_2NiBr_2$	17.6	-	> 98	2.12	Hyper branched	35
31[d]	**M13**	A16	$(PPh_3)_2NiBr_2$	23.3	-	> 98	1.57	Hyper branched	35
32	**M13**	A19	$CuBr(L8)_2$	37.4	1.16	85	1.45	homop.	36
33	**M13**	A16/A19	$(PPh_3)_2NiBr_2$	4.37	-	90	1.81	Hyper branched	36
34	**M15**	A20	$CuBr(L4)_2$	9.1	1.82	51	1.04	homop.(*graft*)	37
35	**M13**	A21	$CuCl(L10)_2$	12.5	-	-	1.18	Block ABA	38
36	**M32**	A23	$CuBr(L3)_2$	27.6	0.82	62	1.32	homop.	39
37	**St/M32**	A22	$CuBr(L3)_2$	23.7	0.65	83	1.22	A-*co*-B	39
38	**M33**	A23	$CuBr(L3)_2$	20	0.99	45	1.14	Block AB	39
39	**M32**	A24	$CuBr(L3)_2$	25.2	0.69	53	1.43	Graft AB	39
40	**M30**	A16	$CuCl(L8)_2$	11	-	95	1.29	Hyper branched	40
41[e]	**M23**	$A9_{23}$	$CuBr(L2)_2$	11.4	-	> 97	1.23	Block AB	41
42[f]	**M23**	$A9_{23}$	$CuBr(L2)_2$	12.6	-	> 97	1.48	Block AB	41
43[g]	**M23**	$A9_{23}$	$CuBr(L2)_2$	13.4	-	> 97	1.82	Block AB	41
44[h]	**M25**	$A9_{23}$	$CuBr(L2)_2$	22.5	-	-	1.24	Block AB	42
45[f]	**M25**	$A9_{23}$	$CuBr(L2)_2$	25.3	-	> 95	1.26	Block AB	42
46[g]	**M25**	$A9_{23}$	$CuBr(L2)_2$	34.8	-	> 95	1.60	Block AB	42
47	**M25**	A17	$CuBr(L2)_2$	24	1.02	80	1.32	Block AB	43
48	**M30**	A18	$CuBr(L9)_2$	40.7	1.88	94	1.17	homop.	44
49	**M31**	A18	$CuBr(L9)_2$	43.1	3.01	86	1.07	homop.	44
50	**M23**	A25	$CuBr(L2)_2$	80	-	64	1.26	4-arm star	45
51	**M31**	A26	$CuBr(L2)_2$	10	-	≅ 80	1.12	homop.	46
52	**M63**	A1	$CuBr(L3)_2$	70	-	≅ 90	1.2	homop.	47
53	**M63**	A27	$CuBr(L3)_2$	≅ 27	-	≅ 75	1.15	homop.	47
54	**M47**	P**M63**[i]	$CuCl(L3)_2$	15	0.87	90	1.31	Block AB	47
55	**M47**	P**M63**[j]	$CuCl(L3)_2$	17.6	0.98	93	1.38	Block ABA	47
56	**M46**	P**M63**[i]	$CuCl(L3)_2$	32.7	1.2	45	1.3	Block AB	48

57	**M64**	A28	$CuCl(L9)_2$	51	-	-	1.5	Brush	49
58	**M28**	A13	$CuBr(L7)_2$	14.9	2.50	> 80	1.16	homop.	50
59	**M28/M15**	A13	$CuBr(L7)_2$	8.9	1.56	> 80	1.09	A-*co*-B	50
60	**M28/M29**	A13	$CuBr(L7)_2$	11.9	1.52	> 80	1.12	A-*co*-B	50
61	**M67**	A29	$CuBr(L7)_2$	26	-	-	1.2	homop.	51

a: degree of control where $M_{n,\,th}$ is the theoretical targeted molar mass, b: homop. stands for homopolymer, c: $[\mathbf{M_i}]_0$ / $[A_i]_0$ = 1.5, d: $[\mathbf{M_i}]_0$ / $[A_i]_0$ = 10, e: methanol, f: methanol/water : 3/2, g: water, h: *N*-Methyl-2-pyrrolidone, i: obtained using A1, j: obtained using A27.

4.3.1 Protected glycomonomers

4.3.1.1 (Meth)acrylate monomers

The first example of a glycopolymer obtained by ATRP was described by T. Fukuda and co-workers [13f] where the polymerization of a protected glucose glycomonomer **M13** in veratrole was examined at 80 °C (3.5 hours) using ethyl 2-bromoisobutyrate **A1** as an initiator and $CuBr(\mathbf{L1})_2$ as a catalyst (Entry 1, Table 4.2). By varying the monomer to initiator ratio, polymers with M_n in the range $2.7 \times 10^4 - 2 \times 10^5$ Da and polydispersities of 1.27-1.82 were obtained. As expected, lower polydispersities were obtained with higher monomer to initiator ratio. The sequential addition of the two monomers styrene and **M13** afforded a bromine block terminated copolymer of the type P**St**-*b*-P**M13** under the same conditions. Deprotecting the homo- and block copolymers by formic acid gave well-defined glucose-carrying water soluble polymers. The same group later on, studied the first example of grafting a well defined glycopolymer onto a solid surface. [52] Where a monolayer initiator substrate, obtained by Langmuir-Boldget technique, was dipped in a veratrole solution of **M13**, $CuBr(\mathbf{L1})_2$ and *p*-toleunesulfonyl chloride as a free initiator. The latter solution was heated at 80 °C for 12 hours. The polydispersity of the free polymers in solution did not exceed 1.2. Ellipsometric and atomic force microscopic analyses showed the formation of a homogenous graft layer onto the substrate. Moreover, the thickness of the graft layer in the dry state was found to increase monotonically with the reaction time and a linear relation could be established between it and the M_n of the free polymers in solution. All this suggested a controlled growth of the graft chains while the graft density stayed constant. Quantitative deprotection of the grafted P**M13** in formic acid produced a solid surface densely grafted with a well defined glucose-carrying polymer as confirmed by grazing-angle reflection-absorption FTIR studies.

F.M. Li and coworkers [28] described the polymerization of **M14**, a protected glucose bearing an acrylate group, in the presence of **A2** as an initiator and CuBr(**L2**)$_2$ as a catalyst in chlorobenzene at 80 °C. The kinetic plot was a first order kinetic with a linear increase of the molecular weight with conversion and the molecular distribution remained narrow up to 70 % conversion. By increasing the monomer to initiator ratio, polymers with M_n in the range 5-25 KDa and polydispersities of 1.26-1.34 were obtained, respectively (Entries 2-4, Table 4.2). The resulting polymer was quantitatively deprotected in a dilute NaOMe solution in $CHCl_3$/MeOH at room temperature. The same group investigated the interaction of a prepared block copolymer (P**M14**-*b*-PEO) with ConA. [53] In this sense, a methoxy capped polyethylene oxide (PEO) macro-intiator **A3** along with CuBr(**L3**)$_2$ was used to polymerize **M14** under the same conditions reported in their previous paper. The obtained glycopolymer contained 27 glycomonomer units and its polydispersity index was 1.12. After deprotection, its interaction with ConA was studied by optical density and fluorescene methods and compared to the interaction obtained by a deprotected decamer of **M14**. While both polymers formed aggregates with the lectin, those from PEO-*b*-P(deprotected **M14)** were stable in water as well, due to the existence of the PEO segments.

Haddleton and coworkers studied the preparation and the use of carbohydrate-functionalized ATRP initiators for the polymerization of a wide range of methacrylate monomers (Entries 5-9, Table 4.2). [29] To this aim, an acylated maltoheptoside **A4** was obtained from a series of transformations of β-cyclodextrin and was used as a glycoinitiator for the polymerization of a series of different methacrylates (**M13**, **M15**, **M16**, and **M18**) and **St**. The polymerizations were conducted in xylene or toluene at 90 °C using CuBr(**L4**)$_2$ as a catalyst. The kinetic study on the polymerization of methyl methacrylate **M15** showed a first order kinetics with a linear evolution of the molecular weight with time. However, polymerization of styrene using the same glycoinitiator resulted in a broadening of the polydispersity to 1.48 while a good control over the M_n was maintained, a phenomenon already observed with other types of 2-bromo-2-methylpropionyl initiators. [54] Finally, deacetylation of the carbohydrate residues was achieved in a dilute NaOMe solution in $CHCl_3$/MeOH at room temperature. Similarly, amphiphilic block copolymers [55] P(**M16**-*b*-**M17**) containing end of chain carbohydrate residues were synthesized using galactose and glucose derived initiators **A5** and **A6**, respectively. In all experiments, the hydrophilic macro-monomer **M16** was first polymerized at 60 °C, since reaction at higher temperatures reduced

the proportion of end of chain bromine groups in the final polymer, followed by extension of the obtained polymer with **M17** at 90 °C in toluene using CuBr(**L4**)$_2$ as a catalyst. In both cases, the polymerizations occurred with a good first order kinetics producing AB blocks with molecular weights close to the targeted ones and with low polydispersity indices 1.1-1.2. It is worth noting that the average DP_n of each of the two blocks was, in all cases, between 5 and 28, indicating narrow polydispersity oligomers rather than polymers. Block copolymer micelles were obtained after the removal of the isopropylidene groups with 50% TFA at room temperature whose size and polydispersity were estimated by dynamic light scattering which showed a unimodal size distribution with hydrodynamic diameters between 35 and 41 nm.

The combination of ring opening and atom transfer radical polymerizations was a subject of a paper by G. Wulff et al. [30] where amphiphilic linear and star block copolymers were synthesized (Entries 10-13, Table 4.2). Hence, bifunctional **I1** and tetrafunctional **I2** initiators (Figure 4.6) were used in the ring opening polymerization of ε-caprolactone **M19** at 110 °C for 24 hours to get hydroxyl terminated narrow polydispersity polyesters (P**M19**). The obtained ATRP macro-initiators **A7**$_2$ and **A7**$_4$, obtained by the reaction of P**M19** with 2-bromo-2-methylpropionyl bromide, were chain extended, at 90 °C in anisole with a protected galactose derived glycomonomer **M20** to yield ABA and star block glycopolymers. The carbohydrate residues in the copolymer were deprotected with 80 % formic acid at room temperature. In the ATRP experiments, maximum conversion was achieved after half an hour (65 % and 51 % for linear and star polymers respectively) after which no further monomer was consumed. Fascinatingly, the lack of high molecular weight peaks from the SEC traces suggests that no star-star coupling took place.

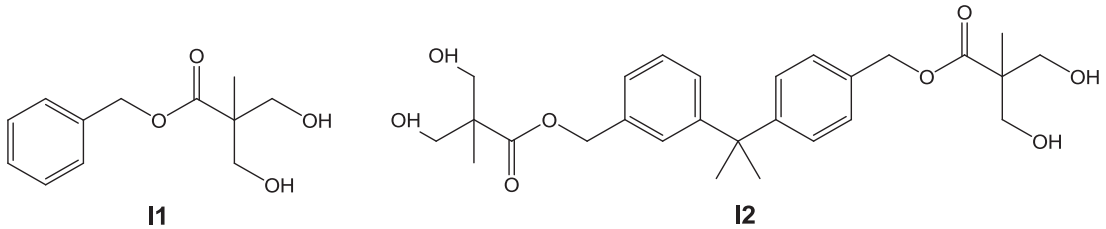

Figure 4.6 *Initiators used by Wulff et al. [30] for the polymerization of **M19**.*

E. L. Chaikof and coworkers [31] described the synthesis of a new class of well-defined glycopolymer-polypeptide triblock copolymer of the structure P(L-alanine)-*b*-P**M21**-*b*-P(L-alanine) by the combination of ATRP and ROP (Entries 14-16 , Table 4.2). First, a protected lactoside glycomonomer **M21** was polymerized in the presence of a bifunctional initiator **A8**

with CuBr(**L2**)$_2$ as a catalyst in chlorobenzene at 100 °C. Well defined glycopolymers were obtained in good yield that were converted into ROP macroinitiators by functionalizing its extremities with primary amino groups. Chain extension with L-alanine *N*-carboxyanhydride **M22** in DMF at room temperature for 64 hours afforded triblock copolymers P**M22**-*b*-P**M21**-*b*-P**M22** (Figure 4.7) whose carbohydrate moieties were deprotected in the presence of hydrazine in DMSO at 0 °C. As anticipated, deacetylation of the protected glycopolymer midblock generated amphiphilic triblock copolymers which self assembled in aqueous solution to form nearly spherical aggregates of several hundred of nanometers as showed by TEM.

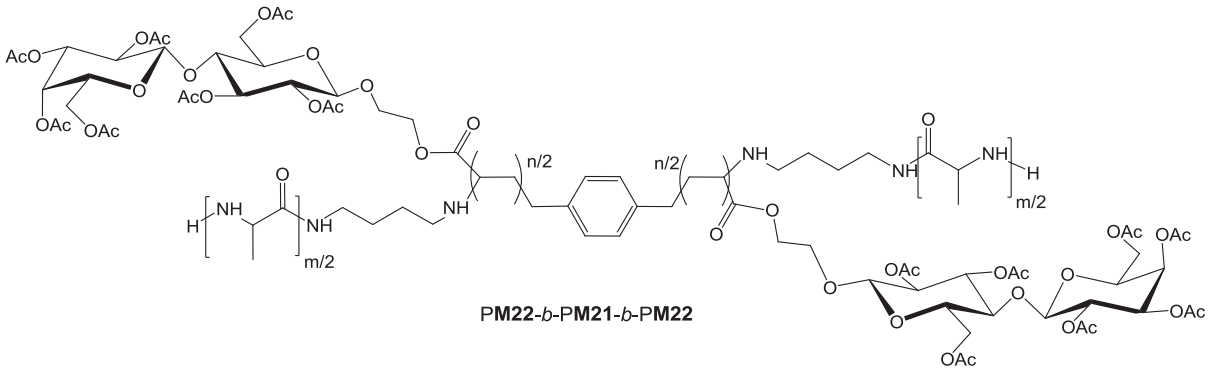

Figure 4.7 *Structure of polymer prepared by Chaikof and coworkers.* [31]

The synthesis and characterization of a number of *N*-(hydroxy)succinimidyl ester-terminated glycopolymers obtained ATRP has been described by Haddleton et al. [32] To this aim, glucose and galactose protected monomers, **M13** and **M20** respectively, were polymerized in toluene at 70 °C in the presence of an ester derived initiator **A12** and CuBr(**L6**)$_2$ as a catalyst. The two polymerizations evolved with a first order kinetics with an increase in the molecular weight with conversion. Adding, the two polymerizations showed similar rates for the two monomers employed, with the reaction being slightly faster, under the same experimental conditions, when **M13** was employed. After high conversions, polymers with molecular weight in the range 7000 Da to 15000 Da were obtained with polydispersity indices inferior to 1.3 (Entries 17-22, Table 4.2). The M_n for the two polymers was comparable by NMR, whereas from SEC, higher molecular weight polymers were seen in the case of **M13**. Deprotection of the sugar moieties in the presence of formic acid was achieved at room temperature and was confirmed by NMR. Moreover, fluorescent statistical copolymers were also synthesized via the copolymerization of the sugar monomers, **M13** or **M20**, with a fluorescent comonomer

M27 under the same conditions used for the homopolymerizations. The copolymerizations proceeded with linear first order kinetic plots and copolymers with fairly low polydispersity index (PDI < 1.25) were obtained after 90 % conversion. Finally, the fluorescent behavior of the obtained materials was explored.

Muller and coworkers [33] described the first paper on employing silsesquioxane nanoparticle based macroinitiators for the synthesis of well-defined glycopolymer-inorganic hybrid stars. In this sense, silsesquioxane based macroinitiator **A14** (M_n = 10200 Da, PDI = 1.25) was synthesized by reacting silsesquioxane nanoparticles (Figure 4.8) with 2-Bromo-2-methylpropionyl bromide in a mixture of pyridine and chloroform. This macroinitiator was used for the polymerization (25 min) of a protected glucofuranose glycomonomer **M13** in ethyl acetate at 60 °C in the presence of CuBr(**L8**)$_2$ as a catalyst to obtain, at low conversions, well defined glycostars with molecular weights up to 600,000 Da and PDI ≤ 1.26 (Entries 23-24, Table 4.2). They showed that at low conversion and at high ratio of monomer to initiator side reactions were suppressed. In order to determine the efficiency of the initiating sites (found to be around 44%), the arms were cleaved from the core by solvolysis with sodium methoxide and thoroughly characterized; indicating that 25 arms per star had been synthesized. Deprotection of the glycostars in the presence of 80% formic acid at room temperature gave water soluble glycostars. Both the protected and deprotected glycostars had a spherical structure in THF and water solution, respectively, and the various methods (SFM, SEM, MALLS-SEC and DLS) being used resulted in comparable sizes with an average size between 30 to 40 nm. However, both in DLS and in SEM a tendency for aggregation was seen for the water soluble glycostars, indicating hydrogen-bonding interactions between the stars.

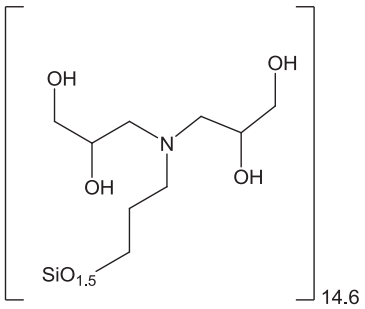

Figure 4.8 *Silsesquioxane nanoparticles described by Muller et al. [33] for the preparation of their ATRP macroinitiator.*

The same group [34] synthesized hyper-branched glycopolymers by self-condensing vinyl copolymerization (SCVCP) of an acrylic inimer **A15** with a protected glucofuranoside **M9** via ATRP. In order to find the suitable polymerization conditions for the synthesis of highly branched glycopolymers by SCVCP, they first investigated the effect of polymerization conditions on ATRP of **M9**. The polymerizations were done in ethyl acetate at 60 °C using **A1** as an initiator and CuBr(**L3**)$_2$ as a catalyst (Entries 25-27, Table 4.2). By varying the monomer to the initiator ratio, polymers with molecular weights up to 30,000 Da were obtained with a good control over molecular weight ($M_n/M_{n,th} \leq 1.3$) and a wider molecular weight distribution as going from 7000 Da (PDI = 1.13) to 30,000 Da (PDI = 1.37). As claimed by the authors, that the extremely slow polymerization rates detected (18-120 hours) compared to other type of acrylates is simply due to the steric hindrance by the bulky side group in the sugar-carrying acrylate. Moreover, the homopolymerization of **M9** was conducted under various conditions aiming at increasing the polymerization rate as well as understanding the effects of solvent and temperature, where bimodal distributions from SEC were observed at higher temperatures (80-100 °C) in ethyl acetate or anisole as solvents. After achieving the best conditions for the homopolymerization of **M9** (EtOAc/CuBr(**L3**)$_2$/60°C), they conducted the copolymerization (SCVCP) of the acrylic inimer **A15** with **M9** using CuBr(**L3**)$_2$ as a catalyst, where different temperatures and solvents were examined as well (Entries 28-29, Table 4.2). In the case of ethyl acetate, copolymerizations at both 60 and 80 °C gave same molecular weight distributions with the Mark-Houwink exponents of the branched polymers in THF being significantly lower than that for linear P**M9** suggesting that the bulky groups on the sugar moieties not only affected the rate of polymerization but also played a role in the behavior of solutions (at low molecular weights $< 10^4$ Da). By increasing

the monomer to the inimer ratio higher molecular weight copolymers could be obtained, but when ratios higher than 5 were examined multimodal distributions were observed from SEC. Finally, water soluble branched glycopolymers were obtained by deprotecting the sugar residues in 80 % formic acid at room temperature.

On the other hand, the SCVCP of a methacrylate inimer **A16** with a protected methacrylate glucofuranoside **M13** [35] was achieved at a higher polymerization rate (total conversion after 2-5 hours) contrary to the acrylate system. This is to say, that the bulky side group has no significant influence on the polymerization rate in the case of solution polymerization of the **M13** and it can be presumed, based on the authors, that the difference in the polymerization rates between the sugar-carrying acrylate and methacrylate is due to both the stability and reactivity of the active species and the reactivity of the **M13** monomer compared to **M9**. The copolymerization of **A16** with **M13** was examined in ethyl acetate at 100 °C using a free ligand based catalyst $(PPh_3)_2NiBr_2$ and polymers with M_n up to 20,000 Da were obtained with PDI ≤ 2.12 (Entries 30-31, Table 4.2). Here also, they varied the monomer to inimer ratios where higher degrees of branching were observed at lower ratios. It is worth noting that, multimodal distributions from SEC were observed at ratios higher than 2.5, but polymers having similar structures as observed from the Mark-Houwink plots were obtained. Finally, deprotection of the isopropylidene protecting groups of the branched P**M13** resulted in water-soluble glycopolymers with randomly branched architectures that were characterized by elemental analyses, ^{1}H-NMR and FTIR measurements.

A continue to their work Muller and coworkers [36] investigated the synthesis of linear and hyperbranched glycopolymers by the "grafting from" strategy, with good controllability and high reproducibility, on multiwalled carbon nanotubes (MWNTs) using ATRP. To this aim, a linear glycopolymer was grafted from the surface of MWNTs by surface initiated atom transfer radical polymerization of a protected glucofuranoside **M13** with CuBr(**L8**)$_2$ at 60 °C in ethyl acetate using 2-bromo-2-methylpropionyl-immobilized MWNTs **A19** as a macroinitiator (with or without a sacrificial initiator **A1**). Kinetic investigation of the polymerizations with and without **A1** revealed that the content of polymer grafted on MWNTs increased with conversion of monomer and polymers up to 37,000 Da were obtained with PDI ≤ 1.45 (Entry 32, Table 4.2). It is worth noting that the polydispersity index increased with conversion from 1.27 (conversion = 18 %) to 1.45 at 85 % converison. FTIR, NMR, TEM, SEM, and SFM confirmed the chemical structure and morphology of the

resulting products. Moreover, hyperbranched glycopolymers were also grafted from MWNTs by self-condensing vinyl copolymerization (SCVCP) of **M13** and BIEM inimer **A16** by ATRP in EtOAc at 100 °C using $(PPh_3)_2NiBr_2$ as a catalyst (Entry 33, Table 4.2). The degree of branching, DB, of the polymer grafted from MWNTs, evaluated by ^{1}H NMR, ranged from 0.49 to 0.21 when the **M13**/**A16** ratio increased from 0.5 to 5, in agreement with the theoretical predictions. After deprotection in formic acid, water soluble hyperbranched glycopolymers with high density of hydroxyl groups functionalized MWNTs were achieved.

The synthesis of amphiphilic grafted glycopolymers having a dextran backbone and PMMA grafts, using the "grafting from" strategy was the subject of an article by Dupayage et al. [37] In this sense, dextran's (M_n = 33800 Da, PDI =1.27) hydroxyl groups were partially acetylated followed by the synthesis of the dextran macroinitiator **A20** from the reaction of the newly acetylated dextran with 2-bromoisobutyryl bromide. Then, methyl methacrylate **M15** was polymerized in DMSO using **A20** as a macroinitiator and CuBr(**L4**)$_2$ as a catalyst at 60 °C. As a result, monodisperse polymer (PDI = 1.04) with M_n = 9,100 Da ($M_n/M_{n,th}$ = 1.82) was obtained (Entry 34, Table 4.2). Interestingly, the authors claimed that neither homopolymerization nor notable termination or transfer reactions were observed. Finally, deprotection of the acetylated groups in mild KOH conditions, gave amphiphilic glycopolymers.

Wang et al. [38] demonstrated the synthesis of an amphiphilic ABA triblock copolymer containing polysulfone as hydrophobic block and well-defined glycopolymer as hydrophilic blocks via ATRP; using a bromo-terminated bifunctional polysulfone as macroinitiator (Entry 35, Table 4.2). First, the bifunctional polysulfone (PSF) macroinitiator **A21** was obtained from the reaction of bisphenol A **1** and 4,4-dichlorophenyl sulfone **2** (Figure 4.9) in basic conditions in a mixture of toluene and NMP at 155-190 °C (11 hours), followed by esterification of the dihydroxyl terminal polysulfone with 2-bromoisobutyryl bromide. The chain extension with a protected glucofuranoside derivative **M13** in anisole at 90 °C for 24 hours using CuCl(**L10**)$_2$ afforded triblock a copolymer with M_n = 12,500 Da (PDI = 1.18) after 51 % conversion. The resulting ABA copolymer was identified by FTIR, ^{1}H-NMR, SEC, and TGA. Deprotection in mild acidic conditions (HCOOH) resulted in amphiphilic triblock glycopolymer that self assembled into micelles in aqueous solution as confirmed by microscopy.

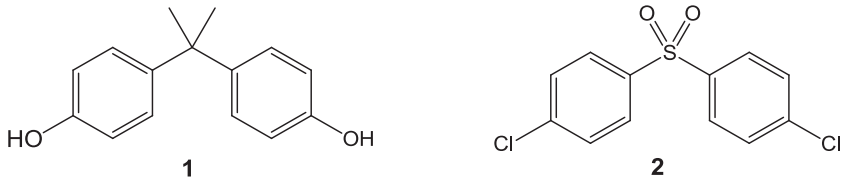

Figure 4.9 *Bisphenol A **1** and 4,4-dichlorophenyl sulfone **2** used by Wang et al. [38] in the synthesis of PSF.*

Recently, three kinds of glycopolymers described by Kee et al., [39] that is linear P**St**-*b*-P**M32** and P**St**-*co*-P**M32**, comb-like P**St**-*b*-(P**M33**-*g*-P**M32**), were synthesized by ATRP from **St**, a protected glucose derivative **M32**, and HEMA **M33** (Entries 36-39, Table 4.2). The synthesis of the comb-like glycopolymer is only described whose conditions are similar to the polymerization conditions of the first two linear copolymers. For that, a P**St**-*b*-P**M33** macroinitiator (**A24**) was synthesized by the chain extension of an already prepared P**St**-Br macroinitiator by **M33** in chlorobenzene at 80 °C using CuBr(**L3**)$_2$ followed by esterification on the free hydroxyl group of HEMA with 2-bromoisobutyryl bromide. The latter obtained macroinitiator, **A24**, was used to initiate the polymerization of the glucose protected glycomonomer **M32** in chlorobenzene at 80 °C using CuBr(**L3**)$_2$ as a catalyst to obtain a comb-like glycopolymer with a molecular weight up to 25,000 Da ($M_n/M_{n,th}$ = 0.69) and PDI = 1.43. The latter glycopolymer entered in the preparation of honeycomb-patterned films by the breath figure method. Furthermore, the preliminary studies on lectin recognition demonstrated that the glucose-containing pattern films have "specific" interactions with ConA.

More recently, Pfaff et al. [40] described the synthesis and characterization of acetylglucosamine-displaying microspheres consisting of poly(divinylbenzene) (PDVB) cores (d = 1.5 μm) onto which chains of linear and branched glycopolymer chains were grafted via ATRP and self-condensing vinyl copolymerization (SCVCP), respectively (Entry 40, Table 4.2). For this aim, a kinetic study on the SCVCP of the protected acetyl-glucosamine derived glycomonomer **M30** with **A16** as an inimer at different [**M30**]$_0$ / [**A16**]$_0$ ratios was investigated at RT in DMSO. The comonomer to catalyst ratio was constant throughout the kinetic study. Furthermore, this approach was adapted to create core-shell particles consisting of poly(divinylbenzene) (PDVB) microspheres onto which hyperbranched polymers have been grafted. Finally, deprotection of the sugar moieties via treatment with NaOMe led to acetyl-glucosamine-displaying spheres that could be easily dispersed in water and therefore

enabled the investigation of the binding behavior of these sugar-covered microspheres toward lectins (Wheat Germ Agglutinin WGA) which increased with increasing degree of branching.

4.3.2 Unprotected glycomonomers

4.3.2.1 (Meth)acrylate monomers

The first example of low polydispersity, controlled-structure sugar-based polymers prepared directly under mild conditions without recourse to protecting group chemistry was the subject of a communication by S. T. Armes et al. [41] The target monomer, 2-gluconamidoethyl methacrylate **M23**, was polymerized using three different ATRP imitators **A9**$_n$, **A10**$_n$ and **A12** in methanol, methanol/water and water solutions in combination with CuBr(**L2**)$_2$ as a catalyst at 20 °C (Entries 41-43 ,Table 4.2). Under the same conditions, the rate of polymerization was faster in aqueous solutions and the evolution of M_n was linear with conversion. However, higher polydispersities were observed as the content of water increased in the polymerization mixtures reaching 1.82 in the case of pure water. The latter phenomenon was referred to premature termination resulting from the ionic character of the catalyst in water which can reduce the efficiency of the de-activation step. The obtained polymer was chain extended with 2-(diethylamino) ethyl methacrylate **M24** in methanol to obtain a pH responsive diblock copolymer. Molecular dissolution, of the obtained diblock copolymer, was achieved in aqueous solution below pH 7 and spontaneous self-assembly occurred above this pH, forming **M24**-core micelles with an average diameter of 29 nm as judged by dynamic light scattering studies. Moreover, **A10**$_{33}$-*b*-**M23**$_{50}$ diblock copolymers formed, at around the cloud point for the PPO (**A10**$_{33}$) block, and near-monodisperse micelles of around 50 nm at 20 °C was obtained. The same work, for the same group [42,56] was extended to an unprotected lactose derived glycomonomer **M25** where they studied the ATRP homopolymerization of **M25** but this time in either *N*-Methyl-2-pyrrolidone (NMP) or methanol/water solutions since the prepared monomer was not totally soluble in methanol. Three different macroinitiators **A9**$_n$, **A10**$_n$ and **A12** were investigated for the polymerization. The summary of the results is shown in Table 4.2 (Entries 44-46). The blocking efficiency of **M25** monomer was also studied by sequential monomer addition with other methacrylates such as glycerol monomethacrylate **M26**, 2-(diethylamino) ethyl methacrylate **M24**, and **M23** in either a 3:2 methanol/water mixture or NMP. The prepared diblock copolymer **M25**$_{25}$-*b*-**M24**$_{50}$ (M_n = 17300 Da, PDI = 1.3) using **A12** as initiator showed a pH induced micellar self

assembly, similar to that described for **M23**. Finally, **A10**$_{33}$-*b*-**M25**$_{50}$ diblock copolymer exhibited a thermoresponsive behavior. It dissolved molecularly at 2 °C and was only weakly surface-active at this temperature since both blocks were well solvated. Above the cloud point of the **A10**$_{33}$ block (PPO) at approximately 15 °C, the diblock copolymer became surface-active due to adsorption of the PPO chains at the air/water interface leading to the formation of PPO-core micelles with an average diameter of 38 nm at 20 °C as observed from dynamic light scattering.

Narain [43] described a versatile new approach for the synthesis of well defined protein glycopolymer bioconjugates via ATRP technique. Where an unprotected lactose derived glycomonomer **M25** was polymerized in *N*-methyl-2-pyrrolidinone (NMP) at 20 °C using a new biotin–PEG ATRP (M_n = 5100 Da, PDI = 1.07) macroinitiator **A17** and CuBr(**L2**)$_2$ as a catalyst (Entry 47, Table 4.2). Polymers up to 24,000 Da were obtained with fairly low polydispersities (PDI ≤ 1.32). It was observed that the complexation of the biotinylated glycopolymer on streptavidin (tetrameric protein) is dependent on the molecular weights of the glycopolymers. Thus higher molecular weights biotinylated glycopolymer bind streptavidin protein at a slower rate as compared to free biotin.

The synthesis of well-defined biotinylated glycopolymers was the subject of a paper by Maynard et al. [44] Poly(methacrylate)s with pendent *N*-acetyl-D-glucosamines were prepared by polymerizing either the corresponding protected or unprotected glycomonomers, **M30** and **M31** respectively, in DMSO (23 °C) or MeOH (30 °C) using CuBr/**L9** or **L2** as catalysts in the presence of a biotinylated initiator **A18**. First, the polymerization of the protected monomer **M30** in DMSO showed from SEC traces fairly narrow molecular distributions although some tailings were detected, at low molecular weights, when high monomer to initiator ratios (50 and 100) were examined which indicated early terminations of some chains. However, the polymerization of the same monomer in MeOH using **L2** as a ligand was slower than that in DMSO where high conversion (80 %) was achieved in 90 minutes, in contrary to DMSO (15 minutes). The molecular weights increased linearly with conversion with a linear first order kinetic plots and polymers up to M_n ~ 50,000 Da with PDI ≤ 1.23 were obtained. Finally, deprotection of the obtained glycopolymers in catalytic amounts of sodium methoxide in a mixture of MeOH/$CHCl_3$ gave water soluble polymers. Similarly, the polymerization of **M31** under the same conditions in both solvents resulted as well in fairly monodisperse polymers (PDI ≤ 1.16) with molecular weights up to 70,000 Da. It

is worth noting that in both cases a deviation of the experimental molecular weights from the theoretical ones was observed with a $M_n/M_{n,th}$ reaching ~ 4 in some cases. Results of both polymerizations in DMSO for a $[M]_0/[\mathbf{A18}]_0$ = 50 are summarized in Table 4.2 (Entries 48 and 49). The ability of the obtained biotinylated glycopolymers to interact with streptavidin was studied using surface plasmon resonance measurements (SPR) and ^{1}H-NMR where absence of the biotin end group in the ^{1}H NMR spectrum was detected.

Mateescu et al. [57] described the direct synthesis of well defined sugar methacrylate-based homopolymer brushes with high grafting densities based on D-gluconamidoethyl methacrylate **M23** and 2-lactobionamidoethyl methacrylate **M25** from functionalized gold substrates in aqueous and methanol/aqueous solutions and by the use of CuBr(**L2**)$_2$ as a catalyst. An early termination of the polymerization was observed in aqueous medium due to side reactions which are frequent at high radical concentrations. The surface roughness found by AFM was below 1 nm suggesting the preparation of very smooth glycopolymer films. Finally, the synthesized glycopolymer films exhibited strong binding interactions with specific lectins (Con A and RCA_{120}).

Qiu et al. [45] synthesized star-shaped polypeptide/glycopolymer biohybrids composed of L-glutamate monomer **M62** and **M23** (Scheme 4.1). For this aim, P**M62** was synthesized by ring opening polymerization (ROP) using a tetra-amine derived initiator **I7**. The obtained polymer was transformed into a macro ATRP initiator that was used in the polymerization of **M23** in *N*-methyl-2-pyrrolidone at RT to afford after 64 % conversion a 4-arm star with a M_n = 80,000 Da and PDI = 1.26 (Entry 50, Table 4.2). These biohybrids self-assembled into large spherical micelles (in aqueous solution), which had a helical polypeptide core surrounded by a multivalent glycopolymer shell. Furthermore, deprotection of the polypeptide chains showed a pH sensitive self assembly behavior as well.

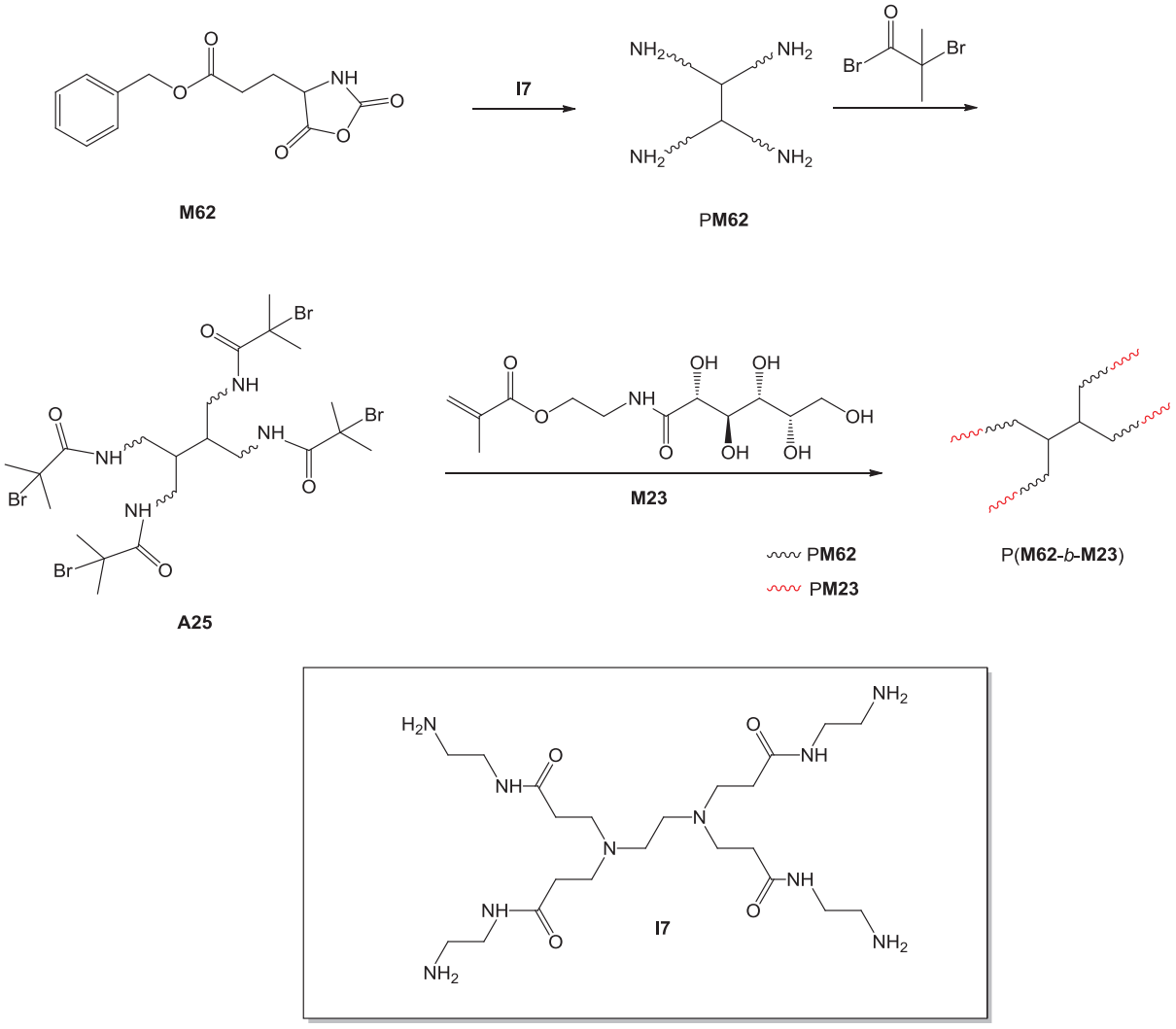

Scheme 4.1 *Synthetic strategy used by Qui et al.* [45] *for the synthesis of arm stars biohybrids.*

Vazquez-Dorbatt et al. [46] described the synthesis of a pyridyl disulfide end-functionalized polymer with *N*-acetyl-D-glucosamine pendant side chains. The polymerization of the unprotected glycomonomer **M31** was conducted in a MeOH/H_2O (3:1) mixture at 30 °C for 90 minutes in the presence of a disulfide derived chain transfer agent **A26** and a fairly monodisperse polymer (PDI =1.12) up to 10,000 Da was obtained (Entry 51, Table 4.2). The glycopolymer was conjugated to a double-stranded short interfering RNA and the resulting conjugate was characterized by electrophoresis which showed up to 97% conjugation of the glycopolymer. Finally, surface micro-patterning of this glycopolymer on gold was also achieved through micro-contact printing.

Leon et al. [47] reported the synthesis of amphiphilic glycopolymers in DMF. For this aim, an unprotected methacrylate derived glycomonomer **M63** was homopolymerized in the

presence of a mono (**A1**) and bi functional (**A27**) initiators, at 40 and 50 °C respectively. Moreover, mono and bifunctional P**M63** macroinitiators were used to synthesize the amphiphilic di and triblock glycopolymers with n-butyl acrylate **M47** in DMF at 90 °C. As a result, fairly monodisperse block copolymers (PDI < 1.4) with good to excellent control over molecular weight ($0.87 \leq M_n/M_{n,th} \leq 0.98$) were obtained (Entries 52-55, Table 4.2). What is more, the self-assembly of these glycopolymers in distilled water and in 0.1 M NaCl solutions was studied by dynamic light scattering and their interaction with Con A lectin was examined, demonstrating the influence of molecular weight and copolymer composition. In addition, recently the same group [48] took the advantage of the fact that these type of di-block copolymers are capable of forming micelles in aqueous solution in order to use them as polymeric surfactants (without the addition of a co-surfactant) in the emulsion polymerization of butyl methacrylate in order to prepare glycosylated polymer particles. For that aim, diblock copolymers based on **M63** and n-butyl methacrylate **M46** were prepared in the same conditions described above to afford polymers with molecular weights up to 32,000 Da with a good control over molecular weight (Entry 56, Table 4.2). From these glycosylated particles, polymer films were prepared, demonstrating by fluorescence microscopy and spectroscopy that the polymer surface is functionalized in carbohydrate moieties which can specifically interact with ConA.

Yang et al. [58] synthesized linear and comb-like glycopolymers, grafted to poly(ethylene terephthalate) (PET), based on an unprotected lactose glycomonomer in water or *N*-methyl-2-pyrrolidone (NMP) at RT by surface-initiated atom transfer radical polymerization (unfortunately no results shown in this study). Thus, a bromoalkyl initiator was directly immobilized onto PET membrane surface, and the ATRP of the corresponding glycomonomer **M25** was then carried out to yield the grafted linear glycopolymer. The synthesis of the comblike glycopolymer was achieved in a similar manner to that of the linear glycopolymer (Scheme 4.2).

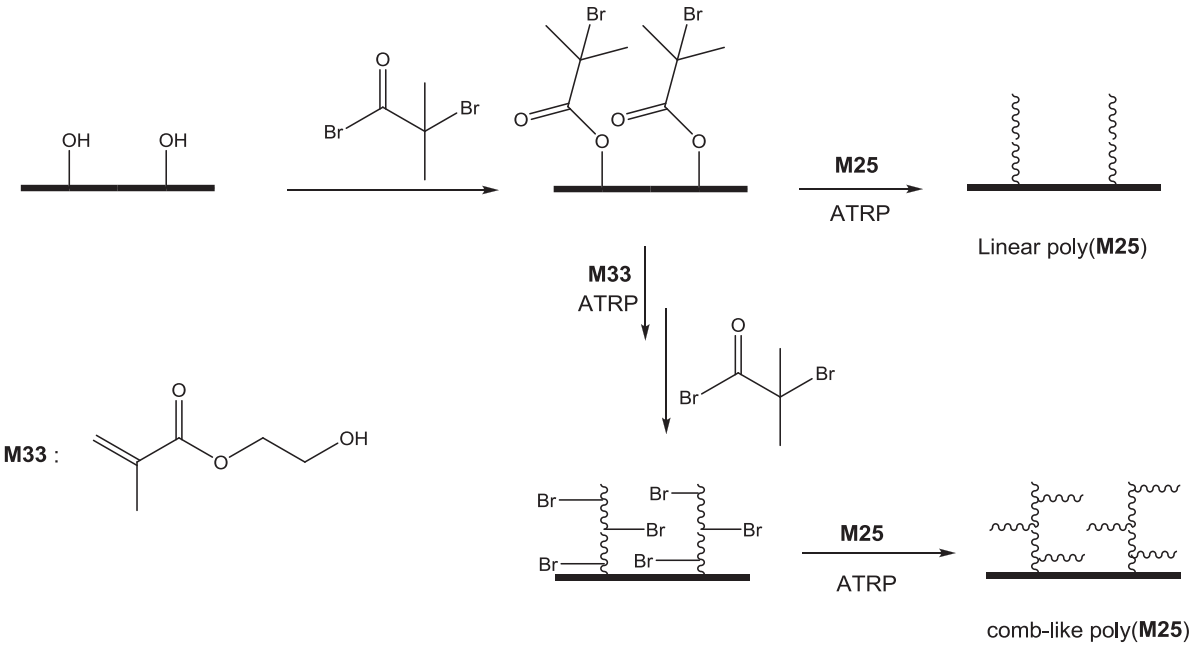

Scheme 4.2 *Schematic representation for the grafting of linear and comblike P**M25** on track-etched poly(ethylene terephthalate) membranes described by Q. Yang et al.* [58]

As shown from their study, compared with water NMP is a less polar solvent and showed a slow ATRP rate even with a much higher monomer concentration, which was 3-fold that in water. The polymer layer thickness and structure were evaluated by dry layer thickness and hydrodynamic layer thickness measurements making use of the well-defined cylinder pores of the PET track-etched membranes. Moreover, the comb-like polymer layer showed a very large increase in dry layer thickness after grafting of the P**M25** branches to the P**M33** main chains which could be ascribed to the obstruction of the collapse of the chains due to the steric hindrance by and among the side branches. Finally, both linear and branched P**M25** grafted PET membranes were then used for lectin binding (peanut agglutinin lectin) studies.

4.3.2.2 (Meth)acrylamide monomers

Yu et al. [49] prepared three novel unprotected monomers containing mannose **M64**, galactose **M65**, and glucose **M66** and studied their homopolymerizations by surface initiated ATRP (SI-ATRP) on silica wafers in order to obtain homo-glycopolymeric brushes. The best results of the homopolymerizations of the unprotected monomers were conducted in water (for 24 hours at RT) using CuCl(**L9**)$_2$ as a catalyst and a silicon wafer modified with ester-based ATRP initiator **A28** as a substrate for this study to yield polymer with PDI = 1.5 and M_n = 51,000 Da (Entry 57, Table 4.2). It is noteworthy, that the thickness of glycopolymeric

brushes prepared in the mixed solvent DMF/H_2O (6.6 nm) was much lower than those prepared in H_2O (24 nm). Whereas using a DMSO/H_2O mixture gave higher PDI = 3.6. Finally, the glycopolymer brushes showed ultralow protein adsorption from bovine serum albumin (BSA) and fibrinogen (Fb) solutions and retained specific protein interactions, as evident from the interaction with ConA.

4.3.3 Glycopolymers from the post-polymerization approach

Haddleton and coworkers [50] prepared a novel series of comb sugar polymers by combining both click chemistry and ATRP. First, alkyne side chain functional polymers were prepared by homo or copolymerization of trimethylsilyl methacrylate **M28** with MMA **M15** or $mPEG_{300}MA$ **M29** in toluene at 70 °C in the presence of CuBr(**L7**)$_2$ as a catalyst and *O*-Benzyl α-bromoester **A13** as an initiator (Entries 58-60, Table 4.2). The kinetic results showed first order plots with an increase of the molecular weight with conversion and polymers with molar masses up to 15,000 Da were obtained with fairly low polydispersities (PDI < 1.16). What followed was a deprotection of the silyl groups, as confirmed by NMR, in the presence of TBAF and acetic acid in THF proceeded by grafting a number of protected and unprotected carbohydrates **3-7** (Figure 4.10) through their C-6 or anomeric azide (α or β) onto these polymers by Cu(I)-catalyzed "click chemistry". The latter, resulted in a number of mannose- and galactose-containing multidentate ligands for lectin binding studies that only differ in their epitope density. The theoretical masses of the new obtained polymers matched the experimental ones obtained from SEC.

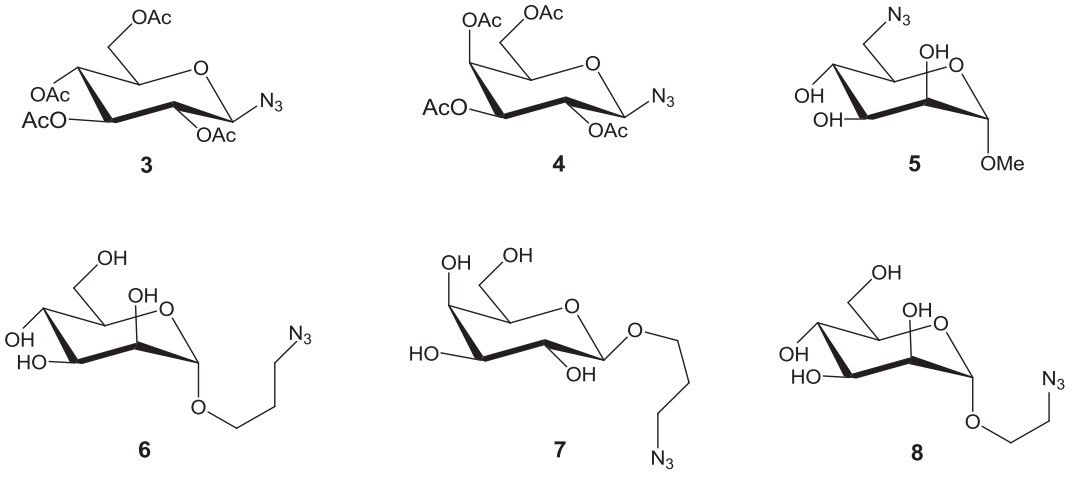

Figure 4.10 *Azido sugars used by Haddleton et al.* [50] *in their click chemistry reactions.*

The same group [51] also studied the synthesis of well-defined neoglycopolymer-protein biohybrid materials and their ability of binding mammalian lectins and inducing immunological function. For that aim, two synthetic pathways were followed for the synthesis of the glycopolymers based on azido sugar **8**. First path based on the homopolymerization of an unprotected glycomonomer **M67** (obtained by click chemistry of **8**) in a MeOH/H_2O 5:2 (v/v) mixture at RT using a protected maleimide initiator **A29**. Quite low polydisperse polymer (PDI = 1.20) was obtained with a molecular weight of 26,000 Da (Entry 61, Table 4.2). The second path was based on the homopolymerization of **M28** using **A29** in toluene at 30 °C followed by clicking the azido sugar **8** to the polymeric backbone after the removal of the silyl group. Moreover, visibly fluorescent tag based on rhodamine B dye was introduced onto the polymers backbone in order to facilitate characterization of the relative protein conjugates. In the polymerization steps, the first-order kinetic plots showed some deviation from linearity, yet M_n increased linearly with monomer conversion and narrow molecular weight distributions were obtained. Deprotection of the maleimide moiety afforded the expected maleimide-terminated glycopolymer. Finally, the conjugation of the obtained glycopolymer with BSA (Bovine Serum Albumin) through the maleimide group afforded a glycoprotein (Scheme 4.3), where a significant and dose-dependent binding of a mannose-binding lectin to the BSA-neoglycopolymer conjugates was clearly revealed by surface plasmon resonance.

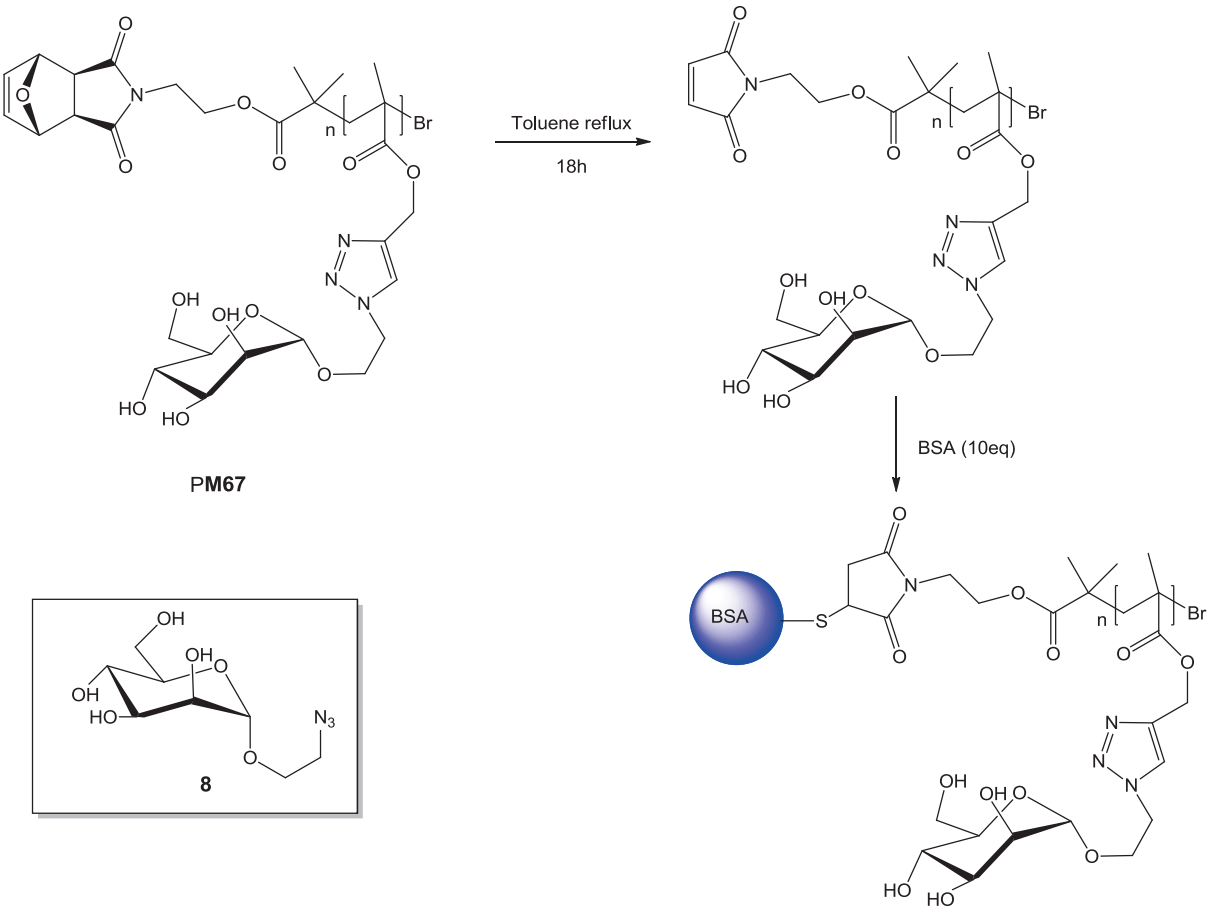

Scheme 4.3 *Schematic representation for the conjugation of a glycopolymer with BSA as described by Haddleton and coworkers.* [51]

4.4 Well defined glycopolymers from RAFT Polymerization

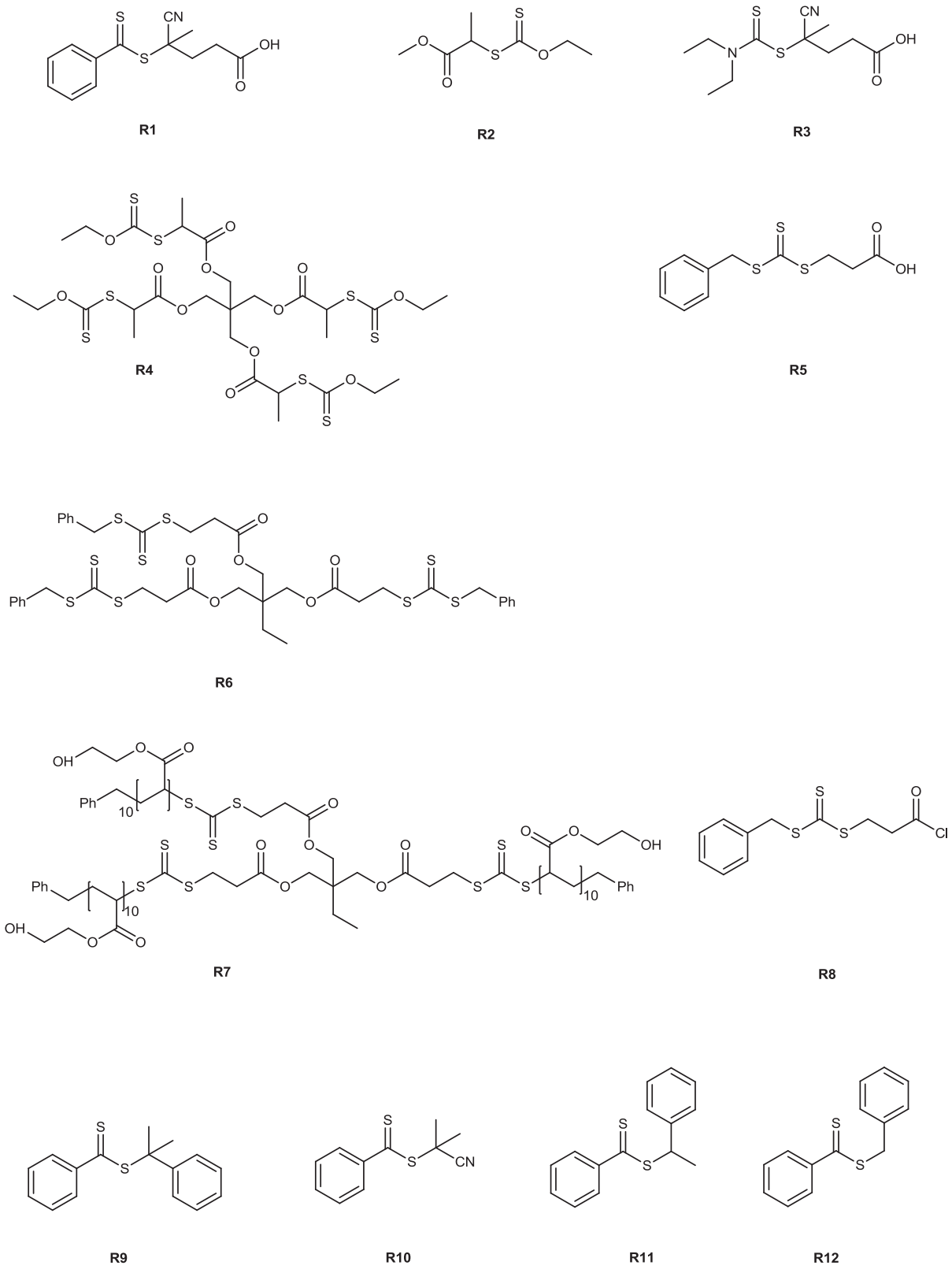

Figure 4.11 *RAFT agents involved the synthesis of well defined glycopolymers.*

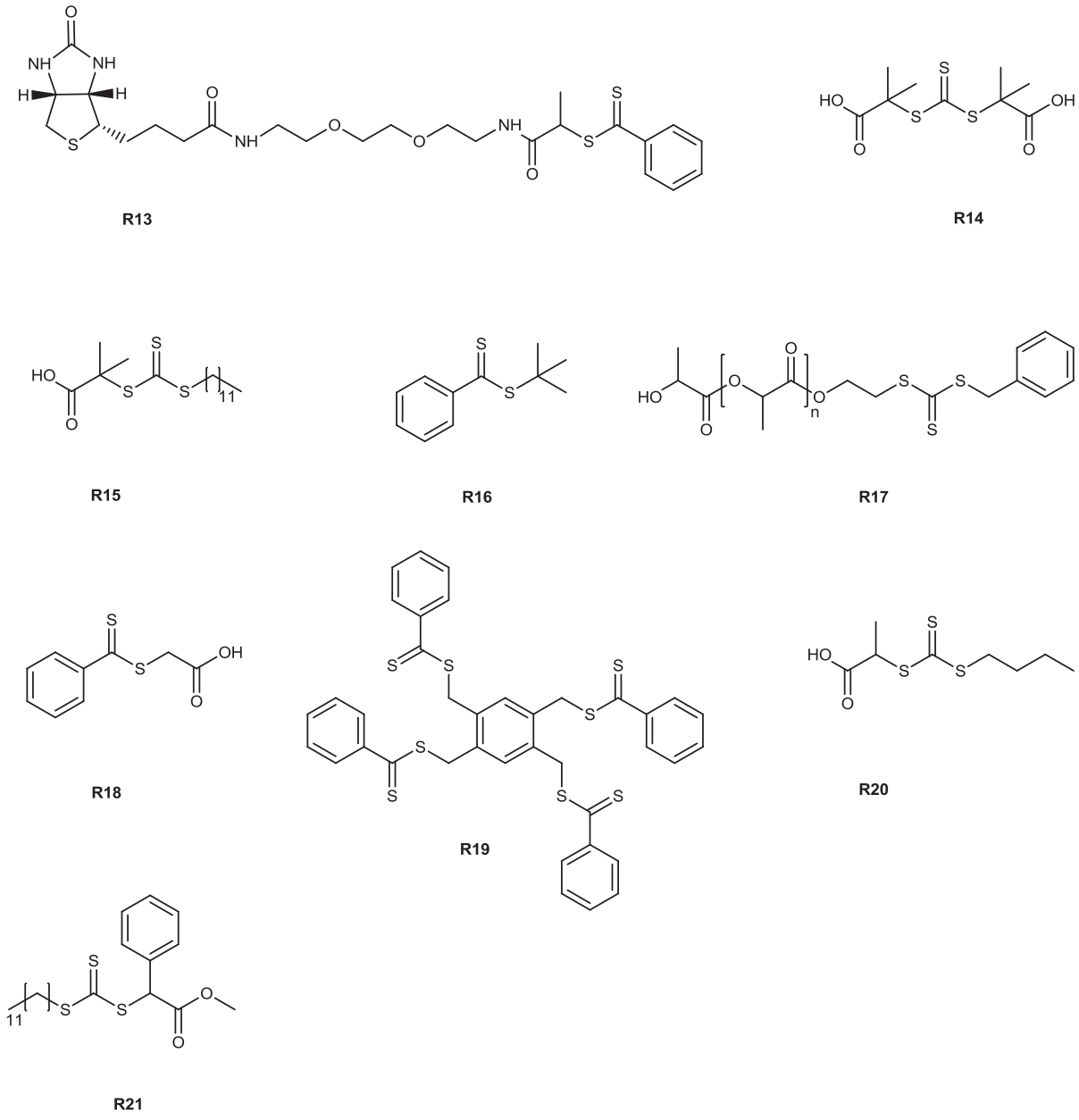

Figure 4.11 *Continued.*

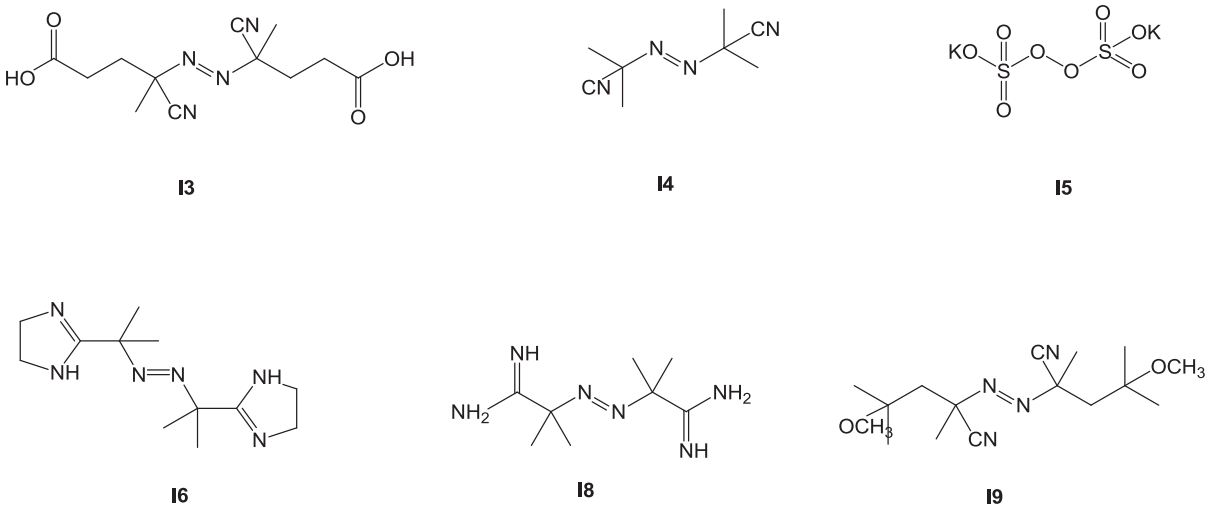

Figure 4.12 *Initiators used in RAFT polymerizations.*

Table 4.3 *Summary of Reversible Addition Fragmentation-chain Transfer (RAFT) polymerization experiments described in literature.*

Entry	Monomer (s)	Control agent	Initiator	M_n ($\times 10^{-3}$)	M_n / $M_{n,th}$ [a]	Conv. %	PDI	Structure [b]	Ref.
1	**M34**	R1	I3	27.4	1.3	70	1.03	homop.	13c
2	**M34**	R1	I3	14.2	1.2	40	1.07	homop.	13c
3	**M34**	P**M34** [c]	I3	34	0.92	-	1.54	Block AB	13c
4	**M35**	P**M34** [c]	I3	37	-	-	1.63	Block AB	13c
5 [d]	**M36**	R1	I3	327	12.5	97	3.67	homop.	59
6 [e]	**M36**	R1	I3	174	6.6	99	1.75	homop.	59
7 [f]	**M36**	R1	I3	26.3	0.93	100	1.14	homop.	59
8	**M34**	P**M36**$_{67}$ [c]	I3	52	0.82	71	1.2	Block AB	60
9	**M37**	P**M34**$_{116}$ [c]	I3	61.3	0.75	52	1.16	Block AB	60
10	**M33**	P**M36**$_{83}$ [c]	I3	45	-	-	1.2	Block AB	61
11	**M38**	R1	I3	24	1.01	80	1.09	homop.	62
12	**M23**	R14	I3	14	-	95	1.19	homop.	63
13	**M25**	R15	I3	24.7	-	95	1.22	homop.	63
14	**M40**	R2	I3	17.1	-	14	1.1	homop.	13a
15	**M40**	R3	I3	19.6	-	27	1.19	homop.	13a
16	**M40**	R4	I3	59.7	1.02	68	1.52	4-arm star	64
17	**M41**	R5 [g]	I3	100.8	1.20	89	1.26	homop.	65
18	**M41**	R5 [h]	I3	6.6	1.40	19	1.15	homop.	65
19	**M42**	P**M41**$_{180}$ [c]	I3	88.4	1.07	88	-	Block AB	65
20	**M41**	R7	I3	72.2	1.22	40	1.21	3-arm star	65
21	**M69**	R1	I3	8.9	0.82	93	1.18	homop.	66
22	**M70**	R1	I3	18.2	0.96	78	1.20	homop.	66
23	**M55**	P**M70**$_{46}$ [c]	I3	19.1	1.26	-	1.39	Block AB	66
24	**M76**	R18	I8	44	-	85	1.3	homop.	67
25	**M76/M75**	R18	I8	9.3	-	82	1.5	A-*co*-B	67
26	**M77/M75**	R18	I8	8.6	-	19	1.5	A-*co*-B	67

27	**M80/M75**	R18	I8	210	-	67	1.0	A-*co*-B	68
28	**M81/M75**	R18	I8	73	-	81	1.7	A-*co*-B	68
29	**M80/M81 /M75**	R18	I8	7.6	-	16	1.4	A-*co*-B-*co*-C	68
30	**M84**	R21	I4	13.5	2.14	79	1.3	homop.	69
31	**St**	$PM84_{23}$[c]	I3	38.5	1.63	83	1.65	Particle	69
32	**St**	$PM84_{23}$[c]	I3	660	-	81	1.33	Cross-linked particle	69
33	**M85**	R5	I3	113	-	85	1.08	homop.	70
34	**M86**	R5	I3	37	-	50	1.35	homop.	70
35	**M86**	R5	I9	56	-	75	1.15	homop.	70
36	**M43**	R9	I4	6.29	0.87	31	1.09	homop.	71
37	**M20**	R9	I4	13.9	-	75	1.2	homop.	72
38	**M20**	R10	I4	12.3	-	-	1.18	homop.	72
39	**M44**	PM20[c]	I4	16.3	-	-	1.2	Block AB	72
40	**M13**	R11	I5	213	17.8	90	1.9	homop.	73
41	**M13**	R11	I4	313	64	60	1.58	homop.	73
42	**M13**	R10	I5	20.9	4.01	30	1.32	homop.	73
43	**M13**	R9	I5	27.7	2.64	99	1.10	homop.	73
44	**M45**	R9	I5	41.2	2.48	91	1.25	homop.	73
45	**M74**	R17	I4	52	0.71	73	1.20	Block AB	74
46	**M13**	$\mathbf{PM79}_{18}$[c]	I3	7.0	-	-	1.19	Block AB	75
47	**M48**	R10	I4	11.6	0.88	60	1.34	homop.	76
48	**M48/M42**	R10	I4	20.5[i]	-	80	1.69[i]	A-*co*-B	76
49	**M49/M42**	R10	I4	18.7[i]	-	65	1.29[i]	A-*co*-B	76
50	**M48**	**PM42**[a]	I4	15.7	-	-	1.57	Block AB	76
51	**M49**	**PM42**[a]	I4	27	-	-	1.69	Block AB	76
52	**M52/M53**	R13	I4	17	-	80	~1.5	A-*co*-B	77
53	**M53/M60**	R13	I4	53.7	0.91	85	1.60	A-*co*-B	78
54	**M53/M61**	R13	I4	12.7	1.26	73	1.20	A-*co*-B	78
55	**M53/M60**	R16	I4	62.3	1.02	93	1.46	A-*co*-B	78
56	**M53/M61**	R16	I4	9.7	1.21	83	1.14	A-*co*-B	78

57	**M50**	R11	I4	27	≅ 0.6	85	1.1	homop.	79
58	**M51**	R12	I4	5.2	-	60	1.11	homop.	80
59	**St**	P**M51**[a]	I4	16.3	-	-	1.35	Block AB	80
60	**M68**	R5	I4	2.8	0.84	-	1.20	homop.	81
61	**M54**	R1	I6	33	0.98	47	1.05	homop.	82
62	**M55**	R1	I3	15	1.3	31	1.08	homop.	82
63	**M56**	P**M54**[a]	I3	48.4	0.85	33	1.05	Block AB	82
64	**M57/M58**	R5	I4	10	0.91	-	1.12	A-*co*-B	83
65	**M57/M59**	R5	I4	11	0.88	-	1.14	A-*co*-B	83
66	**M58**	R19	-	51.4	0.49	85	-	4-arm star	84
67	**M78**	R5	I3	51.5	-	-	1.16	homop.	85
68	**M42**	P**M78**[a]	I4	32.4	-	-	1.12	Block AB	85
69	**M82**	R10	I4	15.4	-	25	11.8	Highly branched	86
70	**M82/M83**	R20	I4	29	-	93	1.9	Highly branched	86

a: degree of control where $M_{n,\,th}$ is the theoretical targeted molar mass, b: homop. stands for homopolymer, c: macroRAFT agent, d: 0.1M Na_2CO_3, e: 0.1M $NaHCO_3$, f: 10 % EtOH, g: $[R5]_0$ =1.78 mM; 7h, h: $[R5]_0$=7.14 mM; 8h, i: for deprotected copolymer.

4.4.1 Unprotected glycomonomers

4.4.1.1 (Meth)acrylate monomers

One of the first reports on the synthesis of glycopolymers by RAFT technique was published by McCormick's group. [13c] Notably, the authors directly polymerized an unprotected glucoside glycomonomer **M34** in basic medium in the presence of **R1** as the chain transfer agent and **I3** as an initiator at 70 °C (Entries 1-2, Table 4.3). The polymerization evolved in a pseudo first order kinetics, without an induction period, and displayed the characteristics of a reversible-deactivation polymerization although deviations from the theoretical M_w were observed at higher conversions (70 %). The prepared macroRAFT agent resulting from the homopolymerization of **M34** was also used for both self blocking experiment and chain extension with a methacrylate derivative **M35** (a sulfono methacrylate) to afford block copolymers with a quite agreement between the experimental M_n and its theoretical value and final PDIs of 1.54 and 1.63 (Entries 3-4, Table 4.3).

Albertin et al. [59] investigated the RAFT polymerization of another glucoside derived methacrylate **M36** with same RAFT agent **R1** used by McCormick at al. [13c] Three different conditions were used for the polymerizations at 70 °C, either Na_2CO_3 (0.1 M) or $NaHCO_3$ (0.1 M) or 10 % EtOH was used in order to increase the solubility of the RAFT agent (Entries 5-7, Table 4.3). The substitution of base by EtOH reduced the possibility of degrading the RAFT agent throughout the polymerization as seen earlier by the group of McCormick [13c] and confirmed by Albertin et al. in this paper; where monommodal distributions (PDI = 1.14) together with a good control over molecular weight ($M_n/M_{n,th}$ = 0.93) were observed at high conversions (100 %) contrary to earlier trials conducted in basic conditions [13c,59]. On the other hand, by increasing the pH longer induction periods with slower polymerization rates were observed, a result contrary to that obtained McCormick et al. [13c] where no induction period was observed.

In order to show the reversible-deactivation character of the macroRAFT agent obtained from the polymerization of **M36**, two block copolymers were synthesized either by the use of an another glucoside derived methacrylate **M34** [60] or by the use of 2-hydroxyethyl methacrylate **M33** (Entries 8 and10, Table 4.3). [61] The polymerizations were conducted in a mixture of H_2O/EtOH at 70 and 60 °C respectively in the presence of **I3** as an initiator. The kinetics for the two chain extensions showed first order plots with slight deviation from the targeted molar masses ($M_n/M_{n,th}$ ~ 0.82) and fairly monodisperse polymers (PDI = 1.2) were obtained.

Moreover, the same polymerization condition (H_2O/EtOH at 70 °C) has been adopted for the homopolymerization of **M34** [60] (same monomer used by McCormick at al.) [13c] and the obtained macro-RAFT agent has been used for the chain extension of an unprotected mannoside derivative **M37**. The chain extension was fairly controlled ($M_n/M_{n,th}$ = 0.75) with a monomodal distribution and a polymer with PDI = 1.16 was obtained (Entry 9, Table 4.3). However, the kinetics of this copolymerization was slower than that observed with the chain extension of P**M36** with **M34** and that was attributed by the authors to the steric hindrance around the propagating radicals at C6. A detailed study on the polymerization of **M34** using **R1** in various polymerization conditions is reported by Albertin et al. [87] In their paper, they examined the effect of temperature, oxygen, CTA and initiator concentration, and the molar mass of the CTA radical leaving group on the kinetic of polymerization.

Spain et al. [62] synthesized glycopolymers based on a galactose glycomonomer **M38** that strongly bound to β-galactosyl specific lectin peanut agglutinin (PNA). First, the polymerization of **M38** was conducted in an aqueous ethanol solution (H_2O:EtOH / 9:1) using **R1** as the control agent and **I3** as an initiator at 70 °C and a monodisperse polymer (PDI = 1.09) with an excellent control over molecular weight ($M_n/M_{n,th}$ = 1.01) was obtained (Entry 11, Table 4.3). The polymerization displayed pseudo first order kinetics, following a short induction period. Adding, the glycopolymer-stabilized gold nanoparticles were synthesized directly by addition of $NaBH_4$ to an aqueous solution of P**M38** and $HAuCl_4$. The biological activity of the obtained nanoparticles was demonstrated using an extremely facile visual method involving the agglomeration of peanut agglutinin (PNA)-coated agarose beads.

Stenzel et al. [88] studied the polymerization of a mannose derived glycomonomer **M39**, synthesized by an enzymatic approach, by the method described by Albertin et al. (H_2O/EtOH, 70 °C) in the presence of **R1** and **I3** as the RAFT agent and initiator, respectively. Polymers with different degrees of polymerizations (DP_n: 100, 200 and 300) were synthesized whose kinetic plots showed first order kinetics with monomodal distributions and PDIs lower than 1.14. Longer induction periods have been observed with DP_n increase. The authors suggested, after studying the interaction of the obtained polymers with ConA (an α-D-mannopyranosides specific lectin), that linking the mannose to the polymer backbone via the 6-carbon position of the mannopyranoside has altered the activity of the mannose and therefore the resulting glycopolymer.

After reporting the polymerization of **M23** and **M25** glycomonomers by ATRP, [41] Narain et al. [63] also tried their RAFT polymerization in a DMF (or MeOH)/H_2O mixture at 60 °C in the aim of synthesizing gold nanoparticles. Two RAFT agents **R14** and **R15** were used (Entries 12-13, Table 4.3). Fairly monodisperse polymers (PDIs ≤ 1.22) with M_n up to 25,000 Da were obtained at high conversions. It is worth noting that conducting the polymerization in water alone led to loss in control of molecular weight most probably due to solubility problems of the RAFT agents. Besides, stable multifunctional glyconanoparticles were synthesized in the presence of varying amounts of biotinylated-polyethyleneglycol having terminal thiol groups (*bio*-PEG-SH) whose aggregation in the presence of streptavidin was studied by UV-vis spectroscopy.

4.4.1.2 Vinyl ester monomers

One of the first examples of a narrow-polydispersity, poly(vinyl ester)-like glycopolymer was the subject of a paper by Albertin et al. [13a] After the synthesis of a glucoside derivative bearing the vinyl ester group **M40** via an enzymatic approach, it was homopolymerized at 60 °C for 48 hours in the presence of **I3** as an initiator and by the use of either xanthate **R2** (in MeOH) or dithiocarbamate **R3** (in basic pH) as chain transfer agents. Due to the little bulkiness and high reactivity of the propagating radicals of vinyl esters, the two RAFT agents were chosen with destabilizing *Z* groups in order to enhance the hemolytic cleavage of the leaving group. Polymers with fairly polydispersities (PDI ≤ 1.19) and M_n up to 20,000 Da were obtained (Entries 14-15, Table 4.3). It is worth noting that higher conversions in water were obtained after 48 hours. The same group [64] used the same monomer **M40** in the synthesis of star glycopolymers in the presence of a tetrafunctional xanthate like RAFT agent **R4** in dimethyl acetamide (to better solubilize the RAFT agent) at 70 °C for 24 hours and in the presence of **I3** as an intiator. By comparing with the same polymerization of **M40** using **R2** in MeOH at 60 °C, [13a] the kinetics seemed to be faster with higher conversions being obtained (35 % in 4 hours). However, the polymerization in DMAc was less controlled (non monomodal distributions, higher PDIs and non linear increase of molecular weights with conversion) as shown in Table 4.3 (Entry 16).

4.4.1.3 (Meth)acrylamide monomers

Stenzel et al. [65] studied the polymerization of an acrylamide derived glucosamine **M41** in aqueous medium (H_2O:EtOH / 5:1) at 60 °C in the presence of **I3** as an initiator. Two trithiocarbonate RAFT agents, **R5** and **R6**, were used for polymerizations. Once using **R5**, homopolymers of **M41** together with thermosensitive copolymers based on *N*-isopropylacrylamide (NIPAAm) **M42** were synthesized. Different trials on the homopolymerization of **M41** showed that, by increasing the amount of RAFT agent in the polymerization mixture longer inhibition periods (up to 3 hours with the highest concentration of RAFT agent) were observed together with a decrease in the rate of polymerization and a deviation from the targeted molecular weights (Entries 17-18, Table 4.3). The kinetic study showed, from SEC, dead chains at low molecular weights with PDIs inferior to 1.3 (final samples). In addition, the prepared macroRAFT agent was chain extended with NIPAAm **M42** in order to obtain thermoresponsive copolymers (Entry 19, Table 4.3). In order to

overcome the water solubility problem of P**M42** at 60 °C the copolymerization was conducted in a DMSO/H_2O mixture (1:1, v / v). From the kinetic study, non quantitative initiation of the macroRAFT agent was observed due to tailings seen from SEC, together with termination by coupling at high molecular weights. Finally, they investigated the possibility to generate 3-arm Poly**M41** stars from a Z-designed trifunctional RAFT agent **R7** derived from **R6** (since it is not water soluble). The prepared RAFT agent **R7** was used for the homopolymerization of **M41** in a H_2O/EtOH (5:1, v / v) mixture at 60 °C (Entry 20, Table 4.3). The homopolymerization evolved without an inhibition period, contrary to what was seen when using **R5**, and similar kinetics were observed for different DP_n which indicated the independency of the concentration of RAFT agent on the kinetics. Fairly monodisperse polymer (PDI = 1.21) with a good control over molecular weight was obtained ($M_n/M_{n,th}$ = 1.22) at low monomer to CTA ratio. However, at high $[\mathbf{M41}]_0$ / $[\mathbf{R7}]_0$ (400) ratios, loss of control at high conversions was seen due to the increasing steric congestion (around the RAFT groups) inherent to this strategy.

The same monomers **M41** and **M42** were used by the same group in order to modify silica wafers by homo-glycopolymers and thermosensitive copolymers. [89] In the aim of obtaining molecular brushes, the RAFT agent **R8** was immobilized on an amine modified silica surface (Scheme 4.4). Few quantity of **R5** was added to the polymerization mixture in order to limit termination reactions. The kinetics of the homopolymerization of **M41 (**in H_2O/EtOH 5:1 at 60 °C; DP_n = 200) evolved similarly to that described before with 65 % conversion in 6 hours. [65] After obtaining a macro-brush-RAFT agent, it was chain extended with **M42** in order to obtain thermoresponsive copolymers. Despite of the steric effect of the Z group of the macro-RAFT agent the copolymerization proceeded similarly to the homopolymerization of **M42** alone with an increase of molecular weight with conversion. Finally, contact angle measurement confirmed that the second block was built in between the first block and the silicon surface.

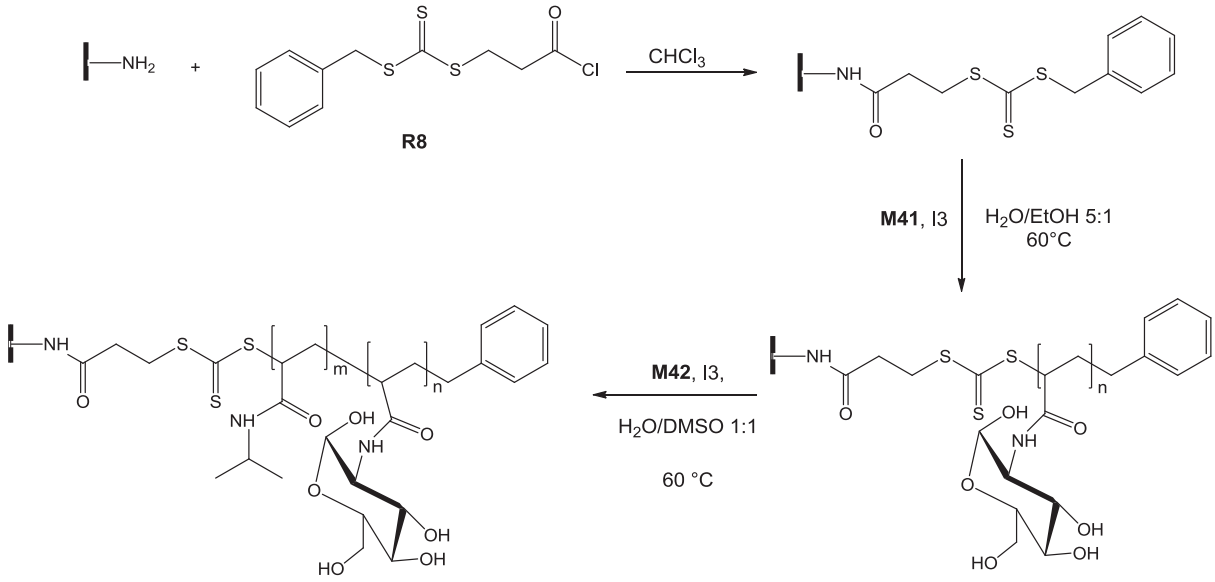

Scheme 4.4 *Immobilization of the RAFT agent on a silica wafer followed by the synthesis of thermo-responsive copolymers as described by Stenzel et al.* [89]

Narain et al. [66] described the synthesis and the homo/copolymerizations of two unprotected methacrylamide glycomonomers **M69** and **M70**. The homopolymerizations were conducted in a H_2O/DMF mixture (14 % in DMF for **M69** and 20 % for **M70**) at 70 °C in the presence of **R1** as the RAFT agent (Entries 1-2, Table 4.3). An induction period was observed for the two homopolymerizations with a linear evolution of M_n with conversion, with first order kinetic plots, and monomodal distributions. Good to excellent control over molecular weights ($0.82 \leq M_n/M_{n,th} \leq 0.96$) with fairly monodisperse polymers (PDI $\leq$ 1.2) were obtained. Furthermore, the synthesized macroRAFT agents were chain extended by three different monomers **M55**, **M71** and **M72** in aqueous and acidic solutions (for **M72** at pH 4) at 70-80 °C and fairly monodisperse polymers were obtained (PDI < 1.4) with quite agreement between theoretical and experimental molecular weights ($M_n/M_{n,th}$ = 1.26). From SEC, tailing to low molecular weight distributions was observed in all copolymerizations and that was attributed by the authors to the hydrolysis of the macroRAFT agent. Moreover, the complexation of the cationic glyco-copolymers with plasmid DNA revealed the formation of well defined nanostructures. Finally, toxicity studies at cellular level showed that the glycopolymers and glyco-copolymers were nontoxic at a concentration range 2-6 μM. The same group, [90] successfully modified quantum dots (QDs) containing surface carboxylic groups with biotinylated glycopolymers via a carbodiimide coupling. For that aim, statistical copolymers based on **M69**, **M71** and a biotinylated methacrylamide **M73** was synthesized by

RAFT polymerization in the presence of **R14** in water at 70 °C. What followed was the activation of the QDs with EDAC (1-ethyl-3-(3-dimethylaminopropyl) carbodiimide) and its coupling with the statistical copolymer in order to obtain surface functionalized QDs with sugar and biotin moieties that showed excellent optical properties and colloidal stability compared to those of the original QDs at whole pH conditions.

M. Toyoshima et al. [67] synthesized sugar decorated gold nanoparticles. For this aim, homo and copolymers (with acrylamide **M75**) of two unprotected acrylamide glycomonomers bearing a mannose and glucosamine units, **M76** and **M77** respectively, were synthesized at 60 °C in the presence of a dithiobenzoate RAFT agent **R18** in a DMSO/H_2O mixture (Entries 24-26, Table 4.3). Partial hydrolysis of the RAFT agent was observed using these reaction conditions which affected both the control over molecular weight and the molecular weight distributions (PDI ≤ 1.5). The thiol-terminated glycopolymers, obtained from reduction with $NaBH_4$, were mixed with gold nanoparticles to yield the glycopolymer substituted gold nanoparticles with various diameters (15-100 nm) which showed specific interaction in the presence of lectins; ORN178 (α-Man binding strain) and ORN208 (a mutant strain without α-Man binding ability) from *E. Coli*.

Miura et al. [68] investigated the synthesis and biological properties of glycosaminoglycans mimic polymers for A*β* (amyloid β-protein). To this end, copolymers bearing unprotected charged glycomonomers, 6-sulfo-GlcNAc **M80** and glucuronic acid **M81**, with acrylamide **M75** were synthesized in a water/DMSO mixture at 60 °C in the presence of **R18** as the control agent (Entries 27-29, Table 4.3). Copolymers up to 200, 000 Da were obtained with fairly low polydispersities in some cases (1.4 ≤ PDI ≤ 1.7) with an exception of the copolymer P(**M80**-*co*-**M75**) whose PDI = 1.0, as claimed by the authors. The interactions of A*β*(140) with glycopolymers were analyzed by inhibition activity of protein aggregation using ThT (Thioflavin T) fluorescence assay, atomic force microscopy observation, and CD (Circular Dichroism) spectra. As a result, glycopolymers carrying **M80** showed inhibition activity toward A*β* aggregate, and those with both **M80** and **M81** showed the strongest inhibition activity.

The one-pot synthesis of glycopolymers by RAFT mediated *ab* initio emulsion polymerization, employing a surface active glucose based RAFT*stab* (reversible addition-fragmentation chain transfer colloidal stabilizer) was described by Stenzel et al. [69] First, homopolymerization of a glucosamine derived acrylamide **M84** was conducted in DMAc

(*N,N*-dimethylacetamide) at 70 °C using **R21** for RAFT*stab* synthesis (Entry 30, Table 4.3). Fairly polydisperse polymer (PDI = 1.3) with a deviation from the targeted molecular weight ($M_n/M_{n,th}$ = 2.14) was attained. The macroRAFT*stab* was used for the emulsion polymerization of styrene with and without a disulfide derived crosslinker. The polymerizations were conducted in water at 80 °C above the critical micelle concentration (CMC > 14.5mM) of the macroRAFT agent. Moreover, SEC analysis reflected an increase in M_w with increasing conversion with tailings toward low molecular weights. What is more, TEM images showed that spherical particles were obtained both with and without the crosslinker. However, the particle size distribution appeared to be somewhat less uniform for the cross-linked particles. By reduction, crosslinking glycoparticles were transformed to linear chains. Finally, results upon interaction with two classes of lectins (ConA and fimH), revealed that the glucose functionalities remained bioactive after being processed into glyconanoparticles. The same group, [91] also investigated the surface copolymerization of the same glycomonomer **M84** with NIPAAm **M42** using a RAFT agent attached to films obtained by crosslinking honeycomb structured porous films prepared via breath figures from poly(styrene-*co*-maleic anhydride). As a result, the conjugation of the grafted P(**M84**-*co*-**M41**) to ConA was switched off below the LCST (lower critical solution temperature) of the surface, while above the LCST the surface grafted glucose moieties bound strongly to ConA.

Recently, Abdelkader et al. [70] described in their paper the synthesis and polymerization of three different acrylamide glycomonomers **M85**, **M86**, and **M87**, two of which bear an azide group. First order kinetic plots, with one hour induction period, were obtained for the homopolymerization of the azide free glucoside derivative, **M85**, in H_2O/MeOH (5:1, v/v) at 70 °C using **R5** as the control agent where monodisperse polymer (PDI = 1.08) was obtained with M_n = 113,000 Da (Entry 33, Table 4.3). In order to examine the reversible-deactivation character of the obtained macroRAFT agent, P**M85**, successful chain extension with NIPAAm **M42** was conducted at 70°C in DMSO/H_2O (1:1, v/v) mixture. However, the homopolymerizations of each of the azido containing glycomonomer, **M86** and **M87**, were more complicated with interference of the azide functionality in the polymerization. In the case where the azide group was at C6, **M87**, no polymerization was observed at either 30 °C or 70 °C. Contrary to **M87**, relatively well-defined polymers from **M86** could be obtained at 70°C with PDI = 1.35 (the azide group was at C2). In order to get better defined glycopolymers out of **M86**, the polymerization was conducted at 30 °C using

I9 as an initiator to afford a fairly monodisperse glycopolymer (PDI = 1.15) with a M_n = 56,000 Da. Moreover, the obtained macroRAFT agent, P**M86**, was chain extended with NIPAAm **M42** successfully and likewise fairly monodisperse copolymer (PDI = 1.18) was afforded. Finally, a carbohydrate moiety bearing a propargyl group **9** (Figure 4.13) was clicked with the azide groups on the polymer backbone.

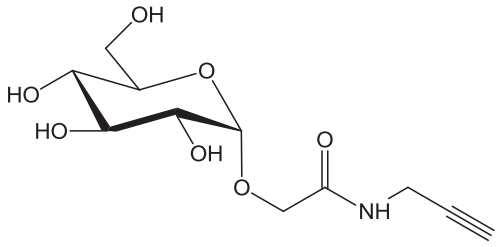

9

Figure 4.13 *N-propargylcarbamoyl methyl-α-D-glucoside **9** used by Abdelkader et al. [70] in their post polymerization step.*

4.4.2 Protected glycomonomers

4.4.2.1 (Meth)acrylate monomers

Guo et al. [71] described the RAFT polymerization of a protected lactoside glycomonomer **M43** in chloroform at 70 °C (above the boiling point of chloroform) for 24 hours in the presence a **R9** as the RAFT agent (Entry 36, Table 4.3). Monodisperse polymer (PDI =1.09) was obtained with a good control over molecular weight ($M_n/M_{n,th}$ = 0.87). The kinetic plots were first order after 4 hours, where the authors claimed that a hybrid behavior between conventional and reversible-deactivation radical polymerization took place for the first 4 hours of polymerization. By increasing the $[\mathbf{R9}]_0$ / $[\mathbf{I4}]_0$ ratio slower kinetics were observed but with a better control over molecular weight distribution. The obtained glycopolymer was grafted on silica particles functionalized beforehand with a methacrylate group in the presence of **I4**. Finally, deprotection of the acetate groups was achieved in the presence of NaOMe/MeOH, thus obtaining silica gel particles modified with well-defined lactose-carrying polymer.

Lowe and Wang [72] studied the RAFT polymerization of a protected galactose derived monomer **M20**, already polymerized by ATRP, [30] using two different RAFT agents, **R9** and **R10**, in DMF at 60 °C (Entries 37-38, Table 4.3). The polymerization evolved in a first order kinetics with an induction period of 50 minutes and that was commonly rationalized by the

authors in terms of slow fragmentation of the intermediate RAFT adduct beside other reasons concerning the purity of the RAFT agent [92] and by the presence of the so called initialization period. [93] Polymers with M_n up to 14,000 Da and PDI ≤ 1.2 were obtained. Moreover, the prepared macro-RAFT agents were chain extended with another methacrylate **M44** (Entry 39) to give fairly monodisperse (PDI = 1.2) hydrophilic-hydrophilic AB diblock copolymers after deprotecting the sugar moieties by TFA/H_2O (5:1, v/v). It is noteworthy that these deprotection conditions did not adversely affect the hydrolysis of the P**M44** block.

Polymers, obtained by RAFT mini-emulsion technique, based on two hydrophobic vinyl saccharide monomers, D-glucose **M13** and D-fructose **M45**, were described in a paper for Al-Bagoury et al. [73] To this end, three RAFT agents **R9**, **R10** and **R11** were used and polymerizations were conducted in a mixture of hexadecane/H_2O/SDS/$NaHCO_3$ at 70 °C (Entries 40-44, Table 4.3). In all cases deviation from targeted molecular weights was observed with the best results obtained with RAFT agent **R9** where fairly monodisperse polymers (PDI ≤ 1.25) with $M_n/M_{n,th}$ = 2.48 were attained (Entries43-44). However, the polymerization of **M13** in the presence of **R11** yielded a polymer with high polydispersity index (PDI = 1.9). What is more, polymerization in the presence of **R10** afforded a polymer with low PDI (< 1.3), but a high **R10** concentration was required. Trials to chain extend the obtained macroRAFT agents (derived from **R9** and **R10**) with butyl methacrylate **M46** and butyl acrylate **M47** were also reported.

Stenzel et al. [74] synthesized hollow nanocages based on D-galactose that can be used in drug delivery applications. Initially, an amphiphilic block copolymer was synthesized by the homopolymerization of a protected galactose glycomonomer **M74** in the presence of a poly(lactide) macroRAFT agent **R17** in α,α,α-trifluorotoluene at 70 °C for 6 hours (Entry 45, Table 4.3). The molecular weight (M_n = 52,000 Da) of the resulting polymer (PDI = 1.2) was in slight agreement ($M_n/M_{n,th}$ = 0.71) with the targeted value. The block copolymer, after deprotection of the sugar moiety, self-assembled in aqueous solution to form micelles with pendent galactose moieties covering the surface. By using hexandiol diacrylate, the micelles were cross-linked at the nexus of the copolymer creating stable aggregates. Subsequent degradation of the core resulted in glycopolymer nanocages. Finally, the obtained nanosopheres were characterized by TEM which showed the cross-linked micelles with a void center.

Liu et al. [75] described the synthesis of pH responsive copolymers and their self assembly in basic solution. First, the RAFT polymerization of a methacrylate monomer **M79** was conducted in dioxane in the presence of **R1** as the RAFT agent at 70 °C. The obtained macroRAFT agent P**M79**$_{18}$ was used in the homopolymerization of a protected methacrylate glucofuranoside derivative **M13** in dioxane at 70 °C for 24 hours (Entry 46, Table 4.3). The copolymerization proceeded with pseudo first order kinetics with a linear evolution of molecular weight with conversion to afford fairly monodisperse polymer (PDI = 1.19). Finally, deprotection of the sugar moieties using aqueous TFA led to unprotected block copolymer whose self assembly in alkaline solutions was studied by ^{1}H-NMR, UV-vis spectroscopy, dynamic light scattering, and transmission electron microscopy. Finally, the obtained micelles containing glucose moieties showed specific recognition to ConA.

Recently, Pfaff and coworkers [94] described the synthesis of mannose and galactose covered PDVB [poly(divinylbenzene)] particles (d = 2.4μm) with high grafting densities. For the mannose decorated particles, an unprotected mannose derived glycomonomer **M39** was added together with the RAFT agent **R1** and initiator **I4** to the dispersed particles in DMF and the solution was heated at 70°C. Moreover, they tested three different proteins (ConA, Lens culinaris agglutinin and Pealectin-I) that bind specifically to mannose moieties but non of them showed positive recognition with P**M39**. On the other hand, galactose based particles was synthesized using three approaches in DMF at 60°C using **R9** as the RAFT agent. The first approach was similar to the one used with mannose but they used a protected galactose glycomonomer **M20**. In the second approach, the RAFT agent was first added to the microspheres by its reaction with the styrenic units on the particles and the last approach was obtained by polymerizing **M20** using **R9** followed by aminolysis in order to click the thiol-terminated polymer to the styrinic moieties via a thiol-ene reaction. The sugar moieties were deprotected in TFA/H_2O mixture that led to glycopolymer covered spheres that could easily be dispersed in water due to the hydrophilic side chains. Contrary to the mannose-grafted particles, galactose-grafted microspheres revealed a strong binding of the glycopolymer towards the lectin RCA120.

More recently, Yang et al. [95] reported the polymerization of a protected lactose monomer **M43** and its introduction to the surface of a protein imprinted polymer beads. In this sense, the polymerization of **M43** was conducted in $CHCl_3$ at 70 °C using **R1** as the control agent to obtain monodisperse polymers (M_n = 4070 Da, PDI = 1.07). What followed

was the introduction of the glycopolymer onto the exterior surfaces of the bovine serum albumin (BSA) imprinted polymer beads by grafting copolymerization with methyl methacrylate and ethylene glycol dimethacrylate. Deprotection of the lactose moieties enhanced the hydrophilicity of the surface of the bead. Finally, rebinding test showed that the glycopolymer modified BSA imprinted polymers present higher performance selectivity properties than that of unmodified ones.

4.4.2.2 (Meth)acrylamide monomers

In the course of investigating thermoresponsive glycopolymers, Voit et al. [76] described the RAFT homopolymerization of two protected glucofuranosides **M48** and **M49**, bearing a hydrophobic linker, and their copolymerization with NIPAAm **M42** (Entries 47-51, Table 4.3). Homopolymerizations were conducted in the presence of **R10** in anisole at 80 °C or dioxane at 70 °C. The RAFT polymerizations of **M48** and **M49** showed that the presence of the linker group increased the reactivity of the monomer (higher conversions obtained in comparison with **M13** under the same conditions). The latter hypothesis was confirmed after conducting a kinetic study on the homopolymerization of **M48**. The kinetics showed first order plots with increase of molar mass with conversion. However, the polymerization slowed down after about 50 % conversion (5 hours) and only about 60 % conversion could be reached after 24 hours to afford polymer with a good control over molecular weight ($M_n/M_{n,th}$ = 0.88, PDI = 1.34). Furthermore, copolymerizations (random and block) with **M42** were conducted in DMF, anisole and dioxane at 70 and 100 °C with different monomer ratios and polymers with broad molecular weight distributions were obtained (PDIs ≤ 1.69). Deprotection of the corresponding copolymers in 80 % formic acid led to water soluble, temperature sensitive copolymers. For the LCST behavior, the critical phase transition temperature, T_c, was strongly dependent on the type and composition of copolymerization being involved.

Gody et al. [77] synthesized biotinylated glycopolymers via RAFT copolymerization of an acrylamide derived galactoside **M52** with NAM **M53** in the presence of a biotin-RAFT agent **R13** in dioxane at 90 °C for 2 hours (Entry 52, Table 4.3). The molecular weight increased linearly with global conversion, with an increase in polydispersity index values of 1.1–1.5 and that was attributed to an increase in viscosity above 70 % conversion that induced micro-heterogeneities in the polymerization mixture. The presence of the biotin ligand at the

α-end of the chains was confirmed (after precipitation of the chains) by ^{1}H NMR spectroscopy and MALDI-ToF MS analyses. Finally deprotection of the sugar residues was achieved in a H_2O/TFA (1:5, v/v) solution at RT. In a continuation to this study, the same group and their coworkers [96] investigated the synthesis of gold nanoparticles, photochemically, by in situ reduction of the deprotected form of the prepared biotinylated glycopolymer P(**M52**-*co*-**M53**) in a solution of P(**NIPAAm**) (obtained also by RAFT polymerization), Methoxy-PEG-SH and $HuCl_4$. Furthermore, they had also shown that the biotin ligands on the surface of the nanoparticles were still accessible for bioconjugation to streptavidin.

Jiang et al. [78] synthesized carbohydrate based copolymers containing *N*-acetyl-D-glucosaminopyranoside or D-mannopyranoside using a biotin-derived **R13** or *tert*-butyl dithiobenzoate **R16** RAFT agents (Entries 53-56, Table 4.3). The copolymerizations of the protected monomers **M60** and **M61** with NAM **M53** were conducted in dioxane at 75-90 °C, and afforded fairly monodisperse polymers ($1.14 \leq PDI \leq 1.60$) with a good to excellent control over molecular weights ($0.91 \leq M_n/M_{n,th} \leq 1.26$) above 70 % conversions. Deprotection of the sugar residues was achieved in a NaOMe/MeOH/CH_2Cl_2 solution at RT for 24 hours. The obtained copolymers were then conjugated to the surface of gold nanoparticles via thiol chemistry that led to the formation of (non)-biotinylated gold glyconanoparticles via a facile photochemical process. Finally, the biotinylated glyconanoparticles, with uniform size and polydispersity, were immobilized on the avidin-coated chip because of the strong affinity between biotin and avidin, and subsequently was used as the model to study the specific biomolecular recognition between lectins (ConA and WGA) and carbohydrates.

4.4.2.3 Styrenic monomers

The RAFT polymerization of a new aldehyde-functionalized glycomonomer **M50** and its auto organization into micelles was a subject of a paper by Xiao et al. [79] The polymerization was conducted in THF at 60 °C in the presence of **R11** as the RAFT agent for 50 hours (Entry 57, Table 4.3). While the polymerization adopted the characteristics of reversible-deactivation radical polymerization, deviation from targeted molecular weights ($M_n/M_{n,th} \cong 0.6$) was observed and polymer with fairly narrow molecular weight distribution (PDI = 1.1) was obtained. Deprotection of the sugar moieties in 88 % formic acid resulted in

amphiphilic polymers that auto-assembled into micelles without the recourse to any surfactant. The obtained micelles had sizes in the 80-205 nm range depending on the molecular weight of the polymer. Finally, protein-bioconjugated nanoparticles were also successfully prepared by the immobilization of BSA (bovine serum albumin) onto the aldehyde-functionalized micelles.

Wang et al. [80] studied the optical activity of homo and copolymers obtained from the RAFT polymerization of an optically active protected glycomonomer **M51**. The examined kinetic studies on the homopolymerizations of **M51**, in toluene at 90 °C and in the presence of **R12** for 50 hours, showed linear plots up to 40 % conversion with a deviation from linearity above that value (Entry 58, Table 4.3). Such deviations could be attributed to chain transfer reactions and besides, the special inflexible structure of the chiral polymer may also have limited the diffusion of monomer as judged by the authors. The resulting macro-RAFT agent was chain extended with styrene in toluene at 70 °C where serious tailing was observed from SEC at low M_w which is due to early terminations (Entry 59, Table 4.3). Moreover, the optically active nature of the obtained P**M51** was studied by investigating the dependence of specific rotation on the molecular weight and the concentration of P**M51** in THF and by the effect of its chain extension on the optical activity.

4.4.3 Glycopolymers from the post-polymerization approach

Davis et al. [81] reported a versatile one-pot synthesis of glycopolymers that can be adapted to any amine-functional sugar. For that, an activated acrylate ester **M68** was polymerized in the presence of **R5** in benzene at 70 °C (Entry 60, Table 4.3). Subsequently, a one-pot modification of the P**M68** was achieved by a nucleophilic reaction of sugar amines **10-11** on the activated ester (high yield **>** 90 % in H_2O/DMF, 1:1) followed by a simultaneous end-group polymer modification (at the sulfur end) using biotin modified maleimide (Scheme 4.5). Finally, the activity of these glycopolymers to bind to a specific lectin ConA was evaluated where D-glucose derived glycopolymers showed positive binding whereas those with D-galactose moieties showed negative interaction as expected.

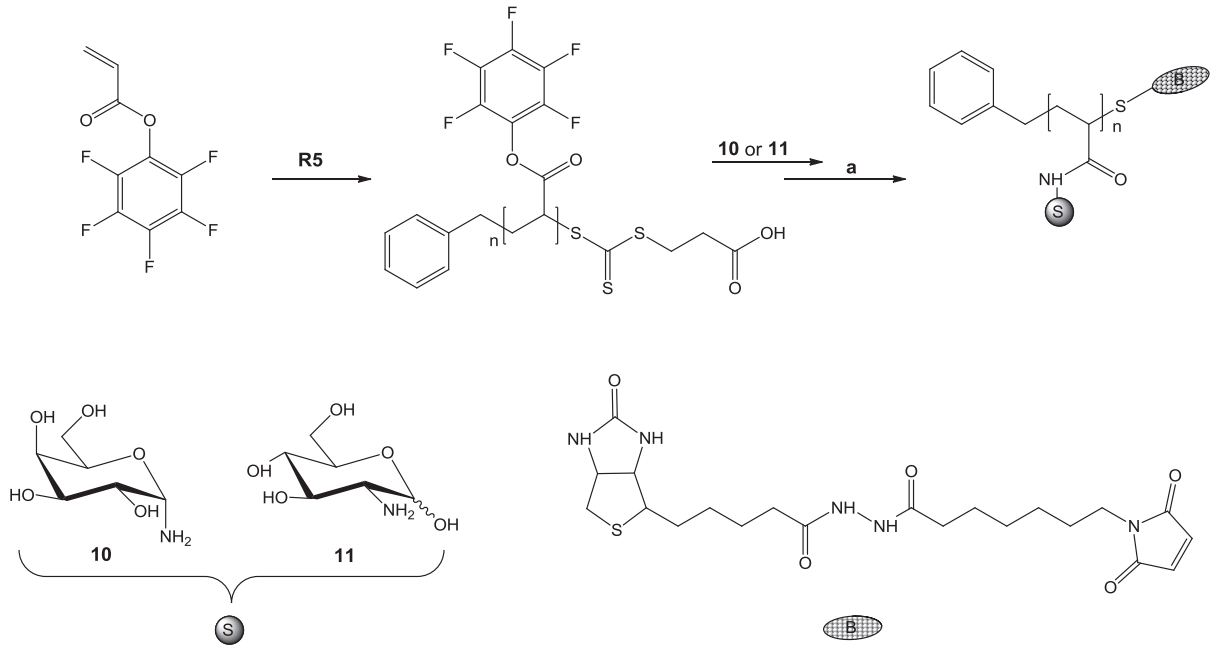

Scheme 4.5 *Synthetic strategy used by Davis et al.* [81] *for the synthesis of their glycopolymers.* ***a****: in situ aminolysis of the RAFT end-group and the addition of thiol onto biotin modified maleimide.*

Alidedeoglu et al. [82] synthesized D-glucuronic acid based glycopolymers. In their study, homo and block copolymers based on **M54**, **M55** and **M56** were synthesized at 50 °C (for P**M54**) and 70 °C in acetic buffer (pH 5) for around an hour (Entries 61-63, Table 4.3). Low polydispersity polymers (PDI ≤ 1.08) with a good control over molecular weights ($0.85 \leq M_n/M_{n,th} \leq 1.30$) were obtained. By reductive amination, the obtained homo and block copolymers (P**M54**, P**M55**, P[**M54**-*b*-**M56**]) were reacted with glucuronic acid in order to obtain carboxylic acid functionalized glycopolymers (Scheme 4.6). Conjugation of the sugar into the polymer was confirmed by ^{1}H-NMR and MALDI-ToF experiments of the dialyzed reaction mixtures.

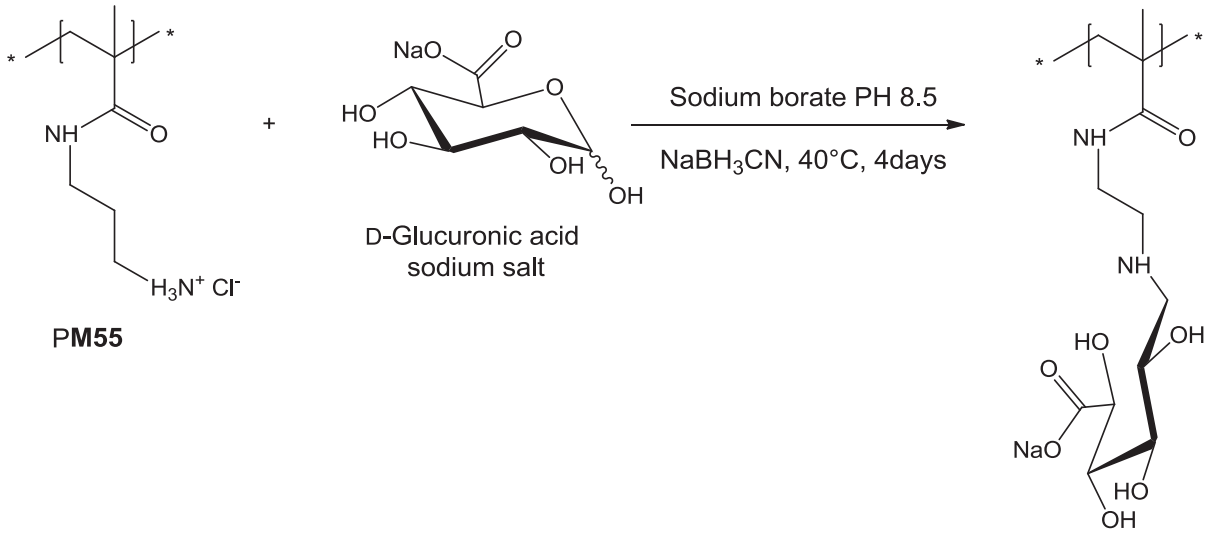

Scheme 4.6 *Reductive amination of D-glucuronic acid with P**M55** reported by Alidedeoglu et al.* [82]

Davis et al. [83] investigated the synthesis of gold nanoparticles decorated by glycopolymers using a layer by layer approach. For this aim, two types of copolymers were synthesized based on **M57**, **M58** and **M59** using **R5** as the RAFT agent in acetonitrile at 60 °C (for P(**M57**-*co*-**M58**)) and in toluene at 70 °C (for P(**M57**-*co*-**M59**)) for 12 hours (Entries 64-65, Table 4.3). Through a nucleophilic reaction, sugar moieties (D-glucose or D-galactose) were introduced to the copolymers as seen in Scheme 4.7. After deprotection of the tert-butyl groups in TFA to form carboxylic acid functionality, the copolymers were assembled onto positively charged gold nanoparticle (GNPs) surfaces using a layer-by-layer methodology to yield sugar-functional GNPs. Finally, the presence of accessible sugar moieties on the surface of the GNPs was confirmed by a binding assay with ConA.

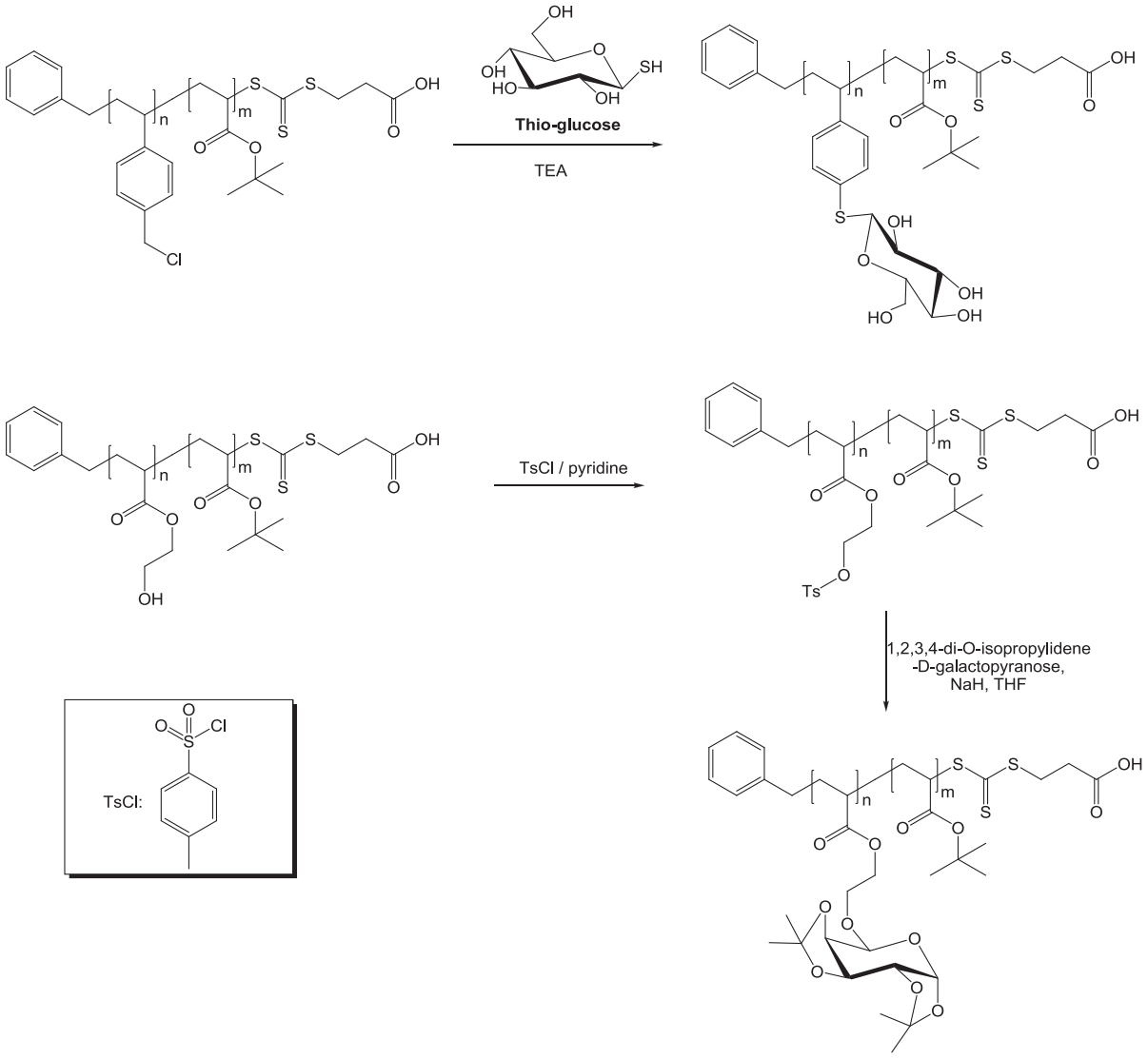

Scheme 4.7 *Strategy reported by Davis and coworkers for the synthesis of glycopolymers via a post polymerization methodology.* [83]

Stenzel et al. [84] reported the synthesis of a 4-arm star glycopolymer by postpolymerization technique. First, a star polymer was synthesized by the RAFT homopolymerization of **M58** using a tetra functional RAFT agent **R19** at 120 °C (Entry 66, Table 4.3). From SEC chromatograms, broadening at high conversions was observed which was assigned by the authors to linear macroRAFT agent and that was accompanied by a steadily increase in PDI from 1.1 to 1.9. Moreover, the obtained star polymer was reacted with 1-thio-β-D-glucose sodium salt in DMSO in order to obtain the corresponding glycopolymer whose ability to combine ConA was tested using turbidity assays. The same group, [85] synthesized thermoresponsive glycopolymers bearing mannose residues and studied their interaction with ConA. Thus, homo and block copolymers of unprotected mannose glycomonomer **M78**,

bearing a triazole moiety obtained by click chemistry, with NIPAAm **M42** were synthesized at 60 °C (Entries 67-68, Table 4.3). The homopolymerization was conducted in a H_2O/MeOH (2:1, v/v) using **R5** as a RAFT agent while the copolymerization was conducted in DMA (dimethyl acetamide). Interestingly, the complexation affinity of the block copolymer at 40 °C (micellar form) with ConA exceeded that for the linear glycopolymer at the same temperature.

Highly branched polymers decorated with sugar moieties was a subject of a paper by Semsarilar et al. [86]. For that aim, homo and copolymers of ethylene glycol dimethacrylate **M82** with and without trimethylsilylpropyne acrylate **M83** were polymerized in toluene at 60 °C. **R10** and **R20** RAFT agents were used for the homo and copolymerizations, respectively (Entries 69-70, Table 4.3). Contrary to copolymerization where the branching took place at the late stages of the reaction, during homopolymerization branching started at the onset of polymerization due to the absence of monofunctional monomer which used to dilute the difunctional species. The alkyne derived copolymers, P(**M82**-*co*-**M83**), were functionalized after deprotection in TFA, by either 1-thio-β-D-glucose sodium salt or an azido-ethyl galactose moiety via a thiol-yne or Cu(I) catalyzed click reactions. On the other hand, the homopolymer, P**M83**, was only functionalized by its reaction with 1-thio-β-D-glucose sodium salt via a thiol-ene click reaction.

4.5 Conclusion

Briefly, we can deduce the importance of reversible-deactivation radical polymerization in the synthesis of glycopolymers with controlled architecture from the ascending number of papers being published especially in ATRP and RAFT domains. This chapter summarized the synthesis of glycopolymers via three reversible-deactivation radical polymerization techniques NMP, ATRP and RAFT. For NMP, mostly styrenic glycomonomers have been polymerized with few examples on acrylate and methacrylate derived glycomonomers. The weak points reside in the fact that all the polymerizations were conducted in organic solvents and high temperature was a must. On the other hand, a wider window of glycomonomers was polymerized in organic and aqueous solutions using ATRP. Glycomonomers with various functional groups were polymerized (acrylates, methacrylates and acrylamides). Low polymerization temperatures were used in some cases. Finally, concerning RAFT polymerization most of the polymerizations were conducted in aqueous

media with a variety of glycomonomers being used (acrylate, methacrylates, acrylamides, methacrylamides, styrenic and vinyl ester) and a possibility to conduct polymerization at low temperatures were reported as well. [70]

4.6 References

(1) Okada, M. *Progress in Polymer Science* **2001**, *26*, 67.

(2) Wadhwa, M. S.; Rice, K. G. *Journal of Drug Targeting* **1995**, *3*, 111.

(3) (a) Choi, S.-K.; Mammen, M.; Whitesides, G. M. *Journal of the American Chemical Society* **1997**, *119*, 4103(b) Fleming, C.; Maldjian, A.; Da Costa, D.; Rullay, A. K.; Haddleton, D. M.; St. John, J.; Penny, P.; Noble, R. C.; Cameron, N. R.; Davis, B. G. *Nature Chemical Biology* **2005**, *1*, 270.

(4) Yun Yang, H.; Goetz Douglas, J.; Yellen, P.; Chen, W. *Biomaterials* **2004**, *25*, 147.

(5) Miyata, T.; Uragami, T.; Nakamae, K. *Advanced Drug Delivery Reviews* **2002**, *54*, 79.

(6) Novick, S. J.; Dordick, J. S. *Chem. Mater.* **1998**, *10*, 955.

(7) Wulff, G.; Zhu, L.; Schmidt, H. *Macromolecules* **1997**, *30*, 4533.

(8) (a) Kanai, M.; Mortell, K. H.; Kiessling, L. L. *Journal of the American Chemical Society* **1997**, *119*, 9931(b) Kiessling, L. L.; Gestwicki, J. E.; Strong, L. E. *Curr. Opin. Chem. Biol.* **2000**, *4*, 696.

(9) (a) Yamada, K.; Minoda, M.; Fukuda, T.; Miyamoto, T. *Journal of Polymer Science Part A-Polymer Chemistry* **2001**, *39*, 459(b) Minoda, M.; Yamaoka, K.; Yamada, K.; Takaragi, A.; Miyamoto, T. *Macromolecular Symposia* **1995**, *99*, 169.

(10) (a) Loykulnant, S.; Hirao, A. *Macromolecules* **2000**, *33*, 4757(b) Loykulnant, S.; Hayashi, M.; Hirao, A. *Macromolecules* **1998**, *31*, 9121.

(11) (a) Iyer, S.; Rele, S.; Grasa, G.; Nolan, S.; Chaikof, E. L. *Chemical Communications* **2003**, 1518(b) Grubbs, R. B.; Hawker, C. J.; Dao, J.; Frechet, J. M. J. *Angewandte Chemie, International Edition in English* **1997**, *36*, 270(c) Fraser, C.; Grubbs, R. H. *Macromolecules* **1995**, *28*, 7248(d) Gestwicki, J. E.; Cairo, C. W.; Strong, L. E.; Oetjen, K. A.; Kiessling, L. L. *Journal of the American Chemical Society* **2002**, *124*, 14922.

(12) (a) Okada, M.; Aoi, K. *Macromolecular Reports* **1995**, *A32*, 907(b) Aoi, K.; Tsutsumiuchi, K.; Okada, M. *Macromolecules* **1994**, *27*, 875.

(13) (a) Albertin, L.; Kohlert, C.; Stenzel, M.; Foster, L. J. R.; Davis, T. P. *Biomacromolecules* **2004**, *5*, 255(b) Cameron, N. R.; Spain, S. G.; Kingham, J. A.; Weck, S.; Albertin, L.; Barker, C. A.; Battaglia, G.; Smart, T.; Blanazsc, A. *Faraday Discussions* **2008**, *139*(c) Lowe, A. B.; Sumerlin, B. S.; McCormick, C. L. *Polymer* **2003**, *44*, 6761(d) Millard, P.-E.; Barner, L.; Reinhardt, J.; Buchmeiser, M. R.; Barner-Kowollik, C.; Müller, A. H. E. *Polymer* **2010**, *51*, 4319(e) Ohno, K.; Tsujii, Y.; Miyamoto, T.; Fukuda, T.; Goto, M.; Kobayashi, K.; Akaike, T. *Macromolecules*

1998, *31*, 1064(f) Ohno, K.; Tsujii, Y.; Fukuda, T. *J. Polym. Sci., Part A Polym. Chem.* **1998**, *36*, 2473.

(14) Ladmiral, V.; Melia, E.; Haddleton, D. M. *Eur. Polym. J.* **2004**, *40*, 431.

(15) Hashimoto, K.; Sugata, T.; Imanishi, S.; Okada, M. *Journal of Polymer Science, Part A: Polymer Chemistry* **1994**, *32*, 1619.

(16) Ohno, K.; Fukuda, T.; Kitano, H. *Macromolecular Chemistry and Physics* **1998**, *199*, 2193.

(17) Miura, Y.; Koketsu, D.; Kobayashi, K. *Polymers for Advanced Technologies* **2007**, *18*, 647.

(18) Chen, Y. M.; Wulff, G. *Macromolecular Chemistry & Physics* **2001**, *202*, 3426.

(19) Chen, Y. M.; Wulff, G. *Macromolecular Chemistry and Physics* **2001**, *202*, 3273.

(20) Narumi, A.; Matsuda, T.; Kaga, H.; Satoh, T.; Kakuchi, T. *Polymer Journal (Tokyo, Japan)* **2001**, *33*, 939.

(21) Narumi, A.; Matsuda, T.; Kaga, H.; Satoh, T.; Kakuchi, T. *Polymer* **2002**, *43*, 4835.

(22) Narumi, A.; Miura, Y.; Otsuka, I.; Yamane, S.; Kitajyo, Y.; Satoh, T.; Hirao, A.; Kaneko, N.; Kaga, H.; Kakuchi, T. *Journal of Polymer Science Part a-Polymer Chemistry* **2006**, *44*, 4864.

(23) Narumi, A.; Otsuka, I.; Matsuda, T.; Miura, Y.; Satoh, T.; Kaneko, N.; Kaga, H.; Kakuchi, T. *Journal of Polymer Science, Part A: Polymer Chemistry* **2006**, *44*, 3978.

(24) Gotz, H.; Harth, E.; Schiller, S. M.; Frank, C. W.; Knoll, W.; Hawker, C. J. *Journal of Polymer Science Part A-Polymer Chemistry* **2002**, *40*, 3379.

(25) Ting, S. R. S.; Min, E.-H.; Escale, P.; Save, M.; Billon, L.; Stenzel, M. H. *Macromolecules (Washington, DC, United States)* **2009**, *42*, 9422.

(26) Becer, C. R.; Babiuch, K.; Pilz, D.; Hornig, S.; Heinze, T.; Gottschaldt, M.; Schubert, U. S. *Macromolecules (Washington, DC, United States)* **2009**, *42*, 2387.

(27) Babiuch, K.; Becer, C. R.; Gottschaldt, M.; Delaney, J. T.; Weisser, J.; Beer, B.; Wyrwa, R.; Schnabelrauch, M.; Schubert, U. S. *Macromolecular Bioscience* **2011**, *11*, 535.

(28) Liang, Y.-Z.; Li, Z.-C.; Chen, G.-Q.; Li, F.-M. *Polym. Int.* **1999**, *48*, 739.

(29) Haddleton, D. M.; Ohno, K. *Biomacromolecules* **2000**, *1*, 152.

(30) Chen, Y. M.; Wulff, G. *Macromol. Rapid Commun.* **2002**, *23*, 59.

(31) Dong, C.-M.; Sun, X.-L.; Faucher, K. M.; Apkarian, R. P.; Chaikof, E. L. *Biomacromolecules* **2004**, *5*, 224.

(32) Ladmiral, V.; Monaghan, L.; Mantovani, G.; Haddleton, D. M. *Polymer* **2005**, *46*, 8536.

(33) Muthukrishnan, S.; Plamper, F.; Mori, H.; Mueller, A. H. E. *Macromolecules* **2005**, *38*, 10631.

(34) Muthukrishnan, S.; Jutz, G.; Andre, X.; Mori, H.; Muller, A. H. E. *Macromolecules* **2005**, *38*, 9.

(35) Muthukrishnan, S.; Mori, H.; Mueller, A. H. E. *Macromolecules* **2005**, *38*, 3108.

(36) Gao, C.; Muthukrishnan, S.; Li, W. W.; Yuan, J. Y.; Xu, Y. Y.; Muller, A. H. E. *Macromolecules* **2007**, *40*, 1803.

(37) Dupayage, L.; Save, M.; Dellacherie, E.; Nouvel, C.; Six, J.-L. *J. Polym. Sci., Part A: Polym. Chem.* **2008**, *46*, 7606.

(38) Wang, J.; Qian, Y.; Zhang, F.; Zhu, B.; Xu, Y. *Chinese Science Bulletin* **2008**, *53*, 1343.

(39) Ke, B.-B.; Wan, L.-S.; Zhang, W.-X.; Xu, Z.-K. *Polymer* **2010**, *51*, 2168.

(40) Pfaff, A.; Müller, A. H. E. *Macromolecules* **2011**, *44*, 1266.

(41) Narain, R.; Armes, S. P. *Chemical Communications (Cambridge, United Kingdom)* **2002**, 2776.

(42) Narain, R.; Armes, S. P. *Macromolecules* **2003**, *36*, 4675.

(43) Narain, R. *Reactive & Functional Polymers* **2006**, *66*, 1589.

(44) Vazquez-Dorbatt, V.; Maynard, H. D. *Biomacromolecules* **2006**, *7*, 2297.

(45) Qiu, S.; Huang, H.; Dai, X.-H.; Zhou, W.; Dong, C.-M. *J. Polym. Sci., Part A Polym. Chem.* **2009**, *47*, 2009.

(46) Vazquez-Dorbatt, V.; Tolstyka, Z. P.; Chang, C.-W.; Maynard, H. D. *Biomacromolecules* **2009**, *10*, 2207.

(47) Leon, O.; Bordege, V.; Munoz-Bonilla, A.; Sanchez-Chaves, M.; Fernandez-Garcia, M. *J. Polym. Sci., Part A Polym. Chem.* **2010**, *48*, 3623.

(48) Munoz-Bonilla, A.; Heuts, J. P. A.; Fernandez-Garcia, M. *Soft Matter* **2011**, *7*, 2493.

(49) Yu, K.; Kizhakkedathu, J. N. *Biomacromolecules* **2010**, *11*, 3073.

(50) Ladmiral, V.; Mantovani, G.; Clarkson, G. J.; Cauet, S.; Irwin, J. L.; Haddleton, D. M. *Journal of the American Chemical Society* **2006**, *128*, 4823.

(51) Geng, J.; Mantovani, G.; Tao, L.; Nicolas, J.; Chen, G.; Wallis, R.; Mitchell, D. A.; Johnson, B. R. G.; Evans, S. D.; Haddleton, D. M. *Journal of the American Chemical Society* **2007**, *129*, 15156.

(52) Ejaz, M.; Ohno, K.; Tsujii, Y.; Fukuda, T. *Macromolecules* **2000**, *33*, 2870.

(53) You, L.-C.; Lu, F.-Z.; Li, Z.-C.; Zhang, W.; Li, F.-M. *Macromolecules* **2003**, *36*, 1.

(54) Patten, T. E.; Matyjaszewski, K. *Accounts of Chemical Research* **1999**, *32*, 895.

(55) Bes, L.; Angot, S.; Limer, A.; Haddleton, D. M. *Macromolecules* **2003**, *36*, 2493.

(56) Narain, R.; Armes, S. P. *Biomacromolecules* **2003**, *4*, 1746.

(57) Mateescu, A.; Ye, J.; Narain, R.; Vamvakaki, M. *Soft Matter* **2009**, *5*, 1621.

(58) Yang, Q.; Ulbricht, M. *Macromolecules (Washington, DC, United States)* **2011**, *44*, 1303.

(59) Albertin, L.; Stenzel, M. H.; Barner-Kowollik, C.; Davis, T. P. *Polymer* **2006**, *47*, 1011.

(60) Albertin, L.; Stenzel, M. H.; Barner-Kowollik, C.; Foster, L. J. R.; Davis, T. P. *Macromolecules* **2005**, *38*, 9075.

(61) Albertin, L.; Stenzel, M.; Barner-Kowollik, C.; Foster, L. J. R.; Davis, T. P. *Macromolecules* **2004**, *37*, 7530.

(62) Spain, S. G.; Albertin, L.; Cameron, N. R. *Chemical Communications* **2006**, 4198.

(63) Housni, A.; Cai, H. J.; Liu, S. Y.; Pun, S. H.; Narain, R. *Langmuir* **2007**, *23*, 5056.

(64) Bernard, J.; Favier, A.; Zhang, L.; Nilasaroya, A.; Davis, T. P.; Barner-Kowollik, C.; Stenzel, M. H. *Macromolecules* **2005**, *38*, 5475.

(65) Bernard, J.; Hao, X. J.; Davis, T. P.; Barner-Kowollik, C.; Stenzel, M. H. *Biomacromolecules* **2006**, *7*, 232.

(66) Deng, Z.; Ahmed, M.; Narain, R. *J. Polym. Sci., Part A Polym. Chem.* **2009**, *47*, 614.

(67) Toyoshima, M.; Miura, Y. *J. Polym. Sci., Part A Polym. Chem.* **2009**, *47*, 1412.

(68) Miura, Y.; Mizuno, H. *Bulletin of the Chemical Society of Japan* **2010**, *83*, 1004.

(69) Ting, S. R. S.; Min, E. H.; Zetterlund, P. B.; Stenzel, M. H. *Macromolecules (Washington, DC, United States)* **2010**, *43*, 5211.

(70) Abdelkader, O.; Moebs-Sanchez, S.; Queneau, Y.; Bernard, J.; Fleury, E. *J. Polym. Sci., Part A Polym. Chem.* **2011**, *49*, 1309.

(71) Guo, T. Y.; Liu, P.; Zhu, J. W.; Song, M. D.; Zhang, B. H. *Biomacromolecules* **2006**, *7*, 1196.

(72) Lowe, A. B.; Wang, R. *Polymer* **2007**, *48*, 2221.

(73) Al-Bagoury, M.; Buchholz, K.; Yaacoub, E. J. *Polymers for Advanced Technologies* **2007**, *18*, 313.

(74) Ting, S. R. S.; Gregory, A. M.; Stenzel, M. H. *Biomacromolecules* **2009**, *10*, 342.

(75) Liu, L.; Zhang, J.; Lv, W.; Luo, Y.; Wang, X. *J. Polym. Sci., Part A Polym. Chem.* **2010**, *48*, 3350.

(76) Ozyurek, Z.; Komber, H.; Gramm, S.; Schmaljohann, D.; Muller, A. H. E.; Voit, B. *Macromolecular Chemistry and Physics* **2007**, *208*, 1035.

(77) Gody, G.; Boullanger, P.; Ladaviere, C.; Charreyre, M. T.; Delair, T. *Macromolecular Rapid Communications* **2008**, *29*, 511.

(78) Jiang, X.; Housni, A.; Gody, G.; Boullanger, P.; Charreyre, M.-T.; Delair, T.; Narain, R. *Bioconjugate Chemistry* **2010**, *21*, 521.

(79) Xiao, N.-Y.; Li, A.-L.; Liang, H.; Lu, J. *Macromolecules (Washington, DC, United States)* **2008**, *41*, 2374.

(80) Wang, J.; Zhu, X.; Cheng, Z.; Zhang, Z.; Zhu, J. *Journal of Polymer Science, Part A: Polymer Chemistry* **2007**, *45*, 3788.

(81) Boyer, C.; Davis, T. P. *Chemical Communications (Cambridge, United Kingdom)* **2009**, 6029.

(82) Alidedeoglu, A. H.; York, A. W.; Rosado, D. A.; McCormick, C. L.; Morgan, S. E. *J. Polym. Sci., Part A Polym. Chem.* **2010**, *48*, 3052.

(83) Boyer, C.; Bousquet, A.; Rondolo, J.; Whittaker, M. R.; Stenzel, M. H.; Davis, T. P. *Macromolecules (Washington, DC, United States)* **2010**, *43*, 3775.

(84) Chen, Y.; Chen, G.; Stenzel, M. H. *Macromolecules (Washington, DC, United States)* **2010**, *43*, 8109.

(85) Hetzer, M.; Chen, G.; Barner-Kowollik, C.; Stenzel, M. H. *Macromolecular Bioscience* **2010**, *10*, 119.

(86) Semsarilar, M.; Ladmiral, V.; Perrier, S. *Macromolecules (Washington, DC, United States)* **2010**, *43*, 1438.

(87) Albertin, L.; Cameron, N. R. *Macromolecules* **2007**, *40*, 6082.

(88) Granville, A. M.; Quemener, D.; Davis, T. P.; Barner-Kowollik, C.; Stenzel, M. H. *Macromolecular Symposia* **2007**, *255*, 81.

(89) Stenzel, M. H.; Zhang, L.; Huck, W. T. S. *Macromolecular Rapid Communications* **2006**, *27*, 1121.

(90) Jiang, X.; Ahmed, M.; Deng, Z.; Narain, R. *Bioconjugate Chemistry* **2009**, *20*, 994.

(91) Min, E. H.; Ting, S. R. S.; Billon, L.; Stenzel, M. H. *J. Polym. Sci., Part A Polym. Chem.* **2010**, *48*, 3440.

(92) Plummer, R.; Goh, Y. K.; Whittaker, A. K.; Monteiro, M. J. *Macromolecules* **2005**, *38*, 5352.

(93) (a) McLeary, J. B.; Calitz, F. M.; McKenzie, J. M.; Tonge, M. P.; Sanderson, R. D.; Klumperman, B. *Macromolecules* **2004**, *37*, 2383(b) McLeary, J. B.; McKenzie, J. M.; Tonge, M. P.; Sanderson, R. D.; Klumperman, B. *Chemical Communications* **2004**, 1950.

(94) Pfaff, A.; Barner, L.; Mueller, A. H. E.; Granville, A. M. *Eur. Polym. J.* **2011**, *47*, 805.

(95) Yang, H.; Guo, T.-Y.; Zhou, D. *International Journal of Biological Macromolecules* **2011**, *48*, 432.

(96) Narain, R.; Housni, A.; Gody, G.; Boullanger, P.; Charreyre, M.-T.; Delair, T. *Langmuir* **2007**, *23*, 12835.

Chapter 5: Synthesis of oligoglycuronan derived glycosylamines in aqueous solution: A detailed systematic NMR/MS study

Table of contents

Disclaimer

Beside my major contribution to this work, this chapter is the fruit of the work of other colleagues as well:

Alexandre Peruchon, a Master 1 student, has worked on the synthesis of β-D-glucopyranuronosylamine **2** in $NH_2CO_2NH_4$ under various conditions (1, 2 3, 4 and 5 M). The results of his experiments (AP10-18) are listed in Table 5.4.

Rédéo Wilfried Moussavou Mounguengui, a Master 1 student, was the first to examine the kinetic study on the amination of D-glucuronic acid in the presence of various ammonium salts. His neat and well resolved NMR spectra helped more in understanding the behavior of the glycosylamine and its carbamate in solution with temperature and in the structural elucidation of β-D-glucopyranuronosylamine **2** and its carbamate **3**.

Eric Condamine, a NMR expert working at IBS Grenoble, conducted the NMR analyses on the 800 MHz spectrometer. He contributed a lot to the analysis of these data.

Anna Wolnik examined the simulation studies on oligoalginates to check for the presence of H-bonding.

Last but not least, Luca Albertin dedicated as well a big part of his precious time to the analysis of my NMR data and crossing it with those of Alexander and Wilfried (after profound consideration). Not to forget his involvement to the writing of two papers on a part of the results of this chapter. [1]

5.1 Introduction

Uronic acids are monocarboxylic acids formally derived from aldoses by replacement of the hydroxymethyl group -CH_2OH with a carboxy group. [2] In nature, they are found in polysaccharides fulfilling diverse biological and structural functions such as glycosaminoglycans (e.g. heparin, hyaluronan, and chondroitin), and homoglycuronans (e.g. alginates and pectins). [3] In order to incorporate uronic acids into glycoconjugates, it would be advantageous to selectively functionalize their reducing end without resorting to protective group chemistry, which tend to be rather cumbersome in the case of monosaccharides [4] and

exceedingly time consuming in the case of oligoglycuronans. [5] A possible solution could be the transformation of unprotected uronic acids into the corresponding glycosylamine directly in water.

Glycosylamines have already been used as intermediates in the synthesis of a number of glycoconjugates, [6] such as glycopeptides, [7] surfactants, [7d,8] glycopolymers, [8a,9] and *N*-glycan probes. [10] Beginning in 1986 with the pioneering work of Kochetkov and collaborators, [7g] four original protocols have been described for the synthesis of β-glycopyranosylamines in aqueous or aqueous methanol solutions (Table 5.1): [8c,11] They are all based on the use of ammonia and/or volatile ammonium salts, and have found widespread application in the derivatization of hexoses, 6-deoxyhexoses, and oligosaccharides of different chain length. [7f,9,10b]

Table 5.1 *Experimental protocols reported in the literature for the synthesis of glycosylamines in aqueous solution. Whenever possible, the exact conditions used for uronic acids are listed.* [a]

Method	$[carb]_0$ / M	$[NH_3]_0$ / M	Salt	$[salt]_0$ / M	T / °C	React. time	Substrate	Yield (%)
Kochetkov [7g]	≤ 0.2	0	NH_4HCO_3	satd (~3.6) [b]	30	6 d	GlcNAc	80
Lubineau [8c,12]	0.2	~16 M	NH_4HCO_3	0.2	42	36 h	D-Glc	100
Gallop [11a]	≤ 0.06	0	$(NH_4)_2CO_3$	satd (~3.3) [b]	~25 [c]	5 d	D-GlcA	60
Likhosherstov [11c,d]	0.8	~7.5 M [d]	$NH_2CO_2NH_4$	3.2	20	48 h	D-GlcA	81 [e]

a Note: [s]0 indicates the initial concentration of species "s". b Solubility in water: NH_4HCO_3, 284 g/kg at 30 °C; $(NH_4)_2CO_3$, 320 g / L at 20 °C. c "Room temperature" in the original paper. d NH_3 15 M / CH_3OH 1:1. e Only the salt with carbamic acid was isolated.

The main advantage of these aqueous based methods resides in their applicability to unprotected and/or charged carbohydrates. Nevertheless, the considerable amount of salt used, the labor-consuming procedures needed to remove it, and the formation of diglycosylamine restricts their scope in preparative synthesis. Surprisingly, a detailed study on the formation of glycosylamines in aqueous solution is lacking [12] and only two papers claim the preparation of glycuronosylamines in aqueous [11a] or aqueous methanolic solution [11c] while providing precious little details.

In order to palliate to this dearth of information, we have carried out a systematic study of the synthesis of glycuronosylamines in aqueous solution. In particular, we tried to verify whether such transformation could be conveniently performed, and to identify the experimental conditions leading to the maximum yield, in the shortest reaction time, and with

the smallest amount of reagents. Besides, an identification of the by-products that formed during the course of this study was investigated by NMR and MS analyses. Further, an embodiment of this study on the amination of oligoglycuronans (oligoalginates) together with a kinetic study is reported.

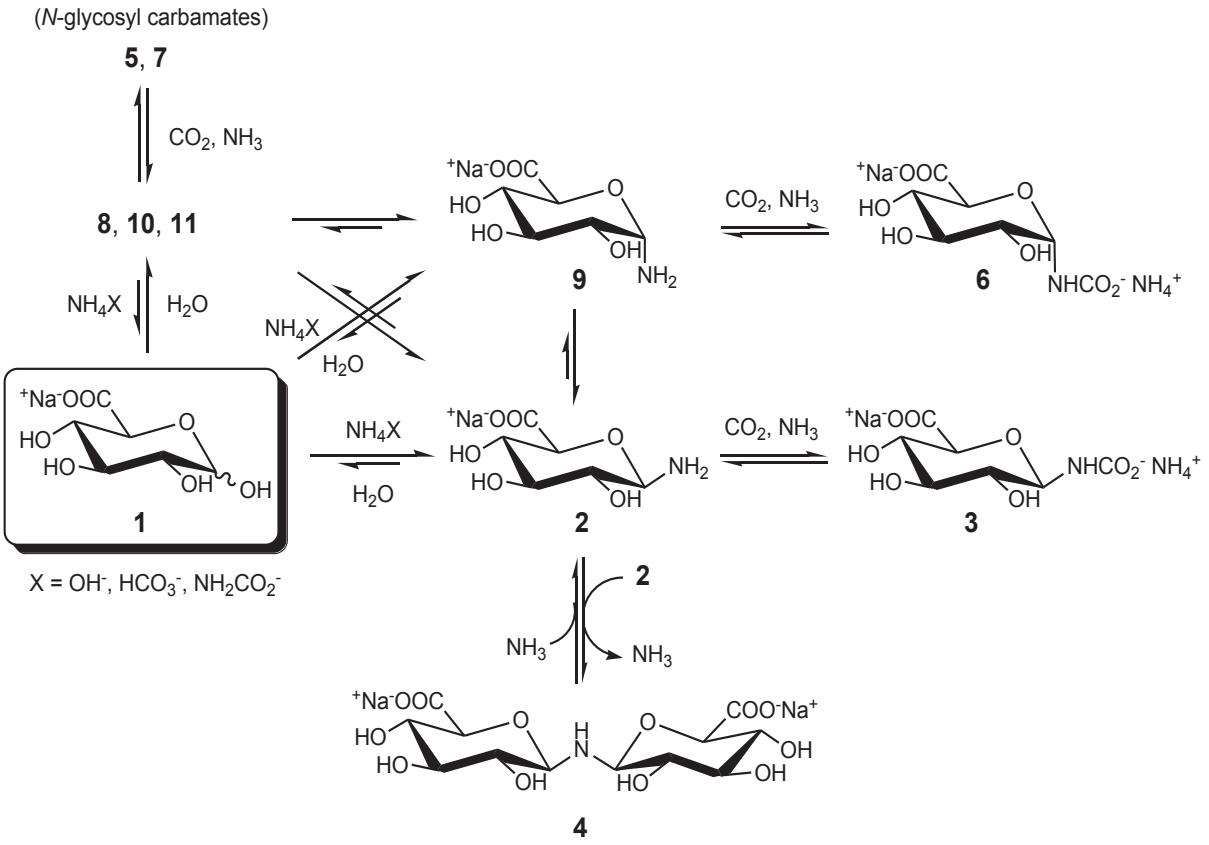

Scheme 5.1 *Reactions taking place during the synthesis of β-D-glucopyranuronosylamine **2** in aqueous solution.*

5.2 Experimental

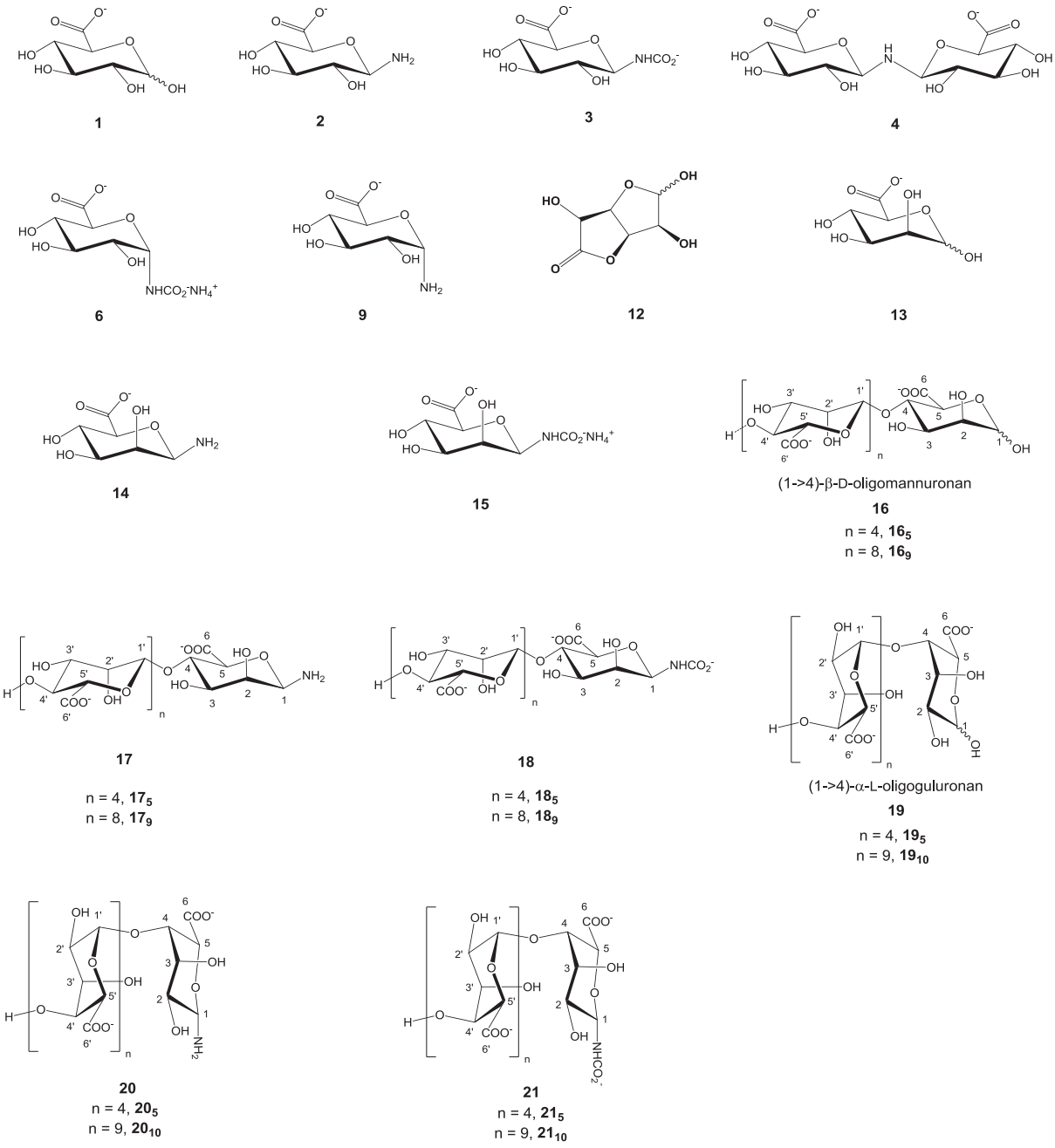

Scheme 5.2 *Molecules involved in this study.*

5.2.1 Materials

The following chemicals were reagent grade and used as received. D-mannurono-6,3-lactone (home obtained from acid hydrolysis of an oligomannuronan block), (1→4)-β-D-mannuronan and (1→4)-α-L-guluronan oligomers were obtained from ELICITYL

OligoTech®. Ammonium bicarbonate (≥ 99.0 %), ammonium carbamate (≥ 99.5%), D-glucose (≥ 99.0 %), D-glucuronic acid sodium salt monohydrate (99 %), and D-glucurono-6,3-lactone (≥ 98.0%) were from Fluka. Ammonia (28 % w/w, Carlo Erba), D_2O (99.9 %-D, Euriso-top), 2-isocyanatoethyl methacrylate (>98.0 %, TCI Europe), methacrylic anhydride (94 %, Sigma-Aldrich), SiO_2 (15-40 μm, 60 Å, Merck), sodium carbonate monohydrate (≥ 99.5 %, Sigma-Aldrich), and TLC plates (SiO_2 F254, 15 μm, 60 Å, Merck) were obtained from the indicated suppliers. Acryloyl chloride (≥96.0 %, Fluka) and methacryloyl chloride (≥ 97.0 %, Fluka) were distilled under reduced pressure. Distilled or deionised water was used in all experiments.

5.2.2 Analysis

The composition of samples from the kinetic study was determined by NMR on a Bruker DPX400 spectrometer equipped with a Variable Temperature (VT) module (resonance frequency of 400.13 and 100.62 MHz for ^{1}H and ^{13}C nuclei, respectively). Two different 5 mm detection probes were used: QNP (direct) and BBIZ (inverse). Unless otherwise specified, 90° pulses and pulse sequence recycle times of 3 s were used. The probe temperature was calibrated in the range 275-300 K using neat methanol. The NMR probe was pre-equilibrated at 278 K, individual samples were re-dissolved in D_2O (~3% w/w), transferred to an NMR tube, and immediately lowered into the instrument magnet for analysis. 1D ^{1}H spectra were obtained with 32 scans and 32 K data points, and were re-processed using MestReNova software (v6.1). Sodium 3-(trimethylsilyl)propanoate (TSP) or sodium 3-(trimethylsilyl)propane-1-sulfonate (DSS) was used as an internal reference. Chemical shifts (in ppm) for ^{1}H and ^{13}C nuclei were referenced to δ_{TSP} = -0.017 ppm (^{1}H) and δ_{TSP} = -0.149 ppm (^{13}C), or to δ_{DSS} = 0.000 ppm (^{1}H and ^{13}C).

Higher field NMR was used to identify peaks belonging to the different spin systems observed at early reaction times. Experiments were carried out on a VARIAN VNMRS 800 MHz spectrometer interfaced to Dell Optiplex 755 computer using VnmrJ and equipped with a 5-mm triple-resonance (^{1}H, ^{13}C, ^{15}N) cryoprobe including shielded z-gradients. All data were processed on Dell HP xw4400 using TopSpin software or Dell Optiplex 755 computer using VnmrJ software. The probe was pre-equilibrated at 278 K, and samples were prepared by dissolving the starting compound in D_2O (0.600 mL) with the addition of sodium 3-(trimethylsilyl)propanoate (TSP) as an internal reference. Immediately after dissolution,

samples were lowered into the instrument magnet and spectra were recorded at 278 K. 1D 799.975 MHz ^{1}H spectra were recorded before and after each set of 2D experiments to check medium modification with time. Each 1D ^{1}H spectrum was collected, without water suppression, with 32 scans of 32 K data points over a 9050 Hz spectral width. 1D 201.172 MHz ^{13}C spectra was obtained with power gated proton decoupling using the WALTZ-16 sequence and 1 K scans of 64 K points on 50000 Hz of spectral width. All 2D experiments were recorded with a continuous wave pulse of 35 Hz presaturation field on the water signal during the 1.5 s relaxation delay. 2D gradient-selected 799.975 MHz ^{1}H-^{1}H COSY spectra were acquired in the absolute value mode. 799.975 MHz ^{1}H-^{1}H TOCSY spectra used a z-filtered DIPSI-2 spin lock of 8.3 kHz power, 120 ms duration and were acquired in the sensitive phase mode using STATES method for quadrature detection. For COSY and TOCSY spectra, 512 equally spaced evolution time period values were acquired, averaging 16 transients of 2 K points, with 9470 Hz of spectral width. 2D gradient selected (799.975 - 201.172 MHz) ^{1}H-^{13}C HSQC with GARP sequence ^{13}C decoupling during acquisition was obtained in the sensitive phase mode using echo-antiecho detection. 512 equally spaced evolution time period values were acquired, averaging 14 transients of 1518 points, with 7300 and 3811 Hz in F1 and F2 respectively. Evolution delay for $^{1}J_{CH}$ amounted to 1.7 ms $[1/(4*^{1}J_{CH})]$. 2D gradient selected (799.975-201.172 MHz) ^{1}H-^{13}C HMBC via heteronuclear zero and double quantum coherence with low-pass J-filter to suppress on-bond correlation and no ^{13}C decoupling during acquisition was achieved in the absolute mode value. 512 equally spaced evolution time period values were acquired, averaging 32 transients of 2426 points, with 44248 and 9470 Hz in F1 and F2 respectively. Evolution delay for low pass $^{1}J_{CH}$ filter and for evolution of long range coupling amounted to 3.6 ms $[1/(2*^{1}J_{CH})]$ and 70 ms $[1/(2*^{n}J_{CH})]$ respectively.

Mass spectrometry analyses were performed with a Waters ZQ (Altrincham, GB) single quadrupole atmospheric pressure ionization mass spectrometer fitted with a Z electrospray interface (ESI). The instrument was calibrated with mass spectra generated by ion spray ionization of a 0.1 mol L^{-1} solution of sodium iodide in aqueous acetonitrile (50%, v/v) in the mass range of 23-1972 amu. Nitrogen was used as the drying and nebulizing gas. Samples (~1 mg mL^{-1}) were dissolved in deionised water and infused to the ESI interface at constant flow rate (50 µL min^{-1}).

For simulation studies, the structure of (1→4)-β-D-mannuronan and (1→4)-α-L-guluronan blocks (DP_n = 4) were created in 2_1 helical conformation based on the work of Braccini et al. [13] Energy minimization was performed using **Dreiding2.21** force field with a dielectric constant equal to **1** using **CERIUS2** software.

5.2.3 Protocol numbering

Sodium D-glucuronate **1**, D-glucose and D-mannuronic acid **13**, and oligoglycuronans **16** and **19** (Scheme 5.2) were reacted at RT, 30 or 40 ºC with ammonia and/or volatile ammonium salts (NH_4HCO_3 or $NH_2CO_2NH_4$) in water according to different protocols. The numbering of each protocol withholds the exact experimental conditions used:

- The first letter indicates the type of solid salt added (**A**, NH_4HCO_3; **B**, $NH_2CO_2NH_4$).
- The middle number indicates the initial formal concentration of liquid ammonia in mol L^{-1}.
- The last number indicates the initial formal concentration of salt in 10^{-1} mol L^{-1}.

For example, **A**.1.06 indicates that the salt used was NH_4HCO_3, and that the initial concentration of ammonia and salt was 1 and 0.6 M, respectively.

5.2.4 MS nomenclature

In the nomenclature used to assign MS peaks, subscript symbols indicate the counterion. For example, $\mathbf{1}_H$ and $\mathbf{1}_{Na}$ indicate D-glucuronic acid and sodium D-glucuronate respectively.

5.2.5 Kinetic study on D-glucuronic acid

In a typical experiment (AG09-30_P2, protocol **B**.5.06), D-glucuronic acid sodium salt monohydrate (0.468 g, 2.0 mmol) and ammonium carbamate (0.468 g, 6.0 mmol) were weighed in a 25 mL round bottom flask. A magnetic bar was added together with 10 mL of aqueous ammonia (5 M), the flask was sealed with a rubber septum, and a disposable needle (21 G) was passed through the septum to prevent pressure build-up. The flask was plunged in an oil bath pre-heated at 30 °C and stirred at 200 rpm. At pre-set intervals, ~250 μL samples were drawn with a syringe, transferred to a glass vial, diluted with 2 volumes of water, and frozen in liquid nitrogen. All samples were then freeze-dried overnight and stored in a freezer (-18 °C) until needed. The mole fraction of each compound for the kinetic study was then

calculated by ^{1}H NMR according to equation 5.2. For protocols **A**/**B**.0.S, saturation was ensured by the constant presence of solid salt at the bottom of the flask.

5.2.6 Kinetic study on oligoglycuronans

(Entries 8 and 9, Table 5.4) In a typical experiment (AG10-21-P1, protocol **A**.5.02), (1→4)-β-D-oligomannuronan (0.100 g, 0.120 mmol) was weighed in a vial (14 mL), dissolved in water (1.2 mL) and the pH of the mixture was adjusted to ~8 by the addition of $NaHCO_3$ (0.047 g, 0.568 mmol). To the latter basic solution, ammonium bicarbonate (0.038 g, 0.481 mmol) and NH_3 (1.2 mL, 10 M) were added respectively. The vial was capped with a perforated aluminum foil, and plunged in an oil bath preheated at 30 °C and stirred at 250 rpm. At pre-set intervals, ~120 μL samples were drawn with a syringe, transferred to a glass vial, diluted with 2-3 volumes of water, and frozen in liquid nitrogen. All samples were then freeze-dried overnight and stored in a freezer (-18 °C) until needed. The composition of the samples was determined by ^{1}H-NMR according to Eq. 5.5.

5.2.7 Synthesis of β-D-glucopyranuronosylamine (2)

D-Glucuronic acid sodium salt monohydrate (1.00 g, 4.27 mmol) and ammonium carbamate (8.32 g, 0.106 mol) were weighed in a 50 mL round bottom flask and dissolved in 21.3 mL of de-ionized water (AP10-12, protocol **B**.0.50). A magnetic bar was added, the flask was sealed with a rubber septum, a disposable needle (21 G) was passed through the septum to prevent pressure build-up, and the mixture was stirred at ambient temperature (~ 25 ºC) and 300 rpm. After 24 hrs of reaction, the content of the flask was frozen in liquid nitrogen and freeze dried overnight. The resulting powder was re-dissolved in de-ionized water (80 mL) and submitted to a second cycle of freeze-drying. The obtained white fluffy solid (1.13 g) had the following molar composition (as determined by ^{1}H NMR): **1** (10 %), **2** (65 %), **3** (17 %), **4** (1 %), **6**+**9** (4 %), **5**+**7**+**8**+**10**+**11** (3 %). The sample was then sealed in a round bottom flask and stored in a freezer (-18 °C) until needed. The increase in the mass of the sample is mostly due to the presence of *N*-glycosylcarbmates **3**, **5**, and **6**, whose molar mass is bigger than that of the starting sugar **1** and of glycosylamine **2**. See Table 5.2 and Table 5.3 for NMR and MS analyses.

5.2.8 Synthesis of β-D-mannopyranuronosylamine (14)

(Entry 4, Table 5.4) D-mannurono-6,3-lactone **12** (1.60×10^{-2} g, 9.08×10^{-5} mol) was dissolved in D_2O (0.6 mL), the pD of the mixture was adjusted to ≅ 9 by the addition of anhydrous Na_2CO_3, and the solution was left stirring at RT for 4 hours. A NMR was acquired to confirm the hydrolysis of the lactone to D-mannuronic acid **13**, and the solution was freeze dried. The resulting solid was re-dissolved in H_2O, stirred at RT for ~8 hours and freeze dried. This process was repeated twice in order to exchange all the deuterium atoms, then the product was re-dissolved in a saturated NH_4HCO_3 solution (360 µl), the vial was closed with a cap, a disposable needle (21 G) was passed through the cap to prevent pressure build-up, and the mixture was stirred (300 rpm) at ambient temperature (~ 23 ºC). After 48 hrs of reaction, the content of the vial was frozen in liquid nitrogen and freeze dried overnight. Yield (86 %) was calculated from ^{1}H-NMR of the gross product. ^{1}H-NMR (400 MHz, D_2O, 0 °C) δ (ppm): ManA-NH_2: 4.36 (H1, 1H, $J_{1,2}$ 0.84 Hz), 3.84 (H2, 1H, $J_{1,2}$ 0.7 Hz, $J_{2,3}$ 2.1 Hz). ManA-$NHCO_2^-$ (4.94, H1, 1H, $J_{1,2}$ 0.93 Hz).^{13}C-NMR (100 MHz, D_2O, 25 °C) δ (ppm): ManA-NH_2: 71.4 (C4), 73.9 (C2), 76.3 (C3), 80.1 (C5), 85.2 (C1), 179.4 (C6). ManA-$NHCO_2^-$: 83.4 (C1), 179.2 (C6). ESI-MS: *m/z* calculated 193.06, found: 192.12 $[M-H]^-$.

5.2.9 Synthesis of the glycosylamines 17 and 20 from (1 → 4)-β-D-oligomannuronan (16) and (1 → 4)-α-L-oligoguluronan (19)

(Entries 27 and 28, Table 5.4) In a typical experiment, (1→4)-β-D-oligomannuronan **16** (98%, 0.250 g, 0.139 mmol) and ammonium carbamate (0.043 g, 0.554 mmol) were weighed in a vial (10 mL) and dissolved in NH_3 (2.77 mL, 5M) (AG11-19-P1, protocol **B**.5.02). A magnetic bar was added, the vial was sealed with a cap, a disposable needle (21 G) was passed through the cap to prevent pressure build-up for the first 4 hours, and the mixture was stirred at ambient temperature (~ 23 ºC) at 250 rpm. After 2 days of reaction, another portion of ammonium carbamate (0.050 g) was added to the reaction mixture that was left reacting for one more day. At the end of the reaction (3 days for oligoM and 4 days for oligoG) the content of the vial was transferred to a centrifugation cell (25 mL), cooled down on ice and precipitated by a slow addition of cold EtOH (80%, 13 mL). Then the resulting mixture was centrifuged (10 krpm, 15 °C, 10 min) and the supernatant was decanted. To the obtained white precipitate an excess of cold water (~5 mL) was added and the portion that was dissolved immediately was transferred to a round bottom flask (using a Pasteur pipette)

already placed in liquid nitrogen. The latter process was repeated several times until all the precipitate was dissolved and transferred (in a period of 5-7 minutes) to the round bottom flask whose contents were freeze dried overnight. A white fluffy solid was obtained and the sample was stored in the freezer (-18 °C) until needed. Yields (~ 80 % for **17** and 77 % for **20**) were calculated from ^{1}H-NMR. ^{1}H-NMR (400.13 MHz, D_2O, 30 °C, ns = 16, D1 = 10 s) for **17** δ (ppm): 3.63-4.02 (m, H2, H2', H3, H3', H4, H4', H5, H5'), 4.36 (d, H1, 1H, J_{12} 0.6 Hz), 4.62-4.70 (m, H1'), 4.90 (s, H1β, 1H, starting sugar **16**), 5.02 (m, H1', G unit), 5.21 (d, H1α, 1H, starting sugar **16**; $J_{1,2}$ 2.5 Hz). For **20** δ (ppm): 3.55 (dd, H2, 1H, $J_{1,2}$ 9.2 Hz, $J_{2,3}$ 2.8 Hz), 3.90 (m, H2', sugar), 4.00 (m, H4', sugar), 4.10 (m, H3', sugar), 4.35 (s, H1, 1H), 4.39-4.45 (m, H5', suagr), 4.88 (d, H1β, 1H, starting sugar **19**, $J_{1,2}$ 8.3 Hz), 4.99-5.17 (m, H1', sugar), 5.22 (d, H1α, 1H, starting sugar **19**, $J_{1,2}$ 2.8 Hz).

5.3 Results and discussion

5.3.1 Structural elucidation of by-products formed during the amination of D-glucuronic acid: NMR study

Sodium D-glucuronate **1** (Scheme 5.1) was reacted at 30 ºC with ammonia and volatile ammonium salts (NH_4HCO_3 or $NH_2CO_2NH_4$) in water according to different protocols (see experimental part). Samples were drawn at preset reaction times, frozen in liquid nitrogen and freeze-dried overnight to eliminate water and most of the salts. No further purification was performed and all reported analyses refer to the gross products obtained this way. In order to monitor the time course of the reaction, individual samples were redissolved in cold D_2O to afford clear solutions of pD ≅ 9, that were immediately analyzed by ^{1}H-NMR. Spectra were acquired at 278 K in order to inhibit hydrolysis of the products and to prevent the peak of residual HDO from interfering with integration.

Figure 5.1 shows an example of the evolution of the ^{1}H and ^{13}C-NMR spectra when going from starting compound (a) to the gross final product (c). In the proton spectrum, the disappearance of the characteristic peaks at 4.63 ($H1_\beta$), 5.23 ($H1_\alpha$), and 3.27 ppm ($H2_\beta$) proves that **1** was completely consumed during the reaction. At the same time, two new doublets appear at 4.09 ppm ($J_{1,2}$ 8.8 Hz) and 4.70 ppm ($J_{1,2}$ 8.8 Hz) that were assigned to the anomeric proton of β-D-glucopyranuronosylamine **2** and *N*-β-D-glucopyranuronosyl

carbamate **3**, respectively. Compound **3** forms from the reaction of **2** with the CO_2 liberated by the decomposition of bicarbonate or carbamate anions. [9b, 10b] Since it decomposes fairly easily upon standing in aqueous solution and/or during repeated freeze drying cycles, [10b] its proportion was included in the calculation of product yields. Besides, the solution equilibrium between **2** and **3** can be easily displaced in favor of **2** by increasing the temperature. For instance, when the product obtained according to protocol **A**.9.06 was analyzed by ^{1}H-NMR at 298 K, its mole content was 37 % and 52 % for **2** and **3**, respectively; whereas the same sample analyzed at 318 K contained 72% and 14 % of the two species. [14] A complete assignment of the peaks observed in ^{1}H and ^{13}C-NMR was performed via ^{1}H-^{1}H homonuclear and ^{1}H-^{13}C heteronuclear correlation experiments and the results are summarized in Table 5.2. As an example, the ^{1}H-^{1}H TOCSY, ^{1}H-^{1}H COSY, and ^{1}H-^{13}C HMQC spectra are shown in Figure 5.2, Figure 5.3 and Figure 5.4, respectively, together with the assignment of some peaks.

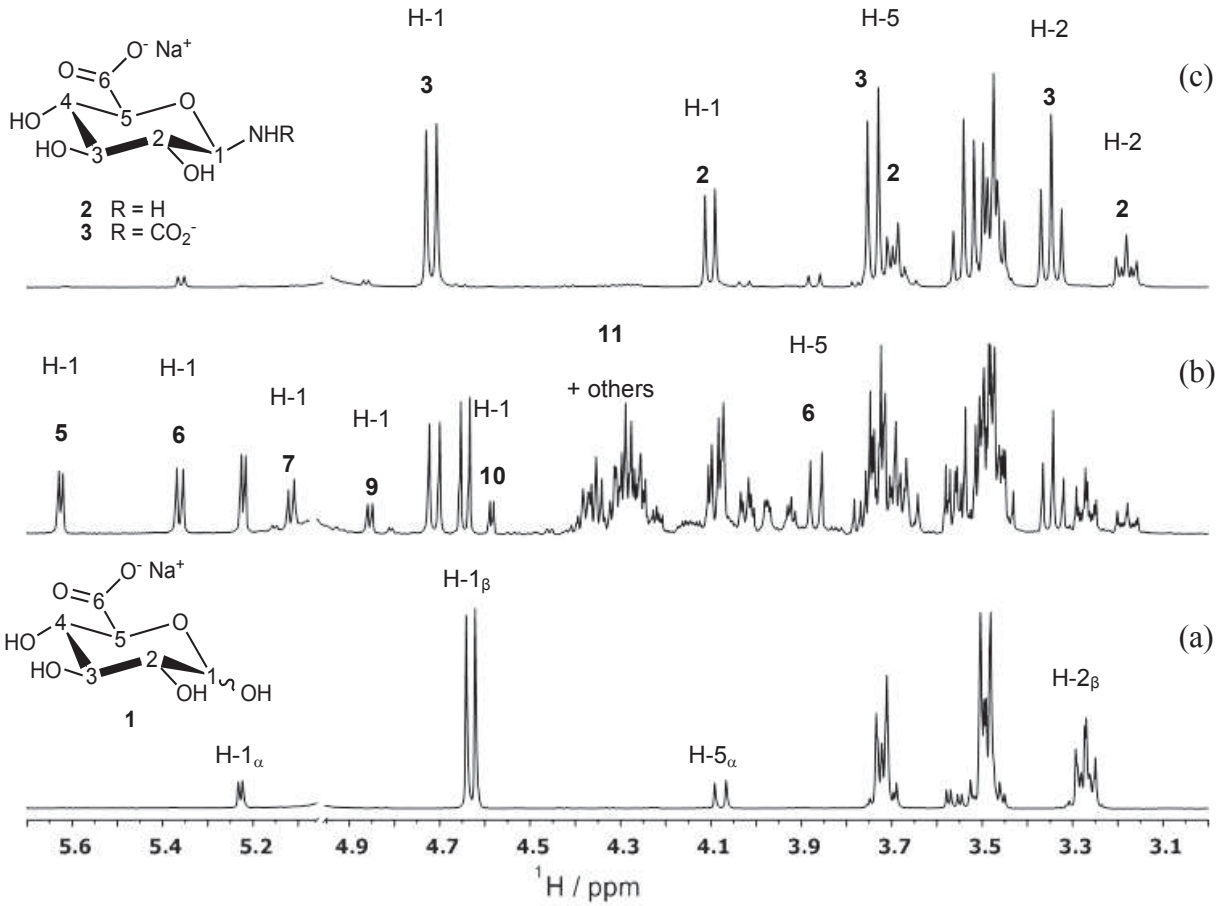
H-1
H-5
H-2
(c)
3
2
NHR
OH
2 R = H
3 R = CO2-
H-1
H-5
H-2
H-1
H-1
H-1
H-1
H-1
H-5
(b)
11
+ others
5
6
7
9
10
6
H-1β
H-2β
H-1α
H-5α
(a)
1
5.6
5.4
5.2
4.9
4.7
4.5
4.3
4.1
3.9
3.7
3.5
3.3
3.1
1H / ppm

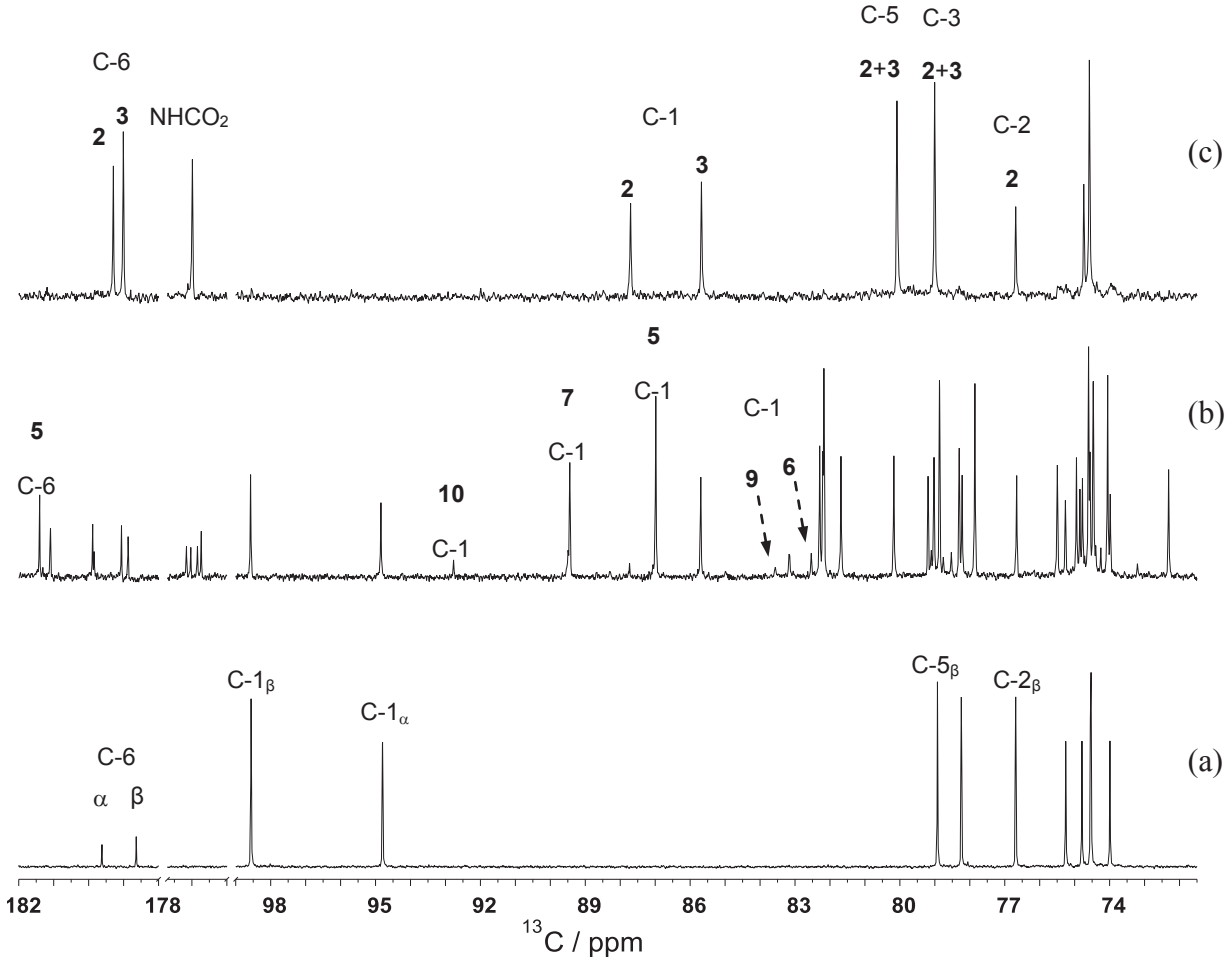

Figure 5.1 *1D ^{1}H (400.13 MHz, top) and ^{13}C (100.62 Hz, bottom) spectra of (a) **1**, (b) the gross product obtained after 140 min. of reaction according to protocol **B**.5.02, and (c) the mixture of **2** and **3** obtained after 33 hrs of reaction according to protocol **B**.0.S. The assignment of some peaks is also shown.* [15]

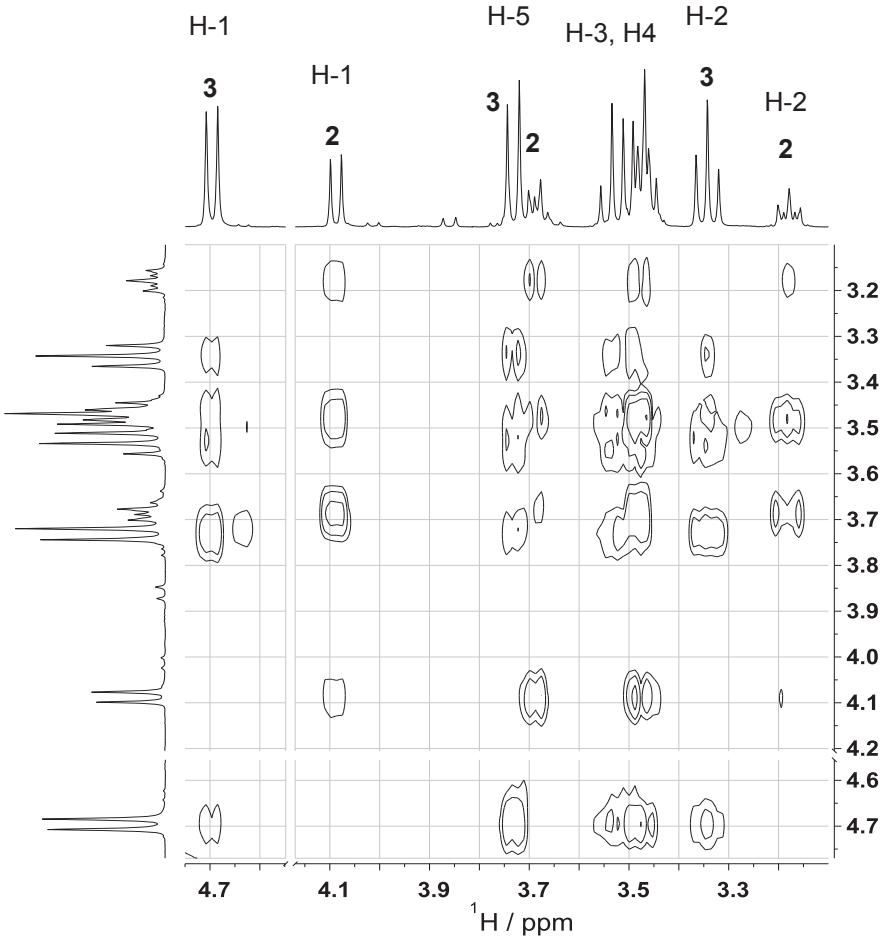

Figure 5.2 *2D ^{1}H-^{1}H TOCSY spectrum of **2**+**3** (400.13 MHz).* [16]

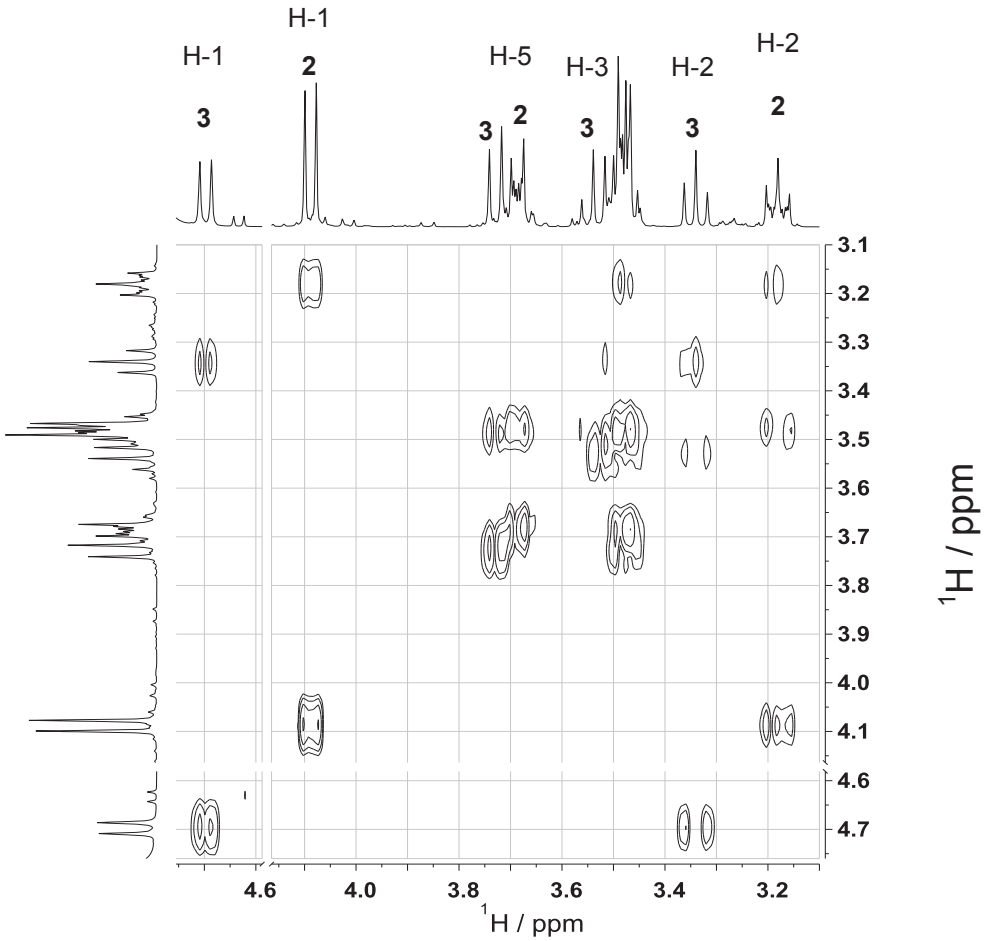

Figure 5.3 *^{1}H-^{1}H COSY spectrum of **2**+**3** (100.62 MHz).* [17]

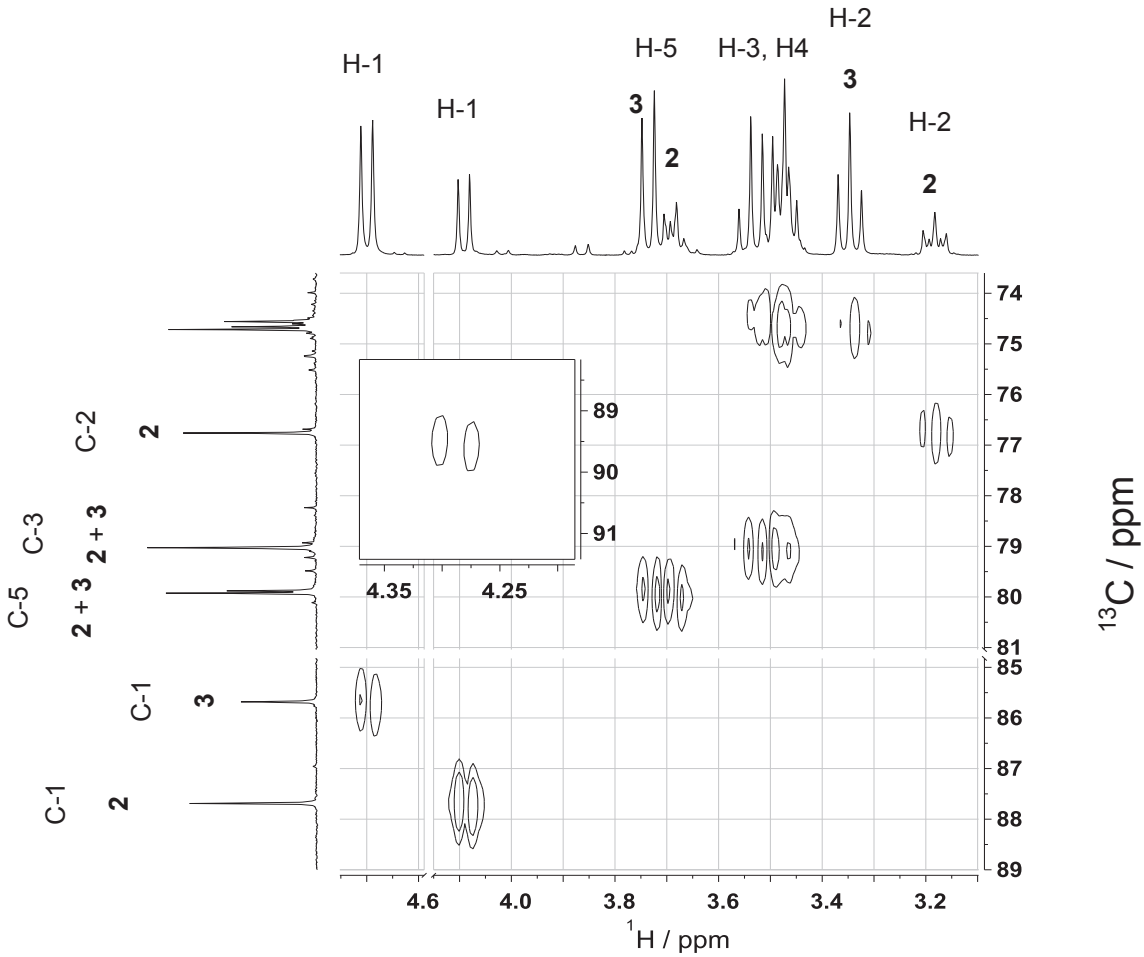

Figure 5.4 *^{1}H-^{13}C HMQC spectrum of **2**+**3** (400.13-100.62 MHz).* [18] *The insert shows the cross-peak due to the anomeric proton and carbon of di(β-D-glucopyranuronosylamine) **4**.*

The presence of 13 peaks in the ^{13}C-NMR spectrum (6 for **2** and 7 for **3**) suggests that both compounds are present in a single cyclic form, and the chemical shift of C-5 (79.9 ppm) points to a hexopyranose ring. [19] Finally, values of 9.4-9.5 Hz for $J_{4,5}$ and $J_{1,2}$ are consistent with an *anti* orientation of the vicinal hydrogens, [20] hence a $^4C_1$ conformation and a β configuration. It is important to note the original assignment reported by Pfeffer et al. [21] for C-5α and C-6α of GlcA at pH 7.8 should be exchanged with that of the β anomer, as evidenced by a three-bond ^{1}H-^{13}C correlation experiment carried out in the course of our study. Also, 1.7-1.9 ppm should be added to the ^{13}C-NMR chemical shifts originally reported in order to refer them to δ_{DSS}=0.0. The comparison of our results with literature data is comforting: Identical values for δ (H1) and $J_{1,2}$ were reported by Likhosherstov et al. for the ^{1}H spectrum of β-D-glucopyranosylamine, [11d] the corresponding *N*-glycosylcarbamate, and the carbamic acid salt of β-D-glucopyranuronosylamine [11c] prepared in aqueous methanolic solution, although in those cases a complete NMR assignment was not realized.

With regard to compound **3**, a weak doublet is visible at 6.25 ppm (*J* 9.8 Hz) in the 1D ^{1}H spectrum of concentrated solutions (~15 % w/w) acquired at 278 K. The same doublet does not couple with any carbon atom in one-bond heteronuclear correlation experiments, and is displaced to 6.04 ppm in spectra acquired at 298 K. This signal correlates to the H1 (4.70 ppm) of the same molecule in three-bond homonuclear correlation experiments though (Figure 5.5a), and was therefore assigned to the proton of the $NHCO_2^-$ group. Further corroboration to the structure of **3** comes from the observation that H1 correlates to a quaternary carbamate carbon (165.9 ppm) in long distance ^{1}H-^{13}C heteronuclear correlation experiments (Figure 5.5b).

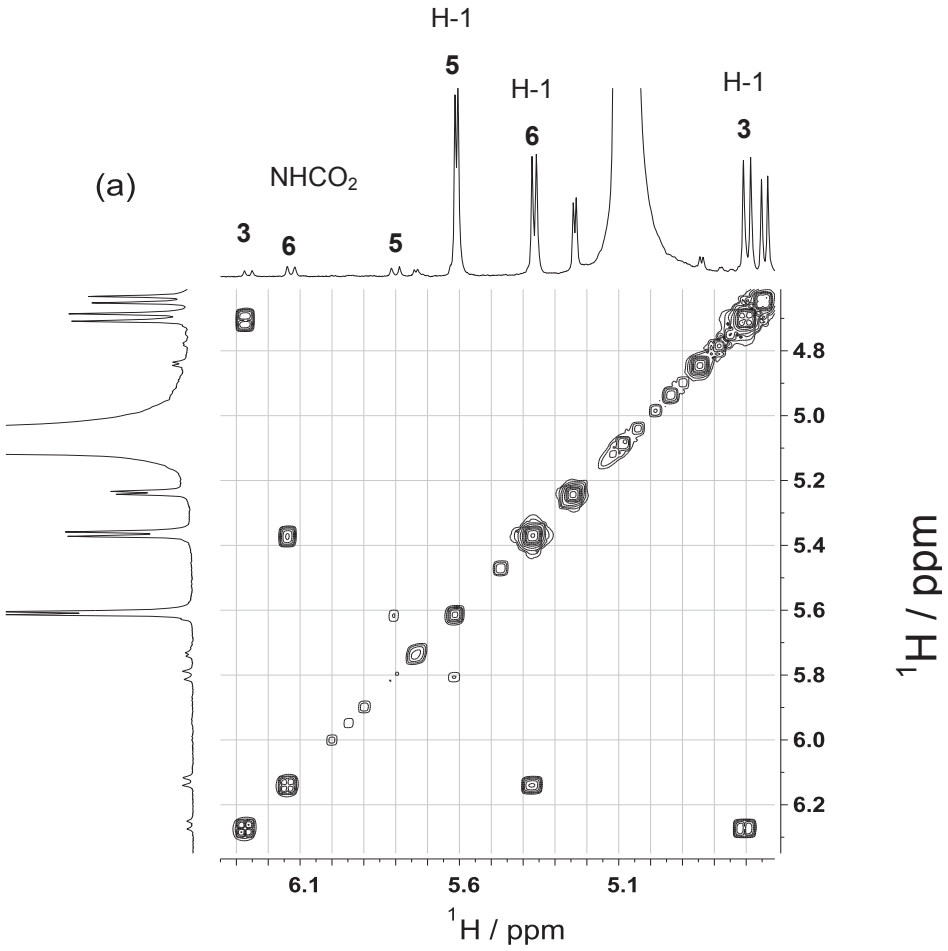
H-1
5
H-1
6
H-1
3
(a)
NHCO2
3
6
5
4.8
5.0
5.2
5.4
5.6
5.8
6.0
6.2
6.1
5.6
5.1
1H / ppm
1H / ppm

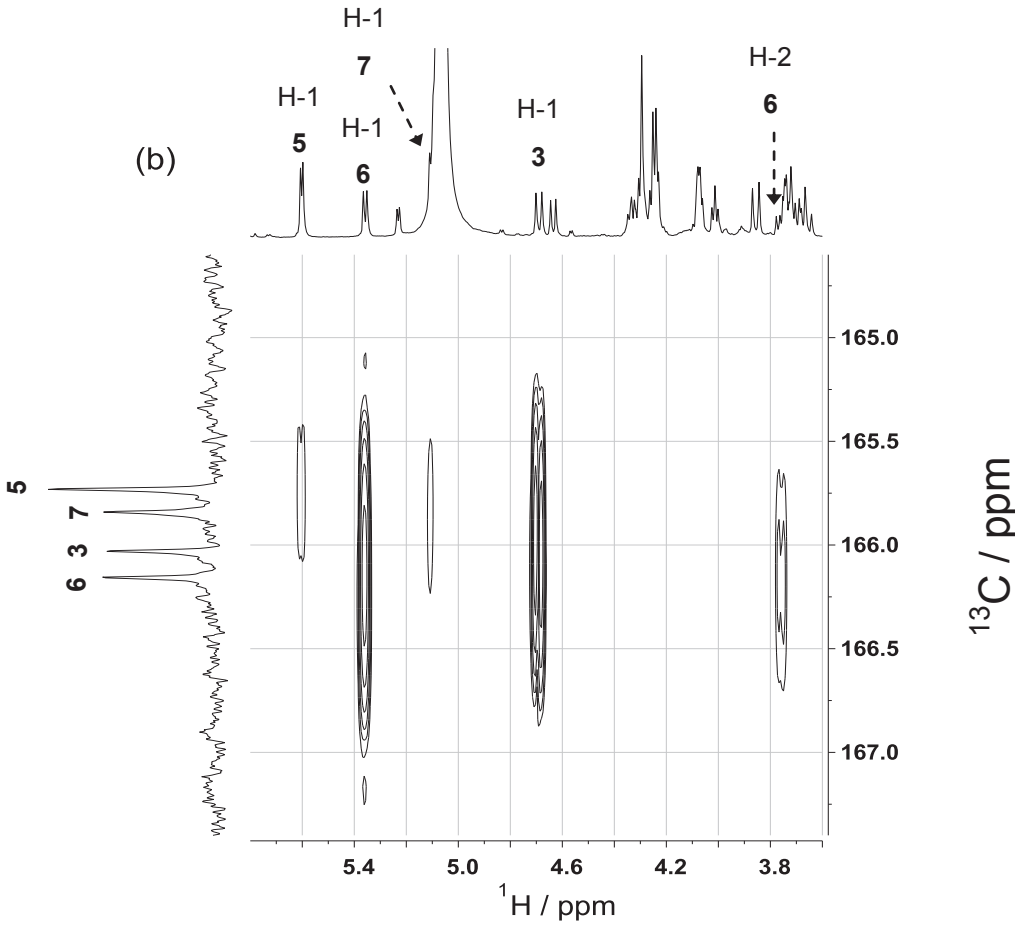

Figure 5.5 *(a) Selected three bond ^{1}H-^{1}H homonuclear correlations (799.975 MHz) and (b) long distance ^{1}H-^{13}C heteronuclear correlations (799.975-201.172 MHz) for a sample obtained after 15 min. of reaction at 30 ºC according to protocol **B**.5.06.* [22]

When the spectra of samples taken at intermediate reaction times are examined, a more complicated picture emerges (Figure 5.1(b)). In particular, five new doublets with a coupling constants ranging from 3.3 to 5.6 Hz appear between 4.5 and 5.6 ppm alongside the peaks due to the anomeric proton of the starting and final compounds. Also, an intense and complex multiplet occupies the region between 4.2 and 4.4 ppm. The nature of these new peaks was elucidated through several ^{1}H-^{1}H (gCOSY, TOCSY) and ^{1}H-^{13}C (gHSQC, gHMBC) correlation experiments and a total of 7 new compounds were identified (compounds **5** to **11**). The relative abundance of these species changes significantly after a few hours at 278 K in solution, and most of them disappear within 24 hours (*vide infra*). This is particularly true of compound **5**, whereas a small amount of compounds **6** and **9** is always observed alongside the main products **2** and **3**. In order to characterize these "transient" species, the use of a higher field spectrometer (800 MHz) equipped with a cryoprobe was necessary for most correlation experiments on samples taken at early reaction times. This way the total acquisition time

could be kept within 7 hours per tube without sacrificing signal intensity, and a higher resolution was attained. As a result, all new doublets appearing between 4.5 and 5.6 ppm could be assigned to anomeric protons. The value of $J_{1,2}$ (3.1-5.6 Hz) for compounds **5** to **10** is consistent with a *gauche* orientation of the vicinal protons, and the three-bond correlation of H1 to a $NHCO_2$ proton and carbon (Figure 5.5) demonstrates that **5**, **6**, and **7** are *N*-(glycosyl)carbamates. Additional weak doublets at 4.45 (d, 4.0 Hz), 4.77 (d, 2.9 Hz), and 5.73 ppm (d, 4.2 Hz) could not be assigned. Concerning compounds **6** and **9**, the chemical shift of C-5 (74.46 and 74.85 ppm respectively, compared to 74.55 ppm observed for $\mathbf{1}_{\alpha}$), the value of $J_{4,5}$ (10 and 9.1 Hz), and that of $J_{1,2}$ (5.5 and 4.4 Hz) point to a hexopyranose ring in a $^4C_1$ conformation and to an α configuration. Based on these results, we postulate that **6** and **9** are the α anomers of compounds **3** and **2**, respectively. Interestingly, in their paper on the synthesis of 1-*N*-glycyl-β-oligosaccharide derivatives, Manger et al. [10b] had already speculated that a low intensity doublet (4.79 ppm, $J_{1,2}$ = 5.1 Hz) appearing in the spectrum of β-GlcNAc-NH_2 prepared according to **A**.0.S was due to the α-anomer of the same molecule, but they did not investigate this hypothesis any further.

The multiplet ranging from 4.2 to 4.4 ppm was particularly difficult to interpret: According to ^{1}H-^{1}H TOCSY and ^{1}H-^{1}H COSY experiments, it only correlates with itself and with species **4** (2 H), **5** (2 H), **7** (3 H), **8** (1 H), and **10** (3 H), which contribute a total of 11 protons. Even so, the value of its integral indicates that other protons must be present. This is supported by one bond ^{1}H-^{13}C correlations, which show that 15 carbon atoms are linked to this group of protons, i.e. five more than could be expected from ^{1}H-^{1}H correlations. We conclude that the multiplet at 4.2-4.4 ppm contains all proton signals of yet another compound (**11**).

Unfortunately, it was not possible to determine the exact structure of intermediates **5**, **7**, **8**, **10** and **11** from the NMR data. The absence of secondary carbon signals in ^{13}C-DEPT135 spectra excludes the formation of ketofuranoses, while the occurrence of base-catalyzed epimerization at C2 was ruled out by examining the spectra of β-D-mannopyranuronosylamine **14** and the corresponding carbamate **15**. To this aim, a sample of D-mannurono-6,3-lactone **12** was hydrolyzed to D-mannuronic acid **13** under basic conditions (pD ≅ 9), and the latter product was reacted with a saturated solution of NH_4HCO_3 at RT (Scheme 5.3). After two days, the reaction was stopped and the gross product was analyzed by NMR.

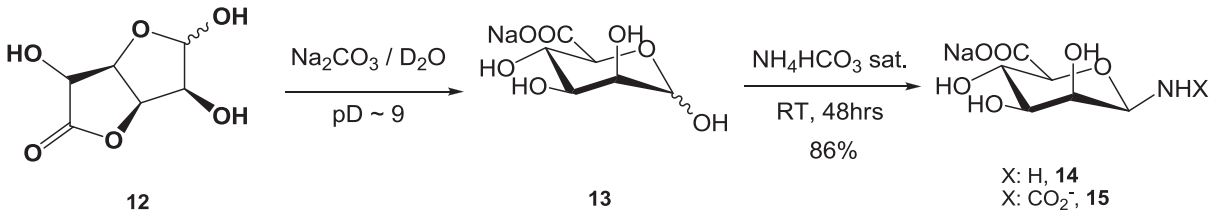

Scheme 5.3 *Reaction scheme for the synthesis of β-D-mannopyranuronosylamine **14** from D-mannurono-6,3-lactone **12**. Conditions: D-mannuronic acid (16 mg, 0.25 M), NH_4HCO_3 satd (360 μL), RT, 48 hrs (Entry 4, Table 5.4).*

Although the coupling constants of the anomeric peaks in the mannose series are small, yet well resolved peaks were obtained from ^{1}H-NMR which facilitated the structural elucidation of the product (Figure 5.6). The signals at 4.36 and 4.94 ppm were assigned to the anomeric peaks of the glycosylamine **14** and its carbamate **15** whose coupling constants (0.8 and 0.9 Hz) are comparable with that of the β anomer of the starting D-mannuronic acid (4.90 ppm, $J_{1,2}$ 0.9 Hz). Furthermore, the peak at 3.84 ppm (dd, $J_{1,2}$ 0.7 Hz, $J_{2,3}$ 2.1 Hz) was attributed to H2β-NH_2 whose coupling constant together with its integration match that of H1β-NH_2 (4.36 ppm, $J_{1,2}$ 0.8 Hz). Unfortunately, the peak at 3.89 ppm is not well resolved and it is suspected to be H2β-$NHCO_2^-$. At the end of the reaction the molar composition of the reaction mixture was: **14** (55 %), **15** (31 %), **13** (6 %) and 8 % for two by-products detected at 4.77 and 5.30 ppm. From the HMQC (see Appendix 5.A, Figure 5.43) the by-product at 4.77 ppm (d, *J* 4.6 Hz) correlates with a carbon at 84.4 ppm. However the by-product at 5.30 ppm (*J* 2.7 Hz) did not show any correlation to a carbon which suggests that this intermediate species has disappeared throughout the analysis in the favor of either the by-product at 4.77 ppm or the glycosylamine **14** and its carbamate **15**. Moreover, the latter transformation is possible since the carbon analysis that preceded the HMQC was acquired at 298 K for ~ 3 hours and at that temperature partial hydrolysis of a glycosylamine could take place. By crossing these data with the NMR data of the α anomers of D-glucopyranuronosylamine and its carbamate (**6** and **9**) we notice that these 2 by-products at 4.77 and 5.30 ppm could be assigned to the α anomers of D-mannopyranuronosylamine **14** and its carbamate **15**. The latter conclusion should be further proved since the coupling constant of the peak at 4.77 ppm is quite high (4.6 Hz).

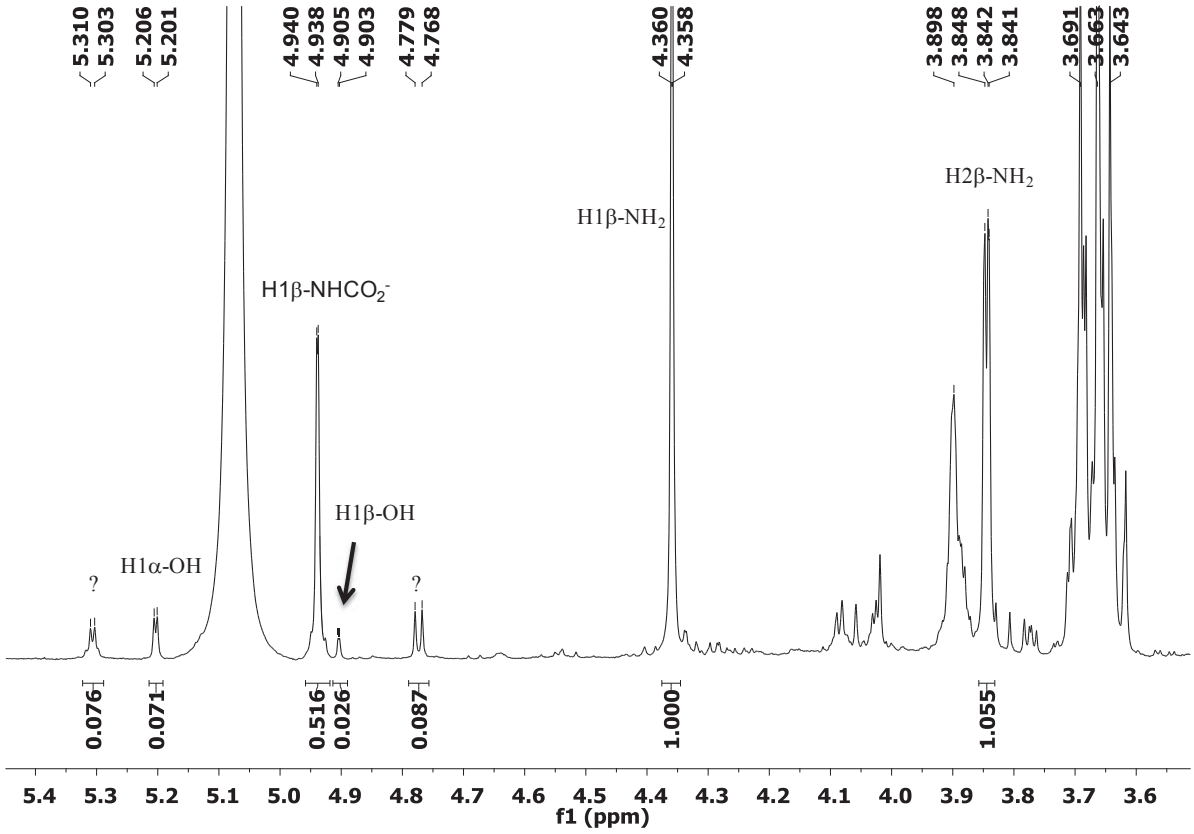

Figure 5.6 *^{1}H-NMR spectrum of the gross reaction mixture of β-D-mannopyranuronosylamine **14** (Entry 4, Table 5.4). Conditions: 400 MHz, D_2O, 2 % w/w, 273 K, ns = 32, D1 = 3s. Composition: **14** +**15** (86%), **13** (6%), by-products (8%).*

The ^{13}C-NMR spectra of the starting D-mannuronic acid and its corresponding glycosylamine are shown in Figure 5.7. C1β-NH_2 (85.2 ppm), its carbamate (C1β-$NHCO_2^-$ 83.4 ppm) and C2β-NH_2 (73.9 ppm) were assigned from the HMQC spectrum while C3, C4 and C5 were assigned according to literature. [23] From both the ^{1}H and ^{13}C NMR spectra, the absence of peaks corresponding to D-glucuronic acid (C1α 94.8 ppm and C1β 98.6 ppm) and to β-D-glucopyranuronosylamine **2** (H1β 4.1 ppm) or its carbamate **3** (H1β 4.70 ppm, C1β 85.7 ppm) confirm the hypothesis that no base catalyzed epimerization took place at C2 for either D-mannuronic acid or its glycosylamine **14**.

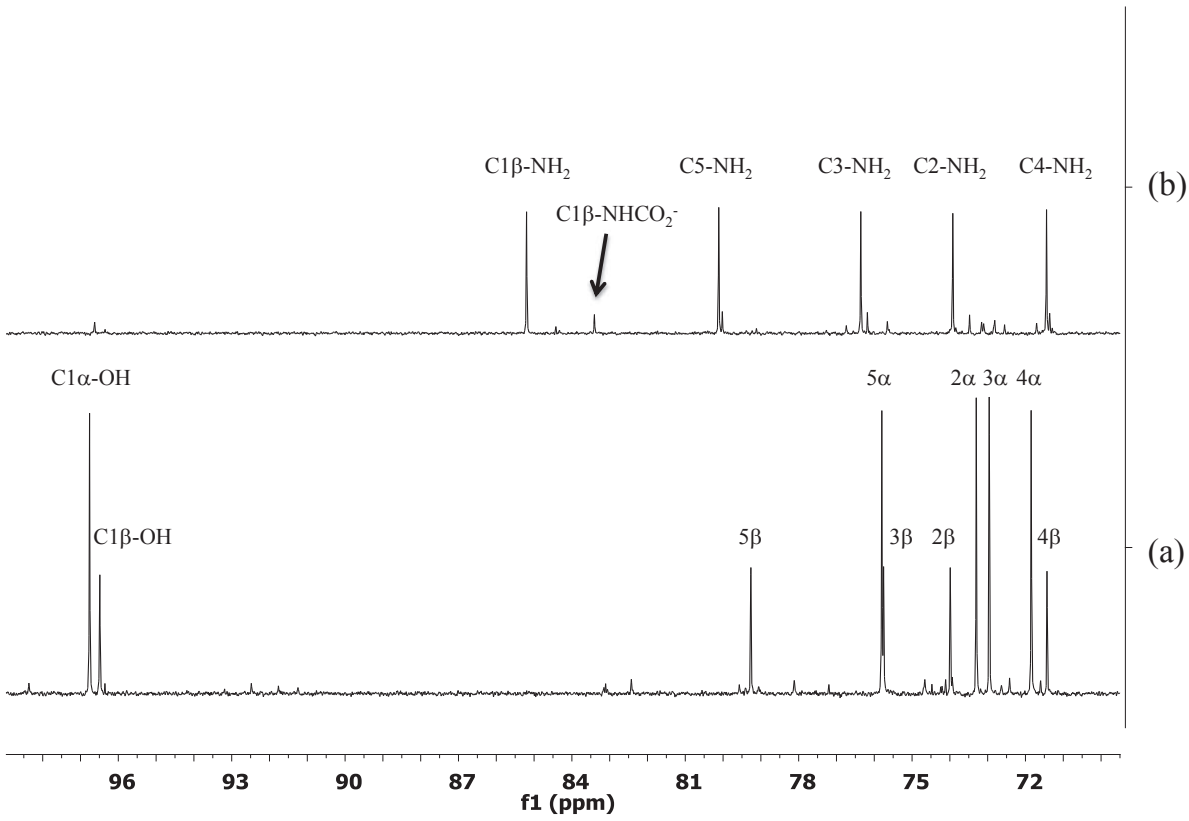

Figure 5.7 *^{13}C-NMR spectra of the gross products of (a) starting α/β-D-mannuronic acid and (b) β-D-mannopyranuronosylamine **14** and its carbamate **15**. Conditions: 100 MHz, D_2O, 2%w/w, 298 K, ns = 2000, D1 = 3 s.*

The most likely hypothesis is the formation of furanose derivatives. The mechanism of formation of glycosylamines involves the opening of the starting aldose ring to give an acyclic aldehyde which in then transformed into an imine followed by ring closure. [24] It is reasonable to assume that kinetically favored furanose forms will initially be more populated than the thermodynamically favored pyranose forms (*vide infra*). Unsubstituted furanose derivatives of D-glucuronic acid are not described in the literature, but assignments of ^{13}C-NMR spectra are available for methyl-α/β-D-glucofuranoside [25] and β-D-glucofuranose. [26] Even so, comparison with our data is tricky. The chemical shift of C2 is the best candidate for this type of analysis; provided that the substituent on C1 is not *N*-carbamate (e.g. δ C2 is 76.6 and 76.7 ppm for $\mathbf{1_\beta}$ and **2** respectively, but 74.6 ppm for **3**). This excludes its applicability to compounds **5** and **7**. Of the remaining unknown species, δ C2 was only assigned in the case of **10** (83.15 ppm), and a difference of +1.5 ppm with respect to methyl-β-D-glucofuranoside and +1.05 ppm with respect to β-D-glucofuranose is observed.

Table 5.2 *NMR characterization of the species observed during the amination of* D*-glucuronic acid in aqueous solution.*

Compound	Nature	δ ^{1}H / ppm (m, *J*/Hz, assignment)	δ ^{13}C / ppm (assignment)
1$_{\alpha}$ [a]	α-aldopyranose	5.23 (d, 3.7, H1), 3.56 (dd, 9.8, 3.8, H2), 3.72 (m, H3), 3.48 (H4), 4.08 (d, 10.1, H5)	94.81 (C1), 73.99 (C2), 75.26 (C3), 74.79 (C4), 74.55 (C5), 179.62 (C6)
1$_{\beta}$ [a]	β-aldopyranose	4.63 (d, 8.0, H1), 3.27 (m, H2), 3.50 (H3), 3.51 (m, H4), 3.72 (H5)	98.57 (C1), 76.70 (C2), 78.25 (C3), 74.53 (C4), 78.93 (C5), 178.64 (C6)
2 [a]	β-glycopyranosylamine	4.09 (d, 8.8, H1), 3.18 (dd, 9.0, H2), 3.48 (H3), 3.48 (d, 9.5, H4), 3.69 (m, H5)	87.68 (C1), 76.76 (C2), 79.03 (C3),74.71 (C4), 79.92 (C5), 179.14 (C6)
3 [a]	*N*-(β-glycopyranosyl) carbamate	4.70 (d, 9.1, H1), 3.34 (t, 9.0, H2), 3.52 (H3), 3.48 (H4), 3.73 (d, 9.4, H5), 6.25 (d, 9.8, $NHCO_2$)	85.68 (C1), 74.64 (C2), 79.02 (C3), 74.55 (C4), 79.87 (C5), 178.88 (C6), 165.86 ($NHCO_2$)
4 [b]	di-(β-glycopyranosyl)amine	4.29 (d, 8.8, H1), 3.27 (H2)	89.51 (C1); 76.80 (C2), 179.60 (C6)
5 [c]	*N*-glycosyl carbamate	5.63 (d, 3.6, H1), 4.07 (H2), 4.27, 4.32, 5.79 (10.0, $NHCO_2$)	86.97 (C1), 77.85 (C2), 181.40 (C6), 165.73($NHCO_2$)
6 [c]	*N*-(α-glycopyranosyl) carbamate	5.37 (d, 5.5, H1), 3.76 (H2), 3.66 (H3), 3.46 (H4), 3.86 (d, 10.0, H5) 6.15 (d, 9.5, $NHCO_2$)	82.17 (C1), 72.31, 75.49, 74.46 (C5), 179.89 (C6), 166.15 ($NHCO_2$)
7 [c]	*N*-glycosyl carbamate	5.12 (d, 5.0, H1), 4.01 (t, 4.79, H2), 4.27, 4.28, 4.36, 6.14 (d, 9.9, $NHCO_2$)	89.45 (C1), 81.69 (C2), 165.84 ($NHCO_2$)
8 [d]	unknown	5.03 (d, 3.1, H1), 3.97 (m, H2), 4.29	89.49 (C1)
9 [c]	α-glycopyranosylamine	4.84 (d, 4.4, H1), 3.67 (H2), 3.70 (H3), 3.55 (H4), 4.01 (d, 9.1, H5)	83.56 (C1), 73.21, 74.57, 74.85 (C5), 179.84 (C-6)
10 [c]	unknown	4.58 (d, 3.3, H1), 3.91 (H2), 4.23, 4.30, 4.32	92.76 (C1), 83.15 (C2)
11 [c]	unknown	4.2-4.4 (m) [e]	Five among the following: 73.21, 73.48, 73.98, 74.25, 74.40, 74.85, 77.50, 78.22, 78.76, 78.86, 79.02, 82.17, 82.29, 83.17

Assignment based on spectra acquired at: [a] 298 K; [b] 298 (^{1}H) and 280 K (^{13}C); [c] 278 K; [d] 288 (^{1}H) and 278 K (^{13}C). [e] Peaks due to compounds **4** (2 H), **5** (2 H), **7** (3 H), **8** (1 H), and **10** (3 H) are found in the same region. Unassigned peaks: ^{1}H (δ / ppm) 4.45 (d, 4.0 Hz), 4.77 (d, 2.9 Hz), 5.73 (d, 4.2 Hz) visible in some concentrated solutions of intermediate samples. ^{13}C (δ / ppm) 181.40, 181.31, 181.09.

5.3.2 Structural elucidation of by-products formed during the amination of D-glucuronic acid: MS study

The identity of species **5** to **11** was further investigated by mass spectrometry. To this end, freeze-dried gross products were redissolved in deionised water and immediately infused through the ESI interface at constant flow rate. Figure 5.8 shows the evolution of the ESI-MS spectrum when going from the starting compound (a) to the gross final product (c) via a sample rich in transient species (b). In negative ion mode, three characteristic peaks are present for D-glucuronic acid which correspond to the uronate anion (*m/z* 193, $[M-H]^-$) and to two cluster ions (*m/z* 387, $(\mathbf{1}_H)_2$, $[M-H]^-$; 409, $(\mathbf{1}_{Na})\mathbf{1}_H$, $[M-H]^-$). Similar ions can be identified in the spectrum of **2+3** (*m/z* 192, 385, 407) by taking into account the difference of 1 Da between starting and final compound. Also, two peaks are visible that can be ascribed to di(glycosylamine) **4** (*m/z* 368 $\mathbf{4}_{H,H}$, $[M-H]^-$; 390, $\mathbf{4}_{Na,H}$, $[M-H]^-$), whereas peaks at *m/z* 207, 209, and 223 could not be assigned. Concerning the sample rich in unknown species (b), its MS spectrum appears as a combination of the spectrum of **1** and of **2+3**, with the added complication of "mixed" cluster ions having a monoisotopic mass identical to that of the most abundant isotopologue cluster ions of **2**. For instance *m/z* 386 ($(\mathbf{1}_H)\mathbf{2}_H$, $[M-H]^-$) and 408 ($(\mathbf{1}_{Na})\mathbf{2}_H$, $[M-H]^-$). Similar considerations can be made for the spectra in positive ion mode (Figure 5.8), where the most intense peaks are those for ($\mathbf{2}_{Na}$) (*m/z* 216, $[M+H]^+$; *m/z* 238, $[M+Na]^+$). A complete list of the peaks observed for each type of sample, together with their assignment, is reported in Table 5.3. By examining this table, it becomes apparent that all peaks observed for the intermediate sample are also present either in the spectrum of the starting compound, or in that of the final product. This proves that species **5** to **11** are isomers of **2** and **3**, and since they have completely different NMR spectra, we conclude that they are constitutional isomers and/or diastereomers of the major products.

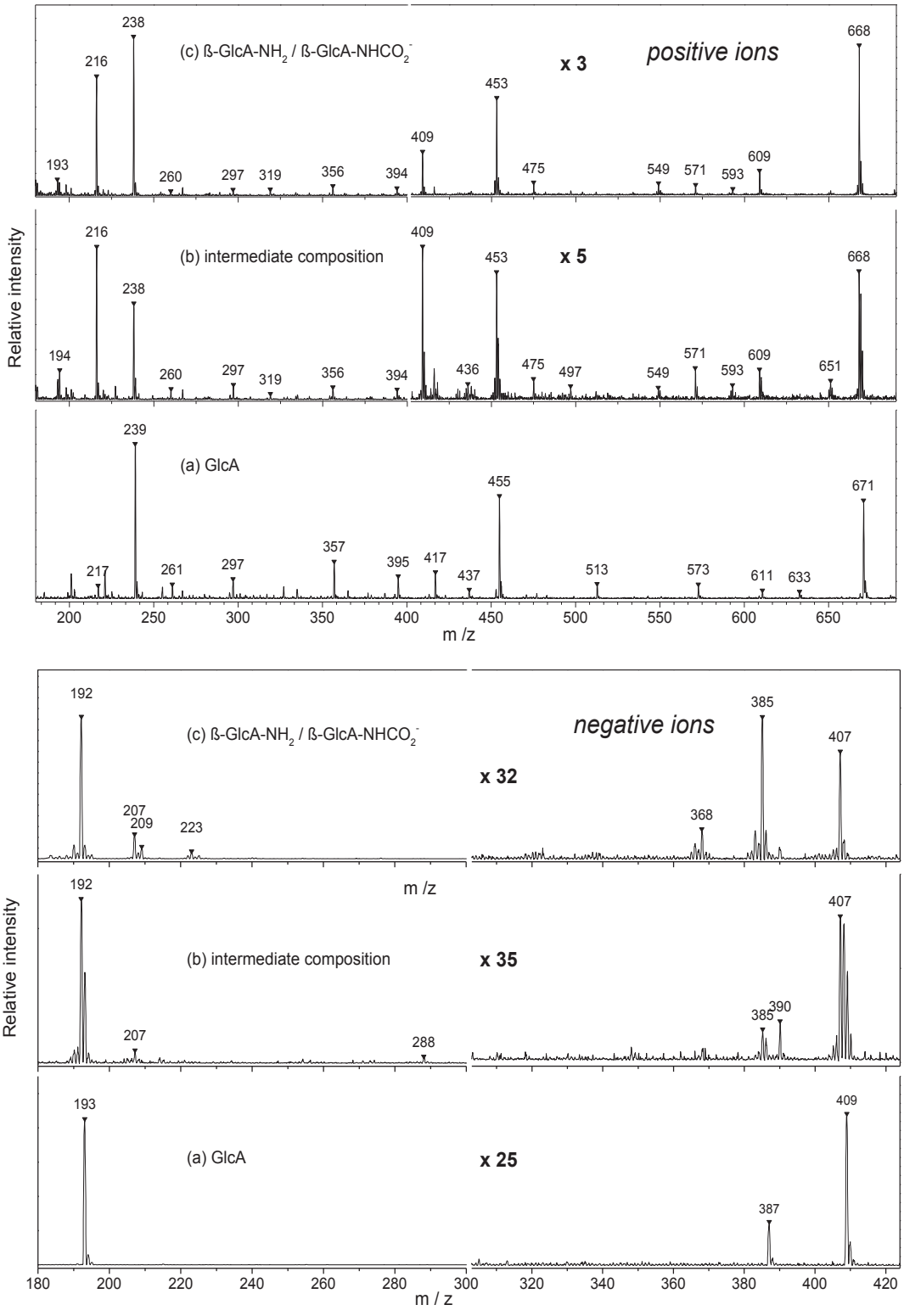

Figure 5.8 *ESI-MS spectrum of **1** (a), a sample containing 65 % transient species (b),* [27] *and **2+3** (c).* [28] *Positive (top) and negative (bottom) ions are shown. In some cases the intensity of the peaks on the right-hand side of the spectrum was magnified.*

Table 5.3 *List of ESI-MS peaks and their assignments.*

m/z		Structure	Ionisation		Spectrum of observation		
Experimental	**Monoisotopic ion mass**				**1**	**Intermediate** [a]	**2 / 3** [b]
192	192.1	$\mathbf{2}_{H}$	-	$[M-H]^-$		✓	✓
193	193.0	$\mathbf{1}_{H}$	-	$[M-H]^-$	✓	✓	
194	194.1	$\mathbf{2}_{H}$	+	$[M+H]^+$	✓	✓	
207		?	-	?		✓	✓
209		?	-	?			✓
216	216.0	$\mathbf{2}_{Na}$	+	$[M+H]^+$		✓	✓
217	217.0	$\mathbf{1}_{H}$	+	$[M+Na]^+$	✓		
223		?	-	?			✓
225		?	-	?			✓
238	238.0	$\mathbf{2}_{Na}$	+	$[M+Na]^+$		✓	✓
	238.0	$\mathbf{3}_{H, H}$	+	$[M+H]^+$			
239	239.0	$\mathbf{1}_{Na}$	+	$[M+Na]^+$	✓	✓	
260	260.0	$\mathbf{3}_{H, H}$	+	$[M+Na]^+$		✓	✓
261		?	+	?	✓		
267		?	+	?		✓	✓
297		?	+	?	✓	✓	✓
319		?	+	?		✓	✓
356		?	+	?		✓	✓
357		?	+	?	✓		
368	368.1	$\mathbf{4}_{H,H}$	-	$[M-H]^-$			✓
385	385.1	$(\mathbf{2}_{H})_2$	-	$[M-H]^-$		✓	✓
387	387.1	$(\mathbf{1}_{H})_2$	-	$[M-H]^-$	✓		
390	390.1	$\mathbf{4}_{Na,H}$	-	$[M-H]^-$		✓	✓
394		?	+	?		✓	✓
395		?	+	?	✓		
407	407.1	$(\mathbf{2}_{Na})\mathbf{2}_{H}$	-	$[M-H]^-$		✓	✓
409	409.2	$(\mathbf{2}_{Na})\mathbf{2}_{H}$	+	$[M+H]^+$	✓	✓	
	409.1	$\mathbf{4}_{Na, NH4}$	+	$[M+H]^+$			
417		?	+	?	✓		
437		?	+	?	✓		

452	452.2	$\mathbf{4}_{Na,\ Na}$	+	$[M+K]^+$		✓	✓
453	453.1	$(\mathbf{2}_{Na})_2$	+	$[M+Na]^+$		✓	✓
455	455.0	$(\mathbf{1}_{Na})_2$	+	$[M+Na]^+$	✓		
475		?	+	?		✓	✓
497		?	+	?		✓	✓
549		?	+	?		✓	✓
513		?	+	?	✓		
571		?	+	?		✓	✓
593		?	+	?		✓	✓
609		?	+	?		✓	✓
611		?	+	?	✓		
633		?	+	?	✓		
651		?	+	?		✓	✓
668	668.1	$(\mathbf{2}_{Na})_3$	+	$[M+Na]^+$		✓	✓
671	667.1	$(\mathbf{1}_{Na})_3$	+	$[M+Na]^+$	✓		

[a] Sample obtained after 15 min of reaction at 30 ºC according to protocol B.5.06 (AG10-08); the initial mole fraction of intermediate species was 65 %. [b] Sample obtained after 48 hrs at 30 ºC according to protocol **B**.0.S (AG10-20_P1_end); the initial mole fraction of **2**+**3** was 89 %.

5.3.3 Quantification of compounds formed during the amination of D-glucuronic acid

The mole fraction of each species observed during the course of the reaction was determined from the proton spectra on the basis of the assignment reported in Table 5.2. To this end, we assumed that each signal in the ^{1}H-NMR spectrum is due to a CH- group, i.e. that there was no rearrangement of C-H bonds during the reaction. This idea is supported by the absence of signals attributable to $R_2C{=}O$ or RCH_2-OH carbons in standard ^{13}C-NMR and DEPT135 spectra. A normalizing constant "S" was then calculated according to the formula:

$$S = \sum_{i=1}^{12} \frac{A_{\delta}^{i}}{n_{\delta}^{i}} = A_{5.23}^{1\,\alpha} + A_{4.63}^{1\,\beta} + A_{3.18}^{2} + A_{4.70}^{3} + \frac{\left(A_{3.27} - A_{4.63}^{1\,\beta}\right)}{2} + A_{5.63}^{5} + A_{5.37}^{6} + A_{5.13}^{7} + A_{4.84}^{9} + A_{4.58}^{10} + \frac{\left(A_{4.20-4.40} - A^{4} - 2\,A_{5.63}^{5} - 3\,A_{5.13}^{7} - 3\,A_{4.58}^{10}\right)}{5} \quad (5.1)$$

where A_{δ}^{i} indicates the area of the methine signal of compound *i* having a chemical shift δ (ppm), and n_{δ}^{i} is the number of such methine groups in species *i* (e.g. there are two equivalent H2 protons in diglycosylamine **4**). It should be noted that since the H2 signal of **4** superimposes with that of $\mathbf{1}_{\beta}$, the former was corrected by subtracting the integral of anomeric proton of $\mathbf{1}_{\beta}$ at 4.63 ppm. Also, the contribution of species **8** and **11** was combined in the last factor since neither can be quantified individually. The mole fraction *x* of each species (with the exception of **8** and **11**) is then calculated from:

$$x^{i} = \frac{A_{\delta}^{i} \,/\, n_{\delta}^{i}}{S} \tag{5.2}$$

Based on this formula we calculated that, depending on the protocol, between 64 % (**A**.1.06) and 89 % (**B**.0.S) of product **2**+**3** is obtained after 24 hours of reaction at 30 ºC, whereas the fraction of diglycosylamine **4** varies between 0 and 3 %. An experiment was also carried out in which an early reaction sample (15 min.) was isolated by freeze-drying, redissolved in D_2O, and monitored by ^{1}H-NMR at 278 K. Figure 5.9 shows the evolution of its composition with time: Just after dissolution, the sample was a complex mixture of all species identified in the system with the sole exception of diglycosylamine **4**. The major single components were D-glucuronic acid **1** (22 %), compound **5** (27 %), and compound **7** (12 %). In the following 7 hours though, unknown species **5**, **7**, and **10** all but disappear; compounds **8**+**11** fall to 3 %, and a small fraction of diglycosylamine **4** forms. At the same time, the proportion of **2**+**3** and **6**+**9** increases steadily from 12 and 11 % to 39 and 30 %, respectively, whereas the fraction of D-glucuronic acid **1** remains virtually constant. Since all sources of ammonia were removed from the sample before the beginning of the experiment, this result indicates that unknown compounds **5**, **7**, **8**, **10**, and **11** are precursors to **2**, **3**, **6**, and **9**, and that they spontaneously transform in the latter compounds upon standing in solution. Concerning species **6** and **9**, their combined proportion is initially identical to that of **2** and **3** (11-12 %), it attains a maximum around 7 hours after dissolution (30 %) and diminishes slowly in the following days to the advantage of **2** and **3**: This behavior is consistent with the mutarotation of an α-glycosylamine into the more stable β anomer, both species being in equilibrium with the respective *N*-glycosylcarbamate. As a result, after five days at 5 ºC the sample contained 69 % of product, 25 % of the starting D-glucuronic acid, 1 % of diglycosylamine, and just 5 % of all other

species combined. Based on this experiment, we propose the reaction scheme reported in Scheme 5.1.

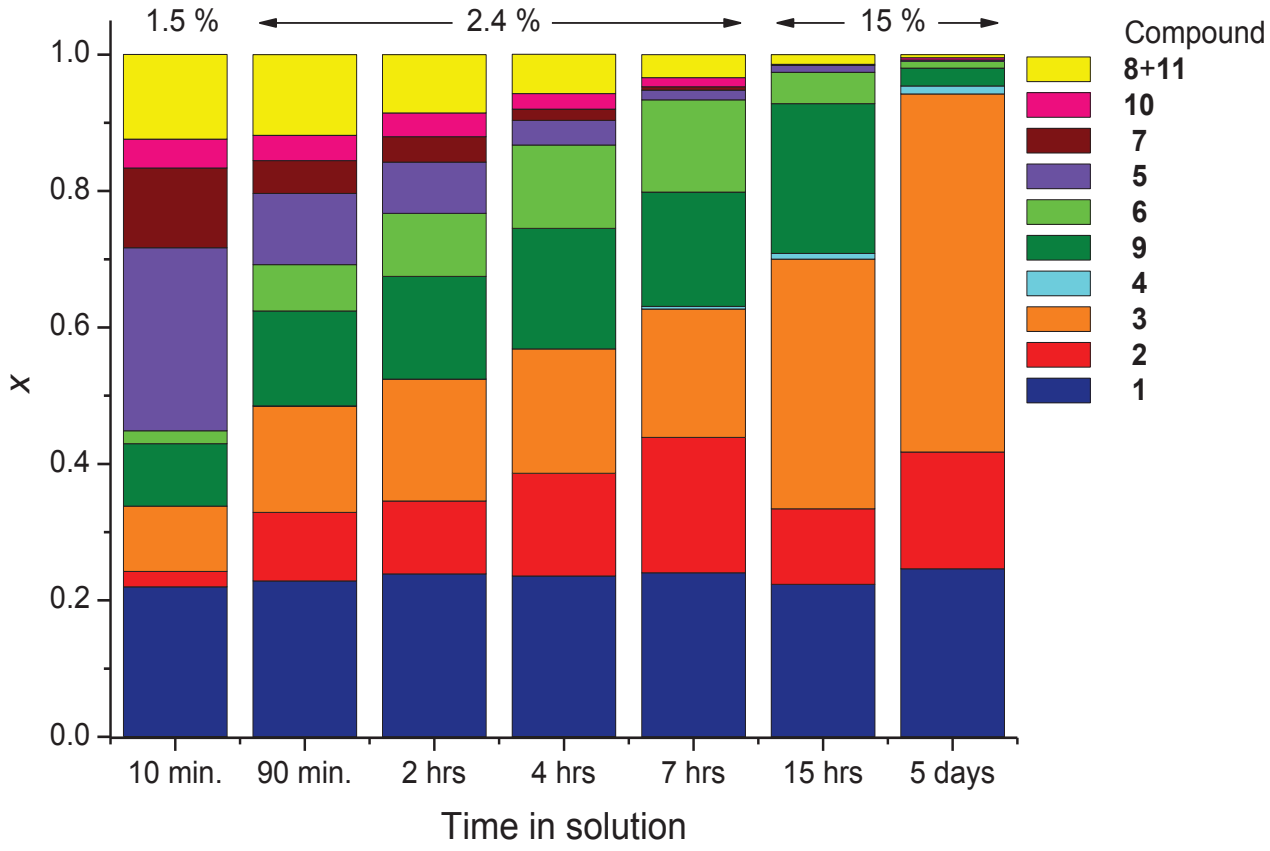

Figure 5.9 *Evolution of the composition with time for a sample obtained after 15 min. of reaction, isolated by freeze-drying, and redissolved in D_2O at 278 K. The percentage values annotated over the graph specify the mass concentration of the sample in solution.* [29]

These results show that species **5**, **7**, **8**, **10**, and **11** are kinetically favored but thermodynamically unstable, and that they disappear after ~24 hours in solution at low temperature in favor of the more stable D-glucopyranuronosylamine **2**/**9** and *N*-(D-glucopyranuronosyl carbamate **3**/**6**. As a consequence, the occurrence of base-catalyzed epimerization as a mechanism for the formation of transient species can be safely ruled out: A catalyst only lowers the activation energy of a reaction and accelerates the formation of a product which is more (or at least comparably) stable. To accommodate the occurrence of epimerization we should consider that **1** is initially transformed into a more stable epimer, that the latter is aminated, and that the resulting glycosylamine is back-epimerized to the more stable α/β-D-glucopyranuronosylamine **2**/**9**. That is a highly unlikely reaction pathway.

5.3.4 Kinetic study on a sample uronic acid (GlcA)

Sodium D-glucuronate **1** was reacted with ammonia and/or volatile ammonium salts (NH_4HCO_3 or $NH_2CO_2NH_4$) in water according to 18 different protocols at 30 and 40 ºC (Scheme 5.1). For comparison, some protocols were also applied to D-glucose. The exact experimental conditions used and the final composition of the gross products are summarized in Table 5.4 (see also the Experimental part for the meaning of protocol numbering). Samples were drawn at preset reaction times, frozen in liquid nitrogen and freeze-dried overnight to eliminate water and most of the salts. No further purification was performed and all reported analyses refer to the gross products obtained this way. In order to monitor the time course of the reaction, individual samples were redissolved in cold D_2O to afford clear solutions of pD $\cong$ 9 that were immediately analyzed by ^1H NMR. Spectra were acquired at 278 K in order to inhibit hydrolysis of the product and to prevent the peak of residual HDO from interfering with integration.

Table 5.4 *Summary of the amination experiments described in this chapter.* [a]

Entry	Protocol [b]	Substrate	T (°C)	$[NH_3]_0$ (M)	Salt	$[salt]_0$ (M)	$[salt]_0$ / $[subst.]_0$	Highest yield (%)			Experiment code
								Time (hrs)	β-carbNHX [c]	By-products [d]	
1	**A**.0.S	GlcA	30	-	NH_4HCO_3	satd (~3.6) [e]	~18	24	75 (19)	11	AG10-20_P2
2		Glc	30	-	NH_4HCO_3	satd (~3.6) [e]	~18	168 [f]	64 (14)	10	AG10-06_P3
3		GlcA	40	-	NH_4HCO_3	satd (>3.6) [e]	>18	7.5	78 (22)	9	AG10-17_P3
4		ManA [h]	~23	-	NH_4HCO_3	satd (>3.6) [e]	~18	48	86 (55)	8	AG09-21
5	**A**.1.06	GlcA	30	1	NH_4HCO_3	0.60	3	33 [f]	67 (21)	21	AG09-31_P2
6	**A**.5.02	GlcA	30	5	NH_4HCO_3	0.20	1	32.5 [f]	80 (34)	15	AG09-12
7		GlcA	40	5	NH_4HCO_3	0.20	1	9.5	75 (22)	16	AG10-17_P4
8		$ManA_5$ [h]	30	5	NH_4HCO_3	0.20	4	3	70 (42)	2	AG10-21-P1
9		$GulA_5$ [h]	30	5	NH_4HCO_3	0.20	4	3	35 (18)	2	AG10-21-P2
10		$ManA_5$ [h]	~24	5	NH_4HCO_3	0.20	4	24	88 (48)	7	AG10-24-P1
11		$GulA_5$ [h]	~24	5	NH_4HCO_3	0.20	4	72	86 (41)	9	AG10-24-P2
12	**A**.5.06	GlcA	30	5	NH_4HCO_3	0.60	3	33 [f]	84 (17)	15	AG09-30_P3
13	**A**.9.06	GlcA	30	8.8	NH_4HCO_3	0.60	3	33	86 (17)	13	AG10-01_P2
14	**A**.14.02	GlcA	30	14.5	NH_4HCO_3	0.20	1	33 [f]	84 (28)	13	AG09-32_P2
15		Glc	30	14.5	NH_4HCO_3	0.20	1	168 [f]	82 (22)	13	AG10-06_P4
16	**B**.0.10	GlcA	~30 [g]	-	$NH_2CO_2NH_4$	1.0	5	24	69 (47)	8	AP10-18_1M
17	**B**.0.20	GlcA	~30 [g]	-	$NH_2CO_2NH_4$	2.0	10	24	84 (51)	8	AP10-18_2M
18	**B**.0.30	GlcA	~30 [g]	-	$NH_2CO_2NH_4$	3.0	15	24	87 (45)	8	AP10-18_3M
19	**B**.0.40	GlcA	~30 [g]	-	$NH_2CO_2NH_4$	4.0	20	24	89 (47)	8	AP10-18_4M
20	**B**.0.50	GlcA	~30 [g]	-	$NH_2CO_2NH_4$	5.0	25	24	88 (48)	8	AP10-18_5M
21	**B**.0.S	GlcA	30	-	$NH_2CO_2NH_4$	satd (>5.4) [e]	>27	5.5	89 (23)	9	AG10-20_P1
22		Glc	30	-	$NH_2CO_2NH_4$	satd (>5.4) [e]	>27	96	87 (6)	13	AG10-06_P1
23		GlcA	40	-	$NH_2CO_2NH_4$	satd (>5.4) [e]	>27	1.5	87 (29)	11	AG10-17_P1

24	**B**.1.06	GlcA	30	1	$NH_2CO_2NH_4$	0.60	3	33 [f]	79 (22)	19	AG09-31_P1
25	**B**.5.02	GlcA	30	5	$NH_2CO_2NH_4$	0.20	1	32.5 [f]	80 (32)	15	AG09-13
26		GlcA	40	5	$NH_2CO_2NH_4$	0.20	1	24	75 (19)	13	AG10-17_P2
27		$ManA_9$ [h]	~23	5	$NH_2CO_2NH_4$	0.20	4	72	~80 (~80) [i]	n.d	AG11-19-P1
28		$GulA_{10}$ [h]	~23	5	$NH_2CO_2NH_4$	0.20	4	96	77 (77)	6	AG11-19-P2
29	**B**.5.06	GlcA	30	5	$NH_2CO_2NH_4$	0.60	3	33	84 (12)	14	AG09-30_P2
30	**B**.9.06	GlcA	30	8.8	$NH_2CO_2NH_4$	0.60	3	33 [f]	86 (17)	12	AG10-01_P1
31	**B**.14.02	GlcA	30	14.5	$NH_2CO_2NH_4$	0.20	1	33 [f]	86 (31)	12	AG09-32_P1
32		Glc	30	14.5	$NH_2CO_2NH_4$	0.20	1	168 [f]	81 (25)	14	AG10-06_P2
33	**X**.14.00	GlcA	30	14.5	-	-	-	48 [f]	82 (78)	16	AG10-11
34		Glc	30	14.5	-	-	-	48 [f]	33 (32)	33	AG10-19

[a] Note: $[s]_0$ indicates the initial concentration of species "s". Unless otherwise specified, $[carb]_0$=0,20 M. [b] The numbering of each protocol withhold the experimental conditions used. Hence **A**.1.06 indicates that the salt used was NH_4HCO_3 ("**A**"), and that the initial concentration of ammonia and salt was 1 and 0.6 M, respectively. In this context, "**X**" indicates that no salt was added and "S" stands for "saturated". [c] Total glycosylamine plus N-glycosyl carbamate; the parenthetical value indicates the yield in free glycosylamine. [d] Total by-products 4-11. [e] Solubility in water: NH_4HCO_3, 284 g kg-1 at 30 °C; $NH_2CO_2NH_4$, 423 g L-1 at 20 °C. [f] End of reaction. [g] Ambient temperature, [h] $[ManA]_0$ = 0.25 M, $[ManA_5]_0$ = 0.05 M, $[GulA_5]_0$ = 0.05 M, $[ManA_9]_0$ = 0.05 M, $[GulA_{10}]_0$ = 0.05 M, [i] conversion.

Figure 5.10 shows the evolution of the proton spectrum with time during the reaction of **1** with 5 M ammonia and 0.6 M ammonium carbamate, as well as the assignment of the peaks used for integration. From these spectra it is clear that, with the exception of **8** and **11**, at least one diagnostic peak per each species can be accurately integrated.

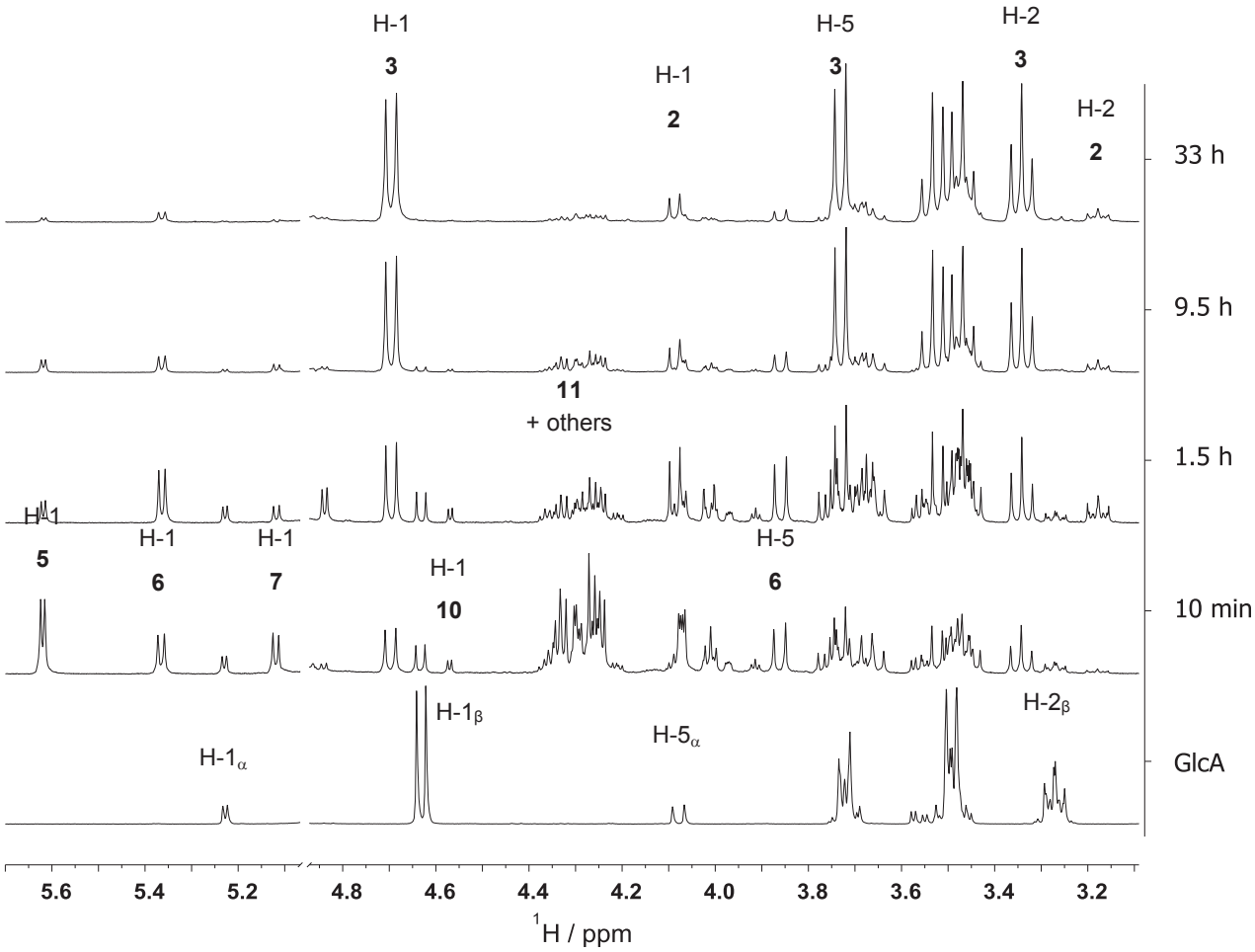

Figure 5.10 *Evolution of the 1D ^{1}H spectrum (400.13 MHz) with time during the transformation of D-glucuronic acid **1** into a mixture of **2** and **3** according to protocol **B**.5.06. The assignment of some peaks is also shown.* [30]

The mole fraction of each compound was then calculated from the proton spectra based on Eq. 5.2. As before, we assumed that each signal in the ^{1}H NMR spectrum is due to a CH-group, *i.e.* that there was no rearrangement of C-H bonds during the reaction. This idea is supported by the absence of signals attributable to $R_2C{=}O$ or RCH_2-OH carbons in ^{13}C and DEPT-135 NMR spectra. It should be noted as well that since the H2 signal of **4** superimposes with that of $\mathbf{1_\beta}$, the former was corrected by subtracting the integral of anomeric proton of $\mathbf{1_\beta}$ at 4.63 ppm. Also, the contribution of species **8** and **11** was combined in the last factor since neither can be quantified individually. Compound **3** forms from the reaction of **2** with the CO_2 liberated by the decomposition of bicarbonate or carbamate anions. [9b, 10b] Since

it decomposes fairly easily upon standing in aqueous solution and/or during repeated freeze drying cycles, [10b] its proportion was included in the calculation of product yields in Table 5.4. Also, throughout this report compound **4** and intermediate species **5-11** will be all considered as by-products of the synthesis of β-D-glucopyranuronosylamine **2**, unless otherwise specified.

As mentioned above, all methods reported in the literature for the synthesis of glycosylamines in aqueous or aqueous methanol solution (Table 5.1) involve the use of volatile ammonium salts that release CO_2 upon decomposition (carbonate, bicarbonate or carbamate) and trap the product as the more stable *N*-glycosylcarbamate. [31] The rationale behind this choice is that studies published in the period 1950-1970 demonstrate that, upon standing in concentrated aqueous ammonia, carbohydrates degrade and epimerize to give a large number of compounds [32] of which the corresponding glycosylamines are sometimes a minor component. Since none of these reports focused on uronic acids though, we decided to react D-glucose and D-glucuronic acid with commercial aqueous ammonia (~14.5 M) at 30 ºC and to analyze the gross products by NMR (protocol **X**.14.00 in Table 5.4). As expected, in the case of glucose equal amounts of by-products and of glycosylamine / *N*-glycosylcarbamate formed: 21 % and 33 % after 25 and 48 hours, respectively. By contrast, for the same reaction times D-glucuronic acid afforded 70 % and 82 % of **2**+**3**, with only 20 % and 16 % of by-products. The latter result is rather positive, especially taking into account the simplicity of the procedure, and will be used as benchmark for all other protocols tested.

5.3.4.1 Saturated salt and concentrated ammonia protocols

We began our study by comparing the kinetics obtained with a saturated solution of $NH_4^+HCO_3^-$ *i.e.* the original protocol of Kochetkov and collaborators (**A**.0.S; entries 1 and 2 in Table 5.4), [7g] with those obtained with a saturated solution of ammonium carbamate (**B**.0.S; entries 21 and 22 in Table 5.4), which is less stable and thus easier to eliminate by freeze-drying. [11b] Surprisingly, when judged from the time required to obtain a 67% of **2**+**3**, the carbamate protocol was about 9 times faster than the bicarbonate one (Figure 5.11). Moreover, the equilibrium (plateau) fraction of **2**+**3** was 75% in the case of **A**.0.S and 89% in the case of **B**.0.S. Part of this difference can be explained by the higher solubility of $NH_4^+NH_2CO_2^-$ (> 5.4 M vs. ~ 3.6 M for $NH_4^+HCO_3^-$), and by the fact that each formula unit of carbamate decomposes to give 2 molecules of ammonia, but other factors must be at work. Similar behavior was observed with D-glucose (Entries 2 and 22): to attain a 52% yield in glycosylamine / *N*-glycosyl carbamate it took protocol **B**.0.S one eighth of the time required

using protocol **A**.0.S. What is more, the rate of formation of glycosylamine / *N*-glycosyl carbamate is ~4-5 times slower in the case of D-glucose than in the case of GlcA **1**, although the same fraction of product is present at equilibrium.

Concerning the amount of by-products **5-11**, in the case of GlcA protocol **B**.0.S lead to an initial increase which was followed by a rapid stabilization around 8%; a value similar to that observed for **A**.0.S (11%). The salt effect was less pronounced in the case of Glc, with ~10% of by-products in the presence of ammonium carbamate against ~6% for ammonium bicarbonate. Finally, in all cases the amount of diglycosylamine remained close to zero during the first 33 h of reaction and only started to increase later on (the latter data is only available for Glc).

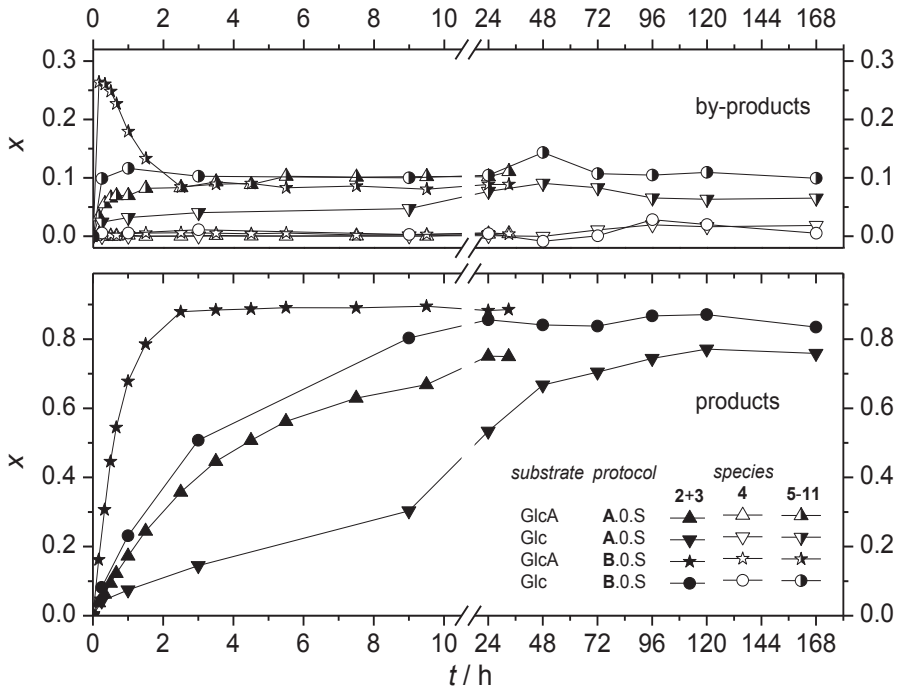

Figure 5.11 *Evolution of the composition with time for the reaction of sodium D-glucuronate and D-glucose with saturated ammonium bicarbonate or ammonium carbamate solutions at 30 ºC (see Table 5.4, entries 1, 2, 21, and 22). The mole fraction (x) of different species is shown.*

Although the high yield and the short reaction time obtained with protocol **B**.0.S are absolutely remarkable, the large amount of salt used could restrict its scope in synthesis. For instance, oligoglycuronans are not soluble at high ionic strength. Thus, we tested the effect of a decreasing amount of ammonium carbamate on the reaction outcome (Entries 16-20, Table 5.4). As it turned out, by using a 2 M initial concentration of $NH_4^+NH_2CO_2^-$, 84% of **2**+**3** is still obtained after 24 h of reaction.

For comparison, a number of protocols based on the combination of concentrated aqueous ammonia (14.5 M) and ammonium salts were investigated as well. Figure 5.12 shows the results obtained with Lubineau's protocol (**A**.14.02; entries 14 and 15 in Table 5.4) [8c] and with a modification in which ammonium bicarbonate was replaced with the less stable ammonium carbamate (**B**.14.02; entries 31 and 32 in Table 5.4). It is evident that the same kinetic profiles were obtained with the two salts, that the conversion in glycosylamine is ~7-8 times faster for GlcA **1** than for Glc, and that the amount of diglycosylamine remains close to zero during the first 33 h of reaction and starts to increase later on (the latter data is only available for Glc). Also, when compared with the corresponding saturated salt protocols (Figure 5.11), it is clear that a much larger fraction of by-products is present with concentrated ammonia during the first ~10 hours of reaction, and that it takes ~24 hours to attain a plateau value (~10% in all cases). This observation is consistent with intermediate species taking longer to transform into the final products **2** and **3**. Concerning the absolute rate of reaction, for both sugars it is comparable to that observed with protocol **A**.0.S (saturated ammonium bicarbonate) although somewhat higher yields of **2**+**3** are obtained for long reaction times. It is interesting to observe that, with respect to concentrated ammonia alone (**X**.14.00; entries 33 and 34 in Table 5.4), the addition of 0.2 M ammonium salt results in a moderate increase in the proportion of glycosylamine / *N*-glycosylcarbamate in the case of GlcA (82% after 24-25 h of reaction), and in a two fold increase in the case of Glc (43%), both measured after 24-25 h of reaction.

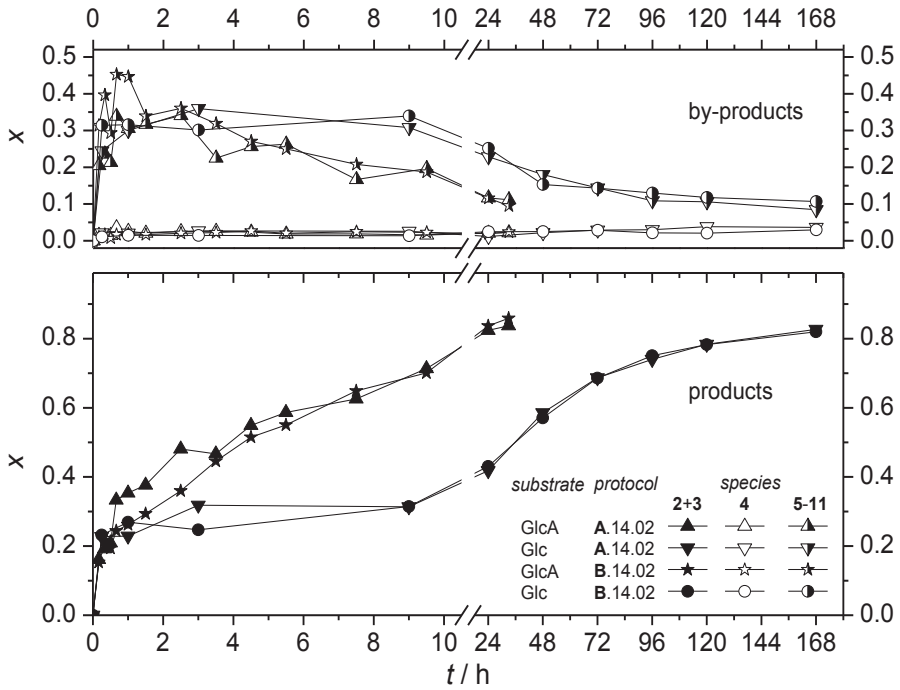

Figure 5.12 *Evolution of the composition with time for the reaction of sodium D-glucuronate and D-glucose with concentrated ammonia (14.5 M) and one equivalent ammonium salt (0.2 M; entries 14, 15, 31, and 32 in Table 5.4). The mole fraction (x) of the different species is shown.*

5.3.4.2 Effect of a lower concentration of reagents

In order to optimize the synthesis of β-D-glucopyranuronosylamine, we looked into the possibility of reducing the amount of reagents used. At first, we examined the effect of a decreased concentration of ammonia for a given concentration of ammonium salt. Figure 5.13a shows that, in the presence of 0.6 M $NH_4^+HCO_3^-$ (Entries 5, 12, and 13 in Table 5.4), the use of 9 M or 5 M ammonia results in almost identical kinetic profiles, whereas a further diminution to 1 M ammonia slows down significantly the reaction and results in ~20% less glycosylamine formed at equilibrium. The opposite can be said about the amount of by-products, which goes from 10% to 20% at equilibrium when the ammonia concentration decreases from 9 M to 1 M. A qualitatively similar effect is observed with $NH_4^+NH_2CO_2^-$ (Entries 24, 29, and 30 in Table 5.4), but the same is much less pronounced (Figure 5.13b). The fraction of diglycosylamine **4** remained close to zero in all cases. Here it should be noted that after 33 h, the yield in **2**+**3** is virtually identical for protocols **A**.14.02 and **A**.5.06, meaning that a small increase in the amount of salt effectively compensates for a threefold decrease in ammonia concentration. The same can be said for protocols **B**.14.02 and **B**.5.06.

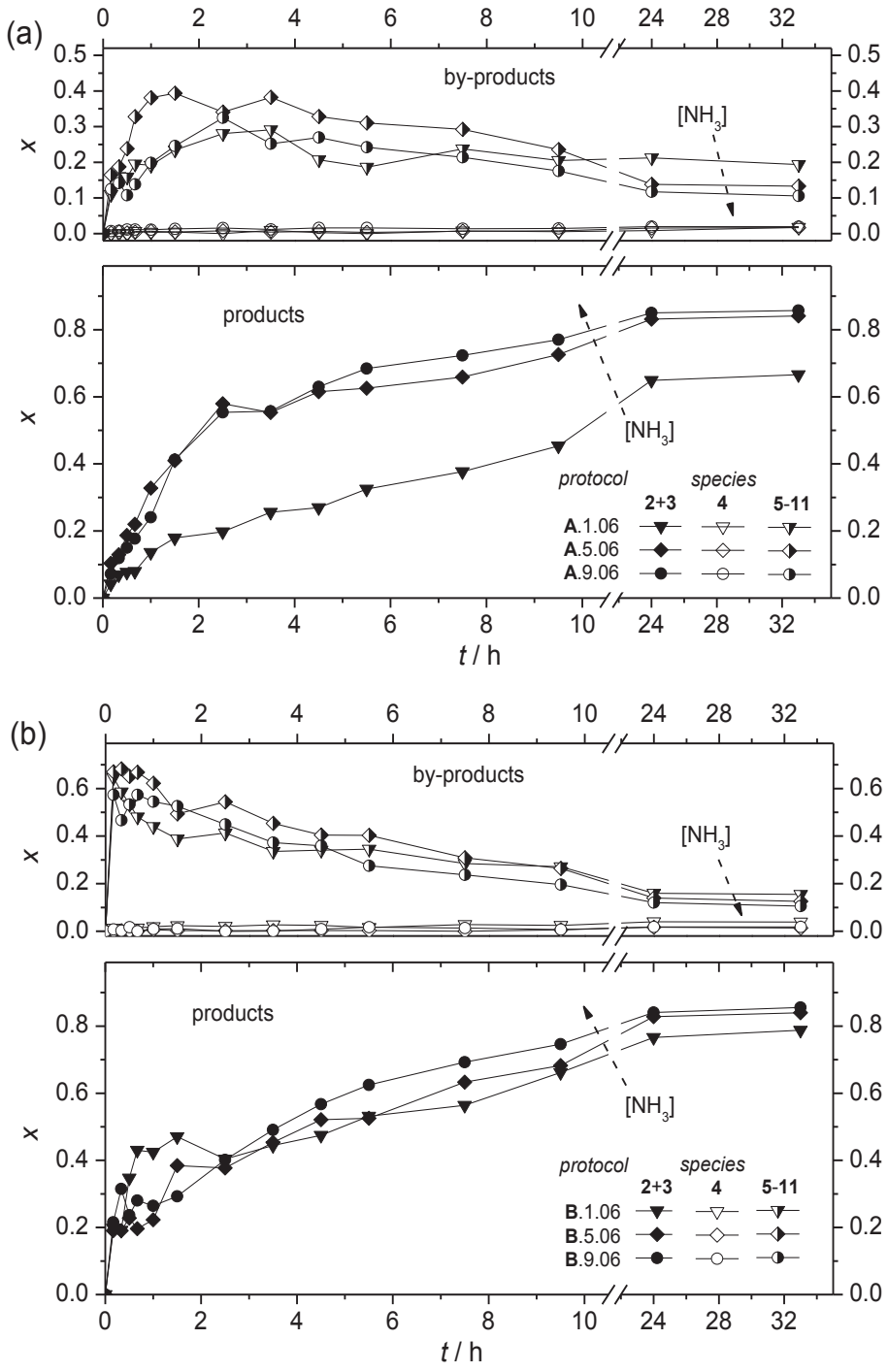

Figure 5.13 *Evolution of the composition with time for the reaction of sodium D-glucuronate with different concentrations of ammonia and (a) 0.6 M ammonium bicarbonate (Table 5.4, entries 5, 12, and 13), or (b) 0.6 M ammonium carbamate (Entries 24, 29, and 30). The mole fraction (x) of the different species is shown.*

Encouraged by the good results of protocols **A**/**B**.5.06, and following the same rationale of minimizing the amount of reagents used, we also tested the effect of a lesser amount of ammonium salt (Entries 6 and 25 in Table 5.4). As shown in Figure 5.14, in the presence of 5 M ammonia a reduction from 0.6 M to 0.2 M of the initial concentration of ammonium

bicarbonate/carbamate only results in a slight decrease in the rate of formation of **2**+**3**, and in a ~5% decrease of their proportion at equilibrium. Concerning the amount of by-products **5-11**, there was no effect in the case of ammonium bicarbonate, while a higher concentration of ammonium carbamate lead to a higher fraction of **5-11** being present during the first hours of reaction. This difference disappeared after ~7 h, though. The fraction of diglycosylamine **4** remained close to zero in all cases, and attained a maximum of ~ 3% after 33 h.

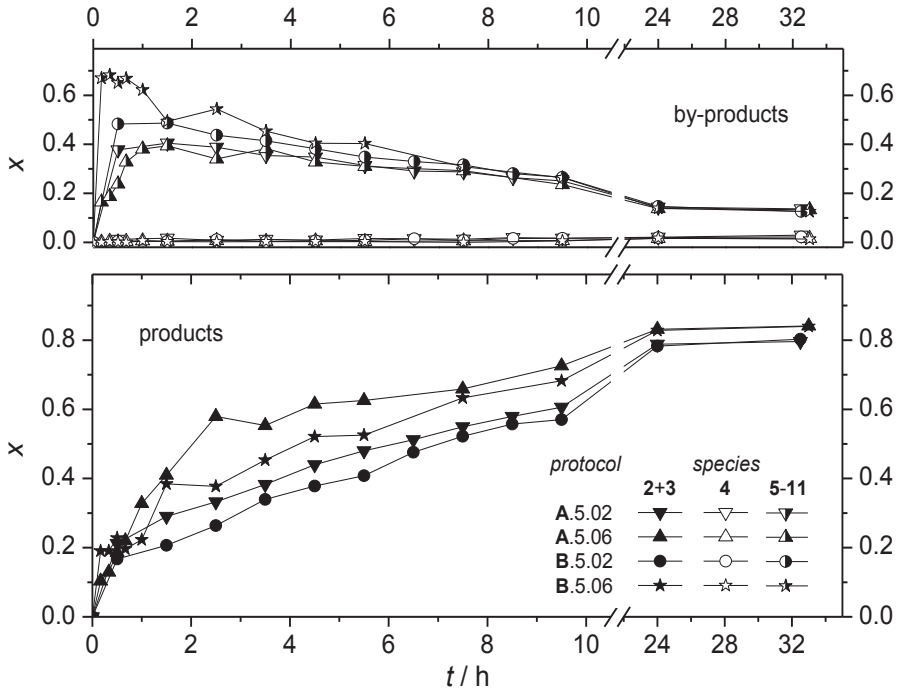

Figure 5.14 *Effect of ammonium salt concentration (0.2 M or 0.6 M) on the evolution of the composition with time for the reaction of sodium D-glucuronate with 5 M ammonia (Entries 6, 12, 25, and 29, Table 5.4). The mole fraction (x) of different species is shown.*

5.3.4.3 Effect of temperature

The last parameter to be tested was the reaction temperature, and in particular whether an increase in temperature would accelerate the rate of reaction without increasing the amount of by-products (Figure 5.15). As it turned out, raising the temperature from 30 ºC to 40 ºC resulted in a 4-fold increase in the rate of production of glycosylamine / *N*-glycosylcarbamate in the case of protocol **A**.0.S (Entries 1 and 3, Table 5.4), and in a 3-fold increase in the case of **B**.0.S (Entries 21 and 23), both measured at 70% conversion. All the same, the highest yield attained remains almost identical for the two temperatures and, for long reaction times, a decrease in the proportion of **2**+**3** is actually observed in the case of **B**.0.S: This certainly results from the poorer thermal stability of ammonium carbamate, which decomposes at T > 30 ºC. [11b] As for the amount of by-products **5-11**, raising the temperature resulted in a

marginal increase, whereas the fraction of diglycosylamine **4** remained close to zero in all cases.

The same type of experiment was carried out with protocols **A**/**B**.5.02 (Figure 5.15b; entries 6, 7, 25, and 26, Table 5.4). In this case, raising the temperature from 30 ºC to 40 ºC resulted in a 2-fold increase in the rate of formation of **2**+**3** (measured at 60% yield), but the evaporation of ammonia was rapid enough to lead to ~ 5% lower yields after 24 h. Accordingly, at 40 ºC the proportion of **5-11** was significantly lower during the first ~ 10 h of reaction and bottomed out around 13% for longer reaction times, i.e. the same value observed at 30 °C. Finally, for both temperatures tested the amount of diglycosylamine **4** remained close to zero during the first ~ 6 h and increased to ~3% by the end of the reaction.

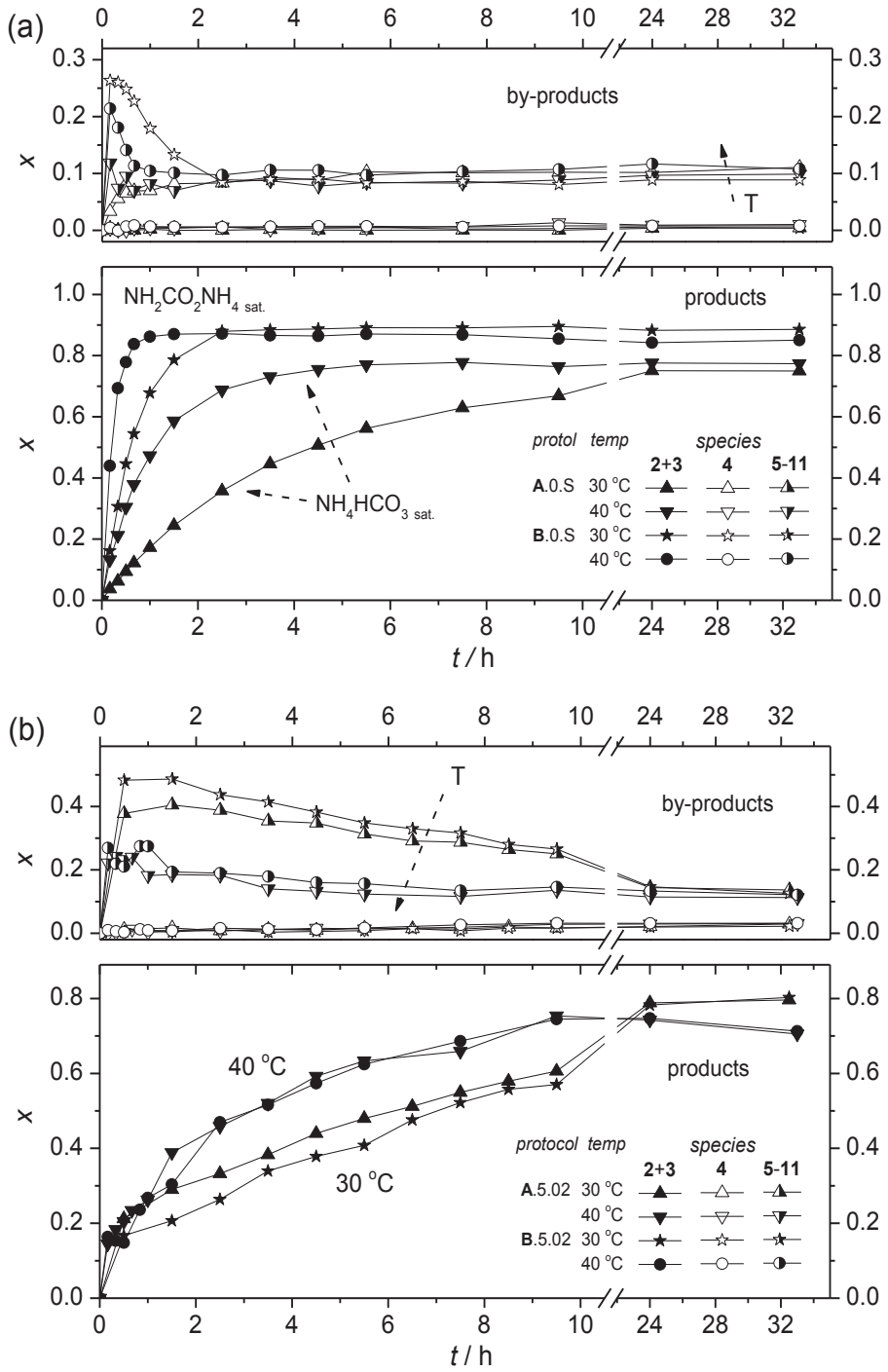

Figure 5.15 *Effect of temperature on the evolution of the composition with time for the reaction of sodium D-glucuronate with (a) saturated ammonium salt (Table 5.4, entries 1, 3, 21, and 23) and (b) 5 M ammonia containing ammonium salt 0.2 M (Entries 6, 7, 25, and 26). The mole fraction (x) of the different species is shown.*

5.3.4.4 Fate of intermediate species

Finally, it is worth looking more closely at the results obtained at 30 ºC for a "slow" protocol (**B**.5.02; entry 25 in Table 5.4) and for the fastest protocol tested (**B**.0.S; entry 21). Figure 5.16 shows that after 30 min of reaction between 65% (**B**.5.02) and 70% (**B**.0.S) of the

initial sugar had already been consumed. In the case of **B**.5.02 though, only half of it was transformed into α/β-D-glucopyranuronosylamine and ammonium *N*-α/β-D-glucopyranuronosyl carbamate, whereas the other half yielded intermediates **5**, **7**, **8**, **10**, and **11**. It then took 32 ½ h for the concentration of intermediates to reach its lowest value of 6% and for the yield in **2**+**3** to attain a maximum value of 80%. By contrast, in the case of **B**.0.S the fraction of intermediates present after 30 min was only 10%, and their concentration reached a minimum of ~2% in just 2.5 h. Consequently, at the same reaction time the system already contained ~ 60% of α/β-D-glucopyranuronosylamine and ammonium *N*-α/β-D-glucopyranuronosyl carbamate, and it reached a maximum yield of 89% in barely 5 ½ h. At the end of the reaction, the proportion of residual GlcA **1** was 5% in the case of **B**.5.02 and 2% in case of **B**.0.S, and both systems contained the same amount (7%) of the α anomers **6**+**9**. We checked the final amount of **6**+**9** for three other protocols and found that nearly the same value was obtained with **A**.5.06 (8%), **A**.14.02 (8%), and **B**.9.06 (7%). This suggests that 7-8% is about the equilibrium fraction of α-D- glucopyranuronosylamine / carbamate in water at 30 ºC.

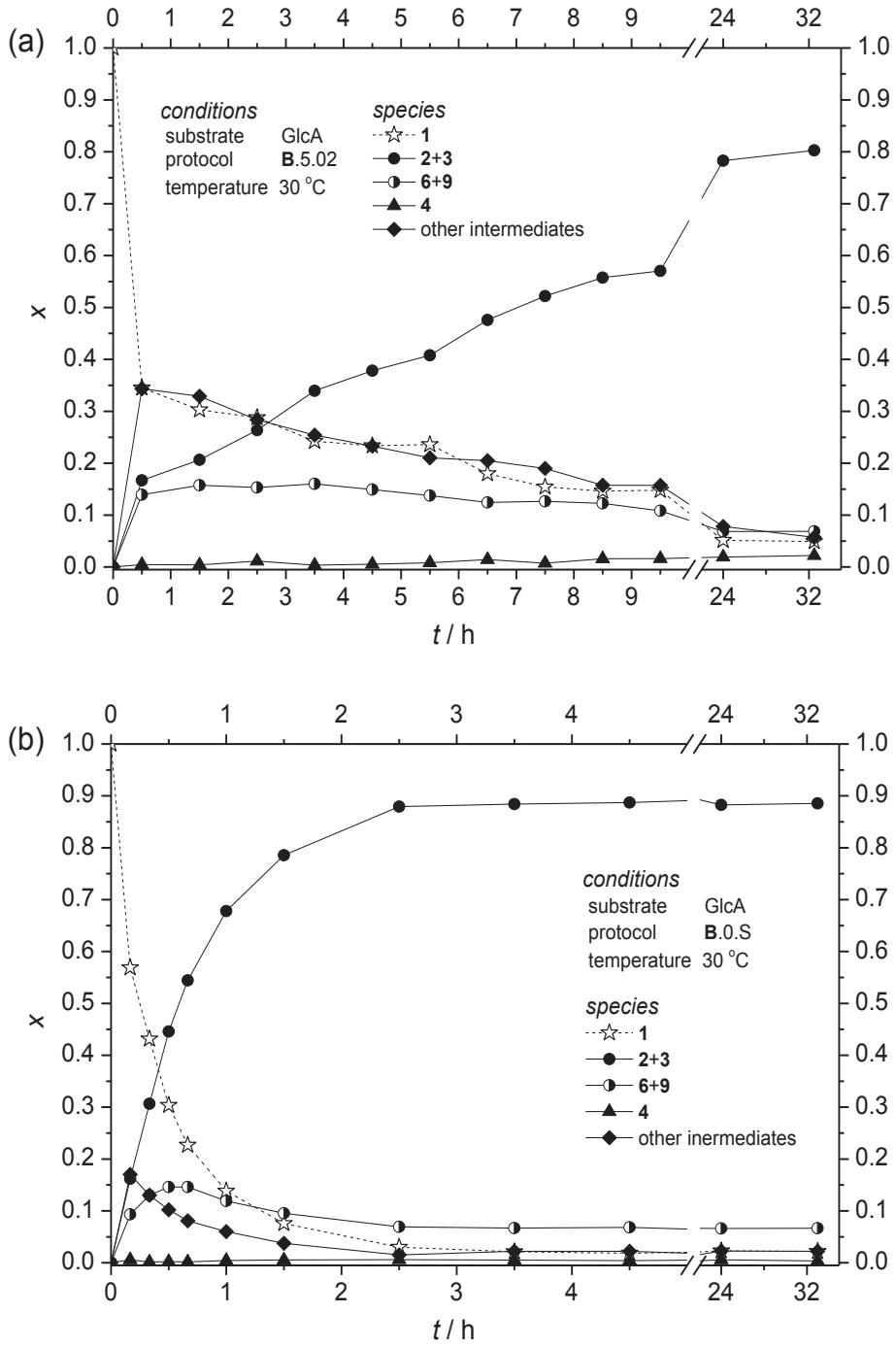

Figure 5.16 *Comparison between the kinetics at 30 ºC of (a) a "slow" protocol (**B**.5.02) and (b) the fastest protocol tested (**B**.0.S; entries 21 and 25, Table 5.4). The mole fraction (x) of different species is shown.*

5.3.5 Amination of oligoglycuronans

The direct amination of oligoglycuronans in aqueous solution was also examined based on the protocols tested on D-glucuronic acid adopting little amount of salt and ammonia, and giving high yield, for instance **A**.5.02 and **B**.5.02. Like that, the salt will not affect the solubility of the oligoglycuronans and the latter could be separated from the salt by selective precipitation. It is worth noting that conducting the amination of oligoglycuronans in saturated ammonium salt solutions (NH_4HCO_3 and $NH_4CO_2NH_2$) resulted in their precipitation due to the high ionic strength of the solutions.

To this end oligomannuronan (oligoM) and oligoguluronan (oligoG) blocks were reacted with the more volatile ammonium salt [11b] according to protocol **B**.5.02 (0.2 M $NH_4CO_2NH_2$, 5 M NH_3) for a period of 3 and 4 days respectively (Entries 27 and 28, Table 5.4). At the end of the reaction the oligomers were separated from the salt via selective precipitation using cold EtOH (80 %) to avoid the hydrolysis of the glycosylamine to the starting oligoglycuronan. To support the hypothesis that no salt precipitated out with the sugar, the quantitative ^{13}C-NMR (D1 = 20s) of β-D-glucopyranuronosylamine synthesized according to **B**.9.06 and precipitated in cold EtOH (90 %) was analyzed. From this NMR, [33] the absence of peaks at 165.80 and 168.36 ppm corresponding to $NH_4CO_2NH_2$ and the products (carbonate and bicarbonate) resulting from its equilibria in water [34] confirm that the precipitation was successfully established without salt precipitation. Furthermore, precipitation tests of both the ammonium salts (with various concentrations) and oligoalginates (DP_n 4) were carried out (Table 5.5). Despite of carrying the tests at temperatures higher than the ones used for precipitating the oligoglycuronans from the amination reaction yet we can find that a 0.6 M $NH_4CO_2NH_2$ solution (Entry 1, Table 5.5) is still soluble even above 95 % EtOH. On the other hand, the saturated ammonium salt solutions (Entries 4-5) and $NH_4CO_2NH_2$ solutions with concentrations 2 and 3M (Entries 2-3) precipitated out starting from 15 and 70 % EtOH, respectively. Interestingly, the short oligoalginate blocks (Entry 6-7) started precipitating out after 45 % EtOH; that is to say that the longer blocks will precipitate at lower amounts of EtOH.

Table 5.5 *Summary of precipitation tests done on ammonium salt solutions.*

Entry	Composition (mol L^{-1})	% EtOH	Temperature (°C)	Precipitation (Y/N)	Experiment code
1	$NH_4CO_2NH_2$ (0.6 M) + NH_3 (9 M)	50	20.5	N	AG10-33
		70	20.5	N	
		80	20.5	N	
		90	20.5	N	
		95	20.5	N	
2	$NH_4CO_2NH_2$ (2 M)	50	20.5	N	AG10-33
		70	20.5	Y [a]	
		83	20.5	Y	
3	$NH_4CO_2NH_2$ (3 M)	50	20.5	N	AG10-33
		70	20.5	Y	
4	$NH_4CO_2NH_2$ (saturated)	15	18	Y	
5	NH_4HCO_3 (saturated)	15	18	Y	
6 [b]	(1→4)-β-D-mannuronan	45	25	Y	AG10-25
7 [b]	(1→4)-α-L-guluronan	45	25	Y	AG10-25

General conditions: stirring rate 600 rpm, [a] slight precipitate, [b] 5 % w/w oligosaccharide, DP_n = 4, pH 9.5..

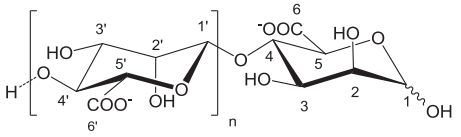

(1->4)-β-D-oligomannuronan

16

n = 4, **16$_5$**
n = 8, **16$_9$**

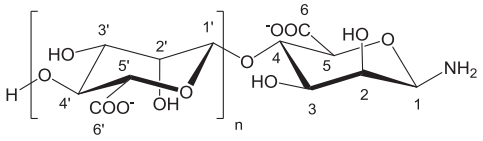

17

n = 4, **17$_5$**
n = 8, **17$_9$**

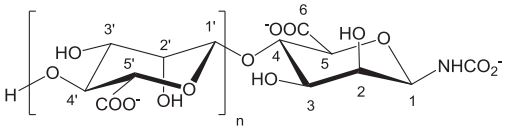

18

n = 4, **18$_5$**
n = 8, **18$_9$**

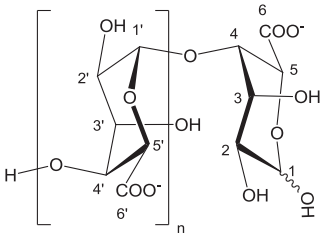

(1->4)-α-L-oligoguluronan

19

n = 4, **19$_5$**
n = 9, **19$_{10}$**

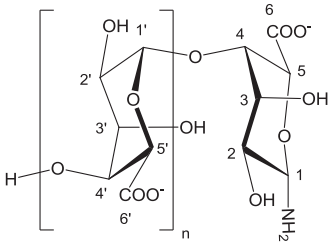

20

n = 4, **20$_5$**
n = 9, **20$_{10}$**

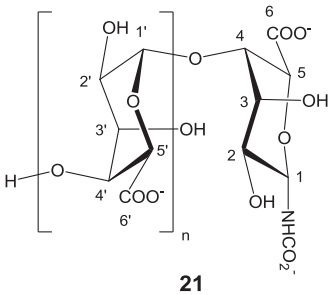

21

n = 4, **21$_5$**
n = 9, **21$_{10}$**

Figure 5.17 *Oligoglycuronan blocks and their corresponding glycosylamines/carbamates. The nucleus numbering is shown where the whole numbers (1-6) represent the reducing end while the primed ones (1'-6') represent the non reducing end. The subscript represents the* DP_n *of the oligoglycuronan.*

Figure 5.18 shows the ^{1}H-NMR spectra of two oligoguluronan derived glycosylamines (**20$_5$** and **20$_{10}$**) obtained according to protocols **A**/**B**.5.02 with some assignments of the reducing end (Table 5.4, entries 11 and 28). Glycosylamine **20$_{10}$** was obtained after precipitation in 80 % EtOH contrary to **20$_5$** whose reaction mixture was not precipitated at the end of the reaction. In both cases, the H1β (4.90 ppm) and H1α (5.22 pm) anomeric peaks of the starting sugar disappeared in the favor of those of the glycosylamine (appearance of H1β-NH_2 at 4.35 ppm) and its carbamate (H1β-$NHCO_2^-$ at 4.95 ppm). Regrettably, the latter assignments were not based on 2D correlation experiments of these compounds but rather based on the evaluation of the ^{1}H-NMR spectrum of β-D-mannopyranuronosylamine **14** whose H1β-NH_2

and its carbamate appear at 4.36 and 4.94 ppm respectively (Figure 5.6). It is worth noting that the chemical shifts of H1α/β of oligomannuronan (δ (ppm): H1β 4.86 and H1α 5.21) and that of oligoguluronan (δ (ppm): H1β 4.88 and H1α 5.22) are the same, hence the previous evaluation makes sense.

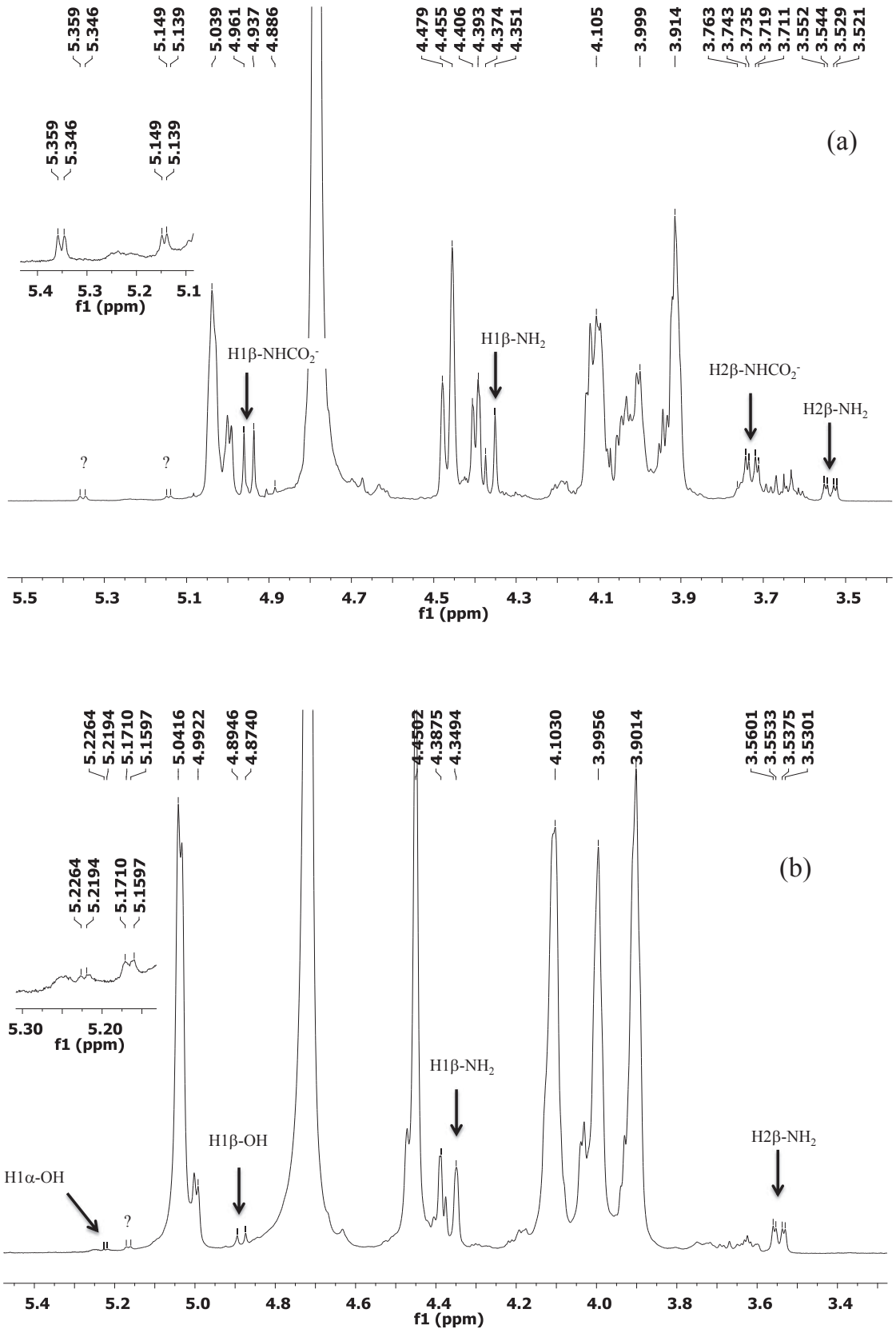

Figure 5.18 *[1]H-NMR spectra of (1 → 4)-α-L-oligoguluronan derived glycosylamine* ***20****. Spectrum (a) refers to the synthesis of* $\mathbf{20_5}$ *(DP_n = 5) according to* ***A****.5.02 without precipitation at the end of the reaction* [35] *while spectrum (b) refers to the synthesis of* $\mathbf{20_{10}}$

*(DP_n = 10) according to **B**.5.02 and obtained from the precipitation of the reaction mixture in 80 % EtOH.* [36] *The assignments above peaks are for the reducing end only where labels ending with OH refer to the starting oligoguluronan **19**, and the ones ending in NH_2 and $NHCO_2^-$ refer to the product **20** and its carbamate **21**.*

Moreover, the coupling constant of H1β-$NHCO_2^-$ ($J_{1,2}$ 9.6 Hz) at 4.94 ppm is comparable with that of the anomeric peak of the starting oligoG (H1β, $J_{1,2}$ 8.3 Hz) which confirms the β configuration of the glycosylamine as well. Unfortunately, the signal of H1β-NH_2 at 4.35 ppm is not well resolved from the spectra and in the two cases it appears as an unresolved singlet rather than a doublet with a high coupling constant ($J_{1,2}$ ~8-9 Hz) and that is suspected to be referred to the fact that the signals of the protons at C5 and C5' (H5, H5') which belong to the reducing end and the closest unit to it superimpose with that of H1β-NH_2. The coupling constant of the signal at 3.53 ppm (dd, $J_{1,2}$ 9.2 Hz and $J_{2,3}$ 2.8 Hz) is comparable with that of H2β of the reducing end of the starting oligoG (dd, $J_{1,2}$ 8.2 Hz and $J_{2,3}$ 3.1 Hz) which suggests that this peak corresponds to the H2β of a glycosylamine or its carbamate ($NHCO_2^-$). Adding, this peak appears as well in the spectrum of $\mathbf{20_{10}}$ which is free from a carbamate derivative (*vide infra*) thus this peak is attributed to H2β-NH_2. We suspect that its corresponding carbamate appears at 3.74 ppm (See Figure 5.18(a)).

From Figure 5.18, the peaks at 5.14 ppm (d, J 3.8 Hz) and 5.35 ppm (d, J 5.0 Hz) come out at the same chemical shift of the anomeric protons of by-products **6** (5.37 ppm, J = 5.5 Hz) and **7** (5.12 ppm, J = 5.0 Hz), that formed during the amination of D-glucuronic acid. Their low coupling constants suggest that these by-products have an α-configuration as it was attributed to by-products **6** and **7**. In both cases their mole fraction did not exceed 9 %. Interestingly, the spectrum of $\mathbf{20_{10}}$ (Figure 5.18b) shows no signal for the carbamate of the glycosylamine at 4.95 ppm. This is attributed to the fact that $\mathbf{20_{10}}$ was isolated after precipitation in 80 % EtOH contrary to $\mathbf{20_5}$ that was not precipitated. This is to say that the advantage of the precipitation step is not only limited to eliminate the salt at the end of the reaction but also in converting the carbamate **21** to the glycosylamine **20**. On the other hand, the precipitation step has a negative outcome on the yield of the reaction where lower yields by 10 % were obtained as a result of the partial hydrolysis of the glycosylamine which is inevitable. For instance $\mathbf{20_5}$ and its carbamate $\mathbf{21_5}$ were synthesized with 86 % yield without precipitation, while upon precipitation $\mathbf{20_{10}}$ and its carbamate $\mathbf{21_{10}}$ were obtained with a lower yield (77 %) although their reaction mixture was left reacting longer periods.

Similar results were obtained from the amination experiment of an oligomannuronan block **16** according to protocols **A**/**B**.5.02 (Entries 10 and 27, Table 5.4). As expected the

anomeric peaks of the glycosylamine **17** (4.36 ppm, H1β-NH_2) and its carbamate **18** (H1β-$NHCO_2^-$, 4.93 ppm) came out at the same chemical shift of the anomeric protons of β-D-mannopyranuronosylamine **14** (Figure 5.19).

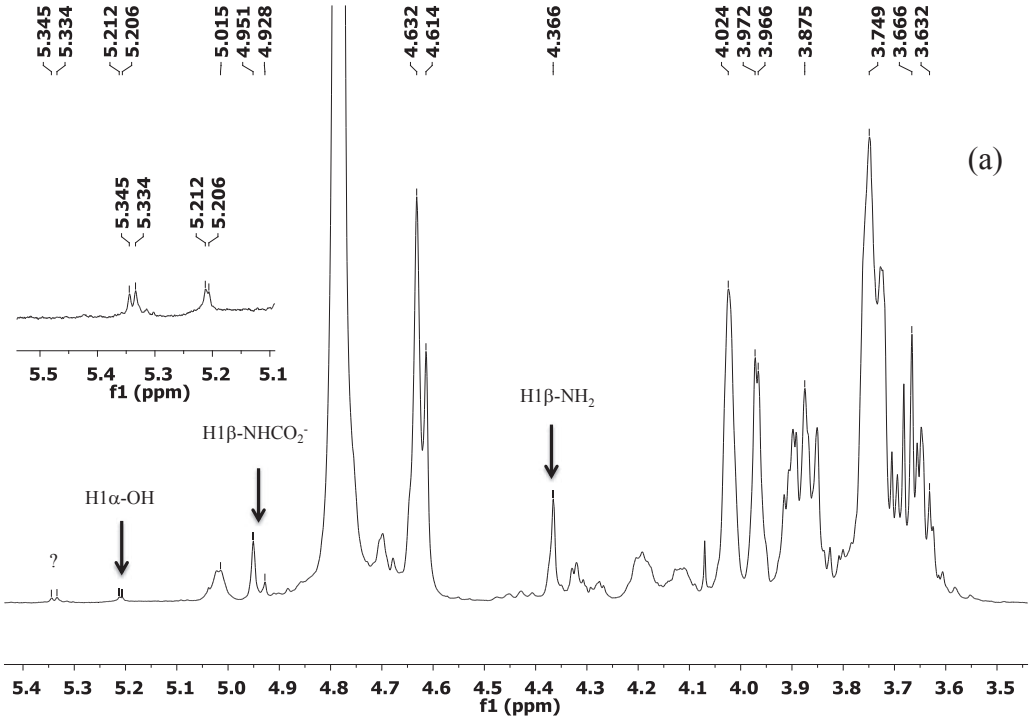

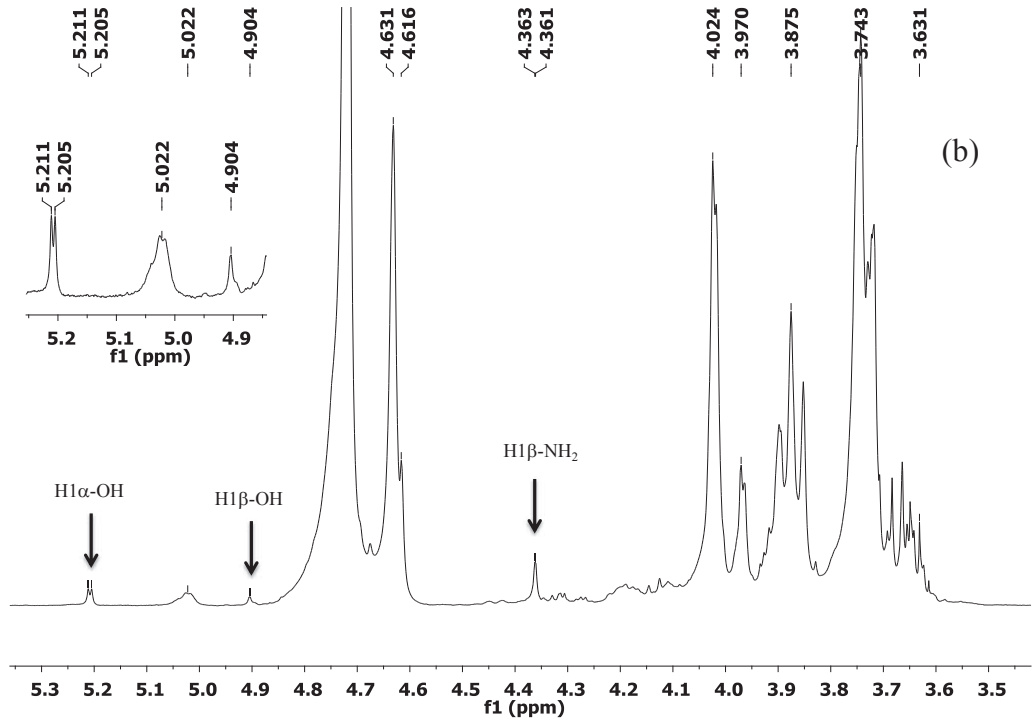

Figure 5.19 *Two ^{1}H-NMR spectra of (1 → 4)-β-D-oligomannuronan derived glycosylamine **17**. Spectrum (a) refers to the synthesis of **17$_5$** (DP_n = 4) according to **A**.5.02 without precipitation at the end of the reaction [37] while spectrum (b) refers to the synthesis of **17$_{10}$** (DP_n = 10) according to **B**.5.02 and obtained from the precipitation of the reaction mixture in 80 % EtOH. [38] The assignments above peaks are for the reducing end only where labels*

*ending with OH refer to the starting oligomannuronan **16**, and the ones ending in NH_2 and $NHCO_2^-$ refer to the product **17** and its carbamate **18**.*

As before, the glycosylamine **17** was obtained without any residual carbamate **18** (Figure 5.19b). As a consequence, a drop in the yield (~10 %) is inevitable once isolating the glycosylamines by precipitation. For instance, the yield for the synthesis of $\mathbf{17_{10}}$ was ~80 % after precipitation and that of $\mathbf{17_5}$ (obtained without precipitation) was 88 %.

5.3.6 Kinetic study on the amination of oligoglycuronans

Two oligoalginate blocks with a short *DP* ($ManA_5$ and $GulA_5$) were investigated due to the ease of monitoring the chemical shifts of their anomeric protons. The aim of this study was to check whether both blocks ($ManA_5$ and $GulA_5$) react in the same way, recalling that both blocks have different conformations and configurations. For instance the pyranose ring of an oligoguluronan block adopts a $^1C_4$ chair conformation with a (1→4) α configuration of the glycosidic linkage and that of an oligomannuronan block adopts a $^4C_1$ chair conformation with a (1→4) β configuration (See chapter 2 for more information).

To this aim, oligoglycuronan blocks $\mathbf{16_5}$ and $\mathbf{19_5}$ were reacted with ammonia (5M) and an ammonium salt (0.2 M) at 30 °C. The exact experimental conditions used and the final composition of the gross products are summarized in Table 5.4 (Entries 8 and 9). Samples were drawn at preset reaction times, frozen in liquid nitrogen and freeze dried overnight to eliminate water and most of the salt. In order to monitor the time course of the reaction, individual samples were redissolved in cold D_2O to afford clear solutions of pD ≅ 9 that were immediately analyzed by ^{1}H-NMR. Spectra were recorded at 298 K to prevent the peak of residual HDO from interfering with integration and to maintain better resolution.

A single byproduct was detected throughout the kinetic study at 5.33 ppm in both experiments. As before, the molar fractions (x) of different species were calculated after establishing two normalizing constants, S_{ManA} and S_{GulA} for oligomannuronan and oligoguluronan blocks respectively:

$$S_{ManA} = \sum_{i=21} A_{\delta}^{i} = (A_{4.36}^{22\beta} - A_{4.37}^{21}) + A_{4.87}^{21\beta} + A_{4.94}^{23\beta} + A_{5.21}^{21\alpha} + A_{5.33}^{byp} \tag{5.3}$$

$$S_{GulA} = \sum_{i=24} A_{\delta}^{i} = A_{3.53}^{24} + A_{4.87}^{24\beta} + A_{4.94}^{26\beta} + A_{5.21}^{24\alpha} + A_{5.33}^{byp} \tag{5.4}$$

where A_{δ}^{i} indicates the area of the methine signal of compound *i* having a chemical shift δ (ppm). For the oligomannuronan block, the anomeric signal of **17_5** (H1β-NH_2) interfered with the signal of an impurity (already present in the NMR spectrum of the starting sugar) at 4.37 ppm, that is why we integrated both peaks together and we corrected for the presence of the impurity at 4.37 ppm in S_{ManA} by subtracting its area from the area of the whole integral after normalizing the spectrum to a known peak. Fortunately, the correction for this peak in the case of the oligoguluronan block is not necessary, rather the integral of the well resolved H2β-NH_2 peak (**20_5**) at 3.53 ppm was considered instead of the H1β-NH_2 signal at 4.36 ppm. Subsequently, the molar fraction (*x*) was calculated according to:

$$x^{i} = \frac{A_{\delta}^{i}}{\mathrm{S}} \tag{5.5}$$

As before, the carbamates (**18_5** and **21_5**) entered in the calculation of the molar fraction of glycosylamines (**17_5** and **20_5**) due to their facile transformation to their corresponding glycosylamines in aqueous solution. Figure 5.20 shows the evolution of the molar fractions of both the glycosylamines and the byproducts for the kinetic studies. It is clearly detected that the oligomannuronan block reacts by far much faster than the oligoguluronan block where yield up to 70 % were obtained for **17_5** + **18_5** in 3 hours contrary to the oligoguluronan block where its corresponding amines (**20_5** + **21_5**) were obtained with 30 % yield for the same reaction time and under the same conditions.

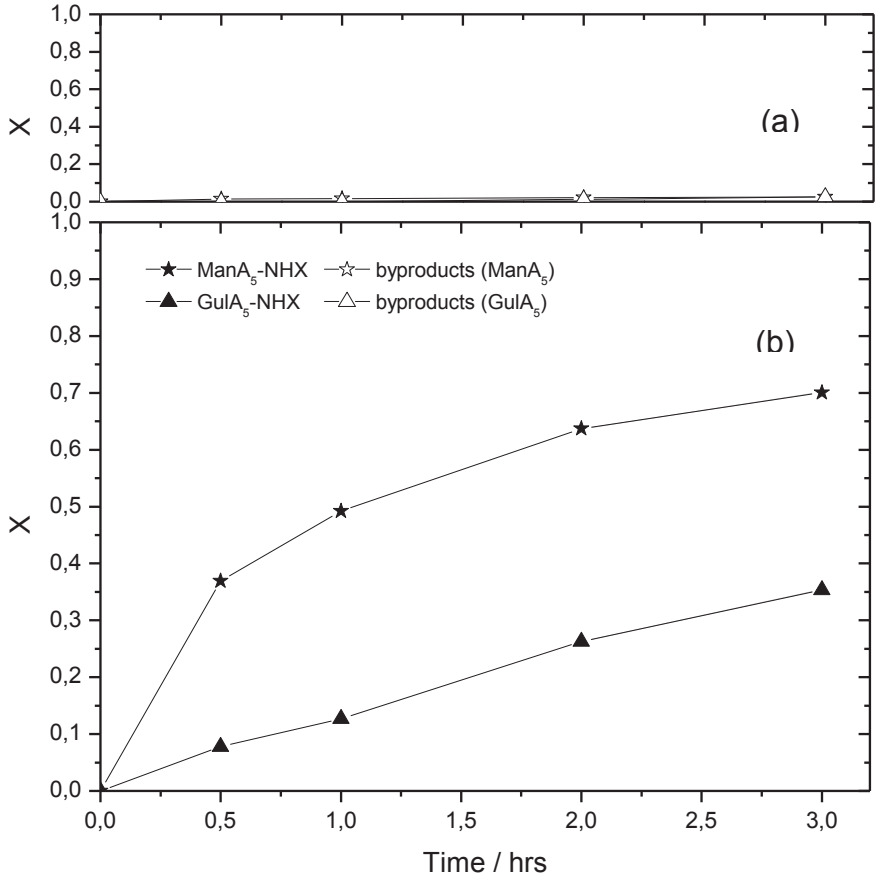

Figure 5.20 *Evolution of the molar fractions of (a) the byproducts and (b) the glycosylamines for the kinetic study on the amination of two oligoglycuronans blocks (**16**$_5$ and **19**$_5$) with time. Conditions: [Carb]$_0$ = 0.05 M, NH_4HCO_3 (0.2 M), NH_3 (5M), 30 °C (Entries 8 and 9, Table 5.4).*

Fascinatingly, and contrary to the amination of D-glucuronic acid the amount of byproducts did not exceed 2.5 % since the beginning of the reaction and that resulted in higher yields in shorter periods. For instance, for the same protocol being used (**A**.5.02), the composition of the reaction mixture for the amination of D-glucuronic acid after 3 hours was: 35 % β-D-glucopyranuronosylamine / carbamate (**2**+**3**), 40 % byproducts and 15 % D-glucuronic acid. In view of the fact that the vials of the kinetic study were not firmly closed and were too much perforated, the results of this kinetic study should be taken with a window of incertitude within 3 hours and should be denied for longer reaction times due to the loss of ammonia with time. In fact, after 8 hours a drop in the molar fraction of the glycosylamine was observed in both cases and that was attributed to the evaporation of the ammonia during the kinetic studies at 30 °C which resulted in the hydrolysis of the glycosylamines to the starting oligoglycuronans.

Recently a PhD student in our group, Anna Wolnik, computed a simulation study aiming to understand the intramolecular H-bonding in oligoguluronan and oligomannuronan blocks. As a result, the anomeric hydroxyl group (at C1α) of the oligoguluronan block was shown to be involved in the formation of a six membered ring with the oxygen atom at C3 via H-bonding (Figure 5.21).

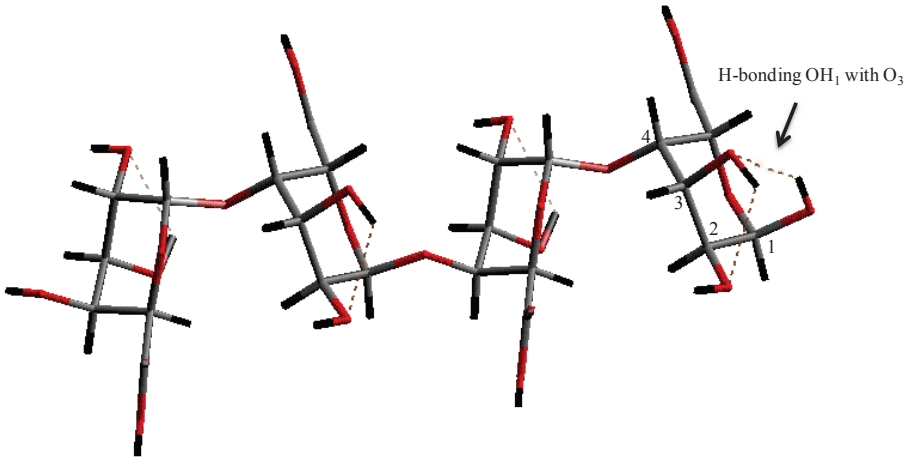

Figure 5.21 *An oligoguluronan block (DP_n = 4) after computer simulation. Carbon, oxygen and hydrogen atoms are represented in grey, red and black respectively. The dashed lines represent hydrogen bonding.*

This H-bonding will increase the stability of the molecule and thus reduces more and more the opened formed of the reducing end and consequently lowering its reactivity with ammonia and hence the kinetics of the reaction as well. It is worth considering the conformation of the oligoguluronan block as well to rationalize this lower reactivity, since it has been shown that the glycosylamine derivative of an oligoguluronan block reacts slower than its oligomannuronan analogue although from the simulation data both were not involved in H-bonding (See Chapter 7).

5.4 Take home messages

A set of take home messages could be extracted out from this work:

For the synthesis of β-D-glucopyranuronosylamine **2**:

i. The synthesis of glycosylamines in aqueous solution results in the formation of by-products that disappear with time in the favor of the final product.

ii. The use of 5 mol L^{-1} NH_3 together with 0.2-0.6 mol L^{-1} salt (NH_4HCO_3 or $NH_4CO_2NH_2$) could be a good compromise for the synthesis of glycosylamines rather than using large quantities of NH_3 (16 mol L^{-1}) or saturated salts.

iii. The amount of diglycosylamine **4** never exceeded 3 % in all the tested protocols.

For the synthesis of oligoalginate derived glycosylamines:

i. The synthesis of oligoalginate derived glycosylamines (using **A**/**B**.5.02) worked successfully with 80 % yield for both oligomannuronan and oligoguluronan blocks.

ii. Oligomannuronans reacts faster than oligoguluronans.

iii. Less amounts of by-products form at the beginning of the reaction compared with the amination of D-glucuronic acid.

iv. The selective precipitation step at the end of the reaction transforms any residual *N*-glycosylcarbamate to the corresponding glycosylamine.

Appendix 5.A NMR spectra

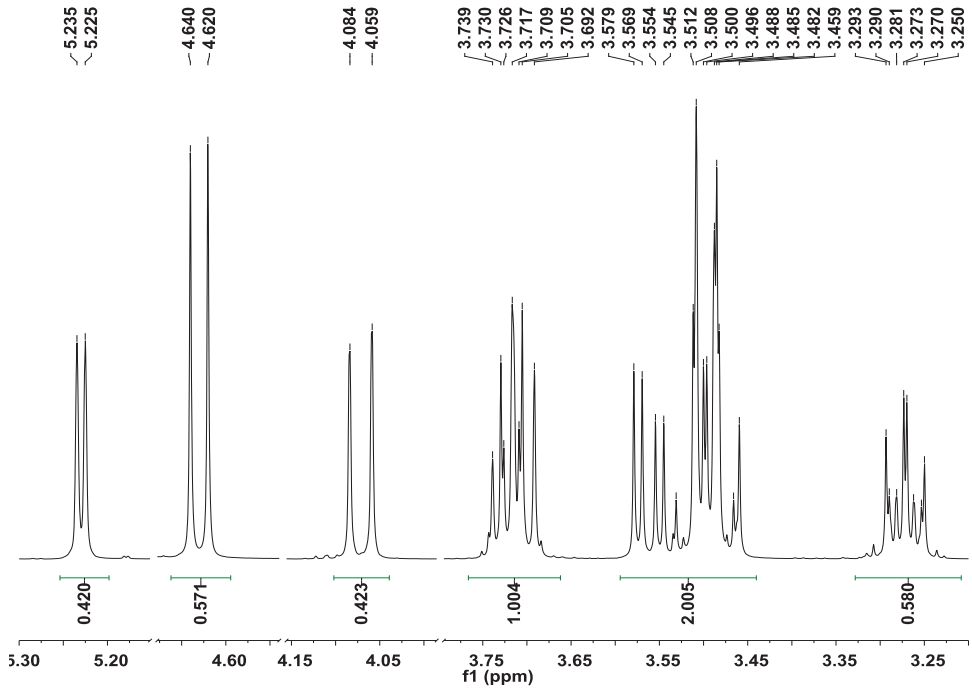

Figure 5.22 *1D ^{1}H spectrum of D-glucuronic acid sodium salt **1** (400.13 MHz, D_2O, 4.2 % w/w, 298 K, $\delta(^{1}H)_{TSP}$ = -0.017 ppm). Three cuts in horizontal axis should be noted.*

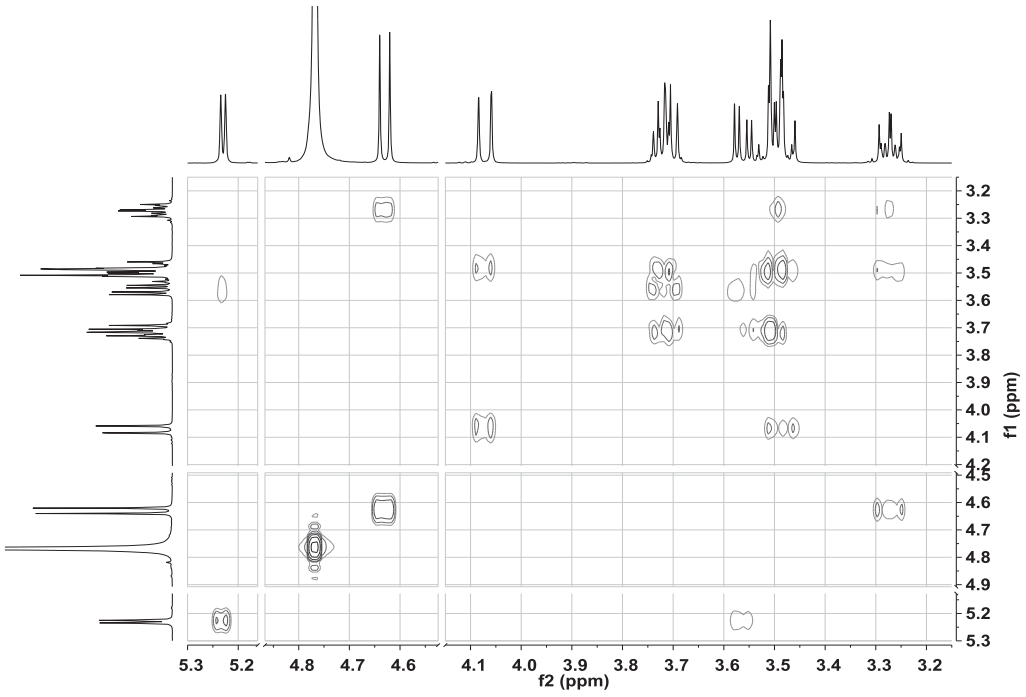

Figure 5.23 *2D ^{1}H-^{1}H COSY spectrum of D-glucuronic acid sodium salt **1** (400.13 MHz, D_2O, 4.2 % w/w, 298 K, $\delta(^{1}H)_{TSP}$ = -0.017 ppm). Two cuts in each axis should be noted.*

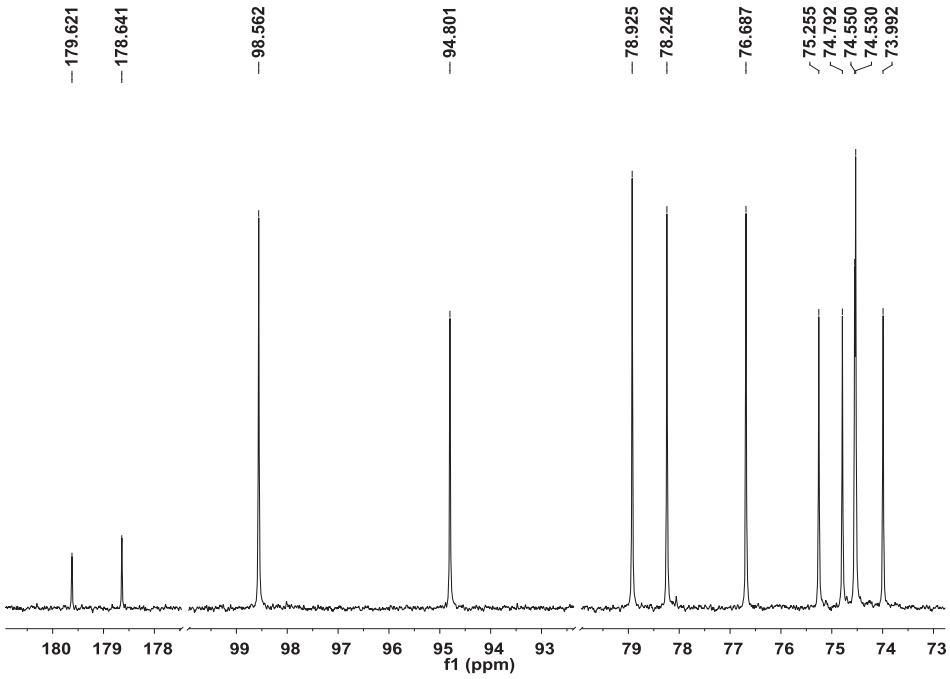

Figure 5.24 *1D ^{13}C spectrum of D-glucuronic acid sodium salt **1** (100.62 MHz, D_2O, 4.2 % w/w, 298 K, $\delta(^{13}C)_{TSP}$ = -0.149 ppm). Two cuts in horizontal axis should be noted.*

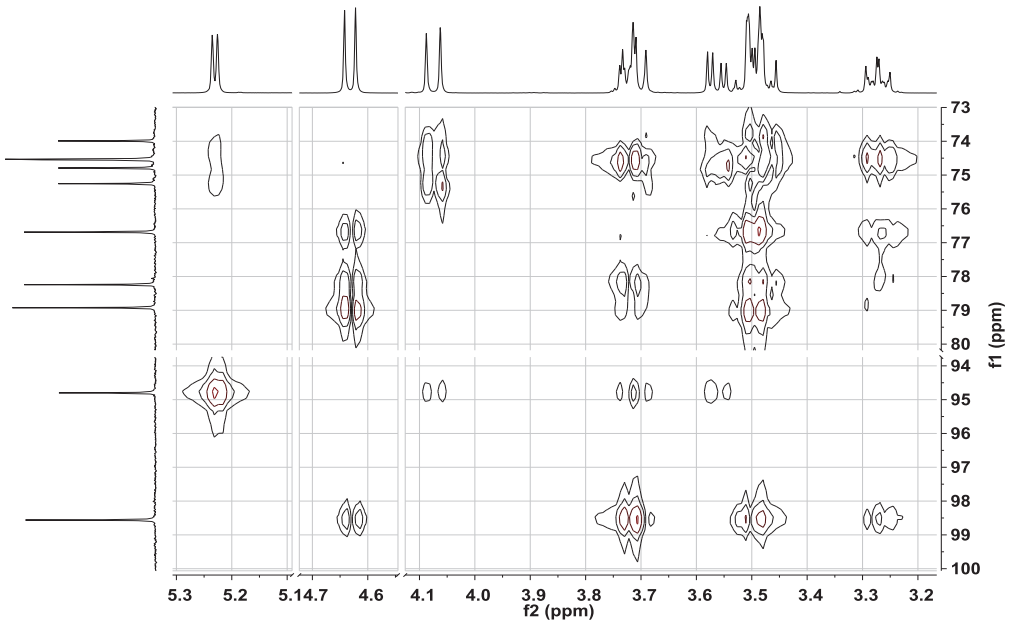

Figure 5.25 *2D ^{1}H-^{13}C HMQC-TOCSY spectrum of D-glucuronic acid sodium salt **1** (400.13-100.62 MHz, D_2O, 4.2 % w/w, 290 K, $\delta(^{1}H)_{TSP}$ = -0.017 ppm, $\delta(^{13}C)_{TSP}$ = -0.149 ppm). Two cuts in each axis should be noted.*

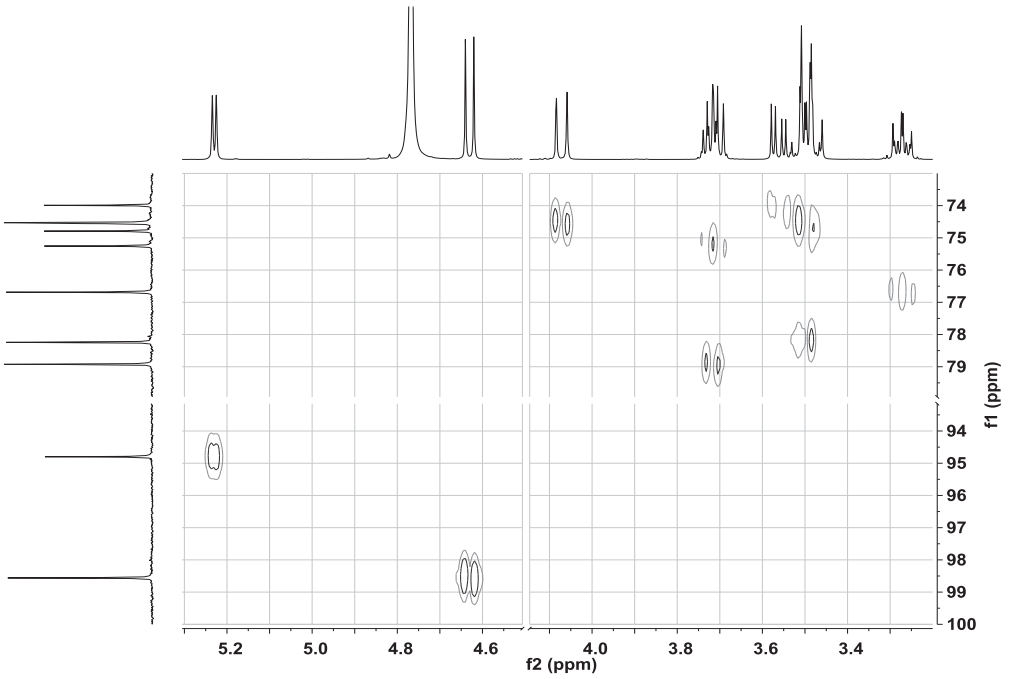

Figure 5.26 *2D ^{1}H-^{13}C HMQC spectrum of D-glucuronic acid sodium salt **1** (400.13-100.62 MHz, D_2O, 4.2 % w/w, 298 K, $\delta(^{1}H)_{TSP}$ = -0.017 ppm, $\delta(^{13}C)_{TSP}$ = -0.149 ppm). A cut in both axes should be noted.*

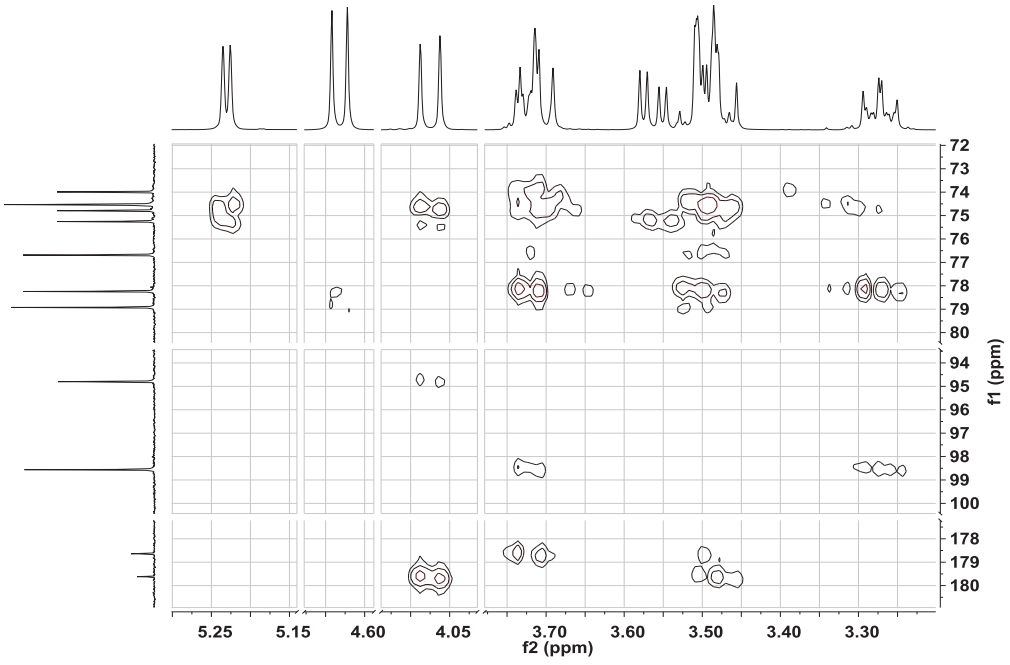

Figure 5.27 *^{1}H-^{13}C HMBC spectrum of D-glucuronic acid sodium salt **1** (400.13-100.62 MHz, D_2O, 4.2 % w/w, 290 K, $\delta(^{1}H)_{TSP}$ = -0.017 ppm, $\delta(^{13}C)_{TSP}$ = -0.149 ppm). Multiple cuts in each axis should be noted.*

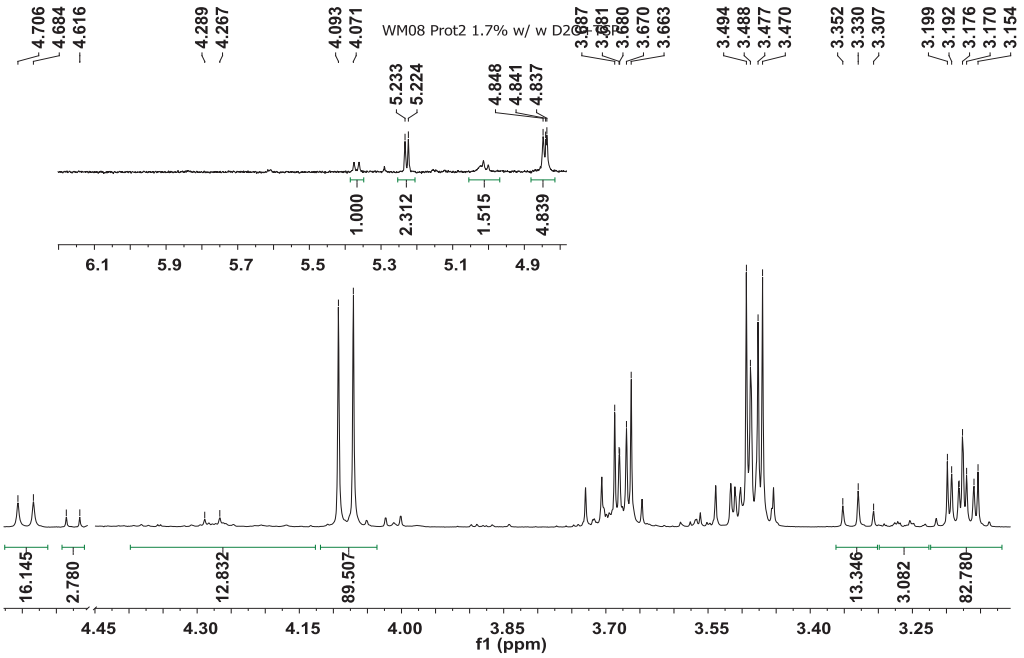

Figure 5.28 *1D ^{1}H spectrum of β-D-glucopyranosylamine uronic acid **2** / N-(β-D-glucopyranosyluronic acid) carbamate **3** obtained according to protocol **A**.9.06 (400.13 MHz, D_2O, 318 K, 1.7% w/w, $\delta(^{1}H)_{TSP}$ = -0.017 ppm). The residual water peak at 4.56 ppm was eliminated with a cut in the horizontal axis.* [39] *Molar composition: **1**, 4%; **2**, 72%; **3**, 14%; **4-13**, 10%.*

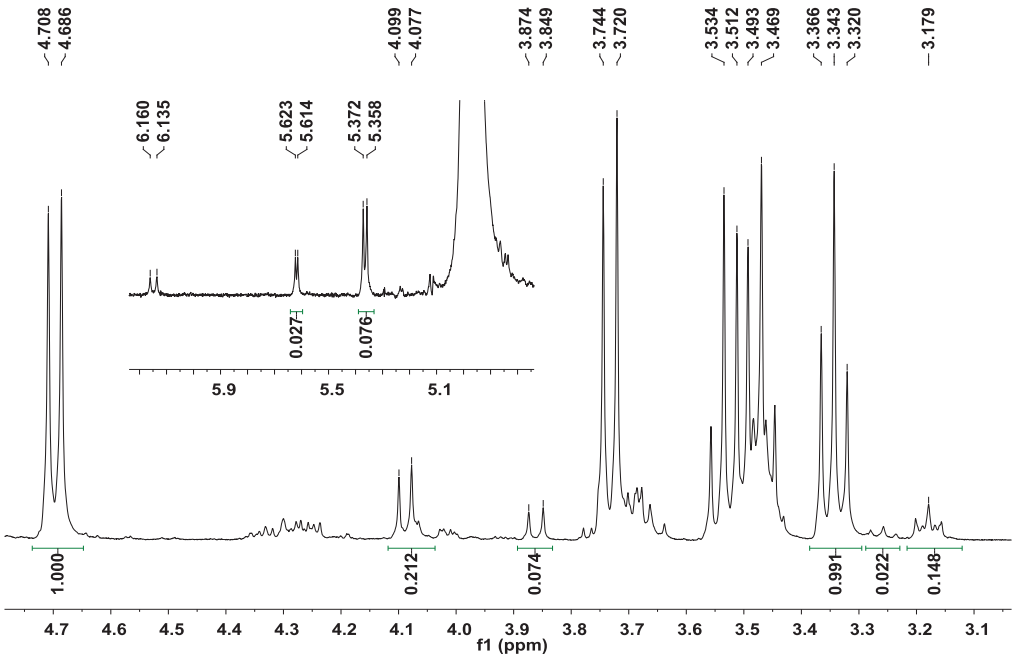

Figure 5.29 *1D ^{1}H spectrum of β-D-glucopyranosylamine uronic acid **2** / N-(β-D-glucopyranosyluronic acid) carbamate **3** obtained according to protocol **B**.5.06 (400.13 MHz, D_2O, 282 K, 2.5 % w/w, $\delta(^{1}H)_{TSP}$ = -0.017 ppm).* [40] *Molar composition: **1**, 2 %; **2**, 17 %; **3**, 69 %; **4-13**, 12%.*

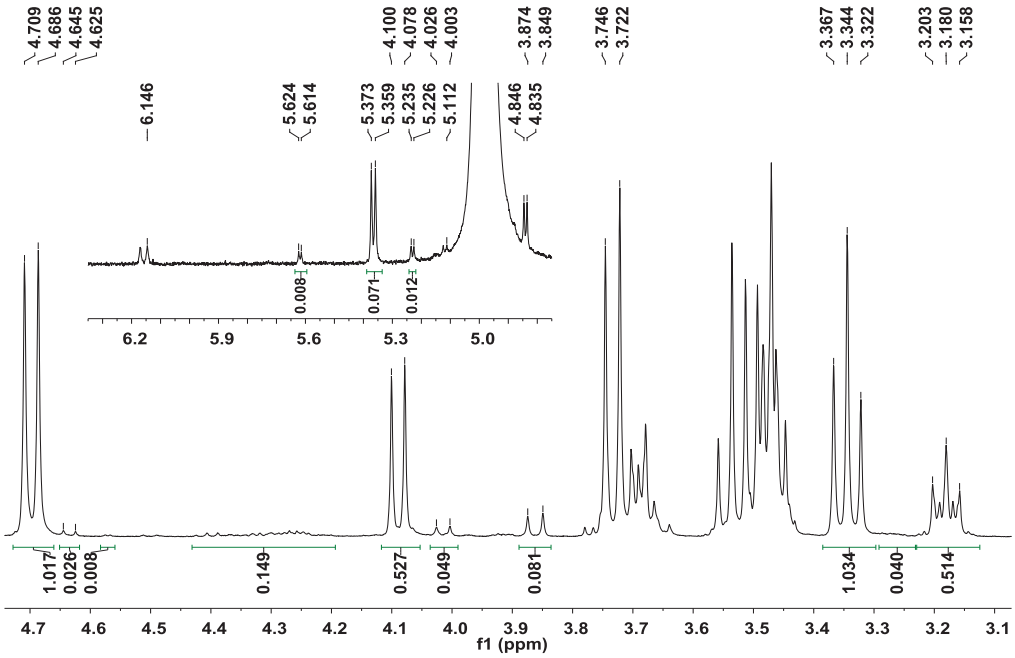

Figure 5.30 *1D ^{1}H spectrum of β-D-glucopyranosylamine uronic acid **2** / N-(β-D-glucopyranosyluronic acid) carbamate **3** obtained according to protocol **B**.0.S (400.13 MHz, D_2O, 282 K, 2.5% w/w, $\delta(^{1}H)_{TSP}$ = -0.017 ppm).* [41] *Molar composition: **1**, 2 %; **2**, 25 %; **3,** 62 %; **4-13**, 11%.*

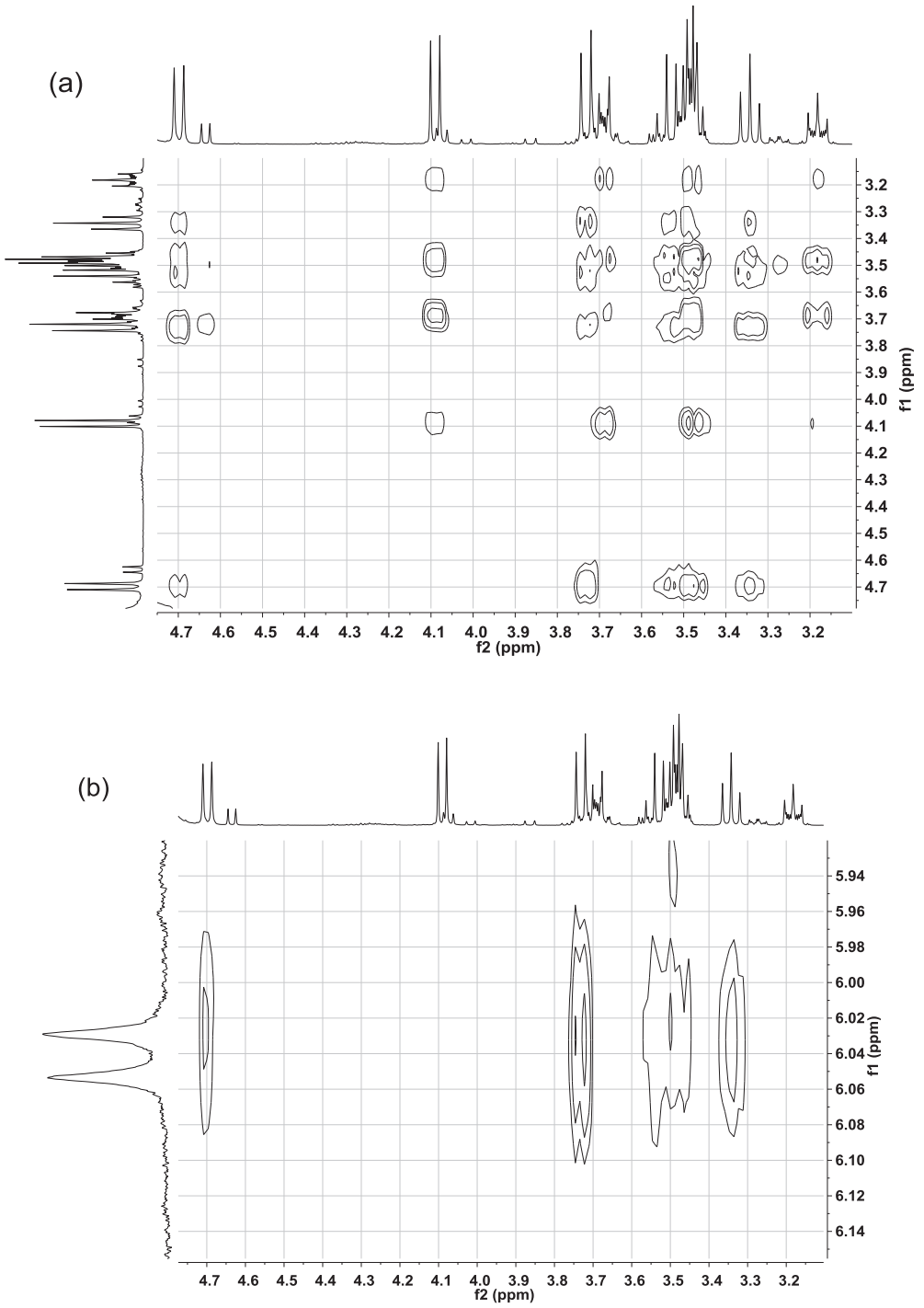

Figure 5.31 *2D ^{1}H-^{1}H TOCSY spectrum of β-D-glucopyranosylamine uronic acid **2** / N-(β-D-glucopyranosyluronic acid) carbamate **3** obtained according to protocol **A**.0.S (400.13 MHz, D_2O, 6.4 % w/w, 298 K, $\delta(^{1}H)_{TSP}$ = -0.017 ppm). Homonuclear correlations for the most abundant spin systems (a), and zoom of the low field area displaying the correlations with the $NHCO_2$ doublet (b).* [42] *Molar composition: **1**, 12 %; **2**, 42 %; **3**, 36 %; **4-13**, 10%.*

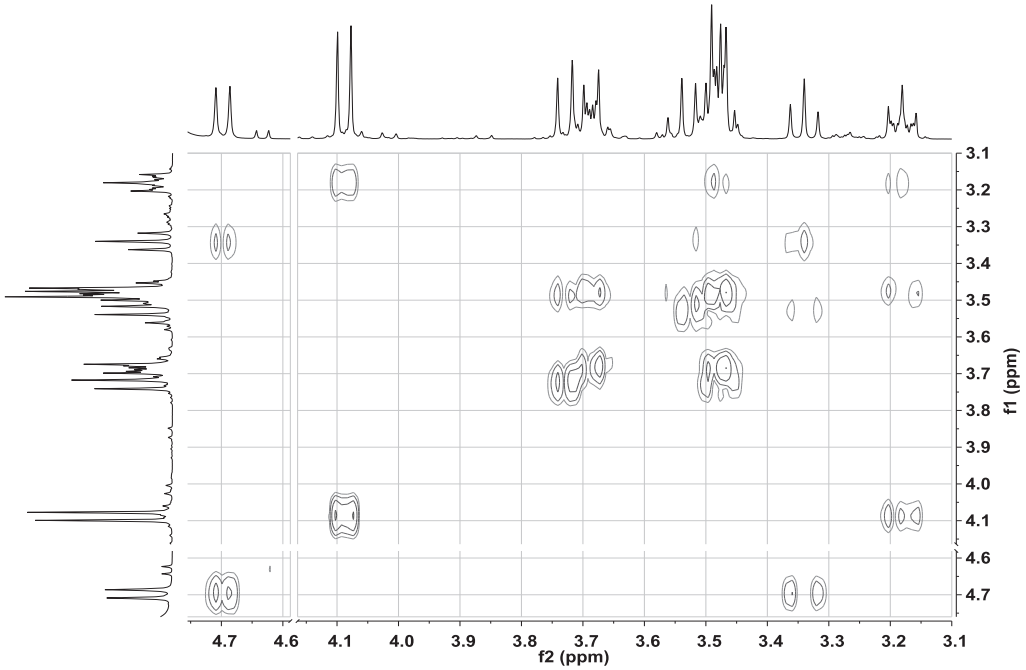

Figure 5.32 *2D ^{1}H-^{1}H COSY spectrum of β-D-glucopyranosylamine uronic acid **2** / N-(β-D-glucopyranosyluronic acid) carbamate **3** obtained according to protocol **B**.9.03 (400.13 MHz, D_2O, 298 K, 5.3% w/w, $\delta(^{1}H)_{TSP}$ = -0.017 ppm). A cut in both axes should be noted.* [43] *Molar composition: **1**, 6 %; **2**, 53 %; **3**, 30 %; **4-13**, 6%.*

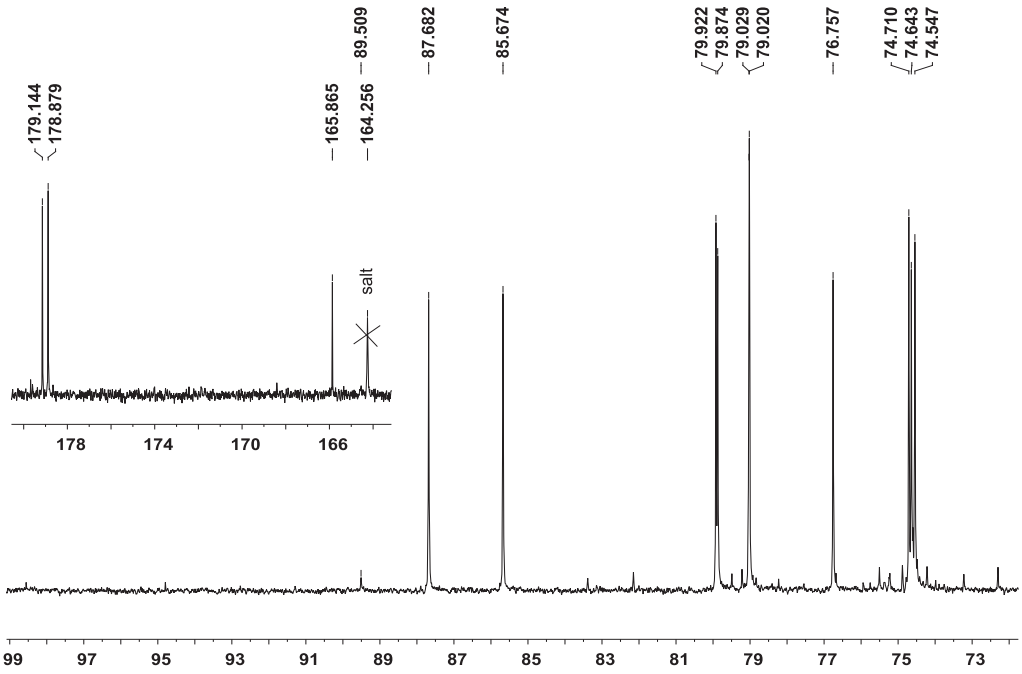

Figure 5.33 *1D ^{13}C spectrum of β-D-glucopyranosylamine uronic acid **2** / N-(β-D-glucopyranosyluronic acid) carbamate **3** obtained according to protocol **A**.9.06 (100.62 MHz, D_2O, 298 K, 5.4% w/w, $\delta(^{1}H)_{TSP}$ = -0.017 ppm).* [44] *Molar composition: **1**, 1 %; **2**, 38 %; **3**, 52 %; **4-13**, 9 %.*

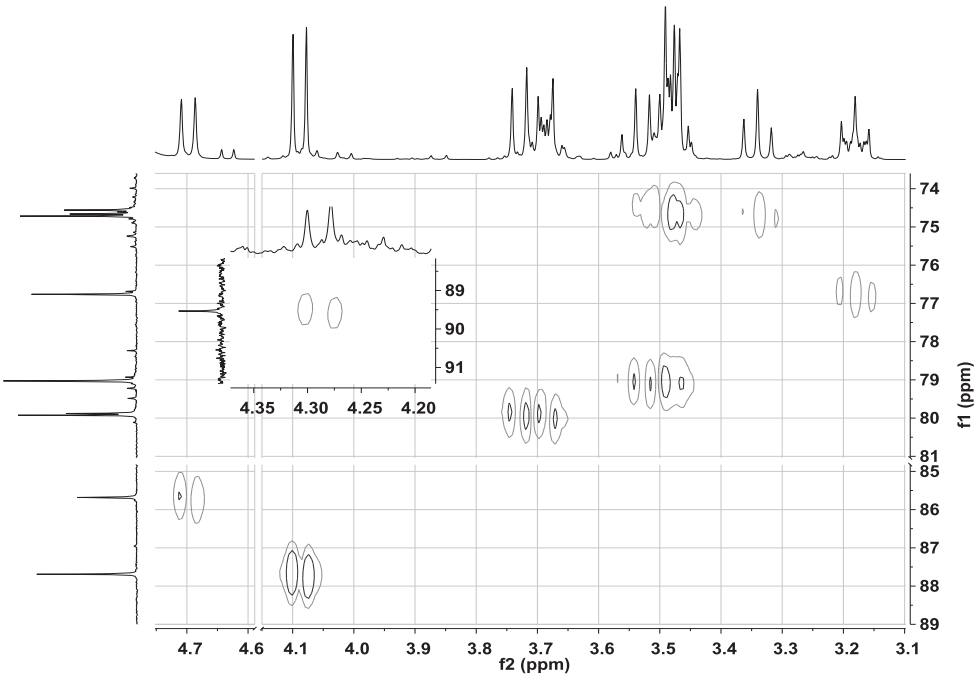

Figure 5.34 . *^{1}H-^{13}C HMQC spectrum of β-D-glucopyranosylamine uronic acid **2** / N-(β-D-glucopyranosyluronic acid) carbamate **3** obtained according to protocol **B**.9.03 (400.13-100.62 MHz, D_2O, 298 K, 5.3% w/w, $\delta(^{1}H)_{TSP}$ = -0.017 ppm). A cut in both axes should be noted; the insert shows the cross-peak due to the anomeric proton and carbon of di(β-D-glucopyranosyl)amine uronic acid **4**.* [45]

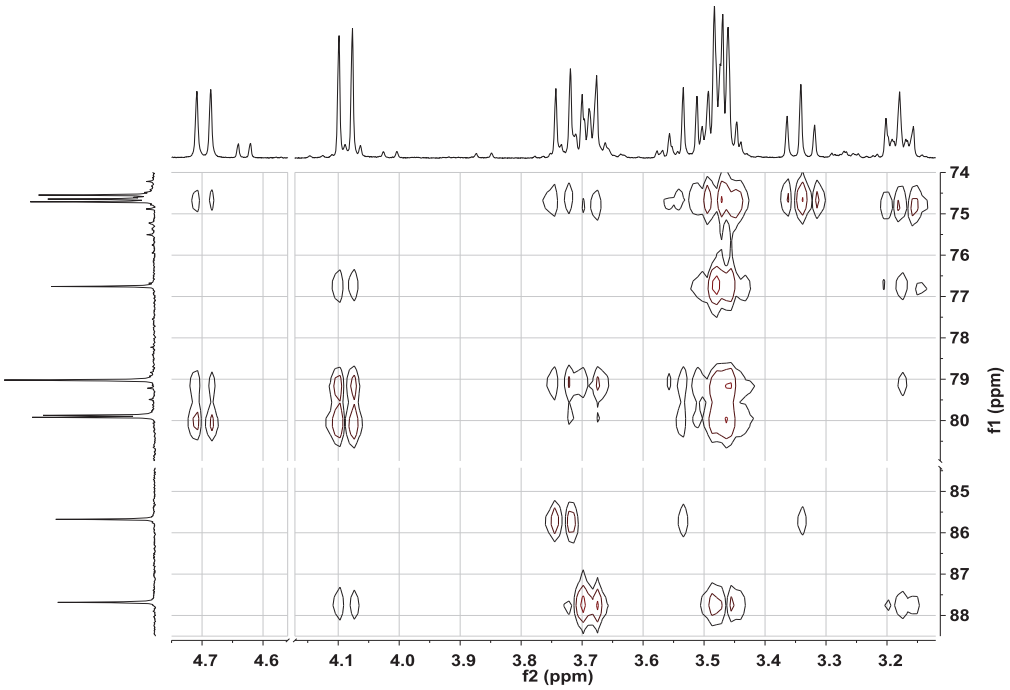

Figure 5.35 *3D ^{1}H-^{13}C HMQC-TOCSY spectrum of a sample of β-D-glucopyranosylamine uronic acid **2** / N-(β-D-glucopyranosyluronic acid) carbamate **3** obtained according to protocol **B**.0.S (400.13-100.62 MHz, D_2O, 280 K, 3% w/w, $\delta(^{1}H)_{TSP}$ = -0.017 ppm). A cut in both axes should be noted.* [46] *Molar composition: **1**, 10 %; **2**, 64 %; **3**, 17 %; **4-13**, 9 %.*

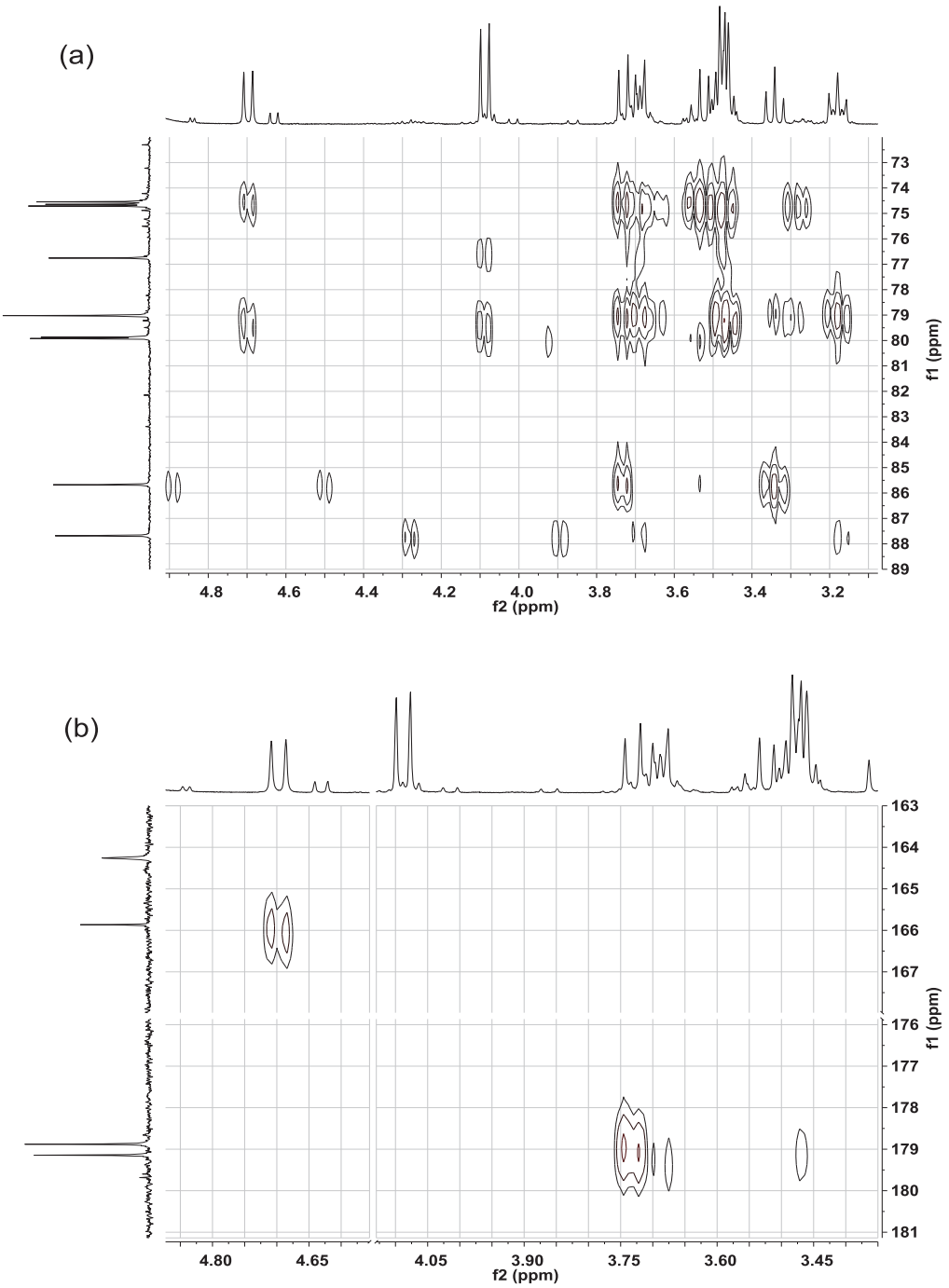

Figure 5.36 *2D ^{1}H-^{13}C HMBC spectrum of a sample of β-D-glucopyranosylamine uronic acid **2** / N-(β-D-glucopyranosyluronic acid) carbamate **3** obtained according to protocol **B**.0.S (400.13-100.62 MHz, D_2O, 280 K, 4.5% w/w, $\delta(^{1}H)_{TSP}$ = -0.017 ppm). Heteronuclear correlations for the most abundant spin systems (a), and zoom of the low field area displaying the correlation of $NHCO_2$ and COOH signals (b). A cut in both axes should be noted. When interpreting spectrum (a), care should be taken about the presence of one-bond ^{1}H-^{13}C coupling responses appearing as satellite pairs.* [47]

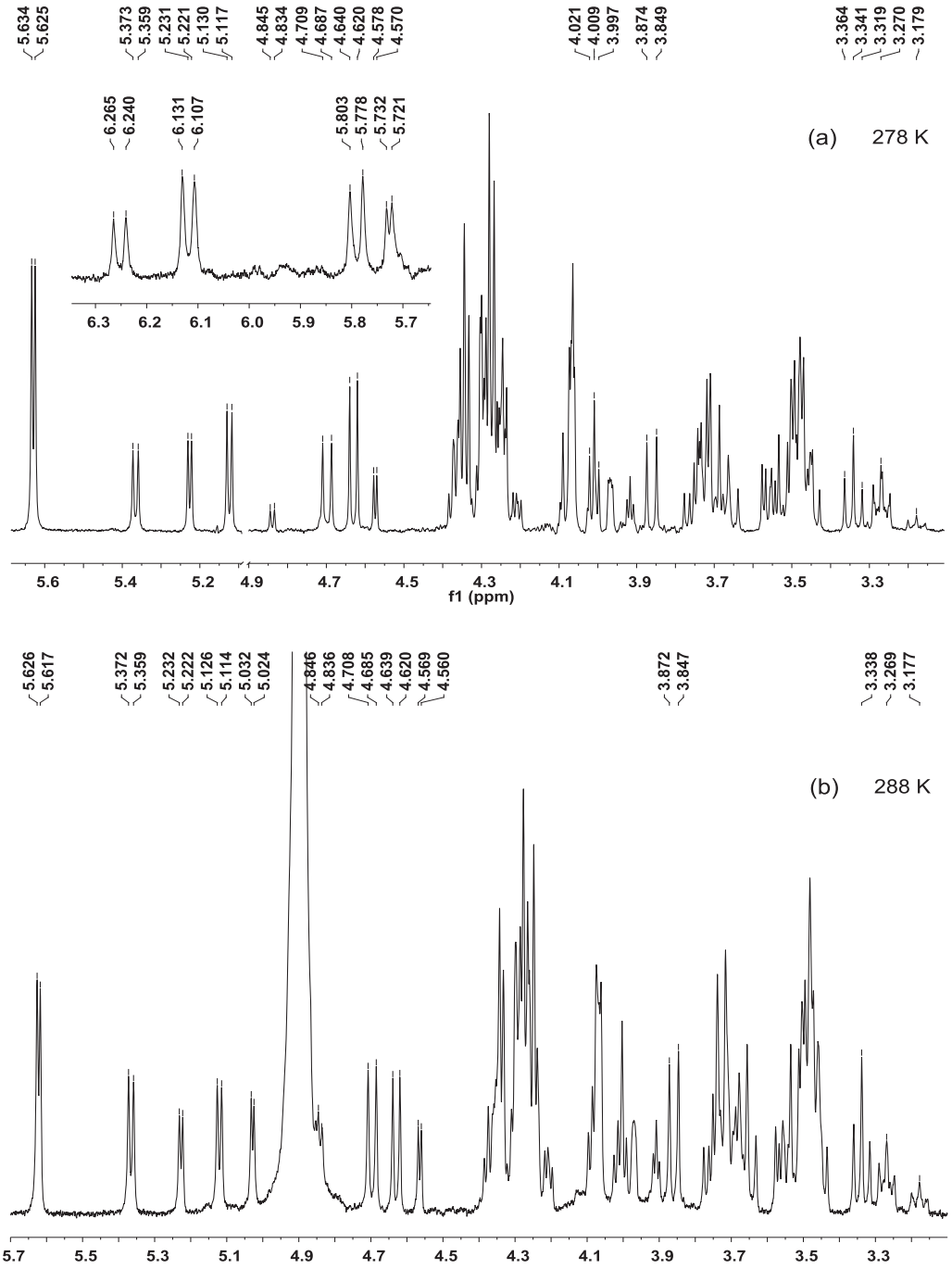

Figure 5.37 *1D ^{1}H spectrum at 278 K (a) and 288 K (b) of a sample of D-glucuronic acid **1** reacted for 15 min. according to protocol **B**.5.06 (400.13 MHz, D_2O, 1.5% w/w, $\delta(^{1}H)_{TSP}$ = -0.017 ppm).* [48] *Initial molar composition: **1**, 20%; **2**, 3 %; **3**, 9 %; **4-13**, 68%.*

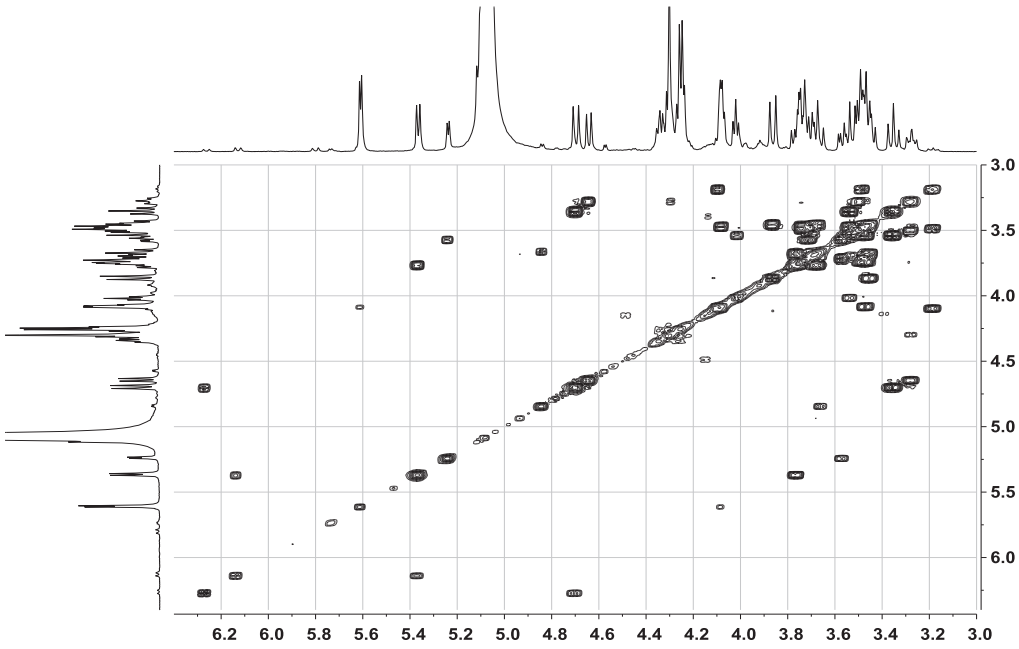

Figure 5.38 *2D gradient-selected ^{1}H-^{1}H COSY spectrum of a sample of D-glucuronic acid **1** reacted for 15 min. according to protocol **B**.5.06 (799.975 MHz, D_2O, 15 % w/w, 278 K, $\delta(^{1}H)_{TSP}$ = -0.017 ppm). The correlation between the $NHCO_2$ signal at 6.24 and the anomeric proton of β-GlcA$NHCO_2$ (4.70 ppm), and between the $NHCO_2$ signal at 6.15 ppm, and the anomeric proton of by-product **6** (5.37 ppm) should be noted.* [49]

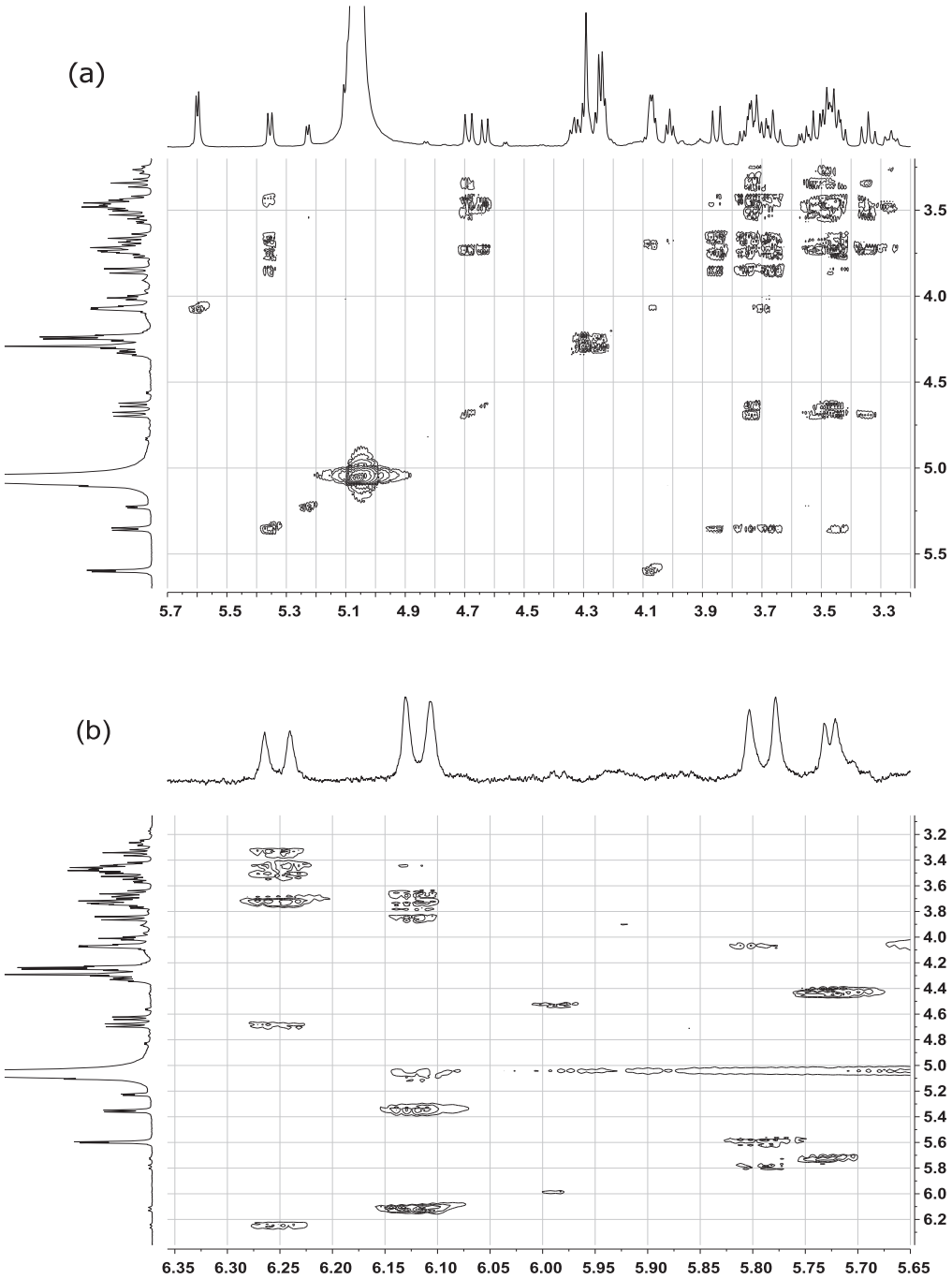

Figure 5.39 *2D ^{1}H-^{1}H TOCSY spectrum of a sample of D-glucuronic acid **1** reacted for 15 min. according to protocol **B**.5.06 (400.13 MHz, D_2O, 18 % w/w, 278 K, $\delta(^{1}H)_{TSP}$ = -0.017 ppm): Homonuclear correlations for the most abundant spin systems (a), and zoom of the low field area displaying the correlation of $NHCO_2$ signals (b).*[50]

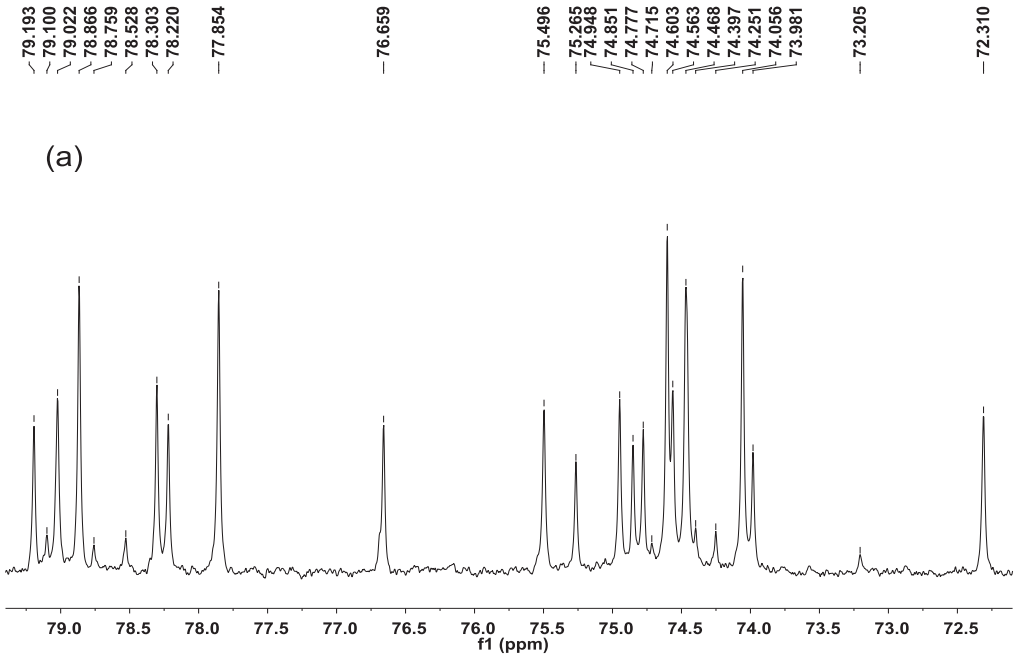
79.193
79.100
79.022
78.866
78.759
78.528
78.303
78.220
77.854
76.659
75.496
75.265
74.948
74.851
74.777
74.715
74.603
74.563
74.468
74.397
74.251
74.056
73.981
73.205
72.310
(a)
79.0
78.5
78.0
77.5
77.0
76.5
76.0
75.5
75.0
74.5
74.0
73.5
73.0
72.5
f1 (ppm)
92.769
89.445
87.735
86.983
85.697
83.562
83.171
83.149
82.535
82.293
82.202
82.172
81.685
(b)
93.0
90.0
89.0
88.0
87.0
86.0
85.0
84.0
83.0
82.0
f1 (ppm)

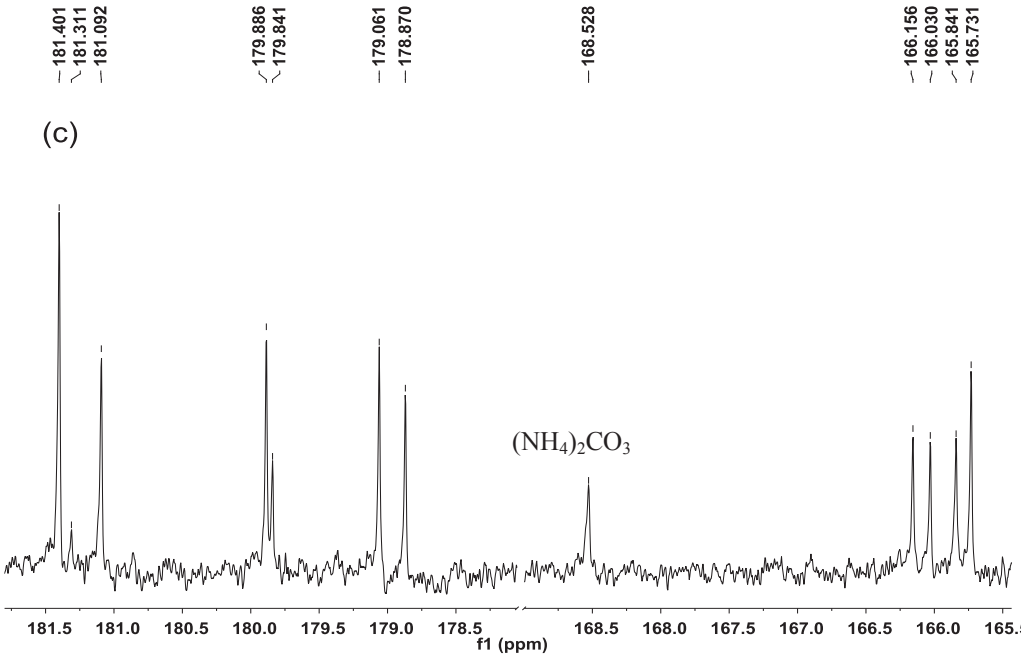

Figure 5.40 *1D ^{13}C spectrum of a sample of D-glucuronic acid **1** reacted for 15 min. according to protocol **B**.5.06 (100.62 MHz, D_2O, 15 % w/w, 278 K, $\delta(^{13}C)_{DSS}$ = 0.000 ppm). Low field zone (a), anomeric carbons zone (b), and carbonyl carbons zone (c).* [51]

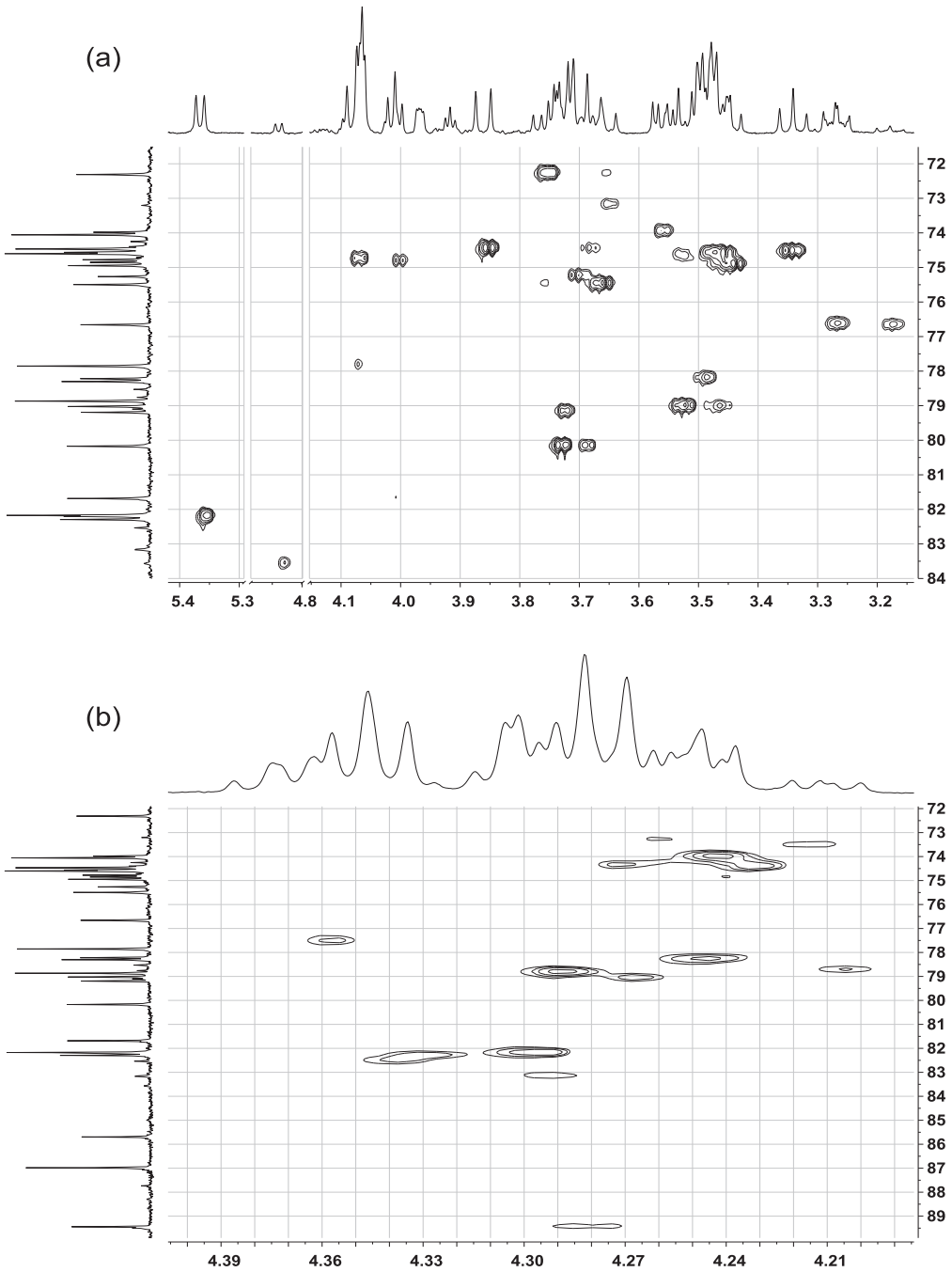

Figure 5.41 *2D gradient-selected ^{1}H-^{13}C HSQC spectrum of a sample of D-glucuronic acid **1** reacted for 15 min. according to protocol **2**.5.06 (799.975-201.172 MHz, D_2O, 15 % w/w, 278 K, $\delta(^{1}H)_{TSP}$ = -0.017 ppm, $\delta(^{13}C)_{TSP}$ = -0.149 ppm): Heteronuclear correlations for the most abundant spin systems (a), and zoom of the area between 4.2 and 4.4 ppm displaying a complex array of peaks from 7 different spin systems (b). In (a), two cuts in the horizontal axis should be noted.* [52]

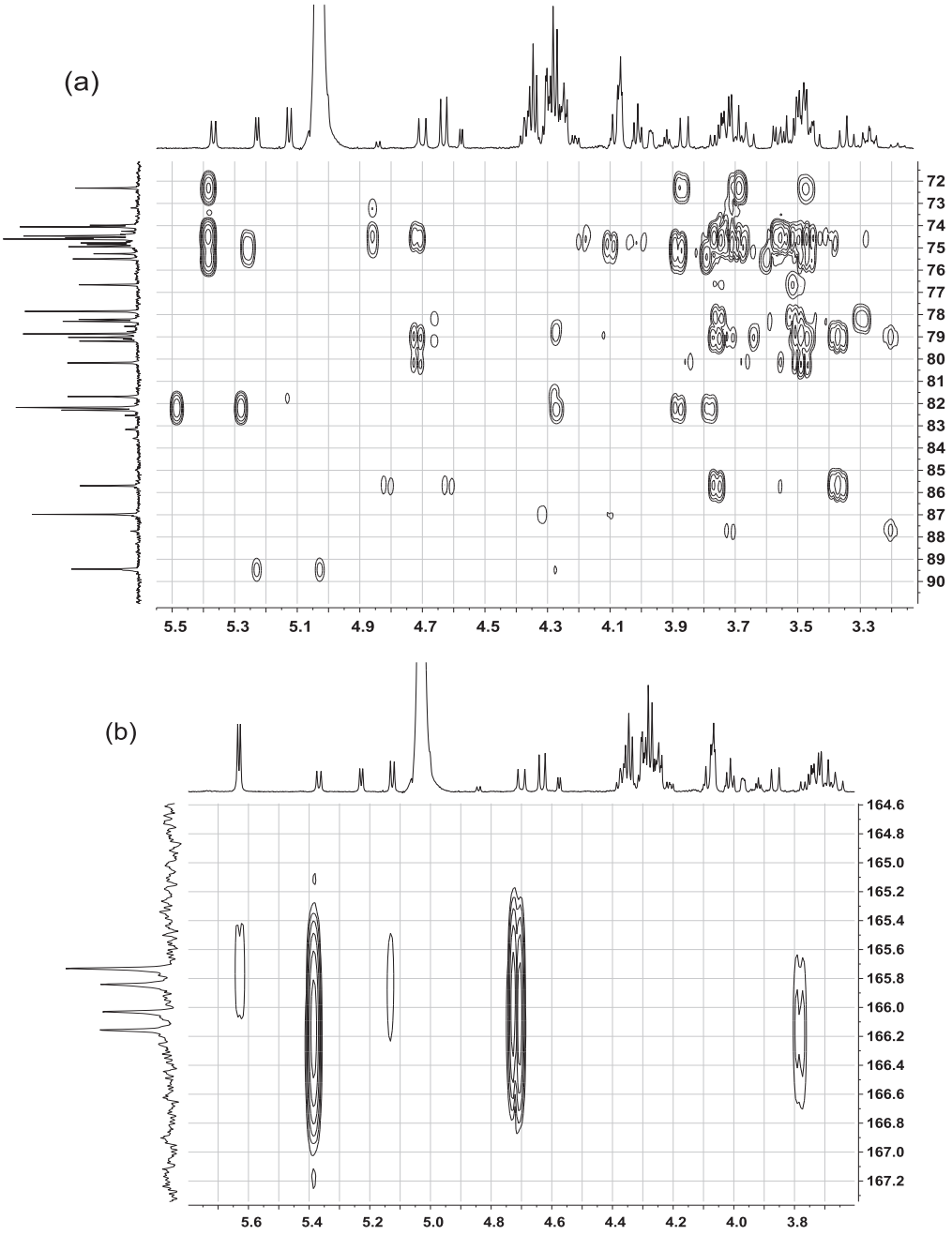

Figure 5.42 *2D gradient-selected ^{1}H-^{13}C HMBC spectrum of a sample of D-glucuronic acid **1** reacted for 15 min. according to protocol **B**.5.06 (799.975-201.172 MHz, D_2O, 15 % w/w, 278 K, $\delta(^{1}H)_{TSP}$ = -0.017 ppm, $\delta(^{13}C)_{TSP}$ = -0.149 ppm): Heteronuclear correlations for the most abundant spin systems (a), and zoom of the low field area displaying the correlation of $NHCO_2$ signals (b). When interpreting spectrum (a), care should be taken about the presence of one-bond ^{1}H-^{13}C coupling responses appearing as satellite pairs.* [53]

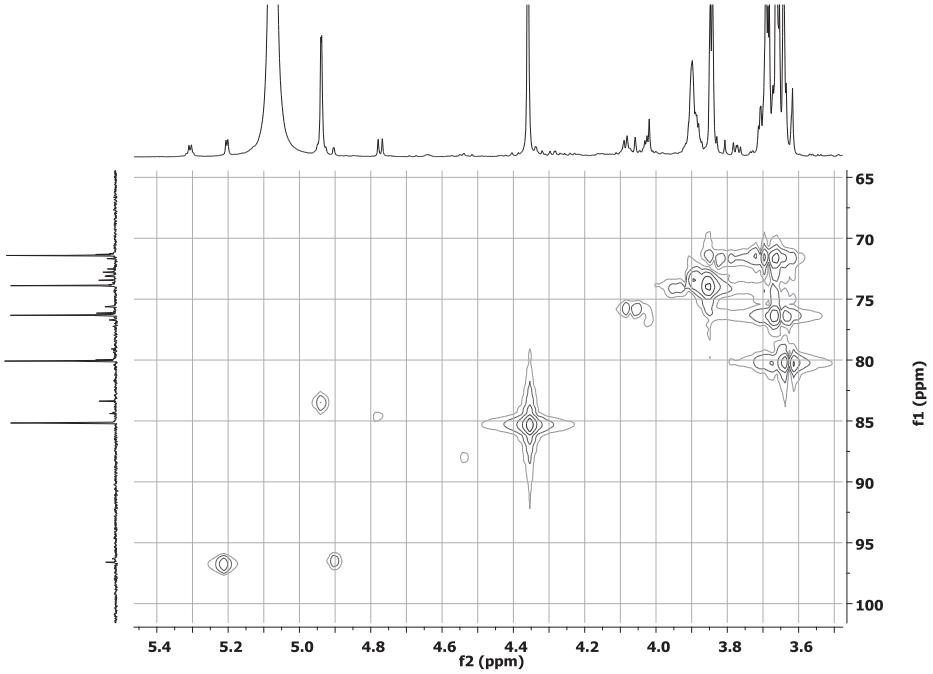

Figure 5.43 *^{1}H-^{13}C HMQC spectrum of β-D-mannopyranuronosylamine **14** / N-(β-D-glucopyranosyluronic acid) carbamate **15** obtained according to protocol **A**.0.S (Entry 3, Table 5.4). Conditions: ^{1}H-^{13}C (400.13-100.62 MHz), D_2O, 298 K, 2 % w/w. $\delta(^{1}H)_{TSP}$ = -0.017 ppm,$(^{13}C)_{TSP}$ = -0.149 ppm.*

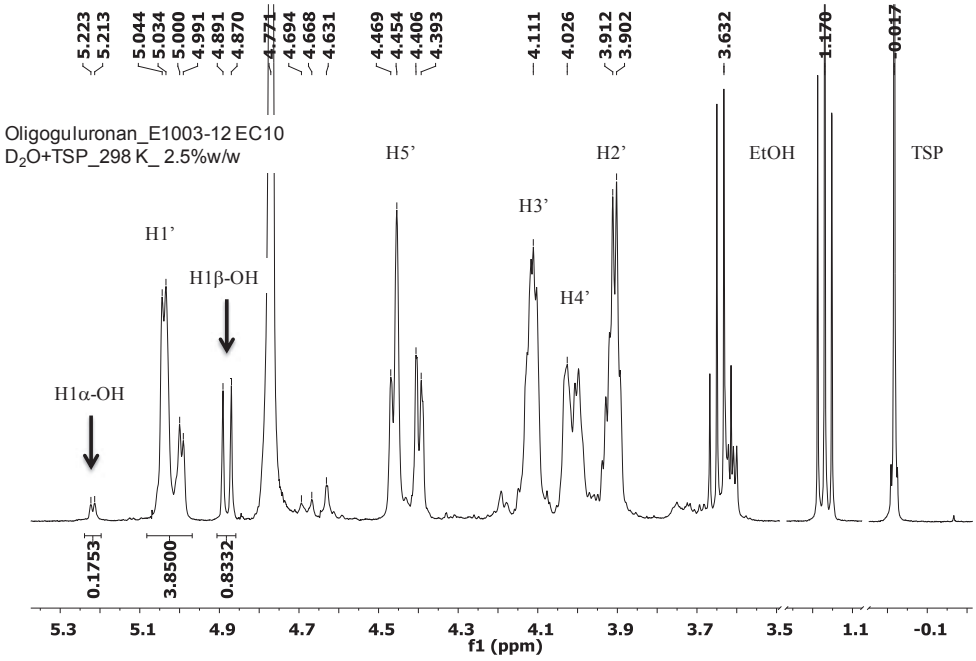

Figure 5.44 *^{1}H NMR spectrum of (1→4)-α-L-guluronan E1003-12 EC10. Conditions: ^{1}H (400.13 MHz), D_2O, 298 K, 2.5 % w/w. $\delta(^{1}H)_{TSP}$ = -0.017 ppm.*

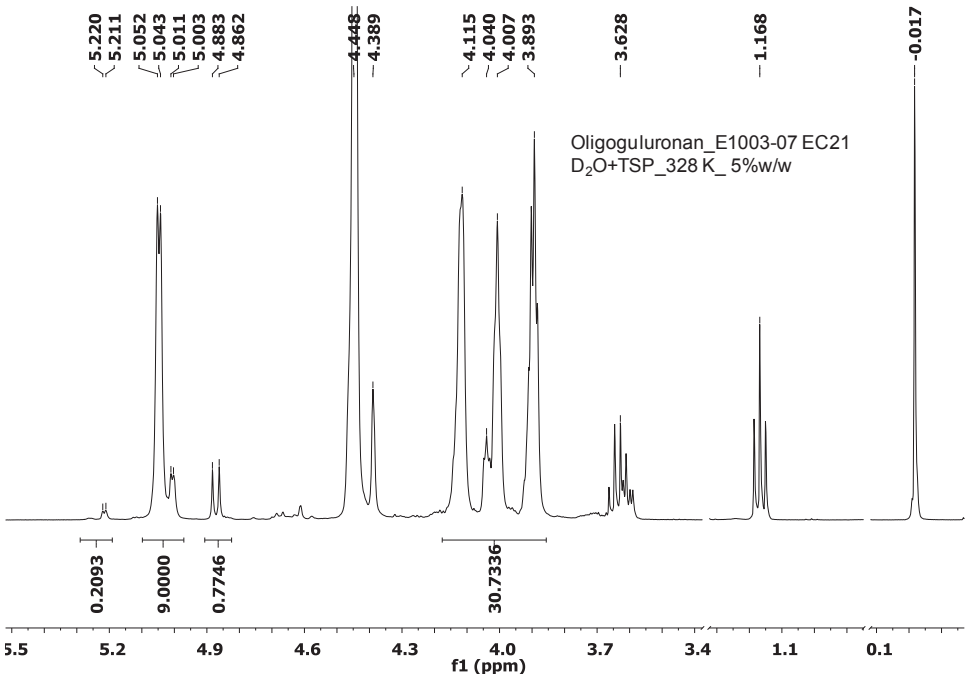

Figure 5.45 *^{1}H NMR spectrum of (1→4)-α-L-guluronan E1003-07 EC21. Conditions: ^{1}H (400.13 MHz), D_2O,328 K, 5 % w/w. $\delta(^1H)_{TSP}$ = -0.017 ppm.*

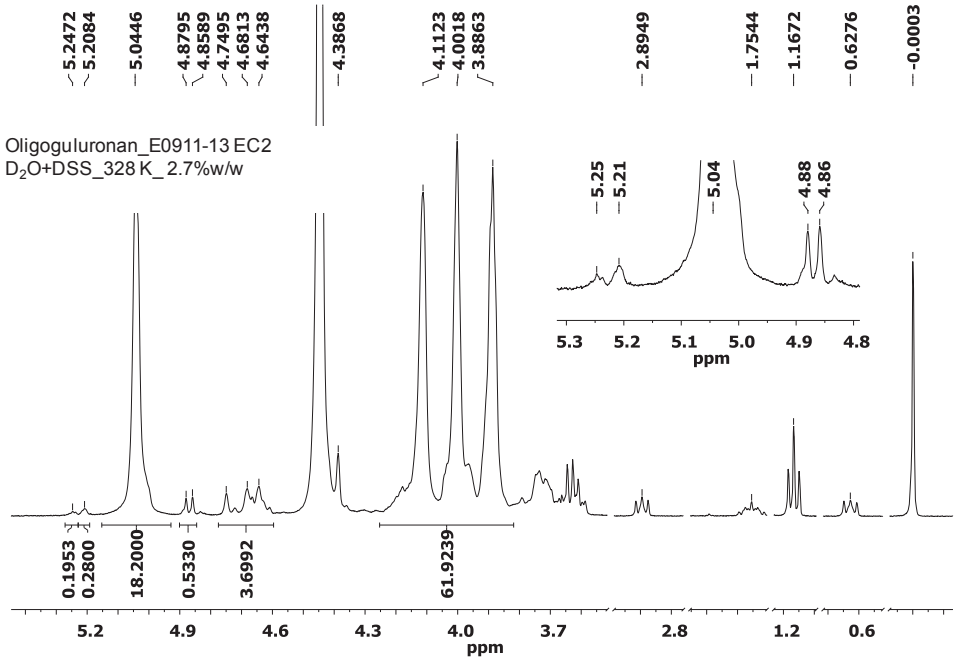

Figure 5.46 *^{1}H NMR spectrum of (1→4)-α-L-guluronan E0911-13 EC2. Conditions: ^{1}H (400.13 MHz), D_2O,328 K, 2.7 % w/w. $\delta(^1H)_{DSS}$ = -0.0 ppm.*

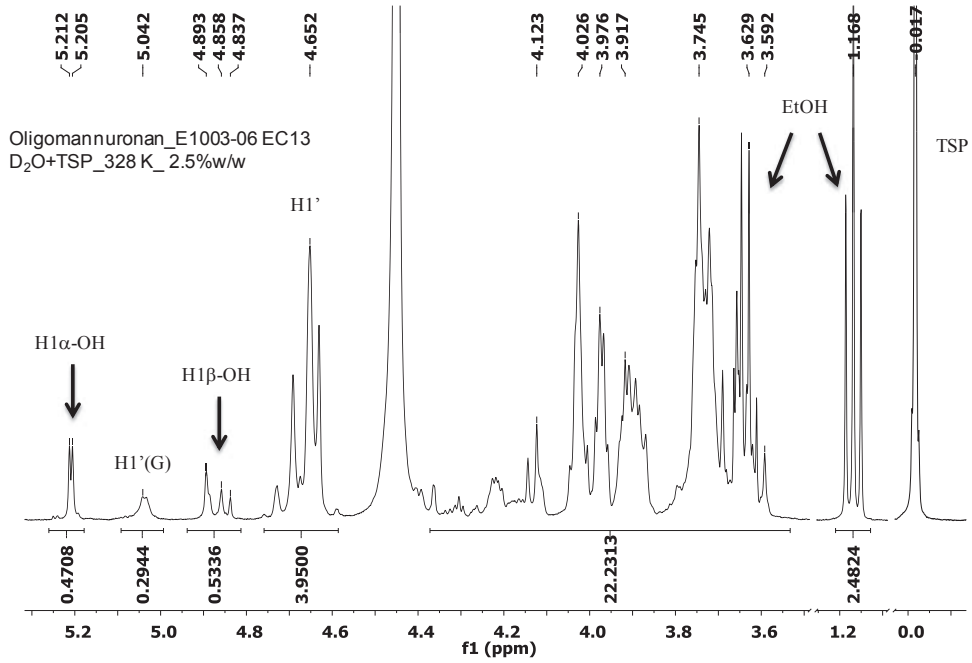

Figure 5.47 *^{1}H NMR spectrum of (1→4)-β-D-mannuronan E1003-06 EC13. Conditions: ^{1}H (400.13 MHz), D_2O,328 K, 2.5 % w/w. $\delta(^{1}H)_{TSP}$ = -0.017 ppm.*

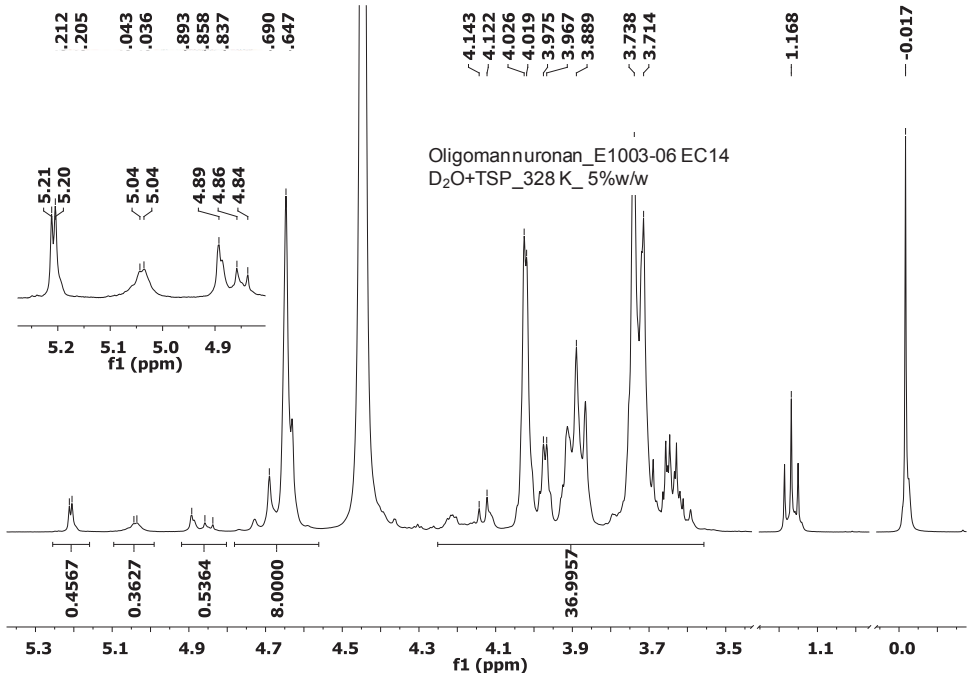

Figure 5.48 *^{1}H NMR spectrum of (1→4)-β-D-mannuronan E1003-06 EC14. Conditions: ^{1}H (400.13 MHz), D_2O,328 K, 5 % w/w. $\delta(^{1}H)_{TSP}$ = -0.017 ppm.*

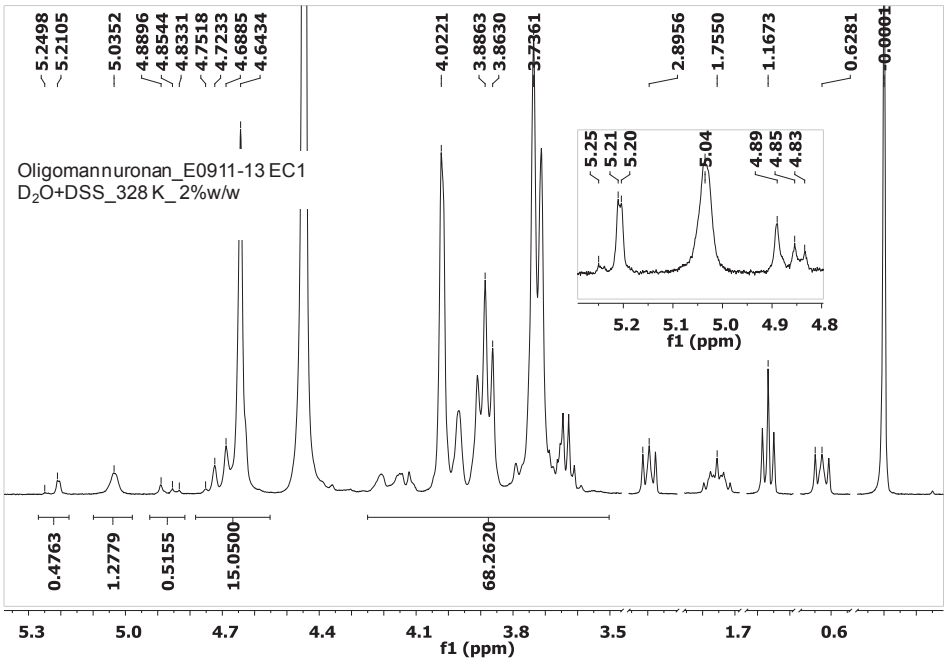

Figure 5.49 *^1H NMR spectrum of (1→4)-β-D-mannuronan E0911-13 EC1. Conditions: ^1H (400.13 MHz), D_2O,328 K, 2 % w/w. $\delta(^1H)_{DSS}$ = -0.0 ppm.*

5.5 References

(1) (a) Ghadban, A.; Albertin, L.; Condamine, E.; Mounguengui, R. W. M.; Heyraud, A. *Can. J. Chem.* **2011**, *89*, 987(b) Ghadban, A.; Albertin, L.; Moussavou Mounguengui, R. W.; Peruchon, A.; Heyraud, A. *Carbohydrate Research* **2011**, *346*, 2384.

(2) McNaught, A. D. *Pure and Applied Chemistry* **1996**, *68*, 1919.

(3) *Polysaccharides II: Polysaccharides from Eukaryotes*; Vandamme, E. J.; De Baets, S.; Steinbüchel, A., Eds.; Wiley-VCH: Weinheim, 2002.

(4) Timoshchuk, V. A. *Russ. Chem. Rev.* **1995**, *64*, 675.

(5) Leendert, J. v. d. B.; Jeroen, D. C. C.; Remy, E. J. N. L.; Jasper, D.; Herman, S. O.; Gijsbert, A. v. d. M. *European Journal of Organic Chemistry* **2007**, *2007*, 3963.

(6) (a) Kamoda, S.; Nakano, M.; Ishikawa, R.; Suzuki, S.; Kakehi, K. *Journal of Proteome Research* **2005**, *4*, 146(b) Likhosherstov, L. M.; Novikova, O. S.; Shibaev, V. N. *Russ. Chem. Bull.* **1998**, *47*, 1214(c) Vetter, D.; Tate, E. M.; Gallop, M. A. *Bioconjugate Chemistry* **1995**, *6*, 319.

(7) (a) Ishiwata, A.; Takatani, M.; Nakahara, Y.; Ito, Y. *Synlett* **2002**, 634(b) Monsigny, M.; Quetard, C.; Bourgerie, S.; Delay, D.; Pichon, C.; Midoux, P.; Mayer, R.; Roche, A. C. *Biochimie* **1998**, *80*, 99(c) Zeng, X.; Murata, T.; Kawagishi, H.; Usui, T.; Kobayashi, K. *Bioscience, Biotechnology, and Biochemistry* **1998**, *62*, 1171(d) Plusquellec, D.; Brenner-Henaff, C.; Leon-Ruaud, P.; Duquenoy, S.; Lefeuvre, M.; Wroblewski, H. *Journal of Carbohydrate Chemistry* **1994**, *13*, 737(e) Mellet, C. O.; Blanco, J. L. J.; Fernandez, J. M. G.; Fuentes, J. *Journal of Carbohydrate Chemistry* **1993**, *12*, 487(f) Urge, L.; Otvos Jr, L.; Lang, E.; Wroblewski, K.; Laczko, I.; Hollosi, M. *Carbohydrate Research* **1992**, *235*, 83(g) Likhosherstov, L. M.; Novikova, O. S.; Derevitskaya, V. A.; Kochetkov, N. K. *Carbohydr. Res.* **1986**, *146*, C1.

(8) (a) Halila, S.; Manguian, M.; Fort, S.; Cottaz, S.; Hamaide, T.; Fleury, E.; Driguez, H. *Macromolecular Chemistry and Physics* **2008**, *209*, 1282(b) Retailleau, L.; Laplace, A.; Fensterbank, H.; Larpent, C. *Journal of Organic Chemistry* **1998**, *63*, 608(c) Lubineau, A.; Auge, J.; Drouillat, B. *Carbohydr. Res.* **1995**, *266*, 211.

(9) (a) Tuzikov, A. B.; Gambaryan, A. S.; Juneja, L. R.; Bovin, N. V. *Journal of Carbohydrate Chemistry* **2000**, *19*, 1191(b) Kallin, E.; Loenn, H.; Norberg, T.; Elofsson, M. *Journal of Carbohydrate Chemistry* **1989**, *8*, 597.

(10) (a) Rice, K. G. *Analytical Biochemistry* **2000**, *283*, 10(b) Manger, I. D.; Rademacher, T. W.; Dwek, R. A. *Biochemistry* **1992**, *31*, 10724.

(11) (a) Vetter, D.; Gallop, M. A. *Bioconjugate Chemistry* **1995**, *6*, 316(b) Fulks, G.; Fisher, G. B.; Rahmoeller, K.; Wu, M.-C.; D'Herde, E.; Tan, J. In *Society of Automotive Engineers, [Special Publication] SP*, 2009; Vol. SP-2254(c) Likhosherstov, L. M.; Novikova, O. S.; Shibaev, V. N. *Doklady Chemistry* **2003**, *389*, 73(d) Likhosherstov, L. M.; Novikova, O. S.; Shibaev, V. N. *Doklady Chemistry (Translation of the chemistry section of Doklady Akademii Nauk)* **2002**, *383*, 89.

(12) Campa, C.; Donati, I.; Vetere, A.; Gamini, A.; Paoletti, S. *Journal of Carbohydrate Chemistry* **2001**, *20*, 263.

(13) Braccini, I.; Grasso, R. P.; Pérez, S. *Carbohydrate Research* **1999**, *317*, 119.

(14) Experiment WM08-P2_final, 30 °C, 25hrs.

(15) Experiments (b) AG09-13, and (c) AG09-30_P1. Conditions: D_2O, 278 K, ((^1H) TSP = -0.017 ppm, ((^{13}C) TSP = -0.149 ppm.

(16) Conditions: D_2O, 6.4 % w/w, 298 K, $\delta(^1H)$ TSP = -0.017 ppm. Sample obtained at 30 ºC according to protocol **A**.0.S (WM-08_P1_final). Its initial molar composition was as follows: **1**, 12 %; **2**, 42 %; **3**, 37 %; **4-11**, 9 %. The projections do not correspond to the same sample.

(17) Conditions: D_2O, 298 K, 5.3% w/w, $\delta(^1H)$ TSP = -0.017 ppm. Sample obtained at 30 ºC according to protocol **B**.9.03 (WM-08_P3 final). Its initial molar composition was as follows: **1**, 6 %; **2**, 55 %; **3**, 30 %; **4-11**, 9 %.

(18) Conditions: D_2O, 298 K, 5.3% w/w, $\delta(^1H)$ TSP = -0.017 ppm. Sample obtained at 30 ºC according to protocol **B**.9.03 (WM-08_P3 final). The projections do not refer to the same sample.

(19) Bock, K.; Pedersen, C.; Tipson, R. S.; Horton, D. *Advances in Carbohydrate Chemistry and Biochemistry* **1983**, *41*, 27.

(20) Altona, C.; Haasnoot, C. A. G. *Org. Magn. Reson.* **1980**, *13*, 417.

(21) Pfeffer, P. E.; Valentine, K. M.; Parrish, F. W. *Journal of the American Chemical Society* **1979**, *101*, 1265.

(22) 2D gradient-selected ^1H-^1H COSY (AG10-08) and ^1H-^{13}C HMBC (AG10-16) spectrum, D_2O, 15 % w/w, 278 K.

(23) (a) Perlin, A. S.; Du Penhoat, P. H.; Isbell, H. S. *Advances in Chemistry Series* **1973**, *No. 117*, 39(b) Heyraud, A.; Gey, C.; Leonard, C.; Rochas, C.; Girond, S.; Kloareg, B. *Carbohydrate Research* **1996**, *289*, 11.

(24) (a) Isbell, H. S.; Frush, H. L. *Journal of the American Chemical Society* **1950**, *72*, 1043(b) Isbell, H. S.; Frush, H. L. *Journal of Organic Chemistry* **1958**, *23*, 1309.

(25) Ritchie, R. G. S.; Cyr, N.; Korsch, B.; Koch, H. J.; Perlin, A. S. *Can. J. Chem.* **1975**, *53*, 1424.

(26) Williams, C.; Allerhand, A. *Carbohydrate Research* **1977**, *56*, 173.

(27) Experiment AG10-08. Its initial molar composition as determined by ^1H-NMR was: **1**, 22 %; **2**, 3 %; **3**, 10 %; **4**, 0 %; **5**, 27 %; **6**, 9 %; **7**, 11 %; **9**, 2 %; **10**, 5 %; **8+11**, 12 %.

(28) Experiment AG10-20_P1_end. Its initial molar composition as determined by ^1H-NMR was: **1**, 2%; **2**, 25%; **3**, 63 %, **4**, 1 %; **5**, 1 %; **6**, 5%; **7**, 0 %; **9**, 2 %; **10**, 0 %, **8+11**, 1 %.

(29) Experiment AG10-08, protocol **B**.5.06, 30 ºC. Mole fractions lower than 0.5 % were disregarded.

(30) Experiment AG09-30_P2. Conditions: D_2O, 278 K, $\delta(^1H)$ TSP = -0.017 ppm.

(31) (a) Johnson, S. L.; Morrison, D. L. *Journal of the American Chemical Society* **1972**, *94*, 1323(b) Ewing, S. P.; Lockshon, D.; Jencks, W. P. *Journal of the American Chemical Society* **1980**, *102*, 3072.

(32) Kort, M. J. *Advances in Carbohydrate Chemistry and Biochemistry* **1971**, *25*, 311.

(33) AG10-34, conditions:100 MHz, 16.6 %w/w, ns = 800, D1 = 20 s, T = 278 K.

(34) Wen, N.; Brooker, M. H. *Journal of Physical Chemistry* **1995**, *99*, 359.

(35) AG10-24-P2, conditions: D_2O, 8.5 %w/w, 298K.
(36) AG11-19-P2, conditions: D_2O, 3.84 %w/w, 303K.
(37) AG10-24-P1, conditions: D_2O, 8 %w/w, 298K.
(38) AG11-19-P1, conditions: D_2O, 3.84 %w/w, 303K.
(39) Experiment WM08-P2_final, 30 °C, 25hrs.
(40) Experiment AG09-30_P2_S14, 30 ºC, 33 hrs.
(41) Experiment AG10-20_P1_S13, 30 ºC, 48 hrs.
(42) Experiment WM-08_P1_final, 30 ºC, 25 hrs.
(43) Experiment WM-08_P3 final, 30 ºC, 25 hrs.
(44) Experiment WM08-P2_final, 30 °C, 25hrs.
(45) Experiment WM-08_P3 final, 30 ºC, 25 hrs.
(46) Experiment AP10-12_lyoph. twice, ambient temperature, 24 hrs.
(47) Experiment AP10-12_lyoph. twice, ambient temperature, 24 hrs.
(48) Experiment AG10-08, 30 ºC.
(49) Experiment AG10-08, 30 ºC.
(50) Experiment AG10-08, 30 ºC.
(51) Experiment AG10-08, 30 ºC.
(52) Experiment AG10-08, 30 ºC.
(53) Experiment AG10-08, 30 ºC.

Chapter 6: Synthesis of oligoglycuronan derived amino alditols in aqueous solution

Table of contents

6.1 Introduction

Reductive amination is the conversion of a carbonyl group into an amine in the presence of a reducing agent and via an intermediate iminium ion formed in-situ (Scheme 6.1). [1] In the first step of the reaction, an amine (or ammonia) condenses with a carbonyl group to give an amino alcohol, which is then protonated at the oxygen atom and eliminates a water molecule. The resulting iminium ion is then rapidly reduced to an amine. If the starting compound is an aldose, the product will be a 1-amino-1-deoxy alditol.

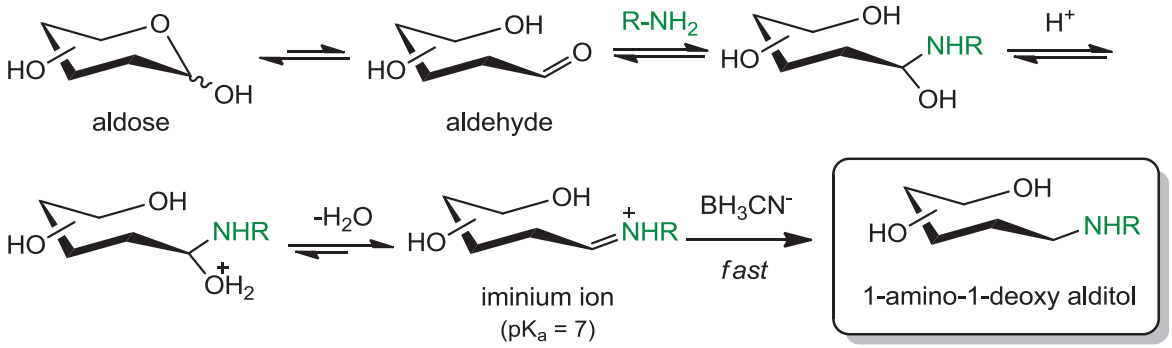

Scheme 6.1 *Mechanism of the reductive amination of an aldose with $NaBH_3CN$.*

The reductive amination of mono-, oligo- and polysaccharides in aqueous solution has already been used, among other things, for the synthesis of glycomonomers, [2] end-labeled oligo- and polysaccharides, [3] graft glycopolymers, [4] and protein glyconjugates. [5] In this context, sodium (or lithium) cyanoborohydride ($NaBH_3CN$) is the reducing agent of choice, thanks to its remarkable stability in aqueous solution (at pH > 2.5) and its pH-dependent chemoselectivity. [6] In particular, at pH 6-8 the reduction of iminium ions is sufficiently faster than that of carbonyl groups to enable their formation in situ followed by their rapid reaction with the cyanoborohydride anion. Compared to glycosylamine synthesis, the reductive amination of aldoses has the inherent advantage of yielding a stable amine. Both reactions do not need protective group chemistry but care should be taken when handling and disposing of cyanoborohydride, since the compound is toxic.

The reductive amination of oligoalginates with a bifunctional amine has already been reported in the literature [3a,b] but the characterization of the resulting materials was basic and functionalization yields were not determined. In this chapter, I will describe the transformation of (1→4)-β-D-mannuronan and (1→4)-α-L-guluronan oligosaccharides into the corresponding 1-amino-1-deoxy alditols by reductive amination with ammonium salts in aqueous solution, the optimization study that was carried on said reaction and the evidence that was gathered on the formation of by-products.

6.2 Experimental

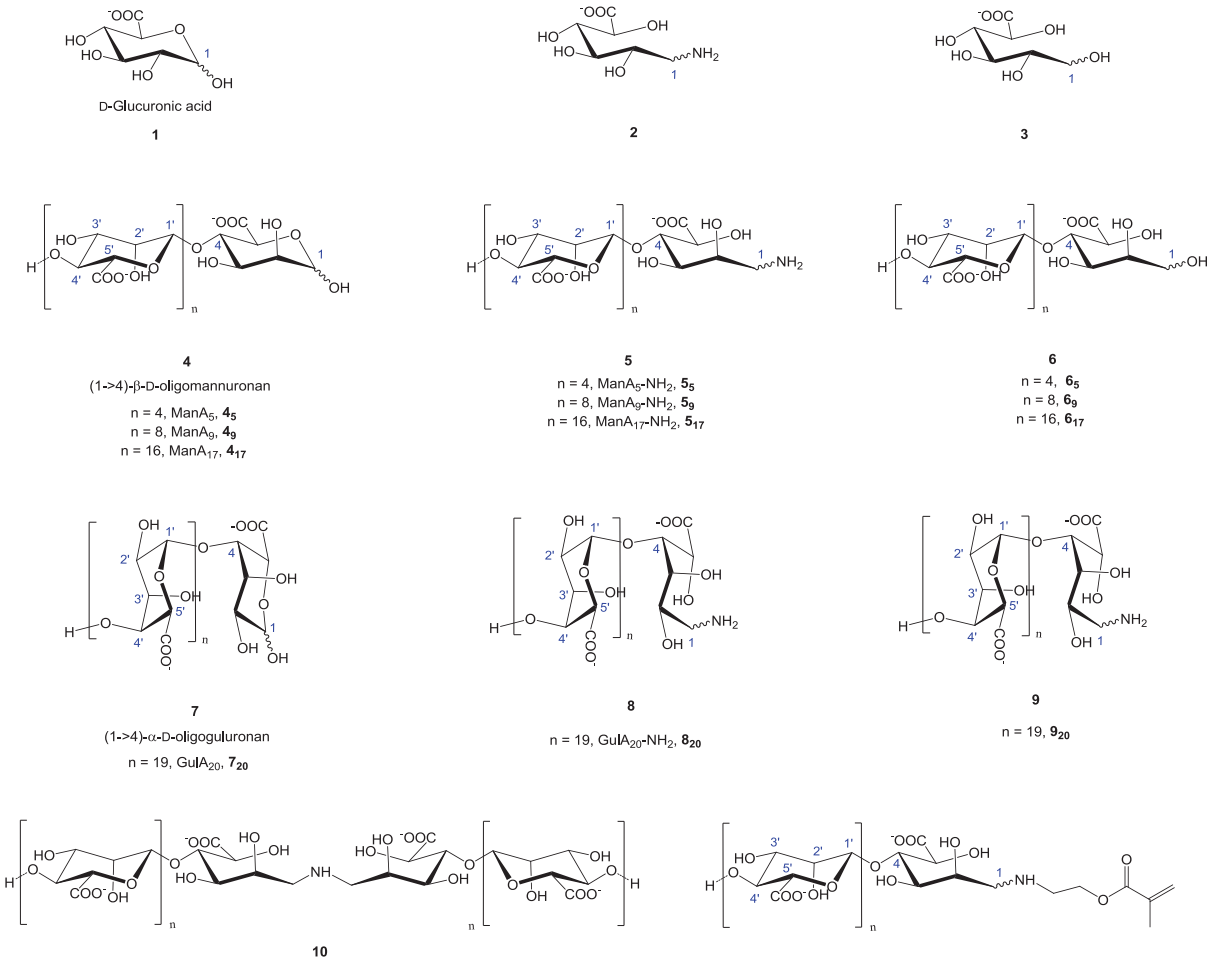

Scheme 6.2 *Molecules involved in this study. Nucleus numbering is used in NMR assignments. The subscript represents the* DP_n *of the oligoglycuronan.*

6.2.1 Materials

The following chemicals were reagent grade and used as received. (1→4)-β-D-mannuronan and (1→4)-α-L-guluronan oligomers were obtained from Elicityl SA (Crolles, France). Ammonium bicarbonate (≥ 99.0 %), ammonium carbamate (≥ 99.5%), and D-glucuronic acid sodium salt monohydrate (99 %) were bought from Fluka. Ammonia (28 % w/w, Carlo Erba), NH_4Cl (≥ 99 %, Prolabo), 2-aminoethyl methacrylate (90 %, Aldrich), NH_4OAc (98 %, Aldrich), $NaBH_3CN$ (95 %, Aldrich), ethanol (96 %, Carlo Erba), and D_2O (99.9 %-D, Euriso-top). Deionized water was used in all the experiments. Dia-filtration membranes were supplied by Millipore®.

6.2.2 Analyses

Mass spectrometry analyses and NMR experiments were performed with a Waters ZQ and a Bruker DPX400 spectrometer respectively (described in Chapter 5). Chemical shifts (in

ppm) for ^{1}H and ^{13}C nuclei were referenced to δ_{TSP} = -0.017 ppm (^{1}H) and δ_{TSP} = -0.149 ppm (^{13}C), or to δ_{DSS} = 0.000 ppm (^{1}H and ^{13}C). Yields from ^{1}H NMR were calculated by setting the integral of the internal anomeric peak H1' (internal anomeric at ~ 4.6 ppm in oligomannuronan and at 5.0 ppm in oligoguluronan) which is not affected by the reaction to $DP_n - 1$ (DP_n calculated from ^{1}H NMR) and the value of the integral of the novel $C\underline{H}_2$-NH_2 signal (H1 at ~ 3.0 or 3.4 ppm) gives the yield. It worth noting that an average integral of the latter signals (at 3.0 and 3.4 ppm) was considered as a yield. For example in Figure 6.1 the oligomannuronan used has a DP_n of 4.95 (from ^{1}H-NMR), so by setting the integral of the internal anomeric peak (H1' at 4.62-4.79) to 3.95 we get the yield from the average of the integral of the $C\underline{H}_2$-NH_2 peaks at 3.0 and 3.4 ppm (~ 38 %).

Accurate pH and conductivity values were measured with a pH-meter (Cyberscan PC 510); alternatively, a special pH indicator paper was used (Macherey-Nagel, ± 0.5 pH units). Diafiltration was carried out using ultrafiltration cells equipped with a cellulose acetate membrane (500 Da cut off, ∅ 63.5 mm, Millipore) and connected to an auxiliary reservoir filled with de-ionized water (p = 2-3 bars; stirring rate ~300 rpm). Purifications were stopped once the conductivity of the eluate had fallen below 5 μS cm^{-1}.

Molecular weight distributions and intrinsic viscosities were measured with a SEC-MALLS-IV system consisting of an Alliance GPCV 2000 chromatograph (Waters) equipped with a differential refractometer (λ = 880 nm) and a 3 capillary differential viscometer, and interfaced with a multi-angle laser light scattering detector (DAWN HELEOS II, Wyatt Technology Corp., Santa Barbara, California; λ = 658 nm). The system was equipped with a 50×6 mm guard column and two 300×8 mm linear columns (Shodex SB-800 HQ series). An aqueous solution ($NaNO_3$ 0.1 M, NaN_3 0.03% w/v, Na-EDTA 0.01 M) was used as eluant at a flow rate of 0.5 mL min^{-1} while temperature of the columns, DRI and viscometer was maintained at 30 °C. Samples solutions (1-5 g L^{-1}) were prepared by dissolving the product in the SEC eluant, filtered through 0.22 μm sterile syringe filters (Millex GS, Millipore) and injected in 100 μL volumes. Results were analyzed with ASTRA 5.3 software (Wyatt Technology Corp.).

Preparative size exclusion chromatography was carried out on a system consisting of two Bio-Gel® P2 (Bio-Rad) columns thermostated at 55 °C (length 1 m, ∅ = 1.5 cm), an isocratic pump, a differential refractive index detector and a fraction collector. Samples (50-100 mg) were injected manually and eluted with water at a flow rate of 0.5 mL min^{-1}. At the

end of the separation, the fractions of interest were pooled, freeze dried and analyzed by NMR and MS.

6.2.3 Reductive amination of D-glucuronic acid 1

In a typical experiment (entry no 1 in Table 6.1), D-glucuronic acid sodium salt monohydrate **1** (0.500 g, 2.13 mmol) was weighed in a 50 mL round bottom flask and solubilized in H_2O (34 mL). To the latter solution, ammonium acetate (7.70 g, 99.0 mmol) and sodium cyanoborohydride (2.82 g, 42.6 mmol) were added and the pH was adjusted to 6.0 with HCl (1.5 mL, 1 M). Note that the reducing agent was only added after the total dissolution of ammonium acetate. The flask was sealed with a rubber septum, a disposable needle (21 G) was passed through the septum to prevent pressure build-up and the mixture was stirred at 250 rpm and 30 ºC. After 6 days, the mixture was diluted with ~10 volumes of water, frozen in liquid nitrogen and freeze-dried overnight. The resulting solid was re-dissolved in water (40 mL) and filtered on a glass sintered filter (P5) to remove suspended material. The collected filtrate was transferred to a centrifugation cell, precipitated in 80 % EtOH under vigorous stirring and centrifuged (10 000 rpm, 10 min, 15 ºC). The supernatant from centrifugation was decanted and the resulting precipitate was re-solubilized in water, frozen in liquid nitrogen and freeze dried overnight. Part of the obtained solid (50 mg) was further desalted by preparative SEC on P2 biogel columns and the collected fractions were pooled, freeze dried and analyzed by NMR and MS. (2ξ)-6-amino-6-deoxy-D-*lyxo*-hexonic acid fraction **2**, ^{1}H-NMR (400 MHz, D_2O, 288 K) δ (ppm): 2.88 (dd, H1a, 1H, $J_{1a,2}$ 8.4 Hz, J_{1a1b} 13.0), 2.98 (dd, H1b, 1H, $J_{1b,2}$ 3.6 Hz, J_{1b1a} 13.1), 3.70 (H3, 1H, $J_{3,2}$ 4.4 Hz, $J_{3,4}$ 3.1), 3.76 (dd, H4, 1H, $J_{4,3}$ 3.0 Hz, $J_{4,5}$ 5.2 Hz), 3.85 (dt, H2, 1H, $J_{2,1}$ 8.3 Hz , $J_{2,3}$ 4.1 Hz), 3.94 (d, H5, 1H, $J_{4,5}$ 5.2 Hz). ^{13}C NMR (100 MHz, D_2O, 298K) δ (ppm): 44.75 (C1), 72.09 (C2), 74.09 (C3), 74.81 (C4), 76.19 (C5), 181.31 (C6). ESI-MS *m/z*: calculated 195.07 (for C6H13NO6); found 193.8 ([M-H]$^-$).

6.2.4 Reductive amination of (1→4)-β-D-mannuronan

In a typical experiment (entry no. 14 in Table 6.1), (1→4)-β-D-mannuronan (DP_n = 9; $ManA_9$, 98 %, 4.50 g, 2.79 mmol) was weighed in a 200 mL Erlenmeyer flask, solubilized in H_2O (50 mL) and mixed with an aqueous solution (35 mL) of ammonium acetate (9.08g, 115 mmol). Sodium cyanoborohydride (3.21 g, 48.0 mmol dissolved in 15 mL H_2O) was added and the pH of the final mixture was checked with a pH paper (≅ 7). A magnetic bar was added, the flask was sealed with a rubber septum, plunged in a water bath preheated at 30 ºC,

and stirred at 200 rpm for 7 days. At the end of the reaction, the mixture was transferred to a centrifugation cell, precipitated in 80 % EtOH under vigorous stirring and centrifuged (10 000 rpm, 10 min). The obtained precipitate was re-dissolved in H_2O (~80 mL) and diafiltered for 3 days. The desalted solution was transferred to a round bottom flask, frozen in liquid nitrogen and freeze dried overnight. Conversion (≥ 90 %) and yield (42 %) were calculated from ^{1}H-NMR by normalizing the spectra of the starting $ManA_9$ and the final product to a known peak (internal anomeric H1', See analysis section for procedure). ^{1}H-NMR (400 MHz, D_2O, 323 K) δ (ppm): 3.00 (dd, H1a, 1H, $J_{1a,1b}$ 12.9 Hz, $J_{1a,2}$ 9.4 Hz), 3.47 (dd, H1b, 1H, $J_{1b,1a}$ 13.1 Hz, $J_{1b,2}$ 3.0 Hz), 3.61-4.06 (H2, H2', H3, H3', H4, H4', H5, H5', sugar), 4.62-4.81 (H1', sugar), 5.02 (H1', residual G). M_n (SEC) 1889 Da, PDI 1.08, $[\eta]_w$ = 9.2 mL g^{-1}, dn/dc = 0.165.

6.2.5 Reductive amination of (1→4)-α-L-guluronan

In a typical experiment (entry no 16 in Table 6.1), (1→4)-α-L-guluronan (DP_n = 20; $GulA_{20}$, 4.00 g, 1.00 mmol) was weighed in a 500 mL Erlenmeyer flask, solubilized in H_2O (87 mL) and mixed with an aqueous solution (87 mL) of ammonium acetate (3.5 g, 44.5 mmol). Sodium cyanoborohydride (1.25 g, 18.9 mmol dissolved in 7 mL H_2O) was added and the pH of the final mixture was checked with a pH paper (≅ 7). A magnetic bar was added, the flask was sealed with a rubber septum, plunged in a water bath preheated at 30 ºC and stirred at 200 rpm. Samples were drawn at preset intervals, frozen in liquid nitrogen and freeze dried overnight. After 6 days the reaction mixture was transferred to a centrifugation cell, precipitated in 75 % EtOH under vigorous stirring and centrifuged (10 000 rpm, 10 min). The supernatant was decanted and the precipitate was re-dissolved in H_2O and further purified by diafiltration for 2 days. The desalted solution was transferred to a round bottom flask, frozen in liquid nitrogen and freeze dried overnight. Since ^{1}H-NMR analysis indicated that conversion was only ~50%, the reaction was restarted using the same quantity of reagents. Total reaction time, 18 days. Conversion (≥ 90 %) and final yield (32 %) were calculated from ^{1}H-NMR by normalizing the spectra of the starting $GulA_{20}$ and the final product to a known peak (internal anomeric H1', See analysis section for procedure). ^{1}H-NMR (400 MHz, D_2O, 318 K) δ (ppm): 3.03 (dd, H1a, 1H, $J_{1a,1b}$ 13.3 Hz, $J_{1a,2}$ 8.7 Hz), 3.34 (dd, H1b, 1H, $J_{1b,1a}$ 13.1 Hz, $J_{1b,2}$ 3.4 Hz), 3.88 (H2', sugar), 3.99 (H4', sugar), 4.11 (H3', sugar), 4.45 (H5', sugar), 5.04-5.12 (H1', sugar). M_n (SEC) 3875 Da, PDI 1.19, $[\eta]_w$ = 19.3 mL g^{-1}, dn/dc = 0.165.

6.3 Results and discussion

Table 6.1 *Summary of reductive amination experiments described in this study.*

Entry	Substrate (mmol L^{-1})	DP_n	Amine (mol L^{-1})	$[NaBH_3CN]_0$ (mol L^{-1})	pH	Reaction time (days)	% Yield	% Conv.	Experiment code
1	GlcA (60)	-	NH_4OAc (2.76)	1.20	6.0	6	n.d	n.d	AG10-41-P5
2	GlcA (58)	-	NH_4OAc (2.68)	1.16	7.5	6	n.d	n.d	AG10-41-P3
3	GlcA (56)	-	NH_4HCO_3 (2.56)	1.11	7.8	6	n.d	n.d	AG10-41-P2
4	$ManA_5$ (56)	5	NH_4OAc (2.39)	1.05	5.5	6	50	> 90	AG11-03
5	$ManA_5$ (56)	5	NH_4OAc (2.39)	1.04	6.0	6	54	> 90	AG10-41-P4
6	$ManA_5$ (53)	5	NH_4OAc (2.39)	0.21	6.0	6	53	> 90	AG11-07
7	$ManA_5$ (56)	5	AEM [a] (0.32)	0.21	6.5	6	53	89	AG11-04-P4
8	$ManA_5$ (60)	5	NH_4OAc (2.70)	1.04	~ 7	7	38	> 90	AG10-31-S1
9	$ManA_5$ (56)	5	NH_4Cl (2.3)	1.00	7.4	6	35	> 90	AG11-04-P3
10	$ManA_5$ (64)	5	NH_4HCO_3 (2.7)	1.20	8.02	6	38	> 90	AG10-41-P1
11	$ManA_5$ (56)	5	$NH_4CO_2NH_2$ (2.0)	1.00	9.4	6	34	> 90	AG11-04-P2
12	$ManA_5$ (56)	5	NH_4OAc (0.2) + NH_3 (5)	1.00	11.1	6	20	> 90	AG11-04-P1
13	$ManA_5$ (56)	5	NH_4OAc (0.2) + NH_3 (5)	0.21	11.3	6	28	77	AG11-04-P5
14	$ManA_9$ (28)	9	NH_4OAc (1.15)	0.48	~ 7	7	42	> 90	AG10-31-S2
15	$ManA_{17}$ (5.3)	17	NH_4OAc (0.24)	0.10	~ 7	5	40	> 90	AG10-27-S1
16	$GulA_{20}$ (5.6)	20	NH_4OAc (0.24)	0.10	~ 7	18	32	> 90	AG10-27-S2

General condition: stirring rate ~ 250 rpm, T = 30 °C. Yields were calculated from ^{1}H-NMR by normalizing the ^{1}H-NMR spectra of the starting oligoglycuronan and the corresponding 1-amino-1-deoxy alditol to the same peak. [a] 2-aminoethyl methacrylate.

6.3.1 Reductive amination of oligoglycuronans

Table 6.1 summarizes all reductive amination experiments carried out. When the substrate was an oligoglycuronan, the sugar was always mixed with the ammonium salt (or amine) first, in order to avoid (or at least limit) direct reduction of the aldose. After adding $NaBH_3CN$, the pH of the solution was adjusted to the target value by adding HCl, if needed. Reactions were stopped by precipitating the oligosaccharide with ethanol (max. 80% v/v), thus eliminating part of the salts as well. This detail is important since excess salt would take longer to eliminate via diafiltration and would favor the loss of the shorter oligosaccharide chains (di- and tri-saccharides) through the 500 Da molecular weight cut-off (MWCO) membrane. Indeed, at low ionic strength the effective MWCO of oligoglycuronans is smaller than the nominal value as a consequence of electrostatic repulsion between the molecule and negative charges on the diafiltration membrane. [7]

Figure 6.1 shows the ^{1}H-NMR spectrum of (1→4)-β-D-mannuronan **4$_5$** (Scheme 6.2) before (a) and after (b) reductive amination with ammonium acetate at pH ≅ 7 (entry 8 in Table 6.1): The anomeric peaks of the starting oligomannuronan disappeared (H1$_\beta$ 4.86 ppm and H1$_\alpha$ 5.20 ppm) while two new peaks with identical integrals appeared at 3.01 ppm (dd, $J_{1a,1b}$ 12.9 Hz, $J_{1a,2}$ 9.4 Hz) and 3.46 ppm (dd, $J_{1b,1a}$ 13.1 Hz, $J_{1b,2}$ 3.0 Hz). In the ^{1}H-^{13}C HMQC spectrum (Figure 6.2), these two peaks correlate to the same carbon at 45.03 ppm, which was identified as a CH_2 by ^{13}C DEPT-135 analysis (Figure 6.4b). Based on these results, the signals at 3.01 and 3.46 ppm were assigned to the newly formed CH_2-NH_2: The two protons are diasterotopic and non-equivalent due to the chiral center on C2 and the coupling constant of 13 Hz corresponds to J_{gem}. An identical result was obtained in the case of an (1→4)-α-L-guluronan (see experimental part). A new singlet at 4.79 ppm appears in the ^{1}H spectrum of the final material (in the case of oligomannuronan) which correlates with a carbon at 102 ppm in HMQC. Judging from the ^{13}C chemical shift of the directly connected carbon, it must the anomeric proton of an internal monosaccharide residue (H1'), most probably the one just next to the amino alditol unit.

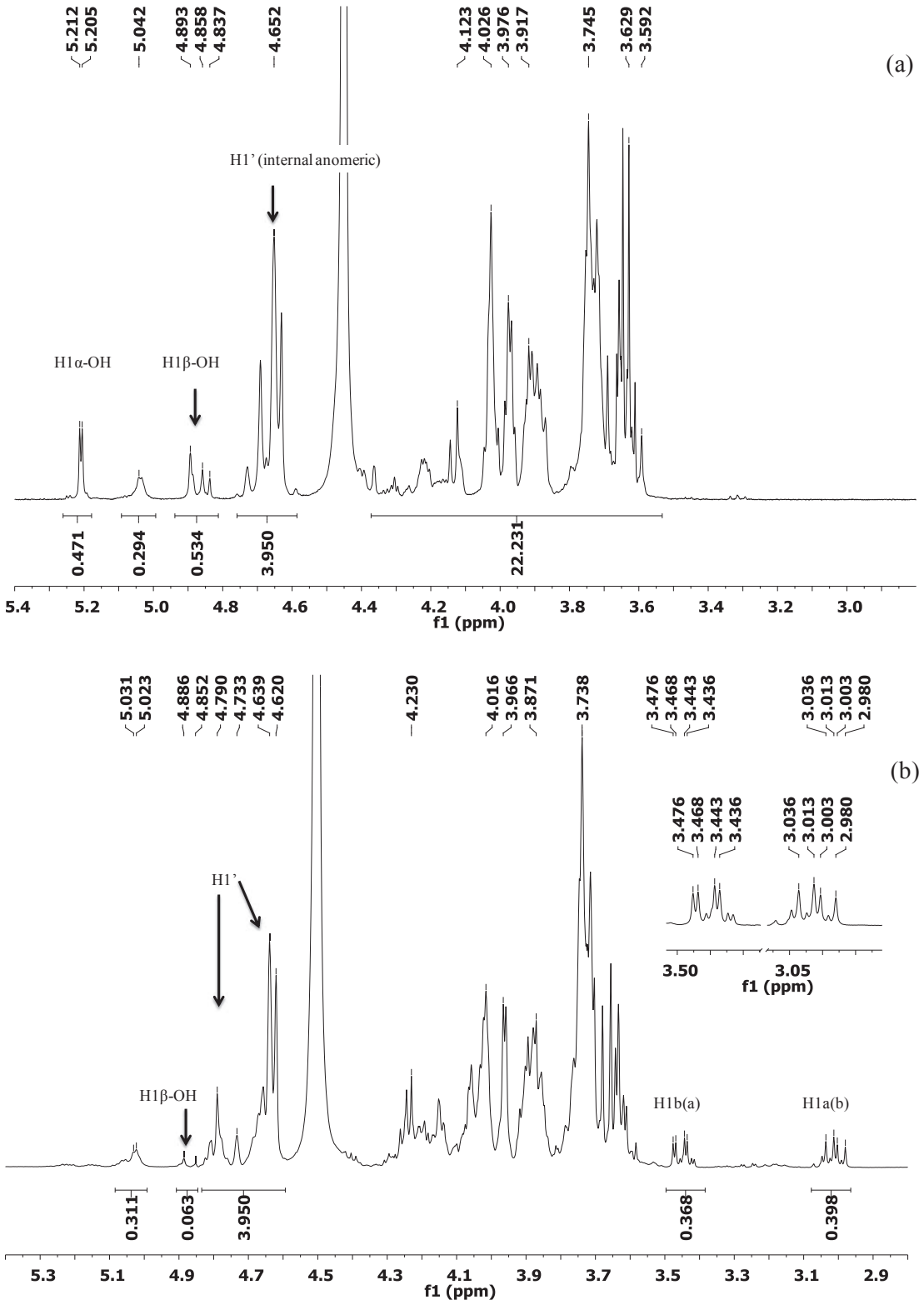

Figure 6.1 *^{1}H-NMR spectra of (1→4)-β-D-mannuronan* ***4₅*** *before (a) and after (b) reductive amination with ammonium acetate (entry no. 8 in Table 6.1). Note the characteristic peaks of the 1-amino-1-alditol* ***5₅*** *(see* Scheme 6.2 *for nucleus numbering). Conditions: 400 MHz, D_2O, (a) 328 K, 2.5 %w/w, ns = 64, D1 = 2s and (b) 323 K, 9 %w/w, ns = 50, D1 =2s.*

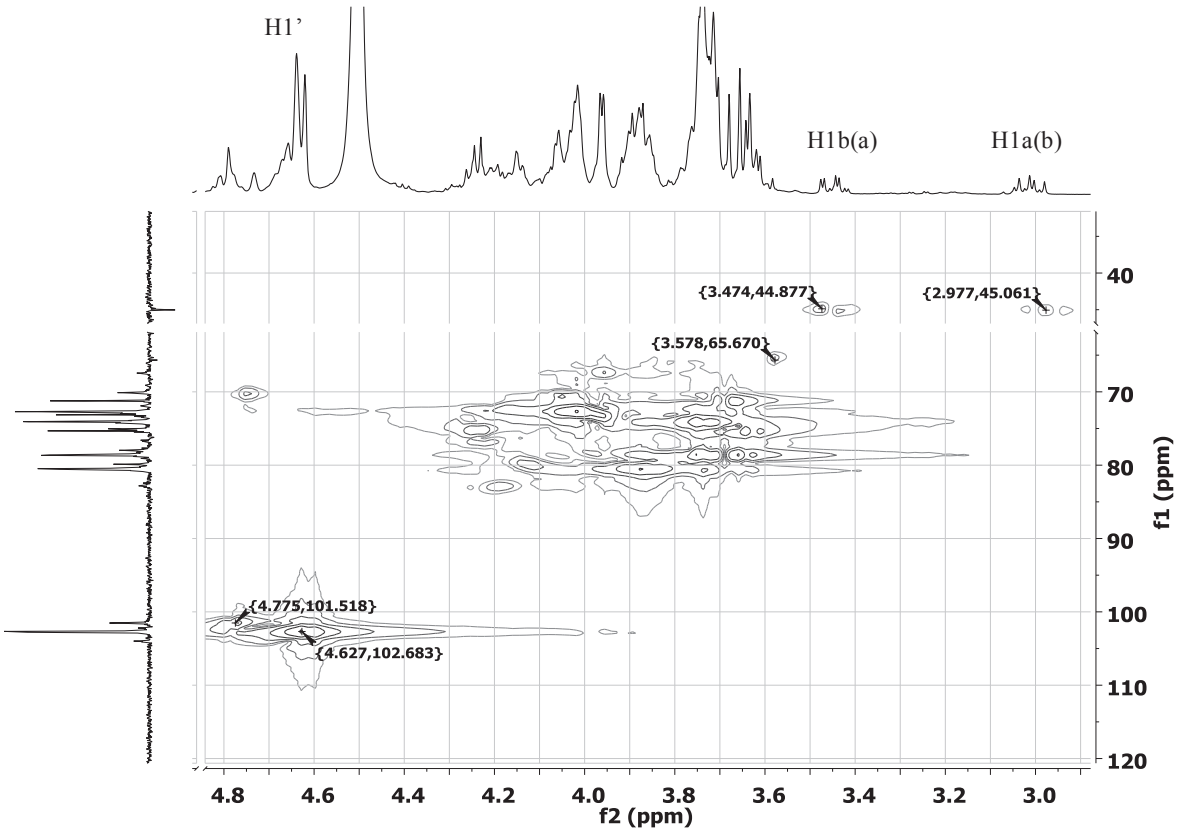

Figure 6.2 *^{1}H-^{13}C HMQC (400.13-100.62 Hz) of the 1-amino-1-deoxy alditol* ***5*****$_5$** *obtained from the reductive amination of (1→4)-β-D-mannuronan* ***4*****$_5$** *(entry no. 8 in Table 6.1). Conditions: D_2O, 298 K, 9 % w/w, ns = 300, D1 = 2 s. A ^{13}C DEPT-135 spectrum is projected on the vertical axis. A cut in each axis should be noted.*

From the disappearance of the anomeric proton signals of the reducing end (4.84 - 4.89 ppm, $H1_\beta$; 5.21 ppm, $H1_\alpha$), the conversion of the starting oligosaccharide was estimated at >90 %. Nevertheless, by setting to 3.95 the integral of the internal anomeric peaks (H1', 4.65 ppm) of both spectra in Figure 6.1, it is evident that only ~ 40% of the starting oligosaccharide was converted into the corresponding 1-amino-1-deoxy alditol, whereas 50% of it was transformed into byproduct(s).

Close inspection of the DEPT 135 spectrum of the product (Figure 6.4b) reveals the presence of only two CH_2 signals, at 45.03 ppm ($\underline{C}H_2$-NH_2 of **5$_5$**) and 65.67 ppm (already present in the spectrum of the starting mannuronan, Figure 6.3. Also, HMQC shows that the latter peak correlates to only one proton signal and is thus unlikely to arise from C1 of putative alditol **6$_5$** (its CH_2-OH protons would be diasterotopic and non-equivalent). As a consequence, reduction of the hemiacetal group should be ruled out. Likewise, no convincing evidence was found of the reduction of some carboxyl groups to the corresponding aldehydes or alcohols: The ^{13}C NMR spectrum of the product (Figure 6.4a) does not contain any signal

compatible with the formation of aldehyde groups (δ = 190-210 ppm), although any such group could have been hydrated in water ($\delta \cong$ 90 ppm) or transformed into a hemiacacetal (δ $^{1}H \approx 4.5 – 6.0$ ppm, δ $^{13}C \approx$ 95-115 ppm) and thus superimpose with existing signals from the molecule. Also, δ (C6) for β-mannosides is 63.5 ppm, and although there is a signal at 65.67 ppm both in starting molecule and in the final material, its intensity in only 1/5 that of $\underline{C}H_2$-NH_2 of the obtained 1-amino-1-deoxy alditol and cannot justify the transformation of half of the starting product.

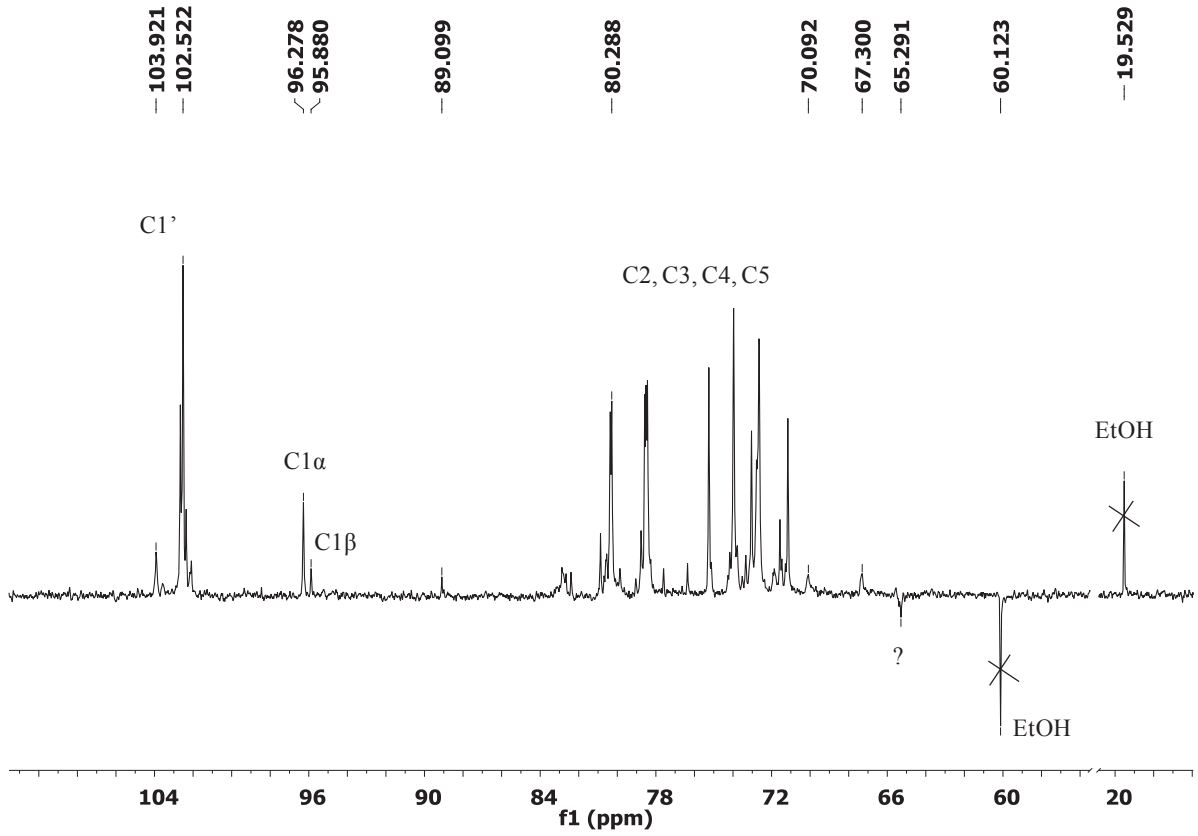

Figure 6.3 *DEPT 135 spectrum of (1→4)-β-D-mannuronan* ***4₅*** *(a cut in the spectrum axis should be noted; CH_2 signals are down whereas CH and CH_3 signals are up).* [8]

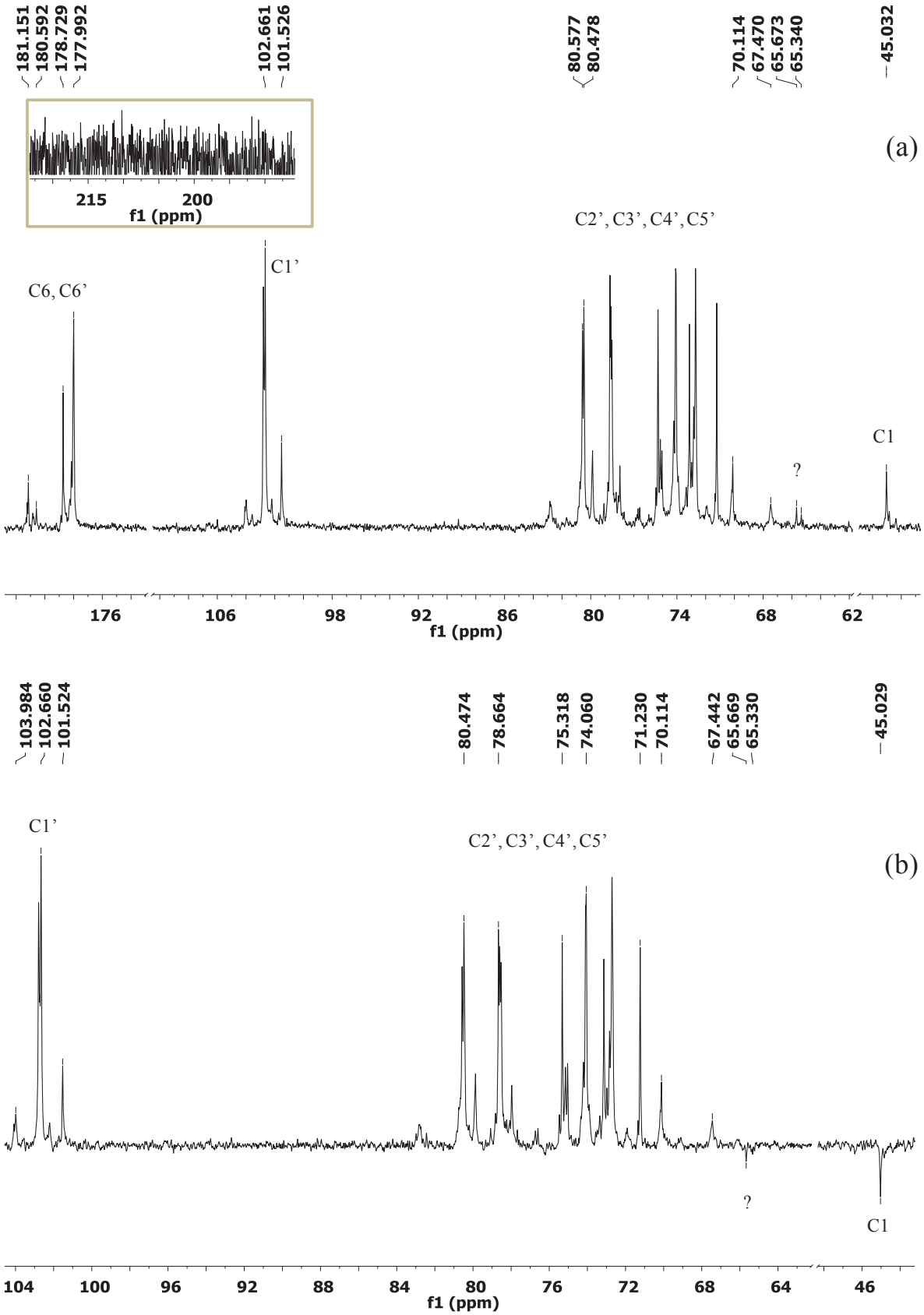

Figure 6.4 *^{13}C (a) and DEPT 135 spectra (b) of (1→4)-β-D-mannuronan 1-amino-1-deoxy alditol* $\mathbf{5}_5$ *(cuts in the spectra axis should be noted; in DEPT 135 CH_2 signals are down whereas CH and CH_3 signals are up).* [9]

The last hypothesis to be considered was the formation of a bisubsituted amine **10** (Scheme 6.2) by the reaction of 1-amino-1-deoxy alditol $\mathbf{5_5}$ with a second molecule of (1→4)-β-D-mannuronan. In this case, the mass of the obtained product would be double that of the starting oligosaccharide and of the corresponding 1-amino-1-deoxy alditol. Size exclusion chromatography gives virtually superimposable traces for the starting and final oligosaccharides though (Figure 6.5) and the average molar mass calculated by laser light scattering (M_n = 1000 Da, PDI = 1.08) is unchanged.

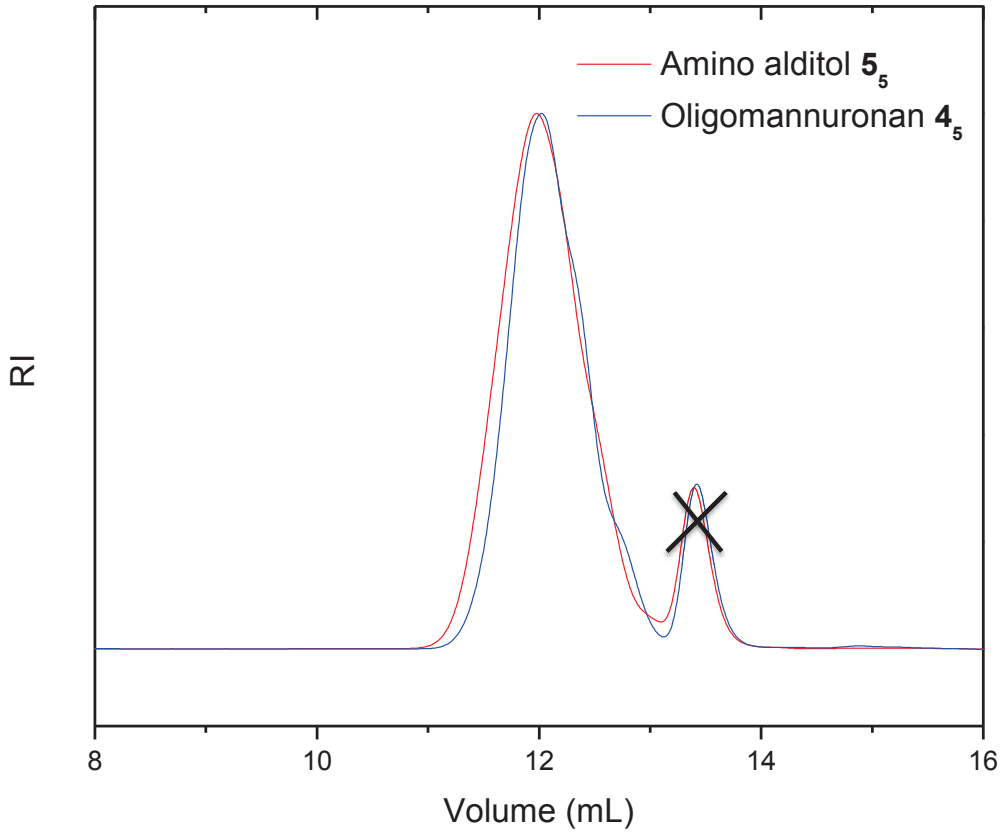

Figure 6.5 *SEC traces for (1→4)-β-D-mannuronan* $\boldsymbol{4_5}$ *and the product from reductive amination (entry 8 in Table 6.1). Conditions: injected sample 2-5 mg* mL^{-1}*, columns Shodex OH pak SB-(G + 802 + 802.5) HQ.*

6.3.2 Optimization study

An optimization study was carried out to improve the yield in oligoglycuronan 1-amino-1-deoxy alditol. Hence, the time course of the reaction was monitored to check whether there was an optimal reaction time and the reductive amination of (1→4)-β-D-mannuronan $\mathbf{4_{17}}$ was compared with that of (1→4)-α-L-guluronan $\mathbf{7_{20}}$ (entries 15 and 16 in Table 6.1). In separate Erlenmeyer flasks, a solution of each oligoglycuronan was mixed with ammonium acetate first and $NaBH_3CN$ second (pH ~ 7). The flasks were sealed, plunged in a

water bath preheated at 30 °C and left stirring. At pre-set intervals a sample was drawn (~ 400 μL), frozen in liquid nitrogen and freeze dried. The resulting powder was dissolved in D_2O and analyzed by ^1H NMR analysis (D1 = 5 s). Figure 6.6 shows the evolution of the molar fraction with time for the starting oligosaccharides (a) and the corresponding 1-amino-1-deoxy alditols $\mathbf{5_{17}}$ and $\mathbf{8_{20}}$ (b). Both reactions were rather slow but the consumption of (1→4)-β-D-mannuronan $\mathbf{4_{17}}$ was faster than that of (1→4)-α-L-guluronan $\mathbf{7_{20}}$ (78% vs. 50% in 75 h). Symmetrically, the formation of 1-amino-1-deoxy alditol $\mathbf{5_{17}}$ was faster than that of $\mathbf{8_{20}}$ (39% vs. 18% in 75 h). As a result, after 75 h of reaction half of the consumed (1→4)-β-D-mannuronan and 64% of the consumed (1→4)-α-L-guluronan had been transformed in byproduct(s). Moreover, it took 18 days for $\mathbf{7_{20}}$ to be totally consumed (final yield 32 %). In both cases the molar fraction of 1-amino-1-deoxy alditol kept increasing monotonically, and no optimal reaction time giving a "peak yield" was identified. As shown in Figure 6.6 for comparison, the synthesis of the analogous glycosylamines is much faster, virtually no byproducts are formed and the solid content of salts is smaller. Of course, in the latter case the molecules are susceptible to hydrolysis in aqueous solution and should be handled with care. In theory, the reductive amination could have been attempted with a water-soluble catalyst [e.g. $Pd(PhCN)_2Cl_2$ and 2,2'-biquinoline-4,4'-dicarboxylic acid dipotassium salt (BQC)], [10] but the high affinity of oligoglycuronans for metal ions dissuaded us from trying this route. [11]

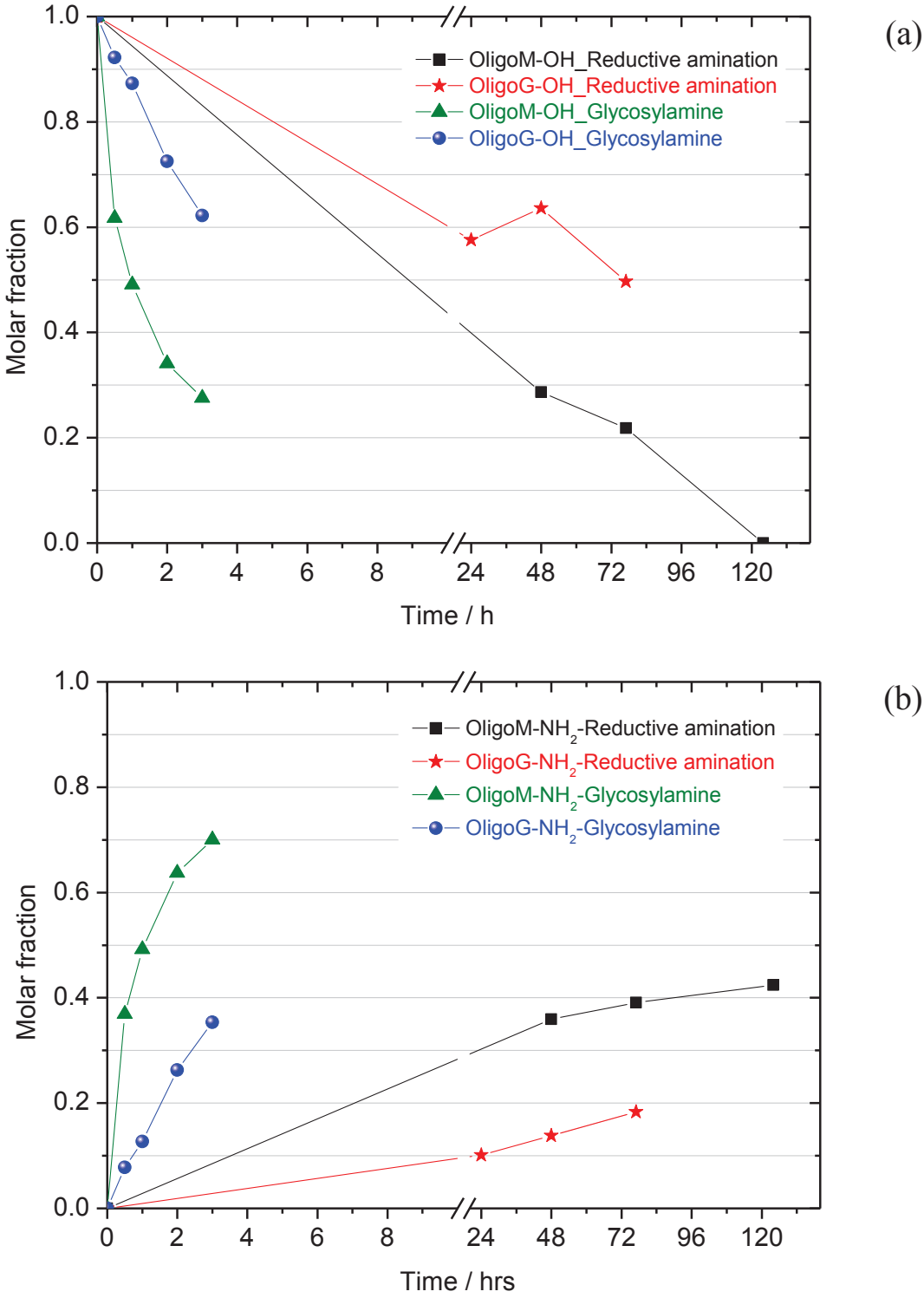

Figure 6.6 *Evolution of the molar fraction with time for the reductive amination of oligoglycuronans* $\mathbf{4}_{17}$ *and* $\mathbf{7}_{20}$ *(entries no 15-16 in Table 6.1): (a) disappearance of the starting sugars and (b) formation of the corresponding 1-amino-1dexoy alditols* $\mathbf{5}_{17}$ *and* $\mathbf{8}_{20}$*. For comparison, the time course of the corresponding direct aminations (glycosylamine) is presented as well (Chapter 5, Table 5.4, entries 8-9).*

A second aspect which was considered is the pH of the reaction medium. To this end, a series of reductive amination experiments were performed on (1→4)-β-D-mannuronan **4$_5$** using different ammonia sources (NH_4OAc, NH_4HCO_3, $NH_4CO_2NH_2$, NH_3, and NH_4Cl) and one primary amine (2-aminoethyl methacrylate). The pH of the solution (pH = 5.5 to 11) was adjusted with HCl soon after the addition of $NaBH_3CN$ as needed. The exact experimental conditions are summarized in Table 6.1, but here it should be pointed out that a big excess of ammonia source (> 40 equivalents) and sodium cyanoborohydride (56 eq.) was used in almost all cases. All reactions were carried out at 30 °C for ~ 6 days and pH values below 5.5 were avoided to reduce any competing reduction of aldehyde groups. [1a,b] Reactions at higher pH values (pH = 11) were instead explored following the results of Dangerfield et al. on the reductive amination of D-glucose in EtOH (87% yield in 1-amino-1-deoxy-D-glucitol). [12] At the end of the reactions, the solutions were precipitated in EtOH (80 % v/v), diafiltered and freeze dried. Samples were re-dissolved in D_2O and analyzed by ^{1}H-NMR using a 90° pulse an inter-scan delay (D1) of 10 s to obtain quantitative integrals for the signals (D1 was only 2 s for entries 5, 8 and 10). In all experiments the conversion of the starting oligosaccharide was higher than 90 %. Figure 6.7 shows the yield in 1-amino-1-deoxy alditol as a function of pH: the best results (50-55 % yield) were obtained in the pH range 5.5 - 6.5, whereas increasing the pH of the reaction medium above 6.5 resulted in a marked drop in the yield. That was attributed to the increasing difficulty for the intermediate amino alcohol to be protonated and form an iminium ion by elimination of a molecule of water (Scheme 6.1). A similar result was obtained when a more nucleophilic primary amine (2-aminoethyl methacrylate) was used (55% yield, entry no 7 in Table 6.1), although the excess of amine was smaller in this case (5.7 eq.). Puzzlingly, a decrease in the amount of reducing agent from 56 to 12 equivalents gave opposite results at pH 6.0 and 11: the yield was unchanged in the first case (entries no 5-6 in Table 6.1) but 8 % lower in the second one (entries no. 12-13 in Table 6.1).

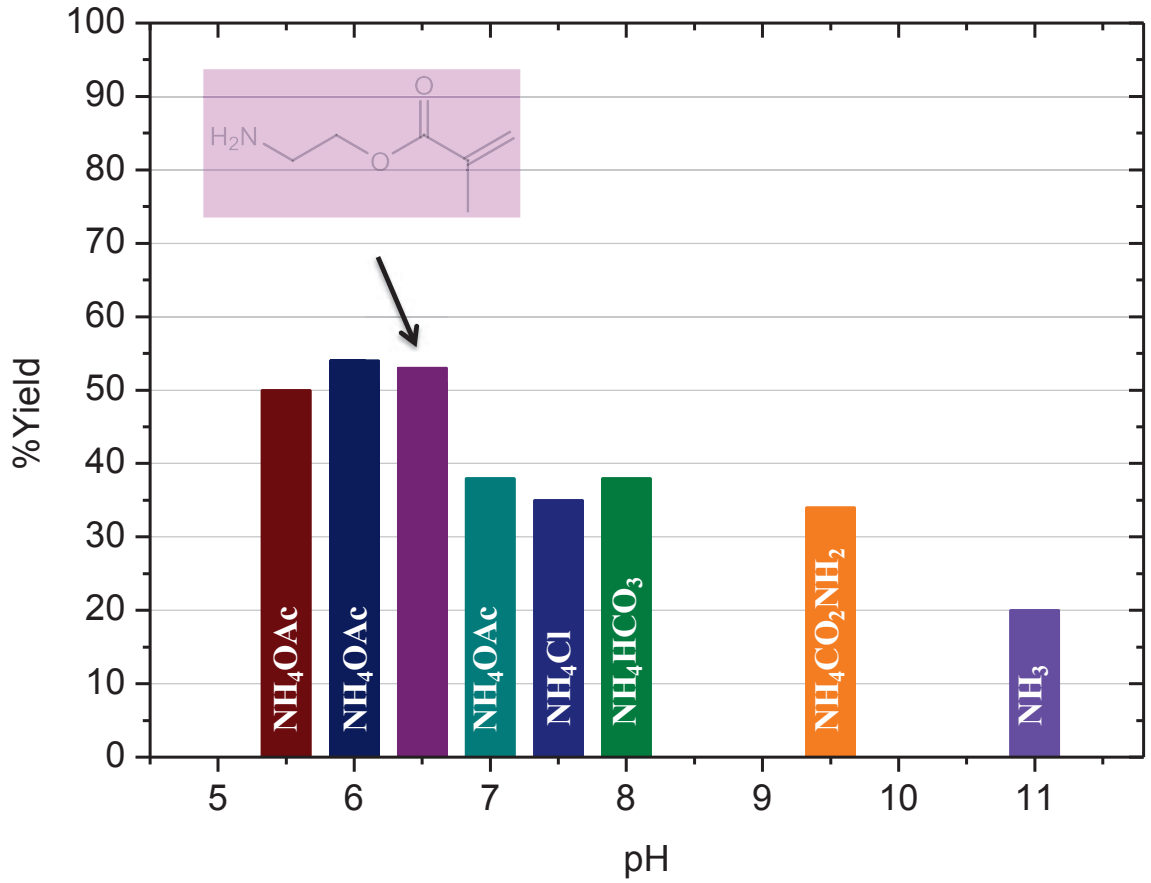

Figure 6.7 *Variation of yield with pH for the reductive amination of (1→4)-β-D-mannuronan* $\mathbf{4_5}$*. Conditions: Man*A_5 *(0.05 M), amine,* $NaBH_3CN$ *(12 or 56 eq), 30 °C, 6 days (Entries 4, 5, 7-12, Table 6.1).*

6.3.3 Reductive amination of D-glucuronic acid, a model uronic acid

To better understand the nature of the by-products formed during the reductive amination of oligoglycuronans, a simpler uronic acid (D-glucuronic) acid was investigated as well (Entries 1-3 in Table 6.1). The rationale behind this choice was that the NMR and MS analyses of a monosaccharide derivative would be easier to realize and to interpret. Hence, the reaction was carried out with two different ammonium salts (NH_4OAc and NH_4HCO_3) and at three different pH values (6, 7.5 and 8). D-Glucuronic acid sodium salt **1** was solubilized in water, NH_4OAc or NH_4HCO_3 were added first, followed by $NaBH_3CN$ and the pH of the resulting solution was adjusted with HCl as needed. After 6 days at 30 °C, the solutions were freeze dried to eliminate most of the ammonium salts, the resulting solid was re-dissolved in water and precipitated in 80 % EtOH. Preparative size exclusion chromatography was then carried out to eliminate all residual salts and separate the target (2ξ)-6-amino-6-deoxy-D-*lyxo*-hexonic acid **2** from the any byproduct(s) (Figure 6.8). Figure 6.9 and Figure 6.10 show the ^{1}H and ^{13}C NMR spectra of the 1-amino-1-deoxy alditol (*m/z* calculated 195.07 for

$C_6H_{13}NO_6$, found 193.8 for $[M-H]^-$). As expected, the two H1 protons are non-equivalent, appear as two double doublets at 2.87 and 2.98 ppm and have a geminal coupling constant of 13 Hz. All other peaks were assigned by ^1H-^1H COSY.

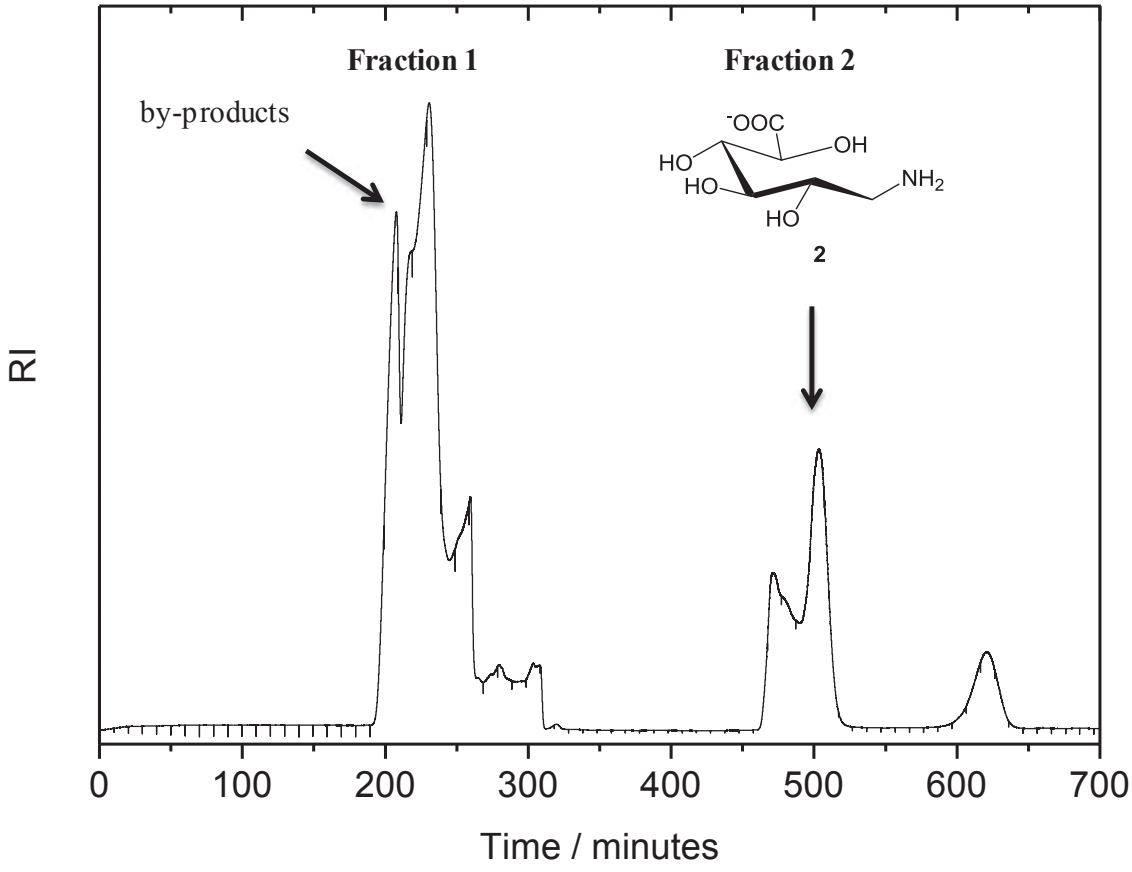

Figure 6.8 *Chromatogram obtained for the preparative* SEC *purification of the gross product from the reductive amination of GlcA at pH 7.8 (entry no 3 in Table 6.1).* [13]

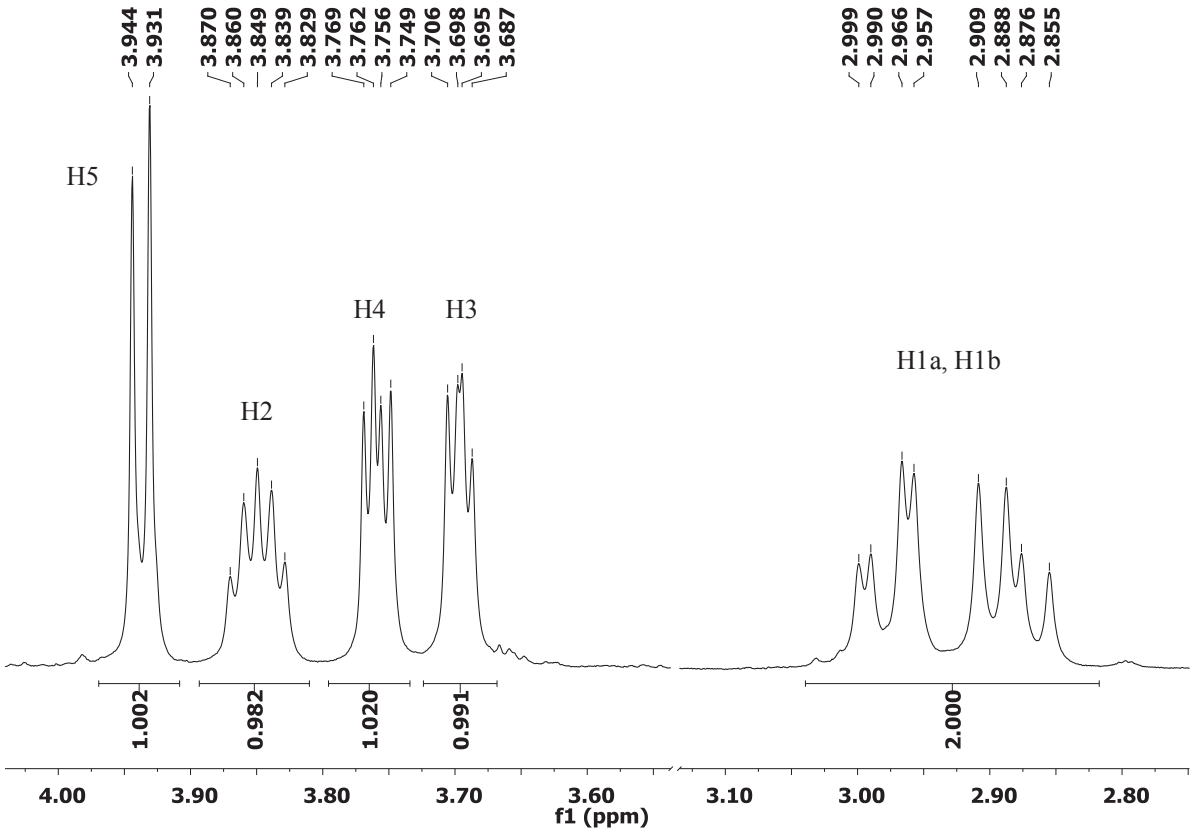

Figure 6.9 *[1]H-NMR spectrum of pure 1-amino-1-deoxy alditol **2** (entry 1 in Table 6.1).* [14]

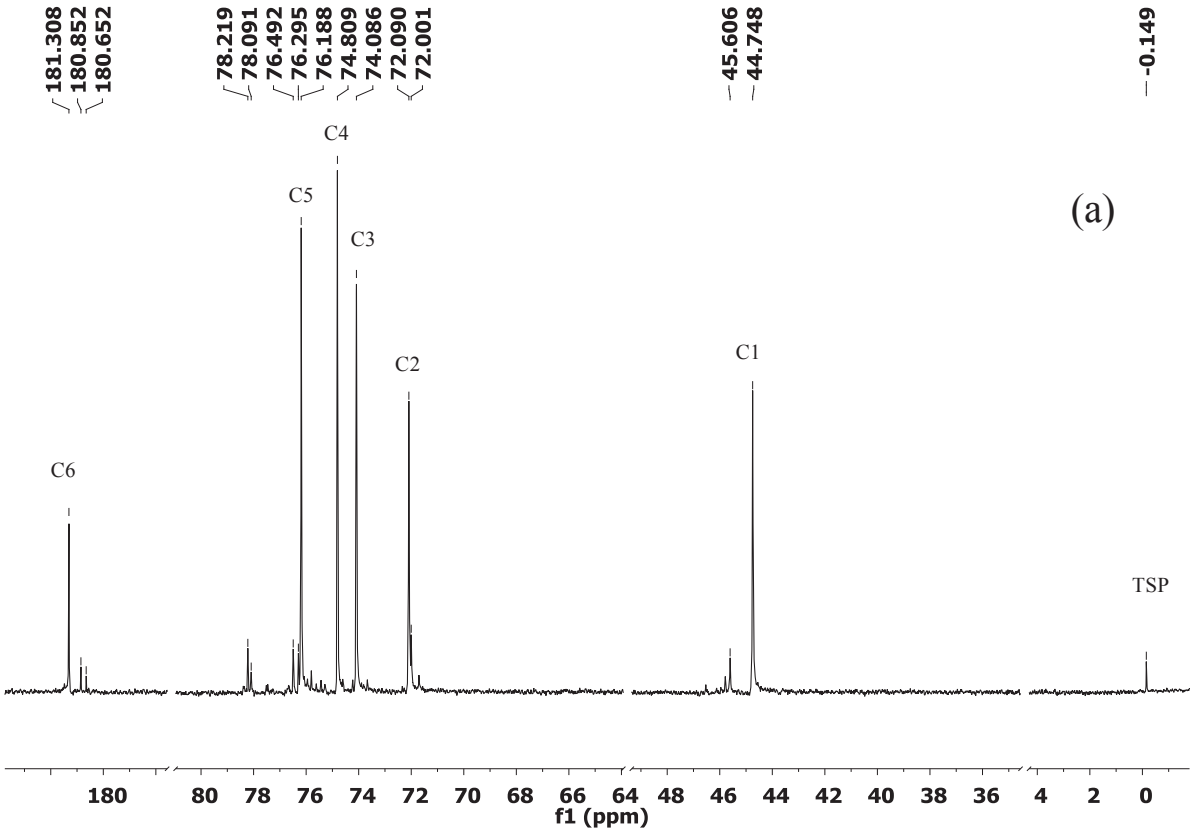

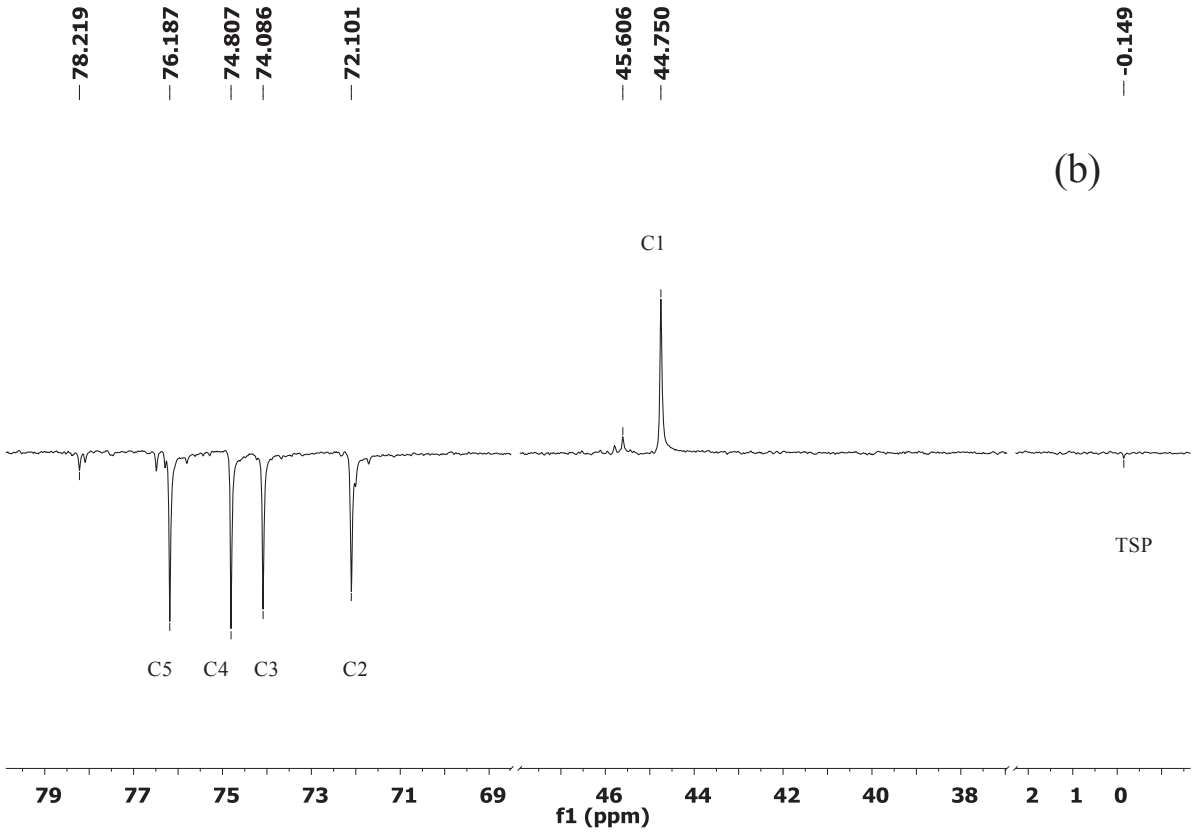

Figure 6.10 *^{13}C (a) and DEPT 135 (b) spectra of a partially pure 1-amino-1-deoxy alditol **2** (entry 3 in Table 6.1). In DEPT 135 CH, CH_3 are pointing downward and CH_2 upward.* [15]

Unfortunately, SEC did not completely separate the byproducts from the salts (fraction 1 in Figure 6.8) and the latter adversely affected the resolution of NMR spectra and the signal to noise ratio of ESI-MS analyses of fraction 1. Figure 6.11 shows the ^{1}H-NMR spectra for the byproducts isolated from experiments carried out at different pH values: The complexity of the spectrum and the number of species formed increased with increasing pH. In particular, the reductive amination at pH 6 yielded two by-products (diagnostic peaks at 2.95 ppm and 3.60 ppm respectively) whereas 3 to 4 by-products formed at pH 7.5 and 7.8 (note peaks at 4.30, 4.40 and 4.85 ppm). The latter result is coherent with what previously discussed for the reductive amination of (1→4)-β-D-mannuronan.

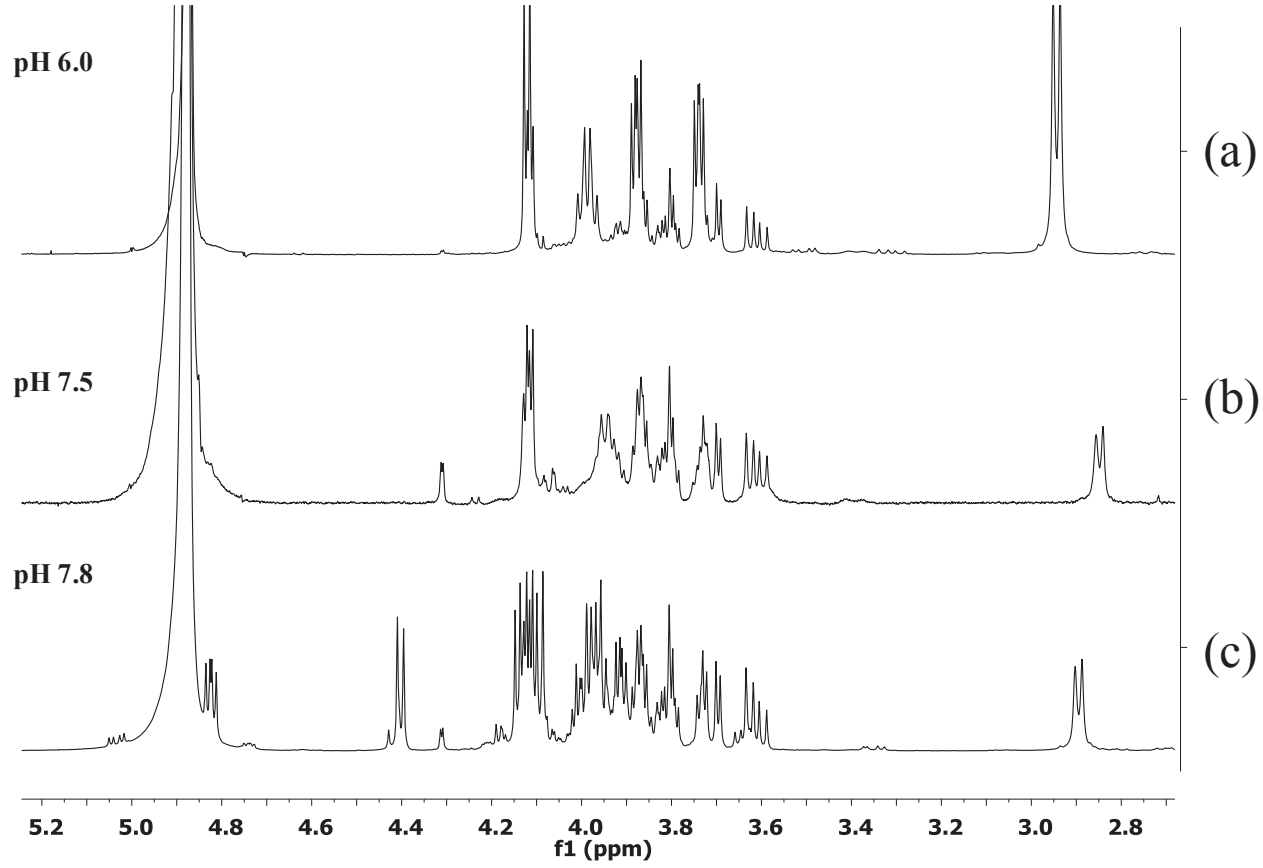

Figure 6.11 *^{1}H-NMR spectrum of fraction 1 collected after the SEC separation of the gross product from the reductive amination of D-glucuronic acid at (a) pH 6, (b) 7.5 and (c) 7.8 (entries no 1-3 in Table 6.1).*

The two by-products formed at pH 6 were further investigated by ^{13}C NMR, DEPT-135, ^{1}H-^{1}H COSY, ^{1}H-^{13}C HMQC and HMBC. The ^{13}C NMR spectrum (Figure 6.12a) shows the presence of 6 peaks for each by-product, including a carboxyl signal at 181 ppm. The DEPT-135 spectrum (Figure 6.12b) revealed that each molecule contained only one CH_2 signal (52 ppm and 65 ppm). The hypothesis of any Amadori products was ruled out from NMR (^{13}C and 135 dept) where neither quaternary carbons (after cyclization) nor keto-carbonyl groups above 190 ppm (for the non-cyclic product) were detected. In the ^{1}H-^{13}C HMQC spectrum (Figure 6.13a), the CH_2 signal at 65 ppm correlated with two nonequivalent protons at 3.58 and 3.74 ppm, similarly to what previously seen for 1-amino-1-deoxy alditol **2**. Furthermore, the ESI-MS spectrum of fraction 1 contained a peak at *m/z* 194.8 ($[M-H]^-$), suggesting the formation of alditol **3**. Unfortunately, compound **3** was the less abundant of the two byproducts and complete assignment of its ^{1}H and ^{13}C spectra beyond H1 and C1 was only based on analogy with 1-amio-1-deoxy alditol **2**.

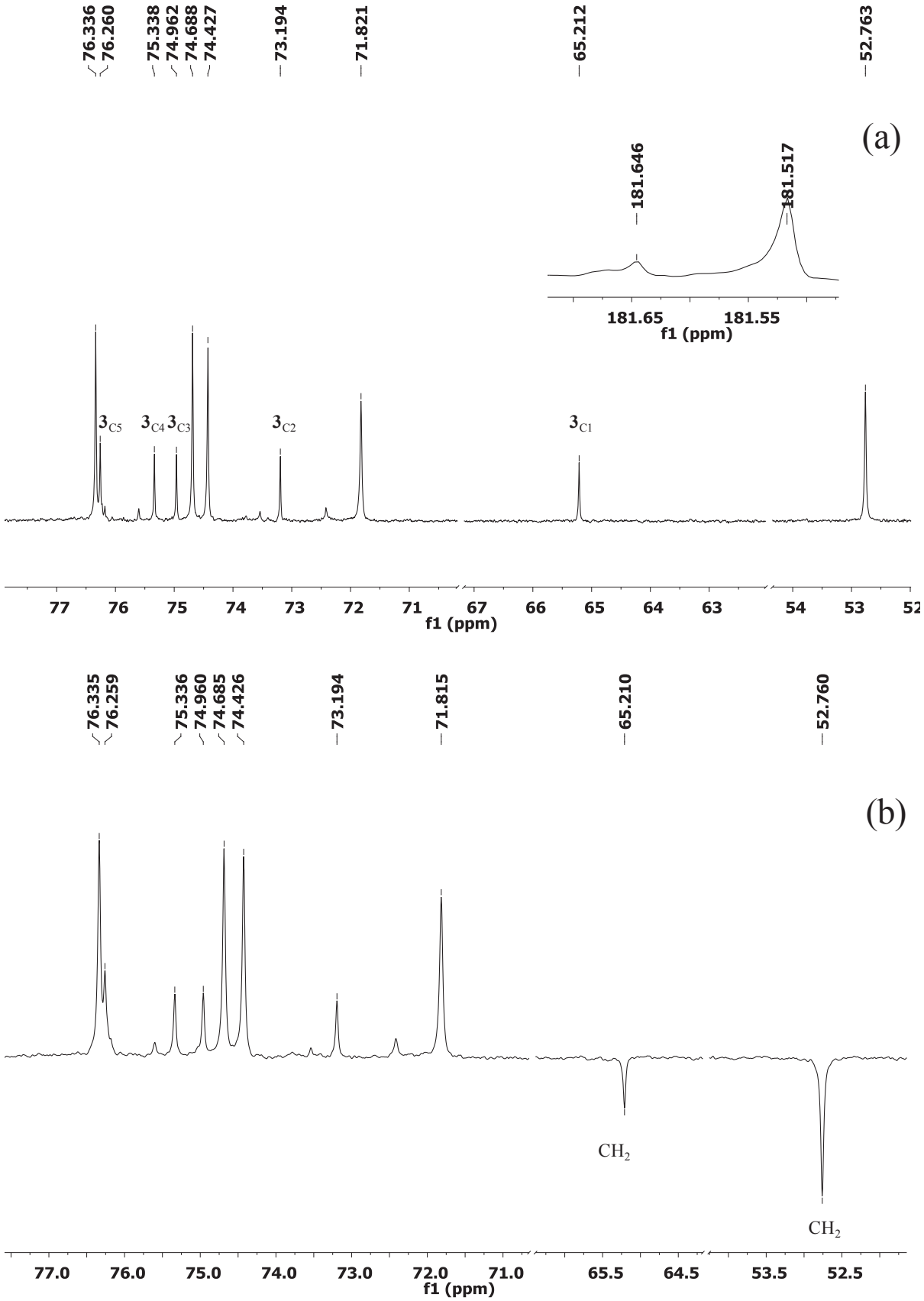

Figure 6.12 *^{13}C (a) and ^{13}C DEPT-135 (b) spectra of by-products (fraction 1, Figure 6.8) formed during the reductive amination of D-glucuronic acid at pH 6 (Entry 1, Table 6.1).* [16] *Two cuts in the axis should be noted.*

The identification of the other by-product in the mixture was not possible. HMBC indicated that the signal at 4.12 ppm was due to the proton(s) in α to the carboxyl carbon (181 ppm) and was thus assigned to H5. ^{1}H-^{1}H COSY showed that H4 appeared at 3.88 ppm and H3 at 3.73 ppm, but no correlation could be done with the other protons. Starting from the other end of the molecule, H1 at 2.99 ppm was identified by its one-bond correlation with C1 (52.8 ppm) and enabled the identification of H2 at 4.01 ppm. By difference, the multiplet at 3.73 should belong to H3 and indeed the signal couples with H2 in the ^{1}H-^{1}H COSY spectrum and a value of $J_{3,4}$ = 3.5 Hz is observed. Nevertheless, the coupling constants of H2 and H3 do not match. Finally, it was noticed that upon prolonged storage of the sample at -18 °C the doublet at 2.99 ppm broadens and transforms into an unresolved multiplet (see for example the horizontal projection in Figure 6.14).

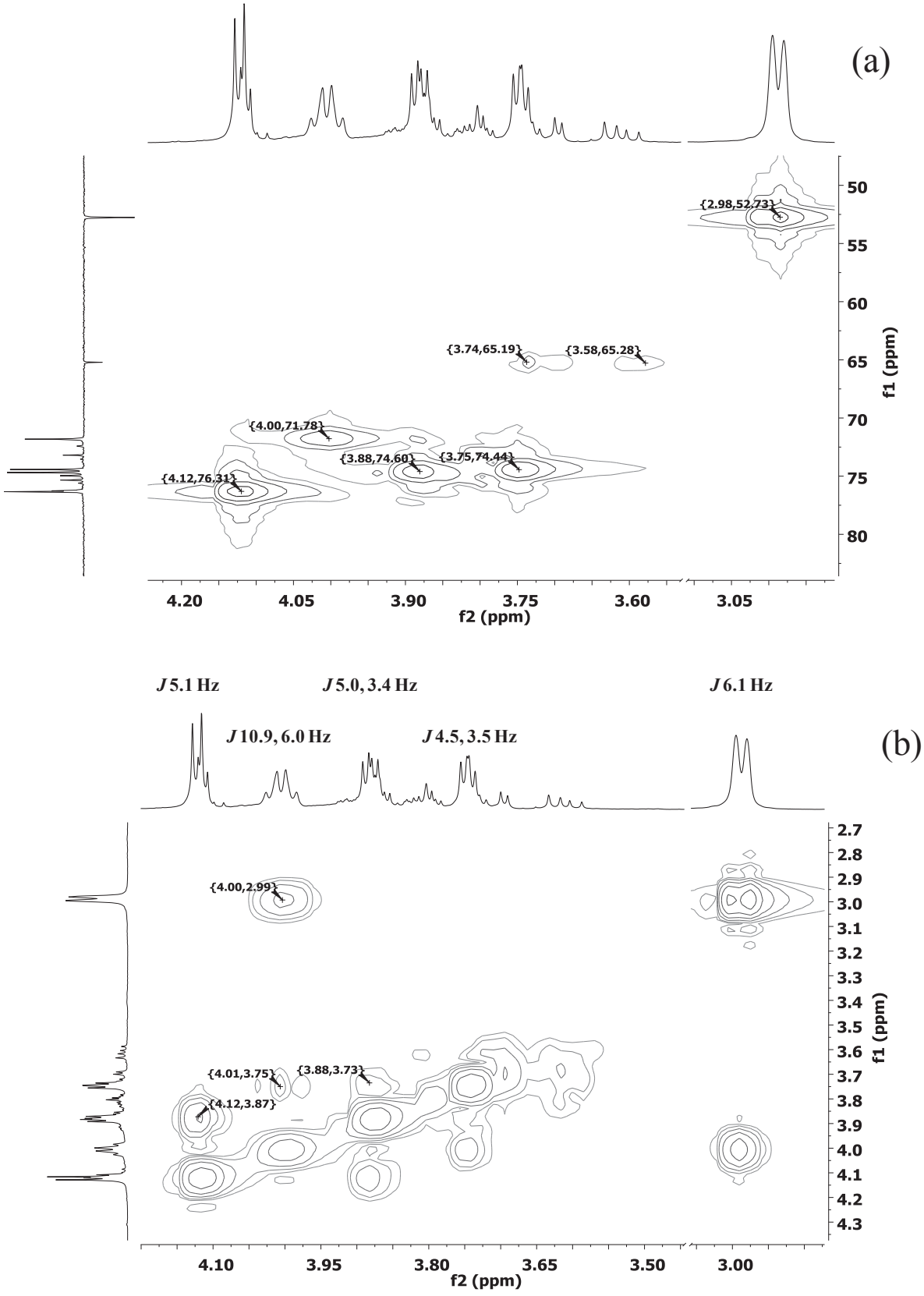

Figure 6.13 *^{1}H-^{13}C HMQC (a) and ^{1}H-^{1}H COSY (b) spectra of the by-products formed during the reductive amination of D-glucuronic acid at pH 6 (fraction 1 in Figure 6.8; entry no 1 in Table 6.1). [17] In HMQC, the DEPT-135 spectrum is projected and one cut in the horizontal axis should be noted.}*

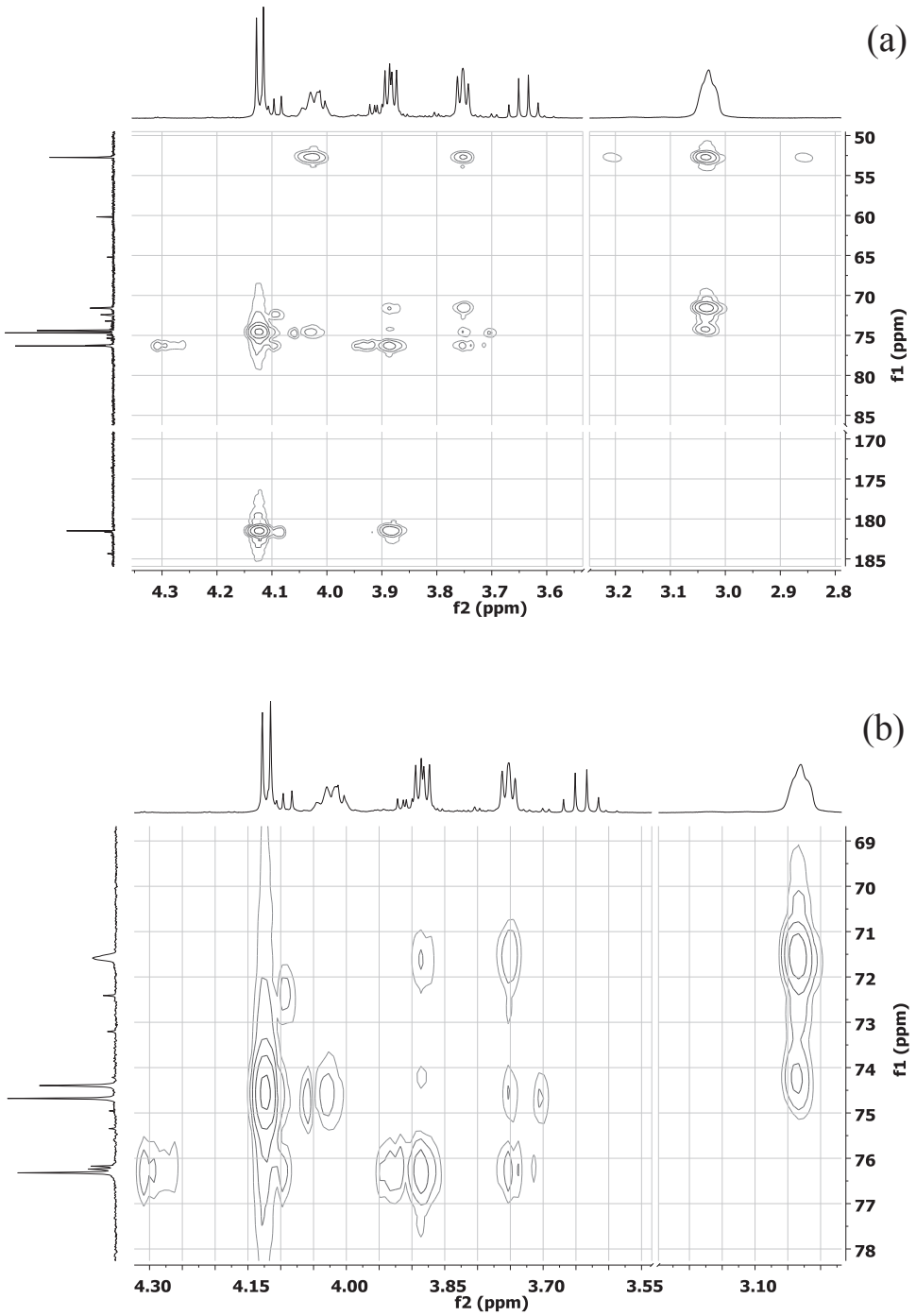

Figure 6.14 *^{1}H-^{13}C HMBC spectrum of the byproducts mixture from the reductive amination of D-glucuronic acid at pH 7.5 (fraction 1 in Figure 6.8, entry no 2 in Table 6.1). Note the cut in each axis and the satellites resulting from self-coupling.* [18]

6.4 Take home messages

The following chapter described the reductive amination of oligoglycuronans in aqueous solution and the following hints could be conveyed:

i. The reductive amination of oligoglycuronan in aqueous solution results in a fair amount of by-products (≤ 45 %) depending on the reaction conditions.

ii. The nature of by-products is not clear where no reduction of either carboxylic groups or aldehydes were observed. Neither dimers nor any Amadori derived products (cyclic or opened form) could be detected.

iii. The best yield (55 %) could be afforded at pH values in the range 5.5-6.5, and the amount of by-products is directly proportional to pH.

iv. The reductive amination of oligomannuronans is faster than that of oligoguluronans.

Appendix 6.A Selected NMR spectra

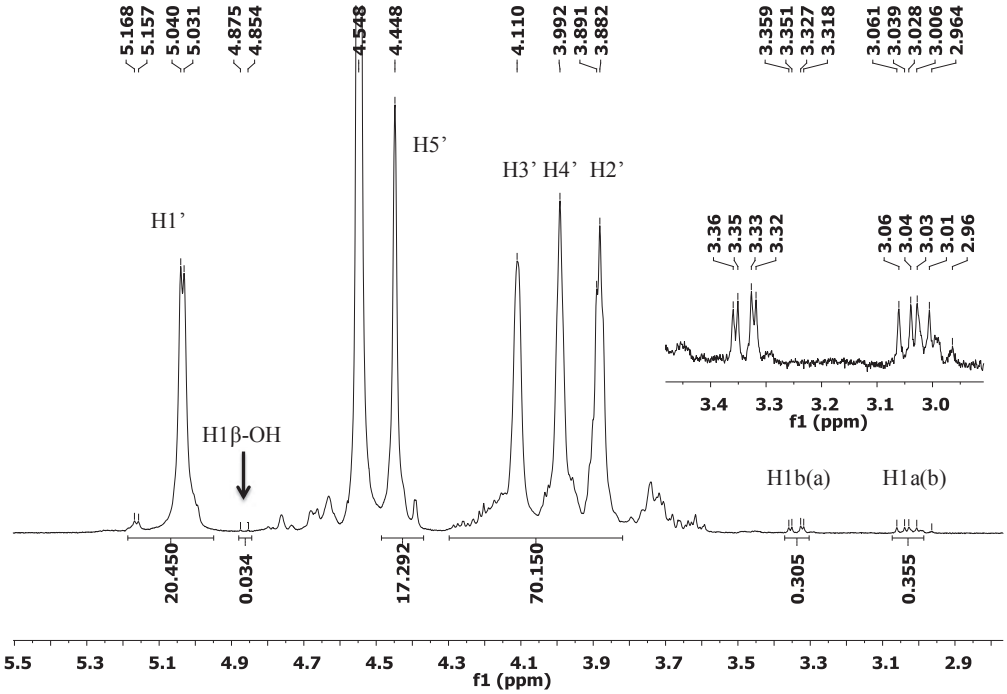

Figure 6.15 *[1]H-NMR spectrum of (1→4)-α-L-guluronan derived amino-alditol* ***8₂₀****. (Entry 16, Table 6.1). See Scheme 6.2 for nucleus numbering.*[19]

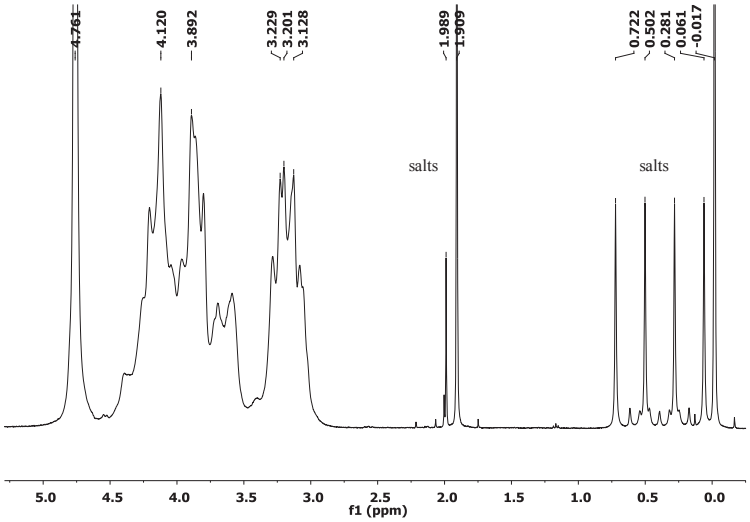

Figure 6.16 *[1]H-NMR spectrum of (2ξ)-6-amino-6-deoxy-D-lyxo-hexonic acid* ***2*** *purified by freeze drying followed by precipitation in EtOH. (Entry 1, Table 6.1). Note the effect of the salt on the resolution* [20]

Appendix 6.B Molecular weights from Size Exclusion Chromatography with MALLS detector

6.B.1 The technique

Size exclusion chromatography is a chromatographic method in which molecules are separated based on their size, in more technical terms on their hydrodynamic volume. A column is filled with porous material that will admit ions and small molecules into their pores but not large ones. Thus, when a mixture of molecules and ions dissolved in a solvent is applied to the top of the column, the smaller molecules (and ions) are distributed through a larger volume of solvent than is available to the large molecules. Consequently, the large molecules move more rapidly through the column, and in this way the mixture can be separated (fractionated) into its components. Disregarding all other forms of interaction (adsorption, partition), a molecule that is small enough to enter every pore of the gel will be eluted after retention volume (V_r):

$$V_r = V_i + V_p \tag{6.1}$$

where V_i is the interstitial volume and V_p is the pores volume. For any intermediate sample:

$$V_r = V_i + K_{sec} V_p \tag{6.2}$$

in which K_{sec} is the partition constant in the mobile phase and has values between 0 and 1. Once separation is established, the solution passes a number of detectors depending on the information needed for a particular sample. In our laboratory three online detectors are used, this means: a differential refractometer (for concentration measurement), light scattering photometer (for molar mass) and a viscometer (for measuring intrinsic viscosity).

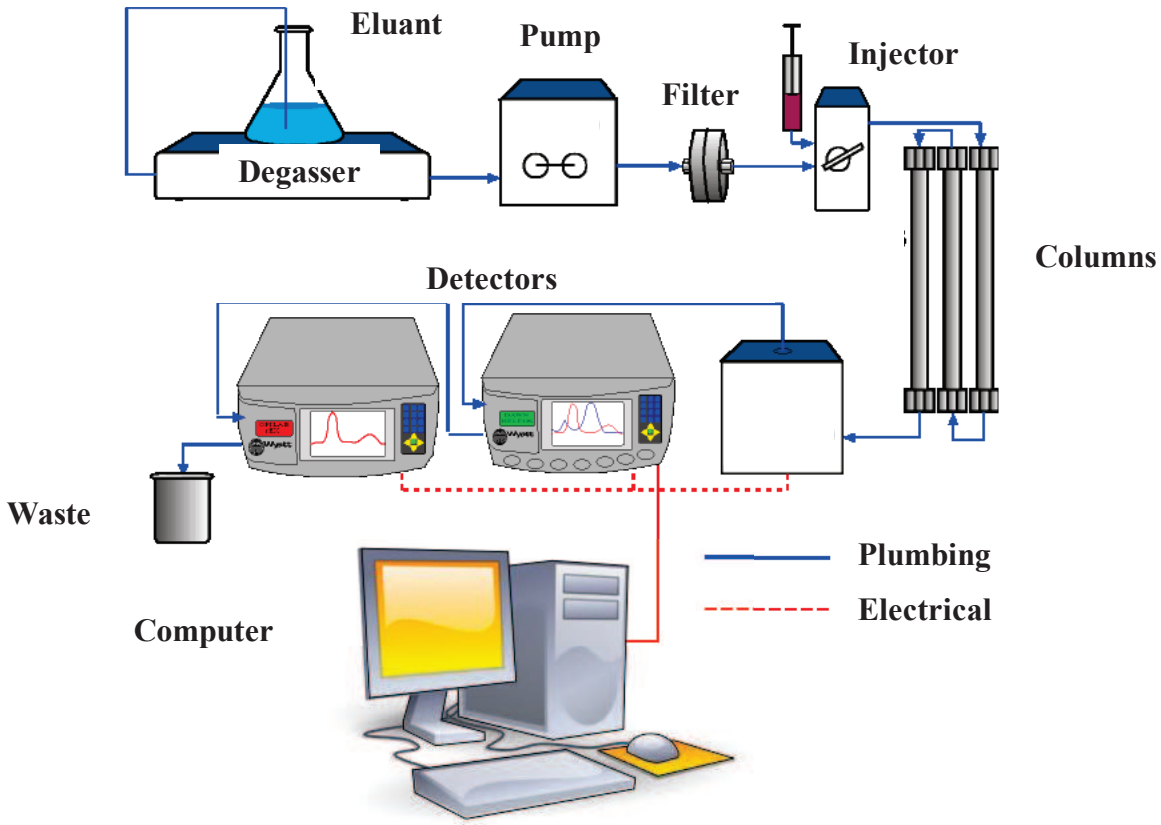

Figure 6.17 *Typical setup of a Size Exclusion Chromatography apparatus. Reprinted under permission from Wyatt Technology ©.*

6.B.2 Molecular weight from light scattering detector

In SEC systems operating without an online light scattering detector, a calibration with molecular weight standards is needed in order to relate the elution volume to the molecular weight of a molecule and that reflects the relativity of the system. However, in the presence of an online light scattering detector, measurement of absolute molecular weight is independent from column calibration. Besides molecular weight dependence, light scattering also has a direct dependence on particle size. For polymer solutions, this dependence on size can be used to measure the radius of gyration (R_g) of the polymer.

In general, when a beam of light (electromagnetic wave) strikes a molecule of a medium, the oscillating electric field (dominates the magnetic one) partially separates positive and negative charges in the particle, with the amount of separation determined by the *polarizability* of the particle. The gained energy will be re-radiated and scattered at different angles and therefore detected. It is worth noting that the amount of light scattered in this fashion is typically quite small (only a fraction of a percent of the incident light). [21]

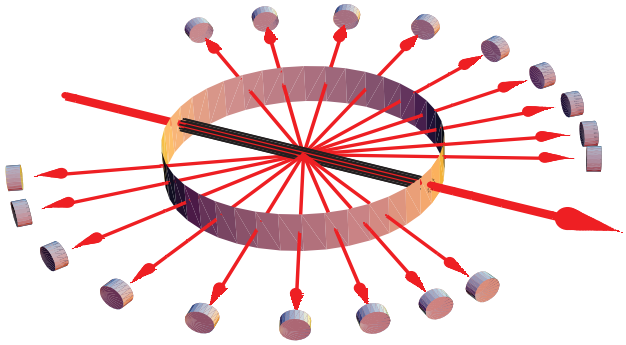

Figure 6.18 *Scattering of light resulting after striking a particle by a laser beam.*

In fact, the phenomenon of light scattering is caused by fluctuation in the refractive index of the medium as shown initially by Smoluchowski [22] and Einstein. [23] Later on, Zimm [24] and Debye [25] replaced the fluctuation in the refractive index of the solvent itself by the changes caused by the polymer molecule, i.e. dn/dc. The latter result related the detected intensity of the scattered light to the osmotic pressure (π) of the polymer as follows: [21]

$$\frac{Hc}{R(\theta)} = \frac{1}{RT}\left(\frac{\partial \pi}{\partial c}\right)_T \tag{6.3}$$

Where R(θ) is called the Rayleigh's ratio and is equal to $I_\theta w^2/I_0 V_s$ where I_θ represents the light intensity detected at angle θ scattered from a volume V_s and at a distance w from the source with an intensity of the incident light I_0. The optical constant H and π/c are respectively given by:

$$H = \frac{2\pi^2 n_0^2 \left(\frac{dn}{dc}\right)^2}{N_A \lambda^4} \tag{6.4}$$

$$\frac{\pi}{c} = RT\left(\frac{1}{M_n} + A_2 c + A_3 c^2 + \ldots\right) \tag{6.5}$$

Where n_0 is the refractive index at wavelength λ, N_A is Avogadro's number, dn/dc is the refractive index increment, A is the virial coefficient and c is the concentration. By multiplying Eq. 6.5 by c then differentiating as shown in Eq. 6.3, the basic equation for molecular weight and size calculation could be given as:

$$\frac{Hc}{R(\theta)-R(solvent)}=\frac{1}{M_w P(\theta)}+2A_2c \tag{6.6}$$

Where $P(\theta)$ is the scattering function which describes the angular scattering arising from the conformation of an individual chain. It is worth noting that A_2 gives information about the interaction between polymer and solvent. If A_2 is > 0 this means that the polymer is well solvated, if it is equal to zero then the solvent is known as a theta solvent and if it is inferior to zero the solvent used is a poor solvent.

For small molecules $P(\theta)$ tends to unity. However, for big molecules $P(\theta)$ differs from unity and it is a generally defined as:

$$\frac{1}{P(\theta)}=1+\frac{1}{3}\left(\frac{4\pi}{\lambda}\right)^2 R_g^2\sin^2\frac{\theta}{2}+... \tag{6.7}$$

The "…" means that there are higher order terms in sin(θ/2). Those terms are normally assumed to be negligible. In a SEC system equipped with a MALLS detector the calculation of M_w and R_g is established from the so called "partial Zimm plot". Since very diluted solutions are analyzed A_2 from Eq. 6.6 could be neglected, thus by replacing $1/P(\theta)$ and A_2 = 0 in Eq. 6.6 we get:

$$\left(\frac{Hc}{R(\theta)}\right)_{c=0}=\frac{1}{M_w}\left[1+\frac{1}{3}\left(\frac{4\pi}{\lambda}\right)^2 R_g^2\sin^2\frac{\theta}{2}+...\right] \tag{6.8}$$

Hence, by the help of the SEC software $Hc/R(\theta)$ is plotted as function of $\sin^2(\theta/2)$ and from the intercept and the slope $1/M_w$ and R_g^2 are calculated respectively.

6.5 References

(1) (a) Borch, R. F.; Bernstein, M. D.; Durst, H. D. *J. Amer. Chem. Soc.* **1971**, *93*, 2897(b) Lane, C. F. *Synthesis* **1975**, 135(c) Abdel-Magid, A. F.; Carson, K. G.; Harris, B. D.; Maryanoff, C. A.; Shah, R. D. *The Journal of Organic Chemistry* **1996**, *61*, 3849.

(2) (a) Thomaides, J. S.; Burkert, J.; Farwaha, R.; Humphreys, R. W. R.; Petersen, P. M.; (National Starch and Chemical Investment Holding Corporation, USA). Application: US US, 1996(b) Whistler, R. L.; Panzer, H. P.; Roberts, H. J. *Journal of Organic Chemistry* **1961**, *26*, 1583(c) Klein, J.; Herzog, D. *Makromolekulare Chemie* **1987**, *188*, 1217(d) Klein, J.; Begli, A. H. *Makromolekulare Chemie* **1989**, *190*, 2527(e) Klein, J.; Kowalczyk, J.; Engelke, S.; Kunz, M.; Puke, H. *Makromolekulare Chemie, Rapid Communications* **1990**, *11*, 477(f) Klein, J.; Begli, A. H.; Engelke, S. *Makromolekulare Chemie, Rapid Communications* **1989**, *10*, 629.

(3) (a) Yoshida, S.; Watanabe, S.; Takeuchi, T.; Murata, K.; Kusakabe, I. *Bioscience, Biotechnology, and Biochemistry* **1997**, *61*, 357(b) Wusteman, F. S.; Gacesa, P. *Carbohydrate Research* **1993**, *241*, 237(c) Roger, O.; Colliec-Jouault, S.; Ratiskol, J.; Sinquin, C.; Guezennec, J.; Fischer, A. M.; Chevolot, L. *Carbohydrate Polymers* **2002**, *50*, 273.

(4) (a) Rinaudo, M. *European Polymer Journal* **2010**, *46*, 1537(b) Rinaudo, M. *Carbohydr. Polym.* **2011**, *83*, 1338(c) Gomez, C. G.; Chambat, G.; Heyraud, A.; Villar, M.; Auzely-Velty, R. *Polymer* **2006**, *47*, 8509(d) Alidedeoglu, A. H.; York, A. W.; Rosado, D. A.; McCormick, C. L.; Morgan, S. E. *J. Polym. Sci., Part A Polym. Chem.* **2010**, *48*, 3052.

(5) Pawlowski, A.; Kallenius, G.; Svenson, S. B. *Vaccine* **1999**, *17*, 1474.

(6) Hutchins, R. O.; Natale, N. R. *Organic Preparations and Procedures International* **1979**, *11*, 201.

(7) Knutsen, S. H.; Moe, S. T.; Larsen, B.; Grasdalen, H. *Hydrobiologia* **1993**, *260-261*, 667.

(8) Conditions: 100.16 MHz, D_2O, 298 K, 17 %w/w, ns = 5000, D1 = 3s

(9) Conditions: 100.16 MHz, D_2O, 298 K; (a) 10% w/w, ns = 7000, D1 = 5s, (b) 10 %w/w, ns = 6000, D1 = 5s. Experiment: AG10-31-S1.

(10) Robichaud, A.; Nait Ajjou, A. *Tetrahedron Letters* **2006**, *47*, 3633.

(11) Kohn, R. *Pure and Applied Chemistry* **1975**, *42*, 371.

(12) Dangerfield, E. M.; Plunkett, C. H.; Win-Mason, A. L.; Stocker, B. L.; Timmer, M. S. M. *Journal of Organic Chemistry* **2010**, *75*, 5470.

(13) Conditions: Biogel P2 columns, 55 (C, eluent: H_2O (0.5 mL min-1), injected mass = 92 mg.

(14) Conditions:400.13 MHz, D_2O/DMSO-d6 1:1, 8 mg mL-1, 288 K, ns = 16, D1 = 2 s. The spectrum was referenced to TSP not to DMSO-d6.

(15) Conditions: 400.13 MHz, 2.5 %w/w, 298 K, ns = 10000, D1 = 3 s.

(16) Conditions: 100.16 MHz, D_2O, 288 K, 2.9 %w/w, for (a) ns = 10000, D1 = 3s, (b) ns = 7000, D1 = 3 s.

(17) Conditions: D_2O, 288 K, 2.9 %w/w, for (a) 100.16, 400.13 MHz, ns = 140, D1 = 2 s, (b) 400.13 MHz, ns = 240, D1 = 2 s.

(18) Conditions: 400.13-100.16 Hz, D_2O, 288 K, 1.6 % w/w, ns = 512, D1 = 1 s.

(19) Conditions: 400.13 MHz, D_2O, 318 K, 2.3 %w/w, ns = 100, D1 = 10 s.

(20) Conditions: 400.13 MHz, D_2O, 6.3 %w/w, 298 K, ns = 16, D1 = 2 s.

(21) Sperling, L. H. *Inroduction to physical polymer science*; 2nd ed.; Wiley & Sons, Inc., 1992.

(22) von Smoluchowski, M. V. *Ann. Phys.* **1908**, *25*, 205.

(23) Einstein, A. *Annalen der Physik* **1910**, *338*, 1275.

(24) Zimm, B. H. *J. Chem. Phys.* **1948**, *16*, 1093.

(25) Debye, P. *J. Phys.Coll. Chem.* **1947**, *51*, 18.

Chapter 7: Synthesis of AlgiMERs in aqueous solution

Table of contents

Disclaimer

Alexandre Peruchon, a Master 1 student, has explored the synthetic potential of β-D-glucopyranuronosylamine **11** in the presence of diverse electrophilic moieties (see synthetic potential section).

Anna Wolnik conducted the simulation study on the glycosylamine derivatives of oligoalginates.

7.1 Introduction

The modification of oligoglycuronans in aqueous solution requires the selection of water soluble reagents that are capable of reacting selectively with functional groups since protective chemistry is exhaustive and time consuming; like that the principles of green chemistry are respected to an extent. The use of water soluble acyl halides, [1] anhydrides, [1a] and isocyanates [2] bearing vinyl moieties could be useful for the synthesis of glycomonomers. Based on the relative stability of these electrophilic moieties in aqueous solutions, *N*-acylation reactions at low temperatures can surmount to an extent this problem providing that the acylation reaction is fast and selective for amino groups. In this chapter a short overview on the synthesis of glycomonomers, from glycosylamines and amino alditols, in aqueous solution is reported. The embodiment of these known strategies for the synthesis of oligoalginates derived monomers (AlgiMERs) is shown (Scheme 7.1). The functionalization step was optimized as well to steer clear of any side reactions during synthesis, as β-elimination [3] under basic conditions and partial functionalization of the hydroxyl groups of the sugar. Knowing that glycosylamines are sensible to water, a study to transform D-glucuronic acid into β-D-glucopyranuronosyl amine derivatives without resorting to protective group chemistry was examined as well.

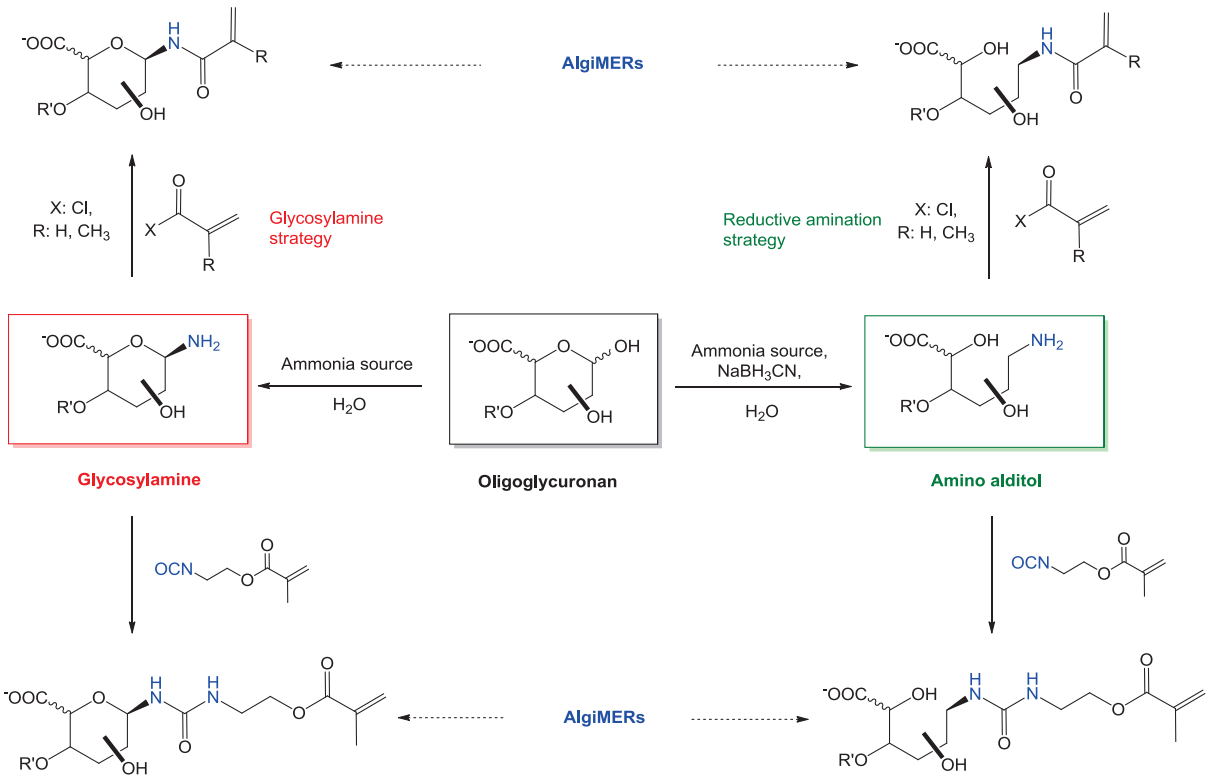

Scheme 7.1 *Synthetic routes used for the synthesis of AlgiMERs in aqueous solution.*

7.2 Synthesis of glycomonomers in aqueous solution by the reductive amination and glycosylamine strategies: an overview

Most glycomonomers described in literature are synthesized in organic solvents after resorting to protective group chemistry. Here, an overview on the synthesis of glycomonomers in aqueous solution is described.

Reductive amination strategy

Whistler et al. [1a] described the synthesis of glycomonomers in aqueous solution. For instance, 1-acrylamido-1-deoxy-D-glucitol **1** was obtained by the reaction of 1-amino-1-deoxy-D-glucitol (0.2 M) [4] with acryloyl chloride (1eq) in a potassium carbonate solution at 4 °C. The product was obtained with 60 % yield after crystallization from ethyl ether. The latter reaction was also conducted in methanol in the presence of methacrylic anhydride, where higher yield (92 %) was obtained. Interestingly, the synthesized amides showed relative stability in basic solution where after 20 hours in NaOH solution (2.3 M) at RT, less than 10 mol % of the amides (0.2 M) were hydrolyzed.

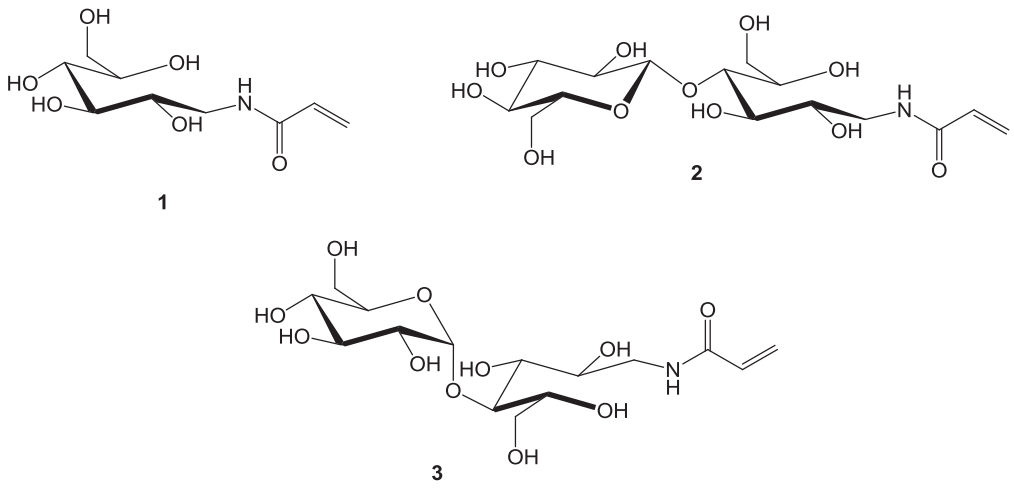

Figure 7.1 *Different glycomonomers synthesized in aqueous solution described by Whistler [1a] and Klein [5] from the reductive amination strategy.*

The same monomer **1** was synthesized as well by Klein [5a] where the amino alditol was obtained from the reaction of glucose with hydrazine in a high pressure autoclave. Fresh Raney nickel was added to the mixture followed by passing hydrogen to the system at 50 °C for 3 hours. The corresponding amino alditol, purified by crystallization, was solubilized in a K_2CO_3 solution at 0 °C under nitrogen followed by a drop wise addition of acryloyl chloride (2 eq). The product was obtained after a series of crystallizations with a yield of 59 %. Nonetheless, the corresponding methacrylamide was synthesized with a yield of 70 % in methanol. In an another paper, Klein [5b] also described the synthesis of 1-acrylamido-1-deoxycellobiitol **2** and 1-acrylamido-1-deoxymaltitol **3** in aqueous solution using the same method (reductive amination followed by functionalization) where yields up to 75 % were obtained. It is worth noting that the corresponding methacrylamides were synthesized in MeOH using methacrylic anhydride and 75 % yields were obtained. The different glycomonomers were polymerized and the influence of the structural differences of the corresponding polymers on the solution properties was examined by viscosity and light scattering measurements.

The synthesis of methacrylate derived glycomonomers in aqueous solution at -3 °C via the reaction of an amino alditol with 2-isocyanatoethyl methacrylate **IEM** was a subject of three papers by Klein. [2] The sugar moieties were attached to the polymerizing functionality through a urea linkage (Scheme 7.2). In the absence of a catalyst, the author claimed that at low temperatures (< 5 °C) the isocyanate group reacted preferentially with the amine group and did not react with the hydroxyl groups of the sugar with the absence of side reactions as

the formation of urea or gaseous compounds resulting from the hydrolysis of the isocyanate in water and its self condensation. [2b]

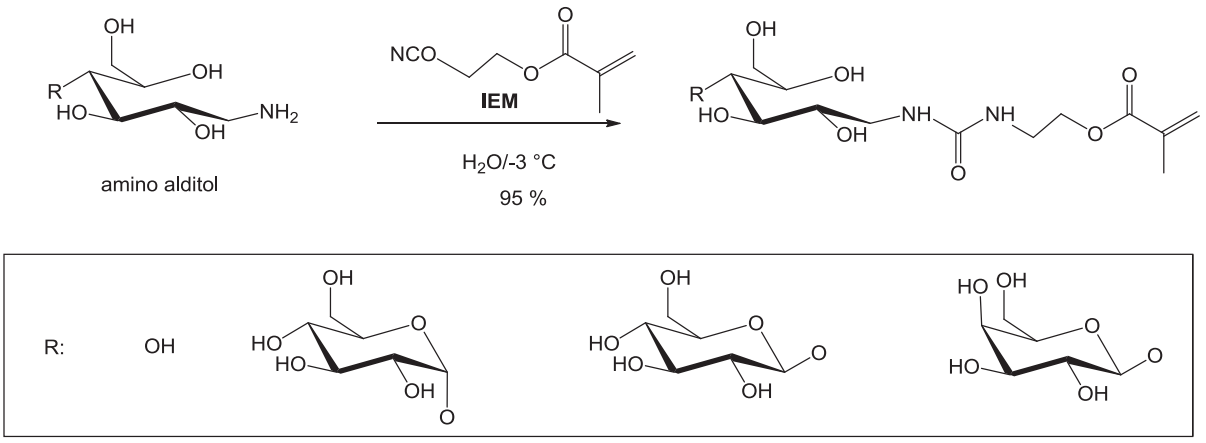

Scheme 7.2 *Glycomonomers synthesized by Klein [2b] in aqueous solution. Conditions: 1 eq amino alditol (1.1 M), 1 eq IEM, -3 °C–RT, 12 hours.*

Furthermore, the polymerization of the corresponding methacrylate glycomonomers (Scheme 7.2) yielded polymers whose molecular weights together with their intrinsic viscosity were higher than the polymers obtained from the (meth)acrylamide derived glycomonomers (**1**, **2** and **3**) due to the presence of a longer spacer as proposed by the author. It is worth noting that a methacrylate vinyl group polymerizes, normally, faster than a methacrylamide one.

In the course of preparing amphiphilic glycopolymers, Klein [2c] prepared methacrylate glycomonomers from a secondary amino alditol **4** acquiring an alkyl chain. Likewise, the saccharides were reacted with primary alkyl-amines in the presence of the reducing agent (H_2/Ni) to afford the corresponding secondary amino alditols. Like that, by choosing the right alkyl-amine the reactivity of the secondary amines could be altered and consequently the amino alditol will react faster with IEM in aqueous (at low temperature) or organic medium to give the corresponding glycomonomer (Scheme 7.3).

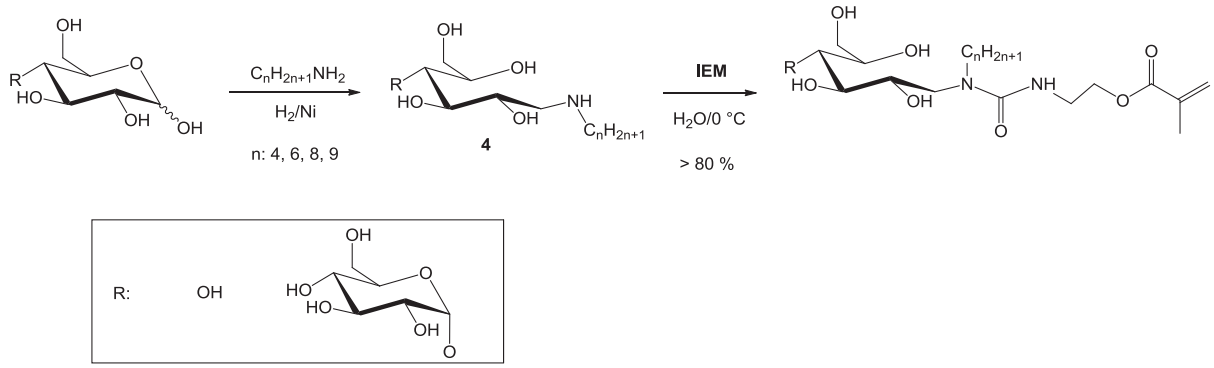

Scheme 7.3 *Glycomonomers synthesized by Klein [2c] in aqueous solution. Conditions: 1 eq amino alditol (0.46 M), 1 eq IEM, 0 °C – RT, 16 hours.*

Klein [2a] also described the synthesis of charged glycopolymers (Scheme 7.4). To this end, isomaltulose (6-O-*α*-D-glucopyranosyl)-D-fructofuranose) **5** was oxidized to its corresponding carboxylated form **6** and functionalized with an amine group via reductive amination. [5b] The latter amine **7** was further reacted in water (-3 °C) with IEM at pH 11 to give, after extraction with diethyl ether, a methacrylate derived glycomonomer **8** with 87 % yield. The obtained water soluble glycopolymers had average molecular weights up to 14 million and showed typical behavior of polyelectrolytes in solution and therefore their solution properties (rheology, light scattering) were measured in the presence of salt.

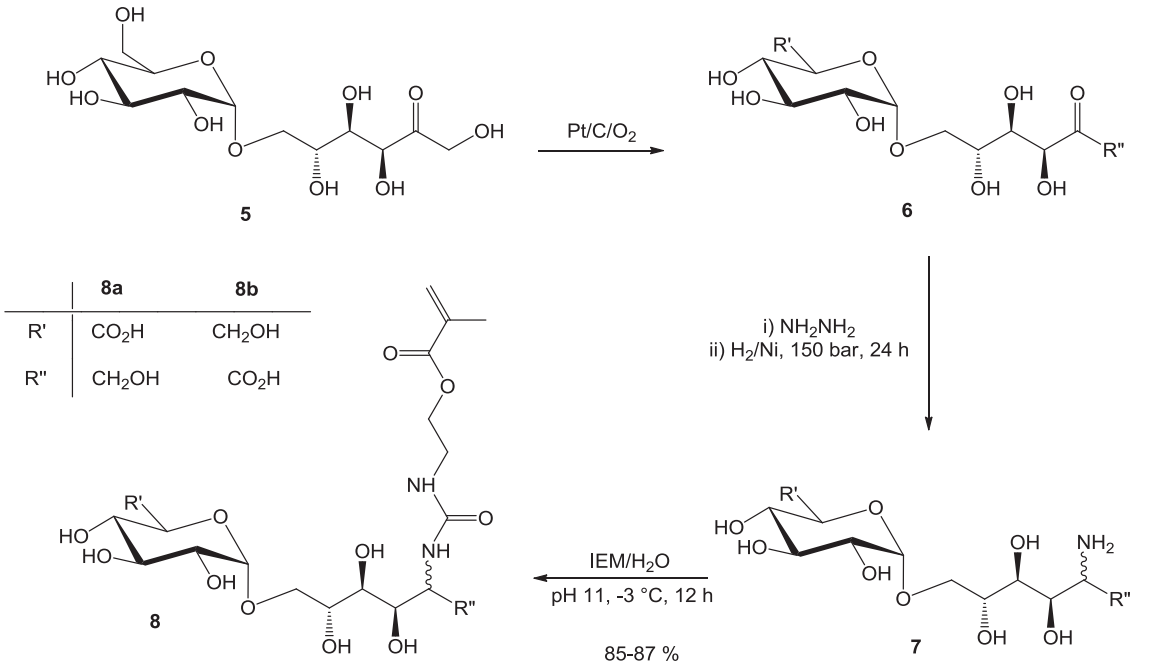

Scheme 7.4 *Isomaltulose derived glycomonomers synthesized by Klein [2a] in aqueous solution. Conditions: 1 eq of 7 (~ 0.33 M), 2.5 eq IEM, pH 11, -3 °C – RT, 12 hours.*

Glycosylamine strategy

Based on the relative stability of glycosylamines in basic solutions at low temperatures, *N*-acylation could be possible providing that the acylation reaction is fast and selective for amino groups. Kallin et al. [1b,6] described the synthesis of a series of *N*-acryloyl glycosylamines in aqueous solution (Scheme 7.5). The reducing end in all the cases was a glucose unit. In a typical experiment, to a solution of glycosylamine (1 eq) in water (1 mL), sodium carbonate (6.7 eq) and methanol (1 mL) were added. The mixture was stirred at 0 °C and a solution of acryloyl chloride (5.3 eq) in THF was introduced. Yields from 50 to 92 % were obtained depending on the glycosylamine being examined. For instance, the reaction of β-D-lactopyranosylamine gave a yield of 88 % and that of lacto-*N*-fucopentaose afforded a yield of 53 %. The radical copolymerization of the resulting glycomonomers with acrylamide in aqueous solution resulted in linear polymers with molecular weights between 100 to 500 KDa.

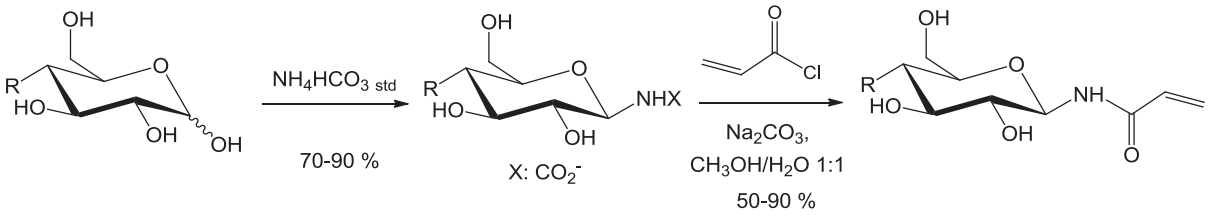

Scheme 7.5 *Synthesis of a series of N-acryloyl glycosylamines described by Kallin et al. [1b] Conditions: Glycosylamine (1eq), acryloyl chloride (5.3 eq), Na_2CO_3 (6.7 eq), $MeOH/H_2O$ 1:1, 0 °C, 10 min.*

Finally, not to forget the syntheses of some (meth)acryl amides of amino sugars as D-glucosamine. For instance, Matsuda et al. [7] described the synthesis and polymerization of *N*-acryloyl-D-glucosamine in aqueous solution based on the method of Whistler et al. [1a] and 38 % yield was obtained in the synthesis step after crystallization. Furthermore the methacrylamide derivative of D-glucosamine was as well synthesized by Stenzel et al. [8] in CH_3OH, where the product was isolated after chromatographic purification with 58 % yield.

7.3 Experimental

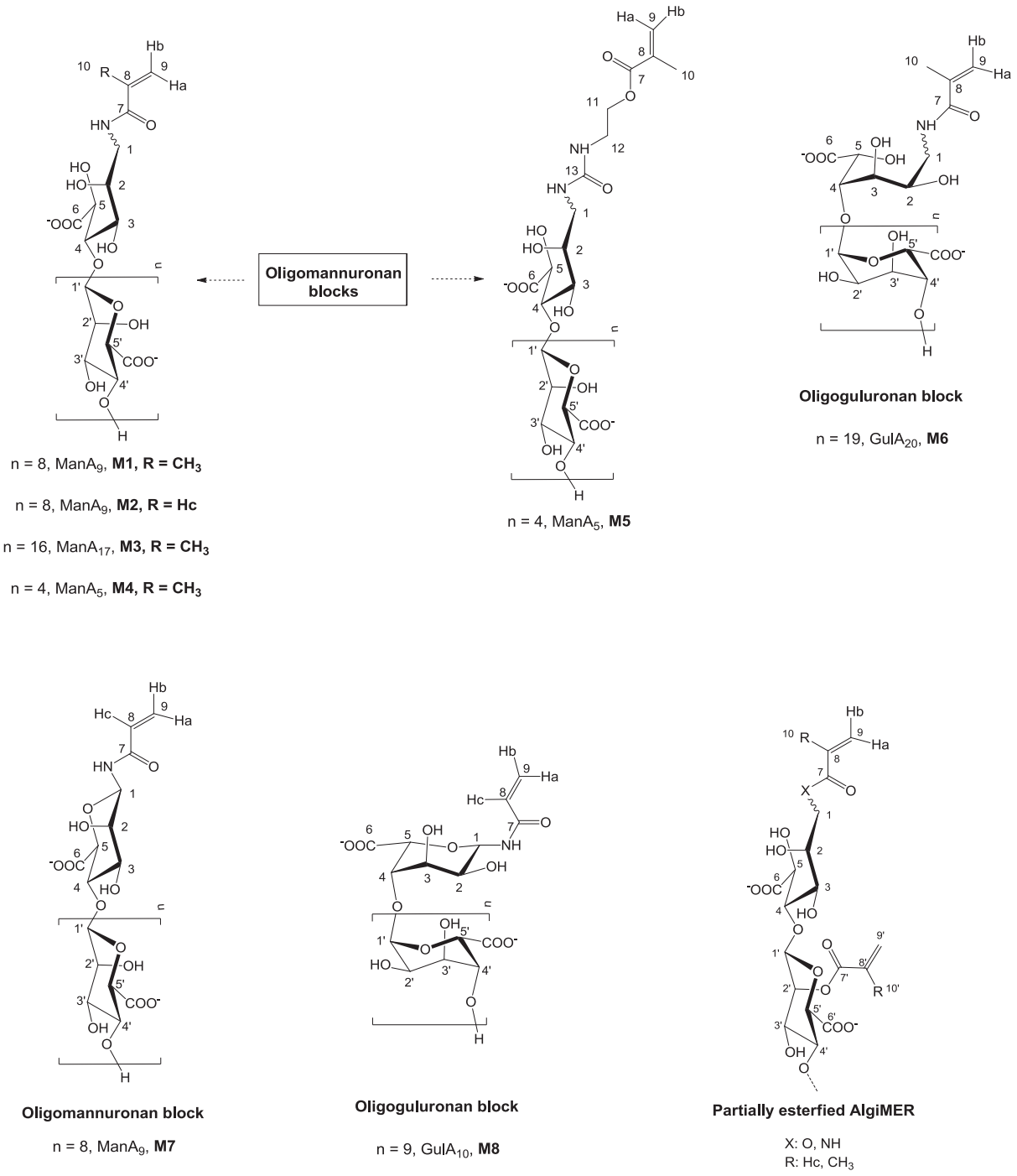

Figure 7.2 *Molecules involved in this study. $ManA_x$ and $GulA_x$ represent oligomannuronan and oligoguluronan blocks with $DP_n = x$, respectively.*

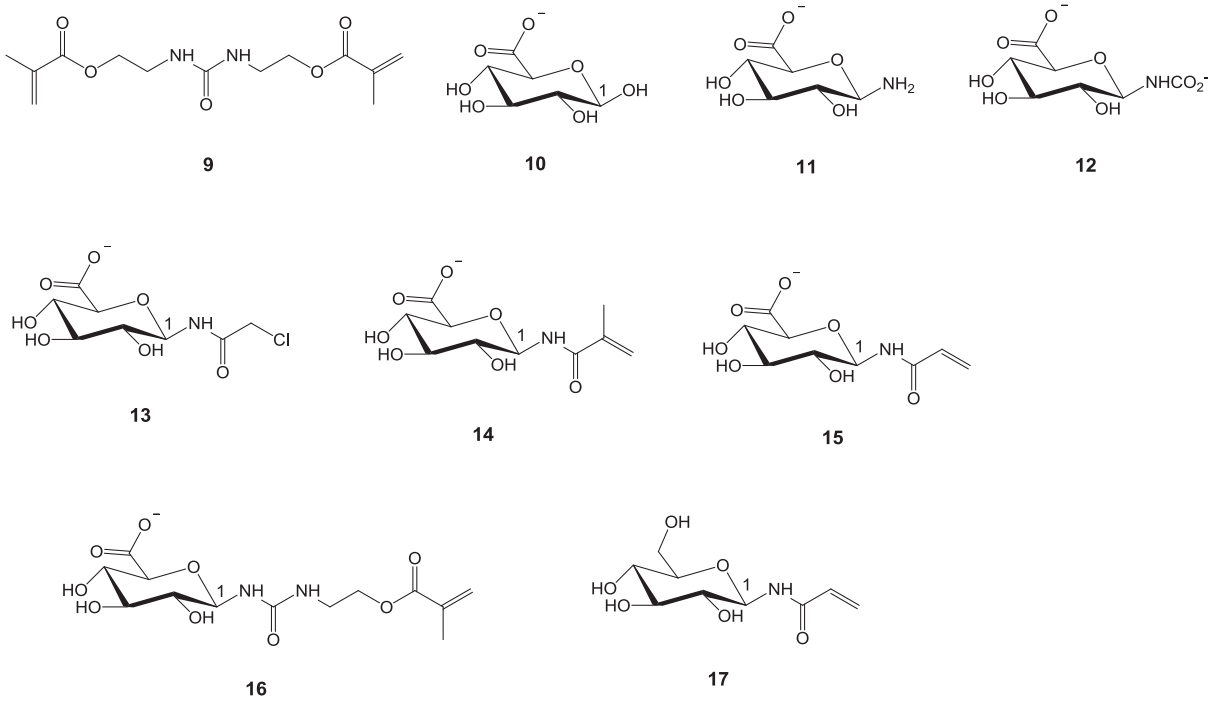

Figure 7.2 *Continued.*

7.3.1 Materials

The chemicals were reagent grade and used as received. NaCl (≥ 99 %, Aldrich), $NaHCO_3$ (≥ 99 %, SdS), Na_2CO_3 (≥ 99 %, Aldrich), 2,6-Di-tert-butyl-4-methyl phenol BHT (≥ 99 %, Fluka), $NaNO_3$ (≥ 99 %, Aldrich), NaN_3 (≥ 99 %, Merck), ethanol (≥ 99 %, Carlo Erba), 2-isocyanatoethyl methacrylate IEM (> 98 %, TCI), methacrylic anhydride (94 %, Aldrich), MeOH (≥ 99 %, Carlo Erba), DMSO (99.5 %, Aldrich). Acryloyl (≥ 96 %, Fluka) and methacryloyl chloride (≥ 97 %, Fluka) were distilled under vacuum prior to use and were stored at -18 °C. Ultra filtration membranes were supplied by Millipore. Accurate volumes were measured using micropipettes (Eppendorf Research).

7.3.2 Analysis

NMR experiments were acquired on a Bruker DPX400 spectrometer (described in Chapter 5). Chemical shifts (in ppm) for ^1H and ^{13}C nuclei were referenced to δ = -0.017 ppm and δ = -0.149 ppm respectively. For glycomonomers obtained by the reductive amination strategy yields were calculated by normalizing the ^1H NMR spectrum of the final product at t = ∞ and that of the starting oligoglycuronan to one peak (*e.g.* internal anomeric H1' of the glycomonomer). For the glycomonomers obtained by the glycosylamine strategy yields were

calculated by comparing the areas of the newly formed vinylic peaks with those of the anomeric peaks (H1α + H1β) of the starting oligoglycuronan (resulting from the hydrolysis of the glycosylamine) in the ^{1}H NMR spectrum of the purified glycomonomer.

Glycomonomers were characterized by size exclusion chromatography (SEC) using a Waters Alliance GPCV2000 (described in a Chapter 6).

The procedure for the simulation experiment is briefly described in Chapter 5.

7.3.3 Synthesis of AlgiMERs from the reductive amination strategy

*7.3.3.1 Synthesis of **M1** from methacryloyl chloride and $ManA_9$-NH_2*

(Run 1, Table 7.1) $ManA_9$-NH_2 (42 %, 1.50 g, 3.57×10^{-4} mol) was dissolved in 30.6 mL Na_2CO_3 / $NaHCO_3$ buffer solution (0.6 mol L^{-1}, pH 9.5) and 3.4 mL MeOH (≅ 10 % v/v) respectively. The mixture was cooled on ice for 10 minutes followed by a drop wise addition of methacryloyl chloride (493 µL, 50.9×10^{-4} mol) under stirring (250-300 rpm). The pH was adjusted to ≅ 9.5 from time to time with Na_2CO_3. After 2 hours on ice and 4.5 hours at RT, the reaction was stopped, the oligosaccharide was precipitated by EtOH (80 % v/v), the mixture was centrifuged (10 Krpm, 15 °C, for 10 minutes), and the precipitate was re-solubilized in water and diafiltered using a 500 Da cut off membrane followed by freeze drying. Reaction time: 6.5 hours. Yield: 100 %. ^{1}H NMR (400 MHz, D_2O, 50 °C) δ (ppm): 1.94 (m, H10, 3H), 3.38 (dd, H1, 1H, J_{11} 14.0 Hz, J_{12} 7.6 Hz), 3.59-4.34 (H2, H2', H3, H3', H4, H4', H5, H5', sugar), 4.64-4.80 (H1', sugar), 5.00 (H1', G unit), 5.44 (m, H9b), 5.70 (m, H9a).

*7.3.3.2 Synthesis of **M2** from acryloyl chloride and $ManA_9$-NH_2*

(Run 2, Table 7.1) Same procedure proceeded with run 1 (Table 7.1) using 1.50 g $ManA_9$-NH_2 (42 %, 3.57×10^{-4} mol). Reaction time: 6.5 hours. Yield: 100 %. ^{1}H-NMR (400 MHz, D_2O, 50 °C) δ (ppm): 3.37 (dd, H1, 1H, J_{11} 14.0 Hz, J_{12} 7.6 Hz), 3.59-4.34 (H2, H2', H3, H3', H4, H4', H5, H5', sugar), 4.64-4.80 (H1', sugar), 5.00 (H1', G unit), 5.76 (d, H9b, 1H, J_{bc} 10.4 Hz), 6.18 (d, H9a, 1H, J_{ac} 17.1 Hz), 6.32 (dd, H8c, 1H, J_{ac} 17.2 Hz, J_{bc}.10.3 Hz).

*7.3.3.3 Synthesis of **M3** from $ManA_{17}$-NH_2 and methacrylic anhydride/methacryloyl chloride*

Protocol A (methacrylic anhydride)

(Run 3, Table 7.1) $ManA_{17}$-NH_2 (38 %, 0.84 g, 9.73×10^{-5} mol) was dissolved in 42 mL Na_2CO_3 / $NaHCO_3$ buffer solution (0.2 mol L^{-1}, pH 10) and 3 mL DMSO respectively. The mixture was cooled on ice for 20 minutes followed by a drop wise addition of methacrylic anhydride (0.76 mL, 500×10^{-5} mol) under stirring. After 2 hours, another portion of methacrylic anhydride (0.76 mL) was introduced to the mixture on ice. The pH of the reaction mixture was adjusted with time to ≅ 9.5-10. After 22 hours the reaction was stopped, the pH was re-adjusted to 10 using NaOH (1 N), the mixture was precipitated by EtOH (75 % v/v) and centrifuged (10 Krpm, 10 min, 15 °C). The recovered precipitate was washed twice with EtOH to remove any suspended anhydride then diafiltered using a 500 Da cut off membrane followed by freeze drying. Reaction time: 22 hours. Conversion: 100 %. ^{1}H-NMR (400 MHz, D_2O, 45 °C) δ (ppm): 1.87 (m, H10'), 1.89 (m, H10'), 1.94 (m, H10, 3H), 3.38 (dd, H1, 1H, J_{11} 14.0 Hz, J_{12} 7.8 Hz), 3.59-4.34 (H2, H2', H3, H3', H4, H4', H5, H5', sugar), 4.69-4.80 (H1', sugar), 5.03 (H1', G unit), 5.44 (m, H9b, 1H), 5.70 (m, H9a, 1H), 5.74 (m, H9'b, 1H), 6.19 (m, H9'a, 1H). M_n (SEC-MALLS) 3371 Da, PDI 1.08.

Protocol B (methacryloyl chloride)

(Run 4, Table 7.1) $ManA_{17}$-NH_2 (40 %, 1.50 g, 1.83×10^{-4} mol) was dissolved in a 21 mL Na_2CO_3 / $NaHCO_3$ buffer solution (0.5 mol L^{-1}, pH 9.5) and 2.3 mL MeOH (9.5 % v/v) respectively. The mixture was cooled on ice for 10 minutes followed by a drop wise addition of methacryloyl chloride (266 µL, 27.5×10^{-4} mol) under stirring. The pH was adjusted to ≅ 9.5 from time to time by Na_2CO_3, and the mixture was left on ice for half an hour then left at RT. A precipitate appeared with time whose significance became important throughout the evolution of the reaction. After 6 hours, the reaction was stopped, the precipitate was totally solubilized by water (25 mL), 35 µL methacryloyl chloride was added, and the mixture was left one extra hour reacting at RT. The final solution was diafiltered using a 500 Da cut off membrane followed by freeze drying. Reaction time: 7.5 hours. Yield: 100 %. ^{1}H-NMR (400 MHz, D_2O, 55 °C) δ (ppm): 1.94 (m, H10, 3H), 3.38 (dd, H1, 1H, J_{11} 14.0 Hz, J_{12} 7.6 Hz),

3.59-4.34 (H2, H2', H3, H3', H4, H4', H5, H5', sugar), 4.64-4.80 (H1', sugar), 5.00 (H1', G unit), 5.44 (m, H9b, 1H), 5.70 (m, H9a, 1H).

*7.3.3.4 Synthesis of **M4** from $ManA_5$-NH_2 and methacrylic anhydride/methacryloyl chloride*

Protocol A (Methacryloyl chloride, pH 11)

(Run 5, Table 7.1) In a 10 mL vial, $ManA_5$-NH_2 (38 %, 0.100 g, 4.08×10^{-5} mol) and Na_2CO_3 (0.084 g, 79.2×10^{-5} mol) were dissolved in H_2O (2.36 mL) and DMSO (0.24 mL) respectively. The latter mixture (pH ≅ 10-11) was cooled on ice for 5 minutes before the addition of methacryloyl chloride (70 µL, 71.9×10^{-5} mol) under stirring (200-300 rpm). The pH was adjusted to 10 from time to time with Na_2CO_3. The final reaction mixture was extracted twice with EtOAc (2.4 mL), the aqueous phase was precipitated with EtOH (80 % v/v), centrifuged (10 Krpm, 10 min, 15 °C), decanted, and the obtained precipitate was re-solubilized in water and freeze dried. A ^{1}H NMR was acquired after freeze drying, and then the solution was further purified by diafiltration using a 500 Da cut off membrane. Reaction time: 5.5 hours. Yield: 100 %. ^{1}H-NMR (400 MHz, D_2O, 50 °C) δ (ppm): 1.94 (m, H10, 3H), 3.38 (dd, H1, 1H, J_{11} 13.9 Hz, J_{12} 7.5 Hz), 3.59-4.34 (H2, H2',H3, H3', H4, H4', H5, H5', sugar), 4.64-4.80 (H1', sugar), 5.00 (H1', G unit), 5.44 (m, H9b, 1H), 5.70 (m, H9a, 1H). ^{13}C-NMR (100 MHz, D_2O, 10 °C) δ (ppm): 20.52 (C10), 44.91 (C1), 71.06-79.57 (C2, C2', C3, C3', C4, C4', C5, C5'), 101.09-103.73 (C1'), 123.95 (C9), 141.65 (C8), 175.04 (C7), 178.16-181.67 (C6, C6').

Protocol B (Methacrylic anhydride, pH 11)

(Run 6, Table 7.1) Same quantities used with run 5 (Table 7.1) using same $ManA_5$-NH_2 (38 %, 4.08×10^{-5} mol). But, with time a white precipitate developed that was solubilized at the end of the reaction with water. The latter solution was extracted with EtOAc to remove any suspended anhydride, the aqueous phase was precipitated with EtOH (85 % v/v) and centrifuged (10 Krpm, 10 min, 15 °C). The recovered precipitate was re-solubilized in water and freeze dried. Reaction time: 24.5 hours. Conversion: 100 %. ^{1}H-NMR (400 MHz, D_2O, 50 °C) δ (ppm): 1.94 (m, H10, 3H), 3.38 (dd, H1, 1H, J_{11} 14.1 Hz, J_{12} 7.5 Hz), 3.59-4.34 (H2, H2',H3, H3', H4, H4', H5, H5', sugar), 4.64-4.80 (H1', sugar), 5.00 (H1', G

unit), 5.44 (m, H9b, 1H), 5.70 (m, H9a, 1H). ^{13}C-NMR (100 MHz, D_2O, 10 °C) δ (ppm): 20.52 (C10), 44.91 (C1), 71.06-79.57 (C2, C2', C3, C3', C4, C4', C5, C5'), 101.09-103.73 (C1'), 123.95 (C9), 141.65 (C8), 175.04 (C7), 178.16-181.67 (C6, C6').

Protocol C (Methacryloyl chloride, pH 9.5)

(Run 7, Table 7.1) $ManA_5$-NH_2 (38 %, 0.100 g, 4.08×10^{-5} mol) was dissolved in 2.16 mL Na_2CO_3 / $NaHCO_3$ buffer solution (0.36 mol L^{-1}, pH 9.5) and DMSO (0.24 mL) respectively. The mixture was cooled on ice for 5 minutes followed by a drop wise addition of methacryloyl chloride (70 µL, 71.9×10^{-5} mol) under stirring (200-300 rpm). The pH was adjusted to 9.5 from time to time with Na_2CO_3. After 6 hours (of which 2 hours on ice), the reaction was stopped, the mixture was extracted twice with EtOAc (2.4 mL), the aqueous phase was precipitated with EtOH (81 % v/v) and centrifuged. The recovered precipitate was re-solubilized in water and freeze dried. Reaction time: 6 hours. Yield: 89 %. ^{1}H-NMR (400 MHz, D_2O, 50 °C) δ (ppm): 1.94 (m, H10, 3H), 3.38 (dd, H1, 1H, J_{11} 13.9 Hz, J_{12} 7.5 Hz), 3.59-4.34 (H2, H2',H3, H3', H4, H4', H5, H5', sugar), 4.64-4.80 (H1', sugar), 5.00 (H1', G unit), 5.44 (m, H9b, 1H), 5.70 (m, H9a, 1H). ^{13}C-NMR (100 MHz, D_2O, 10 °C) δ (ppm): 20.52 (C10), 44.91 (C1), 71.06-79.57 (C2, C2', C3, C3', C4, C4', C5, C5'), 101.09-103.73 (C1'), 123.95 (C9), 141.65 (C8), 175.04 (C7), 178.16-181.67 (C6, C6').

*7.3.3.5 Synthesis of **M5** from 2-Isocyanatoethyl methacrylate (IEM) and $ManA_5$-NH_2*

Protocol A (pH 11)

(Run 8, Table 7.1) $ManA_5$-NH_2 (38 %, 0.100 g, 4.08×10^{-5} mol) was dissolved in H_2O (2.16 mL) and DMSO (0.24 mL) respectively. The pH was adjusted to ≅ 10-11 with Na_2CO_3 (tip of a spatula), the mixture was cooled on ice for 5 minutes, and IEM (51 µL, 36.0×10^{-5} mol) was added under stirring. The reaction mixture, whose pH was adjusted to ≅ 9.5-10 from time to time by the addition of Na_2CO_3, was left on ice for 2 hours before leaving the mixture reacting for another 4.5 hours at RT. At the end of reaction, the formed urea was extracted with three volumes of EtOAc, the aqueous phase was precipitated with EtOH (81 % v/v), and centrifuged (10 Krpm, 10min, 15 °C). The recovered precipitate was re-solubilized in water and freeze dried. Reaction time: 6.5 hours. Yield: 87 %. ^{1}H-NMR (400 MHz, D_2O, 50 °C) δ (ppm): 1.92 (m, H10, 3H), 3.25 (m), 3.44 (m), 3.59-4.34 (H2, H2',H3, H3', H4, H4', H5, H5',

sugar), 4.63-4.83 (H1', sugar), 5.05 (H1', G unit), 5.72 (m, H9b, 1H), 6.12 (m, H9a, 1H). ^{13}C-NMR (100 MHz, D_2O, 10 °C) δ (ppm): 20.16 (C10), 41.3 and 44.91 (C1, C12), 67.11 (C11), 71.06-79.57 (C2, C2', C3, C3', C4, C4', C5, C5'), 101.09-103.73 (C1'), 123.52 (C9), 141.65 (C8), 163.46 (C13), 172.41 (C7), 178.16-181.67 (C6, C6').

Protocol B (pH 9.5)

(Run 9, Table 7.1) $ManA_5$-NH_2 (38 %, 0.100 g, 4.08×10^{-5} mol) was dissolved in 2.16 mL Na_2CO_3 / $NaHCO_3$ buffer solution (0.36 mol L^{-1}, pH 9.5) and DMSO (0.24 mL) respectively. The mixture was cooled on ice for 5 minutes and IEM (51 µL, 36.0×10^{-5} mol) was added under stirring. The pH was adjusted to 9.5 from time to time by the addition of small quantities of Na_2CO_3. At the end of the reaction, the formed urea was extracted twice with EtOAc (2.4 mL), the aqueous phase was precipitated with EtOH (80 % v/v), and centrifuged (10 Krpm, 10 min, 15 °C). The recovered precipitate was re-solubilized in water and freeze dried. Reaction time: 24 hours. Yield: 60 %. ^{1}H-NMR (400 MHz, D_2O, 50 °C) δ (ppm): 1.92 (m, H10, 3H), 3.25 (m), 3.44 (m), 3.59-4.34 (H2, H2',H3, H3', H4, H4', H5, H5', sugar), 4.63-4.83 (H1', sugar), 5.05 (H1', G unit), 5.72 (m, H9b, 1H), 6.12 (m, H9a, 1H). ^{13}C-NMR (100 MHz, D_2O, 10 °C) δ (ppm): 20.16 (C10), 41.3 and 44.91 (C1, C12), 67.11 (C11), 71.06-79.57 (C2, C2', C3, C3', C4, C4', C5, C5'), 101.09-103.73 (C1'), 123.52 (C9), 141.65 (C8), 163.46 (C13), 172.41 (C7), 178.16-181.67 (C6, C6').

*7.3.3.6 Synthesis of **M6** from $GulA_{20}$-NH_2 and methacryloyl chloride*

(Run 10, Table 7.1) $GulA_{20}$-NH_2 (32 %, 1.50 g, 1.32×10^{-4} mol) was dissolved in a 21 mL Na_2CO_3 / $NaHCO_3$ buffer solution (0.5 mol L^{-1}, pH 9.5) and H_2O (14 mL) respectively. After dissolving the sugar, MeOH (2 mL) was added, the mixture was cooled on ice for 10 minutes, and methacryloyl chloride (219 µL, 22.7×10^{-4} mol) was introduced under stirring. The reaction mixture, whose pH was adjusted to 9.5 from time to time by the addition of Na_2CO_3, was left on ice for half an hour. Throughout the evolution of the reaction a precipitate appeared that did not get soluble even after the addition of 10 mL of H_2O. After 6.5 hours, the reaction was stopped, the precipitate was dissolved in 50 mL water; another 25 µL methacryloyl chloride were added, and the reaction was left reacting for one more hour at RT. The final reaction mixture was diafiltered using a 500 Da cut off membrane followed by freeze drying. Reaction time: 7.5 hours. Yield: 100 %. ^{1}H-NMR (400 MHz, D_2O, 55 °C) δ

(ppm): 1.94 (m, H10, 3H), 3.39 (dd, H1, 1H, J_{11} 13.7 Hz, J_{12} 6.2 Hz), 3.89 (H2', sugar), 4.00 (H4', sugar), 4.11 (H5', sugar), 5.04 (H1', sugar), 5.44 (m, H9b, 1H), 5.70 (m, H9a, 1H).

7.3.4 Synthesis of AlgiMERs from the glycosylamine strategy

*7.3.4.1 Synthesis of **M7** from $ManA_9$-NH_2 and acryloyl chloride*

(Run 11, Table 7.1) $ManA_9$-NH_2 (≅ 80 %, 0.090 g, 3.57×10^{-5} mol) was dissolved in 1.29 mL Na_2CO_3 / $NaHCO_3$ buffer solution (0.33 mol L^{-1}, pH 9.5) and MeOH (143 µL, 10 % v/v) respectively. The mixture was cooled on ice for 5 minutes, and acryloyl chloride (28.6×10^{-5} mol, 0.026 g, 23.2 µL) was added under stirring. The reaction mixture, whose pH was adjusted to 9.5 from time to time with Na_2CO_3, was left in cold (0 – 5 °C) till the end of the reaction. The product was purified by diafiltration using a 500 Da cut off membrane followed by freeze drying. Reaction time: 7.5 hours. Yield: 70 %. ^{1}H-NMR (400 MHz, D_2O, 55 °C) δ (ppm): 3.05 (t, *J* 6.6 Hz, unknown), 3.39 (t, *J* 6.6 Hz, unknown), 3.59-4.34 (H2, H2', H3, H3', H4, H4', H5, H5', sugar), 4.64-4.80 (H1', sugar), 4.85 (H1β, 1H), 5.03 (H1', G unit), 5.31 (s, unknown), 5.84 (dd, H9b, 1H, J_{ab} 2.1 Hz, J_{bc} 9.3 Hz), 6.31 (m, H9a, H8c, 2H).

*7.3.4.2 Synthesis of **M8** from $GulA_{10}$-NH_2 and acryloyl chloride*

(Run 12, Table 7.1) Same procedure proceeded with run 11 (Table 7.1) using 0.089 g $GulA_{10}$-NH_2 (82 %, 3.83×10^{-5} mol). Reaction time: 7.5 hours. Yield: 41 %. ^{1}H-NMR (400 MHz, D_2O, 55 °C) δ (ppm): 3.05 (t, *J* 6.6 Hz, unknown), 3.38 (t, *J* 6.6 Hz, unknown), 3.60 (dd, H2, 1H, J_{12} 8.2, J_{23} 3.2 Hz), 3.89 (H2', sugar), 4.00 (H4', sugar), 4.11 (H5', sugar), 4.44 (H3', sugar), 5.04 (H1', sugar), 5.85 (dd, H9b, 1H, J_{ab} 4.0 Hz, J_{bc} 7.5 Hz), 6.30 (m, H9a, H8c, 2H).

7.3.5 Syntheses of β-D-glucopyranuronosylamine derivatives

7.3.5.1 Synthesis of N-acyl-β-D-glucopyranuronosylamines (13-15) and of N-{[2-((2-methylprop-2-enoyl)oxy)ethyl]carbamoyl}-β-D-glucopyranuronosylamine (16)

In a typical experiment, β-D-glucopyranuronosylamine (100 mg of gross product) was dissolved in (a) Na_2CO_3 1 M / DMSO 8:2 (3.9 mL) or (b) Na_2CO_3 1 M / CH_3OH 1:1 (4.4 mL) at 0 ºC under stirring. A calculated volume of acylating agent was added dropwise either as neat liquid (a) or as 1.5 M solution in THF (b). The resulting mixture was then left stirring on ice for 60 min (a) or 30 min (b), and at ambient temperature for another 24 h (a). Methanol

was eliminated by rotary evaporation (b) and any unreacted acylating agent was removed by solvent extraction (EtAcO, 2 × 5 mL). Following further rotary evaporation at ambient temperature, the remaining solution was diluted with 2 volumes of water and freeze-dried overnight (experiments WM_03, WM_06, AP10-11, AP10-16 and AP10-17). Yields were calculated from the ^{1}H NMR spectrum of the gross products by integrating to one the anomeric protons signals.

7.3.5.2 Synthesis of N-(prop-2-enoyl)-β-D-glucopyranosylamine (17)

D-Glucose (2.00 g, 11.1 mmol) and ammonium bicarbonate (2.60 g, 32.8 mmol) were weighed in a 250 mL round bottom flask and dissolved in 55 mL of 5 M ammonia (experiment WM_04, protocol **A**.5.06). A magnetic bar was added, the flask was sealed with a rubber septum, a disposable needle (21 G) was passed through the septum to prevent pressure build-up, and the mixture was stirred at 35 ºC and 300 rpm. After 30 h the flask was fitted to a rotary evaporator and the reaction mixture concentrated to ~ ½ of the initial volume (p = 35 mbar, T_{bath} = 25 ºC). More water was added (~ 30 mL), and the process was repeated once. The resulting solution was freeze-dried overnight. A white fluffy solid (2.15 g) containing β-D-glucopyranosylamime was obtained that was mixed with $Na_2CO_3 \cdot H_2O$ (6.13 g, 49.5 mmol) and redissolved in 108 mL of CH_3OH/H_2O 1:1 under stirring (WM_06). The resulting solution was cooled in an ice bath and acryloyl chloride (4.10 g, 45.2 mmol, diluted in 31 mL of anhydrous THF) was added over a period of 5 min under vigorous stirring. After 30 min the reaction flask was fitted to a rotary evaporator and the volatiles eliminated at ambient temperature. The reaction mixture was then diluted with water (60 mL) and iPrOH (50 mL) and 63 g of chromatographic SiO_2 were added. In order to adsorb the gross product on silica, the flask was re-fitted to the rotary evaporator and water was eliminated as a binary azeotrope with iPrOH (T_b = 80 ºC, 88% w/w alcohol) before evaporating the resulting slurry to dryness (p = 45 mbar, T_{bath} = 40 ºC). The dry silica was then charged on the top of a pre-packed column and eluted with ACN/H_2O 9:1. Fractions containing the product (R_f 0.34 ACN/H_2O 8:2) were pooled, stabilized with a few grains of BHT, concentrated at the rotary evaporator, and freeze-dried overnight. Isolated yield: 1.45 g (52%) of white fluffy powder. The sample was stored in a freezer (-18 °C) until needed. See Table 7.2 for spectroscopic characterization.

7.4 Results and discussion

Table 7.1 *Summary of reactions involved in the synthesis of AlgiMERs.*

Run no.	Monomer (protocol)	Strategy [a]	Substrate (mmol L^{-1})	Reagents		pH	Reaction time (h)	Yield (%) NMR	Experiment code
				(mmol L^{-1})	(mmol L^{-1})				
1	M1	Reductive amination	$ManA_9$-NH_2 (10.5)	**methacryloyl chloride** (150)	buffer [c] (600)	9.5	6.5	100	AG11-05-P1
2	M2	Reductive amination	$ManA_9$-NH_2 (10.5)	**acryloyl chloride** (150)	buffer [c] (600)	9.5	6.5	100	AG11-05-P2
3	M3 (A)	Reductive amination	$ManA_{17}$-NH_2 (2.16)	**methacrylic anhydride** (222)	buffer [c] (200)	10	22	100 [d]	AG10-26
4	M3 (B)	Reductive amination	$ManA_{17}$-NH_2 (7.85)	**methacryloyl chloride** (118)	buffer [c] (500)	9.5	7.5	100	AG11-11-P1
5	M4 (A)	Reductive amination	$ManA_5$-NH_2 (15.7)	**methacryloyl chloride** (276)	Na_2CO_3 (305)	≅ 11	5.5	100	AG10-36-P2
6	M4 (B)	Reductive amination	$ManA_5$-NH_2 (15.7)	**methacrylic anhydride** (276)	Na_2CO_3 (305)	≅ 11	24.5	100 [d]	AG10-36-P3
7	M4 (C)	Reductive amination	$ManA_5$-NH_2 (17)	**methacryloyl chloride** (299)	buffer [c] (360)	9.5	6	89	AG10-39-P2
8	M5 (A)	Reductive amination	$ManA_5$-NH_2 (17)	**2-isocyanatoethyl methacrylate** (150)	Na_2CO_3 (bit)	≅ 11	6.5	87	AG10-36-P1
9	M5 (B)	Reductive amination	$ManA_5$-NH_2 (15.1)	**2-isocyanatoethyl methacrylate** (133)	buffer [c] (360)	9.5	24	60	AG10-39-P1
10	M6	Reductive amination	$GulA_{20}$-NH_2 (2.8)	**methacryloyl chloride** (48)	buffer [c] (220)	9.5	7.5	100	AG11-11-P2
11	M7	Glycosylamine	$ManA_9$-NH_2 (24.9)	**acryloyl chloride** (199)	buffer [c] (330)	9.5	7.5	70	AG11-22-P1
12	M8	Glycosylamine	$GulA_{10}$-NH_2 (24.1)	**acryloyl chloride** (200)	buffer [c] (330)	9.5	7.5	41	AG11-23-P1

General conditions: 0 → RT, ≤ 10 %v/v of MeOH or DMSO. a: run 1 to 10 amines are obtained from reductive amination and runs 11 and 12 amine are obtained by the glycosylamine strategy, b: measured using a pH paper, c: $NaHCO_3$ / Na_2CO_3 buffer, d: conversion.

7.4.1 AlgiMERs from the reductive amination strategy

The functionalization reactions of oligoalginate derived amines (glycosylamine and amino alditols) were conducted in basic solutions in cold to avoid degradation of the oligosaccharides and hydrolysis reactions. [9] The effects of pH and the electrophilic moiety were investigated. In a typical experiment (Run 1, Table 7.1), $ManA_9$-NH_2 was solubilized in a Na_2CO_3/$NaHCO_3$ buffer solution (pH 9.5) followed by the addition of ~ 10 % v/v of an organic co-solvent (MeOH) to better solubilize the acylating agent. The solution was cooled on ice and methacryloyl chloride was added drop wise. Although an excess of buffer (4 eq) was used with respect to methacryloyl chloride, the pH of the reaction was adjusted from time to time back to 9.5 with Na_2CO_3. At the end of the reaction the product was first precipitated in EtOH (80 % v/v), then purified by diafiltration using a 500 Da cut off membrane, and freeze dried overnight. The yield was calculated from ^{1}H NMR by normalizing the ^{1}H NMR spectrum of the final product and that of the starting oligoglycuronan to one peak (*e.g.* internal anomeric H1' of the glycomonomer). Table 7.1 summarizes the exact experimental conditions used in the syntheses of AlgiMERs.

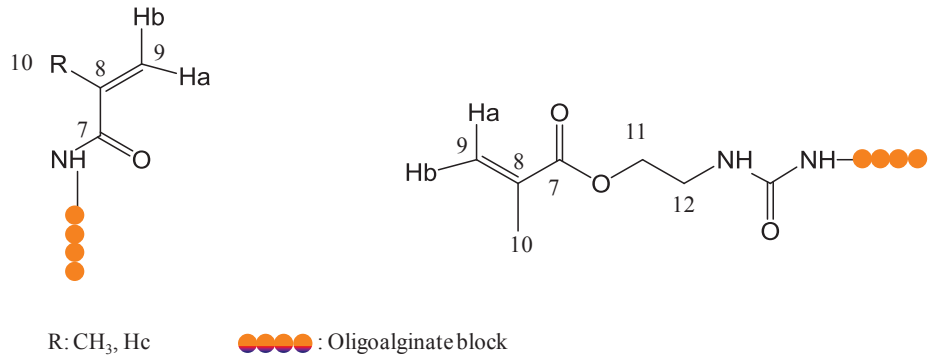

Figure 7.3 *General structures of synthesized AlgiMERs.*

(Meth)acrylamide derivatives

Figure 7.4 shows the ^{1}H NMR spectrum of **M1** (a methacrylamide derivative) after diafiltration where sodium methacrylate was totally eliminated and this was confirmed by the absence of the diagnostic peaks of this product at δ (ppm): 5.4 and 5.7 ppm (CH_2=). The latter product resulted from the hydrolysis of methacryloyl chloride in water. The peaks at δ (ppm) 1.94 (H10, CH_3), 5.44 (H9b, CH=) and 5.70 ppm (H9a, CH=) confirm the success of the reaction. Moreover, the characteristic CH_2-NH_2 signals of the starting amino alditol at 3.0 and 3.4 ppm shifted after functionalization to 3.4 and 3.6 ppm respectively. The latter chemical shift at 3.6 ppm was assigned from HMQC analysis.

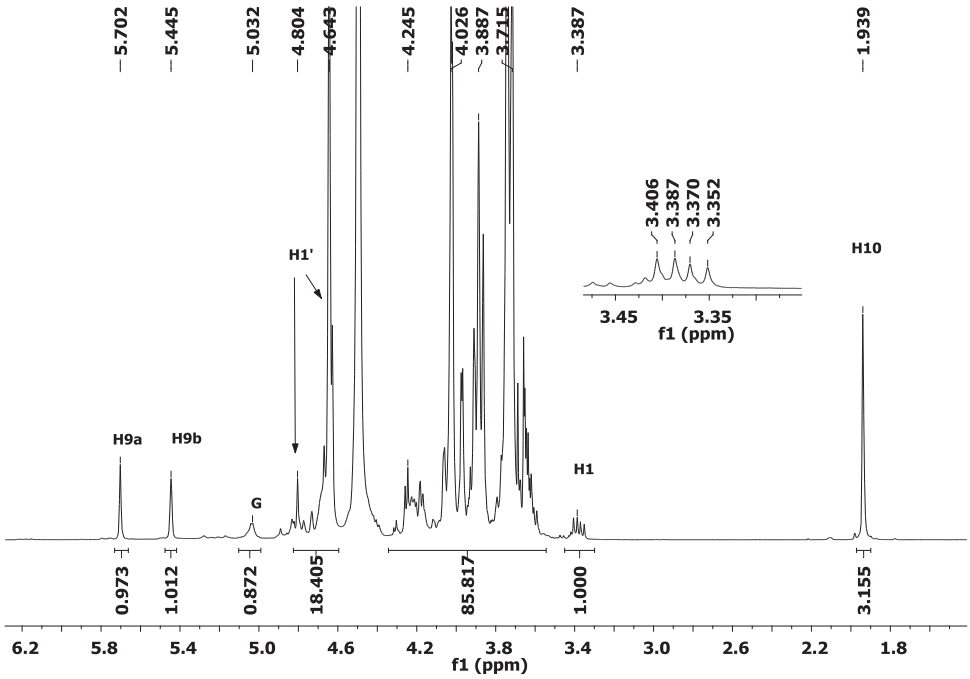

Figure 7.4 *^{1}H NMR spectrum of **M1** after purification (Run 1, Table 7.1). Conditions: 6.5 % w/w, D_2O, 323 K, ns 100, D1 10s.*

Similarly, the acrylamide derivative **M2** (Run 2, Table 7.1) was obtained after purification with no residual sodium methacrylate. As before, the novel CH-NH-R signal was more deshielded and appeared at 3.4 ppm (Figure 7.5). The chemical shifts of the three vinylic protons were detected at δ (ppm): 5.76 (d, 1H, $J_{9b, 8c}$ 10.4 Hz), 6.18 (d, 1H, $J_{9a, 8c}$ 17.1 Hz) and 6.32 ppm (dd, 1H, $J_{9a, 8c}$ 17,1 Hz, $J_{9b, 8c}$ 10.3 Hz).

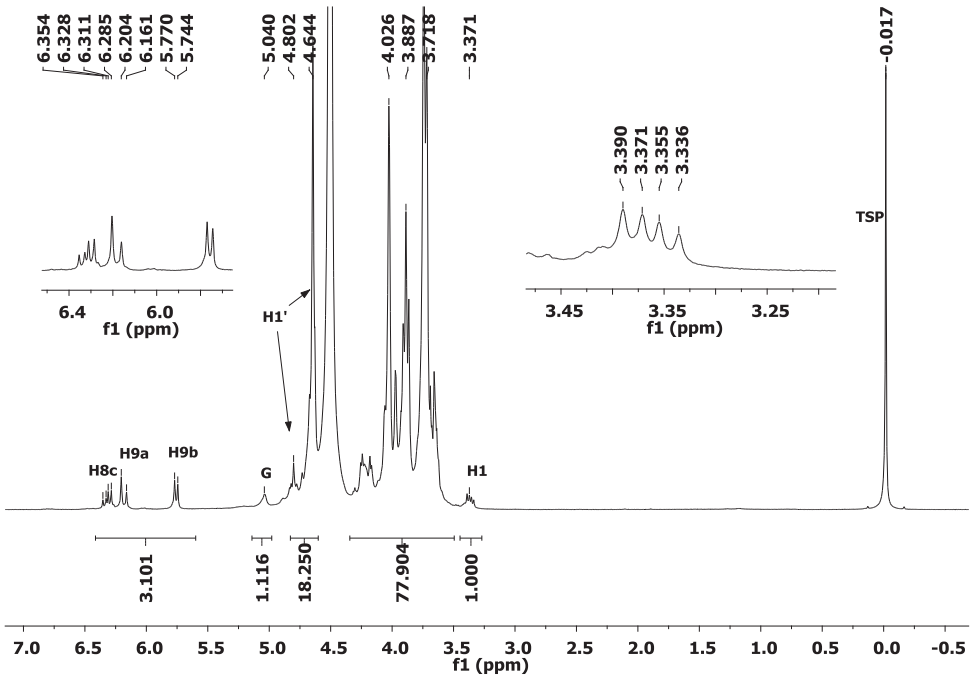

Figure 7.5 *^{1}H NMR spectrum of **M2** after purification (Run 2, Table 7.1). Conditions: 5.8 % w/w, D_2O, 323 K, ns 100, D1 10s.*

A series of different reactions were examined in order to obtain the desired products without any side reactions taking place. First, the use of methacrylic anhydride as an acylating agent was investigated. At pH ≥ 10, the anhydride not only reacted with the amine group but also with the hydroxyl groups of the oligoglycuronan and that resulted in partial esterification of the hydroxyl groups (runs 3 and 6, Table 7.1). The latter result was confirmed by NMR where peaks at 1.87 (CH_3) and 1.89 ppm (CH_3) together with other peaks in the vinylic region at 5.74 (CH=) and 6.19 ppm (CH=) were detected. These peaks are the characteristic peaks of a methacrylate derivative. It is worth noting that no change in the molecular weight of the oligoglycuronan was detected from SEC. At pH ≅ 11 (run 6, Table 7.1), the functionalization step resulted in a precipitate during the evolution of the reaction and that could be attributed to the increased hydrophobicity of the chain due to partial esterification. One reason for this partial esterification is that the anhydride hydrolyzes slowly in water and that provides more chances for the hydroxyl groups to react with it. In all cases the amino alditol was totally consumed.

On the other hand, the use of acyl halides which hydrolyze faster in aqueous solution was examined (runs1, 2, 4, 5, 7 and 10, Table 7.1). To this end the amino alditol in question was reacted with (meth)acryloyl chloride at two different pHs (9.5 and ≅ 11). At the end of the reaction shorter oligoglycuronans (DP_n 5) were only purified by precipitation followed by

freeze drying (except for run 5) since a big part of the sugar was lost during the diafiltration step with a 500 Da cut off membrane (run 5, Table 7.1). Unfortunately, the precipitation step did not eliminate totally the base and the formed sodium methacrylate from our product as confirmed by the basic nature (pH ≅ 10-11) of the freeze dried solution after precipitation and from NMR (*vide infra*) respectively. However, the pH of the solution played a role on the stability of the sugar at low *DP*s where diafiltration could not be adopted as a purification method. For instance, the reaction of $ManA_5$-NH_2 with methacryloyl chloride in Na_2CO_3 (pH ≅ 11) resulted in a colored product after freeze drying (run 5, Table 7.1). The color of the solution persisted even after diafiltration, suggesting that the color is not due to small molecules. The coloration could be due to slight degradation of the sugar, although not detected by ^{1}H-NMR, under basic conditions upon freeze drying. It is worth noting that conducting the same experiment at pH 9.5 did not cause coloration of the product (result not shown, AG11-02). In all cases the pH of the reaction was adjusted with time back to the desired value although excess base was used with respect to the acyl chloride. As a matter of fact, the best protocol examined at pH 9.5 was established by the use of 4 fold excess of buffer with respect to the acyl chloride where no dramatic drop in pH was detected (run 1 and 2, Table 7.1).

As a result, the use of acyl halides minimized a lot, and totally eliminated at low *DP*s, the partial functionalization of the hydroxyl groups. Figure 7.6 shows two ^{1}H-NMR spectra of two AlgiMERs obtained from the reaction of $ManA_5$-NH_2 with methacryloyl chloride and methacrylic anhydride under the same conditions at pH ≅ 11 (run 5 and 6, Table 7.1). The two spectra were superimposed after normalization to a peak, where the red spectrum represents the reaction with methacryloyl chloride and the one in turquoise represents the reaction with methacrylic anhydride. Briefly, by examining the vinylic peaks at 5.76 and 6.15 ppm one notices that once using methacrylic anhydride the hydroxyl groups were more susceptible to esterification. We cannot deny the fact that using methacryloyl chloride also resulted in partial esterification at this pH (≅ 11) that is why the reactions at lower pH (9.5) were explored.

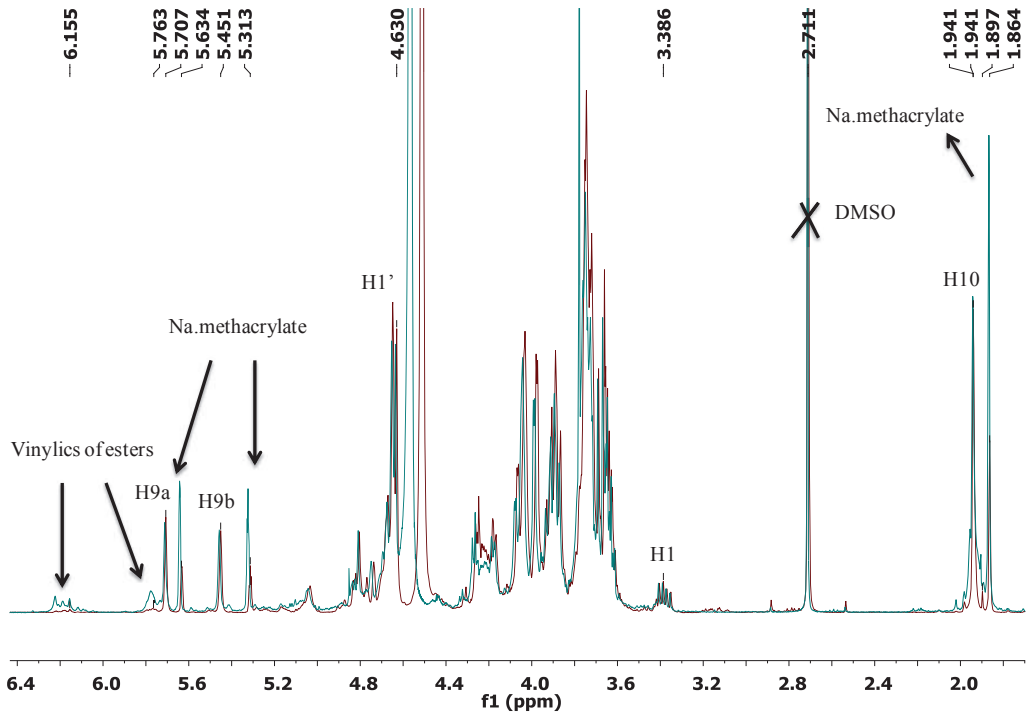

Figure 7.6 *Superimposed ^{1}H-NMR spectra of two AlgiMERs (**M4** (A) and **M4** (B)). **M4** (A) spectrum in red obtained from methacryloyl chloride and **M4** (B) in turquoise obtained from methacrylic anhydride. Conditions: $ManA_5$-NH_2 (15.7 mmol L^{-1}), electrophile (276 mmol L^{-1}), Na_2CO_3 (305 mmol L^{-1}, pH ≅ 11), 0 °C → RT.*

Methacrylate derivatives

Taking advantage of the presence of the isocyanate group in **IEM**, methacrylate derivatives of oligoalginates could be synthesized by the addition of the amino alditol to the isocyanate group (Scheme 7.6). The latter group has a low affinity to the hydroxyl groups. [2b]

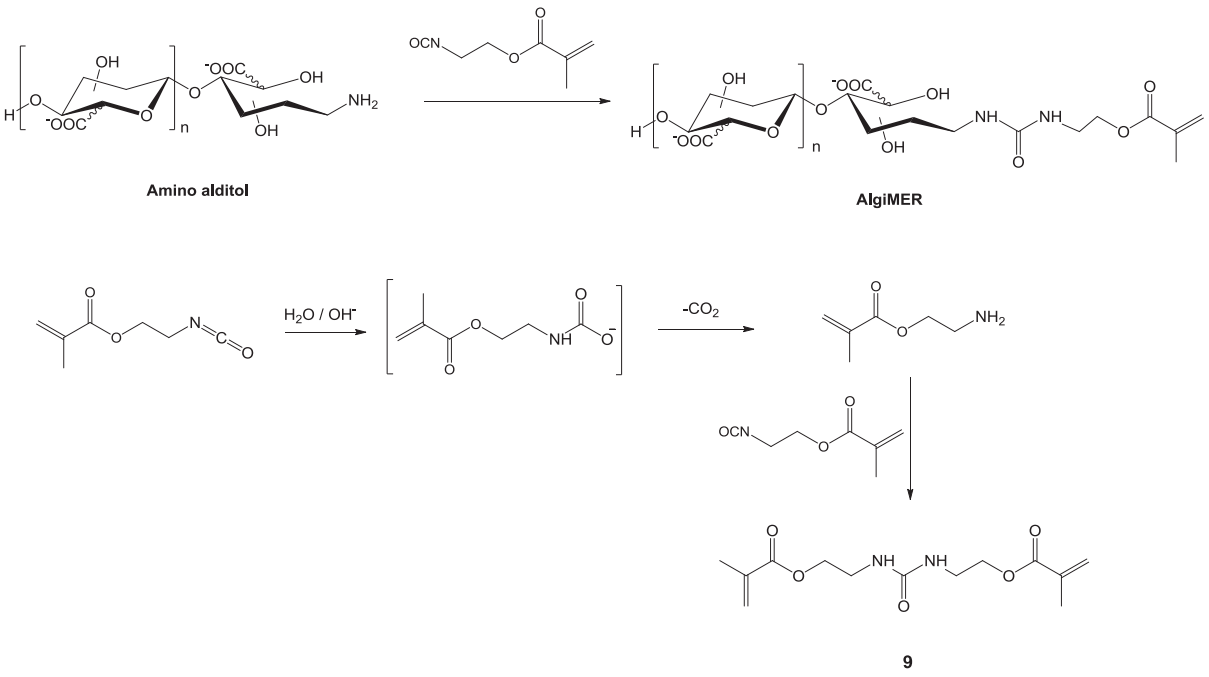

Scheme 7.6 *General synthesis of methacrylate derived alginates from an alginate amino alditol and **IEM**. The formation of the urea **9** as a by-product is shown as well.*

In our case, the synthesis of methacrylate derived glycomonomers was conducted at two different pHs (runs 8 and 9, Table 7.1). Running the reaction at pH 11 afforded comparable yields (87 %) as those obtained by Klein. [2,5] However, the dedicated oligoglycuronan for the study had a $DP_n = 5$ and it was purified only, as before, by precipitation. The latter resulted in coloration of the product (yellowish-brown) after freeze drying due to the presence of residual base from the precipitation step. On the other hand, conducting the reaction at lower pH (9.5) prevented the coloration of the product after precipitation and freeze drying, and that confirms as before the delicacy of the oligoalginate block to high pH (> 10). [3,9] Nonetheless, at this pH (9.5) a lower yield (60 %) was attained.

Unfortunately, the synthesized methacrylate glycomonomers showed instability in basic solutions (pH ≅ 9-10), where slight degradation of the ester bond was observed from ^{1}H NMR (Figure 7.7) upon storing a basic solution of the glycomonomer for 2 weeks at 5 °C. In all cases, product **9** (urea) resulting from the reaction of water with the isocyanate group was detected. [10] The latter formed urea was eliminated effectively by a simple extraction with EtOAc and its structure was confirmed by NMR and MS analyses (see Appendix 7.A for ^{13}C-NMR).

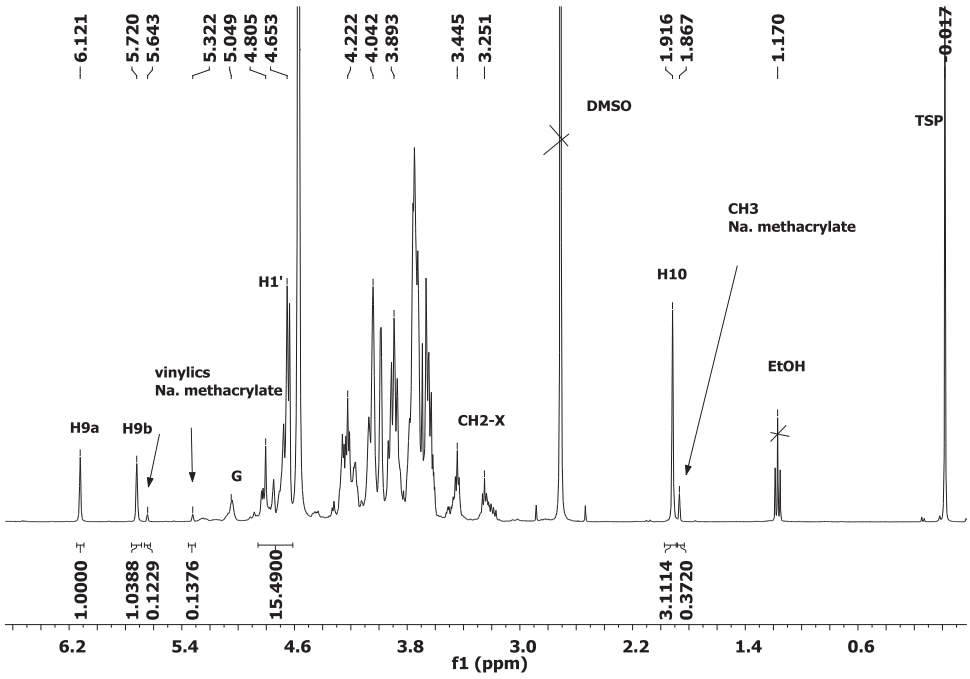

Figure 7.7 *^{1}H NMR spectrum of **M5 (A)** after precipitation (run 8, Table 7.1). Conditions: 20 % w/w, D_2O, 323 K, ns 64, D1 2s.*

From ^{1}H-NMR the formation of the product was accompanied by the disappearance of the $C\underline{H_2}$-NH_2 signals of the amino alditol (at 3.0 and 3.4 ppm) and by the appearance of peaks at 1.91 (CH_3), 3.25 and 3.44 ppm (new CH_2 signals). Besides, the chemical shifts of vinylic protons appeared at 5.7 and 6.1 ppm.

7.4.2 Synthetic potential of β-D-glucopyranuronosylamine

The possibility to transform D-glucuronic acid into β-D-glucosiduronic acid derivatives without resorting to protective group chemistry was as well investigated in aqueous solution. Like that AlgiMERs could be synthesized in a similar pathway. To probe the synthetic potential of our approach, four test reactions were carried out in which the title compound was reacted with various acylating agents and with an isocyanate (Scheme 7.7). In particular, a mixture of **11** + **12** was prepared according to protocol **B**.0.50 (5 M $NH_2CO_2NH_4$, see chapter 5) and purified by two freeze-drying cycles. This procedure slightly reduces the global yield (82% vs. 88% for a single cycle) but effectively removes all ammonium salt. The gross product was then reacted with chloroacetic anhydride, methacrylic anhydride, acryloyl chloride, and 2-isocyanoethyl methacrylate in cold aqueous/organic solutions. This way, *N*-acyl-β-D-glucopyranuronosylamines **13-15** and *N*-alkylcarbamoyl-β-D-glucopyranuronosylamine **16** where obtained in 68-88% yield. The compounds were not isolated, but their formation was confirmed by MS and NMR analysis of the crude products,

as summarized in Table 7.2. In particular, we found that for compounds **13-15** the chemical shift and coupling constant of C1 (82 ppm) and H1 (5.05 ppm, doublet, 9 Hz) are almost identical to those of *N*-(prop-2-enoyl)-β-D-glucopyranosylamine **17**, a pure sample which was prepared in our laboratory. The same can be said for compound **16**, whose diagnostic peaks match those reported in the literature for several *N*-arylcarbamoyl-β-D-glucopyranosylamines. [11] Finally, it is interesting to note that the yields of **13** and **15** are comparable to those reported by Manger [12] and Kallin [1b] for the analogous derivatives of *N*-acetylglucosamine (95%) and lactose (88%), respectively; whereas the yield of **16** matches those obtained by Somsák et al. [11] for the synthesis of *N*-arylcarbamoyl-β-D-glucopyranosylamines in pyridine (45-76%). Here it should be noted that compound **13** represents a classic starting point for the synthesis of 1-*N*-glycyl-β-glycosyl derivatives, [12-13] while **14-16** can be either functionalized by thiol-ene chemistry [14] or used as glycomonomers for radical polymerization. [2b,15]

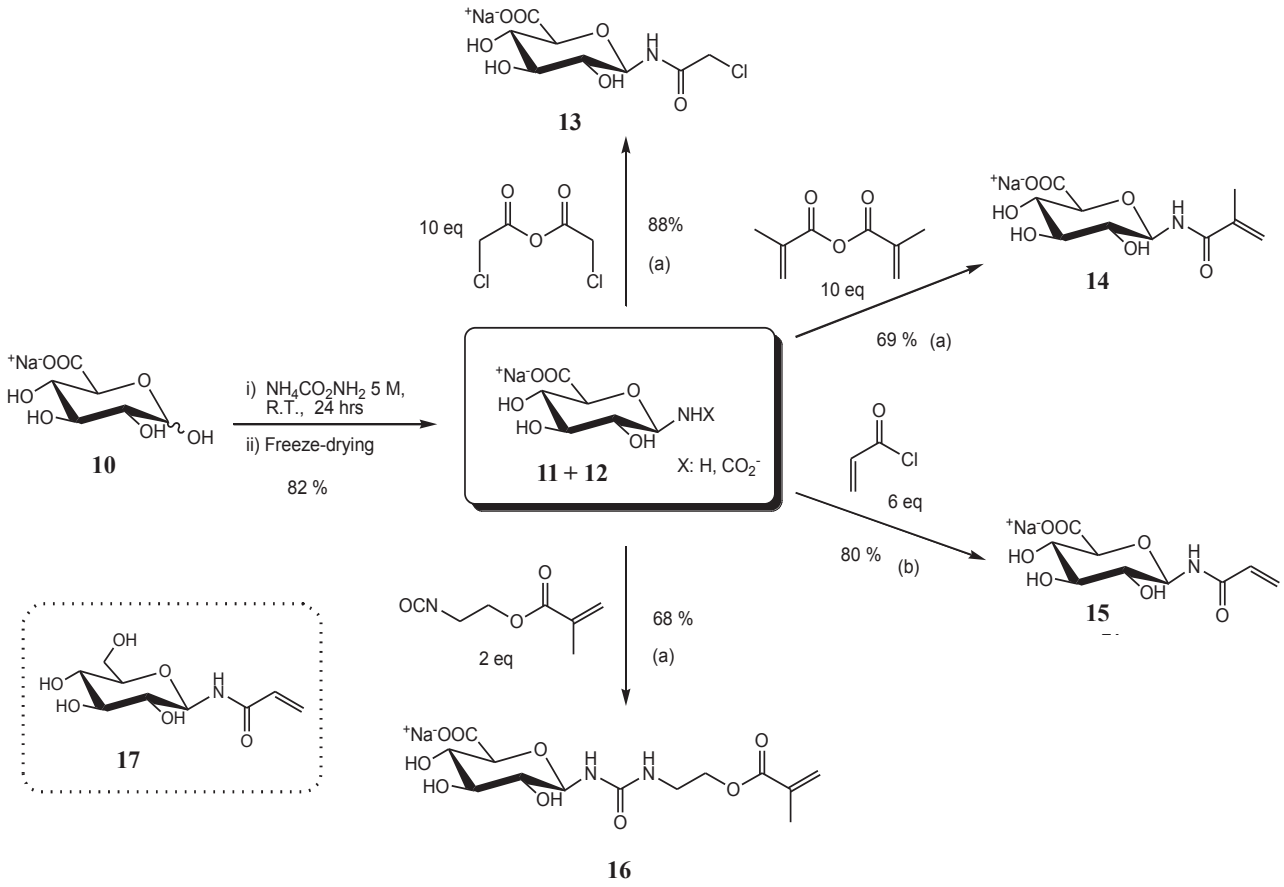

Scheme 7.7 *Synthesis of N-acyl-β-D-glucopyranuronosylamines **13-15** and of N-alkylcarbamoyl-β-D-glucopyranuronosylamine **16**. Conditions: (a) Na_2CO_3, H_2O/DMSO 8:2, 0 ºC → R.T., 25 h. (b) Na_2CO_3, H_2O/CH_3OH 1:1, 0 ºC, 0.5 h.*

Table 7.2 Summary of the characterization of compounds **10_{β}-12** and **13-17**.

Compound [a]	δ ^{1}H / ppm (m, *J*/Hz, assignment)	δ ^{13}C / ppm (assignment)	*m/z* (structure, monoisotopic ion mass, molecular ion)
10_{β}	4.63 (d, 8.0, H1), 3.27 (m, H2), 3.50 (H3), 3.51 (m, H4), 3.72 (H5)	98.57 (C1), 76.70 (C2), 78.25 (C3), 74.53 (C4), 78.93 (C5), 178.64 (C6)	193 (**10_{H}**, 193.0, $[M-H]^-$); 217 (**10_{H}**, 217.0, $[M+Na]^+$); 239 (**10_{Na}**, 239.0, $[M+Na]^+$); 387 (($\mathbf{10}_{H}$)$_2$, 387.1, $[M-H]^-$); 455 (($\mathbf{10}_{Na}$)$_2$, 455.0, $[M+Na]^+$)
11	4.09 (d, 8.8, H1), 3.18 (dd, 9.0, H2), 3.48 (H3), 3.48 (d, 9.5, H4), 3.69 (m, H5)	87.68 (C1), 76.76 (C2), 79.03 (C3),74.71 (C4), 79.92 (C5), 179.14 (C6)	192 (**11_{H}**, 192.1, $[M-H]^-$); 194 (**11_{H}**, 194.1, $[M+H]^+$); 216 (**11_{Na}**, 216.0, $[M+H]^+$); 238 (**11_{Na}**, 238.0, $[M+Na]^+$); 385 (($\mathbf{11}_{H}$)$_2$, 385.1, $[M-H]^-$)
12	4.70 (d, 9.1, H1), 3.34 (t, 9.0, H2), 3.52 (H3), 3.48 (H4), 3.73 (d, 9.4, H5), 6.25 (d, 9.8, $NHCO_2$)	85.68 (C1), 74.64 (C2), 79.02 (C3), 74.55 (C4), 79.87 (C5), 178.88 (C6), 165.86 ($NHCO_2$)	238 (**$12_{H,H}$**, 238.0, $[M+H]^+$); 260 (**$12_{H,H}$**, 260.0, $[M+Na]^+$)
13	5.03 (d, 9.1, H1), 4.20 (s, CH_2Cl)	82.16 (C1), 78.84, 78.60, 73.90, 73.73, 44.96 (CH_2Cl), 173.10 (amide)	268, 270 (**13_{H}**, 268.0, 270.0, $[M-H]^-$); (**13_{Na}**, 290.0, 292.0, $[M-H]^-$); (**13_{H}**, 292.0, 294.0, $[M+Na]^+$); 314, 316 (**13_{Na}**, 314.0, 316.0, $[M+Na]^+$)
14	5.06 (d, 8.6, H1), 3.80 (d, 9.5, H5)	82.12 (C1), 80.97, 78.95, 74.44, 175.54 (amide)	260 (**14_{H}**, 260.1, $[M-H]^-$); 262 (**14_{H}**, 262.1, $[M+H]^+$); 306 (**14_{Na}**, 306.1, $[M+Na]^+$)
15	5.04 (d, 9.0, H1), 3.81 (d, 9.6, H5)	81.95 (C1), 80.65, 78.89, 74.37, 132.08 (CH_2=CH), 172.04 (amide)	246 (**15_{H}**, 246.1, $[M-H]^-$); 268 (**15_{Na}**, 268.0, $[M-H]^-$); 292 (**15_{Na}**, 292.0, $[M+Na]^+$)
16	4.82 (d, 9.1, H1), 3.74 (d, 9.5, H5)	83.69 (C1), 80.62, 138.49 (CH_2=<u>C</u>), 129.67 (<u>CH_2</u>=C), 162.33 (urea)	347 (**16_{H}**, 347.1, $[M-H]^-$); 393 (**16_{Na}**, 393.1, $[M+Na]^+$); 717 (($\mathbf{16}_{H}$)**16_{Na}**, 717.2, $[M-H]^-$)
17 [b]	5.05 (d, 9.2, H1); 3.87 (dd, 12.4, 2.1, H6); 3.72 (dd, 12.4, 5.4, H6); 3.54 (m, H3 and H5); 3.44 (m, H2 and H4); 6.32 (m, <u>CH_2</u>=CH); 5.87 (dd, 6.6, 4.9, CH_2=<u>CH</u>)	82.12 (C1), 80.30 (C5), 79.12 (C3), 74.48 (C2), 71.92 (C4), 63.26 (C6), 132.09, 132.11 (CH_2=CH), 172.02 (amide)	232 (**17** 232.1; $[M-H]^-$); 256 (**17** 256.1, $[M+Na]^+$); 489 (($\mathbf{17}$)$_2$, 489.2, $[M+Na]^+$)

[a] Solvents used for NMR analyses: D_2O (**13**, **15**, **17**); D_2O / DMSO-d6 8:2 (**14**) or 5:4 (**16**). [b] Assignments obtained by HMQC.

7.4.3 AlgiMERs from the glycosylamine strategy

As mentioned before, the synthesis of glycosylamides has been already described in literature in aqueous solutions without resorting to protective group chemistry, and good to high yields were obtained depending on the glycosylamine being investigated and the electrophilic moiety (bulkiness). [1b,12,15] Herein, glycosylamines from oligoalginates were reacted with acryloyl chloride (run 11 and 12, Table 7.1). In a typical experiment, $GulA_9$-NH_2 (24 mmol L^{-1}) was reacted, in cold, with acryloyl chloride (200 mmol L^{-1}) in a carbonate buffer at pH 9.5. Methanol (10 % v/v) was added as a co-solvent to enhance the solubility of the acyl chloride and the pH was kept at 9.5 by the addition of Na_2CO_3 with time. The hypothesis that the precipitate is due to partial esterification was excluded from ^{1}H NMR.

Figure 7.8 shows the ^{1}H NMR spectra of the purified (after diafiltration) AlgiMERs **M7** and **M8** obtained from the reactions of $ManA_9$-NH_2 and $GulA_{10}$-NH_2 with acryloyl chloride at pH 9.5, respectively. The appearance of the vinylic protons at 5.85 and 6.30 ppm is a clear evidence of the formation of the products. Although the reaction was conducted in cold, the hydrolysis of the glycosylamines to the starting oligoglycuronans was inevitable. The latter was confirmed by ^{1}H NMR, where signals of the anomeric protons of the starting oligoglycuronans (H1α-OH and H1β-OH) were detected at 4.8 and 5.2 ppm. In the ^{1}H NMR of **M7** it is suspected that the anomeric signal (H1), whose integration is equivalent to that of one vinylic proton, appears at 5.31 ppm. Besides, it appeared as a singlet due to the well known low coupling constants of mannuronic acids. However, this signal is not observed in the spectrum of the oligoguluronan based monomer **M8**.

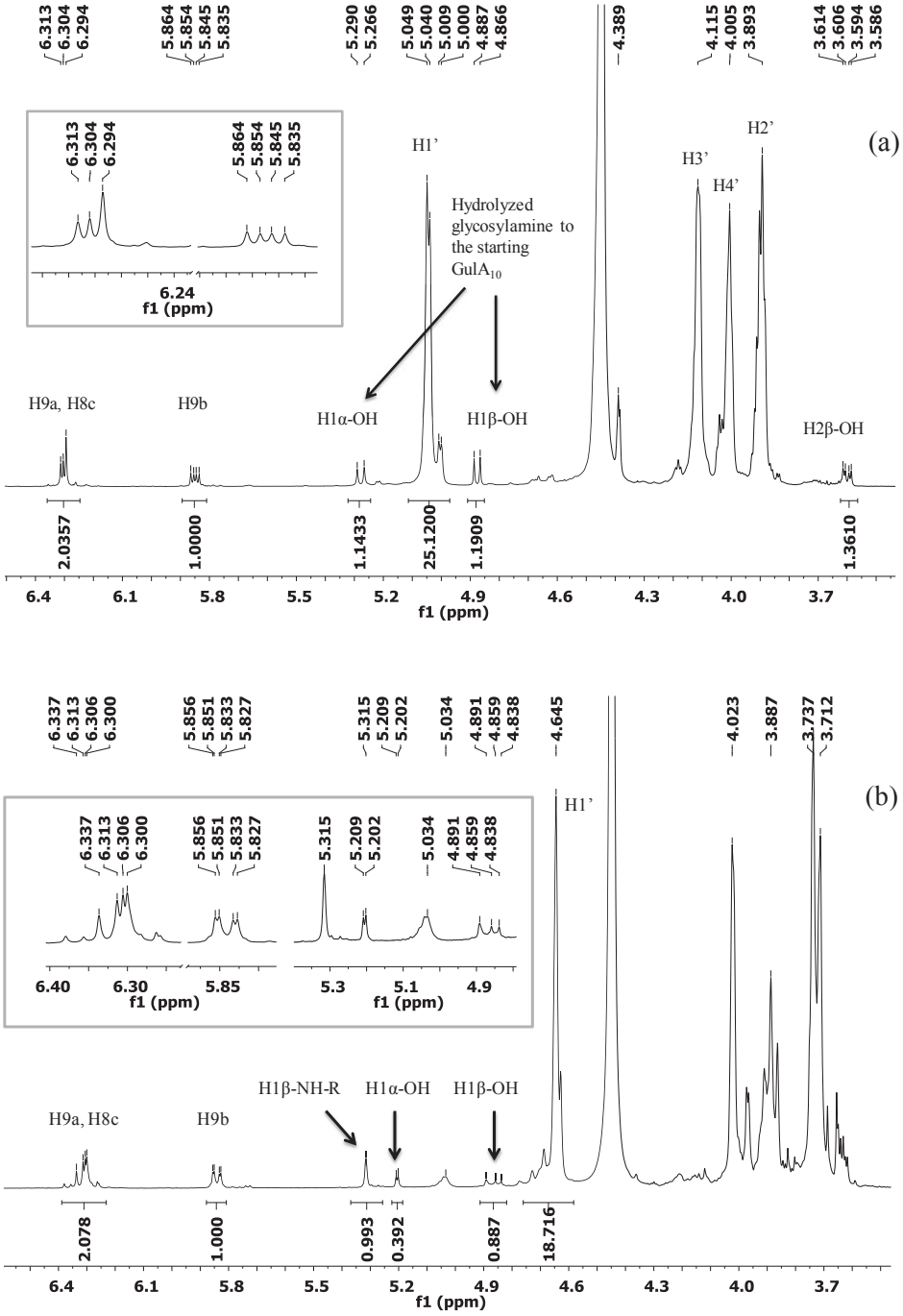

Figure 7.8 *^{1}H NMR spectra of AlgiMERs (a) **M8** obtained from the reaction of $GulA_{10}$-NH_2 (24 mmol L^{-1}) with acryloyl chloride (200 mmol L^{-1}) at pH 9.5 and (b) **M7** obtained from the reaction of $ManA_9$-NH_2 (25 mmol L^{-1}) with acryloyl chloride (199 mmol L^{-1}) at pH 9.5. Conditions: 400 MHz, 5-6 %w/w, D_2O, 328 K, ns 64, D1 10s.*

The reaction with ManA-NH_2 gave higher yield than the reaction with GulA-NH_2 (70 and 41 % respectively), and that could be referred to the higher stiffness of the guluronan block in solution (less flexible due to its conformation). [16] From the simulation study done on $ManA_4$-

NH_2 and $GulA_4$-NH_2 blocks, the beta configuration of the glycosylamines did not show any interaction with the neighboring oxygen atoms (Figure 7.9). By examining both conformations, the NH_2 group of $ManA_4$-NH_2 is freer to react since it is subjected to less hindrance and that could explain some its higher reactivity.

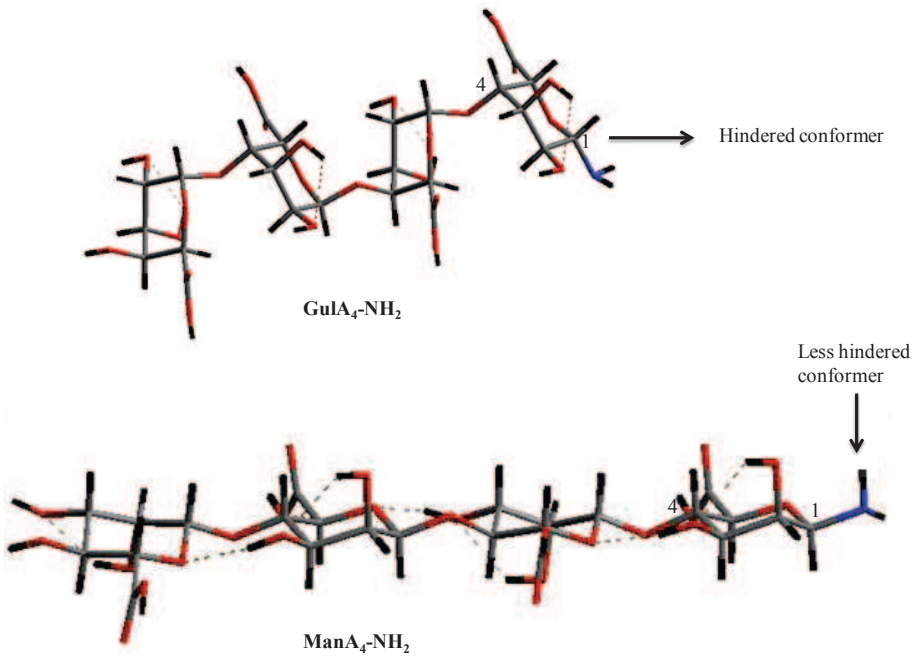

Figure 7.9 *A simulation done on $GulA_4$-NH_2 and $ManA_4$-NH_2 showing the hindrance of the neighboring groups on the reactivity of the NH_2. Grey, red, black and blue represent carbon, oxygen, hydrogen and nitrogen atoms, respectively. Dashed lines represent hydrogen bonding.*

7.4.4 AlgiMERs from glycosylamine *versus* AlgiMERs from reductive amination

Although both strategies (reductive amination and glycosylamine) are promising for the synthesis of AlgiMERs in aqueous solution, yet weak points exist in each method. In the glycosylamine strategy, the amine was obtained with high yield after purification (≅ 80 %) but the functionalization step to synthesize the AlgiMER afforded lower yield due to the sensibility of the glycosylamine to hydrolysis in water; so a total yield (2 steps) of ≅ 56 % was obtained in best cases with oligomannuronans. Similar results were obtained with glycosylamines based on dextran (DP_n 24) and maltodextrin (DP_n 20) as well (results not shown). On the other hand, the reverse was observed with the reductive amination strategy where troubles came out during the synthesis of the amine and the functionalization step was quantitative in almost all the cases. The 2 step yield from this strategy was ≅ 45-50 %

disregarding the one step reaction to synthesize the glycomonomer from reductive amination where 53 % yield was obtained. Moreover, the reductive amination strategy introduces a spacer between the polymerizing functionality which is absent in the case of glycosylamine strategy.

7.5 Take home messages

The synthesis of AlgiMERs in aqueous solution without resorting to protective group chemistry resulted out in the following points:

AlgiMERs from glycosylamines:

i. Acrylamide derived AlgiMERs were synthesized with good yields up to 70 % in a carbonate buffer (pH 9.5).

ii. Oligomannuronans reacted better than oligoguluronans.

iii. In all cases hydrolysis of the glycosylamine to the starting oligoglycuronan was inevitable.

AlgiMERs from amino-alditols:

i. The best protocol avoiding drop in pH during reaction was conducted in the presence of a carbonate buffer (pH 9.5) whose concentration is four folds that of the acylating agent.

ii. Conducting the reaction at pH values above 10 risks degrading and functionalizing the hydroxyl groups of the oligoglycuronan block.

iii. For (meth)acrylamide derived AlgiMERs quantitative yields were obtained in almost all cases.

iv. For methacrylate derived AlgiMERs the best yield obtained without degradation was 60 % at pH 9.5.

Appendix 7.A Selected NMR spectra

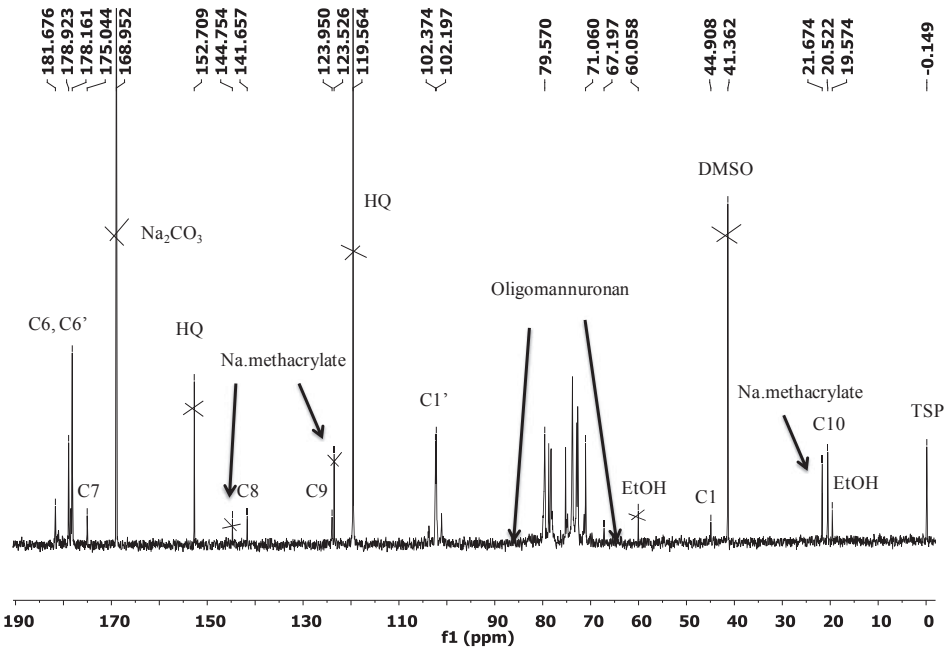

Figure 7.10 *^{13}C-NMR spectrum of **M4 (A)** after precipitation (run 5, Table 7.1). Conditions: 100MHz, 25 % w/w, D_2O, 283 K, ns 5000, D1 5 s. HQ is hydroquinone added to prevent self polymerization.*

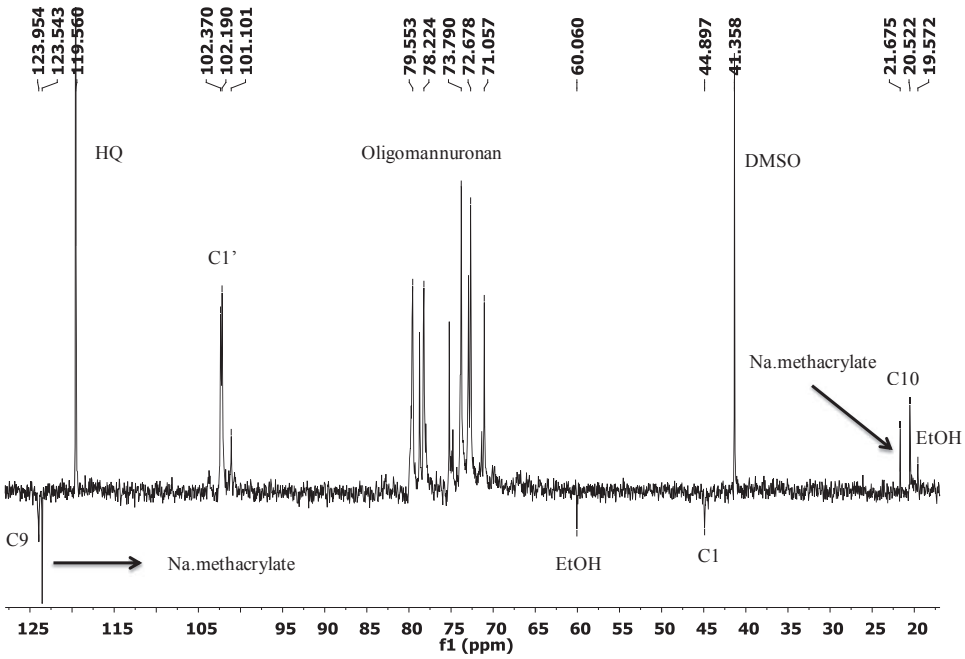

Figure 7.11 *DEPT-135 ^{13}C NMR spectrum of **M4 (A)** after precipitation (run 5, Table 7.1). Conditions: 100 MHz, 25 % w/w, D_2O, 283 K, ns 6000, D1 5 s. HQ is hydroquinone added to prevent self polymerization.*

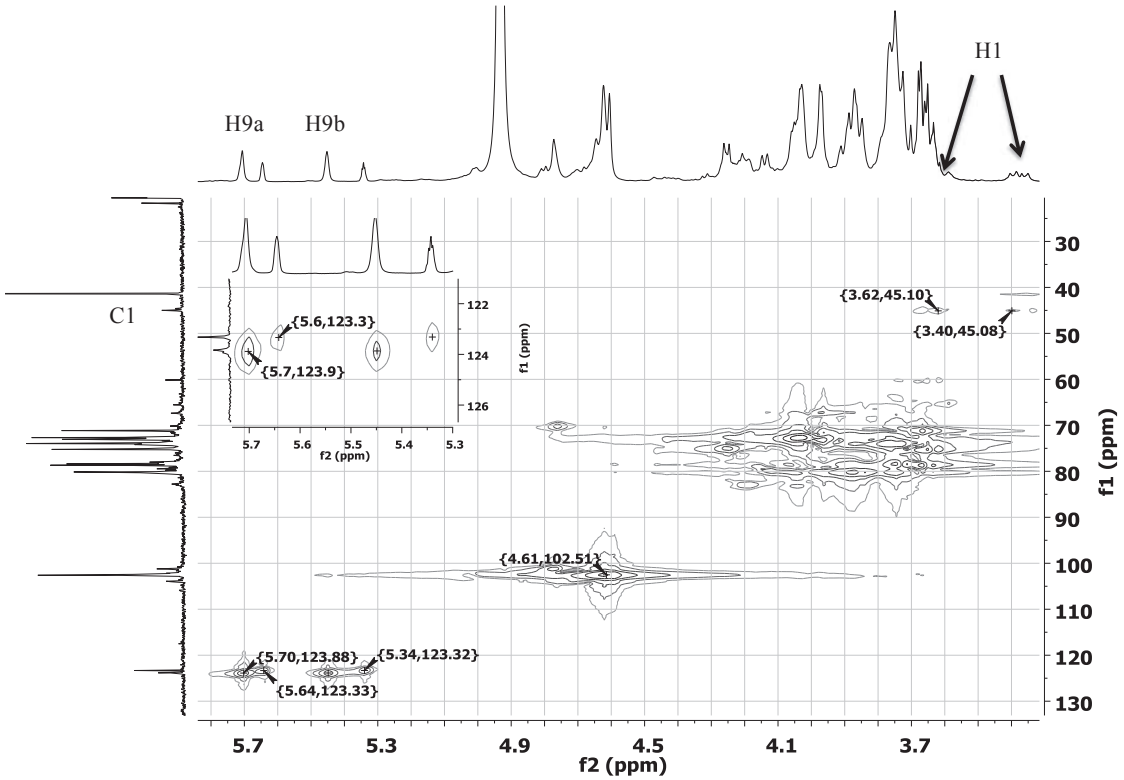

Figure 7.12 *HMQC spectrum of **M4 (C)** after precipitation (run 7, Table 7.1). Conditions: ^{1}H-^{13}C (400.13, 100.16 Hz), 16 % w/w, D_2O, 283 K, ns 300, D1 2 s.*

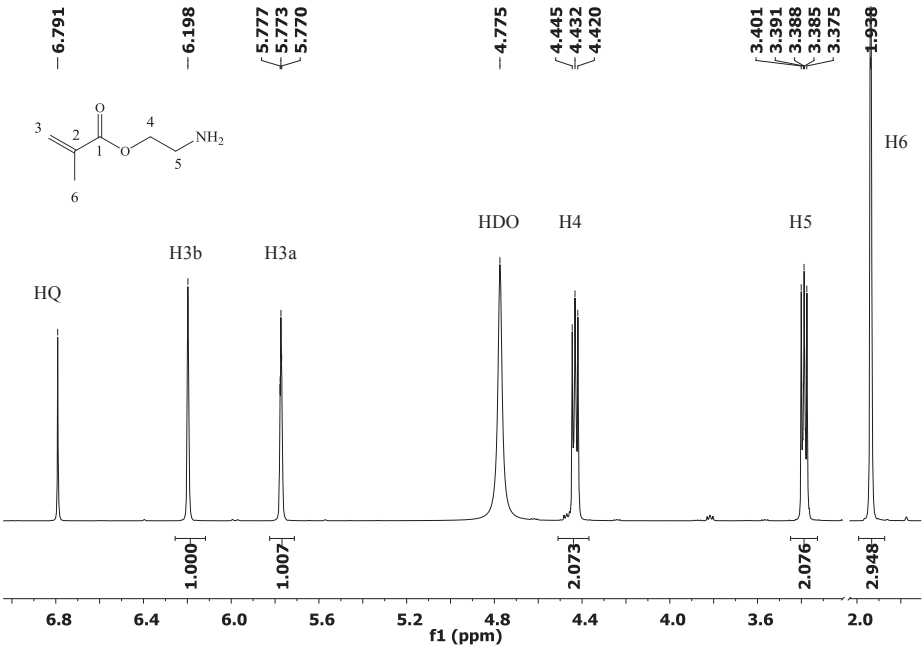

Figure 7.13 *^{1}H NMR of 2-aminoethyl methacrylate (Aldrich). Conditions: 400 MHz, D_2O, 5 %w/w, 298 K, ns 16, D1 2s. HQ is hydroquinone added to prevent self polymerization. One cut in the axis should be noted.*

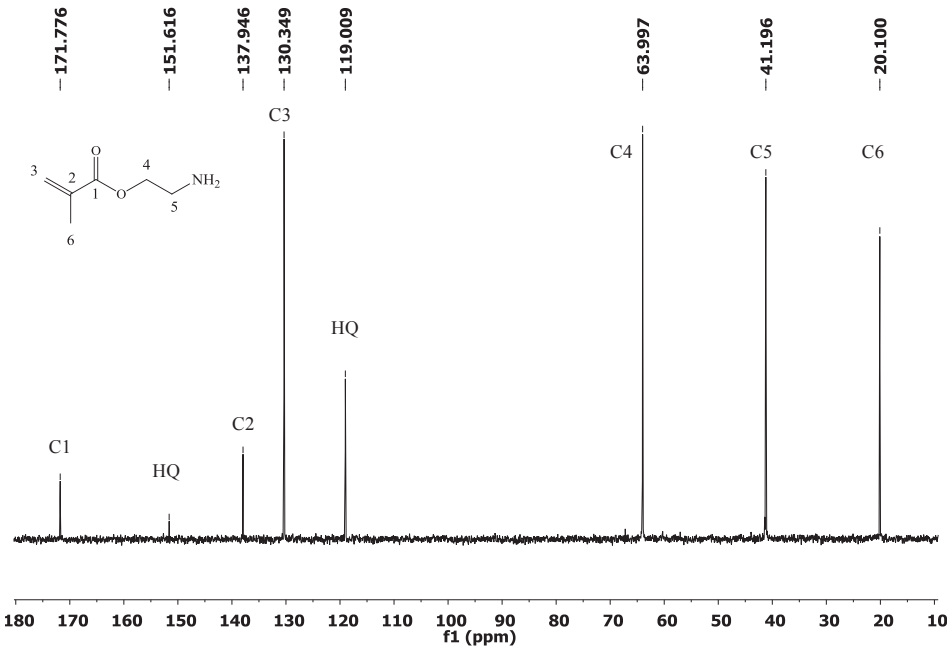

Figure 7.14 *^{13}C NMR of 2-aminoethyl methacrylate (Aldrich). Conditions: 100 MHz, D_2O, 5 %w/w, 283 K, ns 2000, D1 2s. HQ is hydroquinone added to prevent self polymerization.*

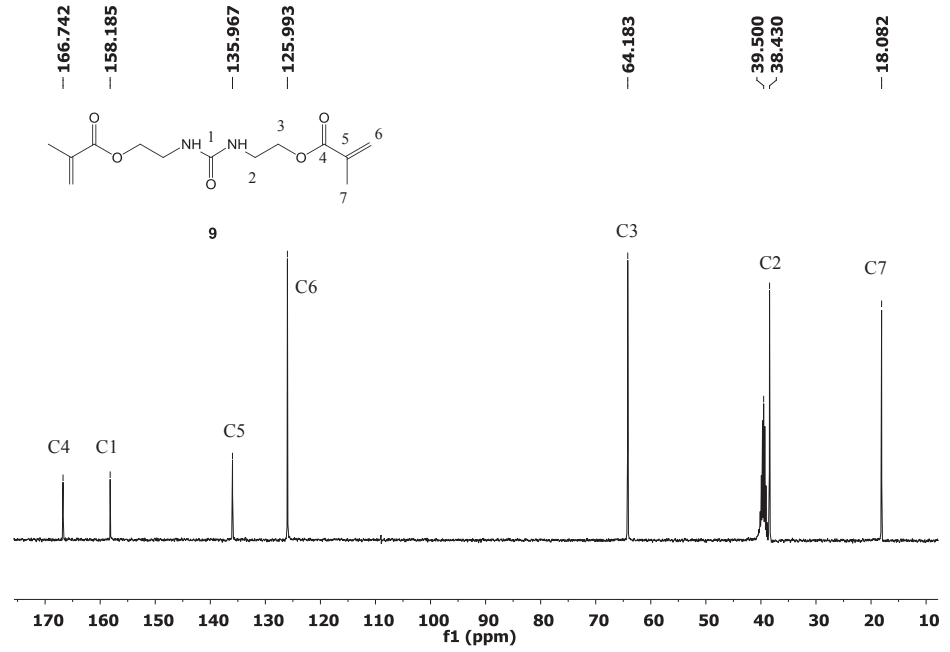

Figure 7.15 *^{13}C NMR of urea **9** formed from the reaction of 2-isocyanatoethyl methacrylate IEM with H_2O. Conditions: 100 MHz, DMSO-d6, 4 %w/w, 298 K, ns 1000, D1 2s.*

7.6 References

(1) (a) Whistler, R. L.; Panzer, H. P.; Roberts, H. J. *Journal of Organic Chemistry* **1961**, *26*, 1583(b) Kallin, E.; Loenn, H.; Norberg, T.; Elofsson, M. *Journal of Carbohydrate Chemistry* **1989**, *8*, 597.

(2) (a) Klein, J.; Kowalczyk, J.; Engelke, S.; Kunz, M.; Puke, H. *Makromolekulare Chemie, Rapid Communications* **1990**, *11*, 477(b) Klein, J.; Begli, A. H.; Engelke, S. *Makromolekulare Chemie, Rapid Communications* **1989**, *10*, 629(c) Klein, J.; Kunz, M.; Kowalczyk, J. *Makromolekulare Chemie* **1990**, *191*, 517.

(3) Haug, A.; Larsen, B.; Smidsroed, O. *Acta Chemica Scandinavica* **1967**, *21*, 2859.

(4) Flint, R. B.; Salhcrg, P. L.; E.I. pont de Nemours United states, 1935; Vol. US 2,016,962.

(5) (a) Klein, J.; Herzog, D. *Makromolekulare Chemie* **1987**, *188*, 1217(b) Klein, J.; Begli, A. H. *Makromolekulare Chemie* **1989**, *190*, 2527.

(6) Norberg, T.; Kallin, E. In *PCT Int. Appl.*; BioCarb AB: Lund, Sweden: WO, 1990.

(7) Matsuda, T.; Sugawara, T. *Macromolecules* **1996**, *29*, 5375.

(8) Ting, S. R. S.; Min, E. H.; Zetterlund, P. B.; Stenzel, M. H. *Macromolecules (Washington, DC, United States)* **2010**, *43*, 5211.

(9) Haug, A.; Larsen, B.; Smidsroed, O. *Acta Chemica Scandinavica* **1963**, *17*, 1466.

(10) Vishnyakova, T. P.; Golubeva, I. A.; Glebova, E. V. *Uspekhi Khimii* **1985**, *54*, 429.

(11) Somsak, L.; Felfoeldi, N.; Konya, B.; Huese, C.; Telepo, K.; Bokor, E.; Czifrak, K. *Carbohydr. Res.* **2008**, *343*, 2083.

(12) Manger, I. D.; Rademacher, T. W.; Dwek, R. A. *Biochemistry* **1992**, *31*, 10724.

(13) Tuzikov, A. B.; Gambaryan, A. S.; Juneja, L. R.; Bovin, N. V. *Journal of Carbohydrate Chemistry* **2000**, *19*, 1191.

(14) Hoyle, C. E.; Bowman, C. N. *Angewandte Chemie International Edition* **2010**, *49*, 1540.

(15) Kallin, E.; Loenn, H.; Norberg, T.; Sund, T.; Lundqvist, M. *Journal of Carbohydrate Chemistry* **1991**, *10*, 377.

(16) Smidsrød, O.; Haug, A. *Biopolymers* **1971**, *10*, 1213.

Chapter 8: Conventional radical copolymerization of AlgiMERs in aqueous solution

Table of contents

Disclaimer

All the rheological characterizations were conducted by Prof. M. Rinaudo (accompanied by Anna Wolnik). Many thanks for her patience in illustrating and interpreting the results with me.

8.1 Introduction

In this chapter, I describe a systematic study on the conventional radical copolymerization of some alginate-derived monomers (AlgiMERs) in aqueous solution. Its aim was to probe the influence of:

- the nature of the (co)monomers (methacrylate, acrylamide or methacrylamide)
- the molecular weight of the AlgiMER
- the ionic strength of the solution
- the comonomer concentration

on the polymerization process (rate, monomer incorporation) and on the properties of the resulting polymer (molar mass, intrinsic viscosity). Also, the glycopolymers carrying "long" oligoglycuronan grafts (DP_n = 17-20) were briefly characterized in terms of rheological behavior in aqueous solution and gelation properties in the presence of Ca^{2+} ions.

The only previous work on the radical copolymerization of AlgiMERs is a patent by Mooney et al. [1] describing the synthesis of alginate containing polymers for biomedical application, and in particular for cell transplantation and drug delivery. Among other things, the patent claims the synthesis of an oligoguluronan-derived acrylamide by the reductive amination of (1→4)-α-L-guluronan (DP_n 25) with hydrazidoacrylate and its conventional radical copolymerization with hydrophilic monomers (acrylic acid, 2-hydroxyethylmethacrylate and diallyldimethyl ammonium chloride). Unfortunately, no real example is provided and all experimental details are omitted (monomer synthesis, copolymerization experiments and polymer characterization).

For this study, 2-Hydroxyethylmethacrylamide (HEMAm) was the comonomer of choice, since it is a highly hydrophilic neutral methacrylamide derivative whose homopolymers are water soluble and can be cross-linked to give hydrogels containing over

80% water. [2] Furthermore, HEMAm copolymers have been studies for drug delivery applications [3] and for the preparation of dental materials. [4] Finally, a few attempts were made to copolymerize AlgiMERs with the less hydrophilic 2-hydroxyethyl methacrylate (HEMA) were also carried out, since poly(HEMA) is recognized as being biocompatible in a number of applications. [2,5]

8.2 Experimental

A list of the AlgiMERs used in this study is provided in Table 8.1, together with the reference to their synthesis as described in Chapter 7. Note that all monomers used in this study were obtained via the reductive amination strategy.

Table 8.1 *Monomers involved in this study with references to their synthesis as described in Chapter 7.*

Run no.	Monomer (Protocol)	Oligoglycuronan	DP_n	Nature	Description	Experiment code
1	**M1**	mannuronan	9	methacrylamide	$ManA_9$-MAm	AG11-05-P1
2	**M2**	mannuronan	9	acrylamide	$ManA_9$-Am	AG11-05-P2
3	**M3** (A)	mannuronan	17	methacrylamide	$ManA_{17}$-Mam	AG10-26
4	**M3** (B)	mannuronan	17	methacrylamide	$ManA_{17}$-MAm	AG11-11-P1
5	**M4** (A)	mannuronan	5	methacrylamide	$ManA_5$-MAm	AG10-36-P2
6	**M4** (C)	mannuronan	5	methacrylamide	$ManA_5$-MAm	AG10-39-P2
7	**M5** (A)	mannuronan	5	methacrylate	$ManA_5$-MA	AG10-36-P1
8	**M5** (B)	mannuronan	5	methacrylate	$ManA_5$-MA	AG10-39-P1
9	**M6**	guluronan	20	methacrylamide	$GulA_{20}$-MAm	AG11-11-P1

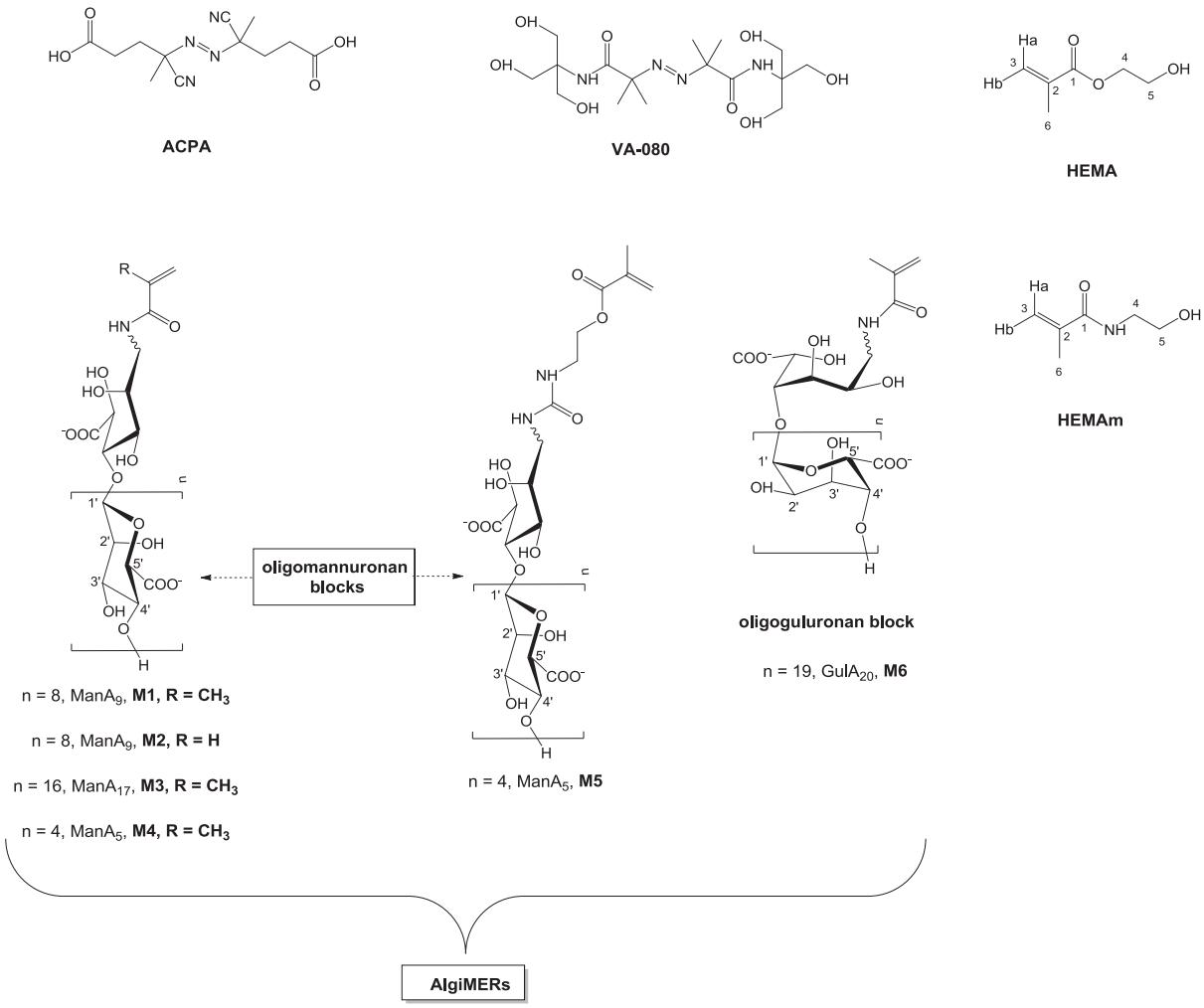

Scheme 8.1 *Molecules involved in this study with the nucleus numbering used for NMR assignment. $ManA_x$ and $GulA_x$ refer to oligo(1→4)-β-D-mannuronan and oligo(1→4)-α-L-guluronan with $DP_n = x$.*

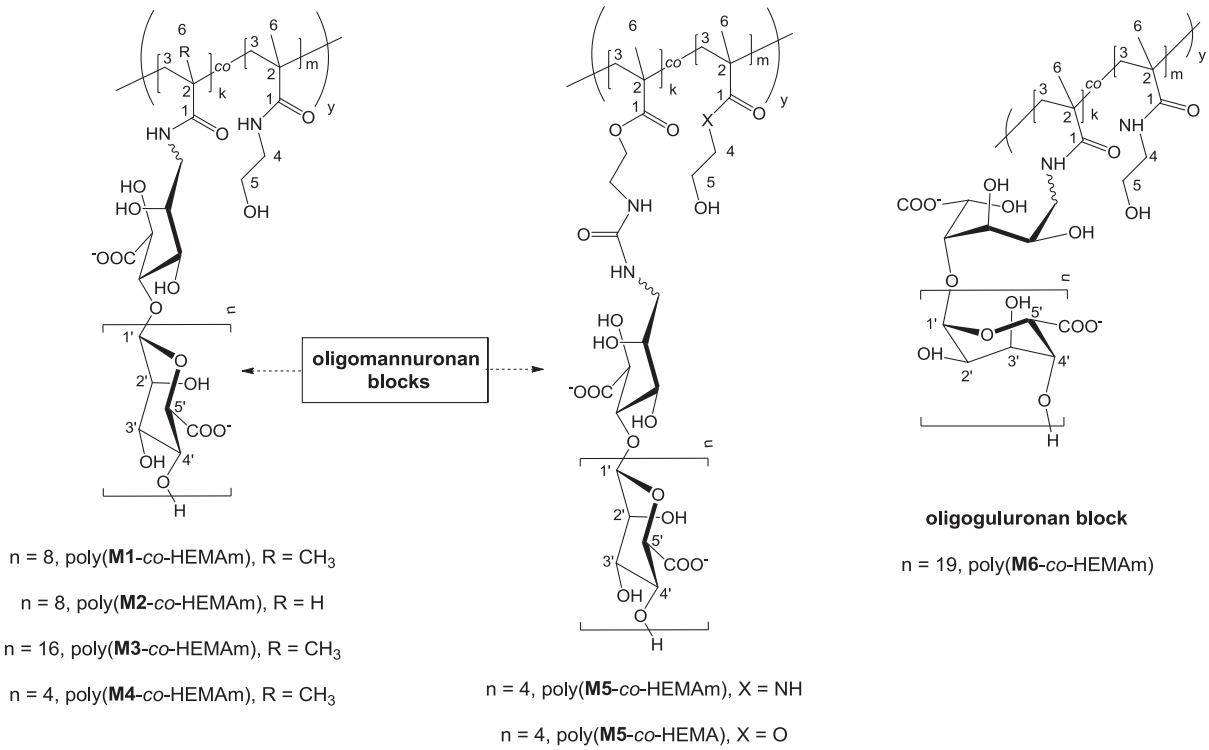

Scheme 8.2 *Polymers synthesized in this study.*

8.2.1 Materials and methods

The following chemicals were reagent grade and were used as received. 4,4'-Azobis(cyanopentanoic acid) (98%, Aldrich), 2,2'-Azobis{2-methyl-N-[1,1-bis(hydroxymethyl) 2-hydroxyethyl] propionamide} (VA-080) (97%, Wako), D_2O (99.8%, Eurisotop), H_2O (de-ionized), NaCl (≥ 99%, Aldrich), $NaHCO_3$ (≥ 99%, SdS), DMSO-d6 (99.8%, Eurisotop), ethanol amine (≥ 99%, Fluka), 2,6-Di-tert-butyl-4-methyl phenol BHT (≥ 99%, Fluka), methyl α-D-glucoside (≥ 99%, Fluka), ethylenediaminetetraacetic acid tetrasodium salt EDTA (99%, Acros), sodium hydroxide solutions (pure, Acros), HCl (37%, Carlo Erba), $CaCl_2$ (97%, Prolabo), $NaNO_3$ (≥ 99%, Aldrich), NaN_3 (≥ 99%, Merck). Flash chromatography was carried with silica gel from Merck (60 Å, 40-60 µm). TLC analyses were performed on aluminum backed silica gel plates (60 Å, 15µm, Merck) containing a UV indicator (254 nm). Methacryloyl chloride (≥ 97%, Fluka) and 2-hydroxyethyl methacrylate HEMA (97%, Aldrich) were distilled under vacuum prior to use and were stored at -18 °C. Slide-A-Lyzer dialysis cassettes were purchased from Thermo Scientific®. Diafiltration and cellulose nitrate membranes were supplied by Millipore and Sartorius, respectively. Accurate volumes were measured using micropipettes (Eppendorf Research).

8.2.2 Analyses

Mass spectrometry analyses and polymer molecular weights were performed with a Waters ZQ and a Waters Alliance GPCV2000 (described in Chapters 5 and 6). NMR experiments were performed on a Bruker DPX400 spectrometer (described in Chapter 5). Chemical shifts (in ppm) for ^{1}H and ^{13}C nuclei were referenced to δ_{TSP} = -0.017 ppm (^{1}H) and δ_{TSP} = -0.149 ppm (^{13}C), or to δ_{DSS} = 0.000 ppm (^{1}H and ^{13}C). The temperature of analysis was either 318 K or 328 K in order to avoid the interference of the HDO peak with the peak of the internal anomeric protons of the AlgiMER.

Total conversions (x) were calculated by normalizing the ^{1}H-NMR spectra of the polymerization mixtures at t = 0 and $t = t_{end}$ to the same reference peak (*e.g.* the internal anomeric proton of the AlgiMER or a peak from the comonomer) and by integrating the ethylenic protons. The following formula was then applied:

$$x = 1 - \left(\frac{A_{\text{ethylenic}}}{A_{\text{reference}}}\right)_t \Big/ \left(\frac{A_{\text{ethylenic}}}{A_{\text{reference}}}\right)_0 \qquad (8.1)$$

where A_i is the area of peak "i". See Appendix 8.C for an example on conversion calculation. In a similar way, the **composition of the purified glycopolymers** was calculated from their ^{1}H-NMR spectra by normalizing them to a suitable reference peak. For example, the peaks from the aliphatic protons of the main chain (CH_3 and CH_2 in the region 0.9-1.9 ppm) were integrated to 5 and the content of AlgiMER was calculated from the integral of its internal anomeric protons divided by the number of repeating units of the oligosaccharide minus one (also estimated by ^{1}H-NMR). Alternatively, when the comonomer was HEMAm the integral of its well resolved NH-C<u>H</u>$_2$- signal at 3.27 ppm (H4 in Scheme 8.2) was compared with the integral of the internal anomeric protons of the AlgiMER. The two methods give comparable results.

For **kinetic studies**, individual monomer conversion was calculated by SEC using a dedicated setup. To this aim, the set of columns and the internal standard to be used were chosen as to attain baseline resolution for the three peaks of interest (monomer 1, monomer 2 and internal standard) with no interference of the internal standard on the polymerization process (e.g. chain transfer). At first, a high molar mass glycopolymer sample, the AlgiMER, HEMAm, a number of internal standards (methyl α-D-glucoside, DMSO, DMF) and D_2O were injected (both individually and mixed together) on two different sets of Shodex OHpak SB-HQ columns. The samples were then eluted under usual conditions (0.1 M $NaNO_3$, 10

mM EDTA, 0.03% w/w NaN_3; 30 °C). The combination *guard column*+ *802* + *803* with methyl α-D-glucoside as an internal standard was found to be the most suitable. Conversion (x) for each monomer was then calculated as follows:

$$x = 1 - \left[\left(\frac{A_M}{A_{ISTD}}\right)_t - (1-P)\left(\frac{A_M}{A_{ISTD}}\right)_0\right] \Big/ \left[\left(\frac{A_M}{A_{ISTD}}\right)_0 - (1-P)\left(\frac{A_M}{A_{ISTD}}\right)_0\right] \quad (8.2)$$

where A_M and A_{ISTD} are the area of the monomer and internal standard peak respectively, P is the purity of the monomer (assumed to be 1 for HEMAm, determined by ^{1}H-NMR for the AlgiMER). This formula takes into account (and corrects for) the fact that AlgiMER samples contain a considerable portion of the oligosaccharide from which they were derived, and that the respective peaks are perfectly superimposed in SEC.

Differential refractive index increments (dn/dc) of poly(HEMAm) (run no. 2, Table 8.3) and poly(**M4**-*co*-HEMAm) (run no. 5, Table 8.4) were determined at 30 °C using an offline Optilab® rEX differential refractometer (Wyatt Technology Corp., (λ = 633 nm). To this end, polymers were isolated by precipitation (pHEMAm) or diafiltration, dried under mechanical vacuum (pHEMAm) or lyophilized and their residual solvent content was determined by thermo gravimetric analysis (130 °C, 2-3 h). Solutions of known concentration were then prepared gravimetrically by dissolving the polymers into the eluant used for SEC analysis (d^{30}= 1.0035 g mL^{-1}) and injected at a flow rate of 0.25 mL min^{-1}. The Optilab rEX measures the refractive index (Δn) for each concentration (c) and from ASTRA 5.3 software (Wyatt Technology Corp.), dn/dc is calculated from the slope of the plot of Δn as a function of c according to the following equation: [6]

$$\Delta n = \frac{dn}{dc} \times c \quad (8.3)$$

The refractive index increment of the copolymers was estimated from their chemical composition and the dn/dc of the corresponding homopolymers according to the formula: [7]

$$dn/dc = F_1(dn/dc)_1 + F_2(dn/dc)_2 \quad (8.4)$$

To this end, a dn/dc value of 0.165 mL g^{-1} was used for alginate, [8] and that of poly(HEMAm), dn/dc = 0.208 mL g^{-1}, was measured.

Thermo Gravimetric Analyses (TGA) were carried out on a Setaram TGA 92-12 instrument. Samples (10-30 mg) were heated from room temperature up to 130 °C at 10

°C/min under nitrogen flow and left at this temperature for 2-4 hours before reading the mass loss (at this point, the first derivative of the curve was zero). Said loss was assumed to be due to residual solvent (water) in the freeze-dried polymer.

Table 8.2 *TGA analysis of some of the polymers prepared in this study.*

Run no.	Sample	Initial mass (mg)	Heating time (h)	solvent content (% w/w)
1	P(HEMAm)	32	3	5
2	P(HEMAm-*co*-M4)	5	2	14
3	P(HEMAm-*co*-M3)	21	4	12
4	P(HEMAm-*co*-M6)	13	4	12

Rheological properties (steady state and dynamic) of polymer solutions and gels were characterized with an AR2000 rheometer (TA instruments). To this end, polymers were isolated by diafiltration, lyophilized and their residual solvent content was determined by Thermo Gravimetric Analysis. Solutions in de-ionized water and NaCl 0.1 mol L^{-1} were then prepared at ~4 times the critical overlapping concentration (C^*) as estimated from the intrinsic viscosity in $NaNO_3$ 0.1 mol L^{-1} ($C^* \approx 1/[\eta]$). The latter was approximated with the $[\eta]_w$ obtained by SEC-IV-MALLS analysis ($[\eta] \approx \eta_{sp}/c$ at low concentration). The resulting solutions were subjected to steady-state and dynamic (oscillatory) measurements at 25 °C using a cone-plate rheometer (diameter = 4 cm, angle = 3°59) with an inter-cone-plate gap of 113 μm.

Gels of poly(HEMAm-*co*-**M6**) and poly(HEMAm-*co*-**M3**) were prepared by dialyzing a glycopolymer solution in deionized water (~ 18 mg mL^{-1}, $[\eta] \approx 200$ mL g^{-1}) against a $CaCl_2$ solution (0.5 mol L^{-1}) for 28-48 hours. To this end, small dialysis cassettes were used (Slide-A-Lyzer, 0.5-3.0 mL, MWCO 2000 Da, Pierce), from which the gel was recovered by cutting off the dialysis membrane with a scalpel. The resulting material was either punched into a disk (∅ = 2 cm, h ≅ 0.25 cm; poly(HEMAm-*co*-**M6**)) with the same diameter of the rheometer plate, or transferred onto the same plate as a film. The rheological properties were then investigated in oscillatory and compression mode using a parallel-plate system at 25 °C. In order to prevent slippage effects, a sanded plate was used for gel characterization. Also, prior to analysis an interval of maximum deformations was tested on a separate sample, so to identify the range within which the measured moduli were independent of the maximum deformation applied.

8.2.3 Synthesis of *N*-(2-hydroxyethyl)methacrylamide (HEMAm)

In a round bottom flask ethanol amine (10 mL, 0.160 mol) was dissolved in MeOH (100 mL) and Et_3N (21 mL, 0.150 mol) was added. The mixture was cooled down on ice and methacryloyl chloride (14.4 mL, 0.150 mol) was introduced drop wise under stirring using a gas tight syringe. After 4 hours, of which 2 hours at 0 °C, the base was precipitated by HCl (2 N), the volatiles were eliminated at reduced pressure, and 10 g of the obtained solid were re-solubilized in EtOH, adsorbed on silica gel (70 g) and re-dried over the rotary evaporator. The resulting white powder was added over a column (∅: 7cm) pre-packed with silica gel (h: 24 cm) for purification and the product was eluted using two gradients of PE/EtOAc/EtOH 6:3:1 and 6:2:2, respectively. The fractions containing the product were pooled, stabilized with BHT, concentrated over the rotary evaporator and further dried under mechanical vacuum (< 10^{-1} mbar). Viscous oil, R_f 0.45 (PE/EtOAc/EtOH 6:2:2). ^{1}H-NMR (400 MHz, D_2O, 25 °C) δ (ppm): 1.93 (m, H6, 3H), 3.40 (t, H4, 2H), 3.68 (t, H5, 2H), 5.45 (m, H3b, 1H), 5.71 (m, H3a, 1H). ^{13}C-NMR (100 MHz, D_2O, 10 °C) δ (ppm): 20.41 (C6), 44.34 (C4), 62.60 (C5), 123.95 (C3), 141.61 (C2), 174.83 (C1). ESI-MS: *m/z* calculated 130.09, found: 130.0 [$M.H^+$]. (See Appendix 8.A for NMR spectra). ***Note:*** if BHT is not added, the monomer tends to homopolymerize in bulk when the oxygen is removed (e.g. under mechanical vacuum).

8.2.4 Homopolymerization of 2-hydroxyethyl methacrylamide (HEMAm)

(Run no. 2, Table 8.3) 4,4'Azobis(cyanopentanoic acid) (ACPA, 3.14×10^{-2} g, 1.12×10^{-4} mol) was dissolved in DMSO-d6 (1 mL), cooled to ≅ 8 °C and diluted with an equal volume of D_2O. HEMAm (0.350 g, 2.71×10^{-3} mol) was dissolved in D_2O (2.4 mL) and filtered through a syringe filter (0.22 µm, cellulose acetate) to remove the suspended inhibitor (BHT). Part of the latter solution (2.0 mL, 1.13 mol L^{-1}), was mixed with a calculated amount of ACPA solution (200 µL, 5.60×10^{-2} mol L^{-1}, 1.12×10^{-5} mol) and transferred to a Schlenk tube. The tube was then sealed with a rubber septum, degassed by 3 freeze-evacuate-thaw cycles and transferred to a water bath preheated at 60 °C. After 3.5 hours the polymerization was stopped by plunging the tube in icy water, a NMR sample was withdrawn from the polymerization mixture and the polymer was recovered by precipitating it twice in an excess of acetone. The fiber-like precipitate was dried under mechanical vacuum at RT for 65 hours (10-15 torr, ~21°C). From Thermo Gravimetric Analysis the solvent content in the polymer was calculated (130 °C, 3 hours) and its d*n*/d*c* was measured (See analysis section for

procedure). Final conversion: 80%. M_n (SEC-MALLS) 232,000 Da, d*n*/d*c* 0.208, PDI 1.74, $[\eta]_w$ 97 mL g^{-1}. ^{1}H-NMR (400 MHz, D_2O, 25 °C) δ (ppm): 0.97 (H3, 2H), 1.12 and 1.74 (H6, 3H), 3.28 (H4, 2H), 3.66 (H5, 2H). (See Appendix 8.B for SEC chromatograms).

8.2.5 Homopolymerization of 2-hydroxyethyl methacrylate (HEMA)

(Run no. 3, Table 8.3) 4,4'Azobis(cyanopentanoic acid) (ACPA, 1.92×10^{-2} g, 6.85×10^{-5} mol) was dissolved in DMSO-d6 (1 mL), cooled to ≅ 8 °C and diluted with an equal volume of D_2O. HEMA (0.200 g, 1.54×10^{-3} mol) was dissolved in CD_3OD (1.25 mL). Part of the latter solution (0.5 mL, 1.23 mol L^{-1}) was mixed with a calculated amount of ACPA (49 µL, 3.43×10^{-2} mol L^{-1}, 1.68×10^{-6} mol) and transferred to a NMR tube equipped with a Young valve. The tube was sealed, degassed by 4 freeze-evacuate-thaw cycles and transferred to a water bath, preheated at 60 °C. Total reaction time: 7.5 hours. Final conversion from ^{1}H-NMR: 76%. M_n (SEC / PMMA standards) 110,220 Da, PDI 2.55.

8.2.6 Homopolymerization of M1 ($ManA_9$-MAm) in 0.2 M NaCl

(Run no. 5, Table 8.3) 2,2'-Azobis{2-methyl-*N*-[1,1-bis(hydroxymethyl) 2-hydroxyethyl] propionamide} (VA-080, 0.029 g, 7.12×10^{-5} mol) was dissolved in D_2O (2 mL). A glycomonomer solution was prepared by mixing **M1** (0.045 g, 2.45×10^{-5} mol) in D_2O (0.6 mL) followed by the addition of NaCl (7.6 mg). The glycomonomer solution (0.6 mL, 0.041 mol L^{-1}) was mixed with a calculated amount of initiator solution (56 µL, 3.56×10^{-2} mol L^{-1}, 1.99×10^{-6} mol) and the whole mixture was transferred to a NMR tube equipped with a Young valve. The tube was sealed, degassed by 3 freeze-evacuate-thaw cycles and a ^{1}H NMR was acquired at t = 0 min prior to heating the polymerization mixture in a water bath at 70 °C. Total reaction time: 48 hours. Final conversion (^{1}H-NMR): 2%. M_n (SEC-MALLS) 11,460 Da, d*n*/d*c* 0.165, PDI 1.26, $[\eta]_w$ 17.4 mL g^{-1}.

8.2.7 Homopolymerization of M2 ($ManA_9$-Am) in D_2O

(Run no. 6, Table 8.3) Same procedure proceeded as run no. 5 (Table 8.3) but without salt. Total reaction time: 48 hours. Final conversion: 6%. M_n (SEC-MALLS) 8,500 Da, d*n*/d*c* 0.165, PDI 1.13, $[\eta]_w$ 17.4 mL g^{-1}.

8.2.8 Homopolymerization of M2 ($ManA_9$-Am) in 0.2M NaCl

(Run no. 7, Table 8.3) Same procedure proceeded as run no. 5 (Table 8.3). Total reaction time: 48 hours. Final conversion (^{1}H-NMR): 5%. M_n (SEC-MALLS) 9,412 Da, d*n*/d*c* 0.165, PDI 1.22, $[\eta]_w$ 17.4 mL g^{-1}.

8.2.9 Homopolymerization of M3 ($ManA_{17}$-MAm) in D_2O

(Run no. 4, Table 8.3) 4,4'Azobis(cyanopentanoic acid) (ACPA, 0.019 g, 6.75×10^{-5} mol) was dissolved in DMSO-d6 (1 mL), cooled to ≅ 8 °C and diluted with an equal volume of D_2O. The glycomonomer **M3** (0.075 g, 2.24×10^{-5} mol) was solubilized in D_2O (1.5 mL) and the pH was adjusted from ≅ 6-7 to ≅ 7-8 by the addition of $NaHCO_3$ (0.1 mL, 0.3 mol L^{-1}) to assure better solubility. The latter solution (1.6 mL, 0.013 mol L^{-1}) was mixed with a calculated amount of initiator (50 µL, 3.37×10^{-2} mol L^{-1}, 1.69×10^{-6} mol) and the mixture was transferred to a NMR tube equipped with a Young valve. The tube was sealed, degassed by 4 freeze-evacuate-thaw cycles and a ^{1}H NMR was acquired at t = 0 min prior to heating the polymerization mixture in a water bath at 60 °C. The polymerization was stopped from time to time to monitor the conversion by ^{1}H-NMR. Total reaction time: 111 hours. Final conversion (^{1}H NMR): 31%. Yield: 2%. M_n (SEC-MALLS) 8,933 Da, d*n*/d*c* 0.165, PDI 1.17, $[\eta]_w$ 34.8 mL g^{-1}.

8.2.10 Conventional radical copolymerization of M4 ($ManA_5$-MAm) with HEMAm in D_2O

Protocol A (total concentration of monomers is 0.3 mol L^{-1})

(Run no. 4, Table 8.4) 4,4'Azobis(cyanopentanoic acid) (ACPA, 1.47×10^{-2} g, 5.24×10^{-5} mol) was dissolved in DMSO-d6 (1.5 mL), cooled to ≅ 8 °C and diluted with an equal volume of D_2O. HEMAm (0.040 g, 3.10×10^{-4} mol) was dissolved in D_2O (0.4 mL) and filtered through a syringe filter (0.22 µm, cellulose acetate) to remove the suspended inhibitor (BHT). The glycomonomer **M4** (0.008 g, 7.60×10^{-6} mol) was dissolved in D_2O (0.5 mL), added to a part of the HEMAm solution (0.3 mL, 0.775 mol L^{-1}) and mixed with a calculated amount of initiator (ACPA, 50 µL, 1.75×10^{-2} mol L^{-1}, 8.74×10^{-7} mol) to get a final concentration of 0.273, 0.0089 and 0.0010 mol L^{-1}, respectively. The polymerization mixture was transferred to a NMR tube equipped with a Young valve that was firmly sealed, degassed by 4 freeze-evacuate-thaw cycles and transferred to a water bath preheated at 60 °C for 3.5

hours and then at 70 °C for 1 hour. At the end of the reaction, a ^{1}H-NMR was acquired for conversion calculation and the polymer was purified by dialysis using a 7,000 Da cut off dialysis cassette for 24 hours, followed by freeze drying. Final conversion (^{1}H NMR): 65%. M_n (SEC-MALLS) 40,460 Da, d*n*/d*c* 0.202, PDI 1.52, $[\eta]_w$ 29.6 mL g^{-1}, *f* (**M4**) 3.2%, *F* (**M4**) 1.9%, *F*m (**M4**) 12.9%. ^{1}H-NMR (400 MHz, D_2O, 50 °C) δ (ppm): 0.96 (H3, 4H), 1.11 and 1.74 (H6, 6H), 3.27 (H4, 2H), 3.64 (H5, 2H), 3.73-4.04 (H2', H3', H4', H5', sugar), 4.67 (H1', sugar).

Protocol B (total concentration of monomers is 0.5 mol L^{-1})

(Run no. 5, Table 8.4) Same procedure proceeded with run no. 4 in Table 8.4, but the polymerization mixture was heated only at 60 °C for 2 hours. At the end of the reaction, a ^{1}H-NMR was acquired for conversion calculation and the polymer was purified by dialysis using 10,000 and 20,000 Da cut off dialysis cassettes for 48 and 50 hours respectively, followed by freeze drying. From Thermo Gravimetric Analysis the solvent content of the polymer was calculated (130 °C, 2 hours) and its d*n*/d*c* was measured (See analysis section for procedure). Final conversion (^{1}H NMR): 68%. M_n (SEC-MALLS) 208,200 Da, d*n*/d*c* 0.197, PDI 2.05, $[\eta]_w$ 104.2 mL g^{-1}, *f* (**M4**) 4.9%, *F* (**M4**) 4.1%, *F*m (**M4**) 24.9%. ^{1}H-NMR (400 MHz, D_2O, 50 °C) δ (ppm): 0.96 (H3, 4H), 1.11 and 1.74 (H6, 6H), 3.27 (H4, 2H), 3.64 (H5, 2H), 3.73-4.04 (H2', H3', H4', H5', sugar), 4.67 (H1', sugar).

8.2.11 Conventional radical copolymerization of M5 (ManA$_5$-MA) in D_2O

Protocol A (with HEMA, pD ≅ 8-9, total concentration of monomers is 0.3 mol L^{-1})

(Run no. 1, Table 8.4) 4,4'Azobis(cyanopentanoic acid) (ACPA, 1.47×10^{-2} g, 5.24×10^{-5} mol) was dissolved in DMSO-d6 (1.5 mL), cooled to ≅ 8 °C and diluted with an equal volume of D_2O. HEMA (3.45×10^{-2} g, 2.65×10^{-4} mol) and the glycomonomer **M5** (1.26×10^{-2} g, 1.16×10^{-5} mol) were dissolved in 1 and 0.25 mL D_2O respectively. To the latter mixed solution (HEMA + **M5**) a calculated amount of initiator (ACPA, 50 μL, 1.75×10^{-2} mol L^{-1}, 8.74×10^{-7} mol) was added. ***Note:*** The pD of the polymerization mixture was ≅ 8-9 since the prepared glycomonomer was only purified by precipitation where some base precipitated out with the glycomonomer **M5**. The polymerization mixture was transferred to a

NMR tube equipped with a Young valve that was firmly sealed, degassed by 4 freeze-evacuate-thaw cycles and transferred to a water bath preheated at 60 °C for 3.5 hours and then at 70 °C for 1 hour. At the end of the reaction, ^{1}H-NMR was acquired for conversion calculation and the resulting polymer was purified by dialysis using 7,000 Da cut off dialysis cassette for 24 hours, followed by freeze drying. Final conversion (^{1}H NMR): 75%, Yield: 56%. M_n (SEC-MALLS) 200,100 Da, d*n*/d*c* 0.186, $[\eta]_w$ 16.8 mL g^{-1}, PDI 1.16, *f* (**M5**) 4.2%, *F* (**M5**) 11.2%, *F*m (**M5**) 51.3%.

Protocol B (with HEMA, pD ≅ 7, total concentration of monomers is 0.5 mol L^{-1})

(Run no. 2, Table 8.4) Same procedure proceeded with run no. 1 in Table 8.4 but the pD of the polymerization mixture was adjusted to ≅ 7 using HCl (0.01 N) and heated at 60 °C for 35 minutes where the mixture precipitated out. The resulting precipitate was neither soluble in methanol nor in water and nor in a mixture of both solvents.

Protocol C (with HEMAm, pD ≅ 7.8, total concentration of monomers is 0.3 mol L^{-1})

(Run no. 3, Table 8.4) 4,4'Azobis(cyanopentanoic acid) (ACPA, 1.47 × 10^{-2} g, 5.24 × 10^{-5} mol) was dissolved in DMSO-d6 (0.5 mL), cooled to ≅ 8 °C and diluted with an equal volume of D_2O. HEMAm (4.60 × 10^{-2} g, 3.56 × 10^{-4} mol) was dissolved in D_2O (0.4 mL) and filtered through a syringe filter (0.22 µm, cellulose acetate) to remove the suspended inhibitor (BHT). The glycomonomer **M5** (0.0126 g, 1.16 × 10^{-5} mol) was dissolved in D_2O (0.54 mL), added to part of the HEMAm solution (0.3 mL, 0.891 mol L^{-1}) and mixed with a calculated amount of initiator (ACPA, 50 µL, 5.24 × 10^{-2} mol L^{-1}, 2.62 × 10^{-6} mol). The pD was adjusted ≅ 7.8 using HCl (0.01 N). The polymerization mixture was transferred to a NMR tube equipped with a Young valve that was firmly sealed, degassed by 4 freeze-evacuate-thaw cycles and transferred to a water bath preheated at 60 °C for 3.6 hours. At the end of the reaction conversion was acquired from ^{1}H-NMR and the resulting polymer was purified by dialysis using 10,000 Da cut off dialysis cassette for 48 hours, followed by freeze drying. Final conversion (^{1}H NMR): 79%. M_n (SEC-MALLS) 42,610 Da, d*n*/d*c* 0.192, PDI 1.46, $[\eta]_w$ 24.6 mL g^{-1}, *f* (**M5**) 4.2%, *F* (**M5**) 6.4%, *F*m (**M5**) 36.7%. ^{1}H-NMR (400 MHz, D_2O, 50 °C) δ (ppm): 0.96 (H3, 4H), 1.11 and 1.74 (H6, 6H), 3.27 (H4, 2H), 3.64 (H5, 2H), 3.75-4.06 (H2', H3', H4', H5', sugar), 4.67 (H1', sugar).

8.2.12 Conventional radical copolymerization of M1 (Man_9-MAm) with HEMAm

Protocol A (D_2O, total concentration of monomers is 0.6 mol L^{-1})

(Run no. 6, Table 8.4) 4,4'Azobis(cyanopentanoic acid) (ACPA, 1.96×10^{-2} g, 6.99×10^{-5} mol) was dissolved in DMSO-d6 (2 mL), cooled to ≅ 8 °C and diluted with an equal volume of D_2O. HEMAm (0.088 g, 6.81×10^{-4} mol) was dissolved in D_2O (0.4 mL) and filtered through a syringe filter (0.22 μm, cellulose acetate) to remove the suspended inhibitor (BHT). The glycomonomer **M1** (0.045 g, 2.45×10^{-5} mol) was dissolved in D_2O (0.5 mL), added to a part of the HEMAm solution (0.28 mL, 1.7 mol L^{-1}) and mixed with a calculated amount of initiator (ACPA, 48 μL, 1.75×10^{-2} mol L^{-1}, 8.39×10^{-7} mol). ***Note:*** pD after mixing was ≅ 6-7. The polymerization mixture was transferred to a NMR tube equipped with a Young valve that was firmly sealed, degassed by 3 freeze-evacuate-thaw cycles and transferred to water bath preheated at 60 °C for 4.5 hours. At the end of the reaction a ^{1}H NMR was acquired for conversion calculation and the polymer was purified by diafiltration using a 10,000 Da cut off membrane (cellulose acetate) for 49 hours, followed by freeze drying. Final conversion (^{1}H NMR): 76%. M_n (SEC-MALLS) 520,000 Da, d*n*/d*c* 0.186, PDI 2.32, $[\eta]_w$ 198.7 mL g^{-1}, *f* (**M1**) 4.9%, *F* (**M1**) 6.6%, *F*m (**M1**) 50.1%. ^{1}H-NMR (400 MHz, D_2O, 55 °C) δ (ppm): 0.96 (H3, 4H), 1.11 and 1.74 (H6, 6H), 3.27 (H4, 2H), 3.64 (H5, 2H), 3.72-4.01 (H2', H3', H4', H5', sugar), 4.64 (H1', sugar). (See Appendix 8.B for SEC chromatograms).

Protocol B (0.2 M NaCl, total concentration of monomers is 0.6 mol L^{-1})

(Run no. 7, Table 8.4) Same procedure proceeded with run no. 6 in Table 8.4 but the polymerization was conducted in NaCl (0.2 M). Total reaction time: 4.5 hours (60 °C). The polymer was purified by diafiltration using 10,000 Da cut off membrane (cellulose acetate) for 49 hours, followed by freeze drying. Final conversion (^{1}H NMR): 76%. M_n (SEC-MALLS) 480,000 Da, d*n*/d*c* 0.187, PDI 2.41, $[\eta]_w$ 193.1 mL g^{-1}, *f* (**M1**) 4.9%, *F* (**M1**) 6.6%, *F*m (**M1**) 48.6%. ^{1}H-NMR (400 MHz, D_2O, 55 °C) δ (ppm): 0.96 (H3, 4H), 1.11 and 1.74 (H6, 6H), 3.27 (H4, 2H), 3.64 (H5, 2H), 3.72-4.01 (H2', H3', H4', H5', sugar), 4.64 (H1', sugar). (See Appendix 8.B for SEC chromatograms).

Protocol C (Kinetic study, D_2O, total concentration of monomers is 0.6 mol L^{-1})

(Run no. 8, Table 8.4) 4,4'Azobis(cyanopentanoic acid) (ACPA, 2.45 × 10^{-2} g, 8.74 × 10^{-5} mol) was dissolved in pure DMSO-d6 (1.0 mL). HEMAm (0.760 g, 5.88 × 10^{-3} mol) was dissolved in D_2O (3.8 mL) and filtered through two syringe filters connected in series (1.22 μm glass fiber filter connected to a 0.22 μm nylon filter) to remove the suspended inhibitor (BHT). The glycomonomer **M1** (0.234 g, 1.28 × 10^{-4} mol) was dissolved in D_2O (2.57 mL), followed by the addition of methyl α-D-glucoside (0.198 g, 1.02 × 10^{-3} mol) as an internal standard. The latter glycomonomer solution (2.57 mL, 0.049 mol L^{-1}) was mixed with a part of the prepared HEMAm solution (1.57 mL, 1.55 mol L^{-1}) and a calculated amount of initiator (ACPA, 49 μL, 8.74 × 10^{-2} mol L^{-1}, 4.28 × 10^{-6} mol). A sample from the polymerization mixture (~ 120 μL) was drawn at t = 0 min, frozen in liquid nitrogen and stored in the freezer until needed. Then the polymerization mixture was transferred to a Schlenk tube, sealed with a rubber septum, degassed by 4 freeze-evacuate-thaw cycles and transferred to a water bath preheated at 60 °C for 5 hours. At preset intervals, samples (~ 6 mg mL^{-1}) were drawn from the polymerization mixture, frozen in liquid nitrogen and stored in the freezer until needed. After 5 hours more initiator (59 mmol L^{-1}, 1.18 × 10^{-5} mol) was added to the polymerization mixture (≅ 0.4 mL) that was reheated for another 11.5 hours (total 16.5 hours) in order to push the conversion to 100%. The samples were analyzed by SEC, using Shodex OH pak SB-(Guard + 802 + 803) HQ columns for conversion calculation using methyl α-D-glucoside as a standard. Final conversion after 5 hours (SEC): 86% (HEMAm), 73% (**M1**). M_n (SEC-MALLS) 743,000 Da, d*n*/d*c* 0.191, PDI 2.05, $[\eta]_w$ 205.2 mL g^{-1}, *f* (**M1**) 5.0%, *F* (**M1**) 4.3%, *F*m (**M1**) 38.9%. (See Appendix 8.B for SEC chromatograms).

8.2.13 Conventional radical copolymerization of M2 (Man_9-Am) with HEMAm

Protocol A (D_2O, total concentration of monomers is 0.6 mol L^{-1})

(Run no. 9, Table 8.4) Same procedure proceeded with run no. 6 in Table 8.4 but the polymerization mixture was heated at 60 °C for 5 hours. At the end of the reaction a ^{1}H NMR was acquired for conversion calculation and the polymer was purified by diafiltration using a 30,000 Da cut off membrane (cellulose acetate) for 68 hours, followed by freeze drying. Final conversion (^{1}H NMR): 85% (HEMAm), 51% (**M2**). M_n (SEC-MALLS) 566,000 Da, d*n*/d*c* 0.188, PDI 2.59, $[\eta]_w$ 211.5 mL g^{-1}, *f* (**M2**) 4.9%, *F* (**M2**) 3.0%, *F*m (**M2**) 30.5%. ^{1}H NMR

(400 MHz, D_2O, 55 °C) δ (ppm): 0.97 (H3, 4H), 1.11 and 1.74 (H6, 3H), 3.27 (H4, 2H), 3.64 (H5, 2H), 3.74-4.01 (H2', H3', H4', H5', sugar), 4.65 (H1', sugar). (See Appendix 8.B for SEC chromatograms).

Protocol B (0.2 M NaCl, total concentration of monomers is 0.6 mol L^{-1})

(Run no. 10, Table 8.4) Same procedure proceeded with run no. 6 in Table 8.4 but the polymerization was conducted in NaCl (0.2 M). Total reaction time: 5 hours (60 °C). At the end of the reaction a ^{1}H NMR was acquired for conversion calculation and the polymer was purified by diafiltration using a 30,000 Da cut off membrane (cellulose acetate) for 93 hours, followed by freeze drying. Final conversion (^{1}H NMR): 87% (HEMAm), 55% (**M2**). M_n (SEC-MALLS) 611,000 Da, d*n*/d*c* 0.188, PDI 2.52, $[\eta]_w$ 218.5 mL g^{-1}, *f* (**M2**) 4.9%, *F* (**M2**) 3.1%, *F*m (**M2**) 31.1%. ^{1}H NMR (400 MHz, D_2O, 55 °C) δ (ppm): 0.97 (H3, 4H), 1.11 and 1.74 (H6, 3H), 3.27 (H4, 2H), 3.64 (H5, 2H), 3.74-4.01 (H2', H3', H4', H5', sugar), 4.65 (H1', sugar). (See Appendix 8.B for SEC chromatograms).

Protocol C (Kinetic study, D_2O, total concentration of monomers is 0.6 mol L^{-1})

(Run no. 11, Table 8.4) Same procedure proceeded with run no. 8 in Table 8.4. At the end of the 5 hours more initiator (59 mM, 1.18×10^{-5} mol) was added to the polymerization mixture (≅ 0.4 mL) that was reheated for another 11.5 hours (total 16.5 hours) in order to push the conversion to 100%. The samples were analyzed by SEC, using Shodex OH Pak SB-(Guard + 802 + 803) HQ columns for conversion calculation. Final conversion after 5 hours (SEC): 84% (HEMAm), 68% (**M2**). M_n (SEC-MALLS) 678,000 Da, d*n*/d*c* 0.192, PDI 2.40, $[\eta]_w$ 197.1 mL g^{-1}, *f* (**M2**) 5.0%, *F* (**M2**) 4.1%, *F*m (**M2**) 37.5%. (See Appendix 8.B for SEC chromatograms).

8.2.14 Conventional radical copolymerization of M3 ($ManA_{17}$-MAm) with HEMAm

Protocol A (D_2O, total concentration of monomers is 1 mol L^{-1})

(Run no. 12, Table 8.4) 4,4'Azobis(cyanopentanoic acid) (ACPA, 1.89×10^{-2} g, 6.75×10^{-5} mol) was dissolved in DMSO-d6 (1 mL), cooled to ≅ 8 °C and diluted with an equal volume of D_2O. HEMAm (12.9×10^{-2} g, 9.99×10^{-4} mol) was dissolved in D_2O (0.87 mL) and filtered through a syringe filter (0.22 μm, cellulose acetate) to remove the suspended

inhibitor (BHT). A part of the latter HEMAm solution (0.71 mL, 1.15 mol L^{-1}) was mixed with the glycomonomer **M3** (0.025 g, 7.46×10^{-6} mol) and a calculated amount of initiator (ACPA, 128 µL, 3.37×10^{-2} mol L^{-1}, 4.32×10^{-6} mol). Then the polymerization mixture was transferred to a NMR tube equipped with a Young valve that was sealed, degassed by 5 freeze-evacuate-thaw cycles and transferred to a water bath preheated at 60 °C for 2 hours. Final conversion (^{1}H NMR): 76%. Gel formation.

Protocol B (D_2O, total concentration of monomers is 0.5 mol L^{-1})

(Run no. 13, Table 8.4) 4,4'Azobis(cyanopentanoic acid) (ACPA, 2.45×10^{-2} g, 8.74×10^{-5} mol) was dissolved in pure DMSO-d6 (1.0 mL). HEMAm (0.760 g, 5.88×10^{-3} mol) was dissolved in D_2O (3.5 mL) and filtered through two syringe filters connected in series (1.22 µm glass fiber filter + 0.22 µm nylon filter) to remove the suspended inhibitor (BHT). The glycomonomer **M3** (0.230 g, 7.02×10^{-5} mol) was dissolved in D_2O (2.3 mL), followed by the addition of methyl α-D-glucoside (0.198 g, 1.02×10^{-3} mol) as an internal standard. The latter glycomonomer solution (2.3 mL, 0.030 mol L^{-1}) was then mixed with a part of the prepared HEMAm solution (1.0 mL, 1.68 mol L^{-1}) and stored overnight at 5 °C. To the latter solution, glycomonomer and HEMAm, a calculated amount of initiator (ACPA, 42 µL, 8.74×10^{-2} mol L^{-1}, 3.67×10^{-6} mol) was added and a sample was drawn from the polymerization mixture (~ 120 µL) at t = 0 min, frozen in liquid nitrogen and stored in the freezer until needed. Then the polymerization mixture was transferred to a Schlenk tube that sealed with a rubber septum, degassed by 3 freeze-evacuate-thaw cycles, and transferred to a water bath preheated at 60 °C. After 4.5 hours, a big part of the polymerization mixture formed a gel, so the polymerization was stopped by plunging the Schlenk tube in cold water, the pH of the mixture was adjusted to ≅ 8-9 by the addition of NaOH (0.1 N) and the mixture was left stirring at RT after the addition of a small spatula of EDTA. After 13 days stirring, the gel was removed by suction filtration using a glass sintered filter (P3) and the recovered solution was further filtered on two cellulose nitrate filters (8 and 1.2 µm) under pressure (2 bar). The recovered solution was diafiltered using a 30 KDa cut off membrane for 66 hours followed by freeze drying. The solvent content (12% w/w) of the purified product was measured by Thermo Gravimetric Analysis (4 hours, 130 °C). Final conversion (SEC): 98% (HEMAm), 100% (**M3**). M_n (SEC-MALLS) 539,000 Da, d*n*/d*c* 0.185, PDI 2.12, $[\eta]_w$ 194 mL g^{-1}, *f* (**M3**)

4.0%, *F* (**M3**) 4.2%, *F*m (**M3**) 52.4%. ^{1}H NMR (400 MHz, D_2O, 55 °C) δ (ppm): 0.98 (H3, 4H), 1.12 and 1.75 (H6, 6H), 3.28 (H4, 2H), 3.66 (H5, 2H), 3.71-4.02 (H2', H3', H4', H5', sugar), 4.64 (H1', sugar). (See Appendix 8.A and B for NMR and SEC spectra).

8.2.15 Conventional radical copolymerization of M6 ($GulA_{20}$-MAm) with HEMAm

(Run no. 14, Table 8.4) 4,4'Azobis(cyanopentanoic acid) (ACPA, 0.0245 g, 8.74×10^{-5} mol) was dissolved in pure DMSO-d6 (1.0 mL). HEMAm (0.760 g, 5.88×10^{-3} mol) was dissolved in D_2O (3.5 mL) and filtered through two syringe filters connected in series (1.22 μm glass fiber filter + 0.22 μm nylon filter) to remove the suspended inhibitor (BHT). The glycomonomer **M6** (0.185 g, 4.66×10^{-5} mol) was dissolved in D_2O (2.3 mL), followed by the addition of methyl α-D-glucoside (0.201 g, 1.04×10^{-3} mol) as an internal standard. The latter glycomonomer solution (2.3 mL, 0.020 mol L^{-1}) was mixed with a part of the prepared HEMAm solution (1.0 mL, 1.68 mol L^{-1}) and stored overnight at 5 °C. Upon storage, the glycomonomer precipitated out so 1 mL D_2O was added to re-solubilize everything and the latter solution, glycomonomer and HEMAm, was mixed with a calculated amount of initiator (ACPA, 55 μL, 8.74×10^{-2} mol L^{-1}, 4.81×10^{-6} mol). A sample from the polymerization mixture (~ 120 μL) was drawn at t = 0 min, frozen in liquid nitrogen and stored in the freezer until needed. Then the polymerization mixture was transferred to a Schlenk tube that was sealed with a rubber septum, degassed by 3 freeze-evacuate-thaw cycles, and transferred to a water bath preheated at 60 °C. After 4.25 hours, a small part of the polymerization mixture formed a gel, so the polymerization was stopped by plunging the tube in cold water and the pH of the mixture was adjusted to ≅ 8-9 by the addition of NaOH (0.1 N). The mixture was left under stirring after the addition of a small spatula of EDTA for 24 hours at RT followed by removing the gel using a syringe filter (1.2 μm, glass fiber). The recovered filtrate was diafiltered using a 30 KDa cut off membrane for 48 hours followed by freeze drying. The solvent content (12% w/w) of the purified product was measured by Thermo Gravimetric Analysis (4 hours, 130 °C). Final conversion (SEC): 82% (HEMAm), 76% (**M6**). M_n (SEC-MALLS) 539,000 Da, d*n*/d*c* 0.185, PDI 2.12, $[\eta]_w$ 202 mL g^{-1}, *f* (**M6**) 2.7%, *F* (**M6**) 2.5%, *F*m (**M6**) 44.1%. ^{1}H-NMR (400 MHz, D_2O, 55 °C) δ (ppm): 0.98 (H3, 4H), 1.12 and 1.75 (H6, 6H), 3.28 (H4, 2H), 3.66 (H5, 2H), 3.88 (H2', sugar), 4.00 (H4', sugar), 4.11 (H3',

sugar), 4.44 (H5', sugar), 5.05 (H1', sugar). (See Appendix 8.A and B for NMR and SEC spectra).

8.2.16 Gel formation

Gels of Poly($ManA_{17}$-co-HEMAm) / poly($GulA_{20}$-co-HEMAm)

In a typical experiment, Poly(**M3**-*co*-HEMAm) (102.5×10^{-3} g, M_n 539,000 Da, water content 12% w/w) and Poly(**M6**-*co*-HEMAm) (83.7×10^{-3} g, M_n 539,000 Da, water content 12%w/w) were dissolved in 5 and 4 mL of de-ionized water respectively. The obtained polymer solutions were dialyzed against $CaCl_2$ (0.5 mol L^{-1}) solution using a 2,000 Da cut off dialysis cassette (capacity 0.5-3 mL) for at least one day.

8.3 Results and discussion

8.3.1 Homopolymerization of AlgiMERs in aqueous solution

Table 8.3 *Summary of homopolymerization experiments.*

Run no.	Monomer (mol L^{-1})[a]	Oligoglycuronan[b]	Nature[c]	Initiator (mmol L^{-1})[a]	Temp (°C)	Reaction time (min)	Conv. (%) NMR	d*n*/d*c*[d]	M_n (Da) SEC	$[\eta]_w$ (mL g^{-1})	PDI	Code
1[e]	HEMAm (bulk)	-	MAm	-	RT	-	-	0.208	2.78×10^6	-	1.19	Bulk
2	HEMAm (1.03)	-	MAm	ACPA (5.09)	60	210	80	0.208	232 000	97	1.74	AG10-29-B1
3[j]	HEMA (1.12)	-	MA	ACPA (3.06)	60	450	76	-	110 220 [f]	-	-	AG11-08-RP
4	**M3** (0.014)[i]	$ManA_{17}$	MAm	ACPA (1.09)	60	6 660	31	0.165	8 933	34.8	1.17[h]	AG10-29-B2
5	**M1** (0.037)[g]	$ManA_9$	MAm	VA-080 (3.04)	70	2 880	2	0.165	11 460	17.4	1.20[h]	AG11-06-RP1-S
6	**M2** (0.038)	$ManA_9$	Am	VA-080 (3.04)	70	2 880	6	0.165	8 500	17.4	1.13[h]	AG11-06-RP2
7	**M2** (0.038)[g]	$ManA_9$	Am	VA-080 (3.04)	70	2 880	5	0.165	9 412	17.4	1.22[h]	AG11-06-RP2-S

General conditions: D_2O (except run no. 3 in CD_3OD), 1 - 4% v/v DMSO-d6, pD ≅ 6-7. [a] Final concentration after mixing. [b] $ManA_x$ represents an oligomannuronan with DP_n = x. [c] MAm is a methacrylamide derivative, Am is an acrylamide derivative and MA is a methacrylate derivative. [d] The value for polyHEMAm was determined experimentally whereas the d*n*/d*c* of alginate was used for poly(AlgiMER)s. [e] Polymer obtained by the spontaneous bulk polymerization of a HEMAm sample during drying under mechanical vacuum at ambient temperature. [f] Poly(methyl methacrylate) equivalent. [g] In the presence of NaCl 0.2 mol L^{-1}. [h] Value affected by the glycomonomer peak. [i] pD ≅ 8, [j] Polymerization conducted in CD_3OD.

Four homopolymerization experiments were conducted to verify whether AlgiMERs could homopolymerize and lead to bottle brush polymers. In particular, the effect of the nature of the polymerizing moiety (methacrylamide or acrylamide) and of the ionic strength of the solution (D_2O or NaCl 0.2 mol L^{-1} in D_2O) was taken into account. All experiments were carried out in NMR tubes equipped with a Young valve and 1-4% v/v of DMSO-d6 was added to help the solubilization of the initiator. Table 8.3 summarizes the experimental conditions and outcome of this study.

Since the mass concentrations of AlgiMER being used was fairly high (5% w/w for run no. 4, 7% w/w for run no. 5-7;), a first attempt was made to polymerize **M3** at pD ≅ 8 so to increase its solubility (run 4, Table 8.3). The pD of the reaction mixture was thus adjusted with $NaHCO_3$ and the reaction was conducted at 60 °C for 111 h (4 ½ days). In the ^{1}H-NMR (Figure 8.1) spectrum of the final mixture appeared well defined sharp peaks at 1.87 ppm, 5.33 ppm and 5.64 ppm whose integrals had a 3:1:1 ratio. The latter were assigned to sodium methacrylate, and its presence suggests that the amide bond of **M3** partially hydrolyzed. It is worth noting that **M3** was prepared according to protocol **A** (Table 8.1) and this signifies that it was partially esterified as well and a part of the formed sodium methacrylate is derived from the hydrolysis of the ester bonds. After 111 hours the molar fraction of formed sodium methacrylate in the polymerization mixture was 0.44. The base-catalyzed hydrolysis 1-(meth)acrylamido-1-deoxy-D-glucitol has already been described by Whistler et al., [9] who found that 20% of it decomposed after 100 hours in NaOH 2 mol L^{-1} at ambient temperature. In our case the polymerization mixture was much less alkaline, but heating at 60 °C might have led to a comparable hydrolysis rate. At the end of the polymerization, by normalizing the two spectra of the polymerization mixture at t = 0 and t = 111 hrs to one peak the conversion of the glycomonomer (30-31%) was calculated, but there was no evidence for polymer formation resulting from the homopolymerizations of **M3** and sodium methacrylate or from their copolymerization (i.e. absence of ^{1}H-NMR peaks from a polymer backbone in the aliphatic region at 0.9-1.9 ppm; absence of polymer peaks in the SEC traces). This finding is inexplicable, even if taking into account that the propagation rate coefficient of ionized methacrylic acid in aqueous solution is low (k_p = 860 L mol^{-1} s^{-1} at 60 °C and 5% w/w monomer concentration). [10] At the same time, the SEC trace of the gross polymerization

mixture showed a shoulder at lower elution volume, with a molecular weight about thrice that of the starting glycomonomer, which suggest the formation of dimers and trimers.

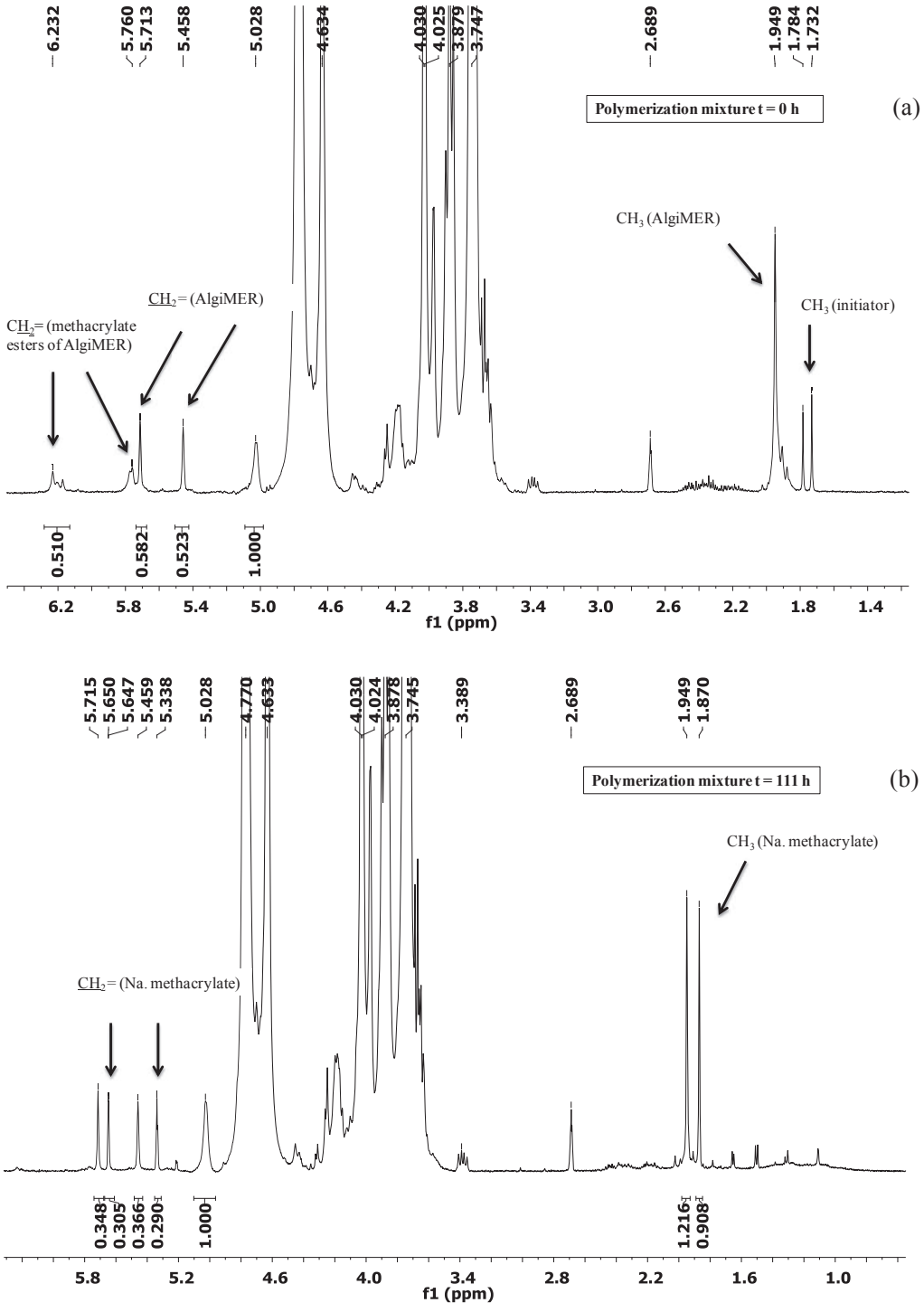

Figure 8.1 *^{1}H NMR spectra of the copolymerization mixture of **M3** and HEMAm at (a) t = 0 hours and (b) 111 hours (run no.4, Table 8.3). Notice the hydrolysis of the amide bond at pD ≅ 8 at 60 °C.*

The causes for the impossibility of **M3** to homopolymerize can be traced to the bulkiness of the monomer and to the fact that at pD ≥ 7 each molecule carries 17 negative charges, thus leading to strong electrostatic repulsion. In an attempt to counter the effects of these physical obstacles, a polymerization was carried out (run 5, Table 8.3) with a smaller mannuronan-derivative (**M1**, DP_n 9) at a higher concentration, in NaCl 0.2 mol L^{-1} (to screen negative charges) and at higher temperature (to help overcome the activation energy barrier to monomer addition). An azo-initiator (VA-080) with a slower decomposition rate was preferred for this experiment and the pD of the solution was left unchanged at 6-7 to prevent hydrolysis of the amide bond. After 48 hours at 70 °C, no sign of degradation was detected in the ^{1}H NMR spectrum, but the same indicated that monomer conversion was only 2%. Also, SEC analysis showed that only pentamers had formed as indicated by the higher molecular weight shoulder (Figure 8.2). This result is only marginally better than the one obtained in run no 4, and was confirmed by two analogous experiments with an acrylamide-type AlgiMER (**M2**, run no. 6 and 7 in Table 8.3), although in the latter cases a somewhat higher conversion was attained (5-6% vs. 2%).

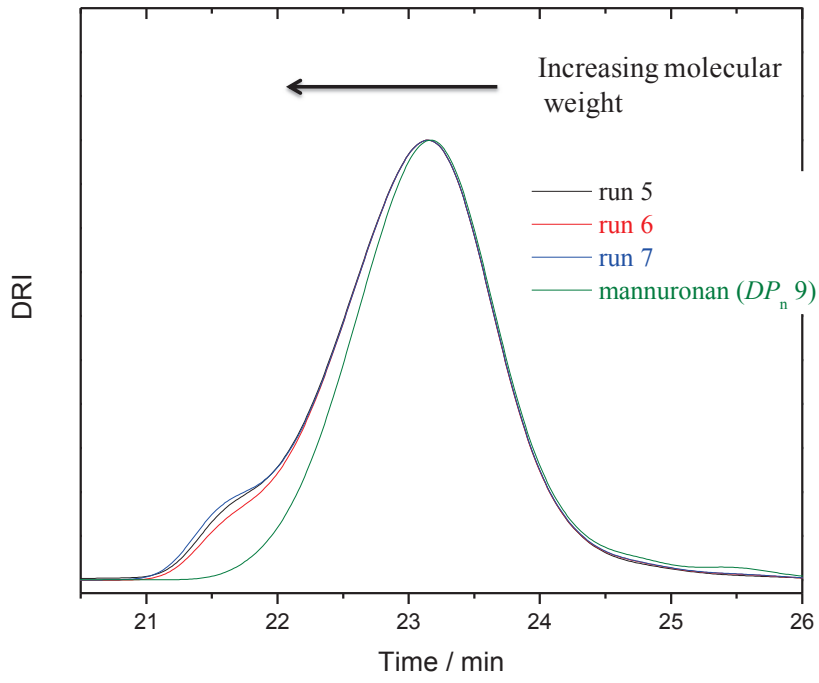

Figure 8.2 *SEC traces for the homopolymerization of **M1** and **M2** (run no. 5-7 in Table 8.3), and for the original oligo(1→4)-β-D-mannuronan. Conditions: 30 °C, injected sample ~5 g L^{-1}, columns Shodex OH pak SB-(Guard + 802 +802.5) HQ.*

8.3.2 Copolymerization of AlgiMERs

Table 8.4 *Summary of copolymerization experiments.*

Run no.	Monomer 1 (mol L^{-1})	Monomer 2			ACPA (mM)	Reaction time (min)	Conv. (%)	d*n*/d*c* [b]	M_n (Da) SEC	$[\eta]_w$ (mL g^{-1})	PDI	*f*(M2) [c] (%)	*F*(M2) [f] (%)	F_m(M2) [c] (%)	Experiment code
		mmol L^{-1}	Nature [a]												
1 [d]	HEMA (0.204)	**M5** (8.90)	MaA_5	MA	0.67	270	75	0.186	200 100	17	1.16 [e]	4.2	11.2 [l]	51.3 [l]	AG10-38-P1
2	HEMA (0.526)	**M5** (27.2)	$ManA_5$	MA	3.09	35	-	-	-	-	-	12.1	-	-	AG10-40-P1
3	HEMAm (0.300)	**M5** (13.0)	$ManA_5$	MA	2.95	220	79	0.192	42 610	25	1.46[h]	4.2	6.4	36.7	AG10-40-P4
4	HEMAm (0.273)	**M4** (8.90)	MaA_5	MAm	1.00	270	65	0.202	40 460	30	1.52[h]	3.2	1.9	12.9	AG10-38-P2
5	HEMAm (0.523)	**M4** (26.9)	MaA_5	MAm	3.10	120	68	0.197	208 200	104	2.05	4.9	4.1	24.9	AG10-40-P3
6	HEMAm (0.576)	**M1** (29.6)	MaA_9	MAm	1.01	270	76	0.186	520 000	199	2.32	4.9	6.6 [l]	50.1 [l]	AG11-09-RP1
7 [f]	HEMAm (0.576)	**M1** (29.6)	MaA_9	MAm	1.01	270	76	0.187	480 000	193	2.41	4.9	6.6 [l]	48.6 [l]	AG11-09-RP1S
8	HEMAm (0.580)	**M1** (30.0)	MaA_9	MAm	1.02	300	86 (76) [g, h]	0.191	743 000	205	2.05	5.0	4.3	38.9	AG11-16-RP1
9	HEMAm (0.576)	**M2** (29.9)	MaA_9	Am	1.01	300	85 (51) [g]	0.188	566 000	211	2.59	4.9	3.0	30.5	AG11-09-RP2
10 [f]	HEMAm (0.576)	**M2** (29.6)	MaA_9	Am	1.01	300	87 (55) [g]	0.188	611 000	218	2.52	4.9	3.1	31.1	AG11-09-RP2S
11	HEMAm (0.580)	**M2** (31.0)	MaA_9	Am	1.02	300	84 (68) [g, h]	0.192	678 000	197	2.40	5.0	4.1	37.5	AG11-16-RP2
12	HEMAm (0.971)	**M3** (18.0)	MaA_{17}	MAm	5.15	120	76	-	- [m]	-	-	-	-	-	AG10-29
13	HEMAm (0.503)	**M3** (21.0)	MaA_{17}	MAm	1.10	270	98 (100) [g, h]	0.185	539 000 [n]	194	2.12	4.0	4.2	52.4	AG11-17-RP1
14	HEMAm (0.386)	**M6** (11.0)	$GulA_{20}$	MAm	1.10	255	82 (76) [g, h]	0.189	575 000 [n]	202	1.95	2.7	2.5	44.1	AG11-17-RP2

General conditions: D_2O / DMSO-d6 (< 2%), pD ≅ 6-7, 60 °C (in run no. 1 and 3 the temperature was 60 °C for 210 minutes and 70 °C afterwards), conversions calculated by NMR. [a] $ManA_x$ and $GulA_x$ represent an oligo(1→4)-β-D-mannuronan and an oligo(1→4)-α-L-guluronan of DP_n = x, respectively; MAm stands for methacrylamide, Am stands for acrylamide and MA stands for methacrylate. [b]: Values calculated according to the formula $dn/dc = F_{m,1}\upsilon_1 + F_{m,2}\upsilon_2$ where: $F_{m,i}$ and υ_i are the weight fraction and the differential refractive index increment of each homopolymer, respectively. [c] *f* and *F* are the molar fraction in the feed; and in the polymer, respectively; F_m is the weight fraction in the polymer. [d]: pD ≅ 8-9. [e] Polymer and AlgiMER peaks partially superimposed . [f]: In NaCl 0.2 mol L^{-1}. [g] Parenthetical values indicate the conversion of monomer 2. [h] Conversion calculated from SEC according to Eq. 8.2. [l] This value is overestimated due to the presence of residual AlgiMER and starting oligosaccharide in the dialyzed / diafiltered sample. [m] Complete gelation. [n] Partial gelation.

8.3.2.1 Preliminary experiments

In order to identify the most promising polymerization condition and comonomer combination(s), five copolymerization reactions were carried out with methacrylate- and methacrylamide-type AlgiMERs in combination with 2-hydroxyethylmethacrylate (HEMA) or 2-hydroxyethylmethacrylamide (HEMAm) (run no. 1-5 in Table 8.4). In particular, we wanted to probe the effect of the nature of the polymerizable ethylenic moiety, the monomer concentration and the size of the AlgiMER on the outcome of polymerization. In all cases, the signal of the ethylenic protons of the comonomers was superimposed in ^{1}H NMR spectra and only a global conversion was calculated. The copolymers were isolated by dialysis or diafiltration followed by freeze-drying, and their composition was determined by ^{1}H NMR in D_2O. Here it should be noted that long dialysis periods were needed to eliminate all unreacted AlgiMER and residual oligoglycuronan even when the nominal molecular weight cut-off of the membrane (e.g. 7000 Da) was much higher than the molar mass of the contaminant (e.g. 1000 Da). This phenomenon is well known for oligoglycuronans and is due to electrostatic repulsion between the molecule and negative charges on the dialysis or diafiltration membrane. [11]

HEMA is a water soluble methacrylate whose homopolymer is only soluble in water up to ~45 repeating units. [12] Higher molecular weight poly(HEMA) swells in water and hydrogels based on this polymer have found a number of biomedical applications (most notably as soft contact lenses). The incorporation of AlgiMER units into poly(HEMA) was expected to yield a water soluble polymer with original properties. Hence, methacrylate glycomonomer **M5** was copolymerized with HEMA in D_2O at 60 °C at two different initial monomer concentrations (run no. 1 and 2 in Table 8.4). In the first case ($c^0_{M,tot}$ = 0.21 mol L^{-1}) the polymerization proceeded smoothly up to 75% conversion with only a minor amount of precipitate forming at the bottom of the tube (possibly poly(HEMA)-rich polymer formed at the early stage of the process). Unfortunately, the pD of the polymerization mixture was basic though (pD≅ 8-9) due to the purification procedure used to purify the glycomonomer (run no. 7, Table 8.1), and that resulted in hydrolysis of the monomers with time upon heating. That was clearly observed from the appearance of well defined sharp peaks from ^{1}H-NMR (Figure 8.3) having the following assignments: δ (ppm) 5.63, 5.30 and 1.86 and these peaks were attributed as before to sodium methacrylate (δ (ppm): 5.65, 5.32 and 1.87 ppm). It is worth

stating that, the degradation of poly(2-aminoethyl methacrylate) was investigated in literature under basic conditions, and hydrolysis was the major reaction taking place. [13]

SEC analysis indicated that a low polydispersity polymer (PDI = 1.16) of M_w 230,000 Da had formed. Still, the retention volume for this polymer was suspiciously high (identical to that of the copolymer from run no. 4 with M_w is 61,000 Da) and its intrinsic viscosity surprisingly low ($[\eta_w]$ = 16.8 ml g^{-1}). Also, such a low PDI value is incompatible with a conventional radical polymerization process. One hypothesis is that water is not a good solvent for this copolymer and the latter assumes a compact conformation leading to a low intrinsic viscosity and high SEC retention volumes. Concerning the low PDI value, it may be an artifact resulting from non-steric interactions between the sample and the stationary phase of the columns. For instance, low molar mass poly(HEMA) obtained by RAFT ($M_n \approx$ 8000 Da) was macroscopically water soluble but did not elute from the aqueous SEC columns used in this study.

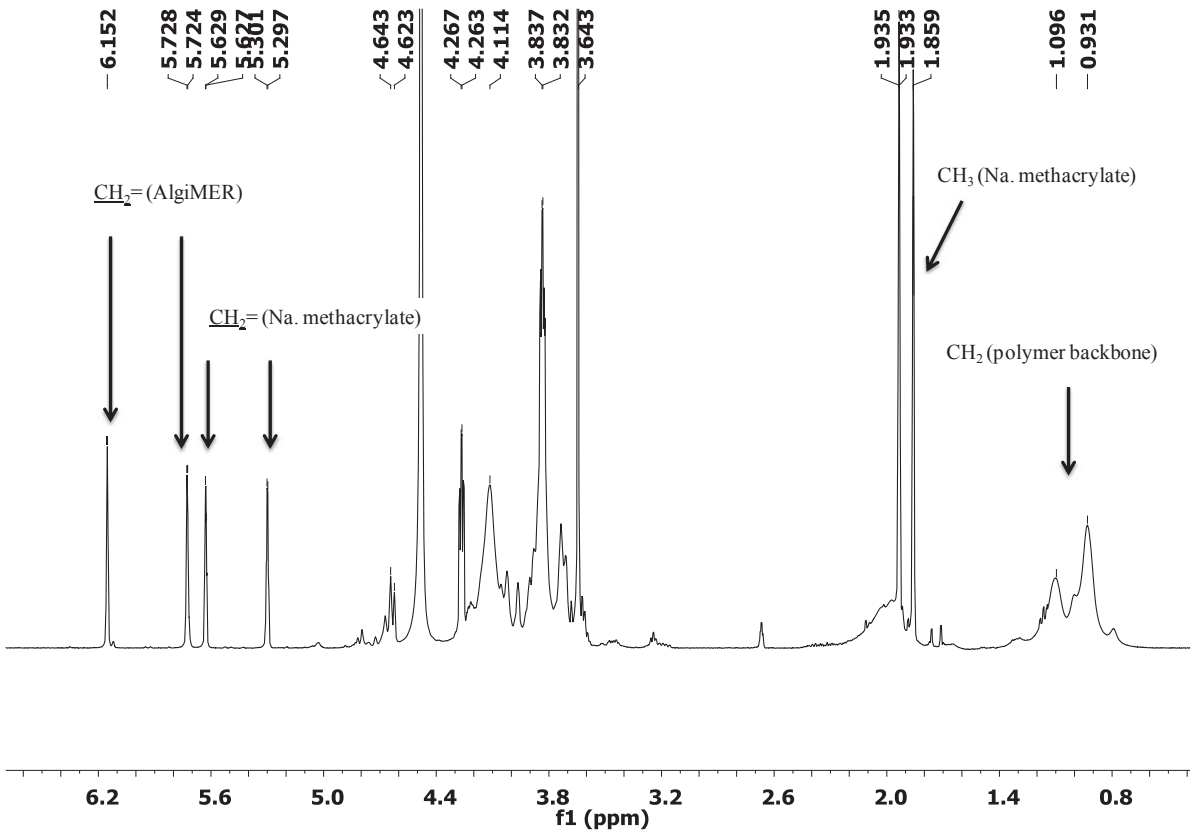

Figure 8.3 *^{1}H NMR spectrum of the copolymerization mixture (pD ≅ 8-9) of **M5** and HEMA after 3.5 hours at 60 °C and one hour at 70 °C (run no. 1, Table 8.4). Conditions: 400 MHz, D_2O (pD ≅ 8-9), 323 K, ns = 50, D1 = 2s.*

When the same copolymerization was conducted at higher monomer concentration ($c^0_{M,tot}$ = 0.55 mol L^{-1}, run no. 2 in Table 8.4) and pD 7 (to prevent hydrolysis of ester bonds), massive precipitation occurred after 30 minutes of reaction. The precipitate did not re-dissolve in water, methanol (a good solvent for poly(HEMA)) nor in a 1:1 mixture of the two. Chemical cross-linking can be safely ruled out since the same AlgiMER and HEMA batches were used for run no. 1 and 2. The absence of bis-methacrylates in distilled HEMA was confirmed by its homopolymerization in methanol (60 °C, 7.5 h, x = 76%; run no.3 in Table 8.1), which led to a soluble polymer with M_n = 110,000 Da (PMMA equivalent). Based on these results, we decided to replace 2-hydroxyethyl methacrylate with the more stable 2-hydroxyethyl methacrylamide (HEMAm), whose homopolymer is fully water soluble. In making this choice, we also expected a better incorporation of the AlgiMER into the copolymer, as judged from the reactivity ratios for the couple methacrylamide / methacrylate (r_1 / $r_2 \cong 3.3$). [14]

In an initial experiment, the same AlgiMER **M5** used in run no. 1 and 2 was copolymerized with HEMAm ($c^0_{M,tot}$ = 0.31 mol L^{-1}; run no 3 in Table 8.4). The reaction was stopped at 79% conversion and SEC analysis indicated that a low molecular weight polymer had been obtained (M_n = 42 000 Da, PDI = 1.46). After dialysis, freeze-drying, and re-dissolution in D_2O, the polymer composition was determined by ^{1}H NMR (Figure 8.4): The molar fraction of AlgiMER (F = 6.4%) was indeed higher than in the initial feed (f = 4.2%). No further investigation was conducted on this system simply because unsatisfactory yield were obtained for the synthesis of methacrylate-type AlgiMERs like **M5** (see chapter 7). In future work though, polymerizations carried out at higher monomer concentration could lead to higher molecular weight copolymers rich in oligoglycuronan grafts.

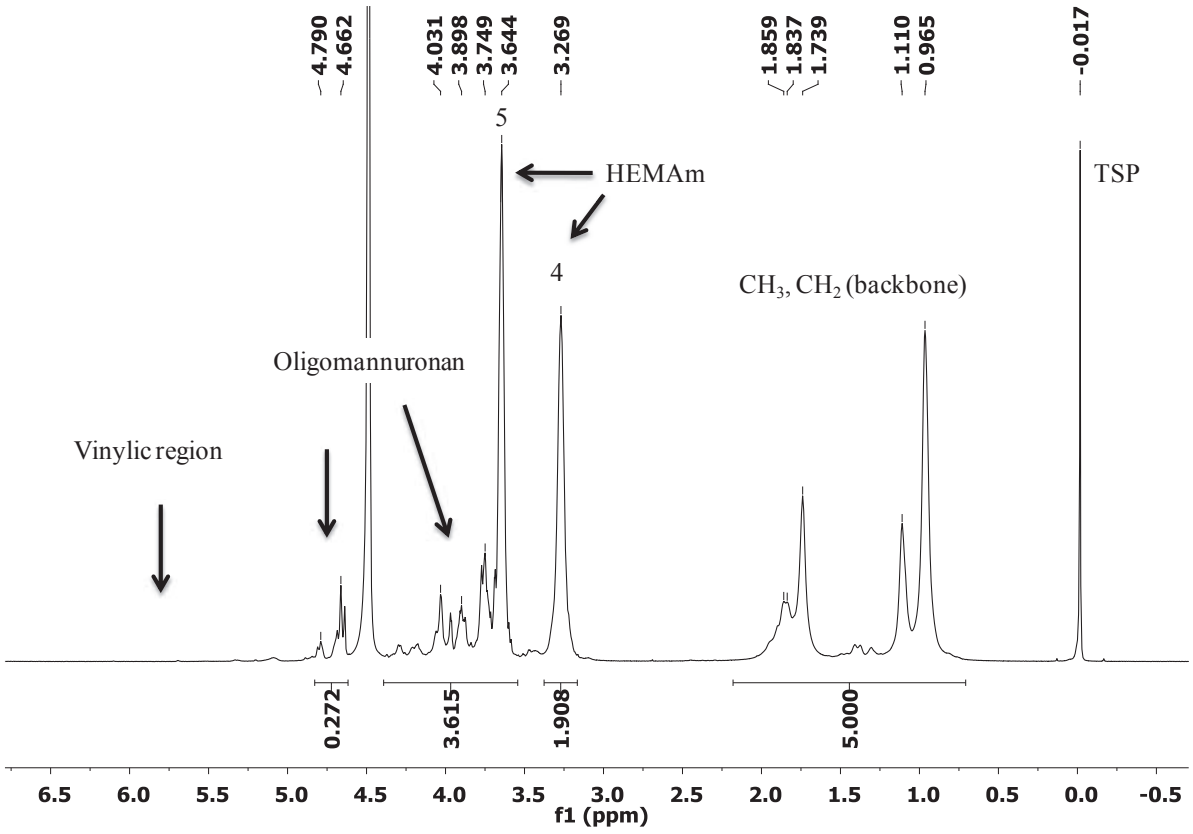

Figure 8.4 *^{1}H-NMR spectrum of poly(HEMAm-co-**M5**) after dialysis (run no 3, Table 8.4). Conditions: 4.7% w/w, D_2O, 323 K, ns 100, D1 10s.*

The last combination to be tested was two methacrylamide-type comonomers (**M4** and 2-hydroxyethyl methacrylamide) at two different concentrations ($c^0_{M,tot}$ = 0.28 mol L^{-1} or 0.55 mol L^{-1}; run no. 4 and 5 in Table 8.4). As expected, the polymerization with a higher initial monomer concentration was the fastest (x = 68% in two hours vs. x = 65% of 4.5 h) and the one leading to the highest molecular weight (M_n = 208 000 Da instead of 40 000 Da). Also, the proportion of AlgiMER units incorporated into the polymer was comparable to that in the feed for run no 5 ($f_{\mathbf{M4}}$ = 4.9%, $F_{\mathbf{M4}}$ = 4.1%), but only ~2/3 of it for run no. 4 ($f_{\mathbf{M4}}$ = 3.2%, $F_{\mathbf{M4}}$ = 1.9%).

8.3.2.2 (Meth)acrylamide-type comonomers

Based on the results from the preliminary experiments, we decided to focus our attention on the copolymerization of (meth)acrylamide-type comonomers with an initial global monomer concentration ≥ 0.5 mol L^{-1}. The study was extended to longer mannuronan-derived (DP_n = 9 and 17) and guluronan-derived (DP_n = 20) AlgiMERs, to an acrylamide-

type AlgiMER (**M2**) and to a reaction medium with a higher ionic strength (run no. 6-7 and 9-10 in Table 8.4).

Firstly, 2-hydroxyethyl methacrylamide was copolymerized with a methacrylamide-type AlgiMER (**M1**; mannuronan, $DP_n = 9$) in D_2O and in NaCl 0.1 mol L^{-1} (run no. 6 and 7): In both cases 76% conversion was achieved in 270 min and a high molar mass polymer was obtained ($M_n \cong 500\ 000$ Da; PDI ≅ 2.4). Secondly, the experiments were repeated with an acrylamide-type AlgiMER (**M2**; mannuronan, $DP_n = 9$): Once again, the same overall conversion (85-86%) and molar mass ($M_n \cong 600\ 000$ Da; PDI ≅ 2.5) were obtained in the two cases (run no. 9 and 10). Moreover, for the latter experiments it was possible to calculate the individual monomer conversion from NMR and it was found that only 51-55% of **M2** had reacted, irrespective of the ionic strength of the medium. This was confirmed by the composition analysis of the copolymer, in which the molar fraction of AlgiMER was only ~60% of the value in the feed ($f_{\mathbf{M2}} = 4.9\%$, $F_{\mathbf{M2}} = 3.0\%$). Note that significantly higher molar masses were achieved in run no. 6-7 and 9-10 than in run no. 5 (Table 8.4): This was the combined result of the longer AlgiMER used ($DP_n = 9$ vs. $DP_n = 5$) and of the lower concentration of initiator (1.0 mmol L^{-1} vs. 3.1 mmol L^{-1}). As a result, when methacrylamide-type AlgiMER **M1** was copolymerized with HEMAm, the resulting glycopolymer contained ~50% by mass of oligosaccharide.

The two couples of experiments just described suggest that the ionic strength of the medium has no significant effect on polymerization kinetics (at least for the feed ratios used in this study) and that HEMAm is incorporated preferentially over acrylamide-type AlgiMERs. To further corroborate this finding, a kinetic study was carried out in which an internal standard (methyl α-D-glucoside) was added to the reaction mixture of HEMAm and **M1** (or **M2**) and samples were drawn at intermediate reaction times for analysis (run no. 8 and 11 in Table 8.4). Since the ethylenic protons of HEMAm and **M1** have identical chemical shifts in ^{1}H NMR, individual monomer conversions were calculated by SEC as described in the Analyses section (Figure 8.5).

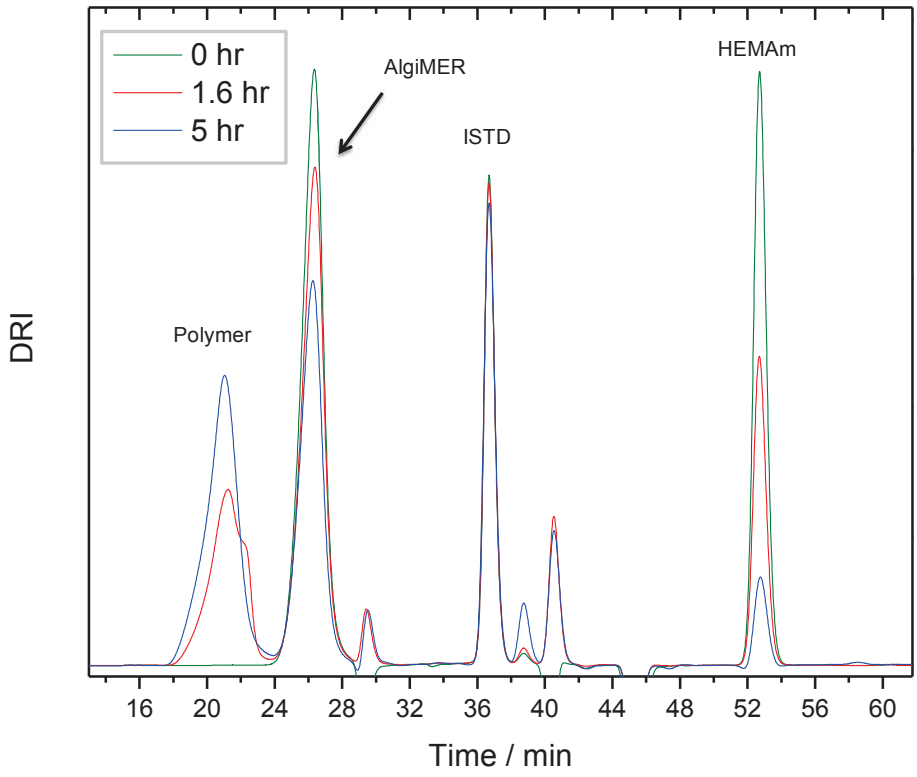

Figure 8.5 *Evolution of the copolymerization kinetics of **M1** with HEMAm at t = 0 h (green), t = 1.6 h (in red), and t = 5 h (in blue). Note that the spectra are area normalized with respect to the internal standard peak (run no.8 , Table 8.4). Notice the disappearance of the HEMAm and **M1**, and the appearance of the polymer peak.*

Figure 8.6 shows the evolution of conversion (x) and polymer composition (F_m) with time obtained with this experimental setup. Both AlgiMERs reacted slower than HEMAm but were incorporated in the copolymer since the early stages of the polymerization. Still, the incorporation of methacrylamide-derivative **M1** was plainly superior, especially at the very beginning of the process. This aspect of the copolymerization is very important since it ensures that macromolecules formed at different stages of the process have similar compositions and physico-chemical properties (neglecting the effect of different molar masses). Similar results were obtained by Klimchuk et al. [15] for the copolymerization of methacrylamide and acrylamide, where the reactivity ratios determined according to the method of Kelen and Tudos were $r_1 = 1.10$ and $r_2 = 0.74$. [16] Figure 8.7 shows the first order kinetic plots for the two copolymerizations: The consumption of each monomer obeyed a pseudo first order plot and there was no inhibition period. This confirmed that the removal of the inhibitor (BHT) from the HEMAm stock solution by simple filtration at 0.22 μm was

effective. Finally, it was reassuring to see that the rate of polymerization of HEMAm was the same in the two cases, confirming that the experiment was reproducible (the mole fraction of AlgiMER in the feed being too small to make a difference).

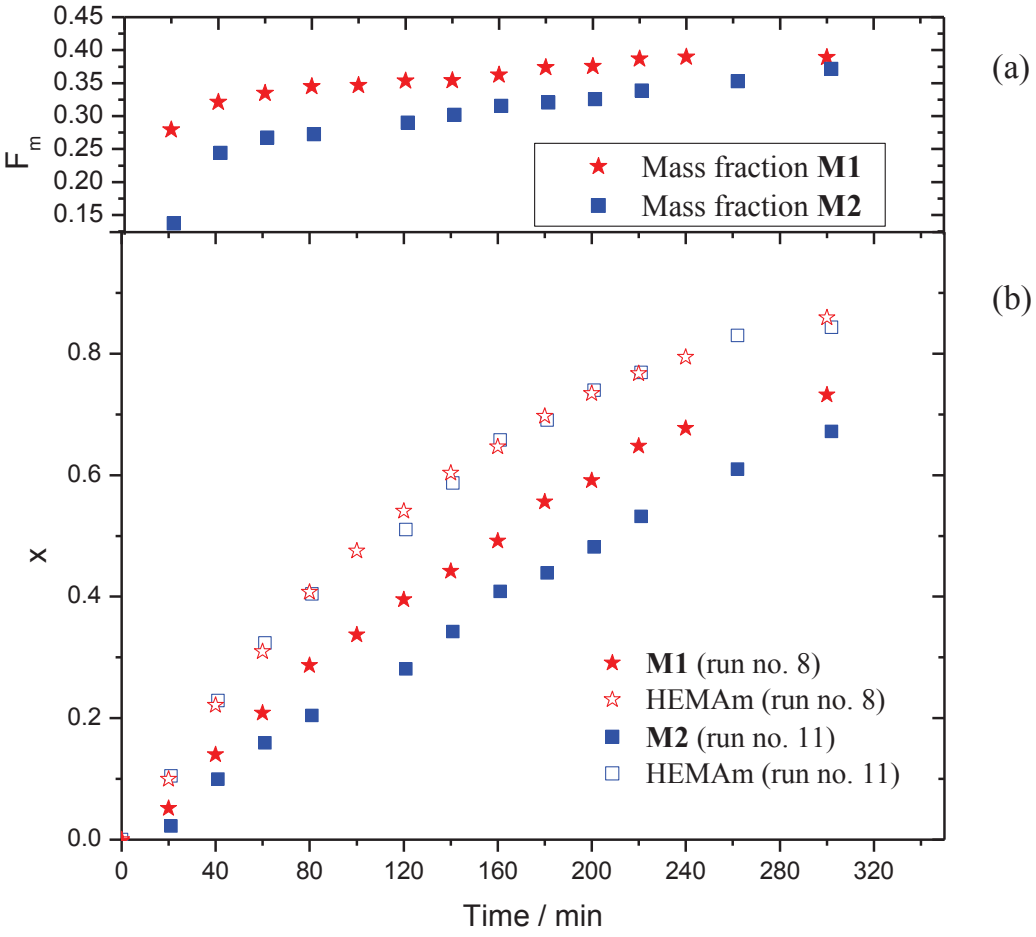

Figure 8.6 *Evolution of (a) copolymer composition F_m and (b) conversion x with time for the copolymerization of HEMAm with **M1** or **M2** at 60 °C (run no. 8 and 11 in Table 8.4).*

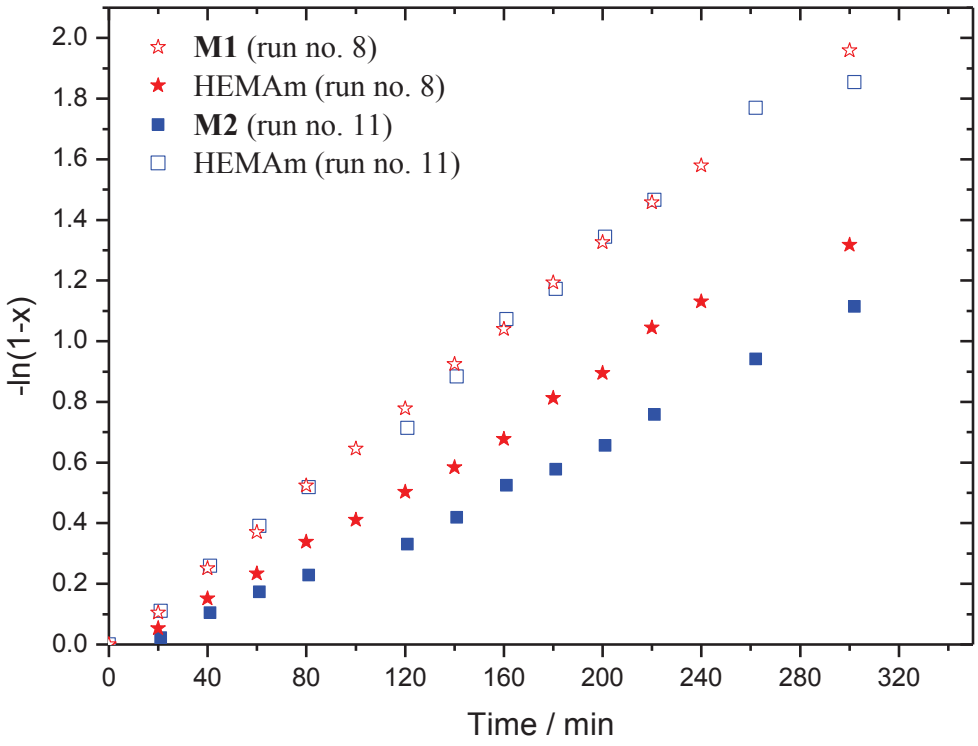

Figure 8.7 *First order kinetic plots for the copolymerization of HEMAm and **M1** or **M2** at 60 °C (run no. 8 and11 in Table 8.4).*

Having established that among the tested combinations methacrylamide comonomers are those performing best, we extended our study to the use of longer AlgiMERs (run no 12-14 in Table 8.4). Surprisingly, the copolymerization of **M3** (DP_n 17) with HEMAm led to complete gelation after 2 hours of reaction ($c^0_{M,tot}$ = 1 mol L^{-1}; run no. 12). To better understand this phenomenon, the homopolymerization of HEMAm was carried out at the same temperature (run no 2 in Table 8.3) and a water soluble polymer formed that was isolated by precipitation in excess acetone (x = 80%, M_n 232 000 Da, PDI 1.74). Our attention was then turned to the batch of AlgiMER used for the copolymerization (Table 8.1): By re-examining the ^{1}H-NMR of **M3** (A) we noticed minor ethylenic peaks with a chemical shift slightly different from those of the main product. Since this batch of AlgiMER had been prepared reacting a big excess of methacrylic anhydride with the 1-deoxy-1-amino alditol of oligomannuronan (DP_n 17) at pH 10, partial esterification of the hydroxyl groups might have taken place, thus leading to formation of a crosslinking monomer. Nevertheless, when a different batch of **M3** (B) and a lower monomer concentration was used, partial gelation was still observed (x = 98%; run no. 13). In this case, the AlgiMER had been obtained by reacting acryloyl chloride

with the usual 1-deoxy-1-amino alditol at pH 9.5, and multiple substitution can be safely ruled out (the acid chloride is hydrolyzed by water before reacting with the hydroxyl groups of the oligosaccharide). Also, when a similar polymerization was conducted with guluronan-derived AlgiMER **M6** (DP_n 20; also prepared with acryloyl chloride), the amount of gel formed was negligible (x = 82%; run no. 14). One hypothesis is that gelation is a consequence of chain transfer to the polymer, and in particular to its oligosaccharide graft chains. In fact, the proton in position 5' of (1→4)-β-D-mannuronan and (1→4)-α-L-guluronan chains is particularly acidic (Scheme 8.1) and is involved in the base-catalyzed β-elimination reaction observed for glycuronans. [17] In a similar way, it may be abstracted by a propagating radical and give rise to a new radical in the middle of an existing chain. Eventually, two of these radicals will couple and form a cross-link. The probability of chain transfer to a given polymer chain will obviously increase with its molar mass and with the size of the oligoglycuronan graft chains. The water soluble fractions from run no. 13 and 14 were recovered by filtration on a 1.2 μm filter and analyzed for conversion and molecular weight (both determined by SEC). In the two cases a high molar mass polymer had formed having $M_n \cong$ 550 000 Da. After dialysis and freeze-drying, the composition of the two glycopolymers was determined by ^{1}H NMR (Figure 8.8 and Figure 8.9) and it was found that they contained 52% and 44% by mass of AlgiMER units, respectively.

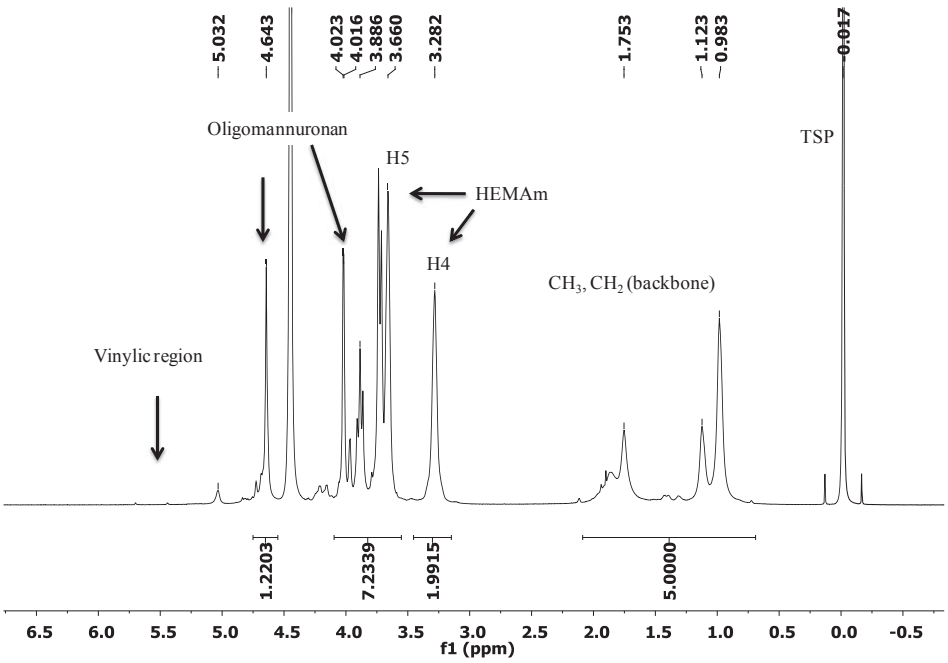

Figure 8.8 *[1]H-NMR spectrum of poly(HEMAm-co-**M3**) obtained by conventional radical copolymerization (diafiltered sample; run no. 13 in Table 8.4). Conditions: 2.3% w/w in D_2O, 328 K, ns 800, D1 10s.*

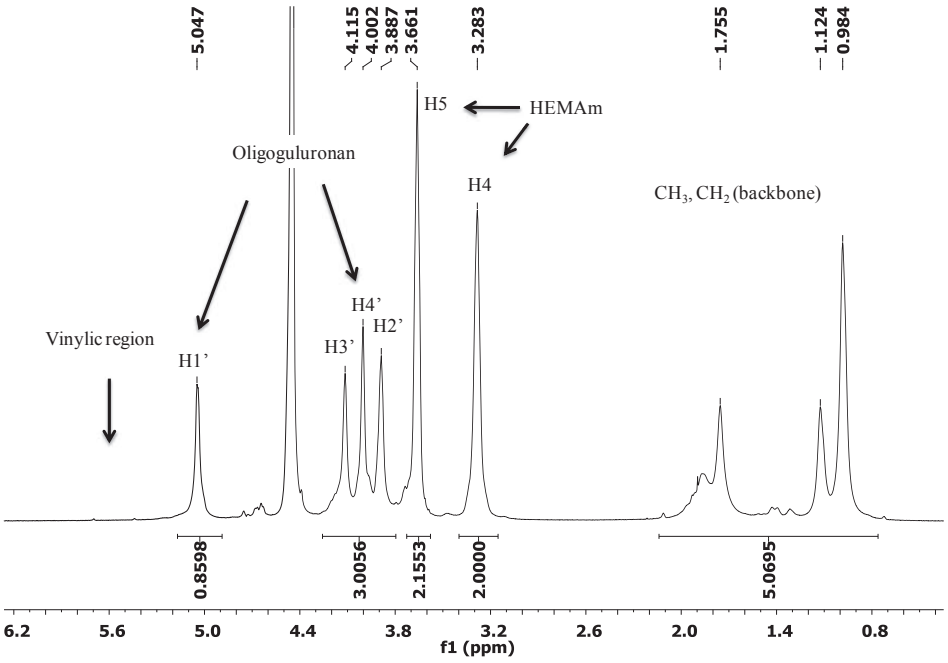

Figure 8.9 *[1]H-NMR spectrum of poly(HEMAm-co-**M6**) obtained by conventional radical copolymerization (diafiltered sample; run no14 in Table 8.4). Conditions: 1.1% w/w in D_2O, 328 K, ns 800, D1 10s.*

8.3.3 Rheological properties of copolymer solutions and gels

The rheological properties of the high molecular weight copolymers obtained in run no 13 and 14 (Table 8.4) were investigated both in solution and after gelation with Ca^{2+} ions. To this aim, semi-dilute solutions in de-ionized water and in NaCl 0.1 mol L^{-1} were prepared at ~4 times the critical overlapping concentration (C^*) as estimated from their intrinsic viscosity in $NaNO_3$ 0.1 mol L^{-1} ($C^* \approx 1/[\eta]$). The latter was approximated by $[\eta]_w$ obtained in SEC-IV-MALLS analyses ($[\eta] \approx \eta_{sp}/c$ at low concentration). To avoid solvent evaporation during the measurement, a film of silicon oil was placed around the rheometer plate. Gels were obtained by preparing semi-dilute glycopolymer solutions in deionized water and by dialyzing them against $CaCl_2$ 0.5 mol L^{-1} for 28-48 h. They were then recovered from the dialysis cassettes by cutting off the membrane with a scalpel. The resulting material was either punched into a disk (∅ = 2 cm, h ≅ 0.25 cm) with the same diameter of the rheometer plate (poly(HEMAm-*co*-**M6**)), or directly transferred onto the same plate as a film (poly(HEMAm-*co*-**M3**). A summary of the samples used for rheological characterization is reported in Table 8.5.

Table 8.5 *Summary of the samples used for rheological characterization.*

Polymer	Run no. (Table 8.4)	Oligoglycuronan	Concentration (g L^{-1})		Sample type	Experiment
			water	NaCl 0.1 mol L^{-1}		
poly(HEMAm-*co*-**M6**)	14	$GulA_{20}$	24.0	23.0	solution	Flow, dynamics
poly(HEMAm-*co*-**M6**)	14	$GulA_{20}$	18.4	-	gel	Dynamics
poly(HEMAm-*co*-**M3**)	13	$ManA_{17}$	24.0	27.0	solution	Flow, dynamics
poly(HEMAm-*co*-**M3**)	13	$ManA_{17}$	18.0	-	gel	Dynamics
poly(HEMAm)	1[a]	-	20	20	solution	Flow, dynamics

a: Table 8.3

8.3.3.1 Polymer solutions

The variation of the steady state viscosity of the polymer solutions was monitored as a function of the shear rate (Figure 8.10). In the shear rate range tested, all solutions behaved as Newtonian fluids (constant viscosity). Here it is worth noting that the samples were only tested at low shear rate ($\dot{\gamma} \leq 10\ s^{-1}$) to check eventually for loose inter chain interactions.

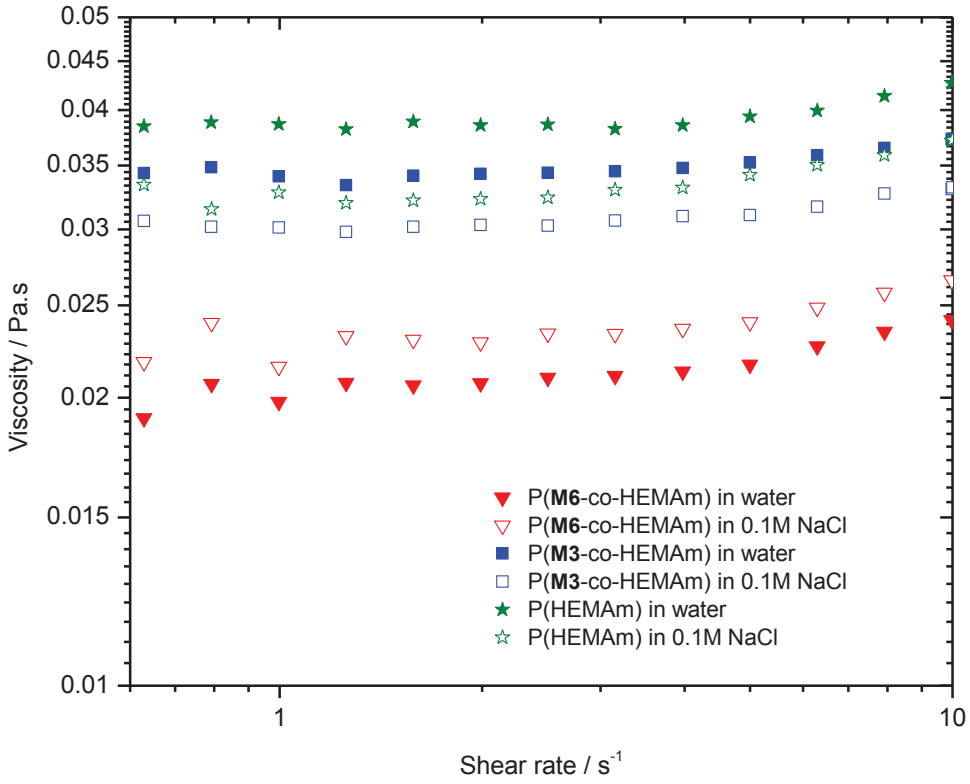

Figure 8.10 *Viscosity as a function of the shear rate for poly(HEMAm-co-**M6**), poly(HEMAm-co-**M3**) and poly(HEMAm) solutions. Full symbols: water. Empty symbols: 0.1 mol L^{-1} NaCl.*

The viscosity (extrapolated at zero shear rate) is higher for poly(HEMAm) compared with the glycopolymers and that is in relation with its higher molecular weight. Besides, its lower viscosity observed in the presence of external salt (compared to its viscosity in H_2O) may be related to the thermodynamic quality of the solvent.

Although the glycopolymers had the same molecular weight distribution and intrinsic viscosity and were dissolved at nearly the same concentration, poly(HEMAm-*co*-**M3**) showed higher viscosities than poly(HEMAm-*co*-**M6**) in both water and in NaCl solutions (even with nearly the same intrinsic viscosities). The only difference between both copolymers is the higher degree of branching in the case of **M3** (see Table 8.4). Even though its molecular weight is nearly third that of poly(HEMAm), yet the glycopolymer's (carrying mannuronan grafts **M3**) high viscosity could be due to electrostatic repulsive forces resulting in some chain expansion (in water). Also, this copolymer gives a lower viscosity in the presence of salt, as expected for a polyelectrolyte due to electrostatic screening which minimizes repulsive forces and results in a smaller molecular volume. [18] Some chain stiffness or/and interchain

attractions may exist in solution increasing the viscosity when compared with the homopolymer with a much higher MW.

The copolymer carrying guluronan graft chains (**M6**) revealed lower viscosities with an "anti-polyelectrolyte" behavior (i.e. higher viscosities in the presence of salt). The comparison of the molecular weight of poly(HEMAm-*co*-**M6**) with that of poly(HEMAm) could rationalize its lower viscosity. However, its lower viscosity compared to poly(HEMAm-*co*-**M3**) could be due to its poorer expansion influenced by its lower degree of branching. In addition, the detected increase in viscosity in the presence of salt could be attributed to interactions between side chains at C > C*. The latter interaction could be attributed to H-bonding which is well known with poly(guluronan) segments. [19] Further studies are needed though.

Oscillatory experiments were carried out to measure the variation of viscoelastic moduli (G', G'') with frequency for the graft-copolymer solutions in water and in NaCl 0.1 mol L^{-1} (only poly(HEMAm-*co*-**M3**)). Unfortunately, the oligoguluronan-derived copolymer gave G' values that were too low to be measured with our rheometer (data not shown). As shown in Figure 8.11, in all cases the viscoelastic moduli increased with increasing frequency and G'' was higher than G' up 10 Hz (highest frequency tested). For poly(HEMAm-*co*-**M3**), a higher ionic strength led to a higher storage modulus possibly due to the increased entanglement of polymer chains brought about by the electrostatic screening. Besides, G'' was slightly lower in the presence of salt as it was observed for the steady state viscosity.

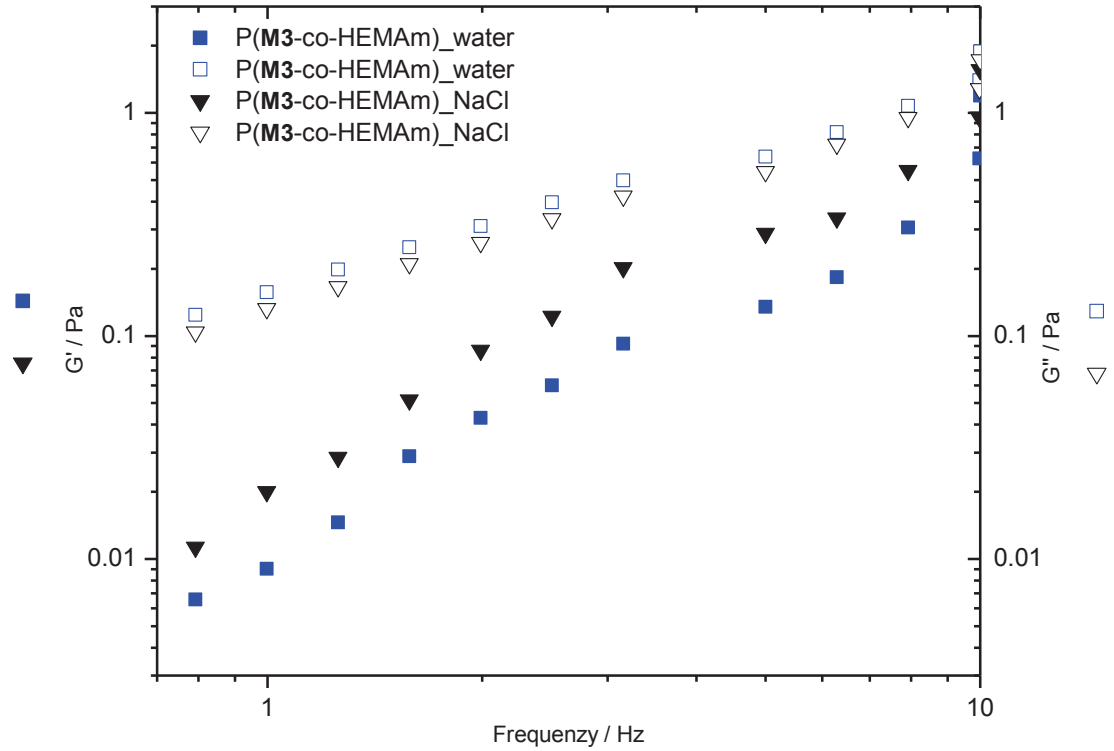

Figure 8.11 *Variation of the dynamic moduli (G', G") with frequency for poly(HEMAm-co-**M3**) and poly(HEMAm-co-M**6**) solutions in water and in NaCl 0.1 mol L^{-1}. G' (Full symbol) and G" (Empty symbol).*

8.3.3.2 Hydrogels

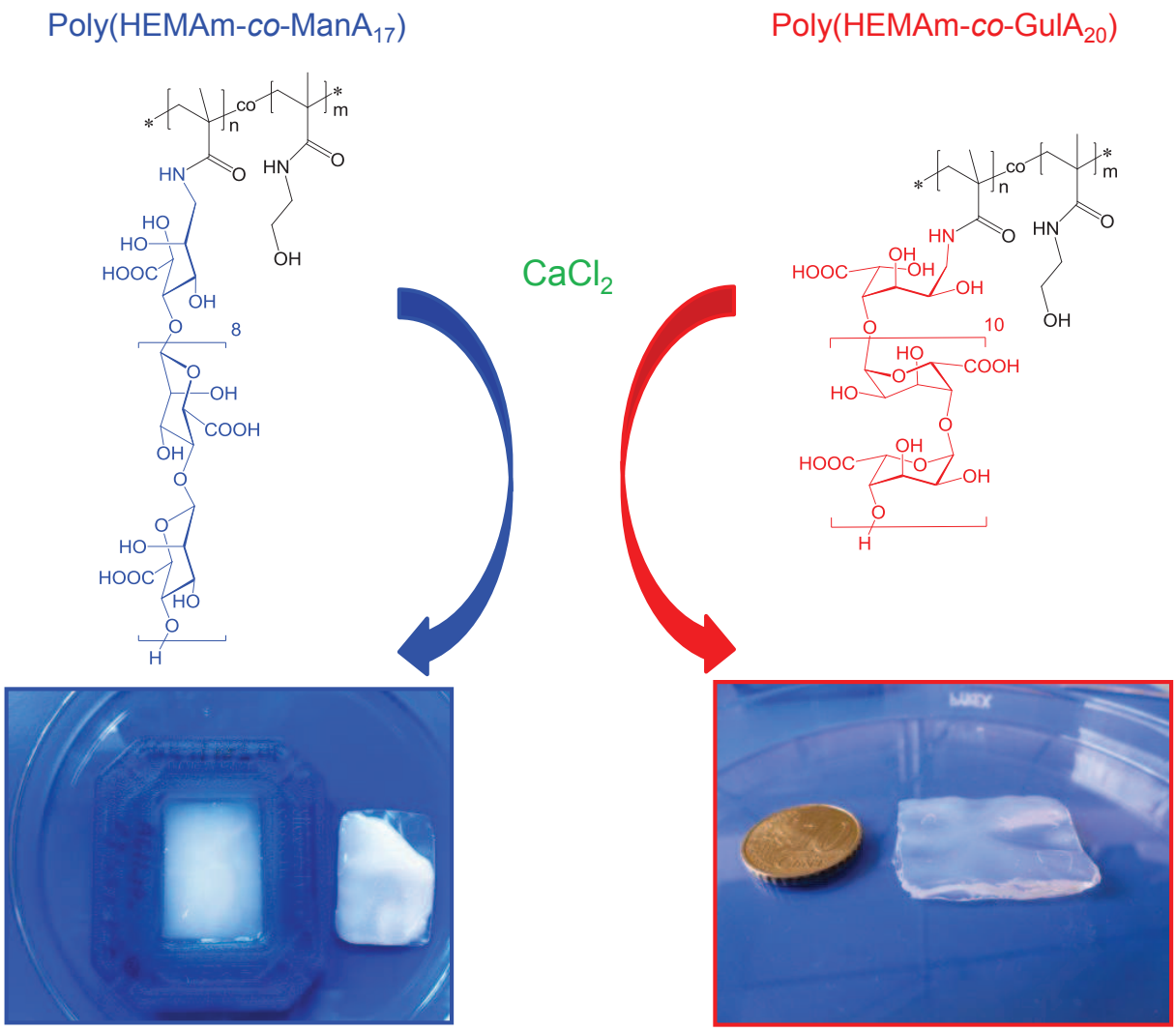

Figure 8.12 *Gels obtained after dialyzing graft-copolymer solutions against $CaCl_2$.*

It is well known that (1→4)-α-L-guluronan molecules containing at least ~20 repeating units have a strong affinity for divalent cations and form stable complexes with them. [20] For instance, this phenomenon is at the base of alginate gelation. Poly(HEMAm-*co*-**M6**) is a high molar mass glycopolymer bearing oligo(1→4)-α-L-guluronan graft chains of DP_n 20 ($F_{m,GulA}$ = 44%; run no. 14 in Table 8.4). It was designed as a neo-alginate to see whether a hybrid polymer could mimic the gelation behavior of alginates while offering most of the advantages of a synthetic polymer (i.e. controlled synthesis, incorporation of different comonomers, tuning of physico-chemical properties). Figure 8.12 shows the hydrogels obtained with a glycopolymer carrying mannuron (poly(HEMAm-*co*-**M3**)) or guluronan grafts

(poly(HEMAm-*co*-**M6**)): the first is a loose opaque paste, whereas the second is a transparent self-standing gel from which a disk was punched out (Figure 8.13).

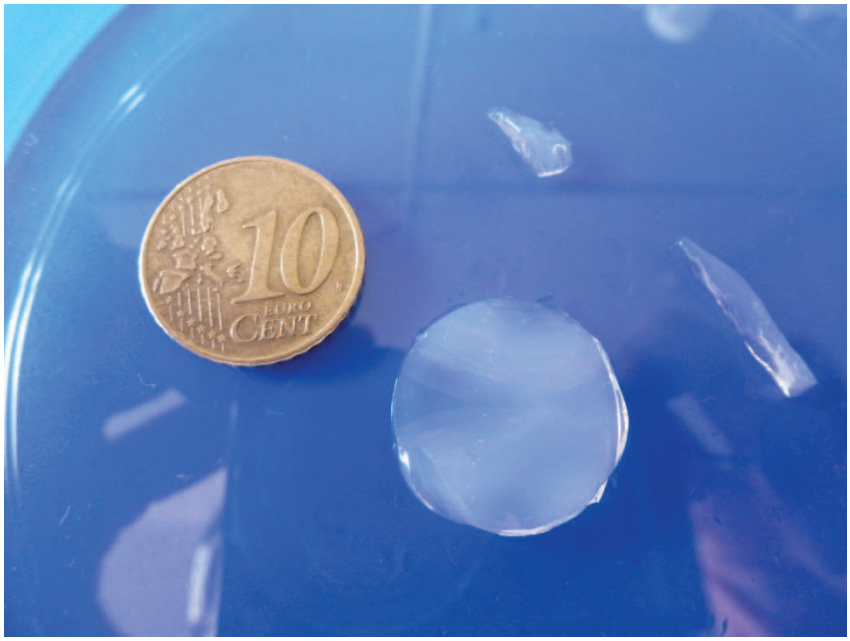

Figure 8.13 *Disk of hydrogel obtained from poly(HEMAm-co-**M6**) used for rheological characterization.*

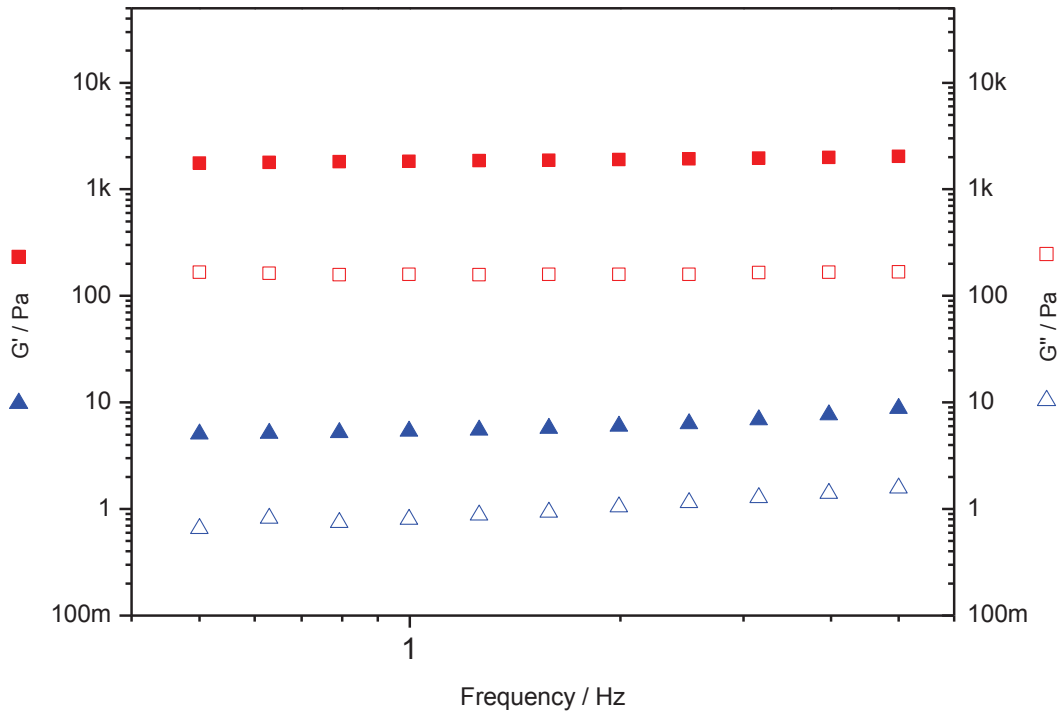

Figure 8.14 *Variation of G' and G'' with frequency for the gels obtained from poly(HEMAm-co-**M6**) (red) and poly(HEMAm-co-**M3**) (blue).*

For both samples, *G*' and *G*" were found to be independent of frequency and the storage modulus was ~11 times the loss modulus, confirming the rubbery behavior (Figure 8.14). Also, the viscoelastic moduli of the guluronan-derived gel were ~300 times higher than those of the mannuronan-derived gel. A sample of the former was weighed in a fully swollen state (m_{sw} = 0.926 g) and after extensive drying (17 weeks at ambient temperature; m_d = 0.133 g). From this data a swelling ratio σ at equilibrium was calculated as follows:

$$\sigma = (m_t/m_d) - 1 = 6.0 \qquad (8.5)$$

In other words, indicating that the gel was made up of ~80-85% water. The drying of the gel was essentially irreversible and re-hydration in aqueous solutions of $CaCl_2$ (0.5 mol L^{-1}), NaCl (1 mol L^{-1}) or Na-EDTA for one week failed. One possibility is that swelling was prevented by strong hydrogen bonding between chains.

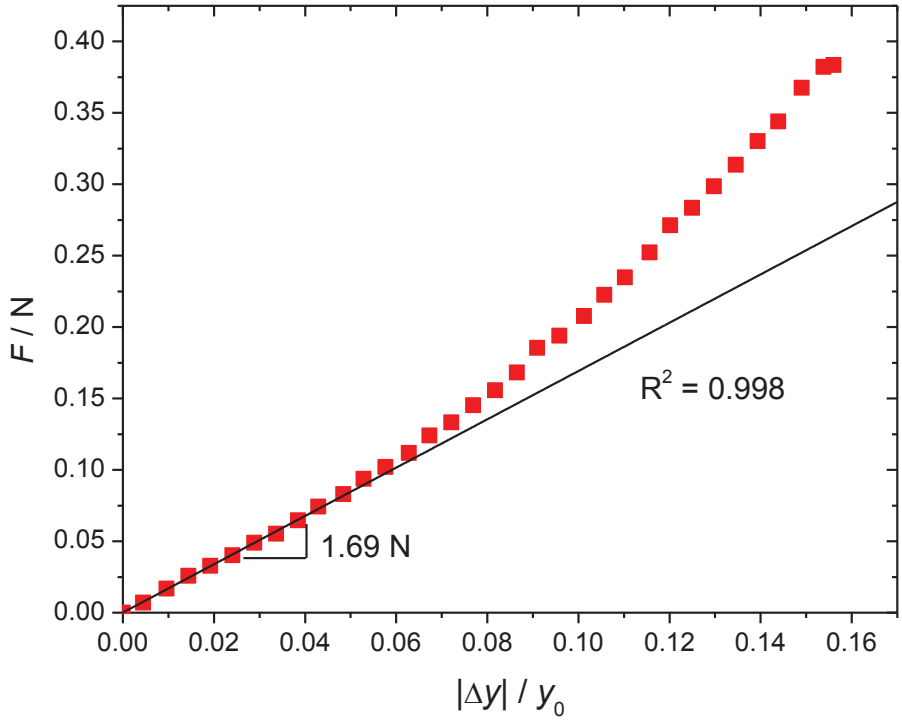

Figure 8.15 *Variation of the force applied by the gel of poly(HEMAm-co-**M6**) under compression.*

The stiffness of the gel obtained from poly(HEMAm-*co*-**M6**) was further investigated with a compression experiment. Hence, a gel disk of surface area S = π r^2 = 3.14 × 10^{-4} m^2 was placed between the two parallel plates of the rheometer. The rheometer started squeezing the

gel while recording the backward force exerted (Figure 8.15). The tangent at the origin of the curve F vs. $|\Delta y|/y_0$ was found to be 1.7 N and the elastic modulus E was calculated as:

$$E = \tan(|\Delta y| / y_0) / S = 1.7 \text{ N} / (3.14 \times 10^{-4} \text{ m}^2) = 5400 \text{ Pa} \quad (8.6)$$

It is worth noting that under similar conditions, an alginate with $F_G = 45\%$ and $M_w = 493\,000$ Da gives a gel with an elastic modulus of 28 000 Pa. [21] In that case though, the crosslinking points are connected by relatively stiff glycuronan chains with a much smaller conformational freedom than poly(HEMAm). By comparing the Young's modulus E and the storage modulus G' obtained from compression and shear experiments, respectively, one can have information about the homogeneity of the formed gel. For short term macroscopic deformations it holds that: [22]

$$E = 2(1 + \nu)\, G' \quad (8.7)$$

where ν is Poisson's ratio. For an ideal rubber, ν = 0.5 and $E = 3\,G'$. In our case $E = 3.06\,G'$ at 0.5 Hz (Figure 8.14), which confirms the formation of a homogenous gel. Here, it is worth recalling that the homogeneity of homoglycuronan gels is strongly influenced by the concentration and molecular mass of the polymer and by the concentration of $CaCl_2$ in the dialysis buffer.[21] In our case, no optimization of the gelation conditions was carried out.

8.4 Take home messages

Several messages could be conveyed from the conventional radical polymerization of AlgiMERs:

i. AlgiMERs did not homopolymerize in aqueous solution even in the presence of salt.

ii. AlgiMERs were incorporated in polymers via their copolymerization with smaller comonomers (HEMAm, HEMA).

iii. High molecular weight copolymers (M_w ~ 1.5 million Da) were obtained when the total concentration of both monomers was ~ 0.5 mol L^{-1}. The ionic strength of the polymerization mixture has marginal effects on the molecular weight of the polymer

iv. AlgiMERs were incorporated in the copolymer since the beginning of the polymerization where methacrylamide derived AlgiMERs were better incorporated than their acrylamide analogues. In all cases, the comonomer (HEMAm) was preferentially incorporated in the polymer.

v. Copolymers bearing long AlgiMER grafts (guluronan DP_n = 20) resulted in stable, homogenous, and self standing hydrogels in the presence of $CaCl_2$ (0.5 mol L^{-1}).

Appendix 8.A Selected NMR spectra

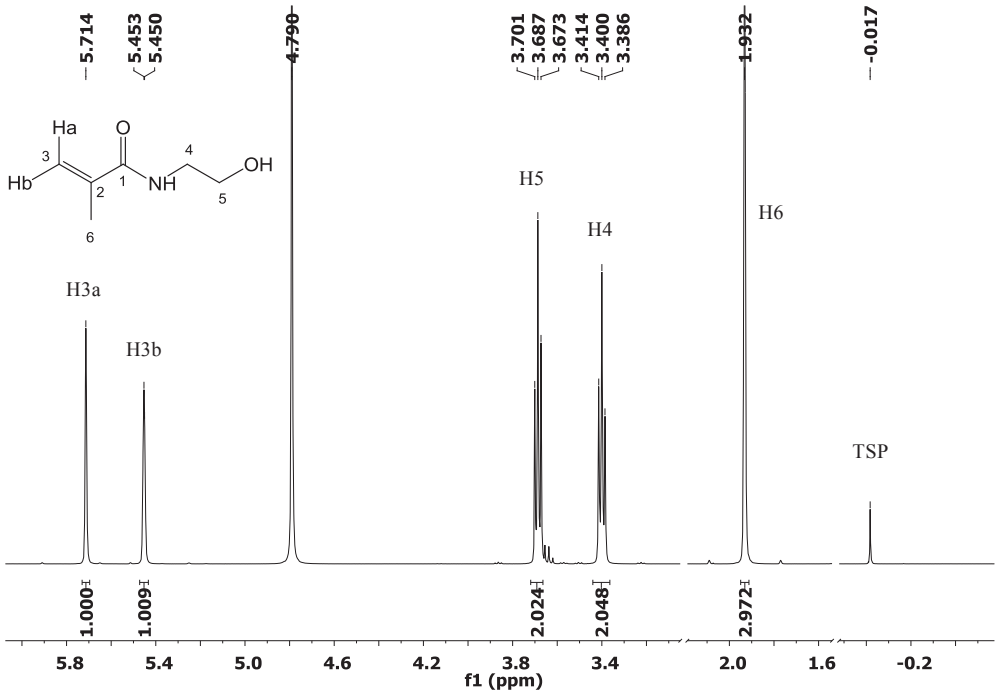

Figure 8.16 *^{1}H-NMR spectrum of HEMAm. Conditions: 6 % w/w, D_2O, 298 K, ns 16, D1 2s.Two cuts in the axis should be noted.*

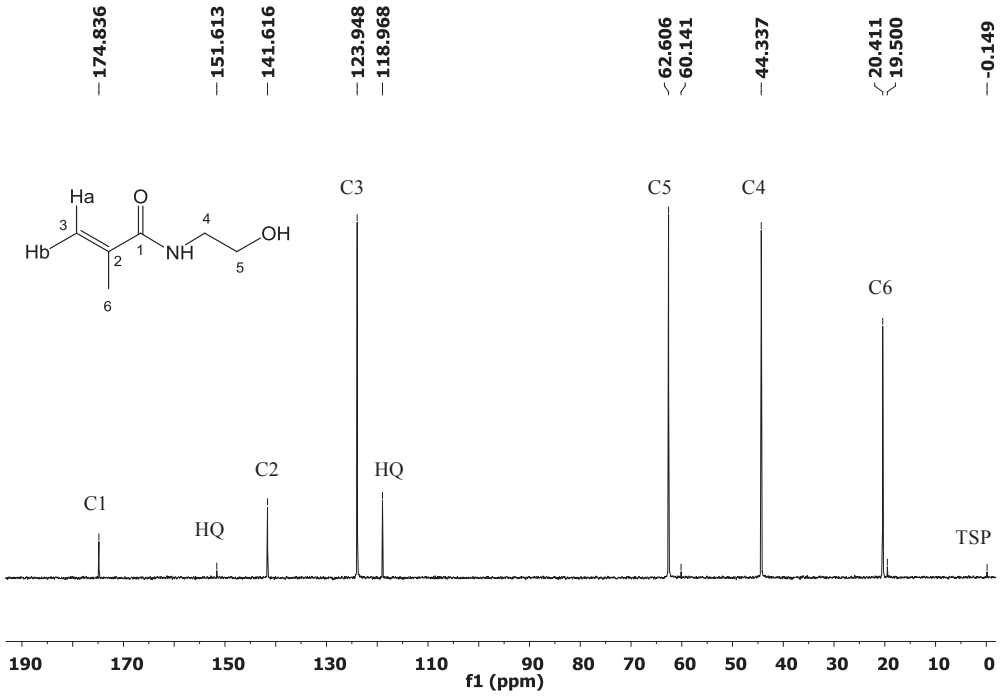

Figure 8.17 *^{13}C-NMR spectrum of HEMAm. Conditions: 6% w/w, D_2O, 283 K, ns 1K, D1 2s. HQ is hydroquinone, added to prevent spontaneous polymerization.*

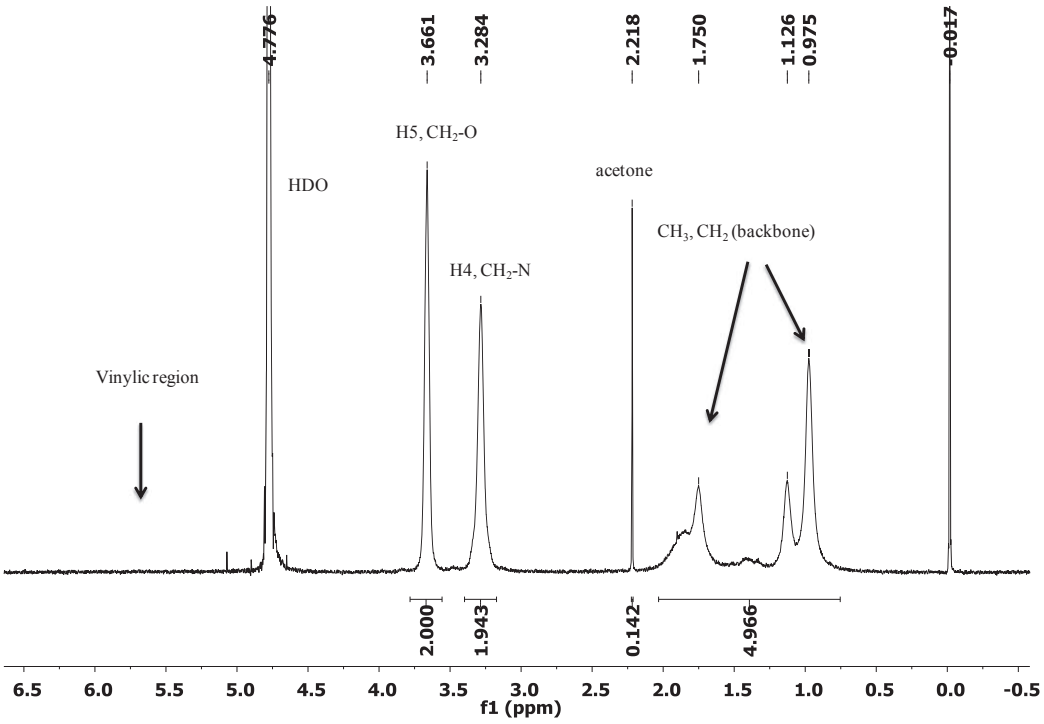

Figure 8.18 *^{1}H NMR spectrum of poly(HEMAm) purified by precipitation in acetone (run no. 2, Table 8.3). Conditions: 400 MHz, D_2O, 298 K, 1 %w/w, ns 16, D1 2s.*

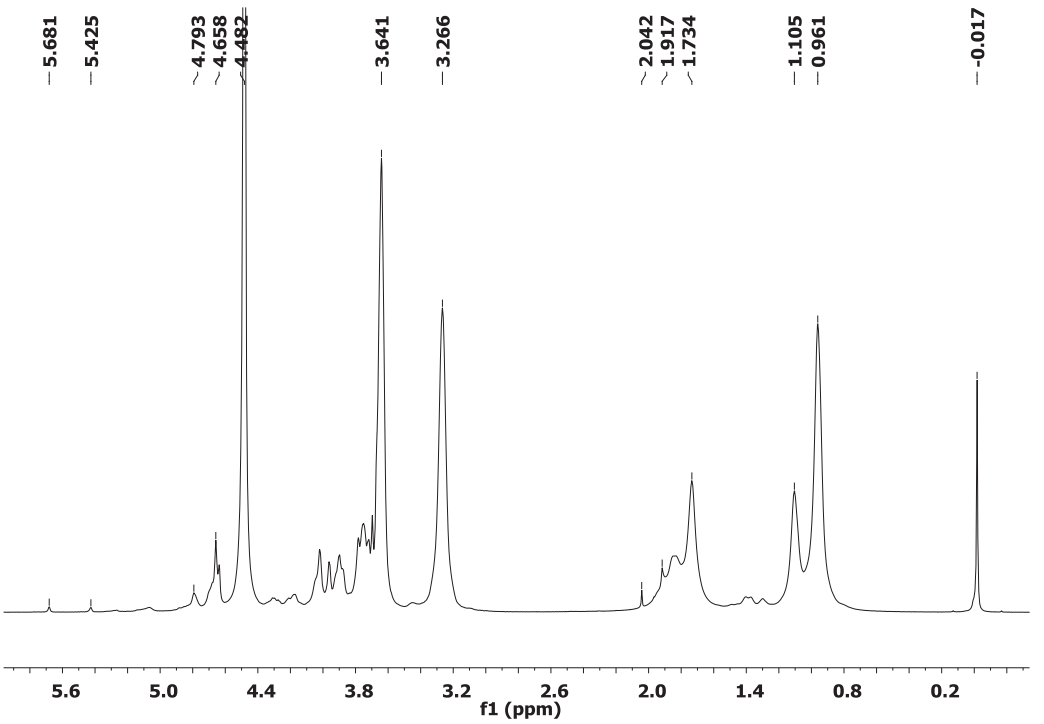

Figure 8.19 *^{1}H NMR spectrum of poly(HEMAm-co-**M4**) after dialysis (run no. 5, Table 8.4). Conditions: 400 MHz, D_2O, 323 K, 8 %w/w, ns 100, D1 2s.*

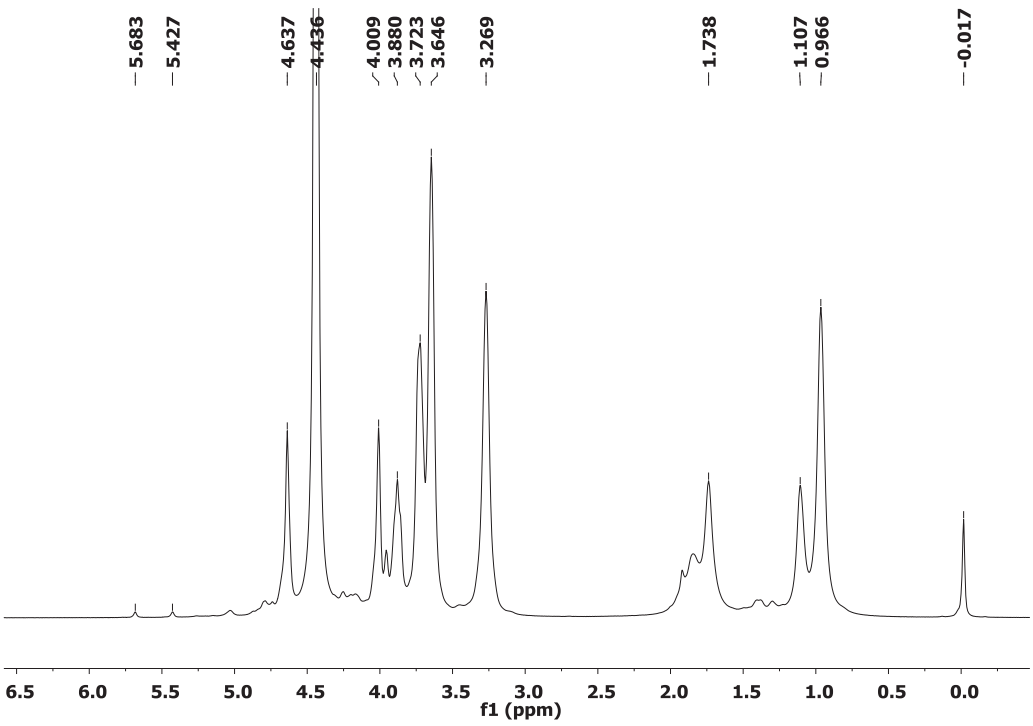

Figure 8.20 *^{1}H NMR spectrum of poly(HEMAm-co-**M1**) after diafiltration (run no.6, Table 8.4). Conditions: 400 MHz, D_2O, 6 %w/w, 328K, ns 100, D1 10s.*

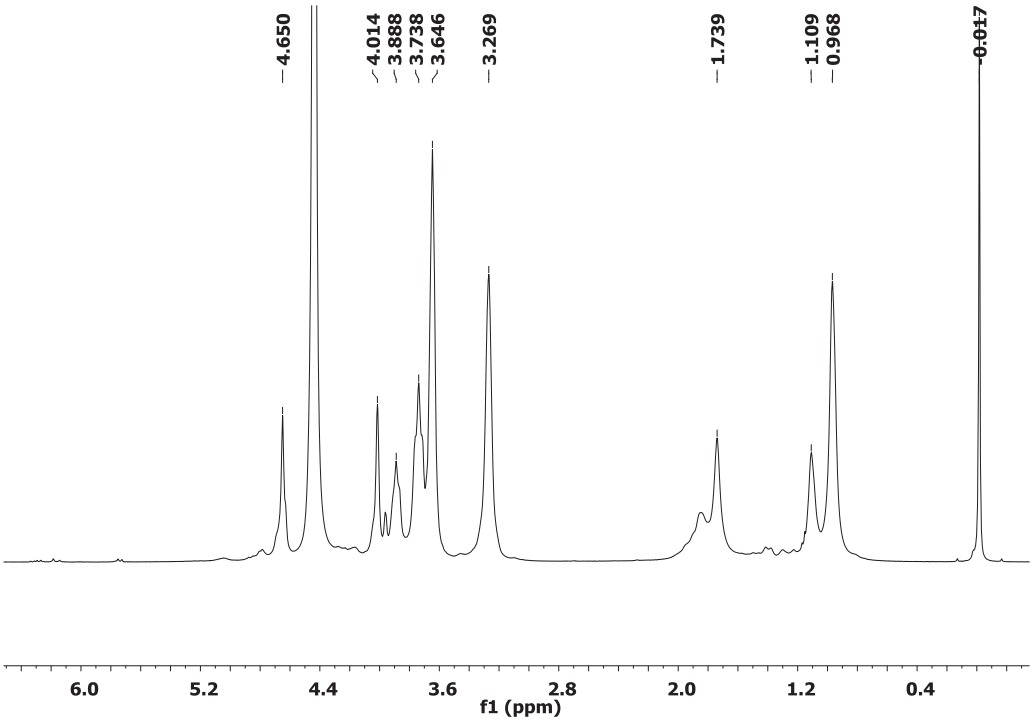

Figure 8.21 *^{1}H NMR spectrum of poly(HEMAm-co-**M2**) after diafiltration (run no.9, Table 8.4). Conditions: 400 MHz, D_2O, 5 %w/w, 328K, ns 96, D1 10s.*

Appendix 8.B Selected SEC chromatograms

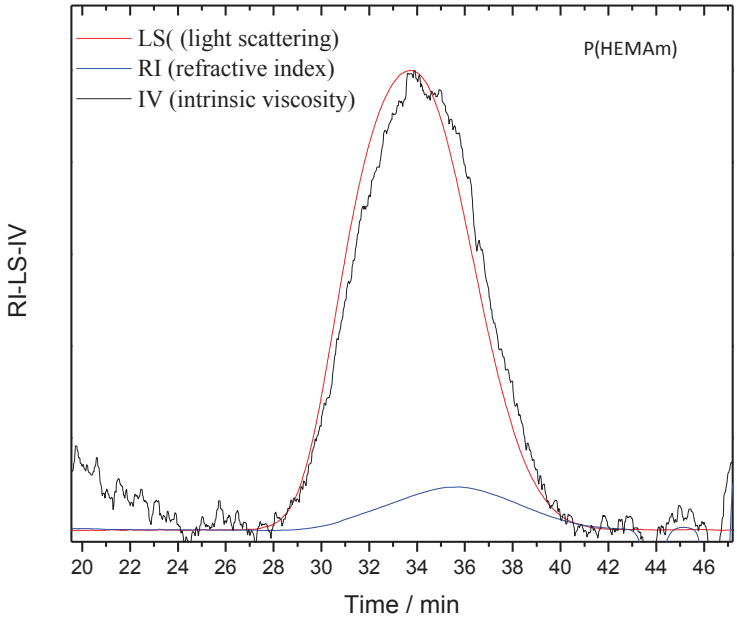

Figure 8.22 *SEC chromatograms of poly(HEMAm) obtained from conventional radical polymerization (run no. 2, Table 8.3). Eluant: 0.1M $NaNO_3$ + 0.03% w/v NaN_3 + 10mM EDTA. Columns: Shodex OH pak SB-(Guard + 805 + 806) HQ.*

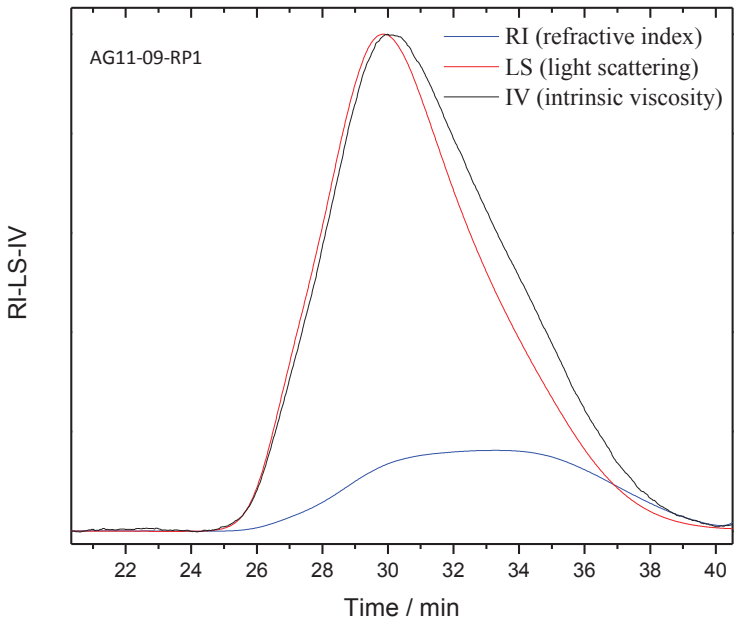

Figure 8.23 *SEC chromatograms of poly(HEMAm-co-**M1**) obtained from the conventional radical polymerization of HEMAm with **M1** in D_2O at 60 °C (run no. 6, Table 8.4). Conditions: 1.2 mg mL^{-1}, 30 °C. Eluant: 0.1M $NaNO_3$ + 0.03% w/v NaN_3 + 10mM EDTA. Columns: Shodex OH pak SB-(Guard + 805 + 806) HQ.*

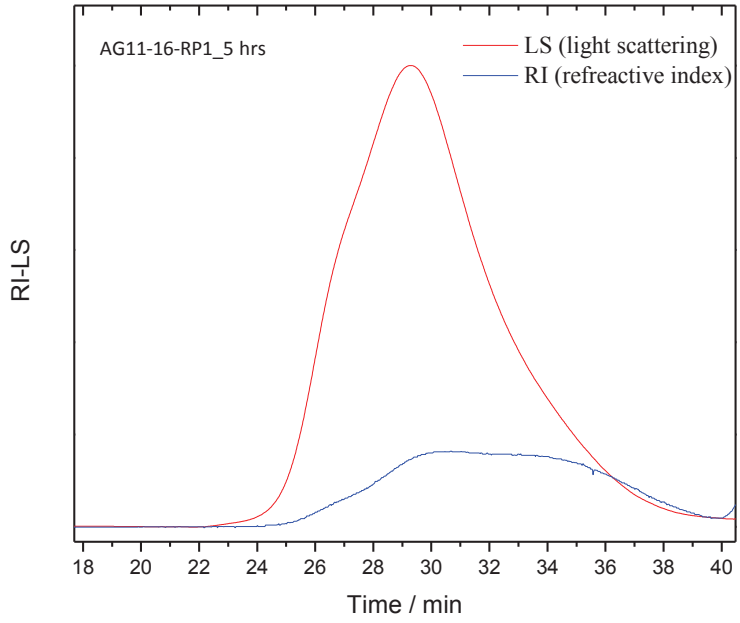

Figure 8.24 *SEC chromatograms of poly(HEMAm-co-**M1**) obtained from the conventional radical polymerization of HEMAm with **M1** in D_2O at 60 °C (run no. 8, Table 8.4). Conditions: ~ 2 mg mL^{-1}, 30 °C. Eluant: 0.1M $NaNO_3$ + 0.03% w/v NaN_3 + 10mM EDTA. Columns: Shodex OH pak SB-(Guard + 805 + 806) HQ. Note that this is the sample after 5 hours.*

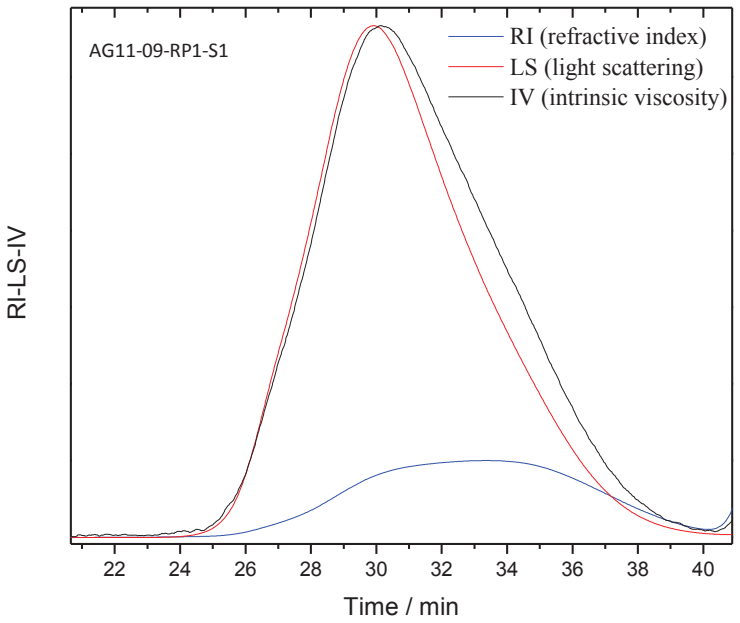

Figure 8.25 *SEC chromatograms of poly(HEMAm-co-**M1**) obtained from the conventional radical polymerization of HEMAm with **M1** in NaCl (0.2 M) at 60 °C (run no. 7, Table 8.4). Conditions: 1.2 mg mL^{-1}, 30 °C. Eluant: 0.1M $NaNO_3$ + 0.03% w/v NaN_3 + 10mM EDTA. Columns: Shodex OH pak SB-(Guard + 805 + 806) HQ.*

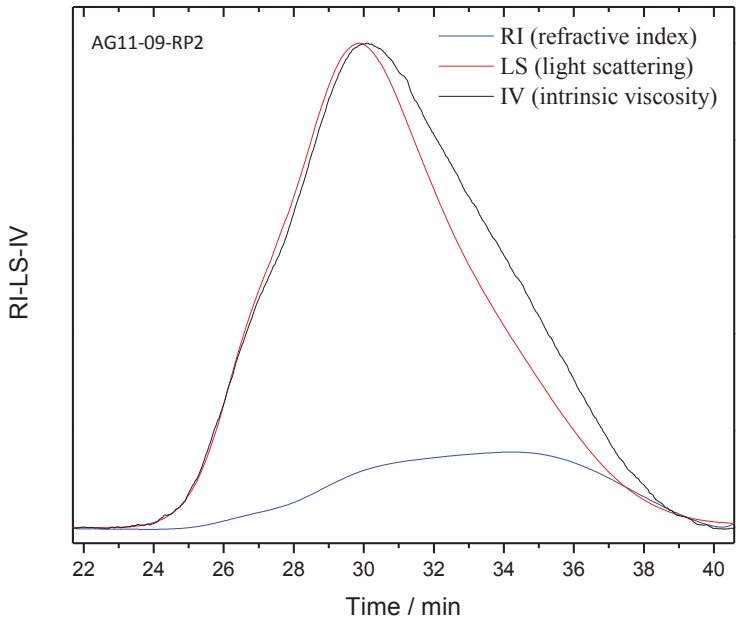

Figure 8.26 *SEC chromatograms of poly(HEMAm-co-**M2**) obtained from the conventional radical polymerization of HEMAm with **M2** in D_2O at 60 °C (run no. 9, Table 8.4). Conditions: 1.2 mg mL^{-1}, 30 °C. Eluant: 0.1M $NaNO_3$ + 0.03% w/v NaN_3 + 10mM EDTA. Columns: Shodex OH pak SB-(Guard + 805 + 806) HQ.*

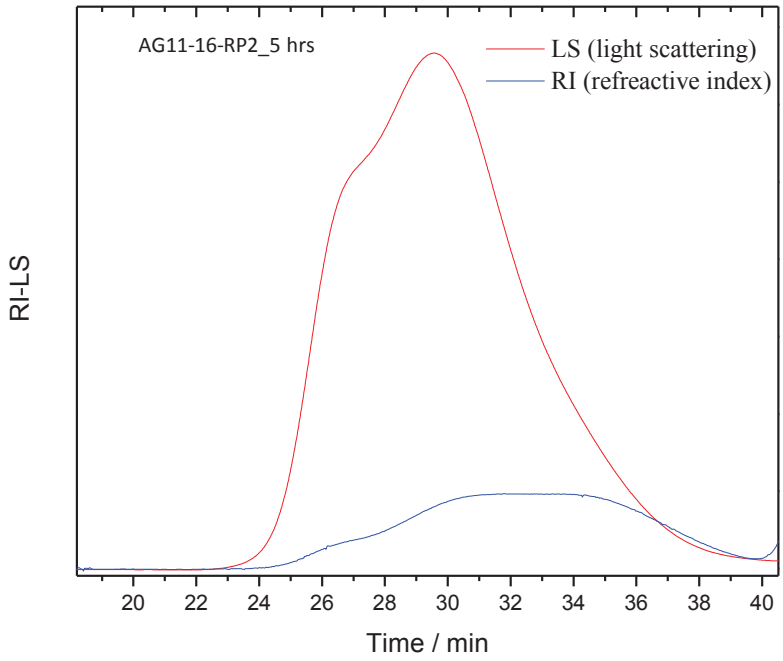

Figure 8.27 *SEC chromatograms of poly(HEMAm-co-**M2**) obtained from the conventional radical polymerization of HEMAm with **M2** at 60 °C (run no. 11, Table 8.4). Conditions: 1.2 mg mL^{-1}, 30 °C. Eluant: 0.1M $NaNO_3$ + 0.03% w/v NaN_3 + 10mM EDTA. Columns: Shodex OH pak SB-(Guard + 805 + 806) HQ. Note that this is the sample after 5 hours.*

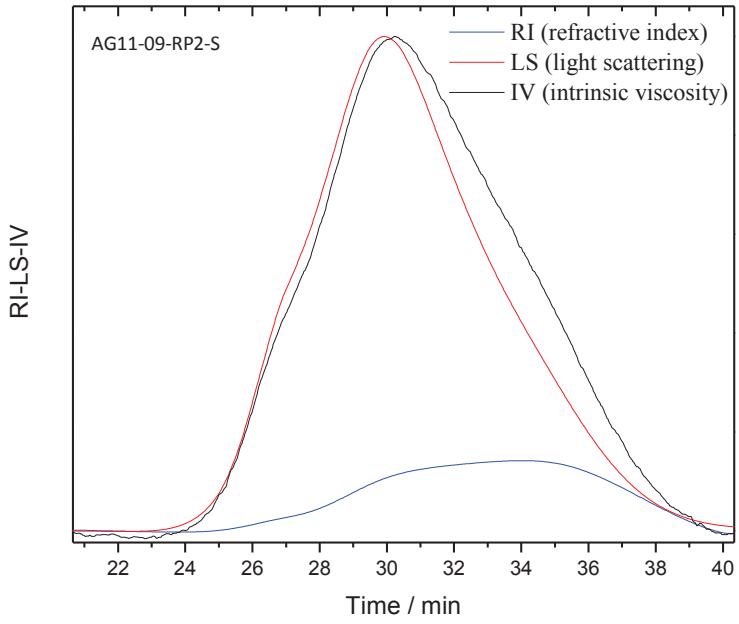

Figure 8.28 *SEC chromatograms of poly(**M2**-co-HEMAm) obtained from the conventional radical polymerization of HEMAm with **M2** in NaCl (0.2 M) at 60 °C (run no. 10, Table 8.4). Conditions: 1.2 mg mL^{-1}, 30 °C. Eluant: 0.1M $NaNO_3$ + 0.03% w/v NaN_3 + 10mM EDTA. Columns: Shodex OH pak SB-(Guard + 805 + 806) HQ.*

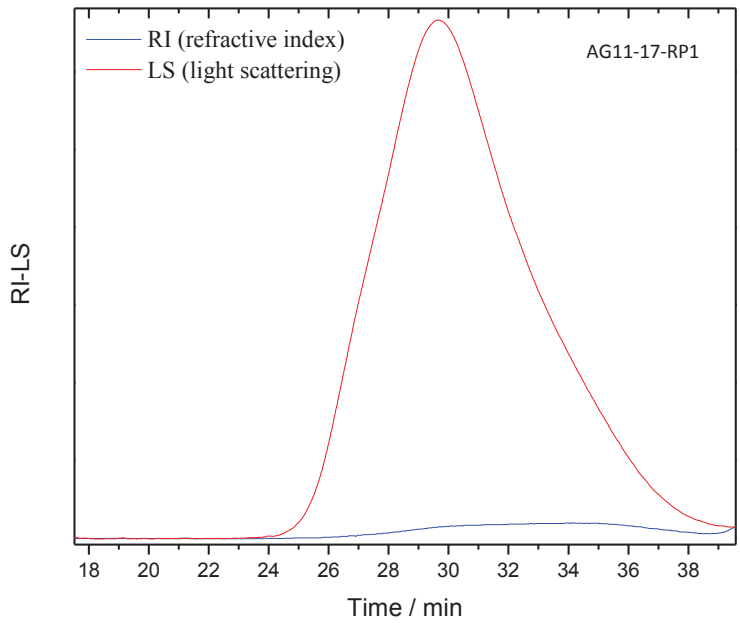

Figure 8.29 *SEC chromatograms of poly(HEMAm-co-**M3**) obtained from the conventional radical polymerization of HEMAm with **M3** in D_2O at 60 °C (run no. 13, Table 8.4). Conditions:~ 2 mg mL^{-1}, 30 °C. Eluant: 0.1M $NaNO_3$ + 0.03% w/v NaN_3 + 10mM EDTA. Columns: Shodex OH pak SB-(Guard + 805 + 806) HQ.*

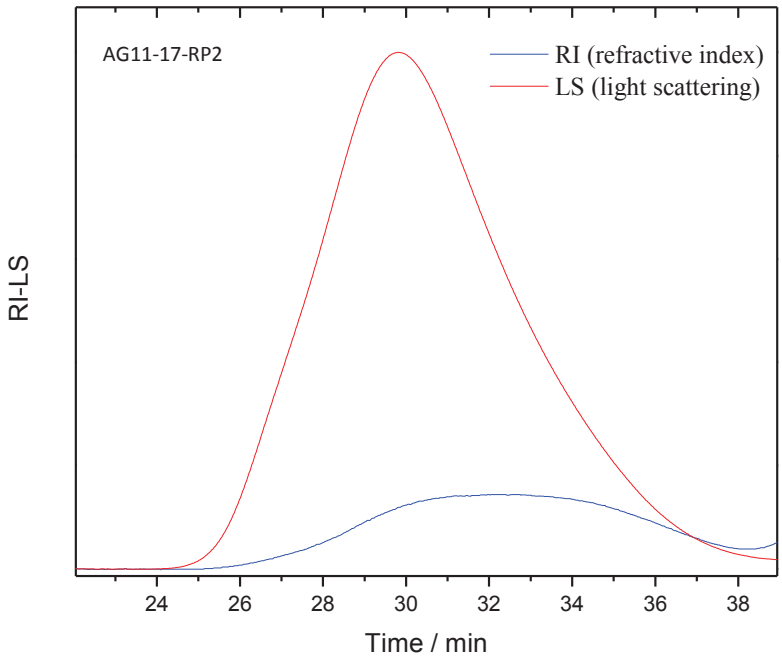

Figure 8.30 *SEC chromatograms of poly(HEMAm-co-**M6**) obtained from the conventional radical polymerization of HEMAm with **M6** in D_2O at 60 °C (run no. 14, Table 8.4). Conditions:~ 2 mg mL^{-1}, 30 °C. Eluant: 0.1M $NaNO_3$ + 0.03% w/v NaN_3 + 10mM EDTA. Columns: Shodex OH pak SB-(Guard + 805 + 806) HQ.*

Appendix 8.C Example on conversion calculation

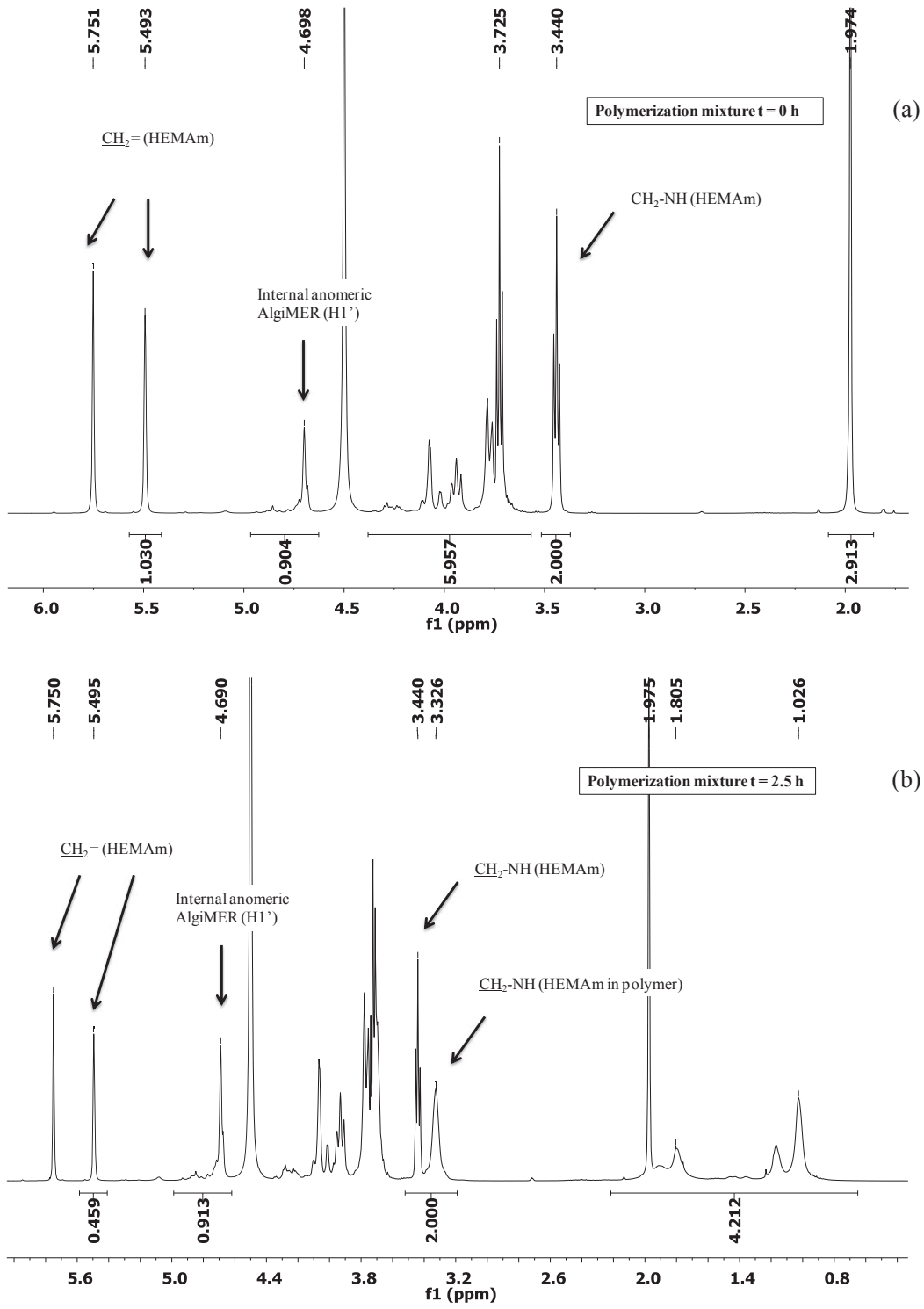

Figure 8.31 *^{1}H NMR spectra of the copolymerization mixture of a methacrylamide AlgiMER **M1** and HEMAm at (a) 0 hours and (b) 2.5 hours (run no. 6, Table 8.4). Conditions: 400 MHz, D_2O, 328 K, ns = 16, D1 = 10 s.*

For conversion calculation from ^{1}H NMR of the copolymerization of **M1** and HEMAm, the NMR spectra of the polymerization mixtures at time t = 2.5 hours (Figure 8.31b) and 0 hours (Figure 8.31a) were normalized with respect to the C$\underline{H_2}$-NH signal of HEMAm in the polymer (3.32 ppm) and the monomer (3.44 ppm) and the integral ethylenic proton (5.49 ppm) was recorded. By applying Eq. 8.1 the conversion (x) was calculated:

$$x = 1 - \left(\frac{A_{\text{ethylenic}}}{A_{\text{reference}}}\right)_t \Big/ \left(\frac{A_{\text{ethylenic}}}{A_{\text{reference}}}\right)_0 = 1\text{-}\{[A_{5.49}/(A_{3.32} + A_{3.44})]/(A_{5.49}/A_{3.44})\} = 0.55$$

8.5 References

(1) Mooney, D. J.; Bouhadir, K. H.; Wong, W. H.; Rowley, J. A., 1998; Vol. WO 012228.

(2) Friends, G.; Künzler, J.; McGee, J.; Ozark, R. *Journal of Applied Polymer Science* **1993**, *49*, 1869.

(3) (a) Rijcken, C. J. F.; Schiffelers, R. M.; van Nostrum, C. F.; Hennink, W. E. *J. Controlled Release* **2008**, *132*, e33(b) Rijcken, C. J.; Snel, C. J.; Schiffelers, R. M.; van Nostrum, C. F.; Hennink, W. E. *Biomaterials* **2007**, *28*, 5581.

(4) Moszner, N.; Angermann, J.; Rheinberger, V.; Zeuner, F.; (Ivoclar Vivadent A.-G., Liechtenstein). Application: EP, 2004.

(5) (a) La Gatta, A.; Schiraldi, C.; Esposito, A.; D'Agostino, A.; De Rosa, A. *Journal of Biomedical Materials Research Part A* **2009**, *90A*, 292(b) Song, J.; Saiz, E.; Bertozzi, C. R. *Journal of the American Chemical Society* **2003**, *125*, 1236.

(6) Wyatt, P. J. *Analytica Chimica Acta* **1993**, *272*, 1.

(7) *Light scattering from polymer solutions*; Huglin, M. B., Ed.; Academic Press: London, 1972.

(8) Rinaudo, M. In *Comprehensive Glycoscience: From Chemistry to System Biology*; Boons, G. J., Lee, Y. C., Suzuki, A., Taniguchi, N., Voragen, A. G. J., Eds.; Elsevier Ltd, 2007, pp 691-735; Vol. 2.

(9) Whistler, R. L.; Panzer, H. P.; Roberts, H. J. *Journal of Organic Chemistry* **1961**, *26*, 1583.

(10) Lacík, I.; Učňová, L.; Kukučková, S.; Buback, M.; Hesse, P.; Beuermann, S. *Macromolecules* **2009**, *42*, 7753.

(11) Knutsen, S. H.; Moe, S. T.; Larsen, B.; Grasdalen, H. *Hydrobiologia* **1993**, *260-261*, 667.

(12) Weaver, J. V. M.; Bannister, I.; Robinson, K. L.; Bories-Azeau, X.; Armes, S. P.; Smallridge, M.; McKenna, P. *Macromolecules* **2004**, *37*, 2395.

(13) Thompson, K. L.; Read, E. S.; Armes, S. P. *Polymer Degradation and Stability* **2008**, *93*, 1460.

(14) Brandrup, J.; Immergut, E. H.; Grulke, E. A.; Abe, A.; Block, D. R. *Polymer Handbook*; 4th ed.; John Wiley & Sons , Inc . 1998.

(15) Klimchuk, K. A.; Hocking, M. B.; Lowen, S. *J. Polym. Sci., Part A Polym. Chem.* **2000**, *38*, 3146.

(16) Kelen, T.; TÜdÕs, F. **1975**, *9*, 1

(17) Haug, A.; Larsen, B.; Smidsroed, O. *Acta Chemica Scandinavica* **1967**, *21*, 2859.

(18) (a) Smidsrød, O.; Haug, A. *Biopolymers* **1971**, *10*, 1213(b) Haug, A.; Smidsrød, O. *Acta chem. Scand.* **1962**, *16*, 1569.

(19) Andriamanantoanina, H.; Rinaudo, M. *Polymer International* **2010**, *59*, 1531.

(20) (a) Kohn, R.; Furda, I.; Haug, A.; Smidsroed, O. *Acta Chem. Scand.* **1968**, *22*, 3098(b) Kohn, R. *Pure and Applied Chemistry* **1975**, *42*, 371.

(21) Bouffar-Roupe, C. Thesis, CERMAV: Université Joseph-Fourier, Grenoble I, 1989.

(22) Sperling, L. H. *Inroduction to physical polymer science*; 2nd ed.; Wiley & Sons, Inc., 1992.

Chapter 9: RAFT copolymerization of AlgiMERs in aqueous solution

Table of contents

Disclaimer

The rheological characterizations were conducted by Pr. M. Rinaudo. Many thanks for her patience in illustrating and interpreting the results with me.

9.1 Introduction

Reversible Addition Fragmentation chain Transfer (RAFT) polymerization is arguably the most robust and versatile reversible-deactivation radical polymerization technique applicable in aqueous solution: It is applicable to the majority of monomers amenable to radical polymerization and it tolerates all functional groups but strong nucleophiles. [1] Since the pioneering work of McCormick and collaborators [2] the number of papers on the subject has kept increasing [3] and now includes over 170 scientific articles. [4] Still, there are few examples in literature describing the synthesis of glycopolymers displaying charged carbohydrates. [5] Herein I describe the RAFT copolymerization of alginate-derived glycomonomers (AlgiMERs) and 2-hydroxyethyl methacrylamide (HEMAm) in aqueous solution. To this end, a preliminary study of the best reaction conditions for the homopolymerization of HEMAm was conducted (pH, RAFT agent) and its results were later applied to the copolymerization with different AlgiMERs (Scheme 9.1).

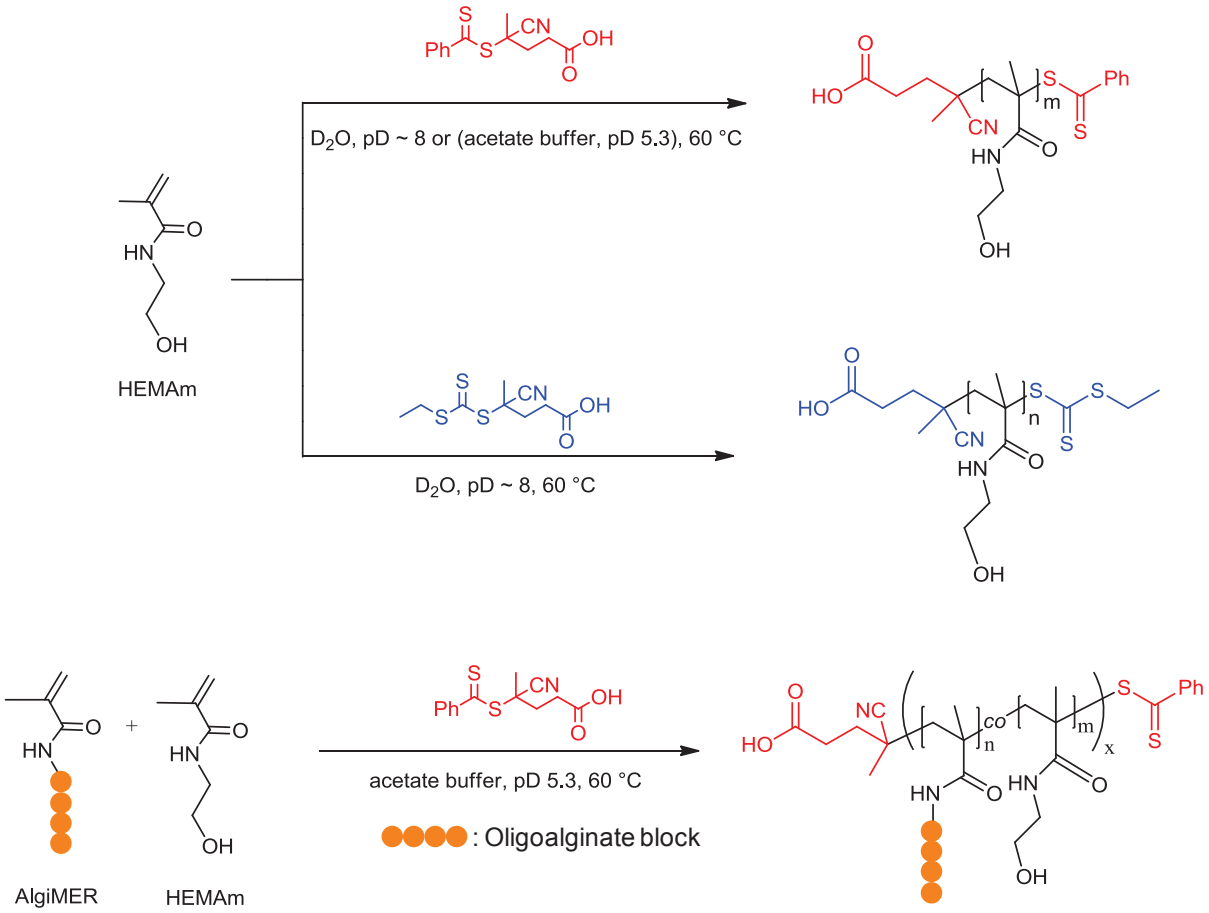

Scheme 9.1 *RAFT (co)polymerization of HEMAm in aqueous solution and synthesis of poly(HEMAm-co-AlgiMER).*

9.2 Experimental

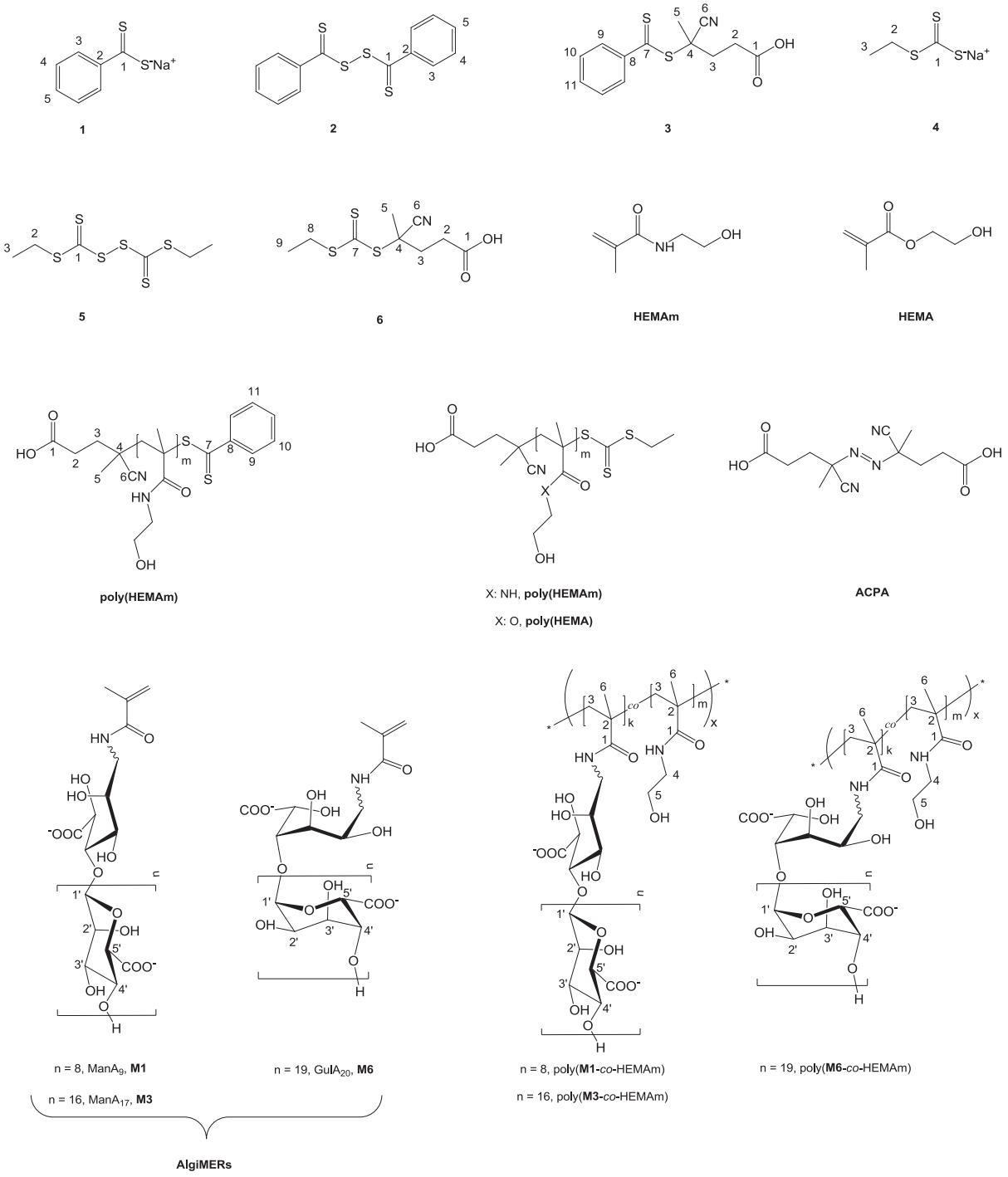

Figure 9.1 *Molecules involved in this study. The nucleus numbering used in NMR assignments is also reported. $ManA_x$ and $GulA_x$ refer to oligomannuronan and oligoguluronan blocks, respectively, with $DP_n = x$.*

9.2.1 Materials and methods

The following chemicals were reagent grade and used as received. 4,4'-Azobis(cyanopentanoic acid) (ACPA, 98%, Aldrich), H_2O (deionized), D_2O (99.8 %, Eurisotop), DMSO-d6 (99.8%, Eurisotop), sulfur (≥ 98%, Prolabo), sodium methoxide (25 %w/w, Aldrich), benzyl chloride (99%, Prolabo), NaOH (≥ 97%, Aldrich), HCl (37 %, Carlo Erba), EtOAc (≥ 99%, Carlo Erba), diethyl ether (≥ 98%, Aldrich), petroleum ether (≥ 97%, SdS), ethanethiol (≥ 97%, Fluka), carbon disulfide (≥ 99.9%, Fluka), iodine (99%, Rectupur), potassium iodide (≥ 99.5%, Normapur), Tetra-*n*-butylammonium bromide TBAB (≥ 99%, Fluka), acetic acid (> 99.8%, SdS), sodium acetate (≥ 98.5%, Fluka), NaCl (≥ 99 %, Aldrich), ethylenediaminetetraacetic acid tetrasodium salt EDTA (99 %, Acros), $NaNO_3$ (≥ 99 %, Aldrich), NaN_3 (≥ 99 %, Merck), 2,6-Di-tert-butyl-4-methyl phenol BHT (≥ 99 %, Fluka), $NaNO_3$ (≥ 99 %, Aldrich), NaN_3 (≥ 99 %, Merck), Na_2CO_3 (≥ 99.5 %, Aldrich).

Flash chromatography carried out using silica gel (60 Å, 40-60 µm, Merck) for **2** and **3**, and (60 Å, 15-40 µm, Merck) for **6**. TLC analyses were performed on aluminum backed silica gel plates (60 Å, 15 µm, Merck) containing a UV indicator (254 nm). Slide-A-Lyzer dialysis cassettes were purchased from Thermo Scientific®.

In calculating reagents concentrations, volume changes taking place upon mixing and heating were ignored. For instance, at 25 °C the excess volume for an equimolar mixture of H_2O and DMSO is only -0.93 cm^3 mol^{-1}, or ~2%. Also, going from 20 °C to 60 °C determines a thermal expansion of water of only 1.5 %. [6]

Theoretical molecular weights were calculated according to the following formula: [7]

$$M_n = M_M .x. \frac{[M]_0}{[RAFT]_0} + M_{RAFT} \quad (9.1)$$

where M_M and M_{RAFT} are the molecular weights of the monomer and RAFT agent respectively, x is the conversion from ^{1}H-NMR and $[M]_0$ and $[RAFT]_0$ are the initial concentrations of the monomer and RAFT agent, respectively.

9.2.2 Analyses

NMR

NMR spectra were recorded on a Bruker DPX400 spectrometer equipped with a Variable Temperature (VT) module and a 5 mm QNP (direct) detection probe. The resonance

frequency was 400.13 MHz and 100.62 MHz for ^{1}H and ^{13}C nuclei, respectively. The temperature control of the probe was calibrated with a 80 % glycol solution in DMSO-d6. Unless otherwise specified, 90° pulses, pulse sequence recycle times of 3 s and an inter-scan delay D1 > 7s were used. Polymerization mixtures were prepared, transferred to a NMR tube equipped with a Young valve, degassed and analyzed by ^{1}H-NMR (D1 > 7s) at t = 0 hrs for DP_n verification and at the end of the polymerization for conversion calculation. The DP_n from ^{1}H-NMR was considered in our calculations in almost all the cases. Sodium 3-(trimethylsilyl)propanoate (TSP) was used as an internal reference. Chemical shifts (in ppm) for ^{1}H and ^{13}C nuclei were referenced to δ = -0.017 ppm (^{1}H) and δ = -0.149 ppm (^{13}C).

Size exclusion chromatography

Molecular weights, molecular weight distributions and intrinsic viscosities were measured with a SEC-IV-MALLS system consisting of an Alliance GPCV 2000 (Described in Chapter 6). Samples were prepared by diluting the polymerization mixtures to 1-8 g L^{-1} depending on the expected molar mass.

Differential refractometry

The differential refractive index increment (dn/dc) of poly(HEMAm) samples from RAFT polymerization (run no 9 and 10, Table 9.1) was determined at 30 °C using an Optilab® rEX differential refractometer (Wyatt Technologies, λ = 633 nm). To this end, polymers were purified by dialysis, freeze dried and their residual solvent content was determined by Thermo Gravimetric Analysis (samples held at 130 °C for 4 h). Solutions of known concentration were then prepared gravimetrically by dissolving the polymers into the same eluant used for SEC analysis (d^{30}= 1.0035 g mL^{-1}) and injected to the refractometer at a flow rate of 0.25 mL min^{-1}. The instrument measures the refractive index (Δn) for each concentration (c) and from ASTRA software, dn/dc is calculated from the slope of the plot of Δn as a function of c according to the following equation: [8]

$$\Delta n = \frac{dn}{dc} \times c \tag{9.2}$$

The refractive index increment of the copolymers was estimated from their chemical composition and the dn/dc of the corresponding homopolymers according to the formula: [9]

$$dn/dc = F_1(dn/dc)_1 + F_2(dn/dc)_2 \quad (9.3)$$

where F_i and $(dn/dc)_i$ are the weight fraction and the refractive index increment of each homopolymer, respectively. To this end, a dn/dc value of 0.165 mL g^{-1} was used for alginate, [10] and that of poly(HEMAm), dn/dc = 0.208 mL g^{-1}, was measured as described above (See chapter 8 for polymer preparation).

Thermo Gravimetric Analysis (TGA)

Thermo Gravimetric Analyses (TGA) for $HEMAm_{121}$ (run no. 9, Table 9.1) and $HEMAm_{153}$ (run no. 10, Table 9.1) were achieved using a Setaram TGA 92-12 instrument. To this aim, samples of $HEMAm_{121}$ (21.7 mg) and $HEMAm_{153}$ (29.0 mg) were heated from room temperature up to 130 °C at 10 °C/min under nitrogen flow. The samples were left at 130 °C for 4 hours before going back to room temperature at 10 °C/min. Solvent content: $HEMAm_{121}$ = 8.4 % and $HEMAm_{153}$ = 4.9 %.

Rheology

Rheological properties (dynamic) of polymer gels were characterized by an AR2000 rheometer (TA instruments). To this end polymers were isolated by diafiltration, lyophilized. Based on the intrinsic viscosities of a glycopolymer with a comparable molecular weight, the intrinsic viscosities [η] was estimated to be ~ 30 mg mL^{-1}. The critical concentrations ($C^* \sim 1/[\eta]$) to assure entanglement of the chains in a semi dilute regime were calculated and polymer solutions with concentrations ≅ 2-2.5 times the critical concentration were prepared in D_2O. The prepared polymer solutions, 70.8 mg mL^{-1} of P(**M6**-*co*-HEMAm) and 62 mg mL^{-1} of P(**M3**-*co*-HEMAm), were added drop wise over a $CaCl_2$ (0.5 mol L^{-1}) solution and were left for ~ 2 hours. The rheological properties of the resulting gel beads from P(**M6**-co-HEMAm) were analyzed in an oscillatory mode using a parallel-plate system (steel, diameter = 2 cm) at 25 °C.

9.2.3 Synthesis of bi(phenylcarbonothioyl) disulfide (2)

Sulphur (12.8 g, 400 × 10^{-3} mol) was transferred to a 3 neck round-bottom flask equipped with a condenser and a magnetic bar. Sodium methoxide (25 % w/w, 92 mL, 400 × 10^{-3} mol) and MeOH (40 mL) were added under nitrogen to the reaction mixture followed by the drop wise addition of benzyl chloride (25.3 g, 23 mL, 200 × 10^{-3} mol) over a period of 30

min. Upon heating at 70 °C, the reaction mixture became brick red. After 10 h the reaction was stopped, MeOH was eliminated by rotary evaporation and the unreacted benzyl chloride was extracted in Et_2O (3 × 150 mL). The collected aqueous phase was acidified with HCl (1 N, 200 mL) and extracted with Et_2O (430 mL in two portions). The product was extracted from the ethereal phase with NaOH solutions (1 N, 100 mL; 0.5 N, 200 mL) and the latter were washed a last time with Et_2O (100 mL) to afford a brick red aqueous solution containing sodium dithiobenzoate **1**. The compound was directly oxidized by drop wise addition of a KI_3 solution and excess I_2 was reduced with $Na_2S_2O_3$ (1 mol L^{-1}). The resulting red precipitate was separated from the aqueous phase by suction filtration; the filter cake was washed with excess water, transferred to a round bottom flask and freeze dried. The gross product was used without further purification. Yield: 15.4 g (50 % with respect to benzyl chloride). ^{1}H-NMR (400 MHz, $CDCl_3$, 25 °C) δ (ppm): 7.45 (t, H3, 2H, *J* 7.8 Hz), 7.61 (t, H5, 1H, *J* 7.4 Hz), 8.09 (d, H4, 2H, *J* 7.3 Hz). ^{13}C-NMR (100 MHz, $CDCl_3$, 25 °C) δ (ppm): 127.73 (C4), 128.80 (C3), 133.31 (C2), 143.83 (C5), 219.70 (C1). Experiment AG08-01.

9.2.4 Synthesis of 4-cyano-4-[(phenylcarbonothioyl)sulfanyl] pentanoic acid (CPADB, 3)

Bi(phenylcarbonothioyl) disulfide **2** (5.00 g, 163 × 10^{-4} mol), 4,4'-azobis(cyanopentanoic acid) (6.85 g, 244 × 10^{-4} mol) and ethyl acetate (80 mL) were introduced into a 3 neck round bottom flask fitted with a condenser connected to an oil bubbler and a nitrogen line. The reaction mixture was purged with nitrogen for 30 min. and refluxed under stirring for 18 hours at 90 °C. At the end of the reaction, volatiles were eliminated by rotary evaporation at reduced pressure and a red solid was obtained. The gross product was solubilized in a minimum quantity of EtOAc and added over a column (∅: 7cm) pre-packed with silica gel (h: 29 cm) for flash chromatography. The product was eluted with a gradient of EtOAc/PE/EtOH from 1:8:1, to 1:7.5:1.5 and 1:6:3. Fractions containing the product were pooled (R_f 0.23 in EtOAc/PE/EtOH 3:6:1) and the volatiles eliminated by rotary evaporation under reduced pressure followed by standing under mechanical vacuum overnight (p = 1.1 × 10^{-1} mbar). Yield: 6.26 g of red amorphous solid (71 % of theoretical yield). ^{1}H-NMR (400 MHz, $CDCl_3$, 25 °C) δ (ppm): 1.94 (s, H5, 3H), 2.41-2.80 (m, H2, H3, 4H), 7.40 (m, H10, 2H), 7.57 (m, H11, 1H), 7.91 (dd, H9, 2H, *J* 8.5, 1.2 Hz). ^{13}C-NMR (100 MHz, $CDCl_3$, 25 °C) δ (ppm):24.29 (C5), 29.68 (C2), 33.14 (C3), 45.73 (C4), 118.51 (C6), 126.81

(C10), 128.73 (C9), 133.22 (C8), 144.61 (C11), 177.35 (C1), 222.30 (C7). Experiment AG08-02.

9.2.5 Synthesis of bi[(ethylsulfanyl)carbonothioyl]disulfide (5)

In a 3 neck round bottom flask, tetra-*n*-butylammonium bromide (TBAB, 0.580 g, 1.80×10^{-3} mol) was added to a NaOH solution (0.750×10^{-1} N, 500 mL). The reaction mixture was purged with N_2 (30 min) and cooled on ice. Ethanethiol (2.26 g, 2.70 mL, 3.60×10^{-2} mol) was then added using a gas tight syringe pre-equilibrated with N_2, followed by carbon disulfide (3.00 g, 39.6×10^{-3} mol, 2.40 mL). The mixture was stirred on ice until total consumption of CS_2 (75 min), after which the yellowish solution of sodium ethyl carbonotrithionate was exposed to the air and oxidized with a KI_3 solution (the latter prepared by solubilizing I_2 (5.0 g, 19.8×10^{-3} mol) in a KI solution (2 N, 36 mL) over a period of 15 min). During the addition of the oxidant, disulfide **5** accumulated on the Teflon magnetic bar and the solution became colorless. $Na_2S_2O_3$ (1 mol L^{-1}, 11 mL) was added to reduce the excess of I_3^- in solution; the product was extracted in EtOAc and washed with more aqueous $Na_2S_2O_3$. The organic phases were transferred to a round bottom flask and the volatiles eliminated by rotary evaporation under reduced pressure to yield a yellow-orange oil that was further purified by flash chromatography in 100 % hexane ($\varnothing_{column}$: 7 cm, SiO_2 packing 23 cm). The fractions containing the product were pooled (R_f 0.2, 100 % hexane) and dried by rotary evaporation followed by standing under mechanical vacuum for 6 h. Yield: 3.56 g of yellow oil (72 % of theoretical yield with respect ethanethiol). ^{1}H-NMR (400 MHz, $CDCl_3$, 25 °C) δ (ppm): 1.36 (t, H3, 3H, J_{23} 7.5 Hz), 3.31 (q, H2, 2H, J_{23} 7.5 Hz). ^{13}C-NMR (100 MHz, $CDCl_3$, 25 °C) δ (ppm): 12.49 (C3), 32.72 (C2), 221.35 (C1). Experiment AG10-22_F15-40.

9.2.6 Synthesis of 4-cyano-4-{[(ethylsulfanyl)carbonothioyl]sulfanyl} pentanoic acid (CPATTC, 6)

Bi[(ethylsulfanyl)carbonothioyl]disulfide (3.00 g, 109×10^{-4} mol), 4,4'-azobis(cyanopentanoic acid) (4.90 g, 175×10^{-4} mol) and ethyl acetate (80 mL) were introduced into a 3 neck round bottom flask fitted with a condenser connected to an oil bubbler and a nitrogen line. The reaction mixture was purged with nitrogen for 40 min and refluxed at 90 °C under stirring for 19 hours. At the end of the reaction, EtOAc was eliminated by rotary evaporation at reduced pressure, the resulting oil was solubilized in a

minimum quantity of EtOAc and charged on the top of a flash chromatography column ($\varnothing_{column}$ 7 cm, SiO_2 packing 23 cm). The product was eluted using a gradient of PE/EtOAc/EtOH from 8:1.5:0.5, to 7:2:1 and 6:3:1. Fractions containing the product were pooled (R_f 0.38 in PE/EtOAc/EtOH 6:3:1) and volatiles were eliminated by rotary evaporation under reduced pressure followed by standing under mechanical vacuum. Yield: 3.73 g of amorphous yellow solid (65 % of theoretical yield). ^{1}H-NMR (400 MHz, $CDCl_3$, 25 °C) δ (ppm): 1.36 (t, H9, 3H, J_{89} 7.4 Hz), 1.88 (s, H5, 3H), 2.36-2.71 (m, H2, H3, 4H), 3.35 (q, H8, 2H, J_{89} 7.4 Hz).^{13}C-NMR (100 MHz, $CDCl_3$, 25 °C) δ (ppm): 12.82 (C9), 24.88 (C5), 29.62 (C2), 31.47 (C8), 33.54 (C3), 46.27 (C4), 118.96 (C6), 177.22 (C1), 216.73 (C7). ESI-MS *m/z* calculated 264.02, found: 264.1 [M.H$^+$]. Experiment AG10-23_F6-10.

9.2.7 RAFT polymerization of *N*-(2-hydroxyethyl)methacrylate mediated by CPATTC

4,4'Azobis(cyanopentanoic acid) (0.980×10^{-2} g, 3.50×10^{-5} mol) was dissolved in CD_3OD (200 µL, $c_{ACPA} = 1.75 \times 10^{-1}$ mol L^{-1}). HEMA (0.305 g, 2.34×10^{-3} mol) was dissolved in CD_3OD (1 mL) and 0.6 mL of the resulting solution ($c_{HEMA} = 2.34$ mol L^{-1}) were used to dissolve the RAFT agent (CPATTC, 0.810×10^{-2} g, 3.08×10^{-5} mol). A calculated amount of ACPA solution (35 µL, 6.12×10^{-6} mol) was then added and the resulting mixture was transferred to a NMR tube equipped a Young valve. The tube was sealed, degassed with 4 freeze-evacuate-thaw cycles and transferred to a water bath preheated at 60 °C. From time to time, the polymerization was stopped by plunging the tube in cold water and a ^{1}H-NMR spectrum was acquired to monitor conversion. The final polymerization mixture was analyzed by SEC in DMF calibrated with narrow PMMA standards to determine the molar mass distribution of the polymer system. Total reaction time: 12.5 hours. Final conversion (NMR, 25 °C, ns = 16, D1 = 25s): 80 %. M_n (SEC) 8057 Da, M_n/M_{nth} 1.61, PDI 1.21. Experiment AG11-10; run no. 1 in Table 9.1.

9.2.8 RAFT polymerization of *N*-(2-hydroxyethyl)methacrylamide mediated by CPATTC

4,4'Azobis(cyanopentanoic acid) (1.92×10^{-2} g, 6.85×10^{-5} mol) was dissolved in DMSO-d6 (1 mL), cooled to ~ 8 °C and diluted with an equal volume of D_2O ($c_{ACPA} = 3.43 \times 10^{-2}$ mol L^{-1}). The RAFT agent (CPATTC, 3.81×10^{-2} g, 1.45×10^{-4} mol) was dissolved in DMSO-d6 (1 mL, $c_{CPATTC} = 1.45 \times 10^{-1}$ mol L^{-1}). HEMAm (0.200 g, 1.55×10^{-3} mol) was

dissolved in D_2O (1.25 mL) and filtered through a syringe filter (0.22 µm, Nylon) to remove the suspended inhibitor (BHT). Part of the latter solution (470 µL, 1.24 mol L^{-1}) was mixed with a calculated amount of CPATTC (40 µL, 5.79×10^{-6} mol) and ACPA (50 µL, 1.71×10^{-6} mol) and the pD was adjusted to ~7-8 with anhydrous Na_2CO_3. The reaction mixture was transferred to a NMR tube equipped with a Young valve and the latter was sealed, degassed with 3 freeze-evacuate-thaw cycles and transferred to a water bath preheated at 60°C. From time to time, the polymerization was stopped by plunging the tube in cold water and a ^{1}H-NMR spectrum was acquired to monitor conversion. The final polymerization mixture was analyzed by aqueous SEC-IV-MALLS to determine the molar mass distribution and intrinsic viscosity of the polymer. Total reaction time: 6 hours. Final conversion (NMR, 25 °C, ns =16, D1 = 25 s): 78 %. M_n (SEC-MALLS) 39,000 Da, $M_n/M_{nth} > 4$, $[\eta]_w$ = 43.2 mL g^{-1}, d*n*/d*c* 0.199, PDI 2.89. Experiment AG11-08-LP1; run no. 2 in Table 9.1.

9.2.9 RAFT polymerization of *N*-(2-hydroxyethyl)methacrylamide mediated by CPADB in different deuterated buffers

Protocol A: carbonate buffer (Run no. 3 in Table 9.1)

4,4'Azobis(cyanopentanoic acid) (1.92×10^{-2} g, 6.85×10^{-5} mol) was dissolved in DMSO-d6 (1 mL), cooled to ~ 8 °C and diluted with an equal volume of D_2O ($c_{ACPA} = 3.43 \times 10^{-2}$ mol L^{-1}). The RAFT agent (CPADB, 3.83×10^{-2} g, 1.37×10^{-4} mol) was dissolved in DMSO-d6 (1 mL, $c_{CPADB} = 1.37 \times 10^{-1}$ mol L^{-1}). HEMAm (0.200 g, 1.55×10^{-3} moles) was dissolved in D_2O (1.25 mL) and filtered through a syringe filter (0.22 µm, Nylon) to remove the suspended inhibitor (BHT). Part of the latter solution (495 µL, c_{HEMAm} = 1.24 mol L^{-1}) was mixed with a calculated amount of CPADB (45 µL, 6.17×10^{-6} mol) and ACPA (53 µL, 1.82×10^{-6} mol), the pD was adjusted ~7-8 with anhydrous Na_2CO_3 and the resulting mixture was transferred to a NMR tube equipped with a Young valve. The NMR tube was sealed, degassed with 3 freeze-evacuate-thaw cycles and transferred to a water bath preheated at 60°C. From time to time, the polymerization was stopped by plunging the tube in cold water and a ^{1}H-NMR spectrum was acquired to monitor conversion. The final polymerization mixture was analyzed by aqueous SEC-IV-MALLS to determine the molar mass distribution and intrinsic viscosity of the polymer. Total reaction time: 6 hours. Final conversion (NMR, 25 °C, ns = 16, D1 = 25 s): 68 %. M_n (SEC-MALLS) 9,600 Da, M_n/M_{nth} 1.07, $[\eta]_w$ = 7.3 mL g^{-1}, d*n*/d*c* 0.174. Experiment AG11-08-LP2.

Protocol B: 0.1 M deuterated acetate buffer (Run no. 4 in Table 9.1)

4,4'azobis(cyanopentanoic acid) (1.92×10^{-2} g, 6.85×10^{-5} mol) was dissolved in DMSO-d6 (1 mL), cooled to ~ 8 °C and diluted with an equal volume of deuterated acetate buffer (0.100 mol L^{-1}, pD 5.3) to give $c_{ACPA} = 3.43 \times 10^{-2}$ mol L^{-1}. The RAFT agent (CPADB, 2.50×10^{-2} g, 8.95×10^{-5} mol) was dissolved in DMSO-d6 (1 mL, $c_{CPADB} = 8.95 \times 10^{-2}$ mol L^{-1}). HEMAm (0.195 g, 1.51×10^{-3} mol) was dissolved in deuterated acetate buffer (1.2 mL) and filtered through a syringe filter (0.22 µm, Nylon) to remove the suspended inhibitor (BHT). Part of the latter solution (400 µL, c_{HEMAm} = 1.26 mol L^{-1}) was mixed with a calculated amount of CPADB (57 µL, 5.1×10^{-6} mol) and ACPA (44 µL, 1.51×10^{-6} mol) and transferred to a NMR tube equipped with a Young valve (CPADB / ACPA = 3.4). The NMR tube was sealed, degassed by 3 freeze-evacuate-thaw cycles and transferred to a water bath preheated at 60°C. At the end of the polymerization, total monomer conversion was determined by ^{1}H-NMR spectroscopy and the molar mass distribution was measured by aqueous SEC-MALLS. Total reaction time: 7.2 hours. Final conversion (NMR, 25 °C, ns = 16, D1 = 25 s): 77 %. M_n (SEC-MALLS) 8,500 Da, M_n/M_{nth} 1.05, $[\eta]_w$ = 7.1 mL g^{-1}, d*n*/d*c* 0.174, PDI 1.03. Experiment AG11-13-LP6.

Protocol C: 0.2 M deuterated acetate buffer (Run no. 6 in Table 9.1)

Same procedure as protocol B, except that from time to time the polymerization was stopped by plunging the tube in cold water and a ^{1}H-NMR spectrum was acquired to monitor conversion. Total reaction time: 6.5 hours. Final conversion (NMR, 25 °C, ns = 16, D1 = 25 s): 77 %. M_n (SEC-MALLS) 8,900 Da, M_n/M_{nth} 1.08, $[\eta]_w$ = 7.2 mL g^{-1}, d*n*/d*c* 0.174, PDI 1.03. Experiment AG11-12-LP1.

Protocol D: 1 M deuterated acetate buffer (Run no. 5 in Table 9.1)

Same procedure as protocol B, except that from time to time the polymerization was stopped by plunging the tube in cold water and a ^{1}H-NMR spectrum was acquired to monitor conversion. Total reaction time: 6.5 hours. Final conversion (NMR, 25 °C, ns = 16, D1 = 25 s): 77 %. M_n (SEC-MALLS) 9,400 Da, M_n/M_{nth} 1.11, $[\eta]_w$ = 7.2 mL g^{-1}, d*n*/d*c* 0.174, PDI 1.03. Experiment AG11-12-LP2.

9.2.10 RAFT polymerization of *N*-(2-hydroxyethyl)methacrylamide in deuterated acetate buffer with different HEMAm / CPADB ratios

All polymerizations were carried out in deuterated acetate buffer (0.20 M, pD = 5.3) starting from the same stock solutions of monomer, RAFT agent and initiator. In all cases, $[CPADB]_0 / [ACPA]_0 = 3.0$.

- **$[HEMAm]_0 / [CPADB]_0 = 100$** (Run no. 7 in Table 9.1). 4,4'Azobis(cyanopentanoic acid) (1.92×10^{-2} g, 6.85×10^{-5} mol) was dissolved in a DMSO-d6 (1 mL), cooled to ~ 8 °C and diluted with an equal volume of acetate buffer to give $c = 3.43 \times 10^{-2}$ mol L^{-1}. The RAFT agent (2.52×10^{-2} g, 9.02×10^{-5} mol) was dissolved in pure DMSO-d6 (1 mL, $c_{CPADB} = 9.02 \times 10^{-2}$ mol L^{-1}). HEMAm (0.680 g, 5.26×10^{-3} mol) was dissolved in deuterated acetate buffer (4.30 mL) and filtered through a syringe filter (0.22 µm, Nylon) to remove the suspended inhibitor (BHT). Part of the latter solution (500 µL, c_{HEMAm} = 1.22 mol L^{-1}) was mixed with a calculated amount of CPADB (57.6 µL, 5.20×10^{-6} mol) and ACPA (50 µL, 1.71×10^{-6} mol), and transferred to a NMR tube equipped with a Young valve ($[CPADB]_0 / [ACPA]_0 = 3.0$). The tube was sealed, degassed with 3 freeze-evacuate-thaw cycles and transferred to a water bath preheated at 60°C. At the end of the polymerization, total monomer conversion was determined by ^{1}H-NMR spectroscopy and the molar mass distribution and the intrinsic viscosity were measured by aqueous SEC-IV-MALLS. Total reaction time: 7 hours. Final conversion (NMR, 25 °C, ns = 16, D1 = 25 s): 79 %. M_n (SEC-MALLS) 10,900 Da, M_n/M_{nth} 1.01, $[\eta]_w$ = 8.0 mL g^{-1}, d*n*/d*c* 0.174, PDI 1.03.

- **$[HEMAm]_0 / [CPADB]_0 = 130$** (Run no. 8 in Table 9.1). Same procedure as run no. 7. Total reaction time: 7 hours. Final conversion (NMR, 25 °C, ns = 16, D1 = 25 s): 78 %. M_n (SEC-MALLS) 13,300 Da, M_n/M_{nth} 0.97, $[\eta]_w$ = 8.8 mL g^{-1}, d*n*/d*c* 0.174, PDI 1.03.

- **$[HEMAm]_0 / [CPADB]_0 = 155$** (Run no. 9 in Table 9.1). Same procedure as run no. 7, but from time to time the polymerization was stopped by plunging the tube in cold water and a ^{1}H-NMR spectrum was acquired to monitor conversion. Total reaction time: 8.5 hours. Final conversion (NMR, 25 °C, ns = 8, D1 = 25 s): 75 %. M_n (SEC-MALLS) 16,400 Da, M_n/M_{nth} 1.04, $[\eta]_w$ = 9.9 mL g^{-1}, d*n*/d*c* 0.174, PDI 1.01.

- **$[HEMAm]_0$ / $[CPADB]_0$ = 200** (Run no. 10 in Table 9.1). Same procedure as run no. 9. Total reaction time: 10.5 hours. Final conversion (NMR, 25 °C, ns = 16, D1 = 25 s): 83 %. M_n (SEC-MALLS) 19,600 Da, M_n/M_{nth} 0.90, $[\eta]_w$ = 11.4 mL g^{-1}, d*n*/d*c* 0.184, PDI 1.03.

9.2.11 RAFT copolymerization of *N*-(2-hydroxyethyl) methacrylamide and M1 in deuterated acetate buffer: Kinetic study.

Run no. 11 in *Table 9.1*: $c_{monomer}$ = 0.58 mol L^{-1}, f_{M1} = 4.9 %

4,4'Azobis(cyanopentanoic acid) (1.97×10^{-2} g, 7.03×10^{-5} mol) was dissolved in DMSO-d6 (2 mL), cooled to ~ 8 °C and diluted with an equal volume of acetate buffer (0.20 mol L^{-1}, pD 5.3) to give $c_{ACPA} = 1.76 \times 10^{-2}$ mol L^{-1}. The RAFT agent (CPADB, 1.91×10^{-2} g, 6.83×10^{-5} mol) was dissolved in pure DMSO-d6 (2 mL, $c_{CPADB} = 3.42 \times 10^{-2}$ mol L^{-1}). HEMAm (0.090 g, 7.00×10^{-4} mol) was dissolved in acetate buffer (400 µL, c_{HEMAm} = 1.75 mol L^{-1}) and filtered through a syringe filter (0.22 µm, Nylon) to remove the suspended inhibitor (BHT). **M1** (0.046 g, 2.52×10^{-5} mol) was dissolved in acetate buffer, added to part of the HEMAm stock solution (280 µL, 4.9×10^{-4} mol) and mixed with a calculated amount of CPADB (57 µL, 1.95×10^{-6} mol) and ACPA stock solutions (52 µL, 9.14×10^{-7} mol). The polymerization mixture (c_{CPADB} / c_{ACPA} = 2.1) was transferred to a NMR tube equipped with a Young valve which was sealed, degassed by 4 freeze-evacuate-thaw cycles and lowered in the NMR probe pre-equilibrated at 60 °C. Clocking was started and ^{1}H-NMR spectra were recorded every 20 min with (ns = 8, D1 = 7s). At the end of the polymerization, the polymerization mixture was analyzed by aqueous SEC-IV-MALLS. Total reaction time: 709 min. Final conversion (NMR): 97 %. M_n (SEC-MALLS) 49,520 Da, M_n/M_{nth} 0.98, $[\eta]_w$ = 30.7 mL g^{-1}, d*n*/d*c* 0.190, PDI 1.11. Experiment AG11-15-LP2.

Run no. 12 in *Table 9.1*: $c_{monomer}$ = 0.42 mol L^{-1}, f_{M1} = 9.1 %

The same initiator and RAFT agent stock solutions prepared for run no. 11 were used. HEMAm (0.091 g, 7.03×10^{-4} mol) was dissolved in acetate buffer (0.20 mol L^{-1}, pD 5.3, 400 µL, c_{HEMAm} = 1.76 mol L^{-1}) and filtered through a syringe filter (0.22 µm, Nylon) to remove the suspended inhibitor (BHT). **M1** (0.090 g, 4.91×10^{-5} mol) was dissolved in acetate buffer (500 µL), added to a part of the prepared HEMAm solution (280 µL, 4.92×10^{-4} mol) and mixed with a calculated amount of CPADB (57 µL, 1.95×10^{-6} mol) and ACPA stock

solutions (52 µL, 9.14 × 10^{-7} mol). Following the addition of the RAFT agent, part of the AlgiMER precipitated out of solution and D_2O (400 µL) was added to attain complete solubilization. Part of the polymerization mixture (c_{CPADB} / c_{ACPA} = 2.1) was transferred to a NMR tube equipped with a Young valve which was sealed, degassed by 4 freeze-evacuate-thaw cycles and lowered in the NMR probe pre-equilibrated at 60 °C. Clocking was started and ^{1}H-NMR spectra were recorded every 20 min (ns = 8, D1 = 7s). At the end of the polymerization, the reaction mixture was analyzed by aqueous SEC-IV-MALLS to determine the molar mass distribution and intrinsic viscosity of the polymer. Total reaction time: 707 min. Final conversion (NMR): 98 %. M_n (SEC-MALLS) 81,510 Da, M_n/M_{nth} 1.08, $[\eta]_w$ = 40.2 mL g^{-1}, d*n*/d*c* 0.183, PDI 1.13.

9.2.12 RAFT copolymerization of *N*-(2-hydroxyethyl) methacrylamide and M1 in deuterated acetate buffer: Different monomer / RAFT agent ratios

HEMAm, RAFT agent and initiator stock solutions were prepared in deuterated acetate buffer (0.20 mol L^{-1}, pD 5.3) and (or) DMSO-d6 and used in the four polymerization experiments. In all cases it was $[CPADB]_0$ / $[ACPA]_0$ = 3.0 and *f* (**M1**) = 6.1 %. 4,4'Azobis(cyanopentanoic acid) (1.97 × 10^{-2} g, 7.03 × 10^{-5} mol) was dissolved in DMSO-d6 (1 mL), cooled to ~ 8 °C and diluted with an equal volume of buffer (c_{ACPA} = 3.51 × 10^{-2} mol L^{-1}). 4-Cyano-4-{[(ethylsulfanyl)carbonothioyl]sulfanyl} pentanoic acid (CPADB, 2.38 × 10^{-2} g, 8.53 × 10^{-5} mol) was dissolved in DMSO-d6 (1 mL, c_{CPADB} = 8.53 × 10^{-2} mol L^{-1}). HEMAm (4.65 × 10^{-3} mol, 0.600 g) was dissolved in acetate buffer (2.65 mL, c_{HEMAm} = 1.75 mol L^{-1}) and filtered through a syringe filter (0.22 µm, Nylon) to remove the suspended inhibitor (BHT). In a typical experiment, **M1** (0.059 g, 3.20 × 10^{-5} mol) was dissolved in acetate buffer (500 µL) and the resulting solution was mixed with calculated amounts of HEMAm (280 µL, 4.91 × 10^{-4} mol), CPADB and ACPA stock solutions (see below for further details). The resulting mixture was then transferred to a NMR tube equipped with a Young valve which was sealed, degassed with 3 freeze-evacuate-thaw cycles and transferred to a water bath pre-heated at 60 °C. At the end of the polymerization, total monomer conversion was determined by ^{1}H-NMR spectroscopy and the molar mass distribution was measured by aqueous SEC- MALLS. To this end, a sample was drawn from each reaction mixture, diluted to $c \cong 4$ mg mL^{-1} with the SEC eluant and injected (50 µL) in the chromatographic system.

- **[monomer]$_0$ / [CPADB]$_0$ = 53** (Run no. 13 in Table 9.1). CPADB (115 µL, 9.82 × 10^{-6} mol), ACPA (92 µL, 3.23 × 10^{-6} mol). Total reaction time: 428 min. Final conversion (NMR, 55 °C, ns = 8, D1 = 14 s): 87 %. M_n (SEC-MALLS) 11,810 Da, M_n/M_{nth} 1.07, d*n*/d*c* 0.187, PDI 1.14.
- **[monomer]$_0$ / [CPADB]$_0$ = 107** (Run no. 14 in Table 9.1). CPADB (57.6 µL, 4.92 × 10^{-6} mol), ACPA (47 µL, 1.65 × 10^{-6} mol). Total reaction time: 428 min. Final conversion (NMR, 55 °C, ns = 8, D1 = 14 s): 95 %. M_n (SEC-MALLS) 23,860 Da, M_n/M_{nth} 0.99, d*n*/d*c* 0.187, PDI 1.06.
- **[monomer]$_0$ / [CPADB]$_0$ = 215** (Run no. 15 in Table 9.1). CPADB (28.8 µL, 2.45 × 10^{-6} moles), ACPA (23 µL, 8.08 × 10^{-7} moles). Total reaction time: 480 min. Final conversion (NMR, 55 °C, ns = 8, D1 = 14 s): 98 %. M_n (SEC-MALLS) 57,280 Da, M_n/M_{nth} 1.16, d*n*/d*c* 0.187, PDI 1.14.
- **[monomer]$_0$ / [CPADB]$_0$ = 320** (Run no. 16 in Table 9.1). CPADB (19.2 µL, 1.64 × 10^{-6} mol), ACPA (15.5 µL, 5.45 × 10^{-7} mol). Total reaction time: 480 min. Final conversion (NMR, 55 °C, ns = 8, D1 = 14 s): 99 %. M_n (SEC-MALLS) 89,250 Da, M_n/M_{nth} 1.20, d*n*/d*c* 0.187, PDI 1.23.

9.2.13 RAFT copolymerization of *N*-(2-hydroxyethyl) methacrylamide and M3 in deuterated acetate buffer: ManA$_{17}$ grafts.

4,4'Azobis(cyanopentanoic acid) (1.97 × 10^{-2} g, 7.03 × 10^{-5} mol) was dissolved in DMSO-d6 (1 mL), cooled to ~ 8 °C and diluted with an equal volume of deuterated acetate buffer (0.20 M, pD 5.3) to give c_{ACPA} = 3.51 × 10^{-2} mol L^{-1}. The RAFT agent (CPADB, 2.38 × 10^{-2} g, 8.53 × 10^{-5} mol) was dissolved in pure DMSO-d6 (1 mL, c_{CPADB} = 8.53 × 10^{-2} mol L^{-1}). HEMAm (4.65 × 10^{-3} mol, 0.600 g) was dissolved in acetate buffer (2.65 mL) and filtered through a syringe filter (0.22 µm, Nylon) to remove the suspended inhibitor (BHT). **M3** (0.046 g, 1.41 × 10^{-5} mol) was dissolved in acetate buffer (500 µL), added to the HEMAm solution (280 µL, 1.75 mol L^{-1}) and mixed with a calculated amount of CPADB (19.2 µL, 1.64 × 10^{-6} mol) and ACPA (15.5 µL, 5.45 × 10^{-7} mol). The polymerization mixture (f_{M3} = 2.8 %, [CPADB]$_0$ / [ACPA]$_0$ = 3.0) was then transferred to a NMR tube equipped with a Young valve which was sealed, degassed with 3 freeze-evacuate-thaw cycles and plunged in a water bath preheated at 60 °C. At the end of the polymerization, the reaction mixture was

analyzed by aqueous SEC-IV-MALLS to determine the molar mass distribution and intrinsic viscosity of the polymer Total reaction time: 540 min. Final conversion (NMR, 55 °C, ns = 16, D1 = 14 s): 98 %. M_n (SEC-MALLS) 76,860 Da, M_n/M_{nth} 1.14, d*n*/d*c* 0.190, PDI 1.23. Experiment AG11-21-LP1, run no. 17 in Table 9.1.

9.2.14 RAFT copolymerization of *N*-(2-hydroxyethyl) methacrylamide and M6 in deuterated acetate buffer: $GulA_{20}$ grafts.

4,4'Azobis(cyanopentanoic acid) (1.97×10^{-2} g, 7.03×10^{-5} mol) was dissolved in DMSO-d6 (1 mL), cooled to ~ 8 °C and diluted with an equal volume of acetate buffer (0.20 M, pH 5.3) to give $c_{ACPA} = 3.51 \times 10^{-2}$ mol L^{-1}. The RAFT agent (CPADB, 2.38×10^{-2} g, 8.53×10^{-5} mol) was dissolved in pure DMSO-d6 (1 mL, $c_{CPADB} = 8.53 \times 10^{-2}$ mol L^{-1}). HEMAm (0.600 g, 4.65×10^{-3} mol) was dissolved in acetate buffer (2.65 mL, $c_{HEMAm} = 1.75$ mol L^{-1}) and filtered through a syringe filter (0.22 µm, Nylon) to remove the suspended inhibitor (BHT). **M6** (0.037 g, 9.39×10^{-6} mol) was dissolved in acetate buffer (0.500 mL), added to a calculated amount of HEMAm (280 µL), CPADB (19.2 µL, 1.64×10^{-6} mol) and ACPA solutions (15.5 µL, 5.45×10^{-7} mol). The polymerization mixture ($f_{\mathbf{M6}} = 1.9$ %, $[CPADB]_0 / [ACPA]_0 = 3.0$) was transferred to a NMR tube equipped with a Young valve that was sealed, degassed by 3 freeze-evacuate-thaw cycles and plunged in a water bath preheated at 60 °C. At the end of the polymerization, the reaction mixture was analyzed by aqueous SEC-IV-MALLS to determine the molar mass distribution and intrinsic viscosity of the polymer. Total reaction time: 540 min. Final conversion (NMR, 55 °C, ns = 16, D1 = 14 s): 95 %. M_n (SEC-MALLS) 55,980 Da, M_n/M_{nth} 0.96, d*n*/d*c* 0.192, PDI 1.21. Experiment AG11-21-LP2, run no. 18 in Table 9.1.

9.3 Results and discussion

9.3.1 Synthesis of RAFT agents

Two water soluble RAFT agents possessing a 4-carboxy-2-cyanobutan-2-yl leaving group were examined for the polymerization of methacrylamide derivatives (Scheme 9.2 and Scheme 9.3). CPADB **3** was first exploited by McCormick's work for the polymerization of sulfonated styrenes [11] and acrylamides [12] in aqueous solution. Later on they used this RAFT agent for the reversible-deactivation radical polymerization of various methacrylamide

derivatives in aqueous solution. [2b,5h,13] The versatility of this RAFT agent made it also useful for the polymerization of several methacrylates, [14] and styrenic derivatives. [11,15] On the other hand, trithiocarbonate RAFT agents bearing a 4-carboxy-2-cyanobutan-2-yl leaving group has been particularly used for the polymerization of methacrylate derivates. [16] Recently, Johnson et al. [17] reported the copolymerization of peptide monomers with *N*-(2-hydroxypropyl(methacrylamide) (HPMA) in aqueous solution in the presence of CPATTC **6** as a control agent. Interestingly, polymers with good to excellent control over molecular weight were obtained with fairly low polydispersity indices (PDI < 1.2).

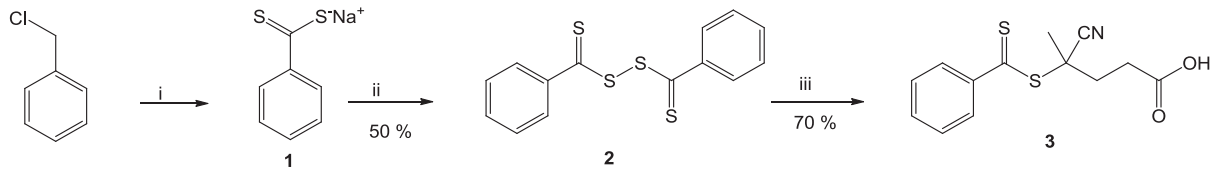

Scheme 9.2 *Synthesis of 4-cyano-4-[(phenylcarbonothioyl)sulfanyl] pentanoic acid (CPADB, **3**). Conditions: (i) sulfur, NaOMe, MeOH, 70 °C, 10 hours. (ii) KI/I_2, H_2O. (iii) 4,4'-azobis(cyanopentanoic acid), EtOAc, 90 °C, 18 hours.*

The synthesis of 4-cyano-4-[(phenylcarbonothioyl)sulfanyl] pentanoic acid **3** was carried out according to literature with only minor modifications (Scheme 9.2). [18] Briefly, Sodium dithiobenzoate **1** was prepared by reacting benzyl chloride with elemental sulfur in the presence of sodium methoxide. The compound was immediately oxidized with potassium triiodide to disulfide **2**, which was then refluxed in the presence of 4,4'-azobis(cyanopentanoic acid) to yield product **3** as amorphous red solid after chromatographic purification (R_f 0.23 in EtOAc/PE/EtOH 3:6:1).

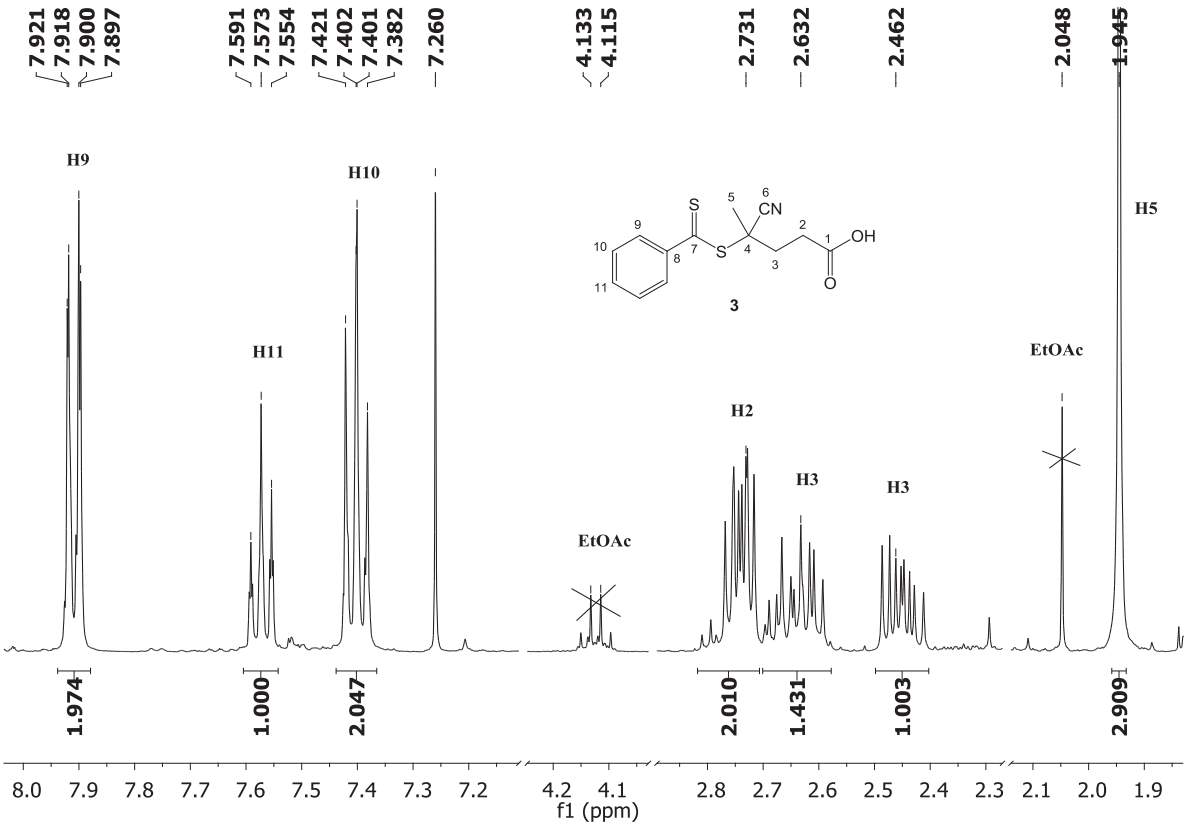

Figure 9.2 *^{1}H-NMR spectrum of the 4-cyano-4-[(phenylcarbonothioyl)sulfanyl] pentanoic acid **3**. Conditions: 400 MHz, $CDCl_3$, 25 °C, 7 mg mL^{-1}, ns = 16, D1= 3 s.*

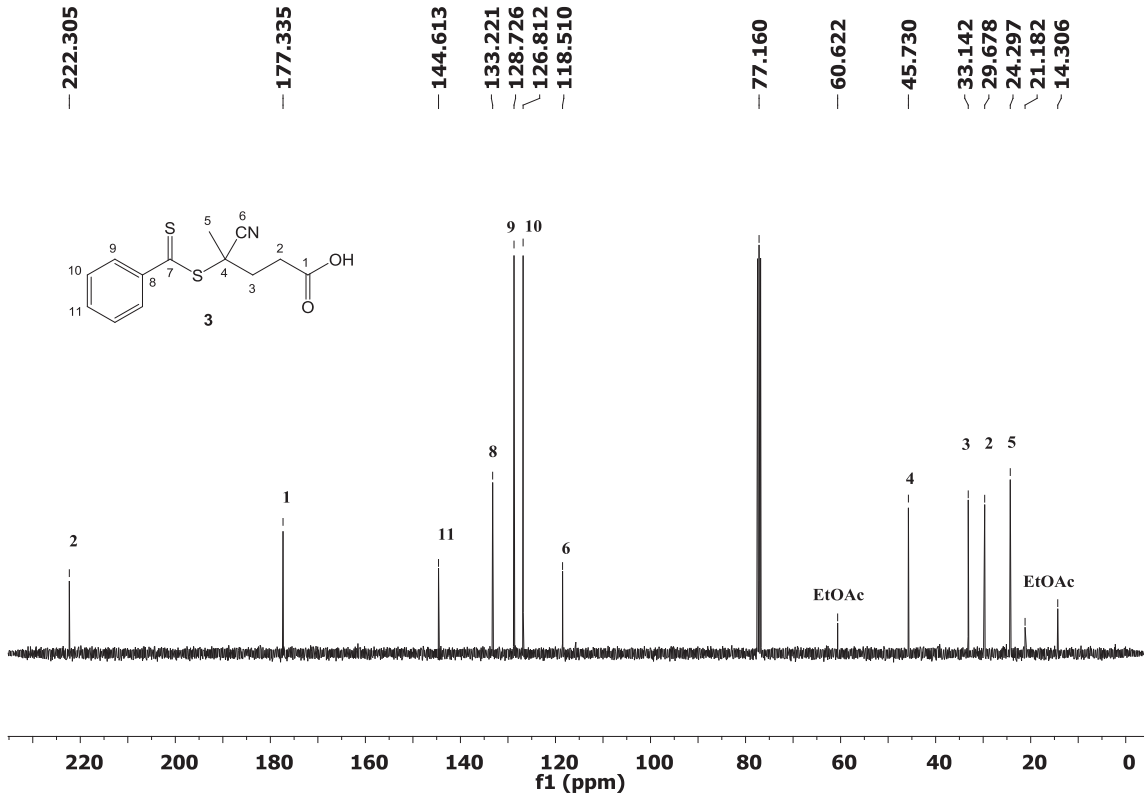

Figure 9.3 *^{13}C-NMR spectrum of the 4-cyano-4-[(phenylcarbonothioyl)sulfanyl] pentanoic acid **3**. Conditions: 100 MHz, $CDCl_3$, 25 °C, 4 %w/w, ns = 64, D1= 10s.*

Figure 9.2 and Figure 9.3 show the ^{1}H and ^{13}C NMR spectrum of the purified product together with the assignment of all peaks. Disregarding residual EtOAc, the product looks fairly pure and the spectra are identical to those reported in the literature.

The synthesis of trithiocarbonate RAFT agent **6** was adapted from the procedure Moad et al. [19] and carried out in aqueous solution (Scheme 9.3).

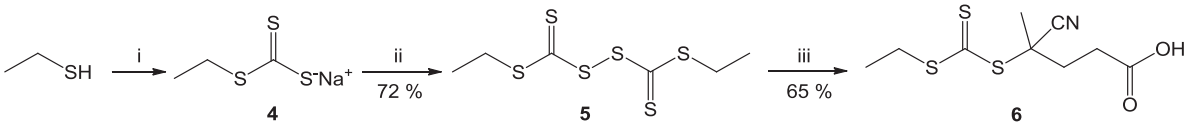

Scheme 9.3 *Synthesis of 4-cyano-4-{[(ethylsulfanyl)carbonothioyl]sulfanyl}pentanoic acid (CPATTC, **6**). Conditions: (i) NaOH, CS_2, TBAB, N_2, 0 °C, 75 min. ii) KI/I_2, H_2O. iii) 4,4'-azobis(cyanopentanoic acid), EtOAc, 90 °C, 19 hours.*

Sodium trithiocarbonate **4** was synthesized by the reaction of ethanethiol with carbon disulfide in basic conditions using a catalytic amount of tetra-*n*-butylammonium bromide (TBAB) as phase transfer catalyst. The resulting trithiocarbonate **4** was oxidized with potassium triiodide to yield the corresponding disulfide derivative **5** as yellowish oil after

flash chromatographic purification. Next, **5** was refluxed in the presence of 4,4'-azobis(cyanopentanoic acid) and the resulting oily crude sample was purified by flash chromatography to yield the desired product **6** as yellow solid (R_f 0.38 in PE/EtOAc/EtOH 8:1.5:0.5).

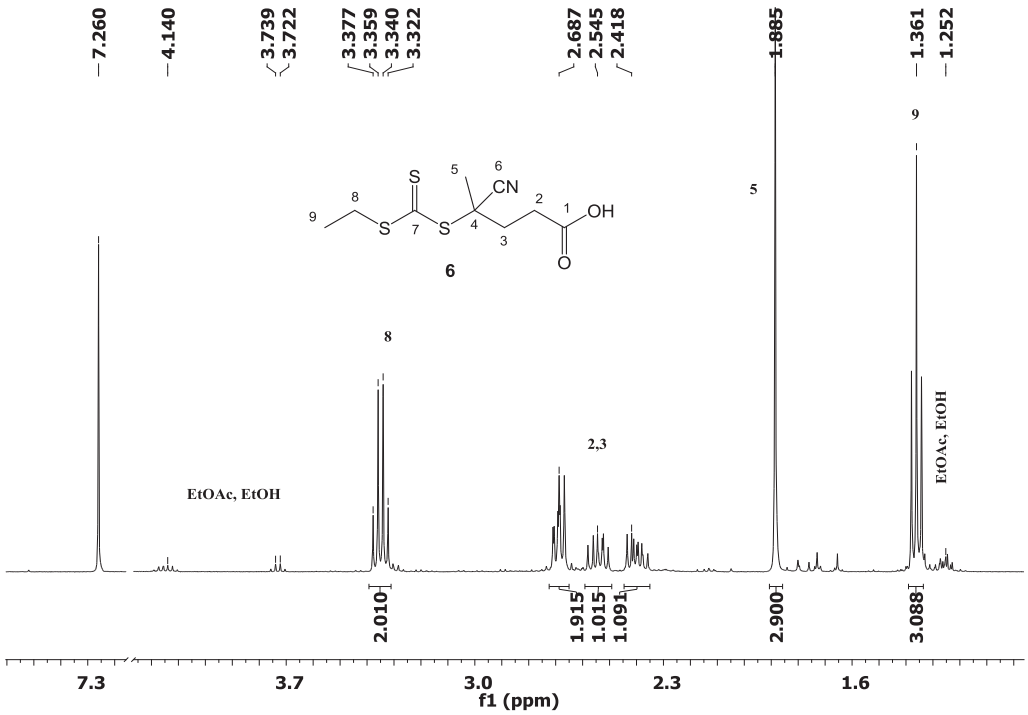

Figure 9.4 *^{1}H-NMR spectrum of 4-cyano-4-{[(ethylsulfanyl)carbonothioyl]sulfanyl} pentanoic acid **6**. Conditions: 400 MHz, $CDCl_3$, 25 °C, 2 %w/w, ns 16, D1 3s.*

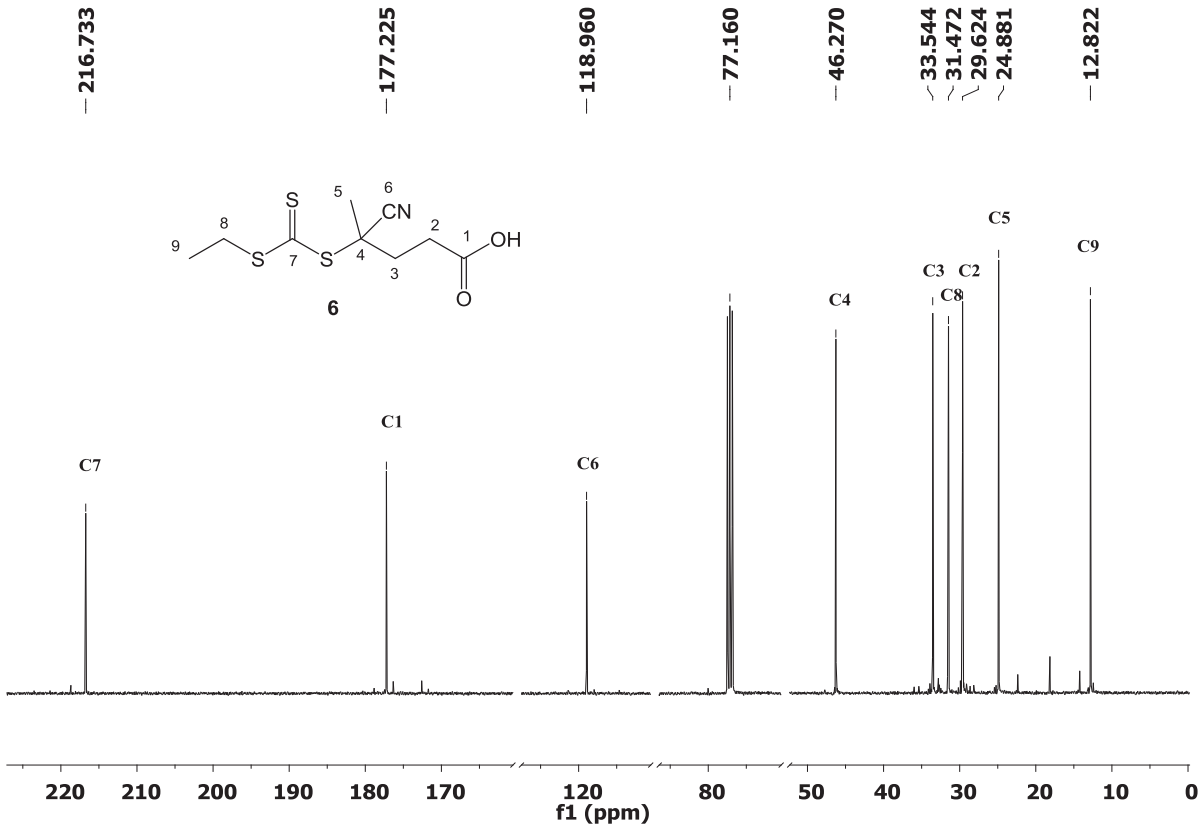

Figure 9.5 *^{13}C-NMR spectrum of 4-cyano-4-{[(ethylsulfanyl)carbonothioyl]sulfanyl} pentanoic acid **6**. Conditions: 100 MHz, $CDCl_3$, 25 °C, 100 mg mL^{-1}, ns 1000, D1 10 s.*

From the NMR spectra in Figure 9.4 and Figure 9.5 the product looks pure, with only some residual EtOAc and EtOH. The triplet at 1.36 and the quartet and 3.35 ppm are due to the CH_3CH_2S- group, whereas the singlet at 1.88 ppm (H5, CH_3) confirms, after integration, the success of the reaction. The multiplet at 2.68 ppm with an integral of 2 was attributed to H2, whereas the two multiplets centered at 2.42 and 2.54 ppm (each with an integral of one) are the diastereotopic protons on C3. From ^{13}C-NMR the characteristic trithiocarbonate signal is visible at 216 ppm. Here it should be noted that the 4,4'-azobis(cyanopentanoic acid) used for the synthesis of 3 and 6 was not optically pure and that the RAFT agents used in this study are a mixture of enantiomers.

Table 9.1 *Summary of RAFT polymerization experiments.*

Run no.	Monomer 1 (mol L^{-1}) [a]	Monomer 2 [b]			RAFT agent (mmol L^{-1})	ACPA (mmol L^{-1})	Solvent system		Reaction time (h)	Conv. (%)	dn/dc [c]	M_n (SEC)	M_n/M_{nth}	$[\eta]_w$ (mL/g) [d]	PDI	Exp. code
		mmol L^{-1}	Nature	DP_n			Buffer (c / mol L^{-1})	DMSO-d6 % v/v								
1	HEMA (2.21)	-	-	-	**6** (48.4)	9.64	- [e]	-	12.5	80	-	8057 [f]	1.61	-	1.21	AG11-10
2	HEMAm (1.04)	-	-	-	**6** (10.3)	3.06	carbonate	9.6	6	78	0.199	39900	> 4	43.2	2.89	AG11-08-LP1
3	HEMAm (1.04)	-	-	-	**3** (10.4)	3.06	carbonate	9.9	6	68	0.174	9600	1.07	7.3	- [g]	AG11-08-LP2
4	HEMAm (1.00)	-	-	-	**3** (10.2)	3.01	acetate (0.1)	16	7.2	77	0.174	8500	1.05	7.1	1.03	AG11-13-LP6
5	HEMAm (1.02)	-	-	-	**3** (10.4)	3.06	acetate (1.0)	9.9	6.5	77	0.174	9400	1.11	7.2	1.03	AG11-12-LP2
6	HEMAm (1.02)	-	-	-	**3** (10.4)	3.06	acetate (0.2)	9.9	6.5	77	0.174	8900	1.08	7.2	1.03	AG11-12-LP1
7	HEMAm (1.01)	-	-	-	**3** (8.55)	2.82	acetate (0.2)	14	7	79	0.174	10900	1.01	8.0	1.03	AG11-13-LP1
8	HEMAm (1.06)	-	-	-	**3** (6.35)	2.08	acetate (0.2)	10	7	78	0.174	13300	0.97	8.8	1.03	AG11-13-LP2
9	HEMAm (1.13)	-	-	-	**3** (3.60)	1.20	acetate (0.2)	5.8	8.5	75	0.174	16400	1.04	9.9	1.03	AG11-13-LP4
10	HEMAm (1.15)	-	-	-	**3** (2.77)	0.93	acetate (0.2)	4.4	10.5	83	0.184	19600	0.90	11.4	1.03	AG11-13-LP5
11	HEMAm (0.551)	**M1** (28.4)	ManA	9	**3** (2.19)	1.03	acetate (0.2)	9.3	11.8	97	0.190	49520	0.98	30.7	1.11	AG11-15-LP2
12	HEMAm (0.382)	**M1** (38.1)	ManA	9	**3** (1.51)	0.71	acetate (0.2)	6.4	11.8	98	0.183	81510	1.08	40.2	1.13	AG11-15-LP1
13	HEMAm (0.498)	**M1** (32.4)	ManA	9	**3** (9.94)	3.28	acetate (0.2)	16	7.1	87	0.187	11810	1.07	-	1.14	AG11-20-LP1
14	HEMAm (0.555)	**M1** (36.1)	ManA	9	**3** (5.56)	1.87	acetate (0.2)	9.2	7.1	95	0.187	23860	0.99	-	1.06	AG11-20-LP2
15	HEMAm (0.590)	**M1** (38.5)	ManA	9	**3** (2.95)	0.97	acetate (0.2)	4.8	8	98	0.187	56800	1.15	-	1.15	AG11-20-LP3
16	HEMAm (0.603)	**M1** (39.3)	ManA	9	**3** (2.01)	0.67	acetate (0.2)	3.3	8	99	0.187	89250	1.20	-	1.23	AG11-20-LP4
17	HEMAm (0.603)	**M3** (17.3)	ManA	17	**3** (2.01)	0.67	acetate (0.2)	3.3	9	98	0.190	76860	1.14	-	1.23	AG11-21-LP1
18	HEMAm (0.568)	**M6** (10.9)	GulA	20	**3** (1.90)	0.63	acetate (0.2)	3.1	9	95	0.192	55980	0.96	-	1.21	AG11-21-LP2

General conditions: D_2O/DMSO-d6, pD ≅ 7-8 (carbonate buffer) or pD = 5.3 (acetate buffer), 60 °C [a] HEMA is 2-hydroxyethylmethacrylate, HEMAm is 2-hydroxyethylmethacrylamide. [b] AlgiMERs of the methacrylamide type. [c] The dn/dc values for run no.9 and 10 were determined experimentally. The latter was then used for run 3-8, whereas the value for run no. 2 was extrapolated according to the formula $(dn/dc)_M = (dn/dc)_\infty - b / M$. [9] Values calculated according to the formula $dn/dc = F_1 \upsilon_1 + F_2 \upsilon_2$ where: F_i and υ_i are the weight fraction and the differential refractive index increment of each monomer, respectively. [d] Weight average intrinsic viscosity from on-line differential viscometer. [e] In CD_3OD. [f] As PMMA equivalent, measured by SEC in *N*,*N*-dimethylformamide (DMF). [g] Bimodal distribution.

9.3.2 Choice of polymerization conditions

As mentioned before, trithiocarbonates possessing a 4-carboxy-2-cyanobutan-2-yl leaving group are known to be effective RAFT agents for the polymerization of methacrylates. [1b,c,20] Also, in aqueous solution they are more stable than the corresponding dithiobenzoates and are less prone to induce retardation in the polymerization kinetics. In one of their papers, [13c] McCormick and collaborators mentioned that trithiocarbonates are effective RAFT agents for acrylamide derivatives but not for methacrylamide ones. Yet, they did not cite any specific nor offered further details. At the same time, a recent report by Johnson et al. [17] describes the successful use of this RAFT agent to mediate the copolymerization of peptide monomers with *N*-(2-hydroxypropylmethacrylamide) (HPMA) in aqueous solution.

Faced with contradicting evidence, I decided to compare the performance of CPATTC **6** and CPADB **3**. The choice of the best RAFT agent and polymerization conditions was made by conducting a series of homopolymerization reactions of HEMAm in D_2O/DMSO-d6 at 60 °C. The use of a co-solvent (DMSO-d6) was dictated by the observation that even at pH ≅ 8-10, the solubility of CPATTC in water is only ~0.06 M. In the initial tests (run no. 2 and 3, Table 9.1) the pD of the mixture was adjusted to ~ 8 with anhydrous Na_2CO_3. The results obtained with **6** were disappointing (run no. 2, Table 9.1), and fairly polydisperse poly(HEMAm) (PDI = 2.89) was obtained having an average molar mass much higher than the predicted value ($M_n/M_{nth} > 4$; Figure 9.6). In order to confirm that the loss of control was not due to impurities in the batch of RAFT agent used, the polymerization of 2-hydroxyethyl methacrylate (HEMA) with CPATTC in CD_3OD was conducted as well (run no. 1, Table 9.1). In this case, a fairly low monodisperse polymer was obtained (PDI = 1.21) having a molar mass not too far from the predicted value ($M_n/M_{nth} = 1.6$). Here it should be noted that when the pHEMA obtained in this experiment was injected to an aqueous SEC system, the sample did not elute from the columns. Hence, the latter data were obtained on an organic SEC system (DMF) calibrated with narrow PMMA standards. The error inherent to this procedure is most probably at the origin of the deviation observed (Figure 9.7).

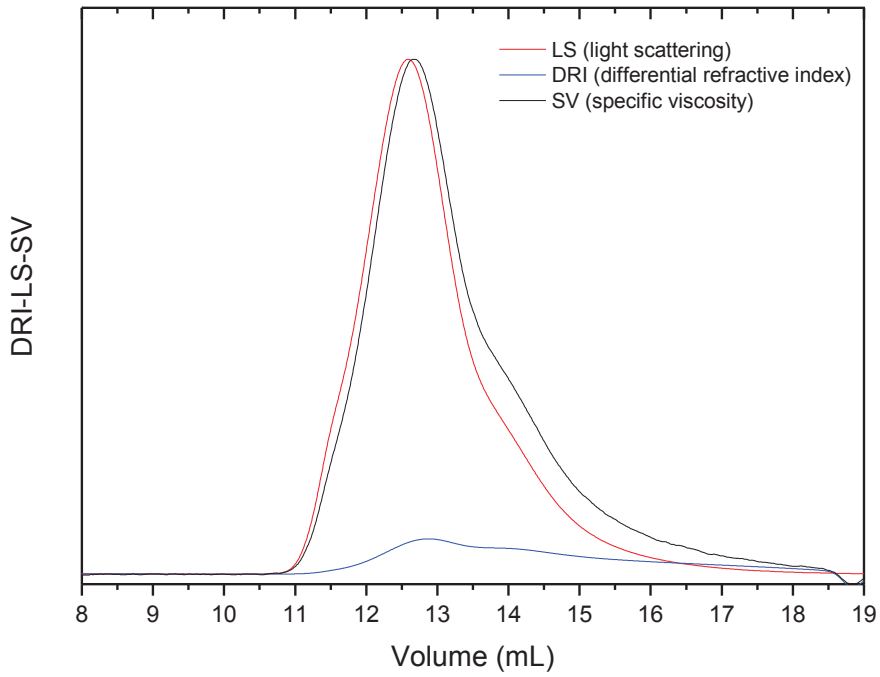

Figure 9.6 *SEC chromatogram of poly(HEMAm) obtained with CPATTC in D_2O/DMSO-d6 (pD ≅ 8; run no. 2, Table 9.1). Sample concentration 7 g L^{-1}, columns Shodex OH pak SB-(803 +804) HQ.*

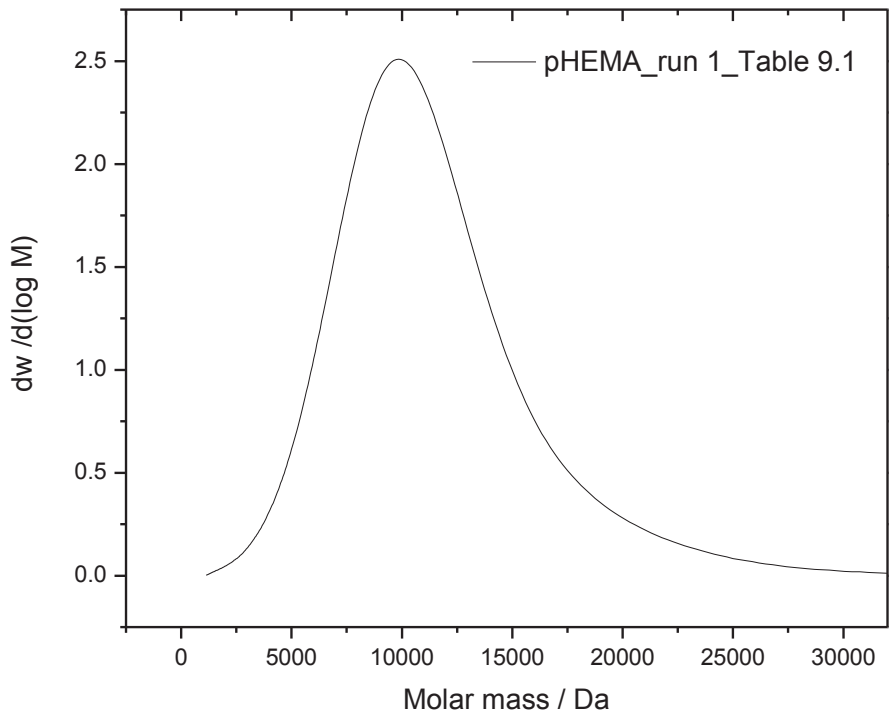

Figure 9.7 *Molecular weight distribution for pHEMA obtained from the CPATTC mediated polymerization of HEMA in CD_3OD at 60 °C (run no. 1, Table 9.1). Organic SEC system (DMF) used that is calibrated with narrow PMMA standards.*

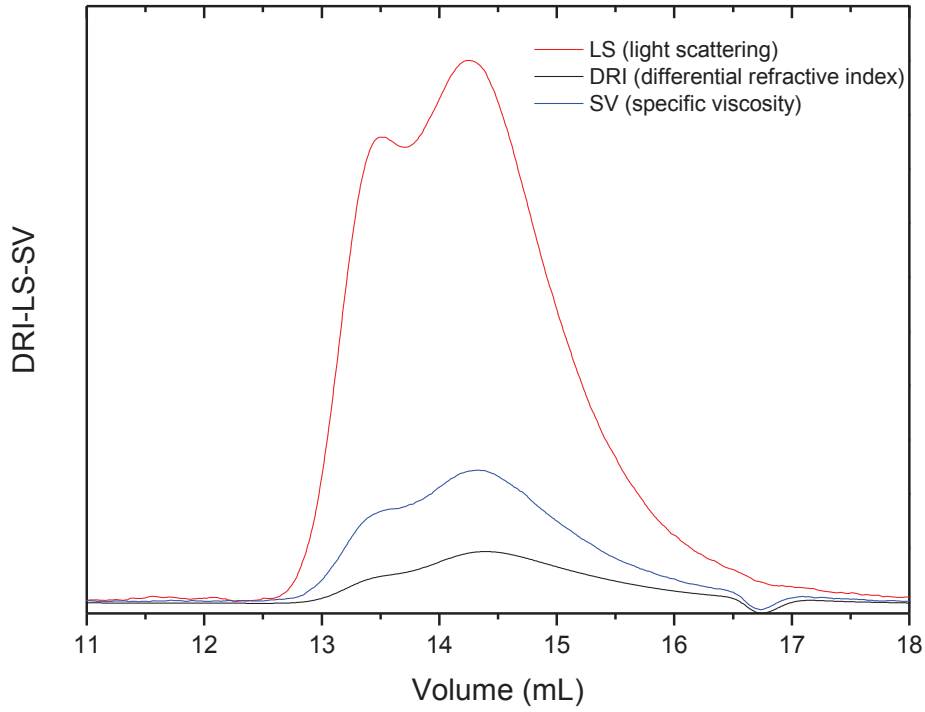

Figure 9.8 *SEC chromatograms of poly(HEMAm) obtained by RAFT polymerization in the presence of CPADB in D_2O (pD ~ 8; run no. 3, Table 9.1). Sample concentration 5 g L^{-1}, columns Shodex OHpak SB-(802.5 +803) HQ.*

Under identical conditions (run no. 3, Table 9.1), CPADB **3** led to a reasonable control over the average molecular weight (M_n/M_{nth} = 1.07) but with a bimodal distribution (Figure 9.8). This could be due to degradation of the RAFT agent during polymerization under basic conditions, as already observed by other investigators. [21] Indeed, CPADB is more stable at pD 5.3 than at pD 8, [21a] as visually confirmed by the change in color from pink to orange when going from slightly acidic to slightly basic conditions (Figure 9.9). According to McCormick and collaborators [13c,d] the RAFT polymerization of methacrylamide derivatives with CPADB works best at pH ≅ 5.2-5.9, the proposed explanation being that the acidic conditions are necessary to suppress the aminolysis of the RAFT agent by the ammonia/amines generated by the partial hydrolysis of the monomer.

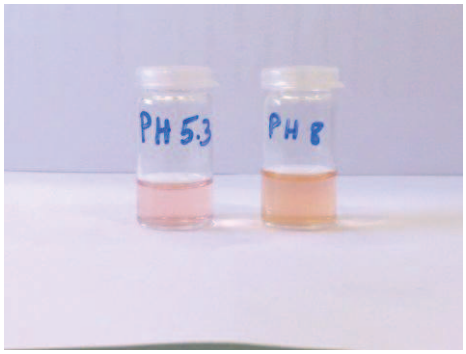

Figure 9.9 *Solutions of CPADB RAFT agent in D_2O/DMSO-d6 at pD 5.3 (left) or pD ≅ 8 (right). Note the change of color from pink to orange with increasing pD (room temperature).*

Indeed, when HEMAm was polymerized in acetate buffer (1 mol L^{-1}, pD 5.3) in the presence of CPADB, good control over molecular weight was obtained (M_n/M_{nth} = 1.11, PDI = 1.03; run no. 5, Table 9.1). Still, a small shoulder was observed in the SEC chromatograms at twice the peak molar mass (Figure 9.10). This result was unexpected, since at 77% conversion bimolecular termination of tertiary macroradicals should be limited. For instance, Gibian et al. [22] showed that in a self-reaction of simple primary, secondary, and tertiary alkyl radicals the values of k_{td}/k_{tc} are 0.06, 0.2 and 0.8 respectively, where k_{td}/k_{tc} is the ratio of disproportionation to combination. [23] An alternative explanation would be the termination of intermediate radical **7** with a low molecular weight species (Scheme 9.4), but in this case it is unclear how the pH of the solution and (or) the presence of acetate ions could influence that. [24]

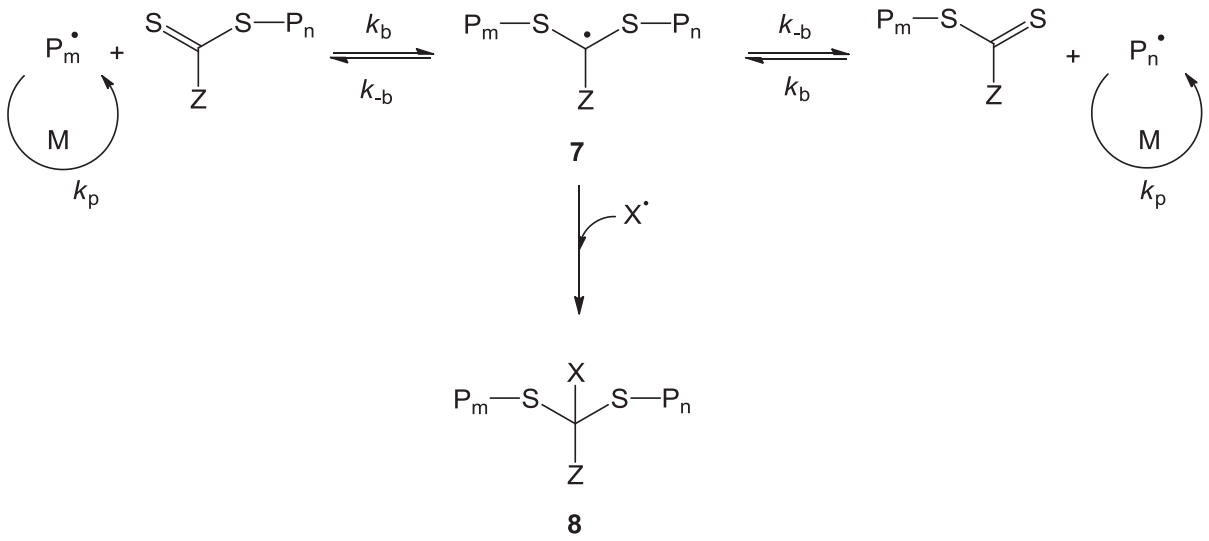

Scheme 9.4 *Termination of intermediate radical 7 during a RAFT polymerization with a low molecular weight species $X^{\bullet}$.*

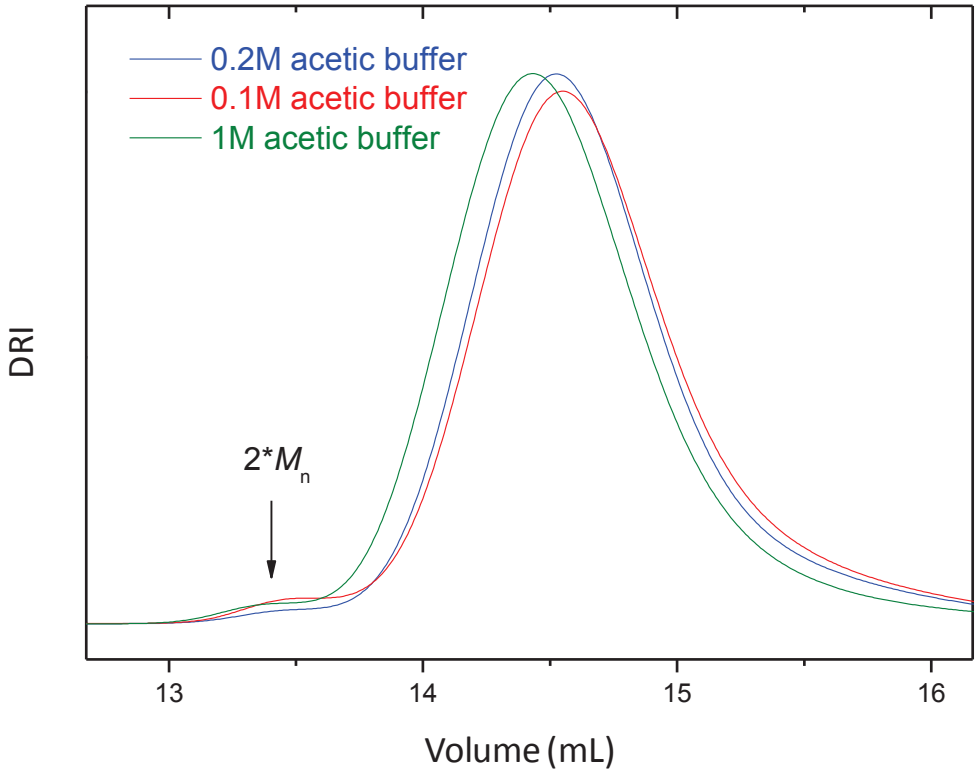

Figure 9.10 *Area normalized SEC traces of the poly(HEMAm) obtained with CPADB in 0.1, 0.2 and 1mol L^{-1} acetate buffer (pD 5.3; run no. 4-6 in Table 9.1).*

Anticipating solubility problems for AlgiMERs at high ionic strength (*i.e.* in a 1 mol L^{-1} buffer), two lower buffer concentrations were tested as well (0.1 mol L^{-1} and 0.2 mol L^{-1}; run no. 4 and 6, Table 9.1). There was no detectable influence of the buffer's concentration on the rate of polymerization and, after 6.5-7 hours of reaction, 77 % conversion was achieved in the three cases. Also, nearly monodisperse polymers (PDI = 1.03) with a predetermined molar mass were obtained (M_n/M_{nth} = 1.05-1.08). Figure 9.10 shows the area normalized SEC chromatograms for the polymerizations at different buffer concentration: Since the use of a 0.20 mol L^{-1} deuterated acetate buffer (pD = 5.3) best minimizes the occurrence of a high molecular weight shoulder, this condition was used in all following experiments. Hence, five polymerizations of HEMAm (~ 1 mol L^{-1}) were conducted in deuterated acetate buffer (0.20 mol L^{-1}) at 60 °C in the presence of different concentrations of CPADB (Scheme 9.5), run no. 6-10 in Table 9.1).

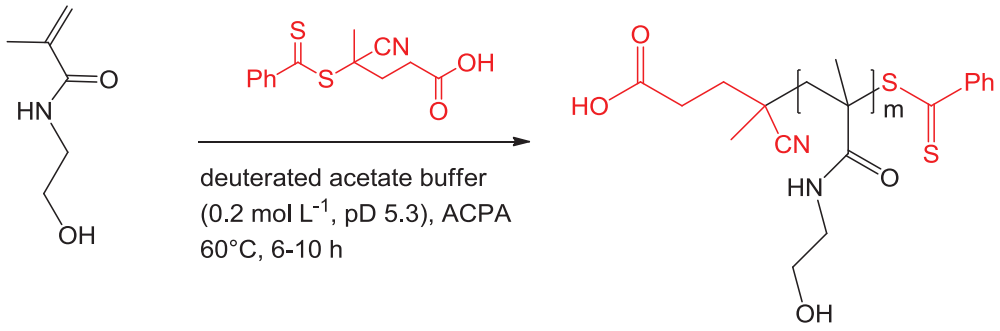

Scheme 9.5 *RAFT polymerization of HEMAm mediated by CPADB in acetate buffer (run no. 6-10, Table 9.1).*

In all experiments, the ratio HEMAm / CPADB was verified by ^{1}H-NMR prior to polymerization and the latter value was used for M_{nth} calculation with Eq. 9.1. A RAFT agent to initiator ratio of 3.0 was used in all cases except for run no. 6, where the same ratio was 3.4. As a result, when higher molecular weight polymers were targeted (and a lower concentration of chain transfer agent and initiator were used) longer reaction times were needed to achieve ≅ 80 % conversion (up to 10 h). The same phenomenon was described by McCormick et al. [13d] for the polymerization of *N*-(2-hydroxypropyl)methacrylamide) with CPADB.

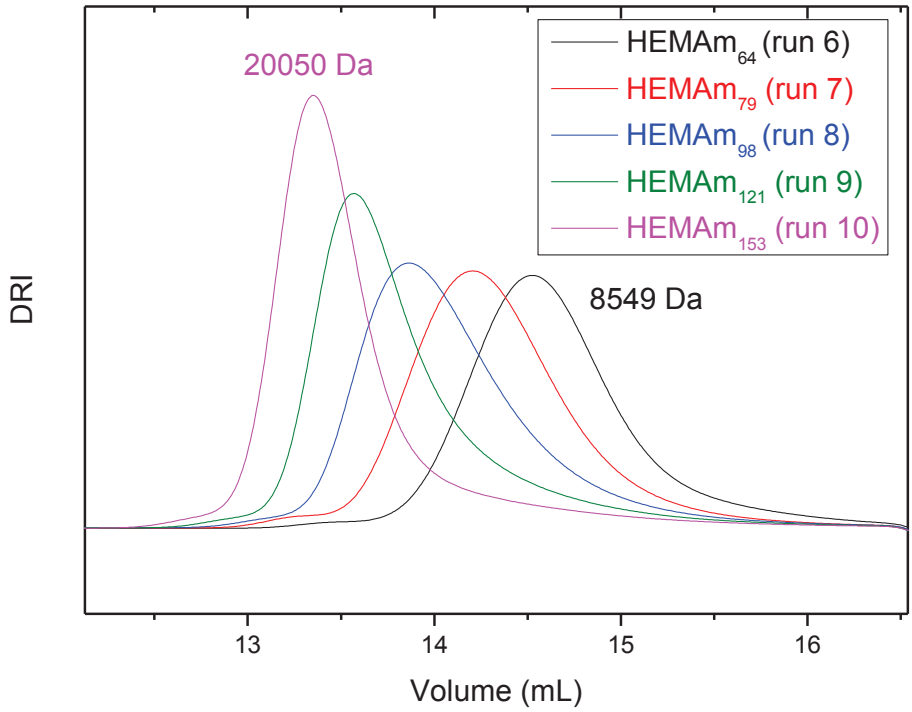

Figure 9.11 *Evolution of SEC traces with decreasing RAFT agent concentration for the homopolymerization of HEMAm (run no. 6-10 in Table 9.1). Columns: Shodex OH pak SB-(Guard + 802.5 + 803) HQ. Injected samples ~ 5 mg mL^{-1}.*

Figure 9.11 shows the evolution of unimodal, symmetrical SEC traces towards lower elution volumes with decreasing RAFT agent concentration. This represents a significant improvement over previous attempts to control the polymerization of HEMAm in carbonate buffer at pD ≅ 8. The high molecular weight shoulder at twice M_{peak} is barely visible from the DRI signal, but is clearly seen in the light scattering and differential viscometer ones (not shown). As shown in Figure 9.12, nearly monodisperse polymers were obtained in all cases (PDI =1.03), and a good agreement between the theoretical and the experimental molecular weights was observed (M_n / M_{nth} = 0.90 - 1.08). Here it should be noted that only the d*n*/d*c* values for samples from run no.9 and 10 were determined experimentally and that the former was then used for run 3-8. The value for run no. 2 was instead extrapolated according to the relationship: [9]

$$(dn/dc)_M = (dn/dc)_\infty - b / M \qquad (9.4)$$

Where b is a constant and $(dn/dc)_M$ and $(dn/dc)_\infty$ are the refractive index increment of polymer of mass *M* and of "high" molar mass, respectively. The latter quantity was determined from a

sample obtained by conventional radical polymerization (M_n 232 000 Da, PDI 1.74, dn/dc = 0.208 mL g^{-1}).

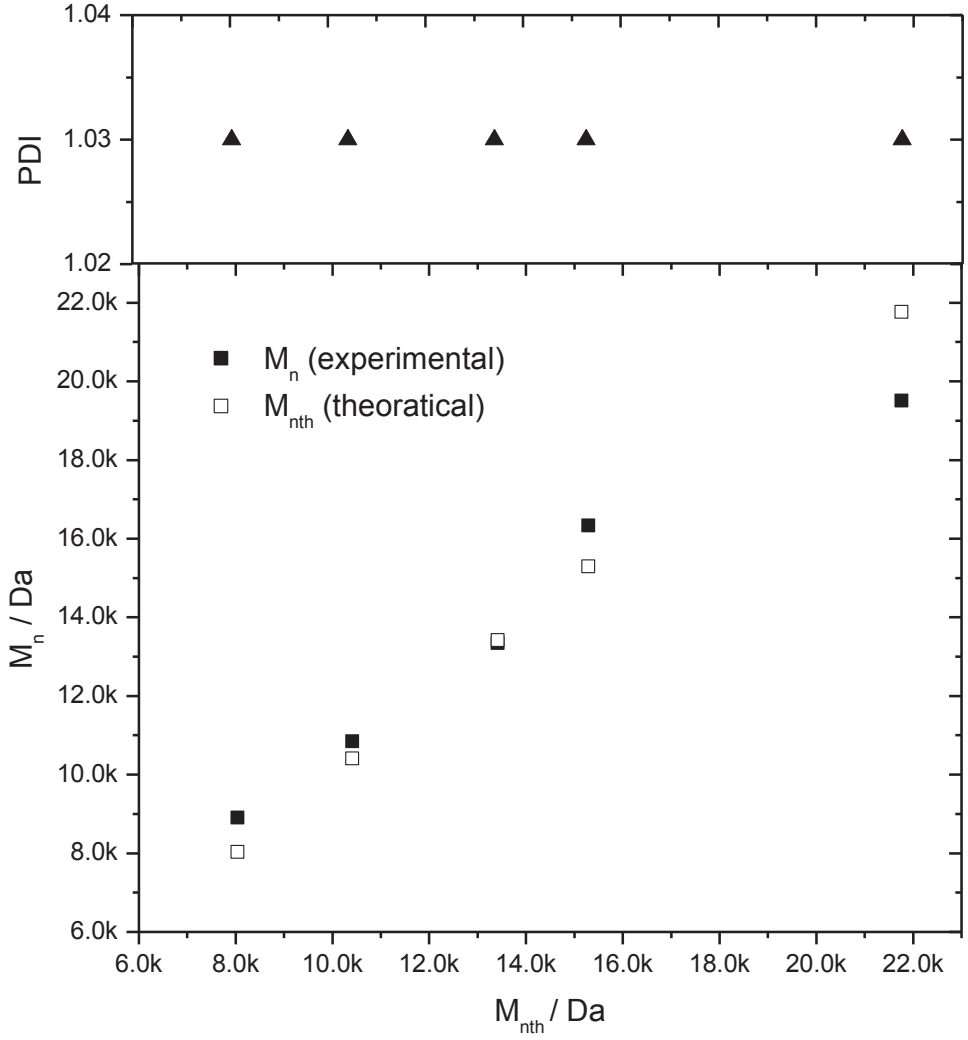

Figure 9.12 *Correlation between experimental and theoretical molecular weight (down) and polydispersity index (up) for the RAFT polymerization of HEMAm using CPADB in deuterated acetate buffer (pD 5.3). Run no. 6-10 in Table 9.1.*

9.3.3 RAFT copolymerization of AlgiMERs and HEMAm

The protocol developed for the RAFT polymerization of HEMAm was applied to the copolymerization of the same monomer with AlgiMERs (i.e. oligoalginate derived macromonomers) of different molar mass (Scheme 9.6).

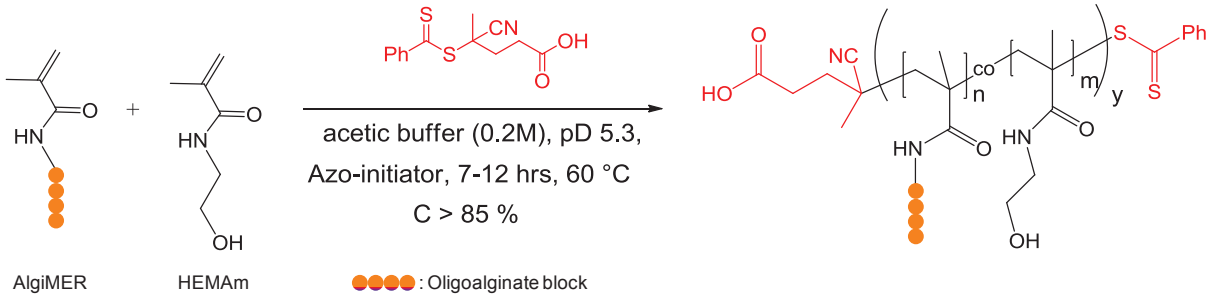

Scheme 9.6 *Schematic representation of the copolymerization of HEMAm and AlgiMERs.*

The theoretical molecular weights were calculated as follows:

$$M_{n,th} = x.\frac{[M_1]_0 + [M_2]_0}{[RAFT]_0}.(f_1 M_1 + f_2 M_2) + M_{RAFT} \qquad (9.5)$$

where M_1, M_2 and M_{RAFT} are the molecular weights of monomer 1, monomer 2 and the RAFT agent respectively; x is total monomer conversion from ^{1}H-NMR, f_1 and f_2 are the molar fractions of monomer 1 and 2 in the feed, $[M_1]_0 + [M_2]_0$ is the overall initial monomer concentration and $[RAFT]_0$ is the initial concentration of the RAFT agent. The ratio $([M_1]_0 + [M_2]_0)/ [RAFT]_0$ was determined by ^{1}H-NMR for all experiments. Since the individual monomer conversion for M_1 and M_2 could not be quantified (the vinylic protons of the two species have identical chemical shifts in ^{1}H-NMR and the AlgiMER and polymer peaks are partially superimposed in SEC), the consumption rate of the comonomers was assumed to be identical. As seen in Chapter 8 this is not strictly true, but the error introduced in the calculation of $M_{n,th}$ is around 5 % and was considered to be acceptable.

A ^{1}H-NMR kinetic study of the RAFT copolymerization of HEMAm with **M1** was conducted (run no. 11 in Table 9.1). To this end, a mixture of **M1** (f = 4.9 %), HEMAm, CPADB and ACPA was introduced in a NMR tube equipped with a Young valve, degassed with a series of freeze-evacuate-thaw cycles and lowered into the NMR probe pre-heated at 60 °C. At regular intervals ^{1}H-NMR spectra were acquired (ns = 8 and D1 = 7s) and total conversion was calculated from the disappearance of vinylic protons (Figure 9.13). To this end, peak integrals were normalized with respect to the CH_2-NH (H4 in Figure 9.1) signal of HEMAm, where the integral of the CH_2-NH signal from HEMAm and polymer at 3.34 and 3.44 ppm was set to one and the integrals of the vinylics were recorded.

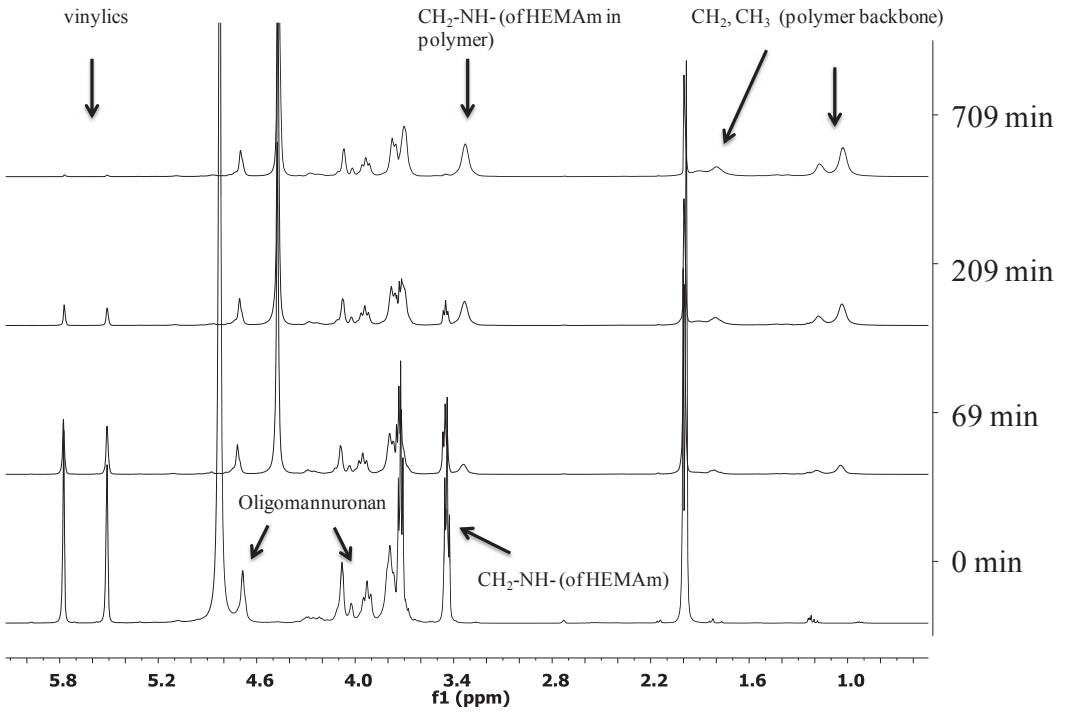

Figure 9.13 *Evolution of kinetic study for the CPADB mediated copolymerization of* ***M1****(551 mmol* L^{-1}*) and HEMAm (28.4 mmol* L^{-1}*) at 60 °C (run no.11, Table 9.1). Conditions: 400 MHz,* D_2O*, 333 K, ns = 8, D1 = 7s.*

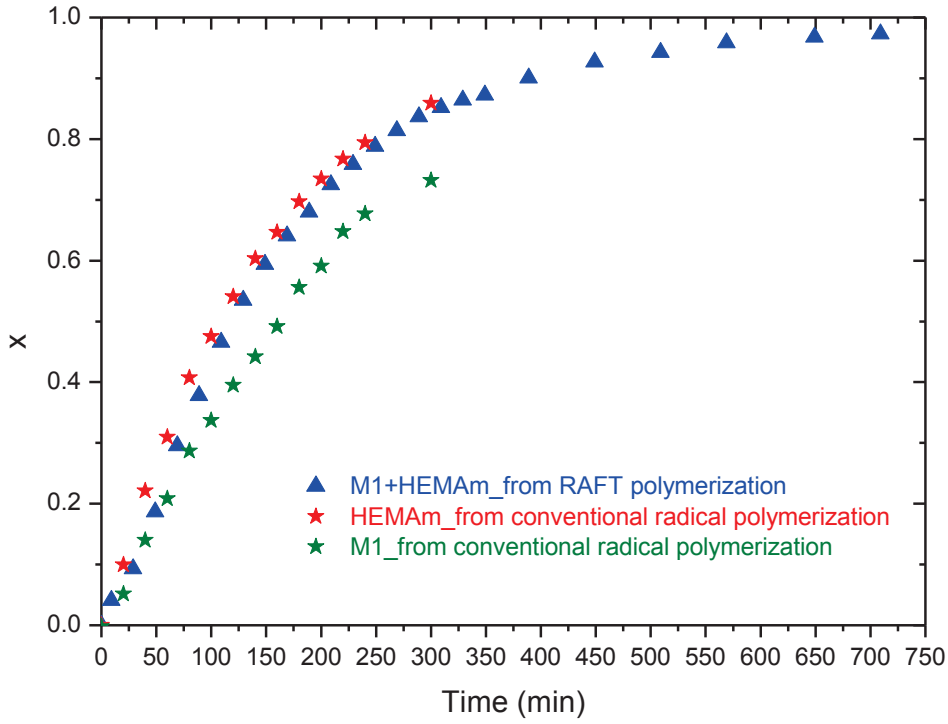

Figure 9.14 *Total monomer conversion (x) versus time for the copolymerization of HEMAm and mannuronan-derived AlgiMER* ***M1*** at 60 °C (run no. 11 in *Table 9.1*). *Star symbols refer*

to the conventional radical copolymerization of the same comonomers under nearly identical conditions (run no. 8 in Table 8.4).

Figure 9.14 shows the evolution of total conversion with time for the RAFT copolymerization and compares them with those obtained for the conventional radical copolymerization of the same comonomers under nearly identical conditions (run no. 8 in Table 8.4). Contrary to what observed by other authors, [3c,21b,25] the addition of CPADB to the polymerization mixture results in a slight induction period during the first 75 min of reaction, but the overall kinetics is barely affected and 80 % conversion was reached in 5 hours. SEC-IV-MALLS analysis confirmed that a well-defined copolymer was obtained (PDI = 1.11) with excellent control over the molecular weight (M_n/M_{nth} = 0.98). When the same copolymerization was conducted with a higher AlgiMER content in the feed ($f_{\mathbf{M1}}$ = 9.1 %) and lower initial concentrations of all reagents (run no. 12 in Table 9.1), a faster kinetics was observed. This contradicting result could be the consequence of the lower concentration of DMSO-d6 used (6.4 % v/v for run no. 12 vs. 9.3% for run no. 11) [26] and (or) of the formation of complexes between monomers and (or) monomers and polymer that alter the local monomer concentration around the propagating radicals. This type of phenomenon has already been described for the radical polymerization of acrylic acid [27] and acrylamide in water. [28]

Figure 9.15 shows the SEC-IV-MALLS chromatogram of the reaction mixture: unimodal symmetrical traces were obtained with the three detectors, whereas no high molecular weight shoulder is visible. The close superposition of concentration, specific viscosity and light scattering intensity traces indicate a nearly monodisperse polymer (PDI = 1.13) and the experimental molar mass was found to be close to the theoretical value (M_n/M_{nth} = 1.08). The same sample was injected on a SEC system equipped with a UV-Vis detector and the absorbance signal at 300 nm was found to superimpose with that from the DRI, as expected for dormant chains carrying a dithiobenzoate end-group (See Appendix 9.B).

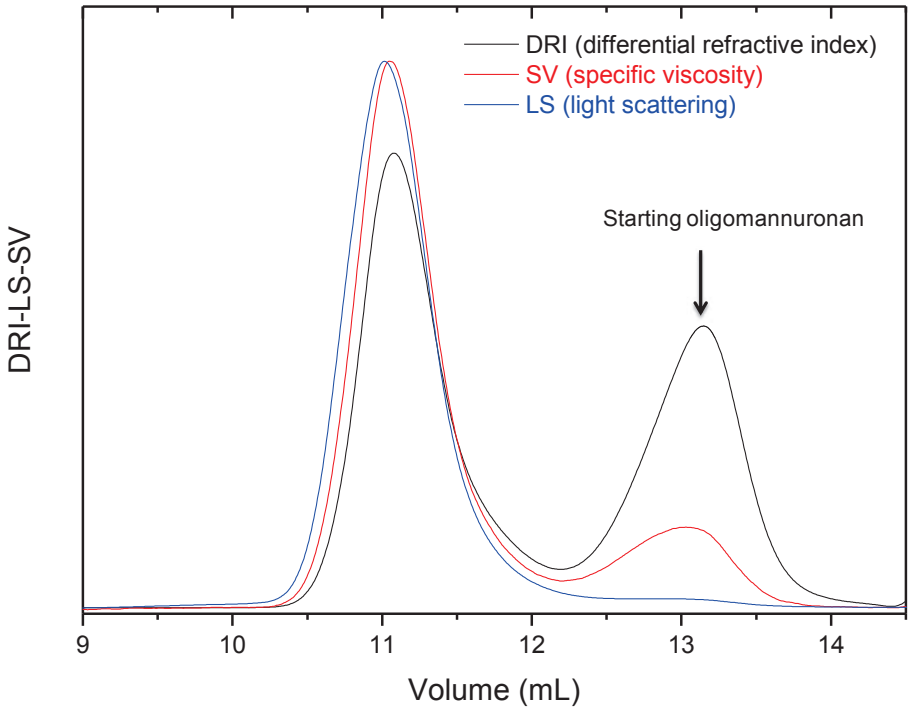

Figure 9.15 *SEC traces of poly(**M1**-co-HEMAm) obtained by RAFT copolymerization at 60 °C (run no. 12 in Table 9.1). Columns: Shodex OH pak SB-(Guard + 802 +803) HQ; injected sample concentration 2 g* L^{-1}.

The reversible-deactivation nature of the copolymerization was further investigated by carrying out a series of experiments with varying $c^0_{monomer}$ / c^0_{CPADB} ratios (run no. 13-16 in Table 9.1). Unexpectedly, for the sample with the highest RAFT agent concentration (run no. 13) the use of 16 % v/v DMSO-d6 as a co-solvent to solubilize the chain transfer agent resulted in part of the glycomonomer precipitating out of solution. Indeed, a preliminary solubility test had been carried out on the starting oligo(1→4)-β-D-mannuronan (DP_n = 9) and it was found to be soluble in the same solvent composition. All samples were reacted to high monomer conversion (87% - 99%) and the corresponding SEC traces are shown in Figure 9.16. The peaks are narrow but not perfectly symmetrical and a high molecular weight shoulder is visible in the first two traces (run no. 13 and 14). These shoulders correspond to the same molecular weight though (M_n ≅ 58 000 Da) and could be due to contamination of the SEC samples. As for previous samples, the absorbance signal at 300 nm was found to superimpose with that from the DRI, as expected for dormant chains carrying a dithiobenzoate end-group (See appendix 9.B).

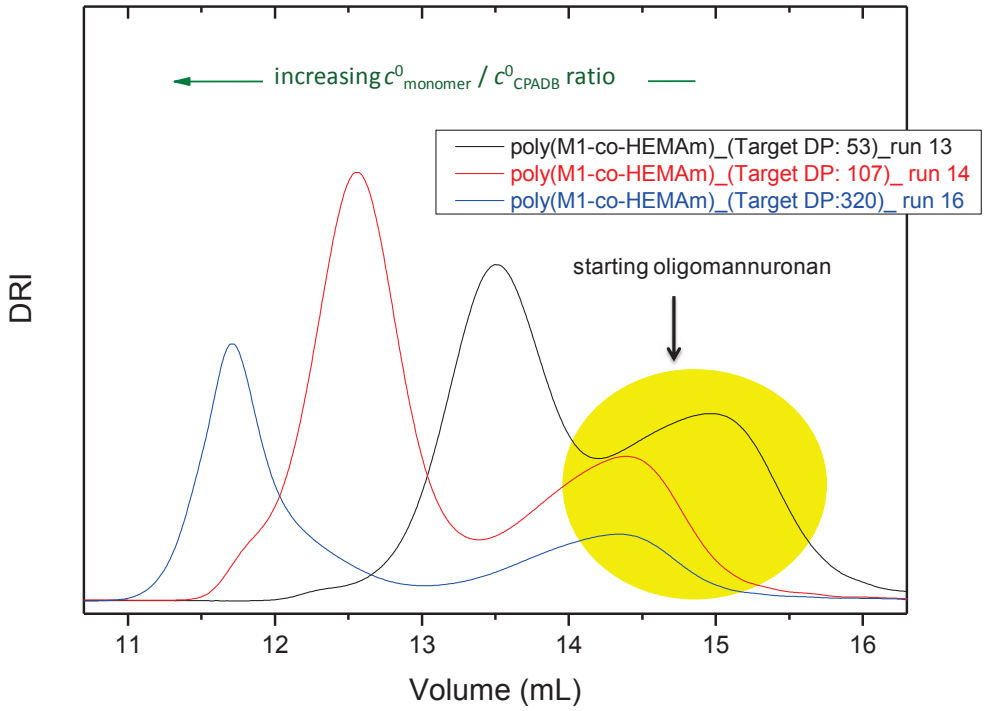

Figure 9.16 *SEC chromatograms for the copolymerizations of HEMAm and **M1** with different $c^0_{monomer}$ / c^0_{CPADB} ratios (from right to left run no. 13-16 in Table 9.1). Conditions: 35 °C, Shodex OH pak SB-(Guard + 802.5 +803) HQ, injected sample 4 g L^{-1}.*

An excellent control over the molar mass was achieved up to 25,000 Da (Figure 9.17), with PDI values in the interval 0.99-1.07 and fairly controlled at 50000 Da (M_n/M_{nth} = 1.15). For the higher molar mass sample instead, PDI was 1.23 and M_n/M_{nth} = 1.20. The latter result was somewhat surprising, since an analogous experiment with a lower HEMAm concentration (hence a higher proportion of glycomonomer in the feed) had led to encouraging results (run no. 12, M_n/M_{nth} = 1.08, PDI = 1.13).

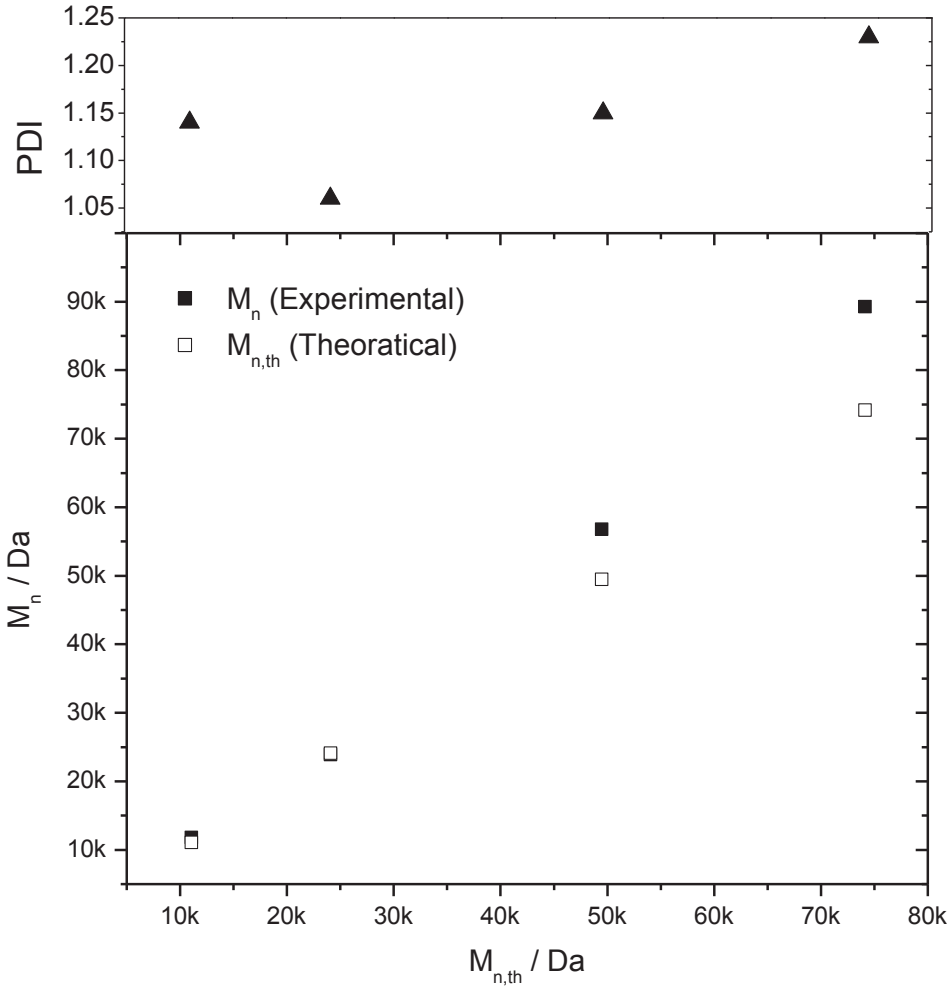

Figure 9.17 *Experimental vs. theoretical molecular weight (down) and polydispersity index (up) for the RAFT copolymerization of HEMAm and **M1** (run no. 13-16 in Table 9.1).*

The RAFT copolymerization of HEMAm with longer AlgiMERs was also attempted (run no. 17-18 in Table 9.1). To this end, (1→4)-β-D-mannuronan-derived monomer **M3** (DP_n = 17) and (1→4)-α-L-guluronan-derived monomer **M6** (DP_n = 20) were used. Contrary to what previously observed with the analogous conventional radical copolymerization (Chapter 8), no gelation occurred during the RAFT processes even at high conversion (X = 95 – 98 %). In run no. 18 though, a small amount of a white precipitate appeared after the first hour of reaction that was later solubilized by diluting the reaction mixture with water. Figure 9.18 shows the SEC chromatogram for the two copolymerization mixtures. Although the polymer and residual oligosaccharide traces are partially superposed (in particular for poly(HEMAm-co-**M6**)), the polymer traces appear to be unimodal, fairly symmetrical and without a high molecular weight shoulder. Low polydispersity glycopolymers were obtained in the two cases

(PDI = 1.21 - 1.23) and good control over the molecular weight was achieved (M_n/M_{nth} = 0.96 - 1.14).

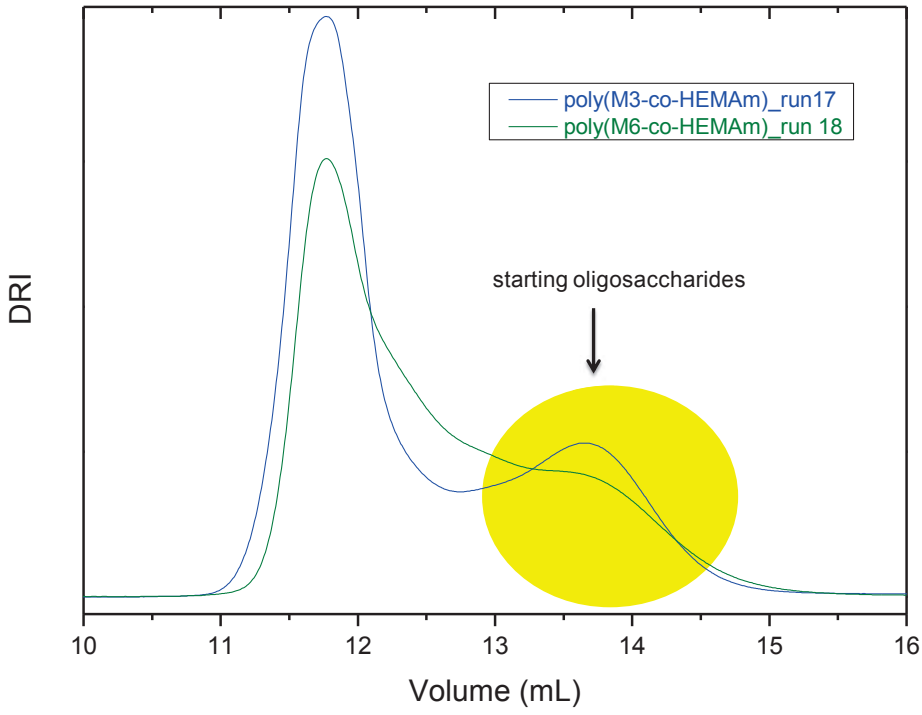

Figure 9.18 *SEC chromatograms for poly(HEMAm-co-**M3**) and poly(HEMAm-co- **M6**) obtained by RAFT copolymerization at 60 °C (run no. 17 and 18, Table 9.1). Note that the peak at higher elution volumes is due to the starting oligosaccharide used for the synthesis of the glycomonomer. Conditions: 35 °C, Shodex OH pak SB-(Guard + 802.5 +803) HQ, injected sample 4 g L^{-1}.*

9.3.4 Gelation and rheology

The gelling behavior of the obtained polymers was investigated. To this end, the polymer solutions from the long AlgiMERs, i.e. poly(**M3**-co-HEMAm) and poly(**M6**-co-HEMAm), were dialyzed to remove any residual oligosaccharides remaining after polymerization and freeze dried. Unfortunately, the intrinsic viscosities of the prepared polymers were not measured and the concentrations of the solutions in the semi dilute regime were prepared based on the intrinsic viscosity of poly(**M1**-co-HEMAm) having a comparable molecular weight as our polymers (run no. 11-12, Table 9.1). Hence the critical concentration to assure entanglement of chains in the semi dilute regime was considered ~ 30 mg mL^{-1}. The fluffy light pink solid was dissolved in D_2O to achieve concentrations above the critical concentration (62 and 70.8 mg mL^{-1} for poly(**M3**-co-HEMAm) and poly(**M6**-co-HEMAm) respectively), the pD was slightly adjusted to ~ 7-8 using anhydrous Na_2CO_3 to directly

dissolve the polymers, and a ^{1}H NMR was acquired to confirm the success of the dialysis step (Figure 9.19).

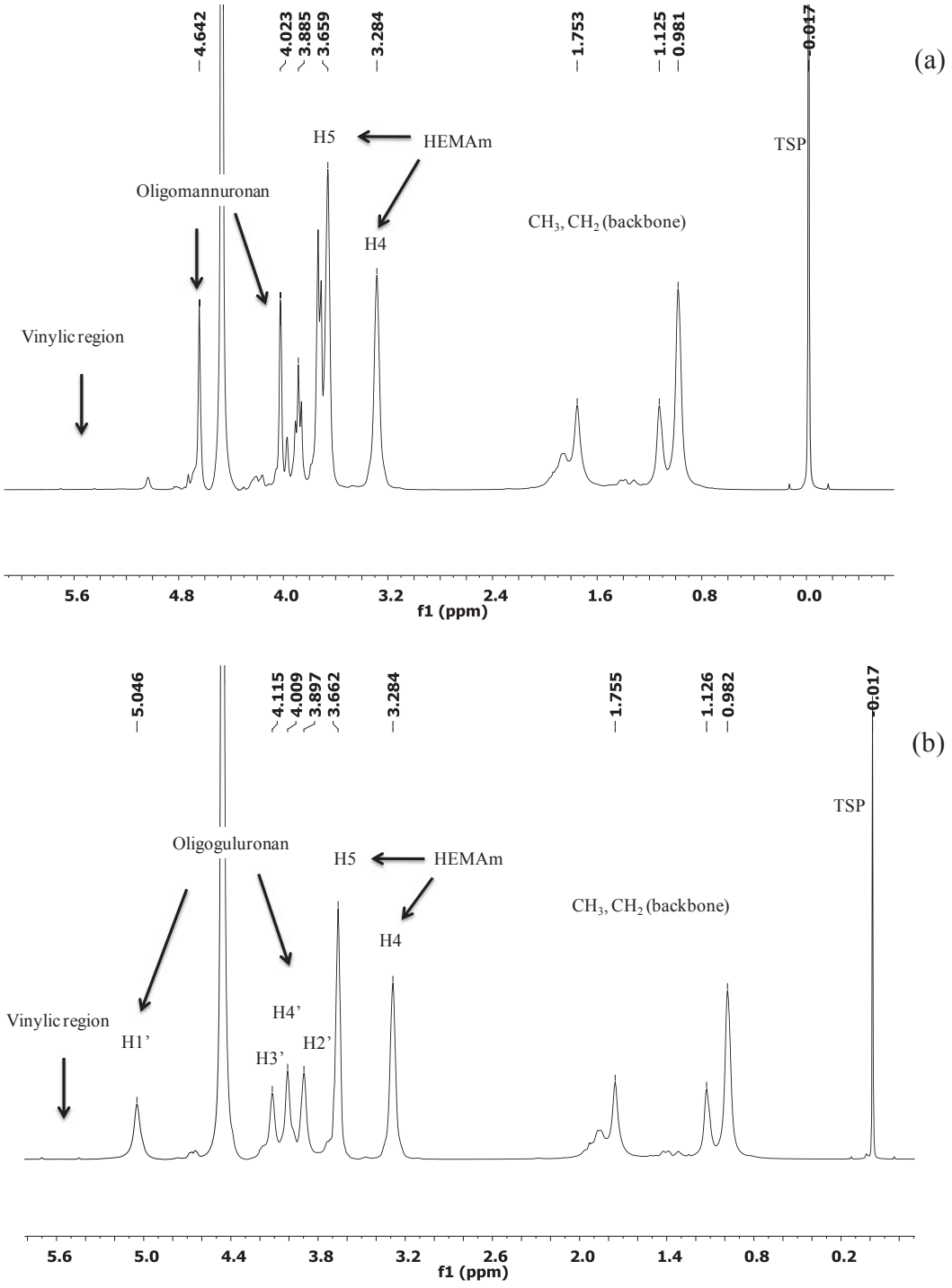

Figure 9.19 *^{1}H NMR spectra of dialyzed (a) poly(**M3**-co-HEMAm) and (b) poly(**M6**-co-HEMAm) obtained from the CPADB mediated polymerization of HEMAm with **M3** and **M6** at 60 °C respectively (run no. 17-18, Table 9.1). Conditions: 400 MHz, D_2O (pD ~7-8), 328 K, for (a) 62 mg mL^{-1}, ns = 436, D1 = 10 s and for (b) 70.8 mg mL^{-1}, ns = 295, D1 = 10 s.*

The polymer solutions from NMR were recovered and added drop wise over a $CaCl_2$ (0.5 mol L^{-1}) solution. Contrary to the oligomannuronan based polymer that did not gel in the presence of $CaCl_2$, the oligoguluronan derived polymer formed nice beads (Figure 9.20).

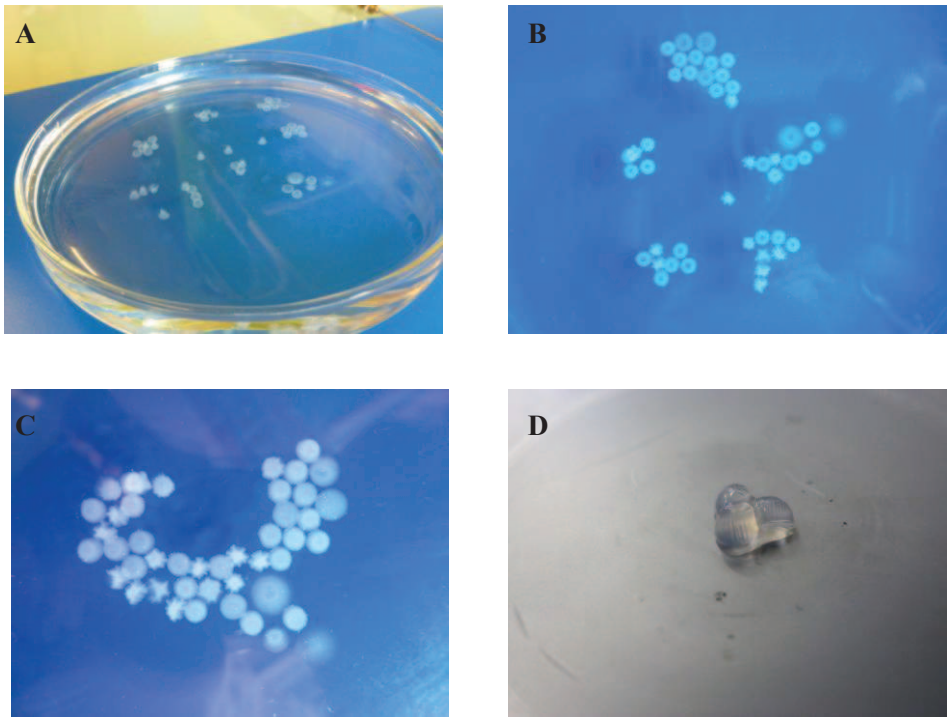

Figure 9.20 *Gel beads formation from poly(**M6**-co-HEMAm) in $CaCl_2$ (0.5 mol L^{-1}). Sample concentration: 70.8 mg mL^{-1}. Notice the diffusion of Ca^{2+} with time and the aggregation of the beads (Going from **A** to **C**).*

The rheological properties of the resultant gel beads were investigated using a dynamic rotational rheometer equipped with a parallel-plate system operating at 25 °C. Three beads at a time were placed on the plate of the rheometer for characterization. From Figure 9.21, the parameters reflecting the elastic (G'; storage modulus) and viscous (G''; loss modulus) components of the rheological properties were obtained at various frequencies. As shown, the variation of G' and G'' is almost independent of the frequency with $G'/G'' \cong 7$ (at 1 Hz) indicating the formation of a gel.

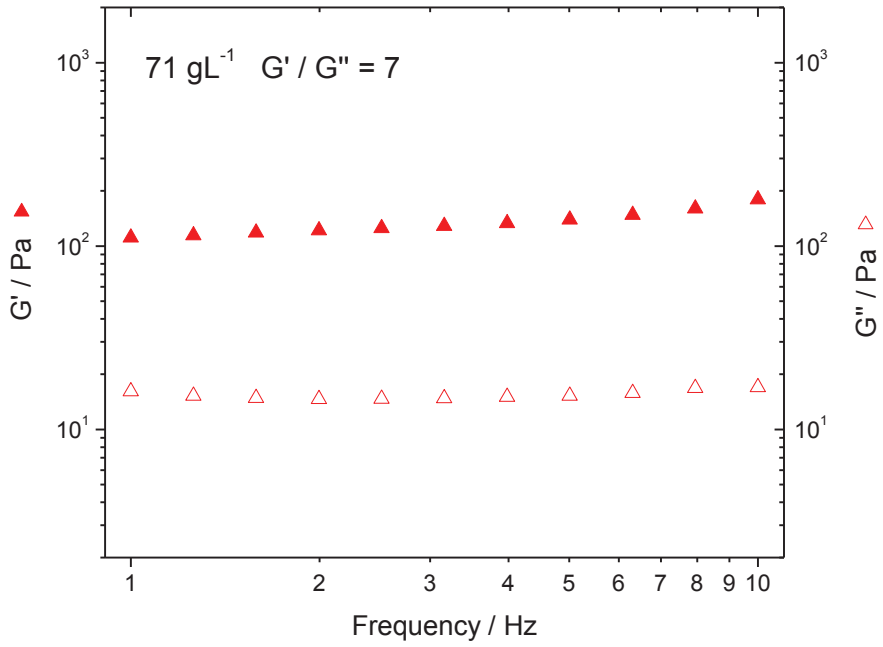

Figure 9.21 *Variation of G' and G" with frequency at 25 °C for P(**M6**-co-HEMAm) gels obtained from RAFT polymerization (run no. 18, Table 9.1).*

As before the stiffness of the obtained gel, P(**M6**-*co*-HEMAm), could be measured from the tangent at $\Delta y/y_0 = 0$ after plotting the variation of the force exerted by the gel upon compression (Figure 9.22). Unfortunately, calculating the elastic modulus from a system of 3 gel beads on the plate can introduce some error in calculating the surface area of contact with the plate and thus on the elastic modulus, that is why the plot was only shown without further calculations.

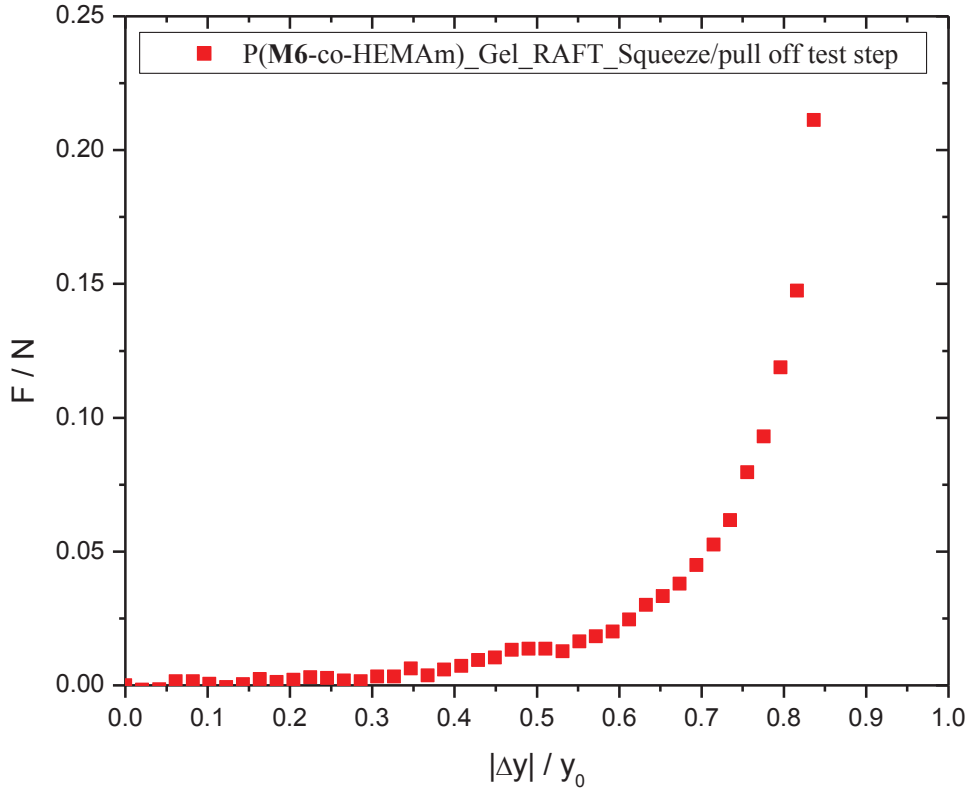

Figure 9.22 *Variation of the force applied by the gel of P(**M6**-co-HEMAm) obtained by RAFT polymerization (run no.18, Table 9.1) under compression.*

9.4 Take home messages

Several messages could be pointed out from the RAFT copolymerization of AlgiMERs:

i. From the preliminary studies, the CPADB mediated polymerization of *N*-(2-hydroxyethylmethacrylamide) (HEMAm) in acetic buffer (pD = 5.3) showed the characteristics of reverse-deactivation radical polymerization.

ii. The CPADB mediated copolymerization of methacrylamide derived AlgiMERs with HEMAm in acetic buffer (pD = 5.3) afforded polymers whose molecular weights were in agreement with the theoretical ones and with narrow molecular weight distributions.

iii. Copolymers bearing long AlgiMER grafts (guluronan DP_n = 20) yielded transparent hydrogel beads in the presence of $CaCl_2$ (0.5 mol L^{-1}).

Appendix 9.A Selected NMR spectra

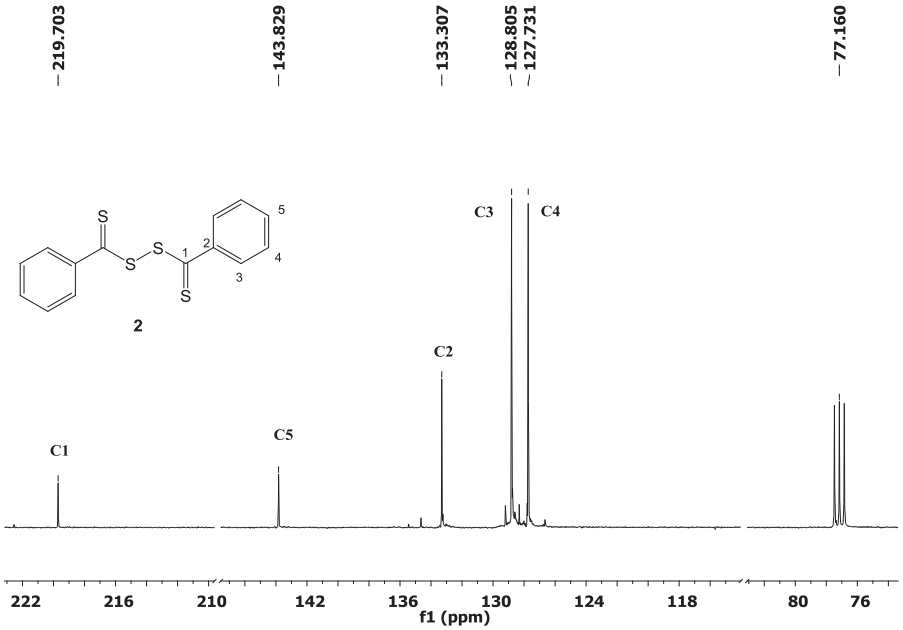

Figure 9.23 *^{13}C-NMR spectrum of bi(phenylcarbonothioyl) disulfide (**2**). Conditions: 100 MHz, $CDCl_3$, 25 °C, 43 mg mL^{-1}, ns 70, D1 10s.*

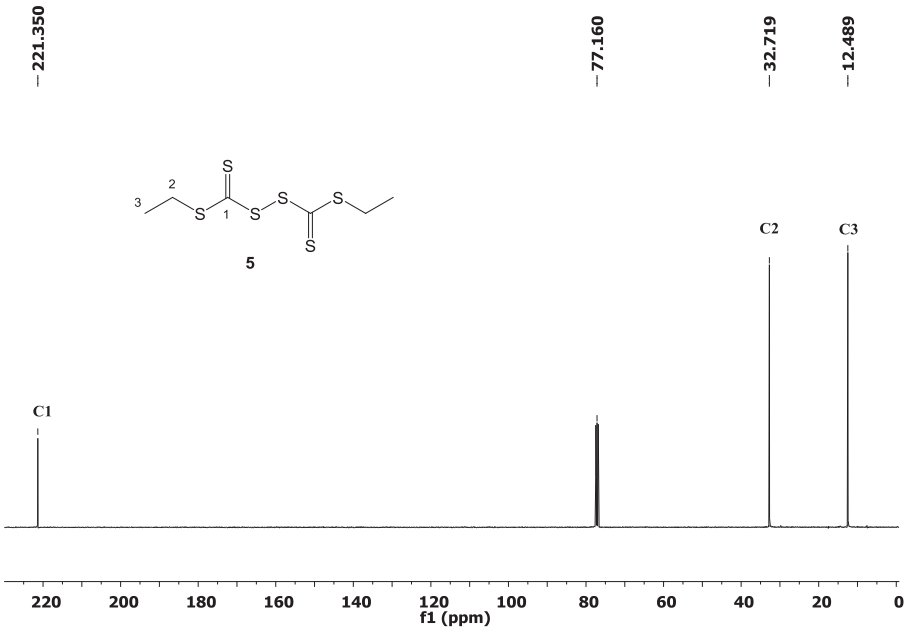

Figure 9.24 *^{13}C-NMR spectrum of bi[(ethylsulfanyl)carbonothioyl]disulfide (**5**). Conditions: 100 MHz, $CDCl_3$, 25 °C, 112 mg mL^{-1}, ns 807, D1 10s.*

Appendix 9.B Selected SEC chromatograms

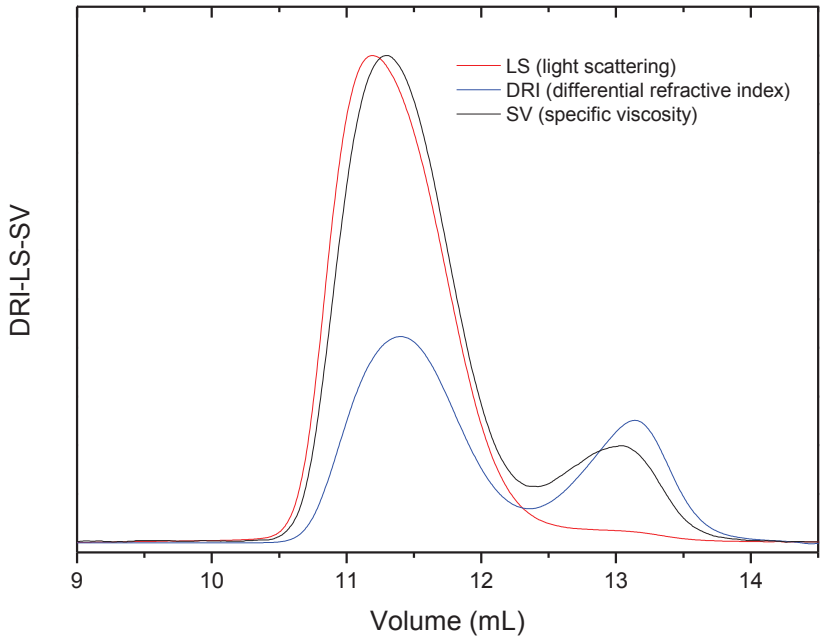

Figure 9.25 *SEC chromatograms of poly(HEMAm-co-**M1**), target DP_n = 243, obtained by RAFT polymerization of **M1** and HEMAm in the presence of CPADB in acetate buffer (pD ~ 5.3) at 60 °C (run 11, Table 9.1). Eluant: 0.1 M $NaNO_3$ + 10 mM EDTA + 0.03 % NaN_3, 30 °C, 3.75 g L^{-1}.Columns: Shodex OH pak SB-(Guard + 802 +803) HQ.*

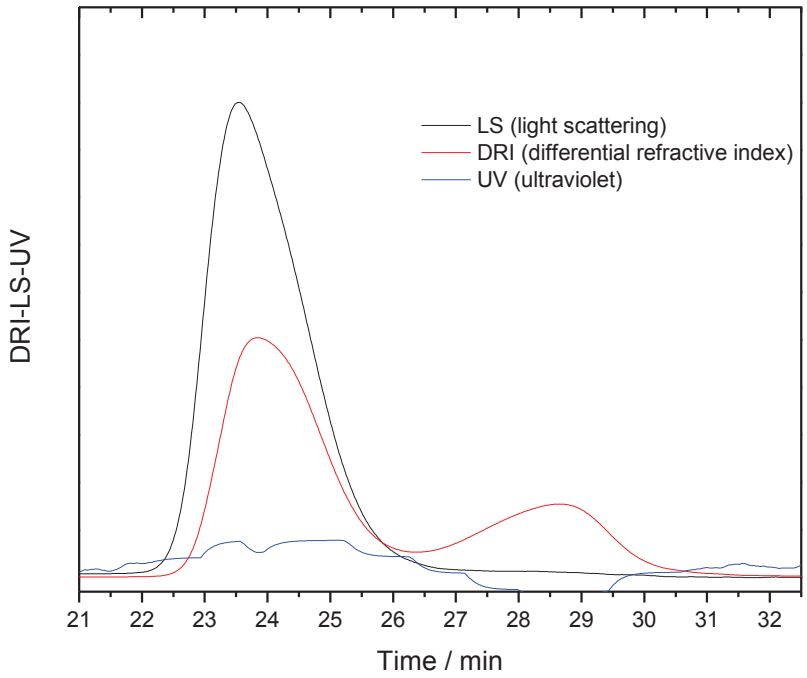

Figure 9.26 *SEC chromatograms of poly(HEMAm-co-**M1**), target DP_n = 243, obtained by RAFT polymerization of **M1** and HEMAm in the presence of CPADB in acetate buffer (pD ~ 5.3) at 60 °C (run 11, Table 9.1). Eluant: 0.1 M $NaNO_3$ + 10 mM EDTA + 0.03 % NaN_3, 30 °C, 3.75 g L^{-1}.Columns: Shodex OH pak SB-(Guard + 802.5 +803) HQ.*

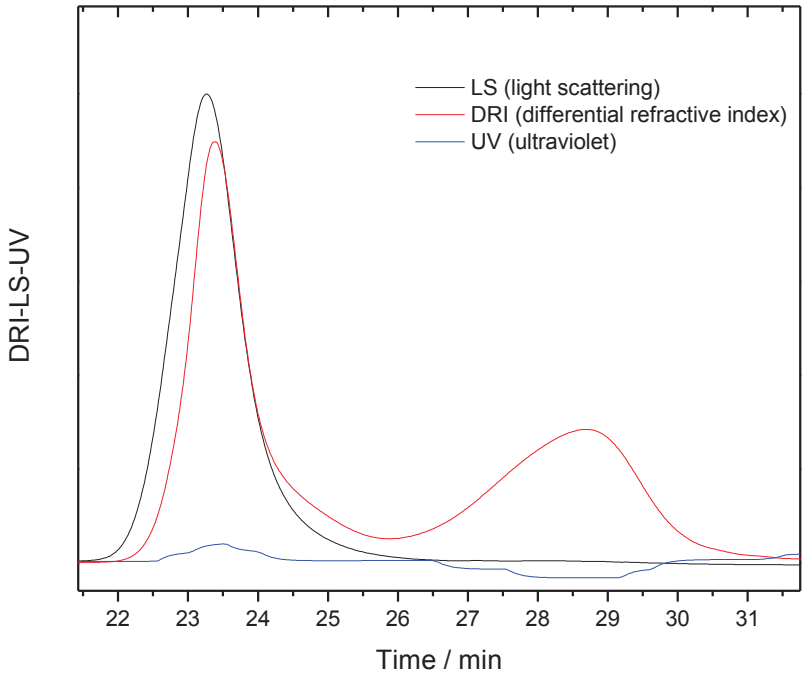

Figure 9.27 *SEC traces of poly(**M1**-co-HEMAm) obtained by RAFT copolymerization at 60 °C (run no. 12 in Table 9.1). Columns: Shodex OH pak SB-(Guard + 802.5 +803) HQ; injected sample concentration 2 g L^{-1}.*

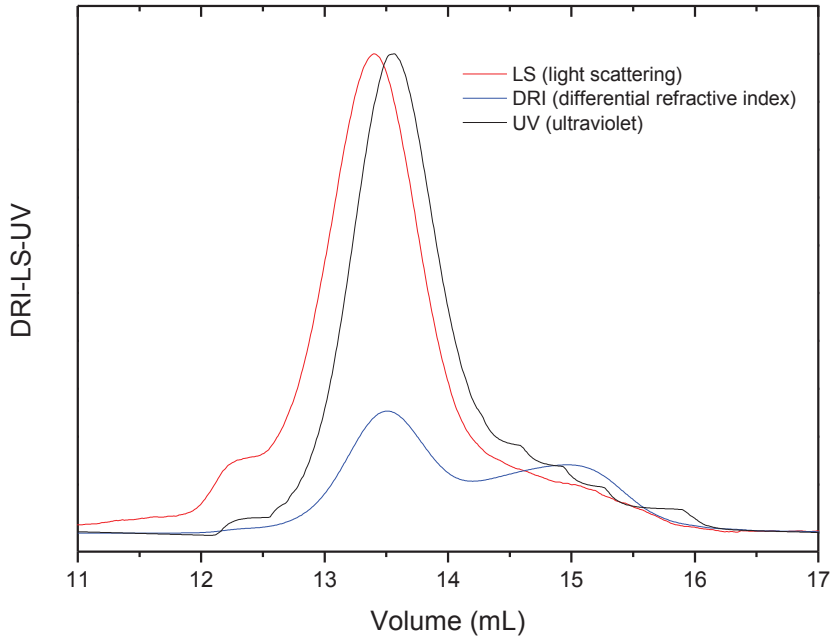

Figure 9.28 *SEC chromatograms of poly(HEMAm-co-**M1**), target DP_n = 53, obtained by RAFT polymerization of **M1** and HEMAm in the presence of CPADB in acetate buffer (pD ~ 5.3) at 60 °C (run no. 13, Table 9.1). Eluant: 0.1 M $NaNO_3$ + 10 mM EDTA + 0.03 % NaN_3, 35 °C, 4 g L^{-1}.Columns: Shodex OH pak SB-(Guard + 802.5 +803) HQ.*

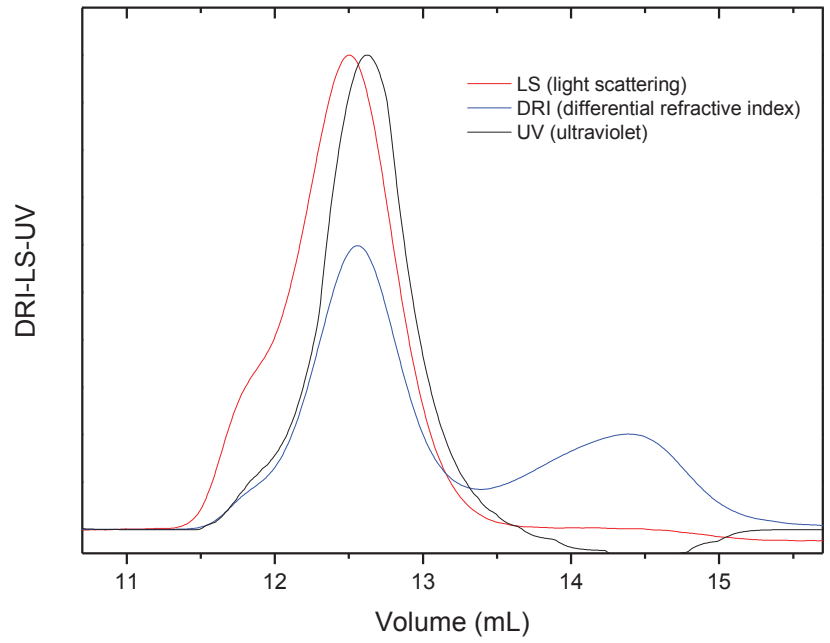

Figure 9.29 *SEC chromatograms of poly(HEMAm-co-**M1**), target DP_n = 107, obtained by RAFT polymerization of **M1** and HEMAm in the presence of CPADB in acetate buffer (pD ~ 5.3) at 60 °C (run no. 14, Table 9.1). Eluant: 0.1 M $NaNO_3$ + 10 mM EDTA + 0.03 % NaN_3, 35 °C, 4 g L^{-1}.Columns: Shodex OH pak SB-(Guard + 802.5 +803) HQ.*

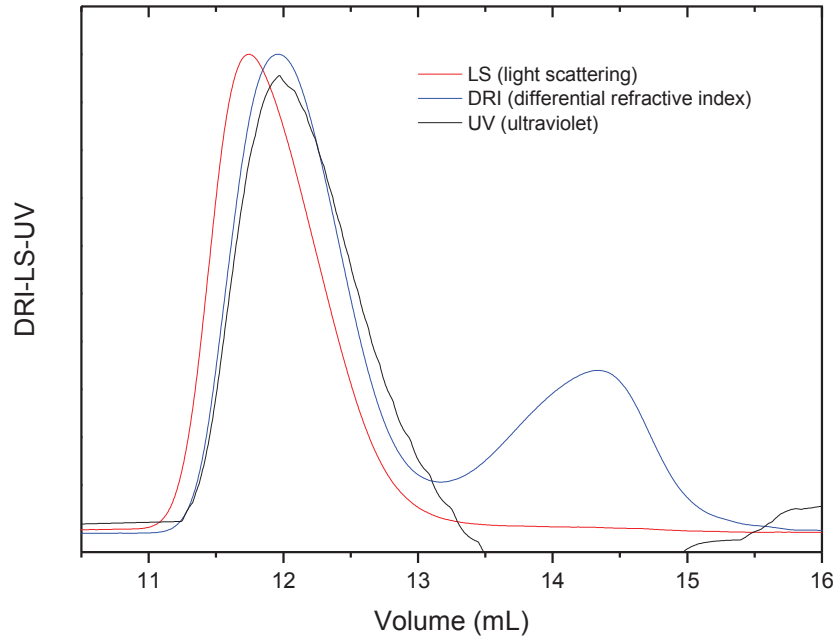

Figure 9.30 *SEC chromatograms of poly(HEMAm-co-**M1**), target DP_n = 215, obtained by RAFT polymerization of **M1** and HEMAm in the presence of CPADB in acetate buffer (pD ~ 5.3) at 60 °C (run no. 15, Table 9.1). Eluant: 0.1 M $NaNO_3$ + 10 mM EDTA + 0.03 % NaN_3, 35 °C, 4 g L^{-1}.Columns: Shodex OH pak SB-(Guard + 802.5 +803) HQ.*

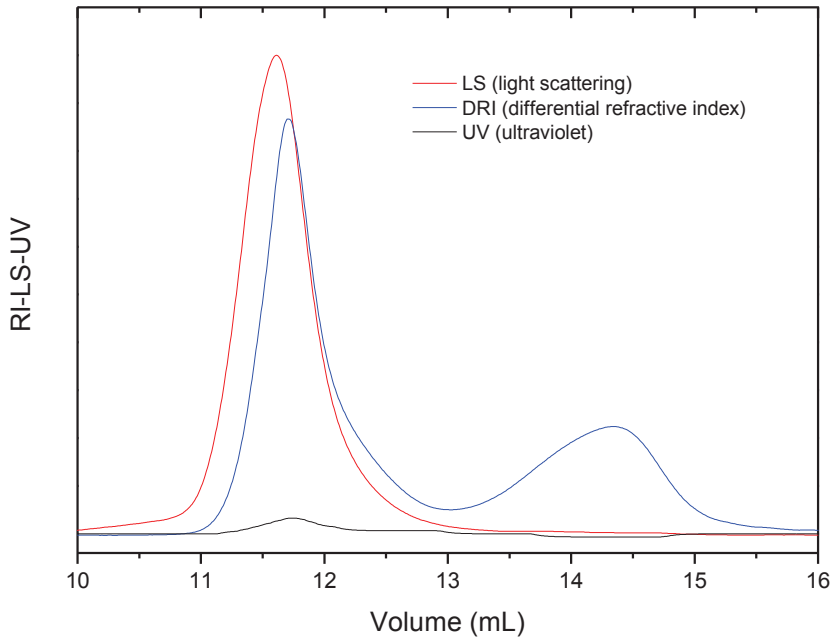

Figure 9.31 *SEC chromatograms of poly(HEMAm-co-**M1**), target DP_n = 320, obtained by RAFT polymerization of **M1** and HEMAm in the presence of CPADB in acetate buffer (pD ~ 5.3) at 60 °C (run no. 16, Table 9.1). Eluant: 0.1 M $NaNO_3$ + 10 mM EDTA + 0.03 % NaN_3, 35 °C, 4 g L^{-1}.Columns: Shodex OH pak SB-(Guard + 802.5 +803) HQ.*

9.5 References

(1) (a) Moad, G.; Rizzardo, E.; Thang, S. H. *Accounts of Chemical Research* **2008**, *41*, 1133(b) Moad, G.; Rizzardo, E.; Thang, S. H. *Australian Journal of Chemistry* **2005**, *58*, 379(c) Moad, G.; Rizzardo, E.; Thang, S. H. *Aust. J. Chem.* **2009**, *62*, 1402.

(2) (a) Donovan, M. S.; Sanford, T. A.; Lowe, A. B.; Sumerlin, B. S.; Mitsukami, Y.; McCormick, C. L. *Macromolecules* **2002**, *35*, 4570(b) Donovan, M. S.; Sumerlin, B. S.; Lowe, A. B.; McCormick, C. L. *Macromolecules* **2002**, *35*, 8663(c) Lowe, A. B.; Sumerlin, B. S.; McCormick, C. L. *Polymer* **2003**, *44*, 6761.

(3) (a) Baussard, J.-F.; Habib-Jiwan, J.-L.; Laschewsky, A.; Mertoglu, M.; Storsberg, J. *Polymer* **2004**, *45*, 3615(b) Cameron, N. R.; Spain, S. G.; Kingham, J. A.; Weck, S.; Albertin, L.; Barker, C. A.; Battaglia, G.; Smart, T.; Blanazsc, A. *Faraday Discussions* **2008**, *139*(c) Albertin, L.; Cameron, N. R. *Macromolecules* **2007**, *40*, 6082(d) Mertoglu, M.; Laschewsky, A.; Skrabania, K.; Wieland, C. *Macromolecules* **2005**, *38*, 3601(e) Lowe, A. B.; McCormick, C. L. *Prog. Polym. Sci.* **2007**, *32*, 283.

(4) SciFinder search for "RAFT polymerization aqueous" carried out on the 5th October 2011. Polymer Preprint articles were excluded from the count.

(5) (a) Sun, X. L.; Faucher, K. M.; Houston, M.; Grande, D.; Chaikof, E. L. *Journal of the American Chemical Society* **2002**, *124*, 7258(b) Sun, X. L.; Grande, D.; Baskaran, S.; Hanson, S. R.; Chaikof, E. L. *Biomacromolecules* **2002**, *3*, 1065(c) Grande, D.; Baskaran, S.; Chaikof, E. L. *Macromolecules* **2001**, *34*, 1640(d) Grande, D.; Baskaran, S.; Chaikof, E. L. *Polymeric Materials Science and Engineering* **2001**, *84*, 141(e) Grande, D.; Baskaran, S.; Baskaran, C.; Gnanou, Y.; Chaikof, E. L. *Macromolecules* **2000**, *33*, 1123(f) Chaikof, E. L.; Sun, X. L. In *PCT Int. Appl.*; Emory University: Atlanta, GA, USA: WO 2003099835, 2003(g) Baskaran, S.; Grande, D.; Sun, X. L.; Yayon, A.; Chaikof, E. L. *Bioconjugate Chemistry* **2002**, *13*, 1309(h) Alidedeoglu, A. H.; York, A. W.; Rosado, D. A.; McCormick, C. L.; Morgan, S. E. *J. Polym. Sci., Part A Polym. Chem.* **2010**, *48*, 3052.

(6) Battino, R. *Chemical Reviews* **1971**, *71*, 5.

(7) Le, T. P.; Moad, G.; Rizzardo, E.; Thang, S. H.; (E. I. Du Pont de Nemours & Co., USA; Le, Tam Phuong; Moad, Graeme; Rizzardo, Ezio; Thang, San Hoa). Application: WO WO, 1998.

(8) Wyatt, P. J. *Analytica Chimica Acta* **1993**, *272*, 1.

(9) *Light scattering from polymer solutions*; Huglin, M. B., Ed.; Academic Press: London, 1972.

(10) Rinaudo, M. In *Comprehensive Glycoscience: From Chemistry to System Biology*; Boons, G. J., Lee, Y. C., Suzuki, A., Taniguchi, N., Voragen, A. G. J., Eds.; Elsevier Ltd, 2007, pp 691-735; Vol. 2.

(11) Mitsukami, Y.; Donovan, M. S.; Lowe, A. B.; McCormick, C. L. *Macromolecules* **2001**, *34*, 2248.

(12) Sumerlin, B. S.; Donovan, M. S.; Mitsukami, Y.; Lowe, A. B.; McCormick, C. L. *Macromolecules* **2001**, *34*, 6561.

(13) (a) York, A. W.; Zhang, Y.; Holley, A. C.; Guo, Y.; Huang, F.; McCormick, C. L. *Biomacromolecules* **2009**, *10*, 936(b) Deng, Z.; Ahmed, M.; Narain, R. *J. Polym. Sci., Part A Polym. Chem.* **2009**, *47*, 614(c) Vasilieva, Y. A.; Scales, C. W.; Thomas, D. B.; Ezell, R. G.; Lowe, A. B.; Ayres, N.; McCormick, C. L. *J. Polym. Sci., Part A Polym. Chem.* **2005**, *43*, 3141(d) Scales, C. W.; Vasilieva, Y. A.; Convertine, A. J.; Lowe, A. B.; McCormick, C. L. *Biomacromolecules* **2005**, *6*, 1846.

(14) (a) Meuer, S.; Oberle, P.; Theato, P.; Tremel, W.; Zentel, R. *Advanced Materials* **2007**, *19*, 2073(b) Li, Y.; Armes, S. P. *Macromolecules* **2009**, *42*, 939.

(15) (a) Zorn, M.; Meuer, S.; Tahir, M. N.; Khalavka, Y.; Sonnichsen, C.; Tremel, W.; Zentel, R. *Journal of Materials Chemistry* **2008**, *18*, 3050(b) Barsbay, M.; Gueven, O.; Davis, T. P.; Barner-Kowollik, C.; Barner, L. *Polymer* **2009**, *50*, 973.

(16) (a) Convertine, A. J.; Benoit, D. S. W.; Duvall, C. L.; Hoffman, A. S.; Stayton, P. S. *J. Controlled Release* **2009**, *133*, 221(b) Xu, X.; Smith, A. E.; Kirkland, S. E.; McCormick, C. L. *Macromolecules* **2008**, *41*, 8429(c) Städler, B.; Chandrawati, R.; Price, A. D.; Chong, S.-F.; Breheney, K.; Postma, A.; Connal, L. A.; Zelikin, A. N.; Caruso, F. *Angewandte Chemie International Edition* **2009**, *48*, 4359(d) Rizzardo, E.; Chen, M.; Chong, B.; Moad, G.; Skidmore, M.; Thang, S. H. *Macromolecular Symposia* **2007**, *248*, 104.

(17) Johnson, R. N.; Burke, R. S.; Convertine, A. J.; Hoffman, A. S.; Stayton, P. S.; Pun, S. H. *Biomacromolecules* **2010**, *11*, 3007.

(18) Thang, S. H.; Chong, Y. K.; Mayadunne, R. T. A.; Moad, G.; Rizzardo, E. *Tetrahedron Letters* **1999**, *40*, 2435.

(19) Moad, G.; Chong, Y. K.; Postma, A.; Rizzardo, E.; Thang, S. H. *Polymer* **2005**, *46*, 8458.

(20) (a) Moad, G.; Rizzardo, E.; Thang, S. H. *Polymer* **2008**, *49*, 1079(b) Moad, G.; Rizzardo, E.; Thang, S. H. *Aust. J. Chem.* **2006**, *59*, 669.

(21) (a) Thomas, D. B.; Convertine, A. J.; Hester, R. D.; Lowe, A. B.; McCormick, C. L. *Macromolecules* **2004**, *37*, 1735(b) Albertin, L.; Stenzel, M. H.; Barner-Kowollik, C.; Davis, T. P. *Polymer* **2006**, *47*, 1011.

(22) Gibian, M. J.; Corley, R. C. *Chemical Reviews (Washington, DC, United States)* **1973**, *73*, 441.

(23) Moad, G.; Solomon, D. H. *The chemistry of radical polymerization: Second fully revised edition*; 2nd ed.; Elsevier Ltd., 2006.

(24) Buback, M.; Vana, P. *Macromolecular Rapid Communications* **2006**, *27*, 1299.

(25) Pearson, S.; Allen, N.; Stenzel, M. H. *J. Polym. Sci., Part A Polym. Chem.* **2009**, *47*, 1706.

(26) Thickett, S. C.; Gilbert, R. G. *Polymer* **2004**, *45*, 6993.

(27) (a) Lacík, I.; Beuermann, S.; Buback, M. *Macromolecules* **2003**, *36*, 9355(b) Kuchta, F.-D.; van Herk, A. M.; German, A. L. *Macromolecules* **2000**, *33*, 3641.

(28) Seabrook, S. A.; Tonge, M. P.; Gilbert, R. G. *Journal of Polymer Science Part A: Polymer Chemistry* **2005**, *43*, 1357.

Chapter 10: Conclusions

In **Chapter 5**, the synthesis of oligoglycuronan derived glycosylamines was investigated. To this end, a preliminary study was carried out on a model uronic acid (D-glucuronic acid **1**). The latter was reacted with different ammonia sources in water and the reaction was monitored by ESI-MS and solution NMR spectrometry. For long reaction times (~24 hrs), the expected products β-D-glucopyranuronosylamine **2** and *N*-(β-D-glucopyranuronosyl)carbamate **3** were obtained, whereas 7 other species (**5**-**11**) were identified in intermediate samples (Scheme 10.1).

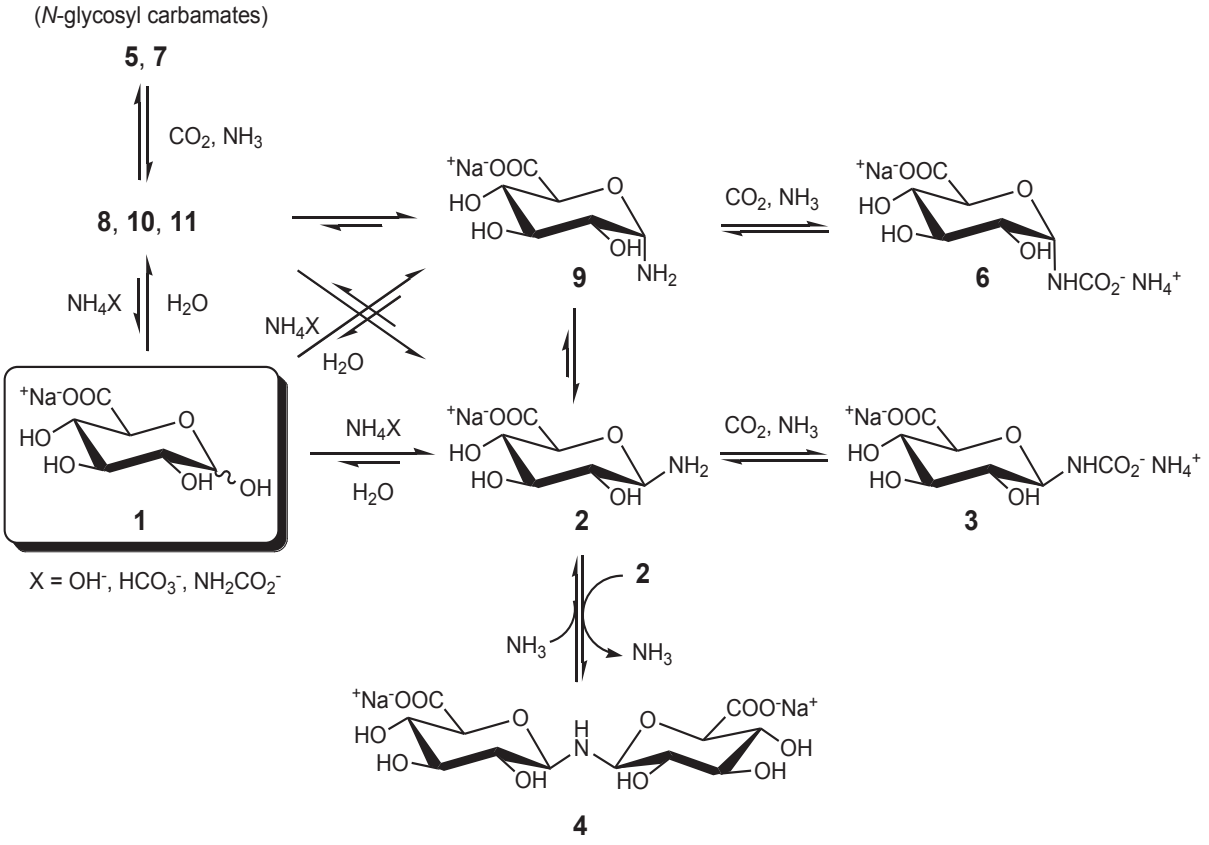

Scheme 10.1 *Reactions taking place during the synthesis of β-D-glucopyranuronosylamine **2** in aqueous solution.*

^{1}H-^{1}H Homonuclear and ^{1}H-^{13}C Heteronuclear correlation experiments enabled complete assignments of the ^{1}H and ^{13}C-NMR spectra of compound $\mathbf{1}_{\alpha}$, $\mathbf{1}_{\beta}$, **2**, and **3**, whereas partial assignments were obtained for the other compounds. Based on these results, a ^{1}H-NMR protocol for the quantification of the different species (reactants, intermediates and products)

taking part to the reaction was developed. It was thus calculated that after 24 hrs at 30 ºC between 64 % (protocol **A**.1.06: 1 M NH_3 + NH_4HCO_3) and 89 % of product **2+3** is obtained (protocol **B**.0.S: saturated ammonium carbamate), whereas the mole fraction of diglycosylamine **4** varies between 0 and 3 %. NMR data confirmed the structure of compounds **2** and **3**, proved that **3**, **5**, **6**, and **7** are *N*-(glycosyl)carbamates, and indicated that **6** and **9** are indeed the α anomer of the main products **3** and **2**. Also, by combining NMR and ESI-MS results, we could prove that all intermediate species are constitutional isomers and/or diastereomers of **2** and **3**. Finally, by monitoring the evolution of the composition of an early reaction sample redissolved in D_2O, we could prove that species **5**, **7**, **8**, **10**, and **11** are precursors of compounds **2**, **3**, **6**, and **9**, and that the α and the β anomer of D-glucopyranuronosylamine are initially formed in the same proportion but the former gradually disappears in favor of the more stable β form. To the best of our knowledge, this was the first time that the α anomer has been observed during the formation of a β-glycosylamine. Based on these results, we concluded that the synthesis of β-D-glucopyranuronosylamine in aqueous solution proceeds according to Scheme 10.1. Correct assignments for the ^{1}H and ^{13}C-NMR spectra of D-glucuronic acid in D_2O were also established in the course of this study.

When sodium D-glucuronate **1** was reacted with ammonia and/or volatile ammonium salts in water the rate of formation of β-D-glucopyranuronosylamine **2** and *N*-(β-D-glucopyranuronosyl) carbamate **3** strongly depended on the experimental conditions. In general higher ammonia and/or ammonium salt concentrations lead to a faster conversion of the starting sugar into intermediate species **5-11**, and of the latter into the final products **2** and **3**. Yet, some interesting trends and exceptions are observed:

i. **B**.0.S (saturated ammonium carbamate) is both the fastest protocol tested and the one leading to the highest final yields of **2**+**3** (89 % in 5 ½ hrs at 30 ºC; 87 % in 1 ½ hrs at 40 ºC).

ii. Whenever a lesser amount of salt (or a lower ionic strength) is needed, protocols **B**.0.20/30 and **A/B**.5.06 should be preferred to **A/B**.9.06 and **A/B**.14.02, since they lead to the same yield in **2**+**3** (84-86 % after 24-33 hrs) while requiring much less reagent.

iii. With the sole exception of **A/B**.1.06, after 24 hrs of reaction all tested protocols lead to higher yields of **2**+**3** than concentrated commercial ammonia alone (**X**.14.00).

iv. The equilibrium fraction of α anomers **6**+**9** is around 7-8 % in water at 30 ºC.

v. Concerning bis(β-D-glucopyranuronosyl)amine **4**, less than 3 % is formed in all cases, with a minimum value of 0.5 % in the case of **B**.0.S (after 24 hrs).

vi. The formation of β-glycopyranosylamine / *N*-β-glycopyranosyl carbamate is consistently faster in the case of D-glucuronic acid than in the case of D-glucose (4 to 8 times faster).

The understanding developed in the preliminary study was used for the transformation of oligoglycuronans of different degrees of polymerization into the corresponding glycosylamines. The starting oligosaccharides were reacted with ammonia according to protocols **A**/**B**.5.02 and good to high yields were obtained for reaction times of a few days. The rate of reaction was different for (1→4)-β-D-mannuronan (MM) and (1→4)-α-L-guluronan oligomers (GG): Under the same conditions, after 3 hours of reaction 70 % of amine was obtained for MM but only 35 % in the case of GG. In the early stages of the reaction, peaks appeared in the NMR which were attributed to two by-products (or intermediates); their amount did not exceed 3 % though. Conveniently, the obtained glycosylamines could be isolated by simple precipitation of the reaction mixture in ethanol followed by freeze-drying. This step not only eliminated most of the salts but favored the conversion of the *N*-glycosyl carbamate to the corresponding glycosylamine.

The major drawback to use of glycosylamine in synthesis is that they are susceptible to hydrolysis in aqueous solution and need to be handled with care. For this reason, the synthesis of oligoglycuronan-derived 1-amino-1-deoxy alditols via reductive amination was investigated as well (**Chapter6**). Conversion of the starting oligosaccharide was much slower than what observed for direct amination (glycosylamines) and depending on the pH, between 40% and 70 % of the sugars were transformed into byproduct(s). The concomitant formation of alditol from the reduction of the hemiacetal group was ruled out since no CH_2OH signals appeared in the DEPT-135 spectrum. Another hypothesis was the formation of di(1-amino-1-deoxy alditol) from the reaction of the target product with another oligoglycuronan molecule, but size exclusion chromatography showed that no higher molar mass species had formed. An optimization study was carried out to improve the yield in oligoglycuronan 1-amino-1-deoxy alditol and the time course of the reaction was monitored by ^{1}H NMR. It was found that the consumption of oligo(1→4)-β-D-mannuronan is faster than that of oligo(1→4)-α-L-guluronan

and that the latter has slightly higher tendency to form byproducts. In both cases the molar fraction of 1-amino-1-alditol kept increasing monotonically, and no optimal reaction time giving a "peak yield" was identified. The effect of the pH of the reaction medium was considered as well and the best results (50-55 % yield) were obtained in the pH range 5.5 - 6.5.

To better understand the nature of the by-products formed during the reductive amination of oligoglycuronans, a simpler uronic acid (D-glucuronic) acid was investigated. In this case, we could prove that the number of species formed grows when the pH of the reaction medium is increased from 6.0 to 7.8 and although (5ξ)-1-amino-1-deoxy-D-*arabino*-hexitol is indeed formed, it is not the major by product.

From the oligoglycuronan-derived glycosylamines and 1-amino-1-deoxy alditols described in Chapter 5 and Chapter 6, glycomonomers (AlgiMERs) were synthesized in aqueous solution without resorting to protective group chemistry (**Chapter 7**). Three types of reagents were considered: Methacrylic anhydride, (meth)acryloyl chloride and 2-isocyanatoethyl methacrylate. The use of methacrylic anhydride led to partial esterification of the hydroxyl groups of the sugar and was soon abandoned in favor of acyl halides. When starting from 1-amino-1-deoxy alditols, the latter gave quantitative yields no concomitant esterification reactions. The reaction medium tested was a carbonate buffer at pH 9.5 with a concentration four folds that of the acylating agent. Starting from the same type of substrate, methacrylate-type AlgiMERs were obtained by reacting with 2-isocayanatoethyl methacrylate, although yields were lower in this case (60-87% depending on the pH). In all reactions, care had to be taken not to exceed pH 10 since higher pH values led to colored products, most probably due to degradation products derived from the oligosaccharides. Concerning the regioselective functionalization of oligoglycuronan-derived glycosylamines, only acrylamide derivatives were prepared and under the same conditions, the yield was markedly higher for oligo(1→4)-β-D-mannuronan (70 %) than for oligo(1→4)-α-L-gululuronan (41%). The origin of this phenomenon is unclear, since in both cases the amine has an equatorial orientation.

In **Chapter 8**, the homo and copolymerization studies on oligoalginate derived monomers (AlgiMERs) in aqueous solution were investigated. The aim of the study was to understand the effect of the nature of the (co)monomers (methacrylate, acrylamide or methacrylamide), the ionic strength of the solution, the molecular weight of the AlgiMER and

the comonomer concentration on the polymerization process. AlgiMERs did not homopolymerize even in high ionic strength and only dimers to pentamers were obtained (depending on the DP of the glycomonomer). Moreover, it was shown than there was a marginal effect of the vinyl moiety (methacrylamide or acrylamide) on the conversion and the molecular weight of the obtained oligomers. On the other hand, copolymerization studies of the same AlgiMERs (acrylamide, methacrylamide) with *N*-(2-hydroxyethyl)methacrylamide (HEMAm) yielded high molar mass copolymers (M_w up to 1.6×10^6 Da). In this context it was shown that:

- Increasing the initial monomer concentrations from ~0.3 mol L^{-1} to ~0.5 mol L^{-1} resulted in a 4-fold increase in the molar mass the obtained polymers.
- The ionic strength of the polymerization mixture had marginal effects on the molecular weight of the polymer, no effect on the rate of polymerization or on the AlgiMER incorporation.
- Acrylamide- and methacrylamide-type AlgiMERs yielded polymers with comparable molecular weights, but AlgiMER incorporation was better in the second case.
- Polymers with longer AlgiMER grafts (up to $DP_n = 10$) had molecular weights at least double those obtained from AlgiMERs with $DP_n = 5$. However, AlgiMERs with DP_n 17 and 20 resulted in polymers with M_w not exceeding 1.0×10^6 Da and in partial gelation, possibly due to chain transfer.

From a kinetic study of the copolymerization of HEMAm with a methacrylamide- or an acrylamide-type AlgiMER, it was found that the consumption of each monomer obeyed a pseudo first order plot without an inhibition period. Both types of AlgiMER were incorporated into the copolymer since the early stages of the polymerization, but their conversion was somewhat slower than that of HEMAm. Such effect was particularly pronounced for the acrylamide derivative, whereas the drift in polymer composition was small with the methacrylamide-type AlgiMER. This is an important aspect of the copolymerization, since it ensures that macromolecules formed at different stages of the process have similar compositions and physico-chemical properties.

Finally, copolymers with long grafts ($ManA_{17}$ and $GulA_{20}$; $M_w \cong 1 \times 10^6$ Da, *F*m(AlgiMER) ≅ 45-50 %) were subjected to gelation experiments in the presence of Ca^{2+}

ions and the rheological properties of the resulting materials were examined. The hydrogel obtained from a glycopolymer carrying mannuronan grafts was loose and opaque whereas that obtained from guluronan grafts was soft, transparent and self-standing (Young's modulus of 5400 N m^{-2}; Figure 10.1).

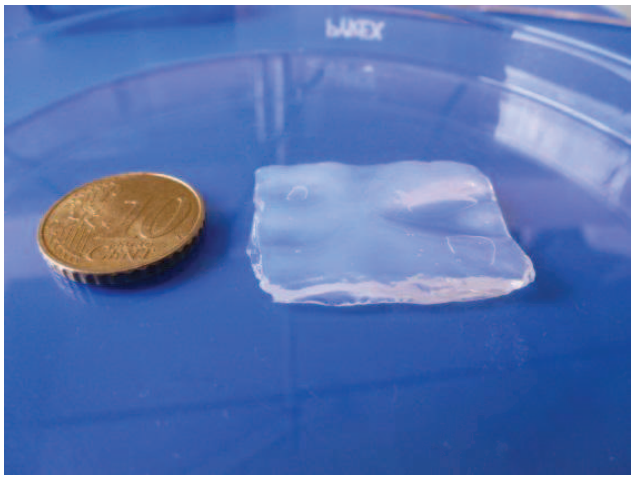

Figure 10.1 *Hydrogel formed by poly(HEMAm-graft-(1→4)-α-L-guluronan) with* Ca^{2+} *ions.*

The study was then extended to the reversible addition-fragmentation chain transfer (RAFT) copolymerization of HEMAm and methacrylamide-type AlgiMERs in aqueous solution (**Chapter 9**). A preliminary study showed that 4-cyano-4-[(phenylcarbonothioyl)sulfanyl] pentanoic acid effectively controlled the homopolymerization of HEMAm in acetate buffer (0.2 mol L^{-1}, pD 5.3) at 60 °C and that nearly monodisperse poly(HEMAm) (PDI = 1.03) with a pre-defined molar mass was obtained ($0.90 \leq M_n / M_{n,th} \leq 1.08$). The same protocol was then applied to copolymerization experiments and kinetics similar to those found for the conventional radical copolymerization were observed (total conversion of ~ 80 % after 5 hours), without any induction period at the beginning of the process. In general, good control over the molecular weight was achieved ($0.96 \leq M_n / M_{n,th} \leq 1.20$) and narrow polydispersity glycopolymers were obtained ($1.06 \leq$ PDI ≤ 1.23). The living character of the process was further proved by conduction a set of copolymerizations with different $c^0_{monomer} / c^0_{CPADB}$ ratios: Good agreement between theoretical and experimental molecular weights was obtained up to 50 000 Da, whereas targeting higher molecular weight polymers resulted in bigger deviations (M_n = 90 000 Da, $M_n/M_{n,th}$ = 1.20, PDI = 1.23). Curiously, an analogous experiment with a lower HEMAm concentration (hence a higher proportion of glycomonomer in the feed) afforded gave better results (M_n = 82 000 Da, $M_n/M_{n,th}$ = 1.08, PDI = 1.13).

The RAFT copolymerization of longer AlgiMERs ($ManA_{17}$ and $GulA_{20}$) with HEMAm was also explored. Contrary to the analogous conventional radical copolymerization, in this case no gel formed during the reaction. A good control over molecular weight was achieved ($0.96 \leq M_n / M_{n,th} \leq 1.14$) and fairly low polydispersity polymers were obtained (PDI ≤ 1.23). Finally, copolymers with long guluronan grafts (M_n = 56 000 Da, PDI = 1.21, *F*m($GulA_{20}$) ≅ 37 %) were subjected to a gelling test in the presence of Ca^{2+} and the resulting soft beads (Figure 10.2) where characterized by rheology (oscillatory experiments), which confirmed their elastic nature (G'/G'' = 7).

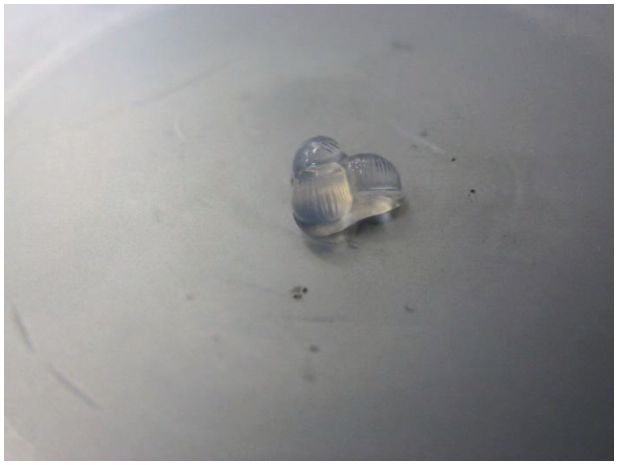

Figure 10.2 *Gel beads obtained from well-defined poly(HEMAm-graft-(1→4)-α-L-guluronan) sitting on the rheometer plate.*